

**PROCEEDINGS
INTERNATIONAL
SOLVENT EXTRACTION
CONFERENCE
1974**

VOL. 3



S.C.I.

Proceedings
of the
International Solvent Extraction Conference
I.S.E.C. 74

Lyon; 8-14th September 1974

SOCIETY OF CHEMICAL INDUSTRY
LONDON
1974

SOCIETY OF CHEMICAL INDUSTRY
14 BELGRAVE SQUARE
LONDON S.W.1.

Editorial Committee
Prof. J. D. Thornton
Dr. A. Naylor
Dr. H. A. C. McKay
Prof. G. V. Jeffreys (Editor)

© 1974 SOCIETY OF CHEMICAL INDUSTRY

In Four Volumes

ALL RIGHTS RESERVED

Printed in England

SESSION 19 EXTRACTION TECHNOLOGY (Nuclear Processes II)

- p. 1985
- 72 TSUBOYA T, TANAKA T, NEMOTO S and HOSHINO T -
Tokai-mura, Japan - Some modification of a Purex
process for the recovery of neptunium.
- 109 SCHMIEDER H, BAUMGARTNER F, GOLDACKER H, HAUSBERGER H
and WARNECKE E - Institute fur Heisse Chemie, W.
Germany - Electrolytic methods for application in the
Purex process.
- 197 PATIGNY P, REGNIER G, TAILLARD D and MIQUEL P - CEA,
France - Utilisation of hydroxylamine nitrate for the
final concentration and purification of plutonium in
the irradiated fuel processing factory at La Hague
- 220 SCHULZ W W, BOUSE D F and KUPFER M J - Atlantic Rich-
field Hanford Co, USA - Reflux amine flowsheet for
plutonium recovery from metallurgical scrap.
- 241 HUPPERT K L, ISSEL W and KNOCH W - G Wiederaufarbeitung
von Kernbrennstoffen mbH, W. Germany - Performance
of extraction equipment in the WAK-pilot plant.
- 257 GERMAIN M, BATHELLIER A, CENF and BERARD P - Centre
de Marcoule, France - Use of formic acid for the
stripping of plutonium.

SESSION 20 EXTRACTION CHROMATOGRAPHY AND ANALYTICAL APPLICATIONS

- 56 KROEBEL R and MEYER A ↗ Bayer A G, W. Germany -
Application of newly developed materials for extrac-
tion chromatography of inorganic salts in columns.
- 66 BENMALEK M, CHERMETTE H, MARTELET C, SANDINO D and
TOUSSET J - Institute Physique Nucleaire, France -
The selective extraction of halide traces.
- 148 McDOWELL W J and COLEMAN C F - Oak Ridge National
Laboratory, USA - Combined solvent extraction - liquid
scintillation methods for radio-assay of alpha emitters
- 187 LEVIN I S, SERGEEVA V V, RODINA T F, TARASOVA V A,
YUKJIN Yu M, VARENTSOVA V I, VORSINA I A, BALAKIREVA N A,
BYKHOVSKAYA I A, NOVOSELTSEVA L A, TISCHENKO L I
and FRID O M - Institute for Mineral Treatment, USSR -
Di-2-ethylhexyldithiophosphoric acid application to rare
and non-ferrous metal analytical chemistry and hydro-
metallurgy; mechanism of extraction and exchange
interphase interaction of metals of the copper, zinc,
gallium, germanium, arsenic sub-groups.

194 EKSBORG S and SCHILL G - Uppsala University, Sweden -
p.2149 Ion-pair chromatography of organic components.

209 BORG K O, GABRIELSSON M and JOHNSON T E - A B Hassle,
Sweden, Ion-pair partition chromatography applied to
separations in the bioanalytical field.

SESSION 21 CHEMISTRY OF EXTRACTION (Rare metals)

27 MARKLAND S Aa - Research Establishment Riso, Denmark -
Separation of niobium and tantalum by solvent extrac-
tion with tertiary amines from sulphuric acid solutions

33 FROLOV Yu G, MORGUNOV A F and SOLDATENKOVA N A -
Mendeleev Institute of Chemical Technology, USSR -
The state of niobium when extracted from solutions
of sulphuric and hydrochloric acids.

36 YAGODIN G A, SINEGRIKOVA O A and CHEKMAREV A M -
Mendeleev Institute of Chemical Technology, USSR -
Zirconium and hafnium polymerization effect on their
extraction by different class organic compounds.

128 BRONZAN P and MEIDER-GORICAN H - Institute Rudjer
Boscovic, Yugoslavia - Solvent extraction of zirconium
and hafnium with some trifunctional phosphine oxides.

182 SATO T, KOTANI S and TERAO O - Shizuoka University,
Japan - The Extraction of anionic vanadium (IV)-
thiocyanato complex from aqueous solutions by long-
chain alkyl quaternary ammonium compound.

186= JORDANOV N, PAVLOVA M - Institute of General and
Inorganic Chemistry and BOIKOVA D - High Institute of
Chemical Technology, Bulgaria - Mechanism of solvent
extraction of perchlorate ions by cyclohexanone.

SESSION 22 EQUIPMENT (Contactor Performance II)

155 LAURENCE G, HABSIEGER D, TALBOT J - ENSCP, France and
p-2269 CHAIEB M T - Tunis University, Tunisia and MICHEL P,
Centre d'Etudes Nucleaires, France - Metal extraction
by di-n-heptylsulphoxide (DH_pSO); applications in a
pulsed column.

216 STEINER L and HARTLAND S - Federal Institute of
p-2289 Technology, Switzerland - Calculation of mass transfer
coefficients in extraction columns under non-ideal-flow
conditions.

248 WEISS, S, SPATHE R, WURFEL R and MOHRING D - Technische
Hochschule fur Chemie, E. Germany - Hydrodynamic
behaviour and mass transfer of extraction columns with
various rotating parts.

- p.2339
- 256 ROWYER H, LÉBOUHELLEC J, HENRY E and MICHEL P - CEA, France - Present study and development of extraction pulsed columns.
- 258 SEIDLVA B and MISEK T - Research Institute of Chemical Equipment, Czechoslovakia - Liquid flow study in the cross-section of ARD extractor.
- 266 TODD D B and DAVIES G R - Baker Perkins Inc. USA - Performance of centrifugal extractors.

SESSION 23 MASS TRANSFER PHENOMENA II

- 51 HANSON C, HUGHES M A and MARSLAND G - Bradford University, UK - Mass Transfer with chemical reaction in liquid-liquid systems.
- 53 COX P R and STRACHAN A N - Loughborough University, UK - The influence of chemical reaction (nitration) on the rate of surface renewal at a liquid-liquid interface.
- 95 FARWELL, MCKAY H A C and WAIN A G - Atomic Energy Research Establishment, UK - Transfer of metal nitrates between aqueous nitrate media and neutral organophosphorus extractants.
- 174 RITCEY G M and LUCAS B H - Mines Branch, Canada - Diluents and modifiers - their effect on mass transfer and separation.
- 192 CLINTON S D - Oak Ridge National Laboratory, USA - Mass transfer of water from single aqueous sol droplets fluidized in a partially miscible alcohol.

FRIDAY, 13th September

SESSION 24 CHEMISTRY OF EXTRACTION (Synergism and Kinetics)

- 6 AMMON R V - Institut für Heisse Chemie, W. Germany - ^1H - and ^{31}P -NMR study of ligand exchange kinetics in the systems $\text{UO}_2(\text{NO}_3)_2$ -TBP and $\text{Pu}(\text{NO}_3)_4$ -TBP.
- 12 SPINK D R and OKUHARA D N - University of Waterloo, Canada - The effect of diluents on the extraction of tracer level copper by an alkyl hydroxy quinoline (Kelex 100).
- 35 YAGODIN G A, TARASOV V V and KIZIM N F - Mendeleev Institute of Chemical Technology, USSR - The state of substances in the organic phase and stripping microkinetics.
- 91 FLETT D S, COX M and HEELS J D - Warren Spring Laboratory UK - Extraction of nickel by hydroxyoxime/carboxylic acid mixtures.

136 SPIVAKOV B Ya, MYASOEDOV B F, SHKINEV B M, KOTCHETKOVA N E and CHMUTOVA M K - Moscow Academy of Sciences, USSR Synergic extraction of metals by the mixtures of tri-n-octylamine with a neutral extractant from nitrate and chloride solutions.

195 NAVRATIL O - Purkyne University, Czechoslovakia - Synergistic effects in liquid-liquid extraction of some heavy metals by 1-phenyl 3-methyl-3-benzoyl-pyrazol-5-one.

269 KOLARIK Z and KUHN W - Institut fur Heisse Chemie, W. Germany - Acidic organophosphorus extractants-XXI. Kinetics and equilibria of extraction of Eu(III) by di(2-ethylhexyl) phosphoric acid from complexing media.

SESSION 25 EXTRACTION TECHNOLOGY (Process Modelling and Control)

9 McDONALD C R and WILKINSON W L - Bradford University, UK - Control studies on a solvent extraction column.

211 GAUDERNACK B, MULLER T B, NULAND S and ORJASAEETER O - Institutt for Atomenergi, Norway - Simulation of the static and dynamic behavior of a solvent extraction process for rare earth separation.

250 BOYADZHIEV L and ANGELOV G - Academy of Sciences, Bulgaria - On the multicomponent extraction with backmixing.

260 ARMFIELD R N and AGNEW J B - Monash University, Australia Application of a two-variable-search optimisation scheme to the on-line control of a continuous extraction process.

SESSION 26 CHEMISTRY OF EXTRACTION (Rare Metals)

64 FOCHE K F, LESSING J G V and P A BRINK - Atomic Energy Board, South Africa, Extraction of platinum group metals from cyanide melts with liquid metals.

88 SINITZIN N M, TRAVKIN V F, PLOTINSKY G L, SVETLOV A A and ROVINSKY F J - Moscow Institute of Fine Chemical technology, USSR - Extraction of ruthenium and osmium nitroscomplexes.

123 GROENEWALD T - Chamber of Mines, South Africa, - A modified diluent for the solvent extraction of gold (I) cyanide from alkaline solution.

129 SEVDIC D - Institute "Rudjer Boskovic", Yugoslavia - Solvent Extraction of silver (I) and mercury (II) with sulphur containing ligands.

- 158 MIKHAILOV V A, KOROL N A and BOGDONOVA D D -
Institute of Inorganic Chemistry, USSR - The
chemical equilibria at distribution of mercury
chloride between water and solutions of TBP and
di-npocetyl sulphoxide in different diluents.
- 252 ESNAULT F, ROBAGLIA M, LATARD J M and DEMARTHE J M -
CEA, France - Separation of molybdenum and tungsten
by a liquid-liquid ion-exchange method.

GENERAL SESSION 27 INDUSTRIAL PROCESSES (Development,
Performance and Economics)

- b. 2789 103 BLUMBERG R, GAI J E and MAJDU K - IMI Institute for
Research and Development, Israel - Interesting aspects
in the development of a novel solvent extraction
process for producing sodium bicarbonate.
- 145 KUYLENTIERNÄ U - Stora Kopparbergs AB - and OTTERTUN
H - Chalmers University of Technology, Sweden - Solvent
extraction of HNO_3 -HF from stainless steel pickling
solutions.
- 199 DASHER J - Bechtel, USA - Economics of SX and its
alternatives for uranium and copper.
- 261 BIECH C P - Nchanga Consolidated Copper Mines, Zambia
The evaluation of the new copper extractant "P-1"
- b. 2873 274 RITCEY G M, LUCAS B H and ASHBROOK A W - Extraction
Metallurgy Division, Mines Branch, Canada - Some
Comments on the, and Environmental Effects of Solvent
Extraction Reagents used in Metallurgical Processing.

SESSION 19

Thursday 12th September: 9.00 hrs

EXTRACTION TECHNOLOGY

(Nuclear Processes II)

Chairman:

Dr. A. Naylor

Secretaries:

Dr. P.G.M. Brown

Mr. P. Nichel

SOME MODIFICATIONS OF A PUREX PROCESS FOR THE
RECOVERY OF NEPTUNIUM

T. Tsuboya, T. Tanaka, S. Nemeto, and T. Hoshino

ABSTRACT

A method for discharging Np into the waste streams of 2D bank (U purification step) or 2A bank (Pu purification step) of the Purex process designed for LWR fuels reprocessing was examined in counter-current solvent extraction experiments using a laboratory scale mixer-settler.

The oxidation of Np(V) to Np(VI) by HNO₂ and higher scrub acid concentrations in either the M.A. bank or the 1A bank were necessary to discharge more Np into the product streams of each bank.

These additive conditions were decided by the use of a computer code, NEPTUN, for simulating the stage concentration profiles of Np. The Np behaviour in the banks was also studied by the quantitative analysis of the Oxidation-reduction reactions of Np in the banks.

(Power Reactor and Nuclear Fuel Development
Corporation, Tokai-mura, Ibaragi-ken, Japan)

INTRODUCTION

The Purex process designed for LWR fuel reprocessing comprises 1st is/^{CO}decontamination, 2nd co decontamination, U/Pu separation, U purification and Pu purification cycles. Np behaviour in these cycles is quite different from either V or Pu behaviour, most of the Np discharges into the H.A. waste stream as Np(V) together with the F.P.s. It is however possible to carry Np into the waste streams of the 2D bank (U purification cycle) or 2A bank (Pu purification cycle) by adding the appropriate reagents to the process streams for the oxidation/reduction of Np. In the HA and 1A banks MnO_2 is added to oxidise Np(V) to Np(VI) in the extraction section and in the scrub-section the scrub acid concentration is increased to prevent reduction of Np(VI) in the organic stream. Hydrazine being added to decompose nitrous acid. In the 2A bank, hydrazine is added as the reductant for Np to improve the separation of Np from Pu and to discharge Np into the waste stream.

The present paper describes the results of continuous counter current solvent extraction experiments using laboratory scale mixer settler equipment.

Each condition was chosen not only from the basic data about the oxidation-reduction reactions of Np, ^{(1),(2),(4)} but also by use of a computer simulation code, NEPTUN, that was programmed to calculate the stage concentration profiles of Np using the extraction equilibrium data, and the oxidation-reduction kinetics data.

Extraction of Np

Extraction data of Np

The extraction coefficients of Np for the 30 vol.% TBP (tri-n-butyl phosphate) in n-dodecane diluent-aqueous nitrate system are generally given as follows: $Np(V) \leq Np(IV) < Np(VI)$. Extraction coefficient of Np(V), E_5 , is approximately $0.01^{(4)}$ E_4 for Np(IV) and E_6 for Np(VI) are given as follows: ⁽³⁾

$$\log(E_4/(\text{TBP})_0^2) = 2.55 \times \log(\text{NO}_3) + \log 0.7$$

$$(0.5 \leq (\text{NO}_3) \leq 2.5) \quad (1)$$

$$\log(E_6/(\text{TBP})_0^2) = 2.19 \times \log(\text{NO}_3) + \log 7.0$$

$$(0.2 \leq (\text{NO}_3) \leq 3.5) \quad (2)$$

, where $(\text{TBP})_0$ is free TBP concentration (M) and (NO_3) is apparent nitrate concentration (M) in the aqueous phase. In the system where U(VI) is present, the following relations are given between E_U and E_4 or E_6 :⁽³⁾

$$E_4/E_U = 0.09 \pm 0.03 \quad (0.5 \leq (\text{NO}_3) \leq 2.5) \quad (3)$$

$$E_6/E_U = 0.5 \pm 0.1 \quad (0.2 \leq (\text{NO}_3) \leq 3.7) \quad (4)$$

From eq.(3) or eq.(4), it is possible to estimate E_4 or E_6 for each stage by using E_U of each stage when the stage concentration profiles of U(VI) is given.

Oxidation-reduction reactions of Np

The reaction of Np with nitrous acid in aqueous solution (4). The rate of reaction and the apparent equilibrium constant at room temperature for the oxidation/reduction reaction $\text{Np(V)} \rightleftharpoons \text{Np(VI)}$ by nitrous acid in nitric acid are given as follows:

$$-d(\text{Np(V)})/dt = d(\text{Np(VI)})/dt = 89(\text{NO}_2)((\text{Np(V)}) - (\text{Np(V)})_e)$$

$$\text{(mole/min)} \quad (5)$$

$$(\text{Np(VI)})_e (\text{NO}_2)_0^{1/3} / (\text{Np(V)})_e (\text{HNO}_3)_0^3 = (1.20 \pm 0.14) \times 10^{-3} \quad (6)$$

, where $()_e$ is the equilibrium concentration and $()_0$ is the initial concentration.

The reaction of Np with U(IV) in aqueous solution:⁽⁵⁾
 Np(VI) is reduced to Np(IV) through Np(V) by U(IV) in nitric acid solution containing a reagent such as hydrazine, urea, and so on. The rate of reaction at room temperature is given as follows:

$$-d(Np(VI))/dt = d(Np(V))/dt = 0.25(Np)_o^{-0.5}(U(IV))_o(Np(VI)) \quad (7)$$

(mole/sec)

and

$$-d(Np(V))/dt = d(Np(IV))/dt = 2.1(Np)_o(U(IV))_o(HNO_3)^3(Np(V)) \quad (8)$$

(mole/sec)

The reaction of Np with hydrazine in aqueous solution: ⁽³⁾

Hydrazine is available as a reduction reagent for Np(VI).

The rate of reaction at room temperature is given as follows:

$$-d(Np(VI))/dt = d(Np(V))/dt = 7.6(NH_2NH_2)_o(Np(VI)) \quad (9)$$

(mole/min)

A computer simulation for the stage concentration profiles of Np ⁽⁴⁾

The stage concentration profiles at the steady state of each bank condition can be estimated prior to the experiment by the use of a computer code, NEPTUN, NEPTUN is also useful to estimate an appropriate condition for Np recovery and to perform the effective experiments. NEPTUN is programmed on the basis of the batchwise counter-current solvent extraction and can give the stage concentration profiles of Np even if the solvent extraction system contains an oxidation(reduction) reaction of Np by an oxidation(reduction) reagent. The calculation scheme is shown in Fig.1. Necessary input data are feed flowrates and its stage numbers, E_G for each stage calculated from eq. (4) using known E_U , the acid concentration and the concentration of the oxidation (reduction) reagent in the aqueous phase for each stage, the concentration and the valence composition of Np in the feed solution, the rate constant and the apparent equilibrium constant of the oxidation(reduction) reaction of Np, and the mixer and the settler volumes. The calculations are carried out of the extraction equilibrium and the oxidation-reduction reaction for each stage at first(N-loop), and then the calculations are repeated till the material balance of Np is satisfied between the feed and the outlets(M-loop). The results are printed out the concentrations, the inventory (X), the quantity of oxidation(ΔX), etc. of Np for each stage.

Counter - current extraction experiments

Experimental procedures ;

The Purex process concept is shown in Fig.2. The process conditions for HA bank, 1A bank, 2D bank, and 2A bank were studied, because they play an important role in a recovery process of discharging Np into the waste streams of 2D bank(2DW) or of 2A bank(2AW).

A laboratory scale mixer settler, "Cyrano 200 - 800" (Sonnal, France) was used as the solvent extraction contactor, having a 6 ml mixer volume and a 17 ml settler volume.

Feed flowrates were measured and recorded automatically. As the organic solvent was used 30 vol.% of TBP(tri-n-butyl phosphate) in n-dodecane diluent, Np was determined by a TTA extraction-a counting method for ^{237}Np and by a counting method for ^{239}Np added as a tracer of Np. Pu was determined by an a counting method, and acid concentrations were given by a potentiometry. U(VI), U(IV), HNO_2 , and NH_2NH_2 (aqueous phase only) were determined by using DBM(di-benzoyl methane)($\epsilon : 3.71 \times 10^6$, 403 m μ), o-phenanthrolin ($\epsilon : 9.40 \times 10^4$, 506 m μ), - naphthylamine($\epsilon : 4.00 \times 10^4$, 520 m μ), and p-di-methyl benzaldehyde($\epsilon : 6.42 \times 10^4$, 460 m μ), respectively.

RESULTS AND DISCUSSION:

HA bank - The flowsheet is shown in Fig.3. The alterations of the basic flowsheet are addition of nitrous acid as sodium into the 1st stage of the extraction section and of hydrazine as a nitrate solution into the feed stage, use of higher scrub acid concentration instead of 3M. Nitrous acid was supplied so as to give optimum conditions for discharging Np into the product stream (HAP) as determined by NEPTUN. Hydrazine was added in order to reduce nitrous acid concentration in the scrub section and the feed stage as low as possible. The observed stage concentration profiles for Np and nitrous acid are shown in fig.4. It was calculated from the flowsheet conditions and the concentration profiles that the Np discharge into HAP was 88.1% of total charge.

The simulated concentration profiles for Np given by NEPTUN are also shown in fig.4. Good agreement is shown for each phase. The ratio of the oxidation quantity of Np(X) to the inventory of Np(X) in each stage plotted in fig.5. also shows good agreement between observed and simulated values. Accordingly, it was proved that the oxidation reaction which gave a value higher than 0.1 for X/X in the extraction section satisfied quantitatively the reaction equations already mentioned. In the scrub section, X/X was observed to be -0.01. The reduction of Np was considerably suppressed as the result of low concentration of nitrous acid.

It was observed that when the scrub acid concentration was 3M, Np discharge into HAP was decreased to 65% of the total Np charge. Increase of the reduction of Np in the scrub section was observed in this operation.

1A bank - The modified flowsheet is given in fig.6. The alterations of the original flowsheet are similar to those for HA bank. The observed stage concentration profiles for Np and nitrous acid are shown in fig.7. The Np discharge into 1AP was 40% of total charge. When the operation was carried out with the original flowsheet, over 99% of total Np charge was released to the waste stream (1AW), $\Delta X/X$ in each stage is shown in Fig.8 about observed and simulated values. Although there are good agreement between both values for the extraction section, the values were only one-third of those given for HA bank. This low oxidation ratio is explained as follows; The ratio of the flowrate of aqueous phase to organic phase in the extraction section for 1A bank was three times higher than that for HA bank, thus considerable quantities of Np(VI) in each stage of the extraction section remained in the aqueous phase without being extracted into the organic phase, interrupting the oxidation reaction of Np(V). In the scrub section $\Delta X/X$ was about -0.05. Since nitrous acid concentration was not sufficiently high to reduce Np(VI) to Np(V) visibly, the reduction reaction was caused by other causes.

When the scrub acid concentration was 3M $\Delta X/X$ decreased to below -0.1 and the Np discharge into 1AP decreased to 5% of total charge.

2D bank: In this bank, U(IV) is fed as 2DS to scrub Pu from U stream in the original flowsheet as shown in fig.9. The stage concentration profiles for Np, NH_2NH_2 , and U(IV) are shown in fig.10. The Np discharge into 2DW was 99.7% of total charge. The reaction half times ($T_{1/2}$) of Np reduction in the aqueous phase calculated from eqs.(7) and (8) using conditions for the contactor; $5.8 \times 10^{-5}\text{M}$ for Np and $2.5 \times 10^{-4}\text{M}$ for U(IV), for example; were 84 sec for Np(VI) to Np(V) and 6.6×10^6 sec for Np(V) to Np(IV). It may be said from these results that Np(VI) fed to the bank is easily reduced to unextractable Np(V) and not to extractable Np(IV). ΔX and X observed are shown in Fig.11. Since 84.9% of X(4.19 mg/hr) in the feed stage is fed as Np(VI) and ΔX in the feed stage was -3.33 mg/hr, it is clear that the reduction reaction was almost completed at the feed stage.

Thus it is now clear that it is not necessary to alter the original condition of 2D bank to discharge Np into 2DW.

2A bank: The modified flowsheet is shown in fig.12. Hydrazine was fed with the scrub acid in order to reduce Np(VI) to Np(V) to discharge more Np into 2AW. The stage concentration profiles for Np and hydrazine are shown in fig.13. Np discharge into 2AW was over 90% of total charge. $\Delta X/X$ in each stage is shown in fig. 14. Figure 14 shows that the reduction of Np(VI) to Np(V) was extremely proceeded in the scrub section. Use of eq.(9) as the rate equation in NEPTUN gives a relationship between the Np discharge into 2AW and hydrazine concentration in the scrub solution (2AS) as shown in fig.15. It was resulted that observed and simulated results were agreed and that the valence of Np in the feed solution affected on Np discharge in case of the addition of lesser amount of hydrazine.

CONCLUSION

In order to discharge more Np into 2DW or 2AW of the Purex process designed for LWR fuels reprocessing, it is necessary to modify the process steps. As a result of continuous solvent extraction experiments using a laboratory scale mixer settler it is proposed to used the ozidation reaction of Np(V) by HNO_2 and to increase the scrub acid concentration in the HS and 1A banks.

For the 2A bank it is also proposed to feed hydrazine in the 2A3 feed to separate Np from Pu by the reduction of Np(VI) to Np(V). A computer code, NEPTUN, was developed and used to simulate the concentration profiles of Np.

ACKNOWLEDGEMENTS

The authors wish to thank Dr. T. Segawa, Manager of Technology Division, and Mr. K. Higuchi, Vice-director of Tokai Works, for the helpful advice, and Messers. M. Omine, K. Ueda, S. Irinouchi, M. Okita, N. Miyagawa, and S. Kumada for the analytical work,

REFERENCES

1. Siddall III, T.H. Dukes, E.K., J.Amer.Chem.Soc., 81, 790 (1959).
2. Swanson, J.L., BNWL-1017 (1969)
3. Tsuboya T., Nemoto, S., Hoshino, T., PNCT841-71-34 (1971)
4. Tanaka, C., Nemoto, S., Tsuboya, T., Hoshino, T., PNCT841-71-35 (1971).
5. Tsuboya T., Nemoto, S., Kumada, S., Hoshino T., unpublished (1973).

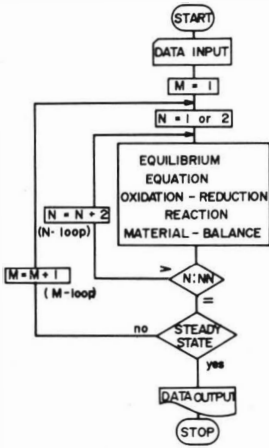


Fig.1. Flowchart of NEPTUN

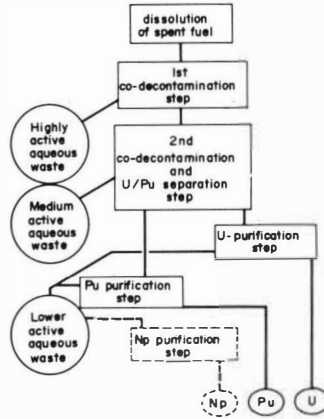


Fig 2 Concept of the Purex process and of Np recovery from lower active waste streams.

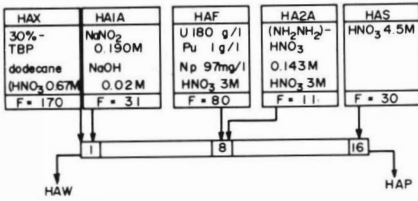


Fig. 3. Flowsheet of HA bank for discharging Np into HAP. (F: flow rate (ml / hr)).

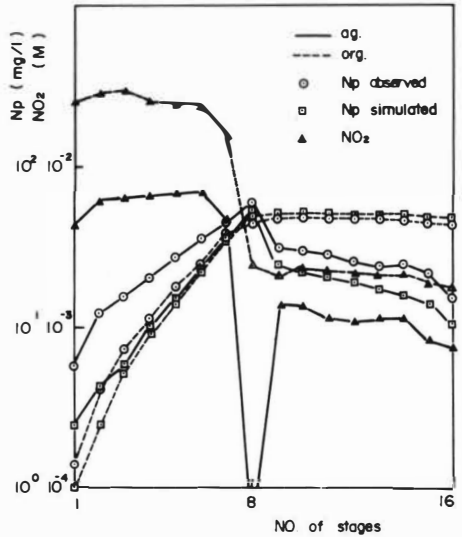


Fig.4. Stage concentration profiles of Np and NO₂ in HA bank.

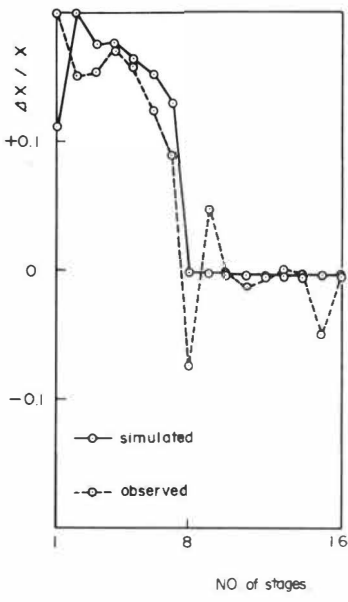


Fig 5. Profiles of oxidation ratios of Np in HA bank

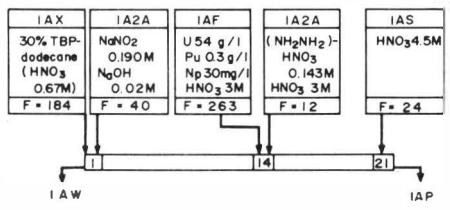


Fig 6. Flowsheet of IA bank for discharging Np into IAP.
(F: flow rate (ml/hr)).

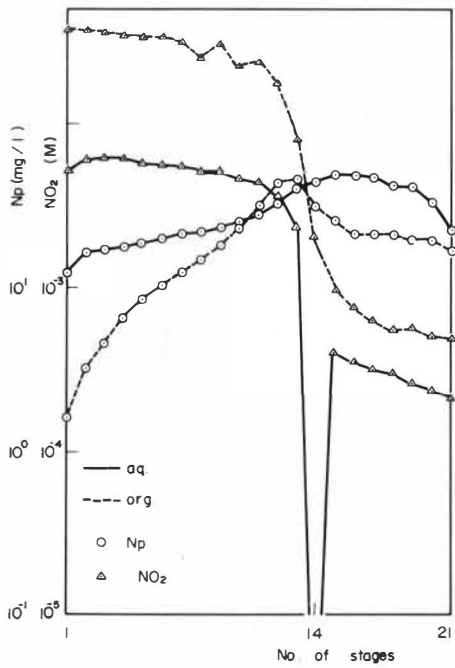


Fig 7. Stage concentration profiles of Np and NO₂ in IA bank.

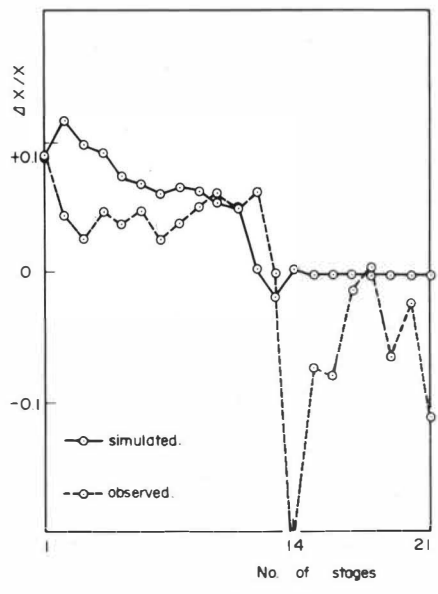


Fig 8. Profiles of oxidation ratios of Np in IA bank.

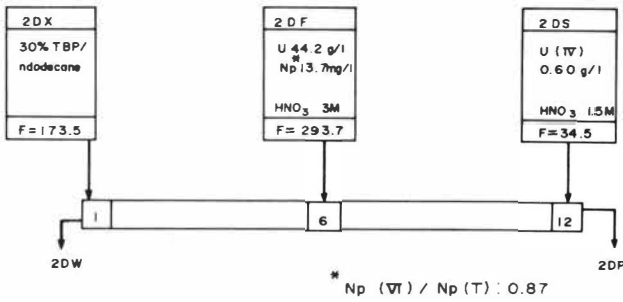


Fig. 9. Flowsheet of 2D bank (the basic flowsheet)
(F: flow rate (ml/hr)).

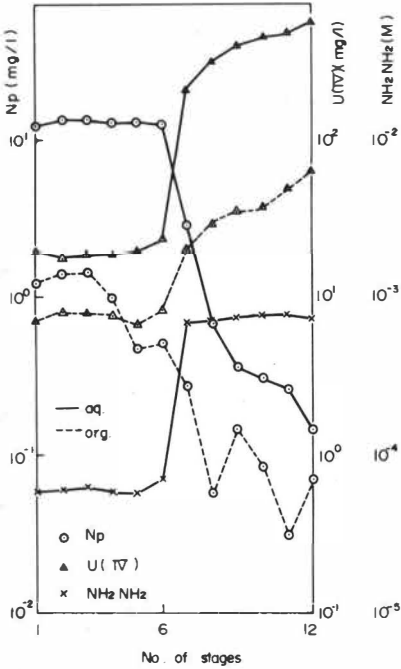


Fig. 10. Stage concentration profiles of Np, U(IV), and NH₂NH₂ in 2D bank.

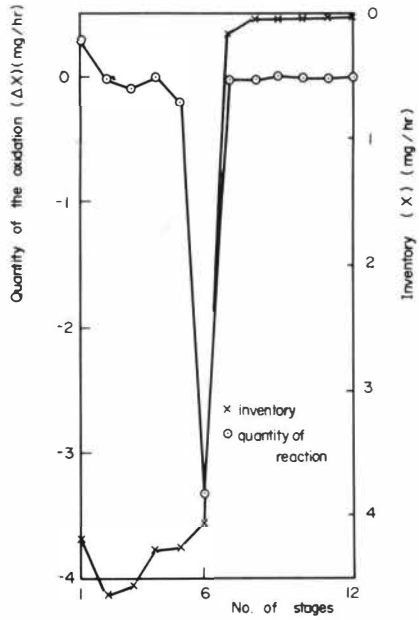


Fig. 11. Nephrium inventory and the quantity of the oxidation-reduction reaction in each stage in 2D bank.

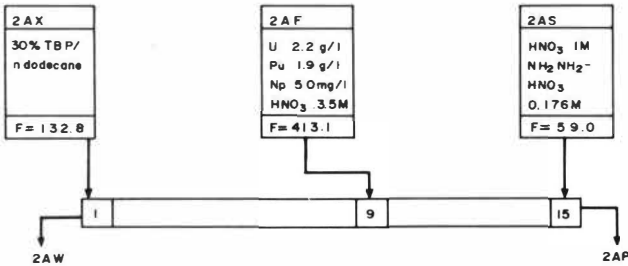


Fig. 12. Flowsheet of 2A bank for discharging Np into 2AW.
(F: flow rate (ml/hr))

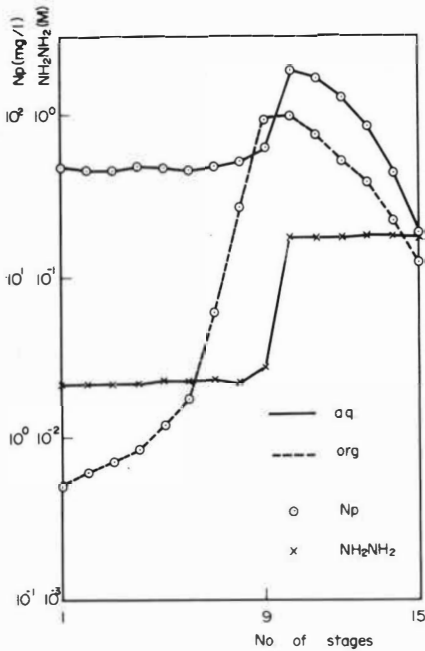


Fig.13. Stage concentration profiles of Np and NH_2NH_2 in 2A bank.

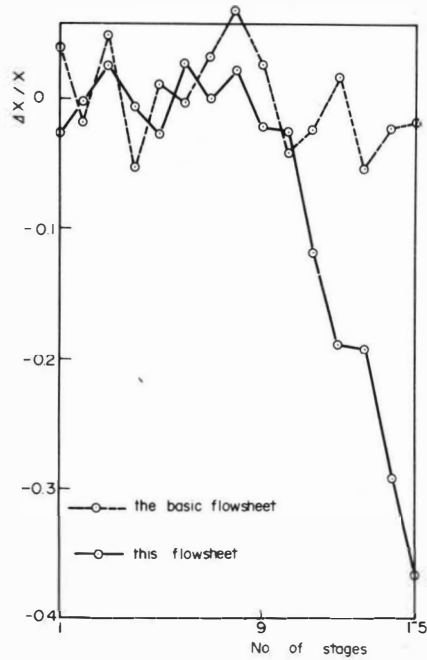


Fig.14. Profiles of oxidation ratios of Np in 2A bank.

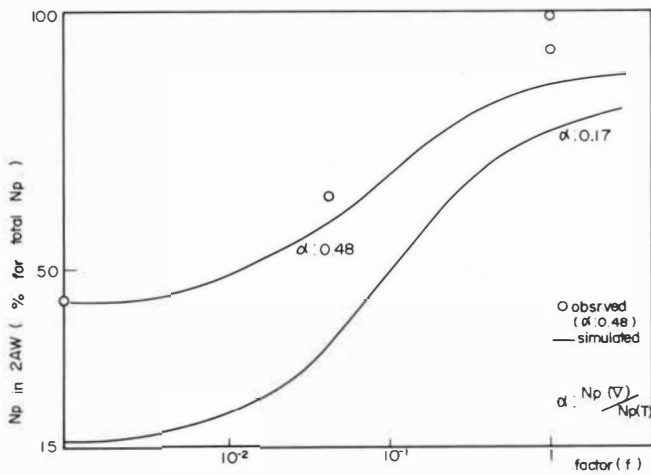


Fig.15 Factor of NH_2NH_2 concentration (f.1 means 0.176M in 2AS)

H. Schmieder, F. Baumgärtner, H. Goldacker,
H. Hausberger, E. Warnecke

Institut für Heiße Chemie, Gesellschaft für
Kernforschung m.b.H. Karlsruhe, Germany

Abstract

Fundamental investigations in the kinetics of the electro-
lyses in the system uranium-plutonium-nitric acid-hydrazine
and corrosion tests with various electrode materials
led to the development of "in-situ" electrolytic ex-
traction equipments without diaphragm.

The behaviour of Pu, Np, and U in a 16-stage electrolytic
mixer-settler is discussed which was made of titanium
(throughput 2 kg/d) and successfully operated as 1B
(Pu/U-separation) and 2B (reductive plutonium reextraction)
batteries. With an electrolytic pulsed column, similar
electrolytic mass-transfer could be achieved.

Experiments with a "fissium" mixture show, that
deleterious effects caused by fission products, are
not to be expected.

The development of an electrolytic cell for the
oxidation of plutonium between the Purex cycles has
been started. Extremely high current efficiencies were
achieved in a cell, which works without diaphragm.

I. Introduction

The classical reducing agent for plutonium in the Purex process is ferrous sulphamate. The process is characterized by obvious drawbacks, viz. the introduction of corrosive ions which are foreign to the process. The only alternative which has so far been realized in technical plants is the use of uranium(IV) as a reducing agent. This entails the disadvantage that above all in processing fuel rich in plutonium considerable enhancements of the process volume must be put up with.

An alternate process more recently developed uses hydroxylammonium nitrate as a reducing agent⁽¹⁾. However plutonium complexed by radiolytic products in the organic solvent is but unsatisfactorily stripped.

Efforts towards an electrolytic reduction technique are quite obvious^(2,3). From the start we attempted to realize a genuine "in-situ" technique allowing the most compact shapes of equipment and a more direct process management^(4,5,6).

A further process step which is not satisfactorily solved is the back-oxidation of Pu between extraction cycles which at present is performed by use of sodium nitrite or gaseous nitric oxides, respectively. The use of NaNO_2 contributes to high solid contents in the medium-activity wastes while with nitric oxides considerable equipment expenditure is required due to the large excess of NO_2 gas which is needed.

The gas must be passed through spray columns and in a subsequent "stripper" the dissolved excess must be destroyed by injection of air.

II. Basic Investigations

The electrolytic reduction of uranium(VI) to uranium(IV) proceeds via the cathode reaction uranium(VI) to uranium(V) and a subsequent disproportionation of uranium(V) to uranium(VI) and uranium(IV). The reaction is irreversible which means that uranium(IV) is not oxidized directly at the anode but through oxygen formed at the anode.

Plutonium(IV) is directly reduced at the cathode to yield plutonium(III). Fig. 1 shows the current-potential curves with platinum and titanium as the cathodes. The plutonium reduction is characterized by a distinct limiting current-density plateau which is controlled by diffusion.

The reduction potential of plutonium(IV) is more positive than the uranium(VI) reduction, i.e., there is a preference for the plutonium reduction. With +0.92 V the $\text{NO}_3^-/\text{NO}_2^-$ reaction is even slightly more positive than the $\text{Pu}^{4+}/\text{Pu}^{3+}$ reaction. Nevertheless, a reduction of nitrate does not take place to a major extent in process solutions containing hydrazine. This is explained by the reaction mechanism proposed by K.J. Vetter⁽⁷⁾. Nitrous acid appears in the reaction chain, which reacts with hydrazine to give hydrazoic acid or nitrogen and N_2O , respectively, resulting in a blockage of the nitrate reduction.

The U(VI)/U(IV) reaction with a redox potential of +0.33 V is followed by the formation of hydrogen starting, under the conditions represented in Fig. 1, at a potential more negative than -600 mV relative to the standard calomel electrode.

In experiments using titanium as the cathode and a stationary electrolyte containing 0.1 M/l uranium in addition to nitric acid and $N_2H_5NO_3$, the gas production was investigated both qualitatively and quantitatively. Under the foregoing conditions gas evolution started visibly at nearly 5 mA/cm^2 .

The composition of the gas remained almost constant over the current density range of 5 to 33 mA/cm^2 . The gas composition was 51 vol.-% hydrogen, 48 vol.-% nitrogen, and less than 1 vol.-% NO . In this range of current densities 0.013 to 0.067 l hydrogen were generated per ampere-hour, which is equal to current yields of 3 to 16 %. The nitrogen fraction in the cathode gas is tentatively explained by the reaction of nitrite with hydrazine.

The gas which was evolved at the platinum anode also showed an almost constant composition over the considered range of current densities, with 95 vol.-% of nitrogen, 4 vol.-% of oxygen, and 1 vol.-% of NO ; the oxygen probably even originated from an air impurity. The rate of gas production was ca. 0.2 l per ampere hour. The nitrogen in the anode gas is due to the direct anodic oxidation of the hydrazine.

The production of nitrogen as an anode reaction and without formation of oxygen, on the one side, and the irreversible nature of the $U(VI)/U(IV)$ reaction on the other side - is of decisive importance in the design of electrolytic extraction equipment, because it principally offers the possibility of renouncing upon a diaphragm.

Despite of the lower specific mass conversion at titanium compared to that occurring at platinum or gold, titanium was chosen as the cathode and construction material due to technical reasons. In corrosion experiments only a relatively low corrosion rate of $0.29 \text{ mg/cm}^2/\text{d}$ was found. Stainless steel was eliminated as a cathode material because of its high corrosion rate of $24 \text{ mg/cm}^2/\text{d}$.

Anode materials which can be taken into consideration are platinum or platinum-plated metals, preferably platinized tantalum.

III. Electrolytic Extraction Equipment

Fig. 2 is a schematic drawing of a laboratory-scale electrolytic mixer-settler for throughputs of 2 kg fuel per day. The mixer-settler is made of titanium. The casing serves as the cathode. An anode cell made of insulating material is installed in each settling chamber and submerged beneath the bottom level of the chamber. The orifice below the bottom level provides the electroconductive connection between the electrodes and acts, at the same time, as a separator preventing the organic phase from penetrating into the anode space under any hydrodynamic conditions. This type of design produces the effect that the electrolysis takes place mainly in the settling chamber.

A 16-stage mixer-settler of this type was operated as a 1B or 2B battery for 1000 hours in total, varying several parameters, such as TBP concentration, plutonium and neptunium content, overall current, current distribution, nitric acid distribution, dibutyl phosphate content, etc. The principal flowsheets used are shown in figure 3.

In the upper part of the figure a flow diagram is given for uranium-plutonium separation. In all experiments the hydrazine concentration in the aqueous scrubbing stream was 0.2 M. The flow ratio of the organic feed solution (BF) to the organic scrubbing solution (BSX) was 5 in all experiments. That section of the mixer-settler which is marked e⁻ was equipped with anodes and thus was electrolytically efficient.

In the lower part of figure 3 a flow diagram is presented for the electrolytic backwashing of plutonium. In all experiments 30 vol.-% of TBP was used and the aqueous scrubbing solution (2BX) contained 0.2 M HNO₃ and 0.2 M N₂H₅NO₃.

Table 1 lists results of typical experiments on plutonium-uranium separation. Similar to the reduction with uranium(IV) nitrate, the acid concentration profile must be regarded as a determining factor for the quality of the separation. The optimum nitric acid concentrations are 0.3 to 0.9 M for the BX section and 1.2 to 1.8 M for the BS section. The uranium(IV) concentrations produced in the first chambers of the battery play a decisive part as regards the amount of residual plutonium in the organic uranium product (1BU), since a large excess of uranium(IV) is required to strip the plutonium which is complexed by radiolysis products. Concentrations ranging from 2 to 8 g of uranium(IV) per liter are sufficient for effective Pu backwash. The 16 g U(IV)/l excess produced in the settling chamber by applying high currents in experiment No. 33 is certainly not necessary, which implies that the current yield of only 5 % with respect plutonium does not constitute an optimum value. Although the separation is better than with conventional mixer-settlers using externally produced uranium(IV), these values do not attain the decontamination factors which are theoretically possible. This is explained by the moderate extraction efficiency of the small-scale mixer-settler used which showed only 50 % stage efficiency.

This is clearly evidenced by a comparison between experiments 30 and 33. In experiment No. 33 the residence time was doubled by decreasing the flow rate to 1/2 of that of experiment No. 30, which resulted in an increase of the plutonium decontamination by a factor of 5, the absolute value being 2400. A typical concentration profile in the electrolytic mixer-settler is shown in figure 4.

The behaviour of Np in this flowsheet has also been studied. About 90 % of the neptunium in the 1B electrolytic mixer-settler were reduced to Np^{IV}. Approximately 99 % of the Np passed into the aqueous Pu product stream under the flowsheet conditions used.

Table 2 shows results obtained in the electrolytic plutonium back-extraction. Here the plutonium losses in the organic outlet (2BW) are determined by the concentration of dibutyl phosphate in the extractant, which is clearly seen from experiment No. 28. However, the presence of small quantities of uranium - about 5 to 10 % of the plutonium - which are quite usually found in the plutonium product after plutonium-uranium separation, drastically improves the result. In experiment No. 18 the plutonium losses drop to 0.0015 %. This is explained by the fact that a portion of the uranium occurs as uranium(IV) so that plutonium complexed by HDBP can be stripped.

The method offers the particular advantage of achieving high plutonium concentrations of about 50 g/l in the Pu product solutions.

The influence exerted by fission products on the electrolysis was investigated in specific experiments with a "fissium" mixture containing, in addition to other significant fission products, in particular the noble metals ruthenium, silver, and palladium, which are of interest in this context. The mere presence of hydrazine is sufficient to produce a visible precipitate of noble metals. A negative influence on the electrolytic production of uranium(IV) could not be detected, although silver and palladium had been overdosed by a factor of 100 in the fissium, and partly precipitated on the cathode.

Problems must be expected when scaling up the electrolytic contactors because of the unfavorable geometries and hydrodynamic conditions. For this reason, extensive mass conversion experiments were performed with electrolytic mixer-settler cells made of titanium and with pulsed column sections, with daily throughputs of 100 kg. Figure 5 shows a schematic drawing of an electrolytic pulsed column.

The principle of the electrolytic column is similar to that of a pulsed column with sieve plates. The aqueous phase is used as the continuous phase. The interface is situated at the head of the column. The inner column diameter is 100 mm. The feeding device for the organic phase provided at the bottom of the column is followed by a cylindrical central space, inner diameter 25 mm, which is used as the anode space. Conically shaped catholyte - anolyte separators are provided which bring about the electrolytic interconnection between the cathode and the anode space by means of bores inclined upwards. At the same level one anode each is provided in

the anode space. In the outer annular space, i.e. the extraction space, the cathodes are installed directly over the conical separators. They are sieve plates with additional radially configured sheets.

The evaluation of the mass conversion experiments carried out in the various types of equipment, with throughputs of 2 and 100 kg per day, yields nearly identical mass transfer coefficients for all types of equipment. With average current densities of 5 mA/cm^2 values of about $1 \times 10^{-2} \text{ cm/min}$ are obtained. The maximum achievable limiting current densities were calculated to be 9 mA/cm^2 for aqueous uranium(VI) concentrations of 0.2 M.

With a view to further scaling up the distribution of current densities was examined for the electrode geometries of interest. A hyperbola like distribution of the current is found at the cathode. In a conservative approach an extrapolation still yields a current efficiency of 55 % for overall cathode lengths of 40 cm. For an overall cathode length of 4.5 cm corresponding to the mixer-settler with a daily throughput of 2 kg a current efficiency of 82 % is calculated. This is based on an average current density of 8 mA/cm^2 and a limiting current density of 5 mA/cm^2 .

IV. Anodic Oxidation of Plutonium

A number of anode potential-current density curves were recorded in order to investigate the behaviour of the individual components contained in the plutonium products. The results are represented in figure 6. Plot 1 in Fig. 6 shows the behaviour of nitric acid. Current densities of 1 mA/cm^2 are reached. Only at potentials higher than +1400 mV. A much more negative potential is found for comparable current densities with HNO_3 solutions

containing hydrazine as shown by plots No. 2, 3, and 4. Plot 2 is characterized by a clear plateau in the potential range between +900 and +1600 mV. Presumably this is caused by the oxidation of hydrazine. This assumption is confirmed by plot 5. With nearly the same hydrazine concentration, but with 0.2 moles/l uranium(IV) added, a similar curve is obtained as in plot No. 2. This can be expected since uranium(IV) is not oxidized directly at the anode. Plot 6 shows the curve for an electrolyte containing 0.2 moles/l plutonium(III) besides 0.2 moles/l $N_2H_5NO_3$. In experiments performed in a specially constructed flow cell at large platinum anodes plutonium(III) could be readily oxidized quantitatively to plutonium(IV). According to expectations, there is no formation of plutonium(VI) below the potential of oxygen formation. Oxidation was possible also in cells without diaphragms, so that also in this case technical implementation offers the possibility of renouncing upon the diaphragm. Anodic current efficiencies up to 150 % were measured. This effect is tentatively explained by the destruction of hydrazine by nitrite which is formed at the cathode.

V. Conclusions

1. From the results obtained it can be concluded that for pulsed electrolytic columns with seven to eight theoretical stages plutonium losses below 0.1 mg/l can be achieved.
2. No difficulties of a principal nature are expected for scaling up to throughputs of several tons per day.

3. The cost of electricity as a redox agent are principally much lower to that of chemical agents. Table 3 shows a comparison of costs for electricity and chemicals. A drastic reduction of costs can be expected from anodic oxidation, namely from more than 600 DM/ton of fuel when oxidizing with N_2O_4 to 6 DM/ton in case of anodic oxidation.

The comparison of hydrazine and electricity costs with the costs for hydroxylammonium sulphate also yields a clear decrease of costs.

4. The process volume and the equipment expenditure required are smaller in the electrolytic process. This is partly due to the high plutonium product concentrations which can be attained and partly to the elimination of make-up facilities.

5. The mass conversion of the electrolytic techniques is governed by the electric current. Therefore, these processes can be controlled more directly and can be run more conveniently and safely than those requiring the dosage of chemicals.

6. In the separation of plutonium any change in the composition of the uranium isotopes is avoided by in-situ electrolysis.

Literature

- (1) I.M. McKibber, J.E. Bercaw
USAEC-Report, DP-1284 (1970)
- (2) H. Schmieder, F. Baumgärtner, H. Goldacker, H. Hausberger,
Reaktortagung, Bonn, April 1971, S. 706
- (3) M. Krumpelt, J.J. Heiberger, M. Steindler
in USAEC-Report, ANL-7871 (1971)
- (4) H. Schmieder, H. Goldacker,
Vortrag beim 2. Deutsch-Indischen Seminar, KFA Jülich,
Sept. 1972 (unpublished)
- (5) H. Hausberger,
Dissertation, Universität Heidelberg (1972)
- (6) H. Schmieder, F. Baumgärtner, H. Goldacker, H. Hausberger,
XXIVth IUPAC Congress, Hamburg 1973
- (7) K.J. Vetter
"Elektrochemische Kinetik", Springer Verlag, 1961

List of Tables and Figures

- Table 1 : Results of Electrolytic Counter-current Extraction Processes, Electrolytic Pu/U-Separation
- Table 2 : Results of Electrolytic Counter-Current Extraction Processes, Electrolytic Pu Re-extraction
- Table 3 : Cost Comparison of Chemical and Electrolytic Processes
- Fig. 1 : Cathode Potential-Current Curves with Different Cathode Material, 25°C
- Fig. 2 : Schematic Drawing of an Electrolytic Mixer-Settler, Laboratory Scale
- Fig. 3 - A : Flowsheet of Electrolytic Pu/U-Separation
- Fig. 3 - B : Flowsheet of Electrolytic Plutonium Re-extraction
- Fig. 4 : Typical Concentration Profile in the Electrolytic Mixer-Settler
- Fig. 5 : Electrolytic Pulse Column, Pilot Plant Scale
- Fig. 6 : Anode Potential-Current Curves with Different Electrolytes, 25°C

Tab. 1: Results of Electrolytic Counter-current Extraction Processes, Electrolytic Pu/U-Separation

Exp. No.	1BF ₀		Pu [N %]	1BXS _a		U-Product, 1BU ₀			Pu-Product, 1BP _a			Current total [A]	Current Effic.* [%]	U-IV Settling Stage No. 1 [g/l]
	TBP [N %]	Flow [cm ³ /h]		HNO ₃ [M/l]	Flowratio 1 BF ₀ /1BXS _a	U [g/l]	Pu [g/l]	DF _{Pu}	Pu [g/l]	U [g/l]	DF _U			
7	20	750	~5	0,5	6	49	0,0005 -0,001	2000- 5000	19	<0,13	2800	1,68	19	3,9
11	20	750	~10	0,4	5	41	0,0013 -0,0025	1700- 3200	~21	<0,13	1900	2,08	20	3,5
30	30	750	~0,8	0,20	7,1	61	0,0008 -0,0009	430- 480	< 3	~1,5	1000	0,54	7	10,5
33	30	375	~0,8	0,20	7,5	69	0,0002 -0,0003	1600- 2400	3,7	~1,5	800	0,49	5	16,6

*) related to Plutonium

Tab. 2: Results of Electrolytic Counter-current Extraction Processes, Electrolytic Pu Re-extraction

Exp. No.	Flowratio $2BF_o/2BP_a$	Pu [g/l]	$2BP_a$ U [g/l]	HNO_3 [Mol/l]	Pu [g/l]	$2BW_o$ Loss [%]	U [g/l]	HDBP [mg/l]	Current total [A]	Current Effic.* [%]	Number of Electrolyt. stages	U aq. Settling stage No. 1 [g/l]	Stirrer [rpm]
18	1	10	0,3	0,5	0,00015	0,0015	1,5	80	0,73	31	11	0,8	1000
28	1	12,5	<0,1	0,4	0,033	0,25	<0,1	170	1,2	20	10	0,03	1100
37	3,5	48	0,6	0,6	0,003	0,02	2,9	70	1,2	22	10	1,3	1100
38	2,5	40	1,3	0,50	0,0008	0,005	2,5	100	0,84	43	9	~1,3	1200

*) related to Plutonium

Tab. 3:

Cost Comparison of Chemical and Electrolytic Processes

Plutonium 0,8 W %; Concentrations of Plutonium Products : 1 BP = 6 g/l, 2 BP = 50 g/l

Process	Effic.	Costs of Redox Agent DM/t	Redox Agent kg/t Fuel	Costs DM/t Fuel		Redox Agent kg/t Fuel	Energy ¹⁾ kWh/t Fuel	Costs of Redox Agent DM/t	Effic.	Process
<u>Hydroxyl-ammoniumnitrate</u>										<u>Electrolytic Extraction</u>
$[\text{NH}_3\text{OH}]_2 \text{SO}_4$	0,06 ⁴⁾	5500 ³⁾	50	277	31	7,8		4000 ²⁾		Hydrazine
					4		135		0,1-0,2	Current
<u>Oxidation with N_2O_4</u>										<u>Electrolytic Oxidation</u>
of $[\text{NH}_3\text{OH}]\text{NO}_3$ and Pu-(III)	0,1 ⁵⁾	1300 ⁶⁾	470	611	6		182		0,5	N_2H_5^+ -and Pu-(III) Oxidation
<u>Sum of Costs</u>				888	41					<u>Sum of Costs</u>

1) 0,032 DM/KWh

3) Fa. Raschig, Ludwigshafen

5) estimated

2) Fa. Bayer, Leverkusen

4) from DP 1248

6) from GWK

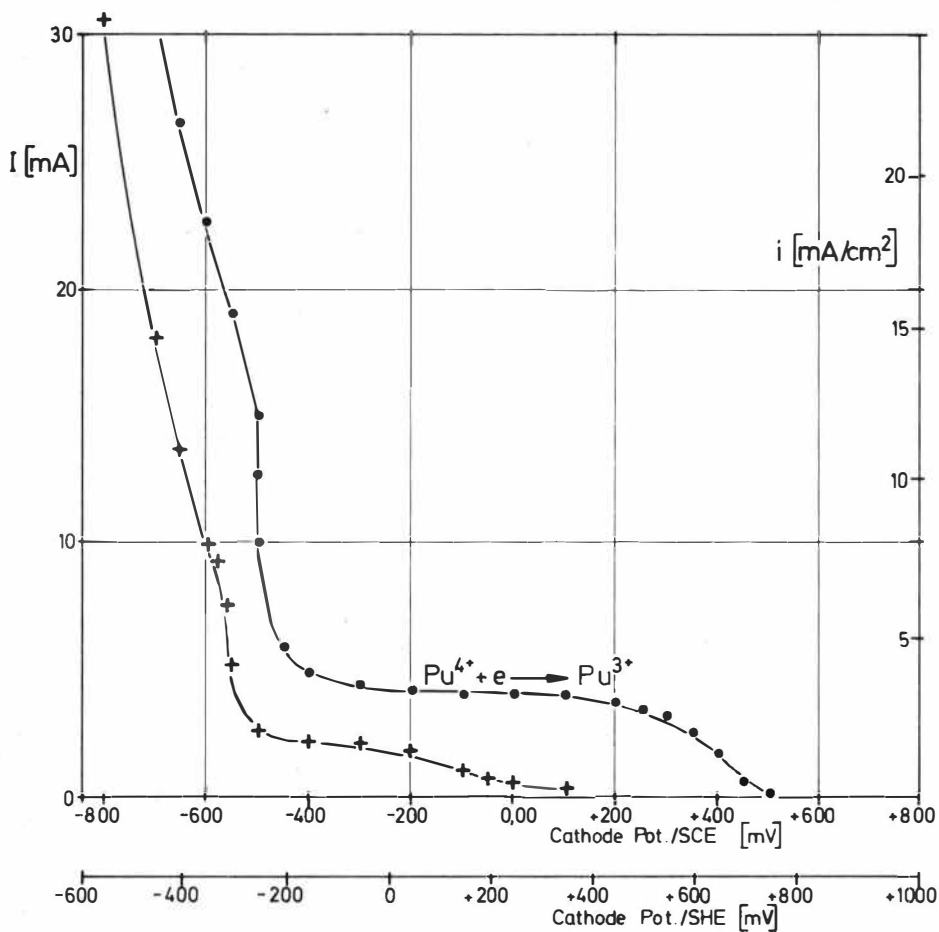
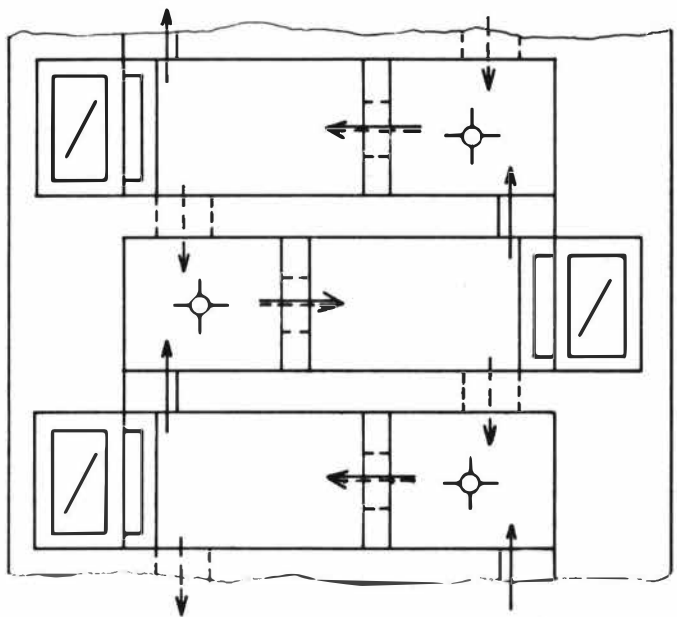
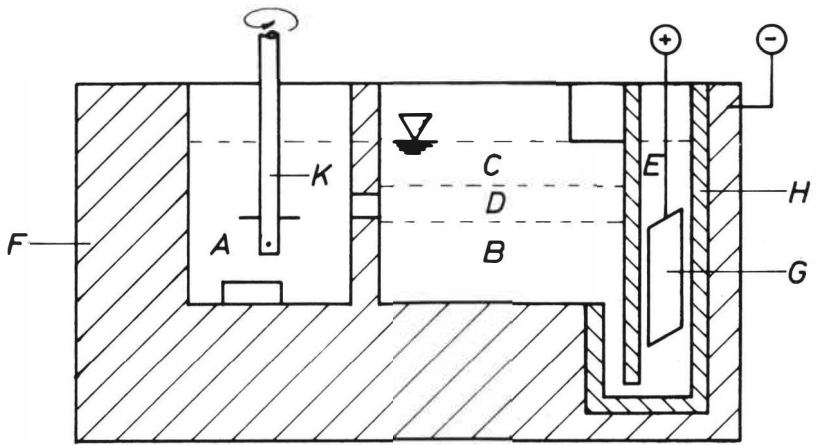


Fig.1 Cathode Potential-Current Curves with Different Cathode Materials, 25°C

Electrolyte : $0,1\text{M UO}_2^{2+}$ - $0,05\text{M Pu}^{4+}$ - 1M HNO_3

●—● Platinum +—+ Titanium



A=Mixer Cell

B=aq. Phase

C=org. Phase

D=Interface

E=Anode Cell

F=Titanium Containment

G=Anode

H=Insulator

K=Stirrer

—→ org. Phase

- - -→ aq. Phase

Fig.2 Schematic Drawing of an Electrolytic Mixer-Settler, Laboratory Scale

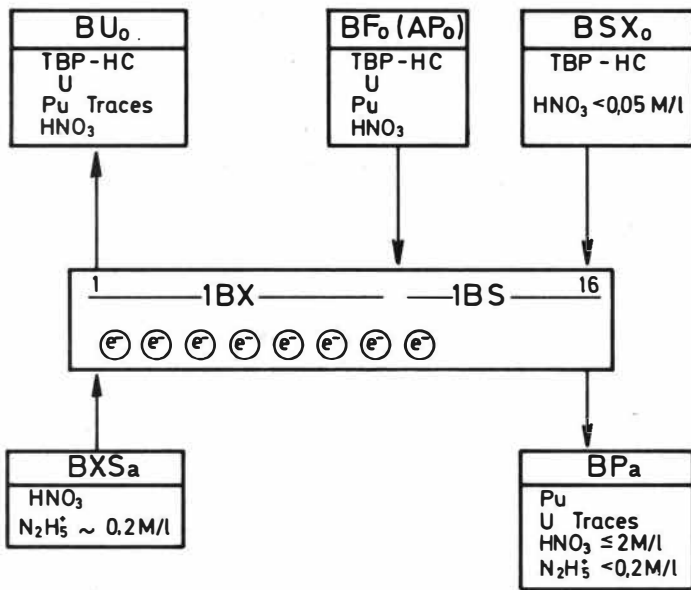


Fig. 3-A Flowsheet of Electrolytic Pu/U-Separation

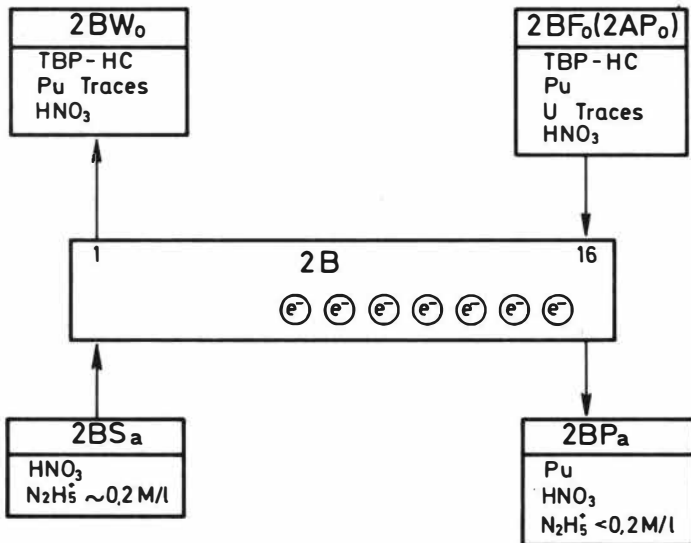


Fig. 3B Flowsheet of Electrolytic Plutonium Re-extraction

e^- electrolytic efficient part of mixer-settler

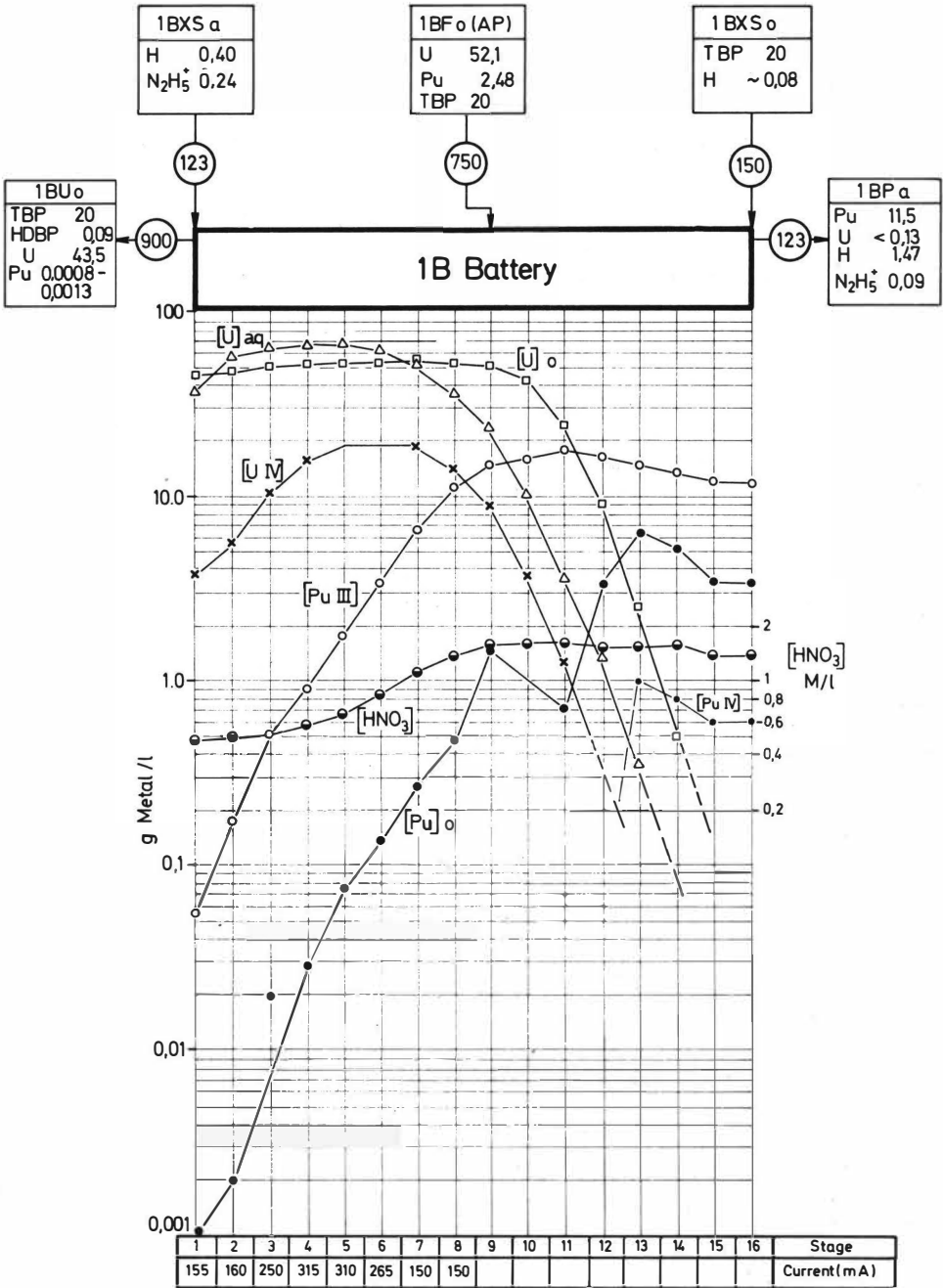


Fig.4 Typical Concentration Profile in the Electrolytic Mixer-Settler

HNO₃ and N₂H₅⁺ Concentration in Mol/l
 U, Pu and HDBP Concentration in g / l
 TBP Concentration in V %
 Flows in cm³/h

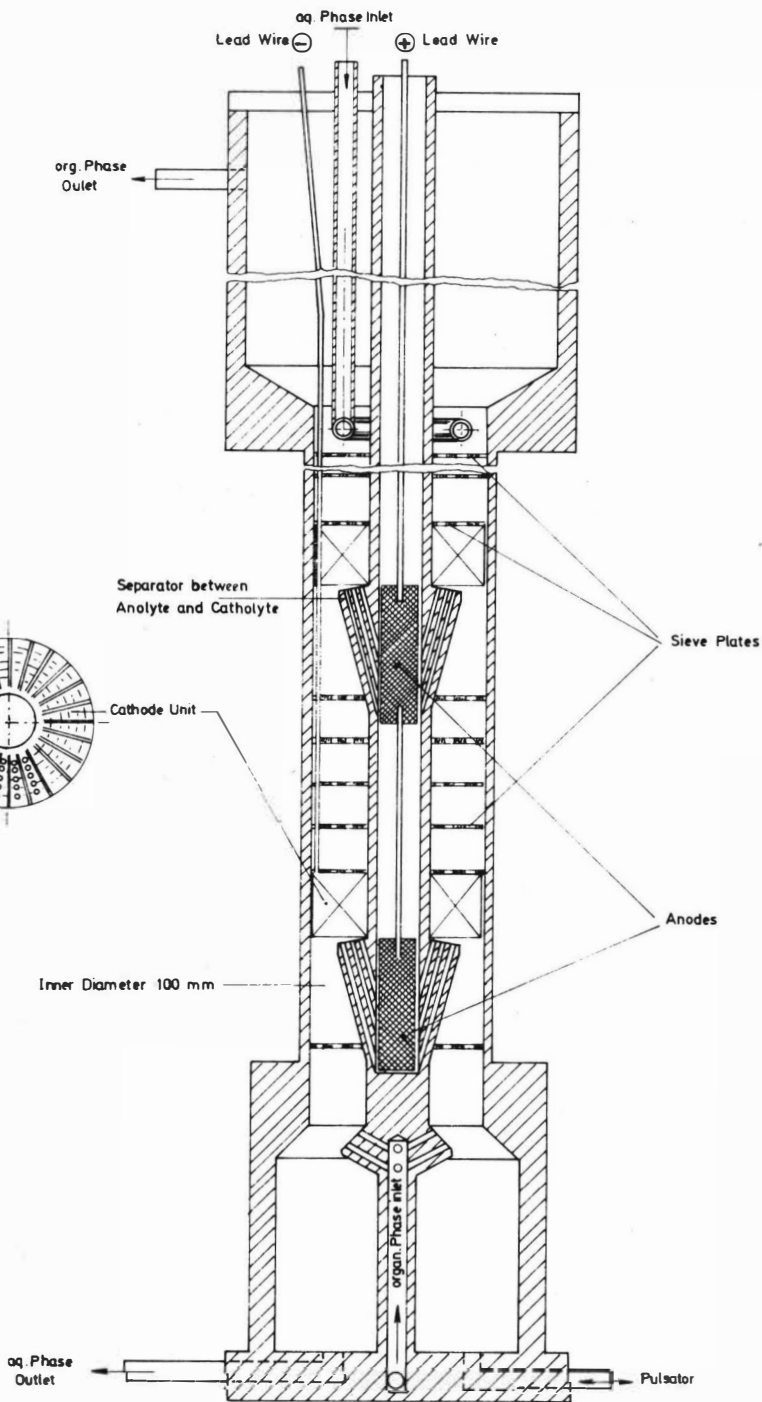


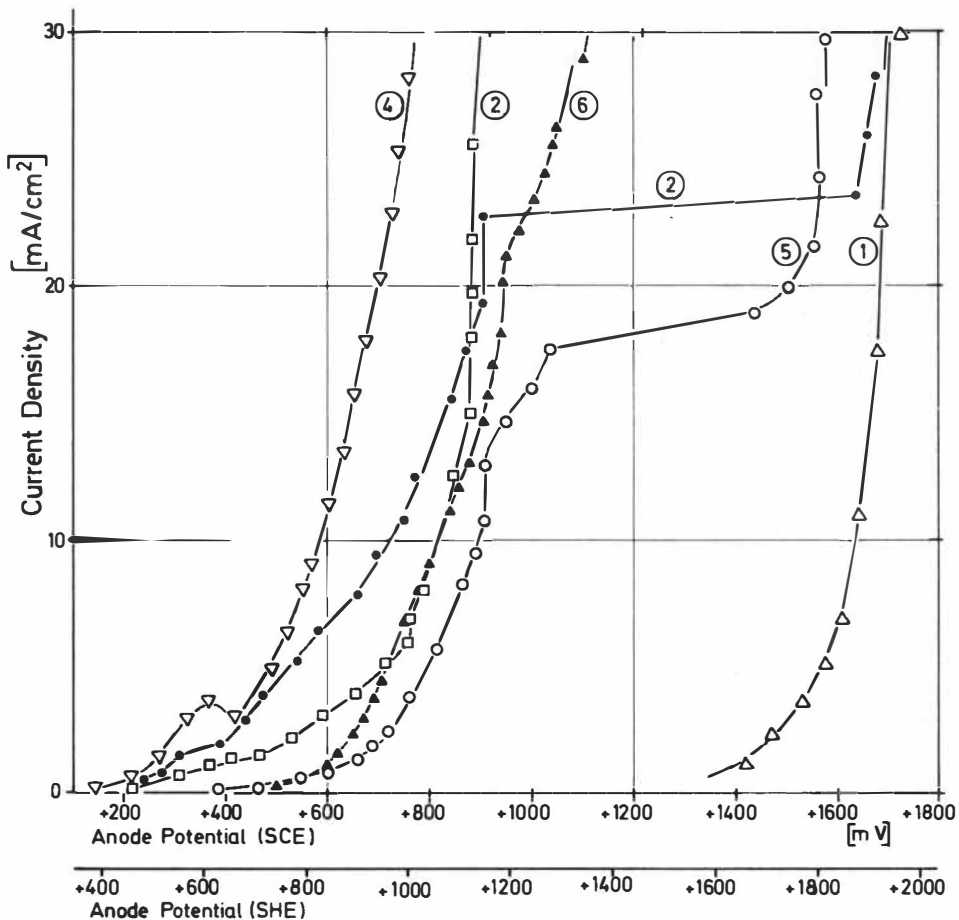
Fig.5 Electrolytic Pulse Column, Pilot Plant Scale

Fig. 6 Anode Potential - Current Curves with Different Electrolytes, 25 °C

Anode: Pt, 1,6 cm²

Electrolyte :

1. $\triangle-\triangle$ 5 M/l HNO₃
2. $\bullet-\bullet$ 0,04 M/l N₂H₅NO₃ - 1 M/l HNO₃
3. $\square-\square$ 0,2 " " " "
4. $\nabla-\nabla$ 1,0 " " " "
5. $\circ-\circ$ ~ 0,04 " " " " - 0,2 M/l U-(IV)
6. $\blacktriangle-\blacktriangle$ ~ 0,2 " " " " - 0,2 M/l Pu-(III)



UTILISATION OF HYDROXYLAMINE NITRATE FOR THE
FINAL CONCENTRATION AND PURIFICATION OF PLUTONIUM
IN THE IRRADIATED FUEL REPROCESSING FACTORY AT LA HAGUE

P Patigny⁺⁺ J Regnier⁺⁺ P Miquel⁺ D Taillard⁺⁺

ABSTRACT

The use of hydroxylamine nitrate has been examined as a means of back-extracting plutonium in a third cycle of purification and concentration using 30% TBP/dodecane. The tests have indicated the parameters which are important in governing the back-extraction; acidity, concentration of plutonium, presence of hydrazine, and temperature. This method has been used for several months on an industrial scale, and has permitted concentration factors of 8 to 10 and the production of very pure plutonium oxide.

+ Commissariat a l'Energie Atomique, Centre de Recherches de
Fontenay-aux-Roses B.P. No 6 - 92260

++ Commissariat a l'Energie Atomique, Centre de La Hague - 50107

I. INTRODUCTION

The conversion of the factory at La Hague (+) to process oxides from water reactors did not bring about any extensive changes in a chemical process (Figure 1) designed for the processing of metallic fuels from graphite-gas reactors.

The increased amount of plutonium did nevertheless require some modifications to be made in the final plutonium purification plant which previously used an extraction cycle based on triaurylamine diluted with dodecane (see Figure 2) (1).

In order to increase the capacity of this plant and for reasons of simplification it was decided to replace the triaurylamine by tributyl phosphate and to seek a process that could be operated in the existing mixer-settlers, and also produce pure and concentrated plutonium nitrate without the risks of super-critical accumulations.

This process had in fact to be capable of processing a nitric acid solution containing from 2 to 6 grams of plutonium per litre, at a maximum rate of 40 kg per day, and of producing pure and sufficiently concentrated plutonium nitrate solution (15 to 40 g/l) to proceed with the ultimate concentration of the product by evaporation (without acid accumulation), or directly with oxalic precipitation of the plutonium.

This could have been achieved by adopting a process of the kind used at Marcoule in pulsed columns (2) (3) and comprising extraction of the Pu with tributyl phosphate, reductive back-extraction by means of uranous nitrate, and extensive recycling of the product of extraction to reach a suitable concentration level.

As the adoption of such a process would involve the setting up of new facilities for recycling the uranium-charged solvent and for re-oxidising the recycled plutonium with NO_2 , a more simple cycle was chosen with reductive back-extraction of plutonium by means of hydroxylamine nitrate.

The definition and development of this hydroxylamine process forms the subject of this paper.

1.

(+) The La Hague factory now has an oxide head to process the oxide fuels for United Reprocessors. It will thus be "bicephalous" and will be able to process metallic fuels and highly irradiated oxides at alternate times.

II. CHARACTERISTICS AND MODE OF ACTION OF HYDROXYLAMINE NITRATE

II.1 General Properties

Hydroxylamine salts were first suggested as reducing agents for plutonium nitrate in 1955 (4) (5) but it was not until the papers of Bruns (6) and Orth (7) were presented at the last Solvent Extraction Conference (ISEC 71) that their industrial utilisation could be envisaged.

Hydroxylamine nitrate is stable in a slightly acid nitrate solution and behaves as a perfectly clean reducing agent for plutonium. It reduces Pu(IV) to Pu(III) at low acidity, giving inert by-products such as H_2O , N_2O or N_2 , and has the particular advantage of helping the re-oxidation of plutonium at high acidity, so that all that is required is to re-acidify the back-extracted plutonium solutions in the presence of nitrate to obtain a fairly rapid re-adjustment of the valencies.

II.2 Suggestions for preparation

During our experiments we noticed that it was difficult to obtain very pure hydroxylamine from commercial sulphate by the known process of ion-exchange of cationic resins (8) and we thought up very efficient processes that could be used if necessary in the processing factories.

One of these processes tested in our laboratories at Fontenay-aux-Roses consists in effecting the $SO_4^{2-} \rightleftharpoons NO_3^-$ exchange in an extraction cycle using diluted D2EHPA (9) and very pure reagents (see Figure 3).

Another even more simple process of effecting the anionic exchange by electrodialysis was thought out by the Applied Chemistry Department at Cadarache (10).

II.3 Mode of action

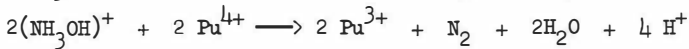
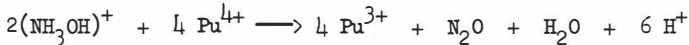
The reactions between hydroxylamine nitrate and plutonium nitrate involve complex kinetic laws, discovered by G S Barney (11), that we were able to confirm in part.

Two chemical reactions are likely to occur in the presence of an oxidising agent:



With plutonium IV in nitric acid, stoichiometric studies of the reaction show that each mole of hydroxylamine reduces 1.3 to 1.6 moles of Pu(IV).

The mechanism is therefore complicated and can result from the two following reactions:



Traces of NO_2 in the gases formed also show the possibility of a reaction with the nitric acid.

G S Barney's kinetic studies of reduction indicate an empirical velocity law,

$$R_i = - \frac{d(\text{Pu}^{\text{IV}})}{dt} = \frac{(\text{Pu}^{\text{IV}})_i (\text{NH}_3\text{OH}^+)_i (K_1 + K_2 (\text{NH}_3\text{OH}^+)_i)}{(\text{H}^+)_i^2 (1 + K_3 (\text{NO}_3^-)_i)}$$

where R_i represents the initial velocity.

As reaction proceeds, the net velocity is limited by the reverse re-oxidation reaction, due to an unidentified substance (NH_2O_x or HNO_x), and the reaction velocity may then be written:

$$R = \frac{K_8 (\text{Pu}^{\text{IV}})}{1 + K_9 \left[\frac{(\text{Pu}^{\text{III}})^2}{\text{Pu}^{\text{IV}}} \right]}$$

where $K_8 = (\text{NH}_3\text{OH}^+) (K_1 + K_2 (\text{NH}_3\text{OH}^+)) / (\text{H}^+)^2 (1 + K_3 (\text{NO}_3^-))$

and $K_9 = K_{10} (\text{H}^+)^2 (\text{NO}_3^-) / (\text{NH}_3\text{OH}^+)$.

These equations show particularly that the reaction velocity is diminished by an increase of (H^+) or of (NO_3^-), and by the presence of Pu(III). It was shown³ that the effect of an increase in temperature on the constants K_1 , K_2 , K_3 and K_6 acted to increase R.

In the heterogeneous back-extraction system it is known that the reactions of Pu(IV) in the solvent are fast and that it is the subsequent aqueous-phase reactions which will determine the overall rate. Therefore, on the face of it, it seems that the reductive back-extraction of the plutonium could be encouraged by:

- (a) reducing the acidity;
- (b) promoting the transfer of the Pu(IV) to the aqueous phase;
- (c) diminishing the $\frac{Pu(III)}{Pu(IV)}$ ratio;
- (d) increasing the temperature;
- (e) preventing the unwanted re-oxidation of the Pu(III) in both phases by means of a fast-acting nitrite suppressor.

In this counter-current process the Pu(III) is carried by the aqueous phase to the concentrated stages whilst the Pu(IV) moves to the diluted stages. This is why the desired reductive back-extraction can be achieved provided that the reduction rate, reduction time and number of stages are sufficient.

III. DEFINITION AND TESTING OF A PLUTONIUM PURIFICATION CYCLE FOR THE FACTORY AT LA HAGUE

On the basis of these data and the constraints on the operation of the installations at La Hague, the basic flow sheet shown in Figure 4 (rather different from that suggested by Bruns (6)) was conceived and tested.

This flow sheet, which can be used directly in the existing installations of the plutonium purification plant, fulfills the wishes:-

- (a) to obtain a concentration factor of around 5 to 6 in relation to the re-acidified feed;
- (b) to extract the plutonium in a diluted medium so as to avoid any possibility of super-critical accumulations in the extractors;
- (c) to back-extract at an acidity favourable to the action of the reducing agent, but sufficient to prevent the risk of plutonium hydrolysis (12).

As a result of experiments on the extraction-stripping cycle carried out at La Hague and at Fontenay-aux-Roses in laboratory mixer-settlers it emerged, inter alia, that:

- there was no need to inject the hydroxylamine nitrate at several points of the back-extraction bank (point b of Fig 4);
- recycling of part of the product (reflux flow diagram) was not required (point a of Fig 4);
- parameters such as the relative quantity of reducing agent, the presence of hydrazine, the acidity and the temperature had a considerable effect on the performance of the process and had to be strictly controlled to ensure stability of the concentration profiles in the extraction stages.

III.1 Effect of contact time between phases

The reduction time is probably fairly long but did not appear to be a limit in mixer-settlers. Tests made with contact times^(x) between phases of one minute and 15 minutes in each stage gave absolutely comparable and acceptable results.

III.2 Effect of the acidity and the amount of hydroxylamine

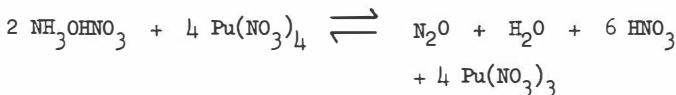
Experiment confirms that diminution of acidity favours the transfer of plutonium into the aqueous phase and its reduction by hydroxylamine nitrate, which is practically inextractable into the solvent. It is not enough, however, to lower the acidity to obtain a good reduction yield, and we have shown that too much reducing agent caused large accumulations of plutonium on back-extraction and loss to the stripped solvent. The hydroxylamine has a net salting-out effect, opposing the transfer of plutonium to the aqueous phase. Its decomposition as a result of both useful and undesirable reactions must also bring about a deleterious increase in the concentration of nitric acid in the medium.

5.

^x The effect of the hydroxylamine reaction time is currently under study at Fontenay-aux-Roses with a view to using this reductant in short-residence contactors such as pulsed columns or centrifugal extractors.

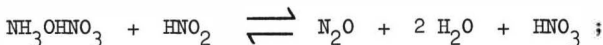
The nitric acid can come from:

- (a) reduction of the plutonium by the reaction



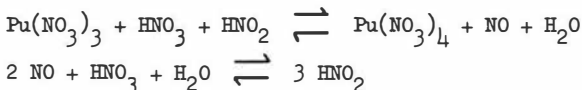
which produces 3 moles of HNO_3 per mole of hydroxylamine used;

- (b) destruction of the nitrous acid contained in the solvent by the reaction

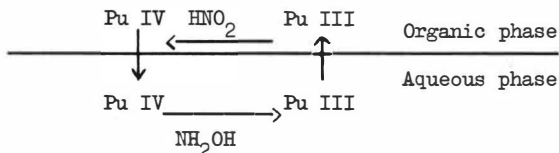


- (c) probably further reactions following the undesired re-oxidation of the plutonium in the organic phase.

The reduced plutonium can actually be re-oxidised by air (13) or more probably be extracted into the solvent (14) and react with HNO_2 in the absence of a nitrite suppressor as follows:



A self-accelerated cycle is then obtained (autocatalytic oxidation reactions of Pu and a medium that is increasingly acidic),



with extensive destruction of the reducing agent accompanied by an increase in acidity and in the inefficiency of the process.

In any case, experiment shows that there is a limiting value of the quantity

$$\left[\frac{\text{HNO}_2, \text{NH}_2\text{OH}}{\text{Pu}} \right]$$

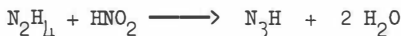
which depends on the apparatus (whether there is recycling of the phases or contact of the surface with air), and beyond which the process is inefficient. The optimum value of $\left[\frac{\text{HNO}_2, \text{NH}_2\text{OH}}{\text{Pu produced}} \right]$

achieved with laboratory mixer-settlers is around 2.5 to 3.

III.3 Effect of hydrazine and temperature

The tests showed also that hydrazine had a very favourable effect on back-extraction efficiency when the plutonium feed to be processed contained HNO_2 .

Hydrazine seems to be a faster-acting nitrite suppressor than hydroxylamine and diminishes the above-mentioned re-oxidation reactions of plutonium in the aqueous phase, and also in the organic phase since the N_2H produced in the following reactions is extractable:



Finally, our experiments confirmed that high temperature had a very favourable effect on the reduction kinetics and ipso facto on the reductive back-extraction.

III.4 Conclusion

Our experiments, and interpretations of the phenomena described, finally enabled us to suggest the plutonium concentration and purification flow sheets shown in Figures 5 and 6.

IV. INDUSTRIAL-SCALE TESTS

This latter flow sheet (Fig 6) was tested and adjusted on an industrial scale in the La Hague factory. After several months of tests the laboratory results were confirmed and the following results obtained:

- the process is stable
- the concentration factor achieved for the plutonium varied from 6 to 10 and can be increased still more.

A remarkably pure end product (PuO_2) is obtained containing 87.6% of plutonium and under 500 ppm of metallic impurities.

V. CONCLUSIONS

The tests described show that a simple extraction-stripping process using hydroxylamine nitrate and tributyl phosphate can enable plutonium to be concentrated and purified satisfactorily in the third cycle normally used in processing factories for irradiated fuel. It emerges that this reducing agent must not be employed in too large an amount in relation to the plutonium, and that the acidity on back-extraction must not be too high. An increase in temperature and the presence of hydrazine are favourable to the process.

The use of hydroxylamine nitrate for the reductive back-extraction of plutonium is comparable in terms of performance and economy with that of uranous nitrate or electrolysis. As such it is one of the range of techniques which make it possible to envisage a process for irradiated fuel using only one solvent (TBP) and clean reagents compatible with the nitric acid medium.

BIBLIOGRAPHICAL REFERENCES

- (1) BATHILLIER A - GRIENEIZEN A - PLESSY L
La Hague: Utilisation de la trilaurylamine pour la concentration et la purification du Pu.
Energie Nucléaire vol. 10 No 3 pp. 145-239 - Mai 1968
- (2) BRESCHET Ch - MIQUEL P
Improvement of the procedure used to treat highly irradiated fuels. Paper 195 - pp. 565-576 - ISEC 71, Society of Chemical Industry London
- (3) AUCHAPT P - GIRAUD J P - TALMONT X
Utilisation du nitrate uraneux dans le second cycle de purification du Pu à Marcoule.
Energie Nucléaire vol. 10 No 3 - pp. 140-145 - Mai 1968
- (4) GOLDSCHMIDT B - REGNAUT P - PREVOT J
Un procédé par solvant pour l'extraction du plutonium irradié dans les piles.
P/349. Conf. internationale sur l'utilisation de l'Energie Atomique à des fins pacifiques. Genève 1955
- (5) MOORE F L - HUDGENS J E
Anal. Chem. 29 - 1767 - 1957
- (6) BRUNS L E
Pu - U. Partitioning by a reflux solvent extraction flowsheet. Paper 103. International solvent extraction conference La Hague, April 1971 - Soc. of Chemical Industry - London
- (7) ORTH D A - McKIBBEN J M - SCOTTEN W C
Paper 147 - ISEC 1971
The Hague, April 1971 - Soc. of Chemical Industry London
- (8) WHEELWRIGHT Earl J
U.S. Patent 80499, 12 Oct. 1970
- (9) DEMARTHE J M - GUE J P - GRIENEIZEN A - MIQUEL P
French patent No 7240759 - 1972
- (10) MOREL A
Procédé et dispositif de transformation continue d'un sel d'hydroxylamine en un autre sel d'hydroxylamine.
French patent No EN 73 33 089 - 14 Sept 1973

- (11) BARNEY G S
The kinetics and mechanism of Pu^{IV} reduction by hydroxylamine.
Atlantic Richfield Hanford Company - Richland
Washington 99352 - ARH SA 100 and ARH SA 97 - 1971
- (12) COSTANZO D A - BIGGERS R E et al.
J. Inorg. Nucl. Chem. 35 No 2, parts I, II, III - 1973
- (13) LOPEZ MENCHERO - SALOMON L - BARDONE G
Etude du nitrate uraneux comme réducteur du plutonium
Eurochemic Mol, Belgique.
ETR 181, 182, 183, 184 - March 1966
- (14) TALMONT X
Proc. int. Conf. Solv. Extr. Chem. of metals
1965 - p. 103 (London : MacMillan)

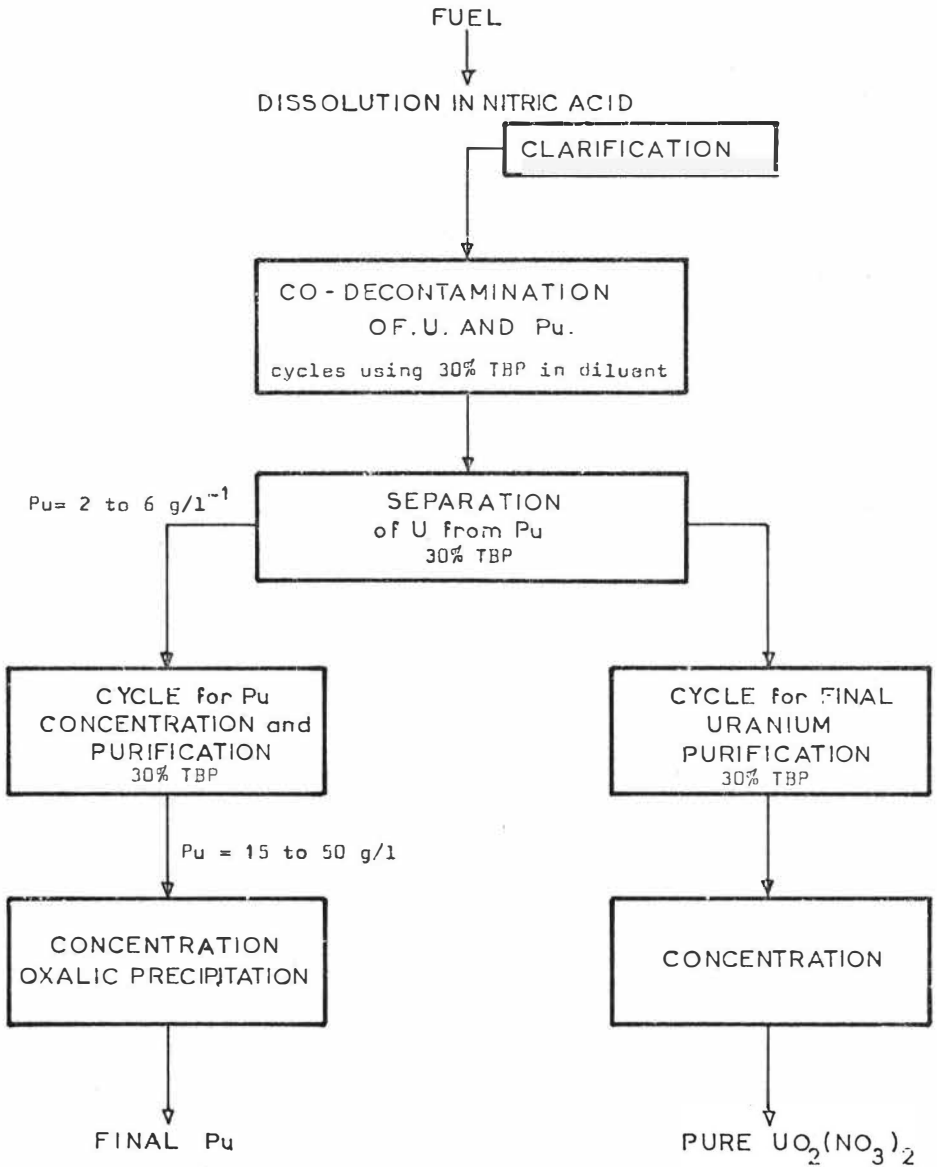


FIGURE 1. General diagram for the processing of irradiated fuels used in the LA HAGUE factory.

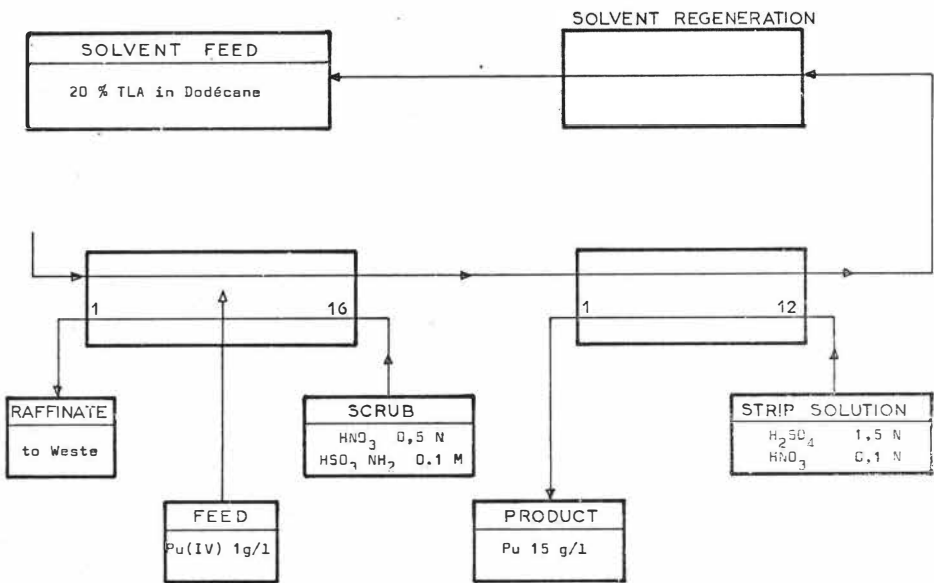


FIGURE 2. Flowsheet for plutonium concentration and final purification used until 1971 at LA HAGUE.

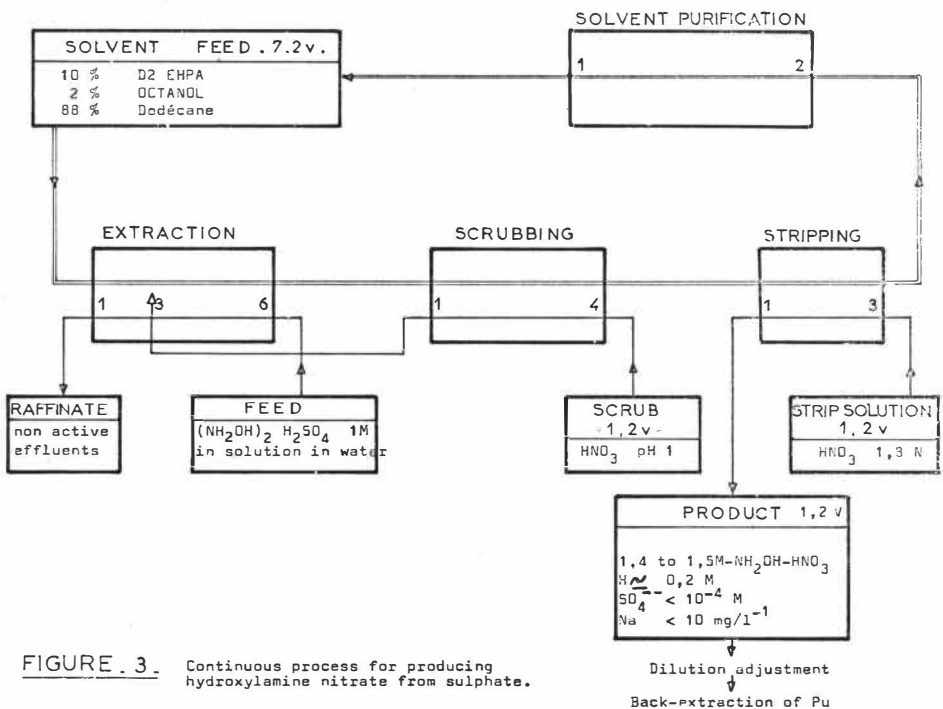


FIGURE 3. Continuous process for producing hydroxylamine nitrate from sulphate.

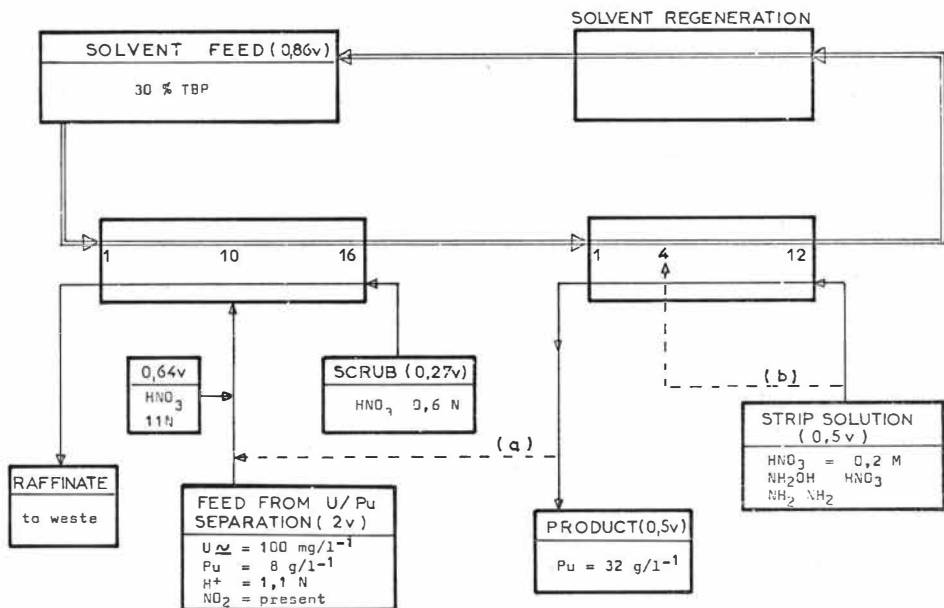


FIGURE 4. Basic flowsheet for the hydroxylamine experiment.

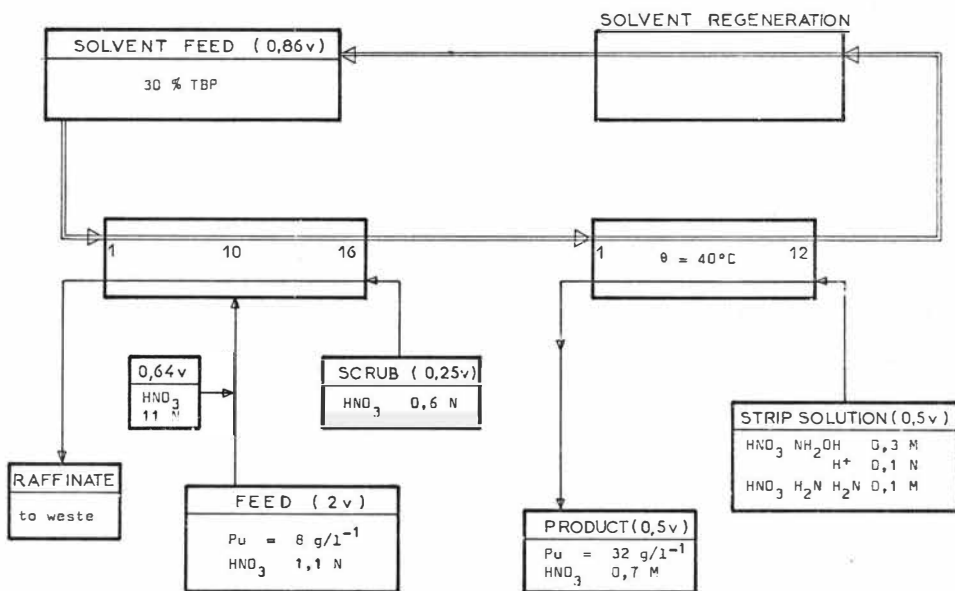


FIGURE 5. Flowsheet for Pu concentration and final purification corresponding to the processing of water reactor fuel (UO_2).

2033

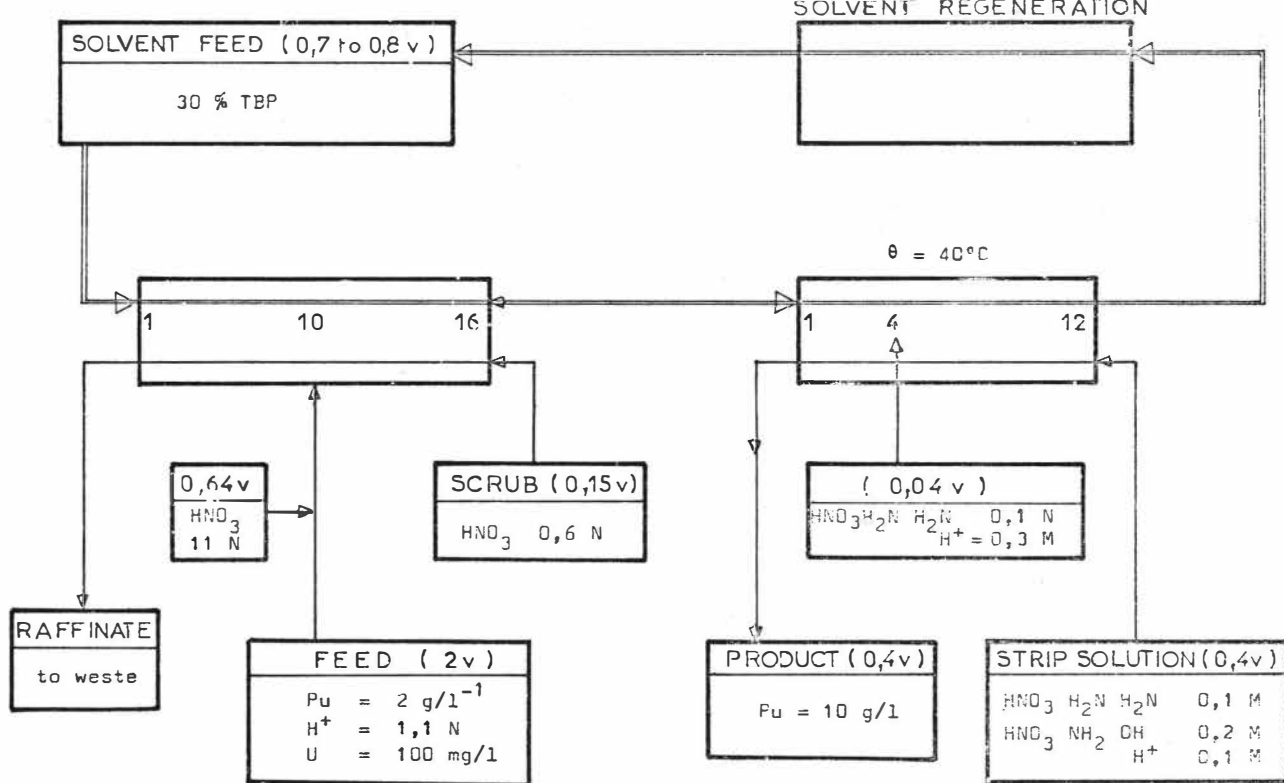


FIGURE 6. Flowsheet for plutonium concentration and purification corresponding to graphite gas reactor fuel processing.

REFLUX AMINE FLOWSHEET FOR PLUTONIUM

RECOVERY FROM METALLURGICAL SCRAP

W. W. Schulz
D. G. Bouse
M. J. Kupfer

Atlantic Richfield Hanford Company
Richland, Washington, U.S.A.

ABSTRACT

With the secondary amine, Amberlite LA-2[®], as extractant, a new reflux-type solvent extraction process is being developed for possible application in Hanford's Plutonium Reclamation Facility. A conceptual amine process flowsheet, considerably simpler than the presently used tributyl phosphate flowsheet, has been successfully demonstrated in mixer-settler tests. Amberlite LA-2, either in CCl_4 or trichlorobenzene solutions, is satisfactorily resistant to degradation by HNO_3 and/or HNO_2 solutions. Unidentified ligands, which complex Pu(IV) and prevent its stripping with dilute HNO_3 , form upon alpha radiolysis of the amine extractant. At expected maximum irradiation doses (20-40 watt hr/liter), however, the concentration of these radiolytic products is small and their adverse effect can be largely overcome by periodic washing of the recycled solvent with HNO_3 -HF solutions.

INTRODUCTION

Hanford's Plutonium Reclamation Facility (PRF) is operated by the Atlantic Richfield Hanford Company to recover and purify plutonium from a wide variety of metallurgical scrap including metal, oxide, and alloys. Chemical flowsheets used in the PRF for solvent extraction recovery of plutonium from HNO_3 and HNO_3 -HF solutions of such scrap have been described elsewhere.^{1,2}

Progress towards development of new PRF reflux-type flowsheets, which employ Amberlite LA-2 diluted with CCl_4 [or trichlorobenzene (TCB)] in place of the presently used 20% TBP (tributyl phosphate)- CCl_4 extractant, is described in this paper. Amberlite LA-2 (hereafter simply LA-2) is an aliphatic secondary amine commercially available from the Rohm and Haas Company. The primary advantage anticipated from substitution of LA-2 for TBP is overall process simplification by elimination of the mechanical and chemical problems engendered by the dibutylphosphoric acid [HDBP] produced by alpha radiolysis of TBP. Other potential benefits which may accrue from such substitution include elimination of the need to produce and use hydroxylamine nitrate solutions in stripping plutonium and improved separation of plutonium from various contaminants.

Earlier considerations of the application of secondary amines to plutonium recovery and/or purification have been listed by Winchester³ and by Ferguson *et al.*^{4,5} Coleman⁶ and Schmidt⁷ have described the general nature of amine extraction systems and reaction mechanisms.

CHEMICAL FLOWSHEETS

A simplified version of the reflux-type TBP flowsheet currently used in the PRF is shown in Figure 1. This flowsheet is used to process scrap containing only plutonium; a modified

flowsheet is used with scrap containing both plutonium and uranium. Packed and air-pulsed sieve-plate columns and other equipment used in the PRF have been described previously.^{1,2}

In the CA Column a 20% TBP-CCl₄ solvent is used to extract Pu(IV) from the feed stock resulting from chemical and/or electrolytic dissolution of the scrap. Dilute HNO₃ containing a small concentration of hydroxylamine nitrate is used to strip plutonium in the CC Column; 70 to 90% of the plutonium in the CCP stream is returned to the CA Column. Subsequently, residual plutonium (held tightly in the solvent as a Pu-HDBP complex) is removed in the CO Column by scrubbing with a small volume of HNO₃-HF solution; the spent scrub stream is routed to the CAF make-up tank. Following water scrubbing of the HNO₃ in the CU Column, the TBP extractant is washed each cycle in the CX Column with K₂CO₃ solution to remove HDBP and then acidified in the OA Column prior to recycle to the CA Column.

Routine solvent washing to remove HDBP is essential with the TBP flowsheet to prevent buildup of plutonium in the CCW stream to a concentration (≈ 0.3 g/liter) where it would precipitate as PuF₄ in the CO Column. Such precipitation tremendously complicates PRF operation. Aqueous waste streams generated in the solvent washing CU-CX-OA system, after evaporation, are routed to underground storage; the volume of these wastes amounts to about one-fourth the total volume of waste generated in PRF operation. The K₂CO₃ wash is recycled until it becomes ineffective in removing HDBP, at which time it is discarded.

As seen from results discussed later, alpha radiolysis products of LA-2 complex plutonium much less strongly than does HDBP generated by radiolysis of TBP. Extensive solvent washing steps to remove degradation products of LA-2 are not required for

satisfactory process operation. Thus, the conceptual LA-2 plutonium recovery process presently envisaged (Figure 2) is considerably simpler than the current TBP process and involves only operation of the CA, CC, and CO Columns. The plutonium concentration of the recycled LA-2 solvent is controlled at 0.01 g/liter or less by scrubbing with 1M HNO_3 -0.05M HF in the CO Column. The CO Column really functions then as the solvent washing column in the amine process.

The PRF-TBP extraction system is operated with a nominal 400-liter extractant inventory. Current physical losses are such that the solvent inventory is replaced 5 to 10 times a year. Similar solvent inventory and loss values are expected for an LA-2 system.

The alpha radiation dose received by the TBP solvent depends, of course, on the isotopic content of the plutonium processed. For typical feed material, however, with the flowsheet conditions of Figure 1 the TBP solvent receives radiation at the rate of about 0.5 watt hr/liter per 24-hr period. [The bulk of this exposure occurs in a pump tank where the pregnant TBP extractant is irradiated in the absence of an aqueous phase.] Thus, over its typical 5- to 10-week life each liter of the TBP solvent is irradiated to a total exposure of 20 to 40 watt hr. The dose rate and exposure expected for the LA-2 solvent in the conceptual flowsheet are calculated⁸ to be nearly the same as for the TBP solvent.

Addition of urea to the CAS stream to destroy radiolytically generated nitrite is an optional feature of the LA-2 process flowsheet. Such addition appears unnecessary, however, in view of the stability of LA-2 extractants to attack by HNO_2 (p. 25¹). Also, trichlorobenzene may be substituted for CCl_4 as the diluent in the LA-2 process. Such substitution is beneficial in the TBP process

to protect, at least partially, the TBP from alpha radiolysis to HDBP.

The aqueous:organic phase ratio in the extraction column of the conceptual LA-2 process is lower than that employed in the current TBP process. This is recognized as a disadvantage for PRF application; flowsheet modifications needed to increase this phase ratio are under study.

Finally, the conceptual LA-2 process flowsheet shown in Figure 2 is intended for processing scrap containing only plutonium. Its application to recovery and decontamination of plutonium from scrap also containing uranium or thorium remains to be established.

EXPERIMENTAL

MATERIALS

Selected properties of LA-2 are listed in Table 1. Extractants were prepared by diluting as-received LA-2 and TBP (Eastman Kodak Company) with either reagent-grade CCl_4 or practical-grade 1,2,4-trichlorobenzene (J. T. Baker Company). Tributyl phosphate extractants were washed with successive equal volume portions of $0.3M$ Na_2CO_3 , $1M$ HNO_3 , and water prior to use.

Locally available purified plutonium stock solutions of known isotopic content were used in extraction and alpha radiolysis studies. Radioisotopes used to follow extraction of various contaminants were obtained from several commercial sources.

DISTRIBUTION COEFFICIENT MEASUREMENTS

Aqueous and organic phases were equilibrated by mechanical stirring or shaking for at least 5 minutes at $\approx 25^\circ\text{C}$. Phases were separated by centrifugation.

Amberlite LA-2 (or TBP)-diluent solutions were contacted with equal volume portions of 0.25 to $4.0M$ HNO_3 - 0.0 or $1M$

TABLE 1
SELECTED PROPERTIES OF AMBERLITE LA-2^a

Property	Value
Appearance	Clear, amber liquid
Odor	Faint, pleasant amine
Formula ^b	$\text{CH}_3(\text{CH}_2)_{11}-\overset{\text{H}}{\underset{\text{R}_3}{\text{N}}}-\overset{\text{R}_1}{\text{C}}-\text{R}_2$ <p style="text-align: center;">R₁ + R₂ + R₃ = 12 to 15 C atoms</p>
Molecular Weight	353-395
Neutral Equivalent	360-380
Acid Binding Capacity, meq/ml	2.2-2.3
Density, g/ml	0.83
Viscosity, cP	18
Flash Point (Cleveland Open Cup)	355°F
Cost, \$/pound ^c	1.50

^aTaken mainly from Reference 10.

^bTypical major component.

^cAs of November 1, 1973.

$\text{Al}(\text{NO}_3)_3$ -0.042M $\text{Pu}(\text{NO}_3)_4$ solutions. Prior to contact with the aqueous plutonium solution, organic phases were contacted twice with fresh equal volume portions of appropriate HNO_3 - $\text{Al}(\text{NO}_3)_3$ solutions. Similar procedures were used to measure distribution of HNO_3 between LA-2-diluent solutions and aqueous media and distribution of various metal ions (*e.g.*, Fe^{+3} , Ca^{+2} , Mg^{+2} , etc.) between 30% LA-2- CCl_4 and HNO_3 - $\text{Al}(\text{NO}_3)_3$ -0.05M metal nitrate solutions containing, usually, appropriate radioactive tracers.

MIXER-SETTLER RUNS

Tests of the amine extraction process were made in 12- and 17-stage all-stainless-steel mixer-settlers. These units were Hanford-designed versions of a type developed earlier by Coplan *et al.*¹¹ In testing chemical flowsheets, mixer-settlers were operated with the particular aqueous and organic solutions required until steady-state conditions were reached. Samples of the effluent streams were taken hourly and analyzed to determine when steady-state was attained. Plutonium losses were computed from analyses of steady-state effluent streams. Organic product solutions collected under steady-state conditions in extraction and strip column runs, respectively, were used as feed solutions in succeeding strip and solvent wash (CO) column runs. Mixer-settler runs generally lasted 6 to 8 hr, and organic solution containing plutonium stood 16 to 24 hr at 25°C before use in a strip or solvent wash column run. Synthetic CAF or CAIS solutions were used in all extraction column runs; no attempt has yet been made to couple extraction and strip column runs to demonstrate the reflux feature of the amine flowsheet.

SOLVENT RADIOLYSIS AND REACTIONS

Radiolysis. Alpha radiolysis of LA-2 diluent solutions was performed both in the presence and absence of an aqueous phase.

In the latter instance 30% LA-2- CCl_4 (or TCB) solvents containing 0.041 to 0.079M $\text{Pu}(\text{NO}_3)_4$ (of known isotopic composition) and 0.4 to 0.5M HNO_3 were obtained from mixer-settler extraction column runs or were prepared by batch contact with appropriate aqueous phases. These organic solutions, in suitably sealed bottles, were allowed to stand at $\approx 25^\circ\text{C}$ for 7 to 147 days corresponding to absorbed energies in the range 7.2 to 100 watt hr/liter. Radiation doses received by these solvents were calculated on the assumption that all of the plutonium decay energy was absorbed within the organic phase. In one test a 30% LA-2- CCl_4 solvent was contacted (stirred emulsion) 104 days at $\approx 25^\circ\text{C}$ with an aqueous phase of the initial composition 3M HNO_3 -0.6M $\text{Al}(\text{NO}_3)_3$ -0.054M $\text{Pu}(\text{NO}_3)_4$.

Periodically, portions of the irradiated LA-2 extractants were removed and contacted three times, at an aqueous-to-organic phase ratio of 1.66, with 0.25M HNO_3 . The concentration of plutonium remaining in the stripped organic phase was determined. Subsequently, the stripped organic phase was washed either with consecutive equal volume amounts of 1M NaOH, 1M HNO_3 and water, or three times with one-fifth volume portions of 1M HNO_3 -0.05M HF. Plutonium extraction capacity of the irradiated and stripped LA-2 solvents, both before and after washing, was determined by contacting them twice with 5M HNO_3 and then once with a 5M HNO_3 -0.042M $\text{Pu}(\text{NO}_3)_4$ solution. The concentration of LA-2 in some of the irradiated extractants was estimated by a gas chromatographic procedure.

Reaction With Nitrite. Amberlite LA-2- CCl_4 solutions were contacted (stirred emulsion) four weeks at either 25 or 40°C with equal volumes of aqueous HNO_3 and HNO_3 - HNO_2 solutions. Spent aqueous phases were replaced weekly. Periodically, samples of the organic phases were removed and stripped twice at 25°C with equal

volumes of 0.25M HNO₃. Subsequently, the capacity of the resulting organic phase to extract plutonium from a 5M HNO₃-0.042M Pu(NO₃)₄ solution was determined. Portions of the stripped organic phases were also washed with successive equal volume portions of 1M NaOH, 1M HNO₃, and water and then titrated with HCl to estimate total amine concentration.

Amine-Diluent Interaction. Solutions of LA-2 in both CCl₄ and TCB were allowed to stand up to six months in laboratory fluorescent light and for 1 to 63 days out-of-doors in alternate periods of bright summer sunlight and darkness. The latter solutions were contained in sealed bottles while the former were exposed to air through water-cooled condensers. Progress of air oxidation and/or amine-diluent interaction was followed by periodic infrared and titration analyses.

ANALYSES

Conventional alpha counting and energy analysis methods were used to measure plutonium concentrations in aqueous and organic phases. Concentrations of ⁵⁹Fe and other gamma emitters in samples obtained in certain distribution coefficient measurements were determined by gamma energy analysis techniques [Ge(Li) detector]. Atomic absorption procedures were used to analyze for Ca, Mg, and Ni in these latter samples. Nitric acid in both organic and aqueous phases was titrated, in some cases after addition of K₂C₂O₄ to complex aluminium, potentiometrically with standardized NaOH.

A Bendix 2200 gas chromatograph equipped for temperature programming was used to estimate the LA-2 content of various extractants. Amine samples were chromatographed at 220 to 350 °C (15°C/min) on 8% Dexil 300 on 100 to 110 mesh Chromasorb 6 using He carrier gas and a flame ionization detector whose output was fed to a multichannel analyzer. Areas, at half-peak height, under

corresponding principal peaks of test and standard samples were compared to estimate LA-2 concentrations.

In some instances samples of the LA-2 extractants were dissolved in an isopropanol- CHCl_3 -water mixture and titrated with HCl in isopropanol to estimate total amine concentrations.

A Beckman IR-10 instrument was used to record the infrared spectra of various LA-2 extractants.

RESULTS AND DISCUSSION

DISTRIBUTION COEFFICIENTS

Plutonium. Data for the distribution of Pu(IV) with 20% TBP and 30 and 40% LA-2 as solvents are plotted in Figures 3 and 4. Additional plutonium distribution data for the 20% TBP-TCB solvent have been obtained by Hamilton.¹² Both sets of data show that TBP-TCB solvents extract Pu(IV) less efficiently than do TBP- CCl_4 solutions; our results (Figure 4) show, however, that TCB has only a slight depressive effect on extraction of Pu(IV) by LA-2. With either TCB or CCl_4 diluent, a 40% LA-2 solvent is equivalent (or nearly so) to a 20% TBP solution in its ability to extract Pu(IV) from HNO_3 media. Addition of $\text{Al}(\text{NO}_3)_3$ to the aqueous HNO_3 phase significantly enhances extraction of Pu(IV) into LA-2 solvents; on this basis and also to facilitate stripping of plutonium with dilute acid, a 30% LA-2 solvent was selected for use in the conceptual plutonium recovery process.

Coleman⁶ notes that distribution data in most amine extraction systems can usually be fitted by an empirical equation of the form $D = E_1 [C_R - mC_O]^n$ where \underline{D} = distribution coefficient, \underline{E}_1 = a constant dependent on salting strength, \underline{C}_R = the concentration (M) of the amine in the solvent, \underline{C}_O = the concentration of plutonium (M) in the organic phase, and \underline{m} and \underline{n} are constants. Our plutonium data, as well as those of German¹³ investigators with LA-2- CCl_4

solvents, are correlated fairly well by the equation

$D_{Pu} = a[M NO_3^-]_{aq}(C_R - 2C_O)^2$ where $[M NO_3^-]_{aq}$ is the molar concentration of nitrate in the aqueous phase and $a = 1.0$ for 20 to 30% LA-2 and $a = 1.6$ for 40 to 50% LA-2. A similar correlation of distribution data for LA-2-TCB solvents has not yet been attempted.

Nitric Acid. Plotted in Figure 5 are data for the distribution of HNO_3 between 30% LA-2 solvents and aqueous HNO_3 solutions. As observed with plutonium, HNO_3 does not extract quite as well into LA-2-TCB solvents as it does into LA-2- CCl_4 extractants.

Extraction of Contaminants. Feedstock to the CA Column contains, in addition to plutonium, small concentrations of various metallic contaminants. Purification from these impurities to the extent of producing plutonium containing less than 2000 parts of metallic impurities per million parts of plutonium is required. Results in Table 2 together with similar data of Japanese scientists¹⁴ indicate that the LA-2 extraction process can readily provide the required decontamination.

Our uranium distribution data (Table 2) are in agreement with the results of Koch, Schön, and Franz¹³ for extraction of uranium into ~20% LA-2- CCl_4 solutions. These workers also find, as expected, that uranium extraction decreases when the LA-2 extractant is loaded with plutonium. Countercurrent extraction and separation behavior of uranium (and also of thorium) under the reflux conditions of the conceptual LA-2 extraction process has not yet been established.

FLWSHEET TESTS

Representative results of the extensive mixer-settler runs made to demonstrate and test performance of the conceptual LA-2 flowsheet (and modifications thereof) under countercurrent

TABLE 2

EXTRACTION OF CONTAMINANTS BY 30% LA-2-CCl₄ SOLVENT

Contaminant	Distribution Ratio Range	
	From 0.25 to 4M HNO ₃ ^a	From 1M Al(NO ₃) ₃ -1 to 4M HNO ₃ ^a
Al ⁺³	<7.2 x 10 ⁻⁷	-
Fe ⁺³	<1.2 to <1.8 x 10 ⁻⁵	-
Am ⁺³	<1.7 to <8.8 x 10 ⁻⁵	-
Na ⁺	<4.0 to <4.3 x 10 ⁻⁵	<4.2 to <4.4 x 10 ⁻⁵
Eu ⁺³	<1.5 x 10 ⁻⁴	<0.9 to <3.1 x 10 ⁻⁴
Ni ⁺²	<3.4 to <3.5 x 10 ⁻⁴	<3.4 to <3.5 x 10 ⁻⁴
Mg ⁺²	<1.5 to <8.9 x 10 ⁻⁴	<0.8 to <1.5 x 10 ⁻⁴
Cr ⁺³	<0.2 to <1.8 x 10 ⁻³	<1.6 to <1.7 x 10 ⁻³
Ce ⁺³	<1.3 to <1.4 x 10 ⁻³	<1.3 to <6.9 x 10 ⁻³
UO ₂ ⁺²	0.0061 to 0.26	0.70 to 1.0

^aExcept with Am⁺³, initial aqueous phase contained 0.01M contaminant.

conditions are shown in Tables 3-5. [Stream designations listed in Tables 3-5 refer to those shown in Figure 2.] Overall flow-sheet performance was very satisfactory with effects produced by flowsheet changes conforming to those expected from distribution data. Thus, extraction (CA) column plutonium losses decreased markedly with either or both increased aqueous phase salting strength and extractant flow. Performance of both the strip (CC) and solvent wash (CO) columns in plutonium removal was adequate with both 30% LA-2-CCl₄ and 30% LA-2-TCB solvents but was slightly better with the latter, possibly because of decreased HNO₃ content of the influent organic streams.

Solids (PuF₄) precipitated in two CO Column runs where the feed organic stream contained 0.4 to 0.7 g_{Pu}/liter, but were not observed at lower feed plutonium concentrations. Adequate removal of plutonium is achieved in the CO Column of the LA-2 process with a COX stream containing 0.05M HF in place of the 0.25M HF currently used in the TBP process.

Hydraulic performance was generally excellent throughout. In some strip column runs with LA-2-CCl₄ solvent the organic raffinate contained a small (1-2 vol%) amount of entrained aqueous phase. Such entrainment was not observed with LA-2-TCB solvent, and, in any case, sparklingly clear organic streams were obtained in all CO Column runs, even in those where the feed contained entrained aqueous phase.

STABILITY OF LA-2 EXTRACTANT

Detailed knowledge of the chemical and radiation stabilities of LA-2 and its solutions is obviously required before serious consideration can be given to using this extractant in the PRF. An excellent review of the stability of amine extractants in various nuclear applications has been prepared by Eubanks.¹⁵ In addition

TABLE 3

LA-2 FLOWSHEET TESTS--TYPICAL MIXER-SETTLER
EXTRACTION (CA) COLUMN RESULTS^a

Phase Ratio ^b Aq:Org	CAF Stream ^c		CAX ^d Stream Flow	CAW Stream Pu g/liter	Pu Loss to CAW Stream ^e %
	Al(NO ₃) ₃ M	HNO ₃ M			
2.0	1.0	3.0	125	1.7	14.
2.0	1.5	3.0	125	0.13	1.0
1.6	1.0	3.0	157	0.20	1.6
1.6 ^f	1.25	2.5	157	0.070	0.55
1.6	1.25	2.5	157	0.075	0.62
1.6	1.5	3.0	157	0.012	0.10
1.5	1.0	3.0	174 ^g	0.035	0.30

^aAll runs: 12 extraction stages, 2 CAIS stages, 3 CAS stages.

CAIS = 3M HNO₃-40 g/liter Pu; Flow = 75.

CAS = 3M HNO₃; Flow = 15.

^bTotal aqueous flow/CAX flow.

^cCAF was also 0.4M HF and 1 g/liter Pu; Flow = 150.

^dExcept where indicated CAX was 30% LA-2-CC1₄.

^eOf total Pu in the CAF and CAIS streams.

^fCAS also contained 0.05M urea.

^gCAX was 30% LA-2-TCB.

TABLE 4

LA-2 FLOWSHEET TESTS--TYPICAL MIXER-SETTLER
STRIP (CC) COLUMN RESULTS^a

HNO ₃ <i>M</i>	CCF Stream ^b			CCX Stream ^c Flow	CCW Stream		Pu Loss to CCW %
	Pu g/liter	Diluent	Flow		Pu g/liter	HNO ₃ <i>M</i>	
0.40	16.0	CCl ₄	174	87	0.092	0.21	0.57
0.50	16.7	CCl ₄	157	78.5	0.10	0.25	0.60
0.45	17.0	CCl ₄	174	87	0.18	0.22	1.05
0.49	17.3	CCl ₄	174	104	0.23	0.32	1.32
0.26	14.0	TCB	174	87	0.08	0.09	0.22
0.25	17.2	TCB	174	87	0.15	0.13	0.88

^a17 mixer-settler stages in all runs.

^b30% LA-2 solvent from preceding CA Column run.

^cCCX = 0.3M HNO₃ in all runs.

TABLE 5

LA-2 FLOWSHEET TESTS--TYPICAL MIXER-SETTLER
SOLVENT WASH (CO) COLUMN RESULTS^a

HNO ₃ <i>M</i>	COF Stream ^b		COX Stream ^c HF <i>M</i>	COW Stream	
	Pu <u>g/liter</u>	Diluent		Pu <u>g/liter</u>	HNO ₃ <i>M</i>
0.28	0.70	CCl ₄	0.25	0.050	0.32
0.27	0.43	CCl ₄	0.25	0.023	0.24
0.27	0.27	CCl ₄	0.05	0.021	0.29
0.11	0.13	TCB	0.05	0.005	0.14
0.12	0.35	TCB	0.05	0.009	0.11

^a5 mixer-settler stages in all runs.

^b30% LA-2 solvent from preceding CC Column run; flow = 125.

^cIn all runs COX was also 1.0M HNO₃ with flow = 25.

to discussing radiolysis effects and mechanisms, Eubanks also reviews reactions of amines with air, water, HNO_3 , HNO_2 and diluents.

Alpha Radiolysis. Gamma radiolysis (^{60}Co) of LA-2 and its solutions to doses as high as 5×10^7 R produces only minor radiation damage according to Ichikawa and Uruno¹⁶, Tsujino and Ishihara¹⁷, and Ishihara, Tsujino, and Komaki.¹⁸ Alpha radiolysis of LA-2 solutions has apparently not been studied previously. Our results (Figure 6 and Table 6) indicate that the principal effect of such radiolysis is generation of an unidentified ligand(s) which complexes Pu(IV) and prevents its stripping with dilute HNO_3 . Irradiation of LA-2 solutions to doses as high as 100 watt hr/liter, however, does not appear to destroy large amounts of amine or impair plutonium extraction capacity.

For LA-2 solvents irradiated either in the presence or absence of an aqueous phase the amount of "unstrippable" plutonium increases linearly, as expected, with absorbed dose (Figure 6). A major difference between the two cases is that when irradiated in the presence of an aqueous phase, the LA-2 solvent apparently retains far less of the radiolysis product that complexes plutonium and prevents it from stripping. In plant-scale operation, however, as pointed out previously, almost all the irradiation dose accrues when the solvent is not in contact with an aqueous phase. The data in Figure 6 also show that the rate of degradation of LA-2 is the same in both CCl_4 and TCB solutions.

After stripping with dilute HNO_3 , LA-2 solvents irradiated in the absence of an aqueous phase retain significantly less plutonium than do similarly irradiated and stripped TBP solvents. According to Barney, irradiated 20% TBP- CCl_4 solvent, after exhaustive (five equal-volume contacts) stripping with 0.2M HNO_3 , retains

TABLE 6

ALPHA RADIOLYSIS OF LA-2 SOLVENTS

Solvent No.	Days Stood	Exposure watt hr/liter	Amine Vol% ^a	D _{Pu} ^b	
				Unwashed ^c	Washed ^d
	0	0	30.0	13.0 ^e ; 10.0 ^f	
1 ^g	7	7.16		18.1	19.3
2 ^h	15	12.5		9.94	9.00
3 ⁱ	21	14.3		16.6	18.0
2	31	25.8		9.29	10.0
3	40	27.2		9.63	14.2
2	56	46.6		10.0	10.1
1	49	50.1	32.6	11.9	14.9
3	77	52.4		13.2	17.1
3	112	75.0	28.8	11.5	12.6
2	111	92.4		8.84	9.00 ^j
3	147	100.	27.4	12.6	13.5
4 ^k	7	4.62	28.0	13.9	14.4
4	21	13.9	30.0	16.4	14.2
4	52	34.3		21.1	16.5

^aAll solvents were initially 30% LA-2.

^bFrom 5M HNO₃-10 g/liter Pu.

^cAfter stripping with 0.25M HNO₃.

^dExcept where indicated, washed with successive equal-volume portions of 1M NaOH, 1M HNO₃, and water.

^eWith 30% LA-2-CCl₄.

^fWith 30% LA-2-TCB[†].

^gCCl₄ diluent; 18.9 g/liter Pu-0.05M HNO₃; no aqueous phase.

^hTCB diluent; 12.1 g/liter Pu-0.40M HNO₃; no aqueous phase.

ⁱCCl₄ diluent; 9.8 g/liter Pu-0.40M HNO₃; no aqueous phase.

^jWashed three times with one-fifth volume of 1M HNO₃-0.05M HF.

^kCCl₄ diluent; contacted continuously with aqueous HNO₃-Al(NO₃)₃-Pu(NO₃)₄ solution.

56 mg Pu per liter for each watt hr of absorbed alpha decay energy. Conversely, even after only three strips with 1.66 volume portions of 0.25M HNO₃, an irradiated 30% LA-2-CCl₄ or TCB-solvent retains only about 0.34 mg Pu per liter for each watt hr of absorbed energy.

Plutonium retained by irradiated and stripped LA-2 solvents is effectively removed by washing them with HNO₃ solutions containing small concentrations of HF. For example, three washes with one-fifth volume portions of 1M HNO₃-0.05M HF solution remove 90 to 99% of the plutonium retained by LA-2 solvents irradiated to exposures as high as 160 watt hr/liter (Table 7). Successive NaOH and HNO₃ washes also remove plutonium retained by irradiated LA-2 solvents but less effectively than sequential HNO₃-HF washes. [The large volume of aqueous waste which would be generated is another, serious disadvantage to periodic caustic washing of the LA-2 solvent.] Gas chromatographic, infrared, and distribution coefficient data all indicate that neither HNO₃-HF nor NaOH-HNO₃ washes remove the amine and/or diluent degradation products which complex and retain plutonium in irradiated LA-2 solvents.

Reaction With Nitrous Acid. That secondary amines react with HNO₂ to form nitrosoamines is well known.¹⁵ According to distribution coefficient and amine concentration data tabulated in Table 8, LA-2 is quite stable to degradation either by HNO₃ or HNO₂. Infrared analyses of the exposed 30% LA-2-CCl₄ solvents also failed to show the presence of any nitroso compounds.

Resistance of the LA-2 extractant to decomposition by HNO₂ is particularly significant since feeds to the PRF always contain small concentrations of radiolytically generated HNO₂. In the conceptual chemical flowsheet (Fig. 2) a small concentration of urea is added to the CAS stream to react with and destroy nitrite.

TABLE 7

WASHING OF PLUTONIUM FROM IRRADIATED LA-2 EXTRACTANTS

Number ^a	Irradiated Extractant		Wash Type ^b	Pu, g/liter	
	Diluent	Dose watt hr/liter		Before Wash ^c	After Wash
1	CCl ₄	50.1	1	0.024	0.0053
		100.	1	0.0229	0.011
		160.	2	0.094	0.00089
2	TCB	25.8	1	0.0090	0.0023
		46.6	1	0.0016	0.0098
		46.6	2	0.016	0.000098
		92.4	2	0.036	0.0019
3	CCl ₄	75.	1	0.012	0.0086
		119.	2	0.041	0.0082
4	CCl ₄	34.3	1	0.0024	0.0011
		73.3	2	0.0080	0.0009

^aIrradiated 30% LA-2 solutions identified as solvents 1-4, Table 6.

^bType 1 - Equal-volume washes with successive portions of 1M NaOH, 1M HNO₃, and water.

Type 2 - Three washes with successive one-fifth volume portions of 1M HNO₃-0.05M HF.

^cIn all cases irradiated solvent was stripped three times with 1.66 volume portions of 0.25M HNO₃ prior to washing.

27

TABLE 8

EFFECTS OF EXPOSURE OF 30% LA-2-CCl₄ SOLVENT TO HNO₃-HNO₂ SOLUTIONS

Contact Time Weeks	Exposure at 25 °C ^a				Exposure at 40 °C ^b			
	With NaNO ₂		Without NaNO ₂		With NaNO ₂		Without NaNO ₂	
	DPu ^c	Amine Vol% ^d	DPu ^c	Amine Vol% ^d	DPu ^c	Amine Vol% ^d	DPu ^c	Amine Vol% ^d
0			12.2 ^e	30.0				
1	11.8	31.8	11.5	31.3	12.3	30.2	16.2	30.7
2	12.2	28.1	11.8	21.1	13.7	29.0	13.2	29.6
4	12.4	32.4	13.8	f	13.8	f	14.8	f

^aAqueous phase: 2.0M HNO₃-1.5M Al(NO₃)₃-0.1M NaNO₃-0.4M HF-0.0 or 0.025M NaNO₂.

^bAqueous phase: 3.0M HNO₃-0.0 or 0.025M NaNO₂.

^cFrom 5.0M HNO₃-0.042M Pu(NO₃)₄.

^dBy titration with HCl.

^eUnexposed 30% LA-2-CCl₄.

^fNot determined.

This flowsheet feature will further guard against loss of LA-2 by reaction with HNO_2 . A similar approach has been used to prevent slow conversion of trilaurylamine to dilaurylamine in certain nuclear fuel reprocessing operations.¹⁹

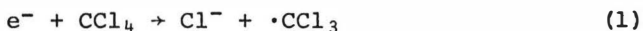
Amine-Diluent Interactions. That amines readily react with halocarbons in the presence of light was first reported by Collins.²⁰ One of the reaction products is always an amine hydrohalide²¹⁻²⁴, and the amine itself may or may not be altered. Stevenson and Coppinger²² found that with halomethanes amines form 1:1 charge transfer complexes.

When exposed to bright sunlight even for as little as one day a ~~30%~~ LA-2- CCl_4 solution changes in color from the initial pale-yellow to a deep-orange and finally to a reddish-black. Although free of solids such as those observed by Collins and others the black solutions contain no detectable free amine when titrated with alcoholic HCl; gas chromatographic analyses show, however, that the total amine concentration of such solutions is comparable to that of a freshly prepared 30% LA-2- CCl_4 solvent. Plutonium extraction-strip behavior of 30% LA-2- CCl_4 extractants exposed to bright sunlight for as long as 37 days is also about equal to that of freshly prepared extractant. Compared with that of unirradiated extractant, new absorption bands occur in the infrared spectra of exposed extractants at 1580 and 2170 cm^{-1} , respectively.

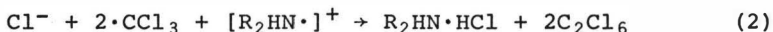
Similar color and other changes occur, but at much slower rates, when LA-2- CCl_4 solvents stand in laboratory fluorescent light or when LA-2-TCB extractants stand in sunlight. For example, after standing in sunlight for nine weeks a 30% LA-2-TCB solvent was colored only slightly more orange than virgin extractant; about 95% of the amine initially present was still titratable with HCl. In fluorescent light both LA-2- CCl_4 and LA-2-TCB

solvents retain their color and base titer for at least three months.

Following Stevenson and Coppinger²², interaction between CCl_4 and LA-2 is believed to involve the reaction sequence:



and



where the electron in (1) comes from the amine portion of the complex. This sequence appears consistent with all the experimental observations including the infrared data; absorption bands due to the NH_2^+ stretch vibration and the NH_2^+ deformation occur at about 1620-1560 and 2700 cm^{-1} , respectively. The amine hydrohalide produced in Reaction (2) is of course not titratable with HCl. Also, since the LA-2 has not been destroyed, only transformed, plutonium extraction behavior of the exposed LA-2 solvent should be comparable to that of unirradiated extractant.

Implications of LA-2-diluent interaction to performance of the proposed amine extraction process appear minimal, particularly if TCB is used as the diluent. In plant-scale application the LA-2 extractant will not be exposed to fluorescent light let alone sunlight. Finally, even if some amine-diluent interaction did occur the transformed LA-2 would still be available for extraction of plutonium.

CONCLUSIONS

Amberlite LA-2 can be satisfactorily substituted for the TBP extractant currently used in the Hanford Plutonium Reclamation Facility. Such substitution is advantageous to realize process simplification and to reduce waste volumes. Stability, both chemical and radiolytic, of the LA-2 extractant is expected to be excellent in the PRF application. Further experimentation is

desirable to define optimum flowsheet conditions with the LA-2 extractant and to establish the capability of an LA-2 extraction process for purifying plutonium from large amounts of uranium and thorium.

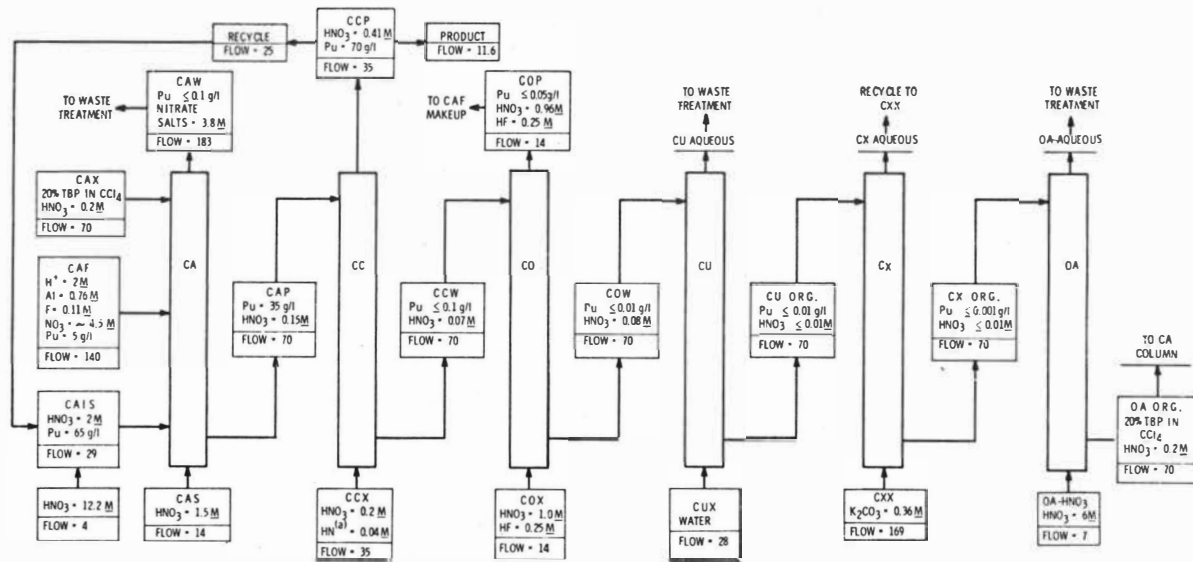
ACKNOWLEDGMENTS

The skilled assistance of Paul Hammitt, James Miller, and Celestine Tillman with the experimental work is acknowledged with pleasure. We are also indebted to Eleanore Earhart for her usual excellent secretarial services.

REFERENCES

1. Bruns, L. E., *Chem. Engng. Prog. Symp. Ser.*, 1967, 63, (80), 156.
2. Bruns, L. E., 'Plutonium-Uranium Partitioning by a Reflux Extraction Flowsheet' in *Proceedings, ISEC 71*, 1971 (London: Society of Chemical Industry), Vol. 1, p. 186.
3. Winchester, R. S., Rep. Congr. Atom. Energy Commn., U.S., 1957, LA-2170.
4. Ferguson, D. E. *et al.*, Rep. Congr. Atom. Energy Commn., U.S., 1968, ORNL-4272.
5. *Ibid.*, Rep. Congr. Atom. Energy Commn. U.S., 1972, ORNL-4794.
6. Coleman, C. F., *At. Energy Rev.*, 1964, 2, 3.
7. Schmidt, V. S., 'Amine Extraction,' 1970 (Jerusalem: Israel Program for Scientific Translations, Ltd.).
8. Richardson, G. L., Private Communication to W. W. Schulz, 1973.
9. Barney, G. S., Unpublished Results, 1973.
10. "Summary of Comparative Properties: Amberlite LA-1 and LA-2, Technical Data Sheet," 1973 (Philadelphia: Rohm and Haas Company).
11. Coplan, B. V., Davidson, J. K., and Zebroski, E. L., *Chem. Eng. Prog.*, 1954, 50, 403.

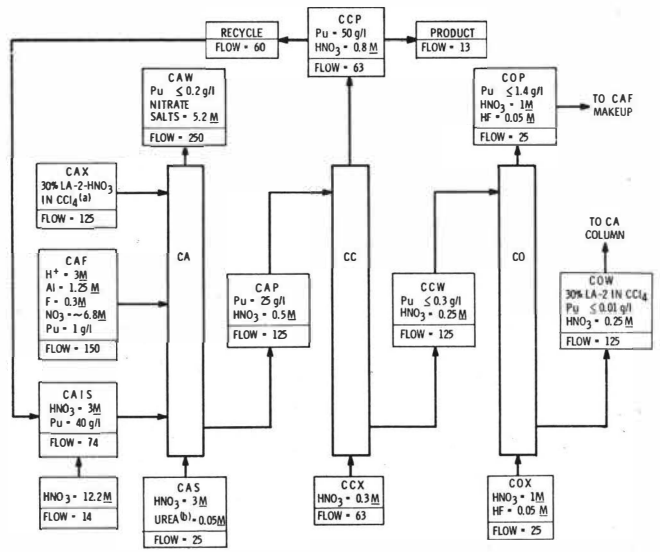
12. Hamilton, R. H., Rep. Congr. Atom. Energy Commn., U.S., 1973, ARH-2785.
13. Koch, G. S., Schön, J., and Franz, G., Report Gesellschaft für Kernforschung mbH, 1970, KFK-893.
14. Ishimori, T., Kimura K., Nakamura, E., Tsukuechi, K., and Osakabe, T., *Nippon Genshiryoku Gakkaishi*, 1963, 5, 89.
15. Eubanks, I.D., *At. Energy Rev.*, 1969, 7, 49.
16. Ichikawa, F. and Uruno, S., *Bull. Chem. Soc. Japan*, 1960, 33, 569.
17. Tsujino, T. and Ishihara, T., *J. Nucl. Sci. Technol. (Tokyo)*, 1966, 3, 320.
18. Ishihara, T., Tsujino, T., and Komaki, Y., *Nippon Genshiryoku Gakkaishi*, 1964, 4, 307.
19. Bathellier, A., Grieneisen, A., and Plessy, L., *Energ. Nucl. (Paris)*, 1968, 10, 186.
20. Collins, R. F., *Chem. Ind. (London)*, 1957, 704.
21. Swan, G. A. Timmons, P.S., and Wright, D., *J. Chem Soc.*, 1959, 9.
22. Stevenson, D. P. and Coppinger, G. M., *J. Amer. Chem. Soc.*, 1962, 84, 149.
23. Cromwell, N. H., Foster, P. W., and Wheeler, M. M., *Chem. Ind. (London)*, 1959, 228.
24. Beichl, G. J., Colwell, J. E., and Miller, J. G., *Chem. Ind. (London)*, 1966, 203.



NOTES: (a) HN - HYDROXYLAMINE NITRATE

FIGURE 1. PRESENT TBP PLUTONIUM RECOVERY PROCESS

2060



NOTES: (a) TRICHLOROBENZENE CAN ALSO BE USED AS A DILUENT
 (b) OPTIONAL

FIGURE 2. CONCEPTUAL LA-2 PLUTONIUM RECOVERY PROCESS

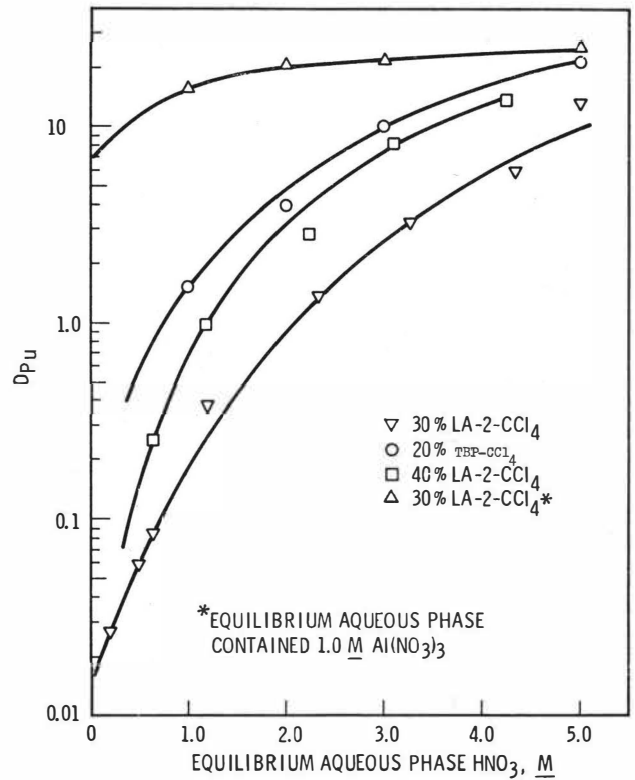
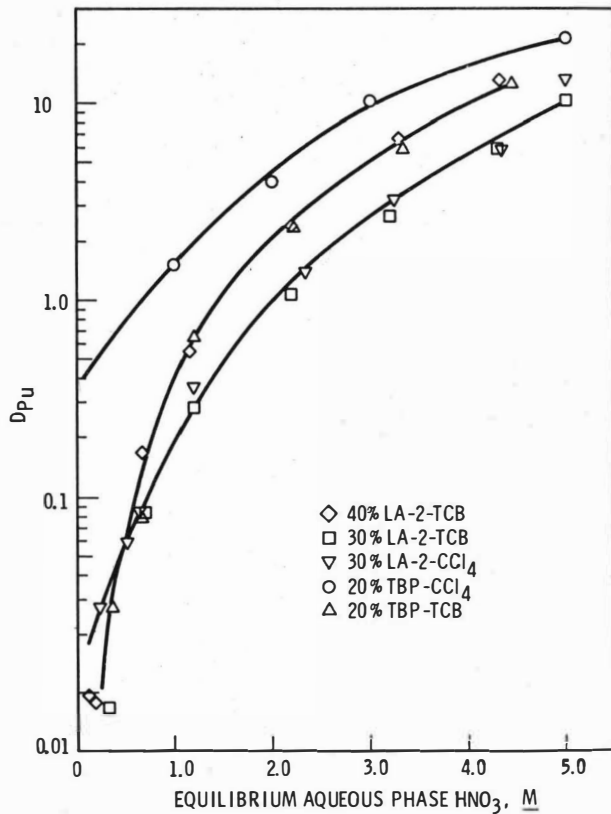
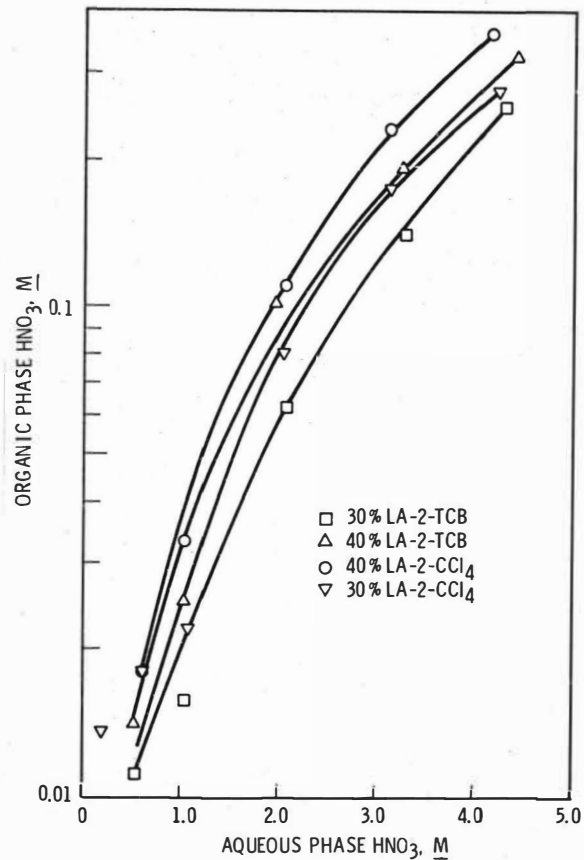


FIGURE 3. PLUTONIUM EXTRACTION BY TBP AND LA-2 SOLVENTS

FIGURE 4. COMPARISON OF CCl_4 AND TCB AS DILUENTSFIGURE 5. EXTRACTION OF HNO_3 BY LA-2 SOLVENTS

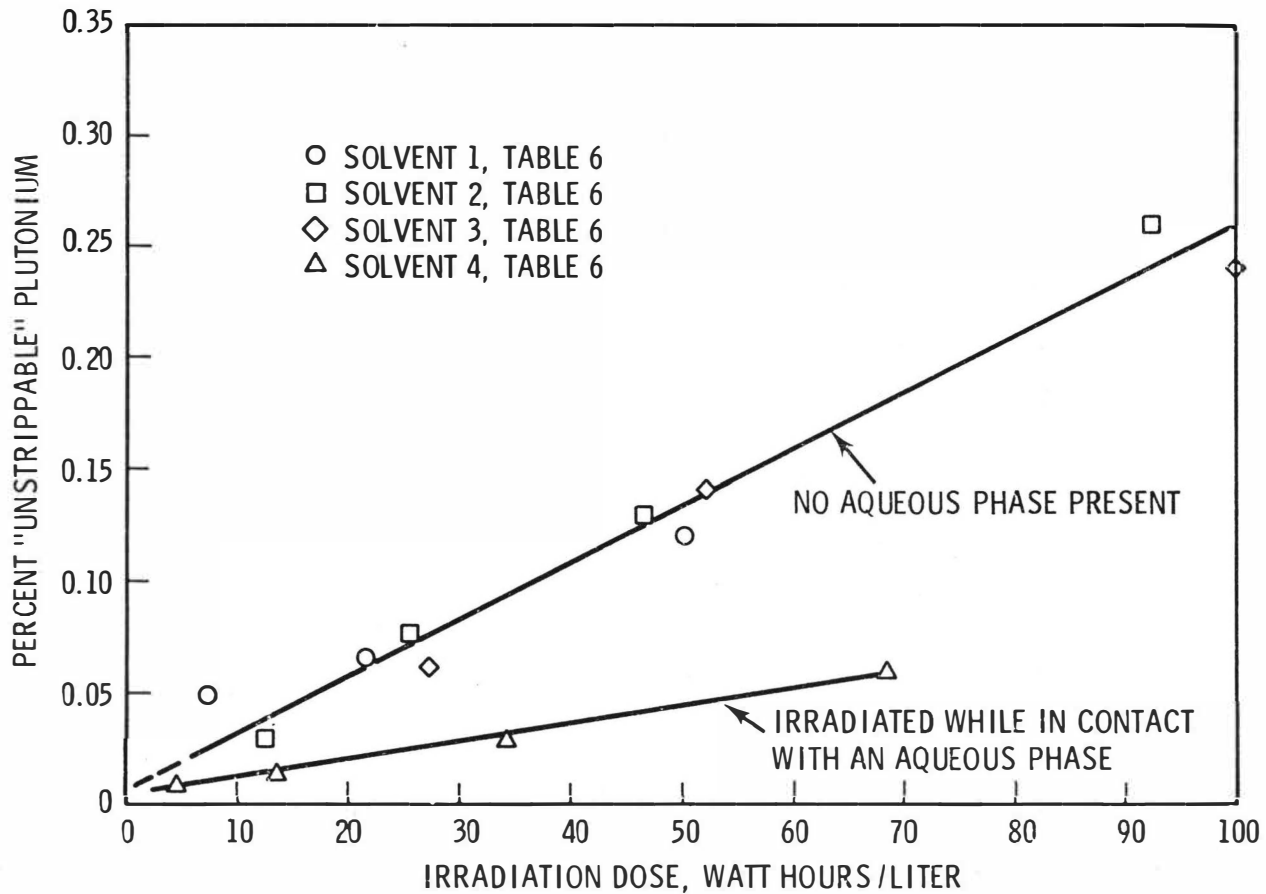


FIGURE 6. "STRIPPABILITY" OF PLUTONIUM FROM ALPHA-IRRADIATED LA-2 SOLVENTS

PERFORMANCE OF EXTRACTION EQUIPMENT
IN THE WAK-PILOT PLANT

K. L. HUPPERT
W. ISSEL
W. KNOCH

GESELLSCHAFT ZUR WIEDERAUFARBEITUNG VON KERNBRENNSTOFFEN MBH
LEOPOLDSHAFEN, GERMANY

Abstract

Mixer-Settlers are used in the German pilot plant for the reprocessing of nuclear fuels. Accumulation of solids presents serious problems and requires design changes. The behaviour of precipitates in pulse columns and centrifugal contactors has been tested. Conclusions are drawn with respect to scale-up and the processing of high-burnup fuels.

The German pilot plant for the reprocessing of spent nuclear fuel, the "Wiederaufarbeitungsanlage Karlsruhe" (WAK), was put into operation in 1971. The chemical separation processes are based on the well-known PUREX-flowsheet.

Various types of extractors are used in reprocessing plants and there is still no general agreement on the best choice. Advantages such as simple and reliable operation, hydraulic stability, easy start-up, high efficiency and a wide range of operational conditions are attributed to mixer-settlers. In the WAK, mixer-settlers have been chosen for the liquid-liquid extraction steps.

The performance of the WAK mixer-settlers will be discussed, considering scale-up and the potential applicability for advanced nuclear fuels.

Mixer-Settlers

Description of apparatus

A total of 9 multi-stage batteries is used for extraction, scrubbing and stripping operations in the system aqueous nitrate solutions / 30 Vol% TBP in n-Dodecane. Overall flowrates vary between 10 and 250 l/h with phase ratios (Vol.) from 10 : 1 to 1 : 3. Two different sizes of mixer-settler are used to cover criticality considerations for uranium and plutonium nitrate solutions respectively. The number of stages per battery varies between 5 and 15. The stages are arranged horizontally in a box. Mixing and phase flow are performed by turbine-impellers. Some design data are summarized in table 1.

Table 1

	Holdup (liter)		Height (cm)	total throughput (l/h)	impeller speed rpm
	Mixing chamber	Settling chamber			
Type A	1	10	15	250	500
Type B	0.75	1.4	5	50	500

A minimum height of the interface level is determined by fixed weirs (see fig. 1), except for the first stage (aqueous outlet) where the position of the interface is measured by an ultrasonic gauge and controlled by adjusting the flowrate of the outgoing aqueous stream in a pressure pot.

Performance

The mixer-settler batteries have been tested in cold runs with uranium but in absence of plutonium and fission products. The extraction performance was good; the overall efficiency with respect to uranium around 85%. Phase separation was excellent due to 2 large baffles in the settler chamber which promoted coalescence. Impeller speeds above 700 rpm resulted, however, in increased entrainment of aqueous phase at the organic outlet. The extraction efficiency in the feed entrance stage was rather poor. In some cases layers of different concentration could be noticed in both phases probably due to the large density differences in this stage. The relation between direction of rotation and the angle of the baffles between mixing and settling chambers influences the hydraulic behaviour and flow capacity. Flooding occurs at much lower throughput when the baffles interfere with the flow direction.

An internal recycling between mixer and settler (of the same stage) is possible through holes at the bottom of the separating wall and through the baffled port itself.

During the first hot reprocessing campaign all the extraction data (losses, decontamination factors and separation factors) were in the expected range. Radiation doses to the solvent were, however, low according to the moderate burnup of 11 000 MWd/t and the cooling time of the spent fuel.

The subsequent processing of high burnup fuel (15 000 - 20 000 MWd/t) resulted in an entirely different hydraulic behaviour of the first extraction battery, which contains the most radioactive solutions. At intervals of 2 to 5 days, control of the interface became difficult, product losses increased and separation factors decreased. Eventually the battery was flooded and

the aqueous flow direction reversed. Proper operation could be restored by emptying and flushing the battery. The cause for the frequent hydraulic failure is very likely the accumulation of interface precipitates in the settler chambers. This leads finally to the blocking of the aqueous port to the neighbouring mixer.

The nature of the solids has not yet been identified. It is reported by other authors, that the crud is formed by the reaction of chemical and radiolytic degradation products of the solvent and diluent with fission products e.g. zirconium. The rapid appearance of substantial amounts of solids leads to the assumption that the introduction of solid particles by the feed, because of insufficient feed clarification, accelerates the accumulation.

Changes of the flowsheet or operational mode did not yield any better performance.

It must be emphasized at this point that all other mixer-settler batteries worked satisfactorily.

There were three possible ways to overcome the difficulties:

- change to another type of extractor (e.g. pulse columns, centrifugal contractors)
- chemical treatment (e.g. pre-precipitation, complexing of fission products)
- improvement of existing equipment.

Our first attempt was to improve the design of the mixer-settler with respect to hydraulic failure in the presence of precipitates.

Cold pilot runs were performed to study the formation and behaviour of cruds, the mechanism of hydraulic failure and the effect of design modifications.

The main source of crud formation is very likely the hydrolysis of the solvent, tributylphosphate (TBP), yielding predominantly dibutylphosphoric acid (HDBP). This acid forms readily compounds

with metals some of which are quite insoluble in the aqueous or organic phase.

In our experiments we used soluble ZrO^{++} -salts and HDBP to produce precipitates within the mixer-settler and thereby simulate the situation in the high-active-battery (HA-battery). Contrary to our expectations we did not succeed in producing enough precipitate to plug the battery inspite of the addition of increasing amounts of Zr and HDBP far beyond the calculated concentrations. The chemistry of Zr-HDBP complexes is not yet well understood although a number of publications do exist⁽¹⁻⁵⁾. Only the introduction of ZrO_2 -powder, which was partially adhering to the voluminous Zr-HDBP precipitate, finally led to a blocking of the aqueous port between settler and mixer (see fig. 1, weir 1). Flowrates and the pumping action of the impeller were too small to lift the solid particles over the aqueous weir (see fig. 1, weir 2).

Consequently a number of changes have been effected:

- increase of free area beneath weir 1 by 50%
- insertion of a bubble pipe positioned diagonally under weir 1. The air bubbles keep this area free from solid particles and apply an airlift-effect on the compartment between weirs 1 and 2.
- elongation of the suction nozzle of the impeller
- increase of the number of extraction stages by 30%
- cutting the area of the baffle in the settler by half
- adding an ultrasonic level gauge into the organic outlet stage.

Experiments proved these changes to be very beneficial with respect to the transport of solids through the battery avoiding accumulation at the critical locations.

The battery has not yet been tested under plant conditions. We expect that the hydraulic failures will not occur any more or at least only at large intervals. It is recognised, however, that any substantial accumulation of solids decreases the efficiency of a mixer-settler. Consequently losses increase and the separa-

tion factors are lowered. This is an inherent disadvantage of mixer-settlers which becomes the more serious the smaller the equipment.

In view of the limited possibilities for the improvement of mixer-settler characteristics alternative solutions were sought.

Centrifugal contactors

Two batteries of single stage centrifugal contactors (Fig. 2) of the Savannah River type have been installed in the WAK.

Although fast contactors are generally proposed for the high active part of a reprocessing plant because of their short contact time, we decided to test their performance by using the batteries for a third uranium cycle. This allows for close inspection, easy maintenance and adjustment.

The original design has been modified and the size reduced substantially (6, 7).

Motor, shaft, rotating bowl and impeller can be removed and replaced in one piece without demounting any other parts.

Some of the characteristics are:

rotor diameter	80 mm
rotor length	130 mm
holdup	0.85 liters
rotor speed	3 000 rpm
max. throughput	400 l/h (0.5% entrainment, vol. phase ratio 0.2 - 2)
max. throughput	300 l/h (0.5% entrainment, vol. phase ratio 0.1 - 5)
contact time	10 sec.

Cold runs have been performed which led to some design corrections.

Solid particles in the process solutions did not accumulate in the centrifuge but were removed continuously by the aqueous

phase. However, the extractor batteries have not yet been used with plant solutions.

The long term behaviour and reliability remain to be established. Difficulties may arise processing plant solutions which contain cruds with unfavourable physical properties.

Multi-stage centrifugal contactors of the ROBATEL-type have been examined in a pilot test facility⁽⁸⁾. Cold runs of a HA-battery with uranium showed satisfactory results using the WAK-flowsheet. Introduction of solid particles (ZrO_2) led to hydraulic failure. The deposits of precipitates could only be removed by immediate rinsing without shutdown of the contactor. We know that the simulated crud does not represent the real conditions in plant operation. Nevertheless, the reliable performance of centrifugal contactors obviously depends on a thorough feed clarification and the absence of further precipitation between filter and first extractor.

Pulse columns

In the nuclear chemical technology pulse columns are widely used for extraction purposes. Advantages such as high efficiency, reliable operation, broad range of operating conditions and the extensive experience existing today favour the choice of this type of extraction apparatus.

The replacement of the mixer-settlers in the high active region by pulse columns is also being explored by WAK.

Pilot runs have been performed with a test rig at Eurochemic. Applying the WAK-flowsheet to a 8 m HA-Column (4 m extraction section; 4 m scrub section; 10 cm diameter; 23% free area; nozzle plates with 3 mm \varnothing holes), very good results with respect to uranium extraction were obtained. The main emphasis was laid on the performance in the presence of cruds.

The same test substance (Zr-HDBP) was used to simulate the crud formation. $ZrO(NO_3)_2$ was added as solute to the feed solution.

HDBP was dissolved in the solvent. Large amounts of precipitate were formed initially and accumulated at the interface in the bottom decanter. The decanter was occupied almost completely by the voluminous precipitate.

The layer did not grow, however, into the column itself, but diminished slowly. Despite the constant feeding of Zr and HDBP the layer shrank to a thickness of about 10 cm and remained more or less constant for two days of operation (fig. 3). Deliberate pushing of the layer into the cartridge section of the column results in a rapid disintegration of the solid particles into invisible parts and probably also partial dissolution in the organic phase. Even in the rather calm zone of the decanter, enough turbulence is effected by the pulse and the air bubbles from level and density measurement to separate large particles from the bulk layer. These particles leave the decanter with the organic as well as the aqueous phase. Thus, the column has a self-cleaning effect with respect to solids. No accumulation or plugging ever occurred in the cartridges. This seems to be a major advantage over centrifugal contactors and mixer-settlers.

Discussion

People who deal with solvent extraction technology for the commercial reprocessing of nuclear fuel will have to face two problems in the immediate future:: scale-up of equipment and increased fuel burnup.

Problems associated with scale-up are

- size restrictions because of criticality risks
- impact of reliability on economy

Advanced fuels very likely will have a high initial fissile material content (^{235}U or Pu), and consequently reach a high burnup. Although little plant experience with fuel burnup above 15 000 MWd/t exists, for the extraction processes two problems seem to become increasingly important with rising burnup:

- accumulation of solids in the extractor, resulting from undissolved fission products and insoluble compounds formed after dissolution or during extraction.
- decreasing separation factors due to a growing complexity of chemical reactions and kinetic effects.

The problems cannot be overcome solely by choosing the most adequate type and design of extractor. Auxiliary processes such as feed clarification and solvent washing will have to be optimized. Chemical pretreatment or flowsheet changes may become necessary.

From our pilot tests and pilot plant experience we evaluate in table 2, very roughly, the various extractor types with respect to scale-up and the processing of advanced fuel.

Table 2

	Scale-up			Processing Advanced Fuels		
	Hold-up	Scale-up Potential	Technical Problems Involved	Contact Time	Accumulation of Solids	Sensitivity towards Flowsheet Changes
Mixer-Settlers	+	+	+++	+	+	++
Pulse Columns	++	++	+++	++	+++	++
Centrifugal extractors	+++	+++	+	+++	+	+(+)

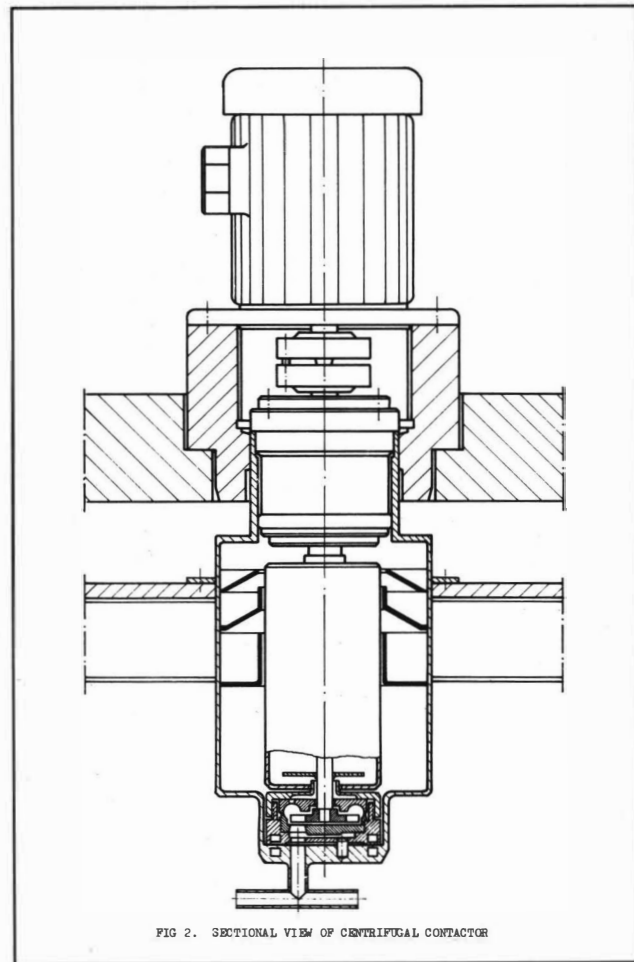
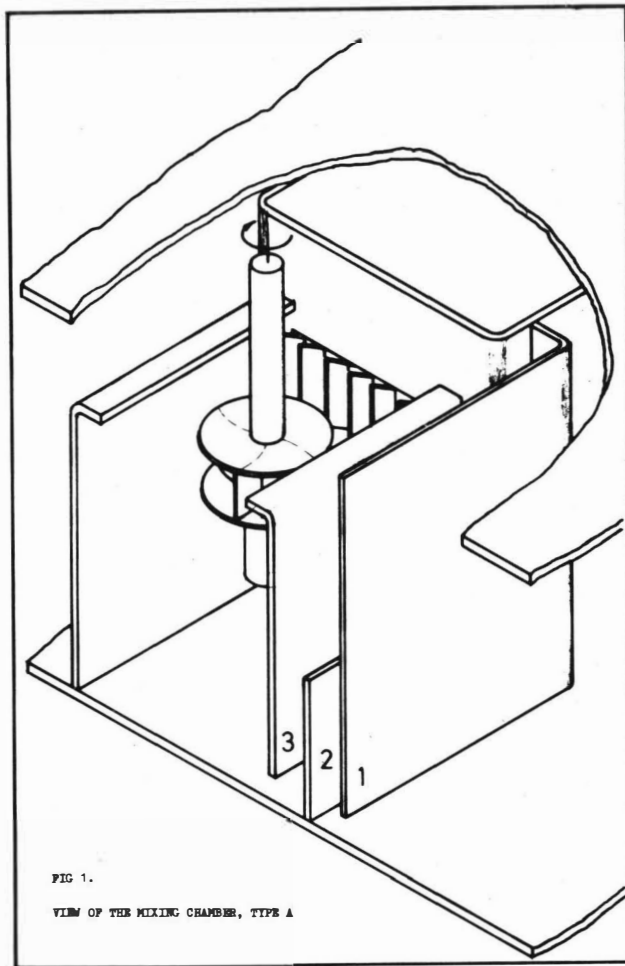
(+ means favourable in the sense of best operation)

We are aware of the fact that this judgement is not based on exact figures and does not take into account other important features like reliability, need for maintenance and replacement, ease of cleaning and startup operations, and more.

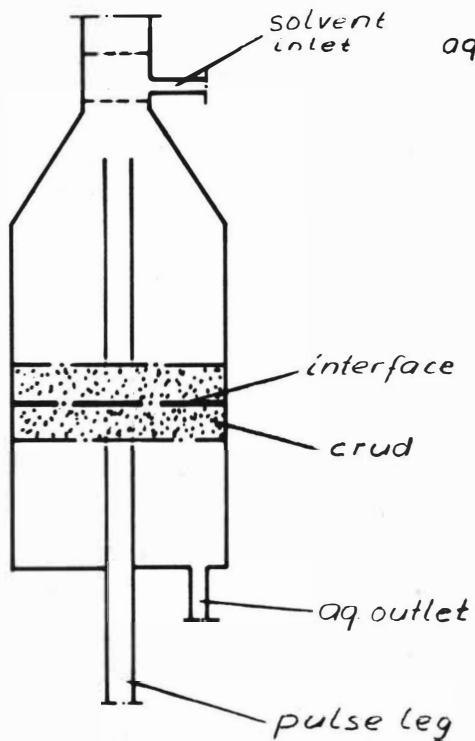
Nevertheless, we deduce from our present knowledge a preference for pulse columns as extractors in large commercial reprocessing plants.

References

- (1) Hardy, C. J., Nucl. Sci. Eng. Vol. 16, 401 - 7 (1963).
- (2) Solovkin, A. S., Krutikow, P. G., and Panteleeva, A. N. Russ. J. Inorg. Chem. Vol. 14, 1780 - 3 (1969).
- (3) "Aqueous Processing of LMFBR Fuels, Progress Report No. 3" ORNL-TM-2624, Mai 1969, pp. 23 - 28.
- (4) "LMFBR Fuel Cycle Studies, Progress Report No. 5" ORNL-TM-2671, August 1969, pp. 22 - 26.
- (5) "Chemical Technology Division, Annual Progress Report" ORNL-4572, October 1970, pp. 62 - 66.
- (6) Roth, B.F., "Zentrifugalextraktoren für die Wiederaufarbeitung von Kernbrennstoffen mit hohem Abbrand und Plutoniumgehalt" KFK-862 (1969)
- (7) Knoch, W. and Roth, B., "Fast Contactors in the WAK", IAEA-115, 1970, pp. 267 - 288.
- (8) Personal Communication by H. Goldacker, Institut für Heisse Chemie, Kernforschungszentrum Karlsruhe.



bottom-decanter
HA-column



top-decanter
1C-column

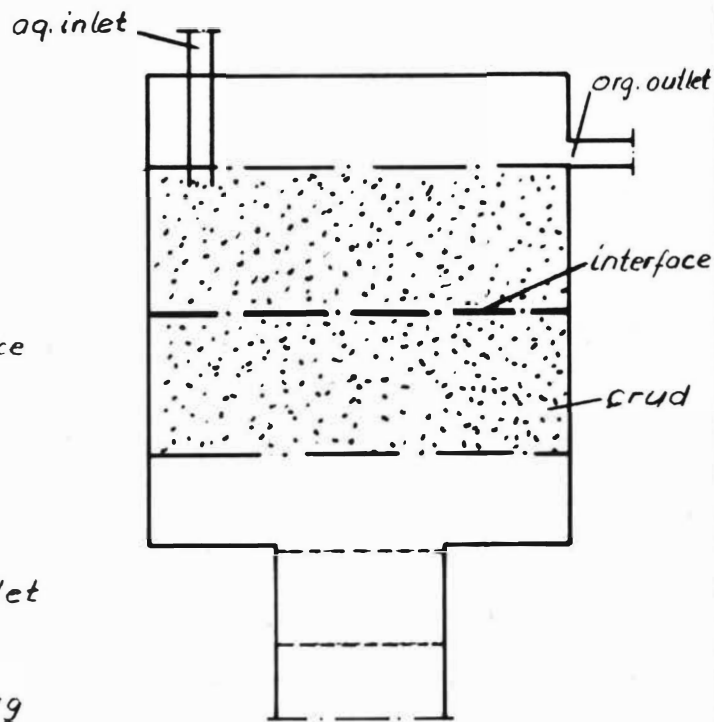


FIG. 3. ACCUMULATION OF CRUD IN THE DECANTERS OF PULSE COLUMNS

USE OF FORMIC ACID FOR THE STRIPPING OF PLUTONIUM

by

M GERMAIN^x - A BATHELLIER^x - P BERARD^{xx}

ABSTRACT

A new extraction process is proposed in which the stripping of plutonium is effected by a mixture of formic acid and nitric acid. When high concentrations of plutonium and/or high concentration factors are required, an alternative process which combines the complexing action of formic acid and the reducing properties of hydroxylamine is used.

The processes have been tested successfully on the laboratory scale in the conditions of the final purification of plutonium as well as those of the separation of uranium from plutonium.

The formic solutions of plutonium can then be boiled to destroy formic acid and increase plutonium concentration, or the plutonium may be precipitated as a solid compound.

^x Centre d'Etudes Nucléaires de Fontenay-aux-Roses

^{xx} Centre de Marcoule

Commissariat à l'Energie Atomique
B.P. No 6
92260 FONTENAY AUX ROSES
France

INTRODUCTION

The processing of irradiated fuels consists mainly of the recovery and purification of uranium, plutonium and transuranium elements (neptunium, americium,).

This separation and purification is usually carried out by co-extraction of uranium and plutonium in the second cycle of a TBP process [1] or selective plutonium extraction in a tertiary amine process [2].

- In TBP processes the following various means of stripping plutonium have been used or proposed [3, 7]:
 - using dilute nitric acid
 - reduction to PuIII (ferrous sulphate, uranous nitrate, hydroxylamine sulphate or nitrate, electrolytic reduction)
 - using complexing agents.
- With tertiary amines, stripping of plutonium is more difficult because of the very high affinity of the solvent for tetravalent plutonium. The flowsheets that have been studied [2, 8, 9, 10, 11, 12] are based on reduction and complexation (sulphuric, formic and acetic acid) processes.

In both cases, in the last cycle which has to effect the purification and concentration of plutonium, the process conditions are very rigid because:

- the concentration of plutonium in the strip liquor has to be high enough not to limit the capacity of the whole plant, and
- the reagents must not introduce impurities, since most of them remain with the concentrated plutonium.

The choice of process depends mainly on the solutions and the performance required of the last cycle of concentration and purification.

In France, it has been found necessary to seek new processes giving high concentration factors and/or highly-loaded strip liquor, to be developed in any type of contactor: mixer settler, pulsed column or centrifugal extractor.

Carboxylic acids and especially formic acid, which are known to be complexing agents for tetravalent elements [13-15], have been examined with special attention to their effects on settling ability, corrosion, chemical stability, process parameters, cost

From all these considerations, formic acid appeared suitable to be used for the stripping of plutonium.

EXPERIMENTAL

Extraction of formic acid

Partition of formic acid between the aqueous and the organic phases affects the stripping of Pu:

- (1) in determining the maximal value of the organic/aqueous flow rate, $(O/A)_{\max} = \frac{1}{D_{\text{HCOOH}}}$ (in order to keep most of HCOOH in aqueous phase);
- (2) by its extraction in the organic phase which may either displace plutonium or form mixed complexes with the solvent [16] resulting in a change of plutonium distribution coefficients.

With 30% TBP-dodecane, the extraction has been shown to be completely reversible (Fig 1) and the distribution coefficient found to decrease when formic acid molarity increases in the aqueous phase.

If the formation of a TBP - HCOOH complex is assumed, as suggested by the general trend of the curve of Fig 1, it is found that

$$D_{\text{HCOOH}} = k (\text{TBP})_f \quad (\text{Table 1})$$

$$\text{with } (\text{TBP})_f = (\text{TBP})_i - (\text{HCOOH})_s$$

where $(\text{TBP})_i$, $(\text{TBP})_f$ are initial and free TBP concentrations respectively and $(\text{HCOOH})_s$, the formic acid concentration in the organic phase. This result confirms that the organic complex is TBP - HCOOH in this range of concentration.

Concerning 20% TLA-Solgil 54B^(*), measurements have been made with tri-laurylammonium nitrate; the distribution is reversible and the results in Figure 1 show the extraction of formic acid to be less significant than in the TBP system. Consequently, for the same range of aqueous formic acid concentration, the variation of D_{HCOOH} with $(\text{HCOOH})_{\text{aq}}$ will be very limited.

PLUTONIUM DISTRIBUTION

Partition of tetravalent plutonium is determined by the relative affinity of this element for the aqueous and the organic phases. Thus, it will vary with the nature of the solvent used and the composition of the aqueous phase, particularly the relative concentrations of plutonium, formic acid and nitric acid.

In 30% TBP-dodecane, distribution coefficients appear to increase [Figs 2, 3 and 4] when

- the nitric acid concentration increases
- the aqueous plutonium concentration increases if the HCOOH concentration is high,
- the formic acid concentration decreases.

These results can be explained qualitatively by the formation of non-extractible formic-plutonium complexes, whose concentration must be an increasing function of the HCOOH/Pu and $\text{HCOOH}/\text{HNO}_3$ ratios, for any plutonium concentration. The increase of extraction coefficients with temperature indicates that the overall extraction reaction is endothermic in nature.

With 20% TLA-Solgil 54B as solvent, the results obtained are qualitatively the same as with TBP, as shown in Figs 5 and 6, while quantitatively they are somewhat different. Because of the high affinity of TLA for tetravalent plutonium nitrate, D_{Pu} will be too high to allow stripping, unless the $\text{HCOOH}/\text{HNO}_3$ ratio is high. This ratio has been calculated for TBP and TLA in the conditions of micro and macro concentration of Pu (Table 2). It appears that in a TLA process the formic acid concentration will have to be more than twice that in a TBP process, if all other conditions remain unchanged.

3.

(*) Solgil 54B is an aromatic diluent, containing more than 95% of 1:1-dimethyl ethylbenzene, supplied by the Progil Company (Pont de Claix - France)

APPLICATIONS

Let us now consider some examples where stripping of plutonium with formic acid serves as an easy and effective method in the field of fuel reprocessing.

Plutonium purification cycle in a TBP process

The object of this study was the purification of a concentrated impure Pu solution (0.15 M) to obtain a pure highly-loaded strip liquor (0.20-0.25 M).

Such conditions required rather high nitric acid concentrations (> 0.4 M) at every stage of the process to prevent plutonium hydrolysis and polymerisation [17-18].

When nitric acidity, plutonium concentration, concentration factor and temperature are fixed, the most important flowsheet parameters to be optimised are the composition and the point of introduction of the stripping solution, which is again dependent on the formic acid and plutonium concentrations allowed in the stripped solvent.

On the schematic flowsheet of the Fig 7, it is observed that three strip solutions are introduced into the stripping battery one at the last stage (R_1), another 3 stages before (R_2) and the last (R_3) in the 6th stage. The stripping streams contain varying amounts of formic acid and nitric acid:

in stages 1 to 6, HCOOH 2-4 M, permitting plutonium stripping
($\approx 98\%$)

in stages 6 to 13, HCOOH 6-8 M, permitting plutonium complexed
by HDBP to be stripped
(Pu ≤ 10 mg/l, HDBP 100 mg/l)

in stages 13 to 16, HCOOH is stripped by dilute nitric acid.

If DBP formation is very limited, formic acid is introduced with R_3 , and R_2 strip solution can be omitted. The final formic acid concentration in the stripped solvent is considerably reduced.

Plutonium purification cycle in a TLA process

The main differences between TLA and TBP flowsheets result from:

- (1) the limited loading of 20% TLA-Solgil (< 0.1 M Pu);
- (2) the higher distribution coefficient of plutonium in a nitric-formic acid mixture;
- (3) the very weak extraction of formic acid by TLA nitrate.

Figure 8 represents a typical flowsheet of plutonium purification by 20% TLA-Solgil 54B.

Selective extraction of plutonium IV is effected in the 10 stages of the mixer-settler unit. Uranium, in the stable hexavalent state, is extracted in negligible quantities.

Additional scrub stages are required for removing entrained and extracted uranium and other impurities.

Plutonium is then stripped with a formic acid-nitric acid mixture; the efficiency of the stripping is aided by a rather low acidity in the unit, and the stripping of plutonium observed at equilibrium is very satisfactory as expected [10] (Fig 9).

Plutonium losses in stripped solvent are usually less than 1 mg/l, while the uranium content of the product is less than 100 ppm.

Uranium-plutonium separation in a TBP process

Formic acid alone is not able to achieve this separation as desired i.e, with a high concentration factor, as shown in Table 3. However, the use of formic acid could be of some interest for this separation, if hydroxylamine were added to it, so that the complexing action of formic acid and the reducing properties of hydroxylamine could be used advantageously.

Moreover, their actions are complementary: the rate of reduction by hydroxylamine which has been shown to be,

$$r = \frac{k_8 (\text{PuIV})}{1 + k_9 \left[\frac{(\text{PuIII})^2}{(\text{PuIV})} \right]} \quad [19]$$

with $k_8 = \frac{[\text{NH}_3\text{OH}^+]}{[\text{H}^+]^2} (k_1 + k [\text{NH}_3\text{OH}^+])$ / $(1 + k_3 (\text{NO}_3^-))$

$$k_9 = k_{10} \frac{[\text{H}^+]^2 [\text{NO}_3^-]}{(\text{NH}_3\text{OH}^+)}$$

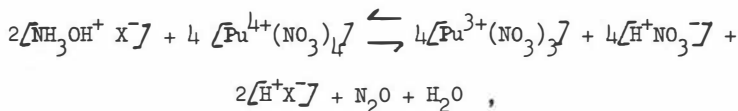
varies nearly as $[\text{H}^+]^{-4}$ and $[\text{NH}_3\text{OH}^+]^2$ and increases when

- PuIV increases
- PuIII decreases.

Therefore the reduction rate will be very slow in the last stages of the battery where PuIV concentration is very low, whereas in these conditions formic acid will be especially efficient, for the acidity is low and HCOOH/Pu is high.

The action of formic acid will increase the reduction rate in the first stages and help solvent stripping by complexing plutonium IV.

If we consider the reduction of PuIV by a hydroxylammonium salt according to the following reaction:



we observe that the number of protons liberated by this reaction is

- 4 : if HX is a weak acid
- 6 : if HX is a strong acid ,

so we have chosen hydroxylamine formate rather than nitrate in our process. The second advantage of this is the formation of formic acid which also favours stripping.

The characteristics of the flowsheet tested in the laboratory are:

uraniumVI and plutoniumIV are coextracted in a multistage extractor with 30% TBP-dodecane as solvent, and the loaded solvent is then scrubbed for removal of impurities. In the second extractor, plutonium is stripped by the combined action of hydroxylamine and formic acid, with two stripping solutions. In the first stage, formic acid and hydroxylamine are introduced, while nitric acid and hydroxylamine enter the battery in the last stage.

This permits the formic acid concentration in the solvent to be low (0.05-0.15 M). The concentration of plutonium (1-30 g/l) in the strip liquor, which has more than 90% Pu in the trivalent state, is a function of the feed solution.

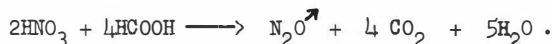
This process has been tested for the reprocessing of various fuels, with U/Pu varying from 10 to 3.

For the fuels coming from natural U, gas cooled reactors, decontamination factors have been found to be

$$\begin{aligned} DF_{Pu} &= 1.8 \times 10^4 && \text{Pu content in U} && 0.6 \text{ ppm} \\ DF_U &= 4.4 \times 10^4 && \text{U content in Pu} && 2100 \text{ ppm} . \end{aligned}$$

Chemical stability of nitric acid - formic acid mixtures

As formic acid is a reductant ($E^0 = -0.2V$), nitric acid and formic acid may react with each other in certain conditions of composition, temperature and presence of catalyst, to give gases whose composition is variable. Whereas in a highly acidic medium ($HNO_3 > 10M$), the main oxide of nitrogen formed is NO_2 , it is NO when $HNO_3 \approx 3-5 M$ and N_2O when $HNO_3 \approx 0.5 M$ [20] according to the following reaction:



The mechanism of the reaction is not well known; the observed decrease of the reaction rate in the presence of an "antinitrous compound" such as N_2H_4 , HSO_3NH_2 is not completely explained.

Measurements made at $60^\circ C$ have shown that the rate of reaction is mainly dependent on the nitric acidity. In the normal condition of a process, even if this rate is very low, it cannot be neglected, especially if storage is prolonged [Table 4]. Hydrazine has been found to be very effective in stopping the reaction, in the absence or presence of plutonium [Table 5].

Hydroxylamine nitrate, which is slightly less efficient than hydrazine, can however be used successfully to prevent the reaction.

When the strip liquor is not to be stored for a long time no protective chemical reagent is necessary to assure the stability of the solution.

PLUTONIUM STREAM

The effect of formic acid in the plutonium stream, especially towards the end of the process, has been investigated.

The acid has been found not to interfere with the precipitation of plutonium oxalate even in 3 M HCOOH. The destruction of oxalic acid in the resulting mother liquor before recycling to the extraction battery is similarly unaffected by the presence of formic acid, which is completely destroyed in the conditions of the process.

When concentrated solutions of plutonium nitrate are desired, the formic acid can be destroyed by boiling with nitric acid during the concentration of the solution.

In the range of 4-5 M nitric acid, the reaction gives mainly NO as follows



It is an autocatalytic reaction, which is rapid in an acid medium in the presence of plutonium.

The recombining of nitric oxide with water in the presence of air permits a considerable reduction in the nitric acid consumption.

In conclusion, we should like to emphasise that the main advantage of using these clean reagents, such as formic acid and hydroxylamine, is that they are easily removed, without giving rise to problems of liquid-waste storage.

Flowsheets given in this paper are only examples that show that this system is applicable in many cases, especially when the process requirements forbid the use of classical reagents.

TABLE 1

Relation between D_{HCOOH} and free TBP^{free} .

$\text{TBP}_i = 1.03 \text{ M}$

free TBP M	0.975	0.87	0.80	0.68	0.51	0.37	0.30
D_{HCOOH}	0.50	0.49	0.47	0.36	0.26	0.22	0.18
$D_{\text{HCOOH}} / (\text{TBP})_f$	1.96	1.77	1.71	1.88	1.96	1.68	1.67

$(\text{TBP})_f^{\text{free}}$ calculated assuming $(\text{TBP})_f = (\text{TBP})_i - (\text{HCOOH})_s$

TABLE 2

Determination of $R = \text{HCOOH}/\text{HNO}_3$ ratio

	TBP	TIA
$(\text{Pu})_{\text{aq}} \quad 0.1 \text{ g/l}$ $D_{\text{Pu}} = 1$	R = 3	R = 7
$(\text{Pu})_{\text{aq}} \quad 30 \text{ g/l}$ $D_{\text{Pu}} = 0.5$	R = 8	R = 20

TABLE 3

Separation factor $\alpha = D_{\text{U}VI} / D_{\text{Pu}IV}$ in nitric acid-formic acid mixture
(without reducing agent)

$U_s = 80 \text{ g/l}$

	HNO ₃ 0.5 M				HNO ₃ 1 M			
HCOOH M	0.5	1	2	5	0.5	1	2	5
$D_{\text{U}VI}$	1.06	0.96	0.98	0.99	1.32	1.24	1.27	1.23
$D_{\text{Pu}IV}$	0.34	0.32	0.31	0.28	0.55	0.44	0.41	0.33
$\frac{D_U}{D_{Pu}}$	3.1	3	3.1	3.5	2.4	2.8	3.1	3.7

TABLE 4

Decomposition of a nitric acid (0.5 M) - formic acid (1 M) mixture
at 60°C

time in hours	0	12	24	40	52
HCOOH M	1	0.88	0.90	0.78	0.73

TABLE 5

Decomposition of the strip liquor with time

Time in hours	0	0.16	4.5	48	110
(HNO ₃ +HCOOH) M	4.5	-	4.15	4.25	3.85
N ₂ H ₄ M	2 x 10 ⁻¹	4 x 10 ⁻²	-	2 x 10 ⁻²	5 x 10 ⁻⁵

- HCOOH : 3.5 M

- HNO₃ : 0.8 M

- Pu : 0.21 M

- N₂H₄ : 0.2 M

- 60°C

REFERENCES

- [1] MIQUEL P - Energie Nucléaire vol 184 p 57-78 Sept 73
- [2] BATHELLIER A et. al - Energie Nucléaire vol 10 No 3
p 145-239 - 1968
- [3] DETILLEUX E et. al - Eurochem rep. ETR 90 - 1962
- [4] RAO Cl. - Radiochemica Acta 12, 135 - 1969
- [5] SCHMIEDER F et. al - XXIVth IUPAC Congress 2-8 Sept 1973
Hambourg p 564
- [6] TALMONT X - "Solvent Ext. Chem. of Met." Ed HAC McKay
p 103-115
- [7] BRUNS L E - "Int. Solv. Ext. Conf." p 103 The Hague
April 1971
- [8] SALOMON L et. al - Rept ETR 234 - 1968
- [9] CALLERI C et. al - Rept ETR 116 - 1961
- [10] CALLERI C et. al - Rept ETR 117 - 1961
- [11] CHESNE A et. al - Nucl. Scie. Eng. 17, 557 - 1963
- [12] BROWN K B et. al - Rept ORNL CF 61-3, 141 - 1961
- [13] PORTANOVA R et. al - J. Inorg. Nucl. Chem. 34, 1685 - 1972
- [14] NEHEL D - SCHWABE K - Z Physik Chem. 224, 29 - 1963
- [15] ISOHANOVA T S et. al - Vest. Moskovh. Univ. Khim. 12, 3,
323 - 1971
- [16] KOEHLI G et. al - Int. Solv. Ext. Conf., The Hague,
Vol B - 1971
- [17] BYRNE J T et. al - Rept RFP 436 - 1964
- [18] COSTANZO D E et. al - J. Inorg. Nucl. Chem. 35, No 2
part I, II, III - 1973
- [19] BARNEY G S - Rept ARH-SA 100 - 1971
- [20] BRADLEY T V - DAVIES B L - US Rep. DP 1299 - 1972

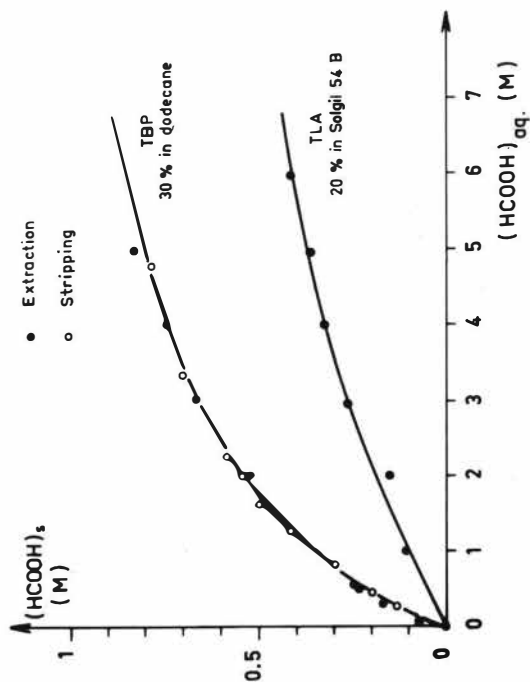


FIGURE 1. DISTRIBUTION OF FORMIC ACID IN THE TBP AND TLA SYSTEMS.

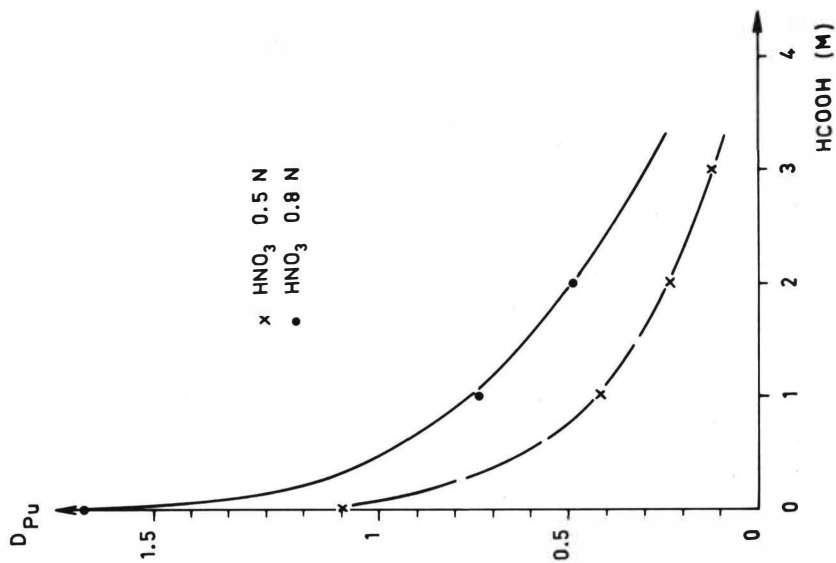


FIGURE 2. PLUTONIUM(IV) DISTRIBUTION IN THE TBP SYSTEM AS A FUNCTION OF $[\text{HCOOH}]$.

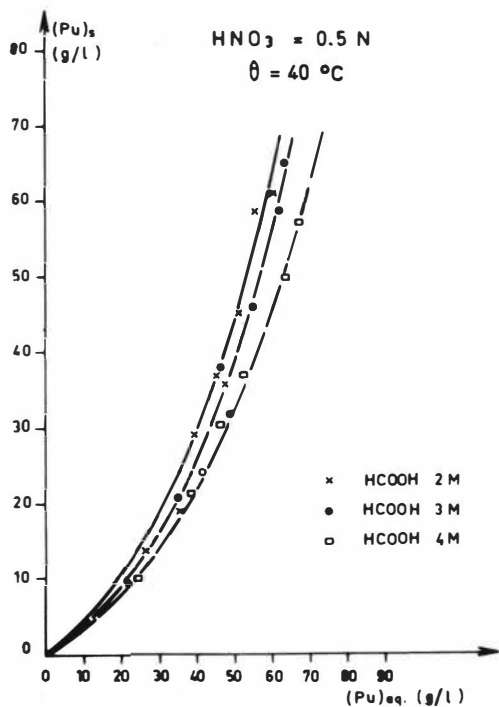


FIGURE 3. PLUTONIUM(IV) DISTRIBUTION IN THE TBP SYSTEM AS A FUNCTION OF AQUEOUS PLUTONIUM CONCENTRATION.

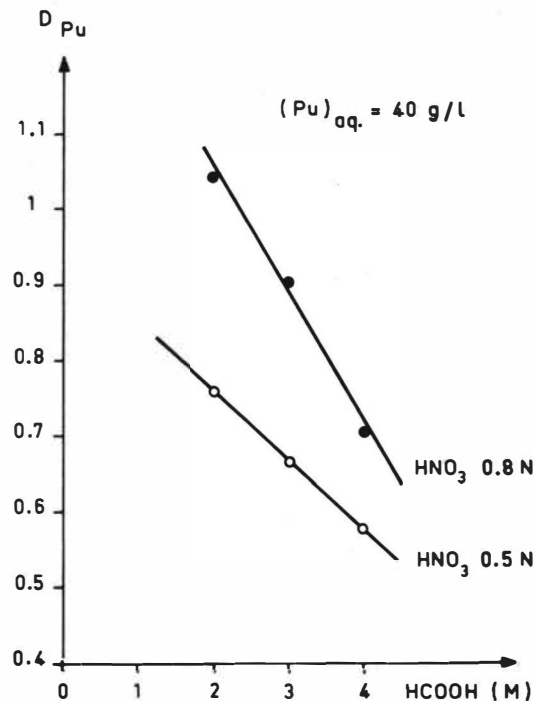


FIGURE 4. PLUTONIUM(IV) DISTRIBUTION IN THE TBP SYSTEM AS A FUNCTION OF FORMIC ACID CONCENTRATION for $(\text{Pu})_{\text{aq}} = 40 \text{ g/l}$.

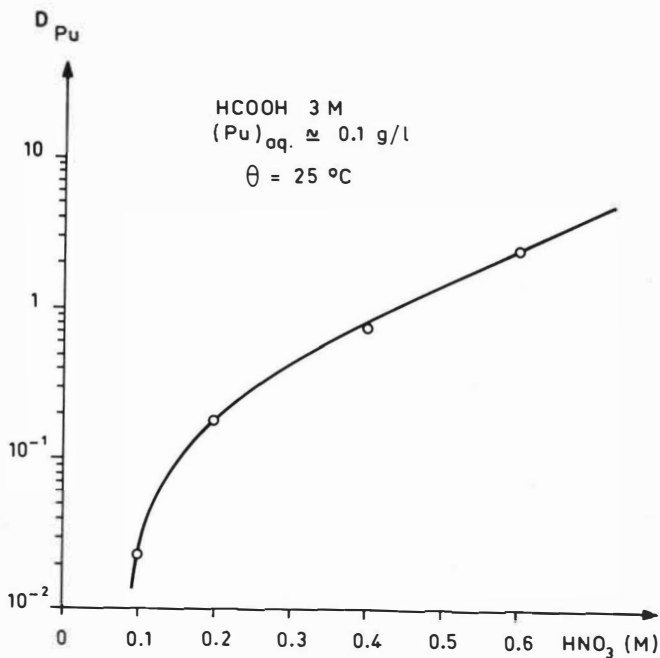


FIGURE 5. PLUTONIUM(IV) DISTRIBUTION IN THE TLA SYSTEM AS A FUNCTION OF NITRIC ACID CONCENTRATION.

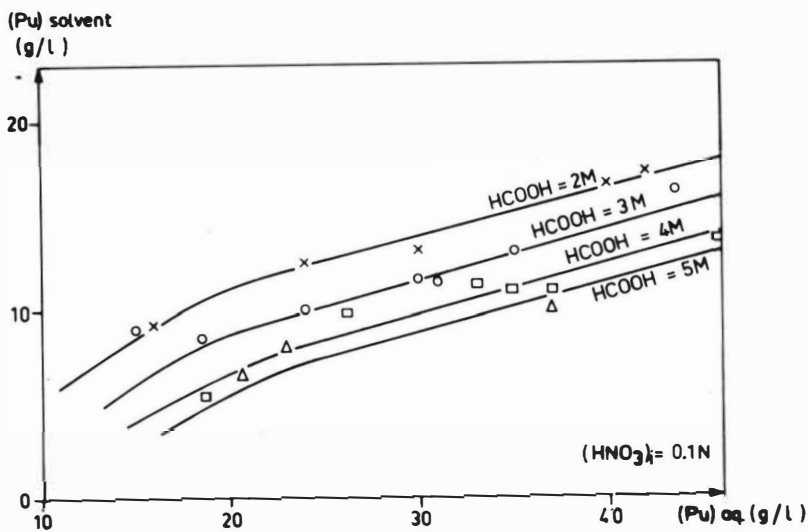


FIGURE 6. PLUTONIUM(IV) DISTRIBUTION IN THE TLA SYSTEM AS A FUNCTION OF β_2 .

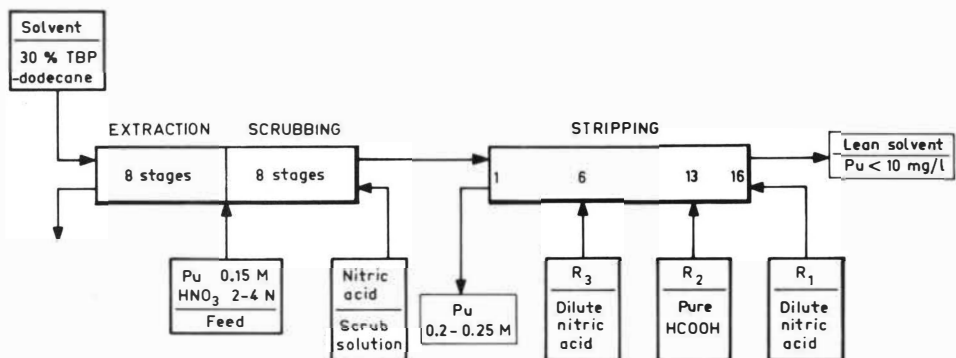


FIGURE 7. SCHEMATIC PLUTONIUM PURIFICATION CYCLE IN THE TBP PROCESS.

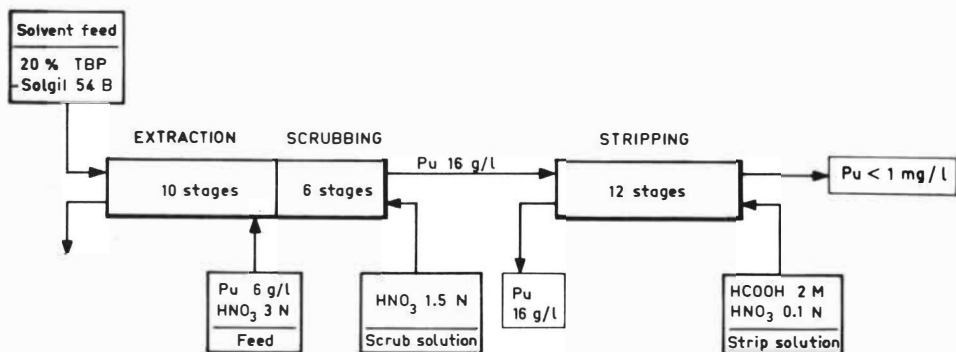


FIGURE 8. TYPICAL TIA FLOWSHEET.

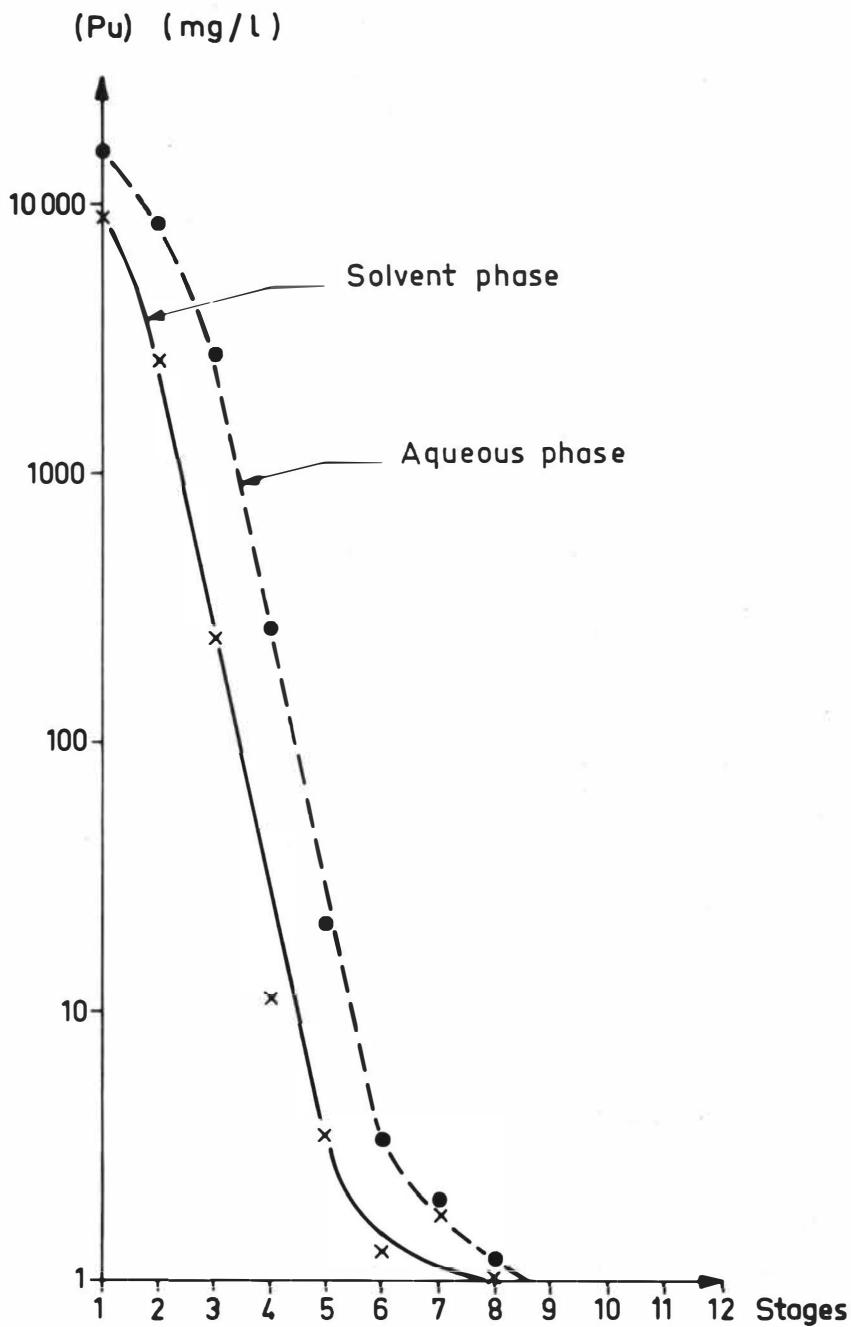


FIGURE 9. STRIPPING OF PLUTONIUM IN THE TLA FLOWSHEET.

SESSION 20

Thursday 12th September: 9.00 hrs

E X T R A C T I O N C H R O M A T O G R A P H Y

(and Analytical Applications)

Chairman:

Professor L.G. Schell

Secretaries:

Dr. M. Streat

Mr. J.C. Leroy

APPLICATION OF NEWLY DEVELOPED MATERIALS FOR EXTRACTIONCHROMATOGRAPHY OF INORGANIC SALTS IN COLUMNS

Reinhard Kroebel, Alfred Meyer, BAYER A.G. 5090 Leverkusen/Germany

Abstract:

The well-known analytical technique of extraction chromatography⁺⁾ of inorganic compounds by means of liquid extractants sorbed on a material to form a fixed bed can now be extended to technical use. This is due to newly developed resins which avoid bleeding of extractant, offer grain sizes and low flow resistance similar to usual ion exchangers and have a kinetic behaviour like droplets of extractant of the same size. As a non-exclusive example, the results of an extraction chromatographic pilot unit for the refining of uranyl nitrate are presented. The resin contains as extractant pure undiluted tri-n-butylphosphate (TBP).

1. Introduction

Extraction chromatography has hitherto only been used on laboratory scale, mainly as an analytical tool for selective or specific fast separations. Literature is extensive, to recall only a few outstanding investigators such as Cerrai, Eschrich, Ghersini, Fritz, Sickierski, Stronski, Testa, with many publications on this subject.

Latest compilations in this field have been made by Eschrich (1), Cerrai and Ghersini (2), Marki (3) which should be consulted for possible applications.

+) Extraction chromatography = reversed phase partition chromatography.

Known technology consists in taking a support material for the stationary phase = extractant. The extractant is fixed on the support by sorption, then filled into columns of a suitable size and a mobile aqueous phase is run through this filling. By means of extraction, a chromatography of salts, ions or molecules dissolved in the mobile phase is executed. Apparatus and technique are simple and resemble those for ion exchange. Due to the enormous variety of known extractants for specific or selective separation, the technique of extraction chromatography seemed promising as a simple method for solving separation problems.

Unfortunately enough, however, the admixture of support and extractant did not fulfil technical specifications such as e.g. low flow resistance, low loss of extractant, no interference with extraction by lack of sorptive power of the support, cheapness and reproducibility, fast extraction kinetics, minor tailing when eluted etc.

The new absorbents (4) called Levextrel[®] (from Leverkusener-Extract-Elution) meet all specifications listed above and can be used technically like conventional ion exchange resins, that is, by combining their well-known simple technology with the selectivity of liquid extractants. Using them as chromatographic columns, any separation problem can be solved by offering sufficient theoretical plates obtainable by simple elongation of the column length. The theoretical background for these techniques is given by Cerrai and Ghersini (2), and Markl (3).

Further literature which deals specifically with the example presented in this paper can be found in numerous Eurochemic technical reports from Eschrich et al. (1, 5, 6, 7, 8)

2. Experiment

2.1 Materials used:

2.1.1 Absorbent:

The chromatographic absorbent (Levextrel[®]) used for the pilot installation of three 70 l columns was a technical resin with the following main characteristics:

- inert matrix : polystyrene-divinylbenzene
- extractant : pure technical TBP (Bayer)
- tap density dry : 630 g/l
- grain size : 0.3-1.2 mm (beads)
- fabrication lot : the first technical 300 l batch of Oct. 71

- weight percent of TBP (dry) : 60-61
- specific weight of Levextrel[®] : 1.03 - 1.035g/cm³
- volume of Levextrel[®] : 61-62 % of bed volume
- volume of stationary phase (TBP) : 370-380 ml/l bed volume
- interstitial volume^{†)} : 38-39 % of bed volume

2.1.2 Column characteristics:

- number : 3
- volume : 70 l
- height : 2000 mm
- diameter : 210 mm
- approx. theoretical plate-height for uranyl-nitrate : 20-30 mm
- material : PVC transparent

†) the interstitial volume is equal to the volume of the mobile phase or the so-called free column volume.

2.1.3 Reagents

- feed : uranyl nitrate + varying contaminants in
1-4 M HNO_3 (40 - 300 g U/l)
- scrub : technical grade 1-7 M HNO_3
- strip : demineralized water (hot or cold)

2.2 Experimental procedure

2.2.1 Running characteristics :

- velocity of mobile phase : 1-3 bed volumes/hour
- operating temperature
 - extraction : room temp.
 - scrub : room temp.
 - strip : 20 - 40°C
- pressure drop : 20 - 60 cm w.g.
- time for one cycle : 75 min. - 180 min.
- direction of feed : upward
- direction of other flows : downward
- regeneration : superfluous, not executed

2.2.2 Typical Extract-Elution

The first column is fed upward with acid uranyl nitrate solution, which may hold 1.2 M uranyl nitrate and 1-3 M nitric acid for optimum conditions.

The column is fed until uranium breakthrough occurs at the top of the first column. The feed velocity for the above-described Levextrel ^(R) may be as high as three bed volumes (BV) per hour ^{+) ,} one or two BV/h being preferable. The scrub solution of 1-7 M nitric acid ⁺⁺⁾ flows downward and feeds the second column in upward direction with the interstitial uranyl nitrate solution of the first column. The quantity

^{+))} under these conditions the feed operation takes only 8 minutes.

⁺⁺⁾ 3 M nitric acid being preferred.

of scrub solution and its acidity is chosen according to the required ultimate purity. The interstitial volume of scrub acid is displaced into the second column by the first 0.4 BV strip water. The elution proceeds via hot or cold demineralized water into receiving vessels.

Hot water of 60°C strips the contents of the first column with 99.9% recovery within 1.5 BV and the exit temperature rises from room temperature to 37° - 41° C. It is convenient to cut the tails after 1.0 - 1.2 BV. They can either remain on the column which is then ready for new feed, or can be used to displace the interstitial scrub acid from the second to a third column.

The elution = (strip) solution in this case contains about equal molarity of uranyl nitrate (0.36 - 0.40 M) and free nitric acid.

Higher elution temperatures of 60 - 80°C can be used and in this way 0.45 - 0.5 M uranyl nitrate can be obtained.

Contaminants which can be eliminated by this purification step are all kinds of acids, metal-ions or non ionic impurities except gold. Typical solutions are those of ore refineries or uranium mills and uranyl solutions originating from the nuclear fuel cycle. To give one example, ore refining solutions, which require separation of contaminants by a DF of 50-100-use scrub volumes of only 0.25 - 0.5 BV nitric acid + 0.4 BV demineralized water, with the exception of some readily extractable metals such as zirconium or thorium. Their DF only reaches factors of 10 - 20 with the same scrub.

A quick survey of interfering inorganic salts can be derived from data given by Mark (3) and more extensively by Tomitaro Ishimori and Eiko Nakamura (9).

A flowsheet for an extract-elution is given as Fig. 1. Fig. 2 represents a typical elution curve for the technical column. The elution reagent is demineralized water entering at the top of the column with 60°C. The determining temperature however is that at the bottom of the column which rises from room temp. to about 37°C after 1 BV.

2.3 Distribution behaviour of uranyl nitrate between Levestrel[®] and aqueous solutions

2.3.1 Influence of nitric acid on distribution

The influence of nitric acid on distribution of uranyl nitrate between aqueous phases and undiluted TBP was extensively investigated by Eschrich et al. (5, 6, 7). As the type of Levestrel[®] used for the experiments described in this paper holds undiluted TBP as extracting reagent, Eschrich's data can be taken as basis for predictions. For the quoted example of uranium refining by extract-elution, Table 1 and Fig. 3 show the experimental values for the Levestrel[®] described, calculated as uranium per litre of TBP for 3 M HNO₃ and 0 M HNO₃(H₂O). This calculation method was chosen to give more conventional figures for experts in the field of liquid-liquid extraction insofar as no special rules for extraction chromatography or extract-elution techniques are yet in existence.

Table 1 (values of Fig.3)

3 M HNO ₃ 22°C			0 M HNO ₃ 24°C		
U aq. g/l	U org. g/l	D o/a	U aq. g/l	U org. g/l	D o/a
0.5	38	76	3.0	2.1	0.70
2.0	108	54	6.1	4.1	0.67
7.0	232	33	14.0	25.2	1.80
23.5	342	14.6	22.3	43.3	1.95
31.7	377	11.8	38.8	140	3.61
60.5	408	6.8	67.4	225	3.35
85.3	416	4.9	92.3	274	2.97
107.	418	3.9	112.5	318	2.55
162	420	2.6	137	330	2.41

435 g U/l TBP is the theoretical limit for the complex UO₂(NO₃)₂.2 TBP, therefore 420 g U/l means .96 % saturation.

2.3.2 Relationship between grain size and velocity of mobile phase during extract-elution.

Fig.4 shows experimental values of possible elution velocities for a given elution curve versus grain size. It can be concluded, that technical resins with a mean grain size distribution of approx. 0,8 mm can be used up to 3 BV/h.

The technical experiments showed indeed that optimum concentrations of uranyl nitrate of 1.2 M could be handled up to 3 BV per hour before a decrease of 20 % in capacity is observed during feeding.

3. Long-term behaviour of technical columns

3.1. Loss of solvent

The tested Levextrels[®] with TBP as extractant show a lower value of TBP solubility than pure TBP for water as well as for nitric acid or uranyl nitrate solutions. The solubility of pure TBP in demineralized water is 0.38 g/l, its solubility from solutions of 40 % TBP in industrially produced dodecane is 0.27 g/l (10). The first technical batch of TBP-Levextrel as used for the experiments described above loses only 0.2 g/l of water, whereas batches expressly produced for low solubility vary from undetectable (0.02 g/l) to 0.1 g/l, without losing their good extract-elution behaviour. The technical columns were checked for TBP-loss after use of 225 kg purified uranium per 70 l column.

The decrease in capacity amounts to less than 5 %.

The mean value for all solutions was 0.163 g/l TBP loss (from solubility and degradation together), which accounts for 4.9 kg of TBP per metric ton of purified uranium.

3.2. Build-up of degradation products

The only degradation product in uranium refining operations is dibutyl-phosphoric acid (HDBP). It is easily washed off by water or slightly caustic solutions. If no special care is taken, its amount reaches an equilibrium value of 100 ± 20 ppm due to steady leaching by the elution operation.

3.3. Radiation stability

Experiments on radiation stability showed no significant (<30 %) decrease in extraction capacity up to a radiation dose of 1×10^8 rad (Irradiated in a reactor pond by spent fuel elements). The dibutylphosphoric acid formed amounted to 3 % w/w and could be washed off by water. This radiation dose will not even be accumulated in reprocessing within the usual life-span of Levextrel.[®]

4. Discussion of the technical use of Levextrel[®]

Levextrel[®] should fulfil the hopes of many investigators that extraction chromatography can become the missing link between the simple ion exchange technique and the versatility of liquid-liquid extraction with its expensive technology. Many other extractants, often in pure or only slightly diluted form compared to the liquid-liquid technology, which is sensitive to density changes, third phase formation and foaming, can be made available as Levextrels[®]. Special attention should be drawn to the possibility of obtaining an indefinite number of theoretical plates by simple elongation of the bed, the scrub sequence variety, and the possibility of displacement chromatography as it is executed in the foregoing example, where contaminants with lower distribution coefficients than uranium are pushed back into the aqueous phase and can be scrubbed off.

Literature

1. H. Eschrich und W. Drent
Extraction chromatography-bibliography
Eurochemic Technical Report ETR-271 (June 1971)
2. E. Cerrai, G. Ghersini
Reversed phase partition chromatography in inorganic chemistry
Advances in chromatography - Vol.9 P.3-189
Marcel Dekker New-York 1970
3. Peter Markl
Extraktion und Extraktionschromatographie in der anorganischen Analytik
Methoden der Analyse in der Chemie Band 13
Akad. Verlaganstalt Frankfurt/Main 1972
4. R. Kroebel, A. Meyer
Verfahren zur Darstellung von Adsorbentien
DT 2162951 (18. Dec. 71)
5. H. Eschrich, P. Hansen, P. H. Heylen
Simultaneous distribution of nitric acid and uranyl nitrate between aqueous and undiluted tributyl phosphate phases
Eurochemic Technical Report
ETR-231 (Dec. 1968)
6. H. Eschrich
The distribution of U-IV and U-VI between tributyl phosphate and nitric acid and their separation by extraction chromatography
Eurochemic Technical Report
ETR-249 (May 1969)

7. H. Eschrich, F. Kenis, E. Schmid
The distribution of uranium (VI) at low concentrations
between undiluted tributyl phosphate and aqueous nitric acid
phases
Eurochemic Technical Report
ETR-247 (January 1969)

8. H. Eschrich, I. Hundere
Separation of impurities from plutonium by extraction
chromatography
Eurochemic Technical Report
ETR-222 (March 1968)

9. Tomitaro Ishimori, Eiko Nakamura
Data of inorganic solvent extraction
Japan Atomic Energy Research Institute
JAERI 1047 (1963)

10. P. Leroy
Etude du solvant TBP-dodecane
Rapport CEA-R 3207 (1967)
(data taken from Fig.7 of this report)

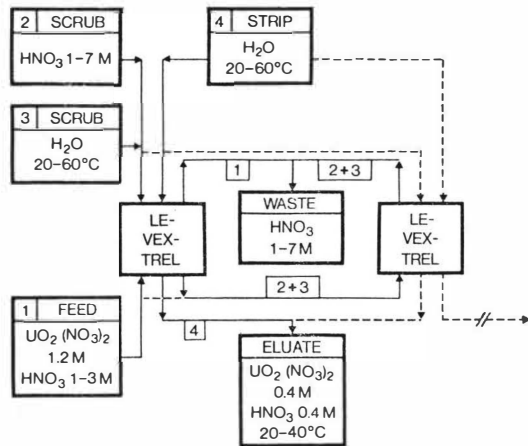


Fig.1 Flowsheet for Extract-Elution
 Numbers indicate sequence of flows or flow directions.
 Full lines indicate flows for the first column, dotted
 lines flows for following columns.

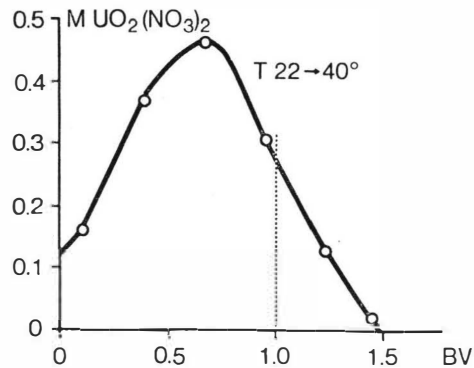


Fig.2 Typical elution curve of a technical Levextrel[®] column
 for 60°C water entering at the top of a 22°C column.
 Dotted line indicates preferred cut of strip operation.
 The eluate of the first bed volume (BV) contains 90-95 g U/l

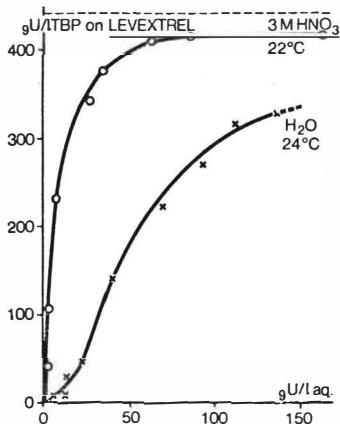


Fig.3 Equilibrium lines for the system Levextrel^(R)/uranyl nitrate/nitric acid (water) at room temperature. Values see Table 1.

- Equilibrium line for 3 M nitric acid expressed as uranium weight in 1 l TBP versus uranium weight in 1 l aqueous phase (Extraction equilibrium)
- ×—× Equilibrium line for aqueous uranyl nitrate without free nitric acid. (Elution equilibrium)
- Dotted line at 435 g U/l TBP indicates theoretical max. value for UO₂(NO₃)₂ · 2 TBP

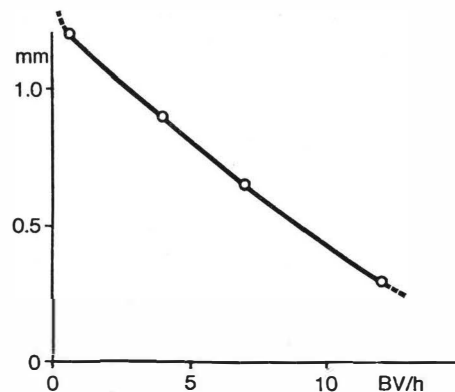


Fig.4 Influence of bead diameter on elution (strip) flow velocity. Identical conditions for different sieve fractions of one production lot. Criterion is an identical elution curve for different flow velocities.

THE SELECTIVE EXTRACTION OF HALIDE TRACES

M. Benmalek, H. Chermette, C. Martlet, D. Sandino and J. Tousset

ATSTRACT Quantitative and selective extraction of halides is possible with some IV and Vb organoelements, mainly with alkyl or aryl-antimony and silicon derivatives. Halide extraction using phenyl derivatives of elements IV and Vb is reviewed and some stability constants values are given. Many of these products may extract fluoride from aqueous solutions at pH values from 2 up to 7 with a nearly quantitative ratio. The triphenylantimony derivatives more soluble in organic solvents, remain the more appropriate extractant. The separation technique allows not only the removal of interferences but also a concentration of halides.

Institute de physique Nucleaire, Universite Claude Bernard Lyon-I (Institut National de Physique Nucleaire et de Physique des Particules), 43 bd du 11 Novembre 1918, 69621 Villeurbanne, France

The determination of halides is a topical problem. Indeed, these elements play an essential role in pollution, even at very low concentrations. This determination often needs a preliminary separation in order to avoid various interferences or inconvenient complexing. Moreover, the separation of these elements (fluoride ions being excepted) is difficult, due to their nearly identical physicochemical behaviour.

In this field, most techniques already known (precipitation column exchange, distillation, pyrohydrolysis ...) ¹ are not suitable for applications in the traces range, due to their lack of selectivity. Besides, many cations in the solutions may be complexed by halides, which lessen the sensitivity of these methods.

In defined conditions, solvent extraction seems to be the technique best adapted to this kind of problem, because it is an easy, fast and quantitative method. Moreover, a good selectivity can be obtained ², provided one chooses a well defined pH range for each halide.

Unfortunately, there are only a few halide extractants operating on the chloride, bromide, iodide and more particularly fluoride ions. Besides the latter has the disadvantage of complexing a great number of cations (like aluminium, thorium or zirconium) which are often found in the studied media. At average concentrations, halides can be extracted by basic compounds ³ like long chains amines or tributylphosphate. But in this case the selectivity is low and many cations are co-extracted which forbids the use of such an extractant for traces separation.

In acidic media, fluoride can be separated with the tetraphenylstibonium ion ^{4,5} or the diphenyldichlorosilane ⁶. A systematic and comparative study of halide extraction possibilities by means of organometallic compounds has been reviewed.

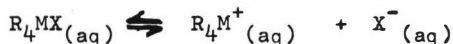
We present here the main results obtained. We show that for fluoride, the best results are achieved with the diphenyldichlorosilane ⁷ or the triphenylantimony dihalides ⁸. A quantitative extraction of chloride in acidic media can be performed only by means of the triphenylantimony system ⁹.

EXPERIMENTAL

All the reagents used are commercial products. The use of antimony-124 allows a radiochemical labelling of the organoantimony species. Fluorine-18 and chlorine-34 radioelements follow the physicochemical behaviour of these halides ⁵⁻¹⁰. Extractions are performed by agitating the aqueous and organic phases in polypropylene separatory funnels, mechanically shaken. Except for silicon derivatives which need shaking approximately 30 minutes, the extraction kinetics are fast and equilibrium is obtained after 10 minutes shaking. Water and all materials used in this study had the required purity for a traces study.

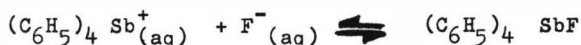
EXTRACTION CONDITIONS

Halide solvent extraction is effected in practice through ion pair formation. According to the ionic character of the complex created, the solubility in aqueous media will be either great or small. For instance the tetra-substituted elements VB have good solubility, and the equilibrium can be schematically written:

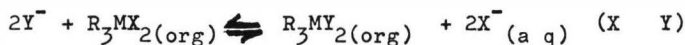


with $X = F, Cl, Br, I, OH$ and $M = N, P, As, Sb, Bi$.

A typical case is given by fluoride extraction by means of tetra-phenylstibonium⁵:



For trisubstituted derivatives of elements VB with an oxidation degree of 5, the extraction equilibrium is written as follows:

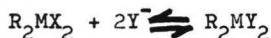


X or $Y =$ Halide or hydroxide for fluoride extraction, $X = Cl$ and $Y = F$ or Cl . R represents an alkylic or arylic group.

To prevent the liberation of the Z^- halide in aqueous media, it is possible to oxidize the R_3M derivative directly by means of hydrogen peroxide. However, this technique could result in formation of hydroxide ions which are competitive with halides towards extraction, but this can be avoided by the use of an acidic medium.



Some derivatives of group IVb elements (mainly the silicon) also enable a halide extraction, but in this case, the hydrolysis becomes preponderant.



In the case of silicon, the reaction mechanism does not consist in an ion exchange, but rather in a nucleophilic substitution¹¹⁻⁷.

These equilibria show that the pH values of the solutions will be an important parameter. From an analytical separation may be obtained.

Table 1 shows the main results obtained with organometallic compounds of elements IV and Vb¹².

DISCUSSION OF THE EXTRACTION CURVES

a) Salts of tetraphenylstibonium

Although, in this case, colloidal effects limit the analytical applications, fluoride can be extracted by means of tetraphenylstibonium ions in two distinct ranges of pH values, each of them corresponding to a particular mechanism.

At a low pH, the first maximum of the curve of extraction ratio as a function of pH can be easily explained as a simple effect of competition between the tetraphenylstibonium fluoride and the HF and HF₂⁻ species (at low pH) or the tetraphenylstibonium hydroxide⁵.

The pH value corresponding to the extraction maximum enables evaluation of the extraction constant of the tetraphenylstibonium hydroxide ($K' = 10^{10}$). (Figure 1).

The second maximum depends mainly on the other ions of the solution, and has been interpreted as a colloidal formation, the micelles of which are made of tetraphenylstibonium hydroxide or fluoride.

Then we have a competition between the two following equilibria:



As the stability constant value of tetraphenylstibonium fluoride is not very high, we were led to study other extractants.

b) Other organometallic derivatives R_mMX^{n+}

In all the studied cases, the extraction curves can be interpreted with a simple mechanism of competition. At low pH value, a competition between fluoride extraction and fluoride hydrogen formation (HF and HF_2^-) could explain the decrease of the extraction rate, but the observed decrease is smaller than the theoretical one.

Sometimes, in acidic media, an instability of the solutions (tricyclohexyl or trioctylantimony dichloride) affects the reproductibility. Then in a pH range which depends only on the extracting agent concentration, a quasi-quantitative extraction is observed. Therefore the hydroxide competition occurs at pH values all the higher as the extracting agent concentration is increased. (Figure 2)

The pH value corresponding to the decrease of the extraction yield, added to a knowledge of the hydrolysis curves of these compounds, enables computation of the stability constants and extraction constants of these species ¹³.

Halide extraction constants X_2 are defined by the following formula :

$$X_2 = \frac{(L_{X_2})}{(L^{2+})(X^-)^2}$$

with $X = F, Cl, Br, I, OH$

and $L = R_2M$ if M is an element of group IVb (Si, Sn)

$L = R_3M$ if M is an element of group Vb (Sb, Bi)

Table II shows the data obtained for some organoelements, mainly organoantimony compounds which are less sensitive to hydrolysis than silicon compounds. One can see also that the organoantimony compounds have a similar behaviour towards halide extraction. Therefore derivatives will be chosen according to the facility for obtaining them, to their stability and to the influence of interfacing ions. For this last point, three mechanisms are generally involved:

The complexing of halide to be extracted. Some metallic ions are strongly complexed by halides (Al, Th, Zr, U). Nevertheless an effective masking of these ions (for example with cyclohexanediaminetetra-acetic acid) can generally be made⁸⁻¹⁴.

The direct action on the extracting agent. Some compounds (e.g. sulfide, permanganate, hydrogen peroxide) may inhibit the extraction by oxidation, reduction or polymerisation of the extracting compounds.

The competitive effect. This is the most important one, mainly for chloride extraction. High concentration levels of ions like nitrate, phosphate or halides reduce the extraction yield of the studied ion. Some results are shown on Fig.3.

In neutral media, triphenylantimony appears to be the most selective compound and also the most convenient for fluoride trace separation but diphenylsilane is still one of the best extractants for a separation of fluoride, either at heavy concentrations, or in very acidic medium.

A systematic study of such a derivative and its possibilities and also of the extraction conditions, enables the prediction that traces of fluoride can be quantitatively separated, even from a complex medium containing ions like Al or Zr.

The chloride separation remains a more difficult problem because of :

- the small pH range allowing a quantitative extraction,
 - the competition of the other halides like bromide and iodide.
- (Note that a preliminary extraction with hydrogen peroxide alone can avoid such an interference).
- in the pH range used, no chelating agents of ions complexed by chloride (mercury, cadmium, ...) are known.

RESULTS

Fluoride concentrations as small as 10^{-8} N have been reached this way, after concentrating up to 10^{-6} N, which is the usual limit of sensibility of the fluoride specific electrode.

CONCLUSION

This method, although one of the best for fluoride determination, still shows a lack of selectivity for chloride determination when other halides are more preponderant in the solution.

The separation of the different halides could be improved by the use of a specific resin of anion exchange¹⁷ which could be obtained by fixation of organoantimony group on a skeleton of chloromethyl-polystyrene.

Traces of fluoride have been quantitatively separated from a strongly complexing medium, and determined by means of a specific electrode¹⁶.

As an example, we give in table III the schematic procedure for the determination of traces of fluorine in an aluminium matrix¹⁴.

Solvent extraction increases the sensibility of the potentiometric determination because it enables the concentration of the ion to be determined, and removes the interfering ions.

BIBLIOGRAPHY

1. G. Charlot, Les methodes de la Chimie analytique, Masson et Cie Paris (1966) p. 747.
2. H. Chermette, C. Martelet, D. Sandino, J. Tousset, Anal. Chem. 44 (1972) 857.
3. D.G. Tuck, R.M. Diamond, J. Phys. Chem. 65 (1961) 193
4. C. Martelet, These, Univ. of Lyon (1970)
5. D. Aulagnier, H. Chermette, C. Martelet, J. Tousset, Bull. Soc. Chim. France 1135 (1971)

6. R. Bock, H.J. Semmler, Z. Anal. Chem. 230 (1967) 161
7. M. Benmalek, These, Univ. of Lyon (1972)
8. H. Chermette, These, Univ. of Lyon (1971)
9. H. Chermette, C. Martelet, D. Sandino, J. Tousset
C.R.A.S. 273 (1971) C543
10. C. Martelet, These Doctorat, Univ. Lyon (1973)
11. L.H. Sommer, J. Am. Chem. Soc. 89 (1967) 57
12. H. Chermette, These Doctorat, Univ. Lyon (1973)
13. H. Chermette, C. Martlet, D. Sandino, J. Tousset,
M. Benmalek, J. inorg. Nucl. Chem. (to be published)
14. M. Benmalek, H. Chermette, C. Martelet, D. Sandino,
J. Tousset, Communication to the Intern. Conf. "Sur les
tendances modernes de l'analyse par activation",
Paris (1972).
15. D. Sandino, These, Univ. of Lyon (1971)
16. H. Chermette, C. Martelet, D. Sandino, M. Benmalek,
J. Tousset, Anal. Chim. Acta 59 (1972) 373
17. D. Sandino, These Doctorat, Univ. of Lyon (to be published)

Extracted compound	Kinetic F = fast S = slow	pH range for F ⁻ extraction	pH range for Cl ⁻ extraction
R ₃ N ⁺ { octyl lauryl			0 - 3*
(C ₆ H ₅) ₃ SbX ₂	F	1 - 7	0 - 3
(o-CH ₃ -C ₆ H ₄) ₃ SbX ₂	F	1 - 6	0 - 2
(p-CH ₃ -C ₆ H ₄) ₃ SbX ₂	F	1 - 7	0 - 2
(α C ₁₀ H ₇) ₃ SbX ₂	F	1 - 6	0 - 2
(β C ₁₀ H ₇) ₃ SbX ₂	F	1 - 5	0 - 2
[o-(CH ₃) ₂ -C ₆ H ₃] ₃ SbX ₂	F	2 - 5	0 - 1
[m-(CH ₃) ₂ -C ₆ H ₃] ₃ SbX ₂	F	1 - 7	
(C ₂ H ₅ -C ₆ H ₄) ₃ SbX ₂	F	1 - 4	0 - 05
(p-(COOH)-C ₆ H ₄) ₃ SbX ₂	F	1 - 5	
(NO ₂ -C ₆ H ₄) ₃ SbX ₂	F	1 - 4	
[(CH ₃) ₃ -C ₆ H ₂] ₃ SbX ₂	F	1 - 5	
(C ₂ H ₃ -C ₆ H ₄) ₃ SbX ₂	F	1 - 7	
(o-CH ₃ -O-C ₆ H ₄) ₃ SbX ₂	F	2 - 6*, 3 - 5**	
(C ₈ H ₁₇ -C ₆ H ₄) ₃ SbX ₂	F	5 - 7	
(C ₆ H ₁₁) SbX ₂	S	5 - 7	
(C ₆ H ₅) ₄ SbX	F	75% 3 - 4* 95% 5 - 7	
(C ₆ H ₅) ₃ BiX ₂	F	4 - 7	0 - 6*
(C ₆ H ₅) ₂ SiX ₂	S	0 - 2	
(C ₂ H ₅) ₃ SiX	S	0 - 1	
(C ₆ H ₅) ₂ GeX ₂	S		
(C ₆ H ₅) ₂ SnX ₂	S	3 - 4	

* : Extracting agent concentration 10⁻³ M

** " " " " 10⁻⁴ M

for all others 10⁻² M

Table 1

Organometallic	Halide α			$\lg \beta(\text{OH})_2$
	F	Cl	OH	$\lg \beta_{X_2}$
$(\text{C}_6\text{H}_5)_3\text{SbX}_2$	7 ± 1	2.5 ± 1.0	19.5 ± 1.0	12.5 ± 0.5
$(p\text{-CH}_3\text{-C}_6\text{H}_4)_3\text{SbX}_2$	7 ± 1	1.5 ± 1.0	19.5 ± 1.0	12.5 ± 0.5
$(o\text{-CH}_3\text{-C}_6\text{H}_4)_3\text{SbX}_2$	7 ± 1	1.5 ± 1.0	19.5 ± 1.0	12.5 ± 0.5
$(o\text{-CH}_3\text{-O-C}_6\text{H}_4)_3\text{SbX}_2$	7 ± 1		19.5 ± 1.5	12.5 ± 1.0
$[\text{m}-(\text{CH}_3)_2\text{-C}_6\text{H}_3]_3\text{SbX}_2$	7.0 ± 1.5		19.5 ± 1.5	12.5 ± 1.5
$(\alpha\text{-C}_{10}\text{H}_7)_3\text{SbX}_2$	6.7 ± 1.0	0.5 ± 1.0	19.5 ± 1.0	12.8 ± 0.5
$[(\text{CH}_3)_3\text{C}_6\text{H}_2]_3\text{SbX}_2$				13.0 ± 1.5
$(\text{C}_2\text{H}_3\text{-C}_6\text{H}_4)_3\text{SbX}_2$				13.0 ± 1.0
$(p\text{-COOH-C}_6\text{H}_4)_3\text{SbX}_2$				13.5 ± 1.5
$(\beta\text{-C}_{10}\text{H}_7)_3\text{SbX}_2$	7.0 ± 1.5	2.5 ± 1.5	20.5 ± 1.5	13.5 ± 1.5
$(\text{NO}_2\text{-C}_6\text{H}_4)_3\text{SbX}_2$				13.5 ± 1.5
$[o\text{-(CH}_3)_2\text{-C}_6\text{H}_3]_3\text{SbX}_2$	7.0 ± 1.5	2.0 ± 1.5	20.5 ± 1.5	13.5 ± 1.5
$(o\text{-C}_2\text{H}_5\text{-C}_6\text{H}_4)_3\text{SbX}_2$				14.5 ± 2.0
$(\text{C}_8\text{H}_{17})_3\text{SbX}_2$				$12.0 - 13.5$
$(\text{C}_6\text{H}_{11})_3\text{SbX}_2$				c.a 12.5
$(\text{C}_6\text{H}_5)_3\text{BiX}_2$				12.0 ± 0.5
$(\text{C}_6\text{H}_5)_3\text{SiX}_2$	16.0 ± 1.5	6.5 ± 2.0	33 ± 1	17.0 ± 0.8
$(\text{C}_6\text{H}_5)_2\text{SnX}_2$				14.2 ± 1.0

Table 2 - Extraction constants ($\lg \beta_{X_2}$).

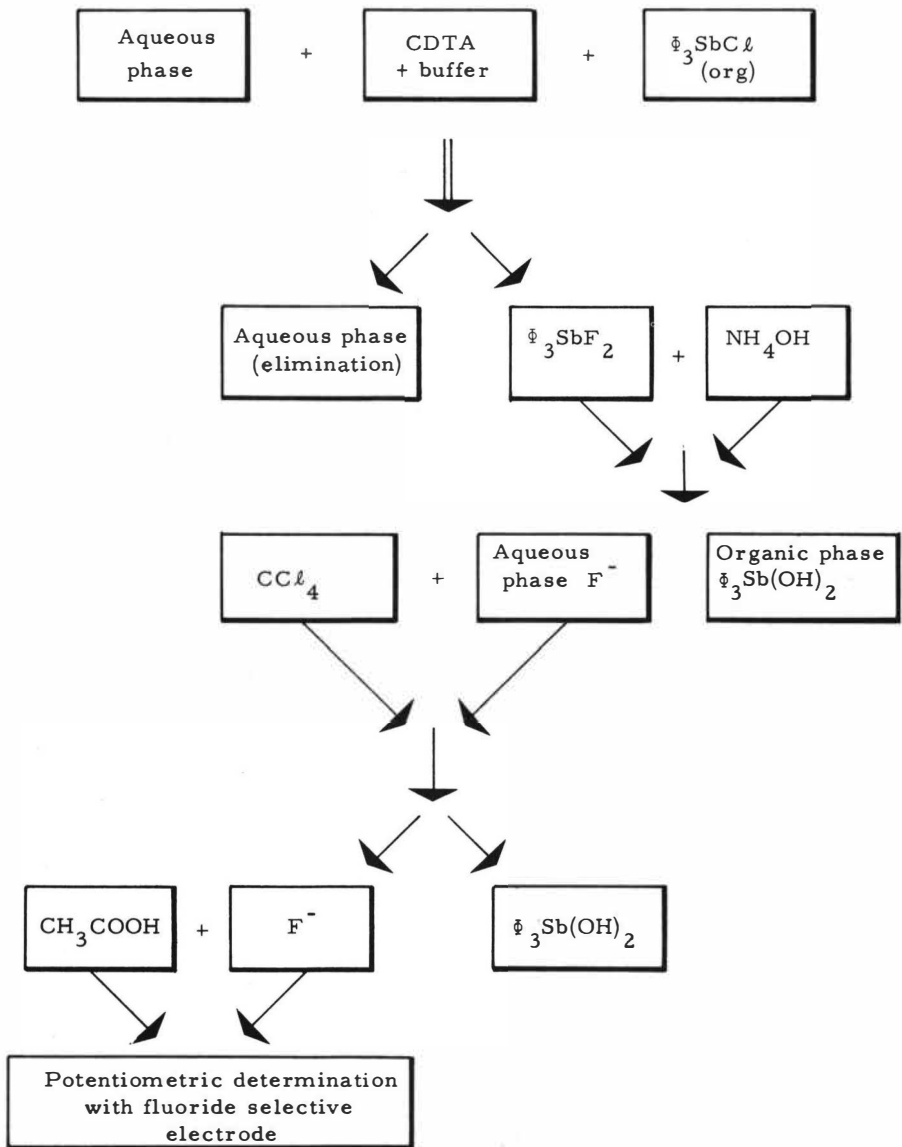


Table 3

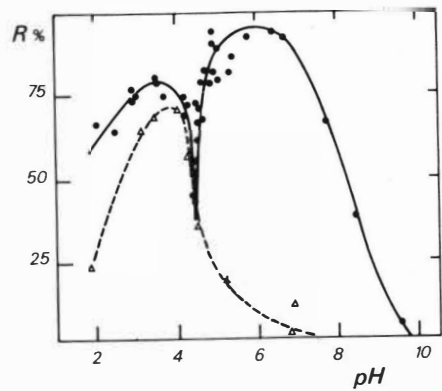


Figure 1 F^- extraction by means of tetraphenylstibonium in $CHCl_3$
 [extracting agent] ● $10^{-3} M$ ($[F^-] = 10^{-4} N$)
 [extracting agent] Δ $2.10^{-6} M$ ($[F^-] = 10^{-7} N$)

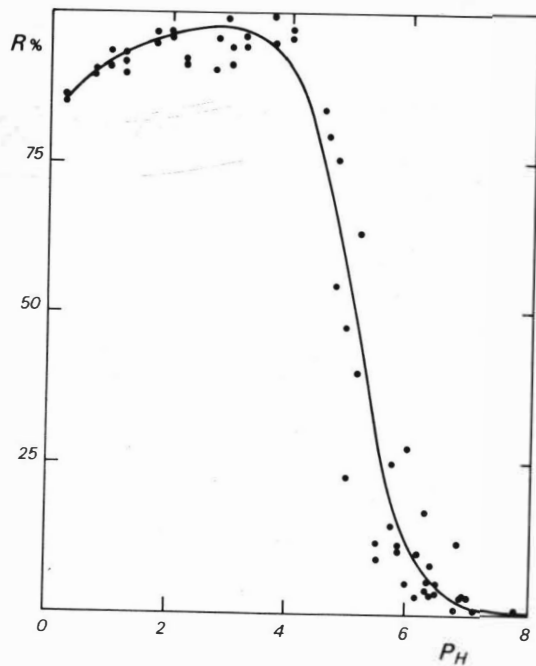


Figure 2 F^- ($10^{-5} N$) extraction with triphenylantimony dichloride ($10^{-4} M$) in CCl_4 .

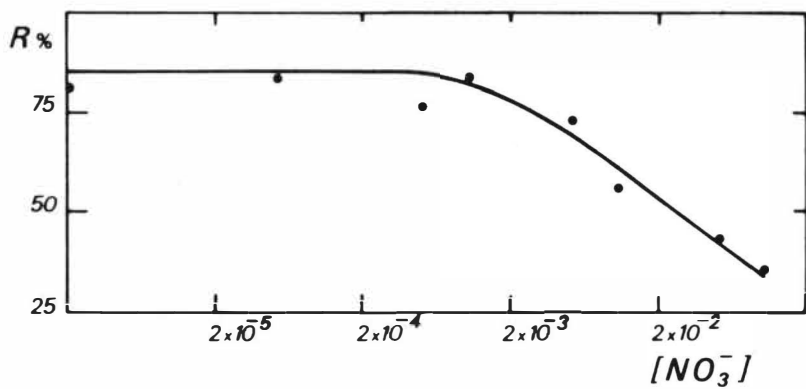


Figure 3 NO_3^- influence on chloride extraction with triphenylantimony diiodide ($10^{-3}M$) in CCl_4 at $pH = 1 - 1.5$.

COMBINED SOLVENT EXTRACTION-LIQUID SCINTILLATION METHODS FOR RADIOASSAY
OF ALPHA EMITTERS*

W. J. McDowell and C. F. Coleman

Chemical Technology Division
Oak Ridge National Laboratory
Oak Ridge, Tennessee 37830

Abstract

Alpha emitting nuclides frequently can be separated from one another and from interfering ions by solvent extraction procedures. If the last step of such a scheme automatically incorporates the nuclide of interest in a liquid scintillator (containing an extractant), a simple procedure for radioassay of the nuclide results. It is shown that correct choices of scintillators and detector systems produce further advantages.

Quenching is minimized and held constant, so that the pulse height obtained from a given alpha energy is reproducible, and the energy resolution is improved over that obtainable with conventional liquid scintillation methods, so that alpha peak widths are decreased from around 1 MeV to 0.2 or 0.3 MeV at half maximum. Compatibility of several extractants with scintillator solutions is described. Procedures are described for separation and analysis of several nuclides, e.g., plutonium, uranium, and trivalent actinides, including a specific application to the assay of plutonium in environmental samples.

*Research sponsored by the U. S. Atomic Energy Commission under contract with the Union Carbide Corporation.

INTRODUCTION

That there are certain advantages to be gained by introducing radio-nuclides into liquid scintillators by means of solvent extraction reagents was recognized some years ago by Ihle¹ and by Horrocks.^{2,3} Others quickly recognized the convenience and the control over quenching to be gained by these procedures.⁴⁻⁹ However, the idea of designing a solvent extraction separation procedure in which the last separation step is extraction into a scintillator containing an extractant, i.e., an extractive scintillator, has evolved only recently^{4,10} and is not yet widely used or appreciated. In addition to the advantage of simplicity, this procedure achieves nearly complete constancy of the scintillating medium. Aqueous solutions and all agents for incorporating them into the scintillator (solubilizing, dispersing, gelling agents) are avoided, eliminating their large and variable quenching effects, and even the addition of increments of organic solvent is avoided. In the limit, nothing is added to the standardized scintillator except the trace nuclide. Consequently, the pulse height and the corresponding peak position due to a given alpha energy can be made constant. Further, with the assurance that the scintillator composition will remain constant, it is possible to develop and use a scintillator solution with very high pulse height response and optimum energy resolution. These features along with the use of appropriate phototube-detector and electronics equipment allow the collection of alpha liquid scintillation spectra containing both number and energy information, and having energy resolution of 0.2 to 0.3 MeV full peak width at half maximum (FWHM). Figure 1 shows a spectrum of ²³²Th and

daughters that illustrates the results presently possible. Although the possibility and usefulness of such spectra were recognized very early by Ihle¹ and Horrocks,^{2,3} little use has so far been made of them. This is partly because of lack of recognition of their availability, partly because of lack of suitable commercial detector equipment, and partly because of insufficient familiarity with appropriate solvent extraction separation procedures. The present paper describes such procedures, suitable extractive liquid scintillators for the last separation step, and suitable detector equipment.

EXPERIMENTAL

Apparatus and Instrumentation

Although commercial liquid scintillation detectors designed for beta counting can be used for alpha counting, the energy resolution is poor (usually ~ 1 MeV FWHM) and background is relatively high ($\sim 4-5$ cpm under an alpha peak). Thus, such detectors cannot fully realize the advantages obtainable by combining liquid scintillation with solvent extraction. A very simple, single phototube detector with a reflector-sample holder of high reflectivity is used in all of our work in which spectra are collected. A low-noise preamplifier and a linear amplifier feed the signal to a multichannel analyzer. (The detector construction and accompanying electronics are described in Refs. 4, 10, and 11.) Background from phototube noise is not a problem, since the alpha pulse is much larger than any noise pulse.

Reagents

Extractants incorporated in the scintillator to make extractive scintillator solutions need to be purified as much as possible to minimize quenching effects. All the extractants used were obtained from commercial sources. Di-n-decylamine (DDAS) was purified by crystallization of the bisulfate from benzene solution. Tri-n-octylamine (TDA), 1-nonyl-decylamine (LNDA), and tri-n-butyl phosphate (TBP) were purified by one-stage, high vacuum distillation. The di(2-ethylhexyl) phosphoric acid (HDEHP) contained about 1% neutral impurities as received, probably 2-ethylhexanol and other alcohols. This was decreased to < 0.5% (with no detectable amount, < 0.1%, of any dibasic acid) by scrubbing a 0.5M solution in toluene with water three to four times, conversion to the sodium salt, scrubbing with saturated sodium sulfate solution three times, and reconversion to the acid form.

The naphthalene used in the scintillator solution was resublimed in our laboratory. The scintillator used in most of this work was PBBO [2-(4'-biphenyl)-6-phenylbenzoxazole]; it was chosen from a large number of commercially available scintillators as providing the best pulse height and resolution.¹¹ It was used in all cases at 4g/l in a toluene solution containing 200g/l of naphthalene. In some earlier work⁴, a scintillator consisting of extractant plus 7g of PPO (2,5-diphenyloxazole) and 0.5g of Me₂POPOP [1,4-bis-2-(4methyl-5-phenyl-oxazolyl)benzene] per liter was used; however, energy resolution was not as good with these solutions. All the scintillators were obtained from commercial sources and were used without further purification.

All other chemicals were the usual reagent grade.

RESULTS AND DISCUSSION

We first used the combined solvent extraction-liquid scintillation alpha counting method in response to a direct analytical need connected with studies of aqueous complexes of the trivalent actinides.^{4,12,13} The further usefulness of the method was obvious, and various applications to solve research analytical problems were made in our own and other laboratories at ORNL. Separation of the nuclide of interest from unwanted material and incorporation into a scintillator was usually easy with the solvent extraction separations already familiar to us.¹⁴⁻¹⁶ In cases where the only radionuclide present was the alpha emitter under study, samples were sometimes counted in a commercial beta liquid scintillation detector if extra counting capacity was needed or for convenience. When resolution or identification of energies was necessary the single-phototube high resolution detector was used.

HDEHP has been most frequently the extractant of choice for an extractive scintillator. It extracts a wide variety of metal ions by cation exchange (without concomitant extraction of anions or ligands), often with good selectivity, and it has very little quenching effect (Fig. 2). We have used some pyrophosphoric acids successfully, and presumably many other phosphoric and phosphonic acids can be used. We have also used several amine salts successfully, e.g., for uranium, thorium, and trivalent actinides as sulfates, and presumably many other amines will be similarly acceptable. Sulfate as counter ion to the

amines causes only mild quenching (Fig. 2), and chloride somewhat more but still tolerable. However, nitrate causes severe quenching.

TBP caused even less quenching than HDEHP, but its usefulness is limited by its usual need for high nitrate salting and the fact that it extracts nitrate both with the metal values and directly. TOPO (trioctyl phosphine oxide) also extracts anions, but it is less dependent on salting and might be the extractant of choice in some situations. TOPO forms synergistic extractant mixtures with HDEHP, and we have used this mixture in a few applications. TOPO also forms synergistic mixtures with thenoyltrifluoroacetone that might work well in some applications.

Procedures combining solvent extraction and liquid scintillation counting can be considered in two categories: (1) for aqueous samples that contain few impurities and can be extracted directly into an extractive scintillator, and (2) for aqueous or organic samples that require one or more preliminary steps prior to extraction into the scintillator. The following examples show two of each type.

(1) In studies of the leachability of $^{238-239}\text{Pu}$ and ^{244}Cm from (synthetic) waste solutions fixed in concrete, 100 ml samples of leachate were extracted with 15 ml of extractive scintillator (161g HDEHP, 200g naphthalene, 4g PBBO per liter in toluene), from which 10 ml portions were pipetted for counting. Analytical recovery from these solutions was shown to be quantitative.¹⁸

(2) In studies of the sulfate, thiocyanate, and chloride^{12,13,19} complexes of the trivalent actinides, analysis of the aqueous phases by directly incorporating the highly salted aqueous phase in a dioxane-based scintillator was not feasible. In contrast, extraction from these

aqueous phases into an extractive scintillator (2.9g INDA sulfate, 7g PPO, 0.5g Me₂POPOP per liter in toluene) allowed quantitative counting with little quenching.⁴ A commercial beta liquid scintillation counter was used in some of these measurements. In these, the extraction was carried out in the 20-ml counting vial and the barren aqueous phase was not removed; it did not interfere with the determination. In other measurements, where the alpha spectra were to be obtained, the aqueous sample was extracted with 1.2 ml of the extractive scintillator and 1.0 ml of that was transferred to a 10 x 75 mm culture tube for counting in the high resolution detector. Figure 3 shows a direct comparison between the energy resolution obtainable in the high resolution detector and a commercial beta liquid scintillation detector. The nuclides ²³²Th (4.00 MeV) and ²³⁹Pu (5.15 MeV) were used for this comparison, and the high-efficiency PBBO scintillator with naphthalene was used in both detectors. The energy spectrum from the commercial liquid scintillation detector is even more smeared if the usual dioxane-based scintillator is used in it.

(3) A procedure has been developed for measuring extremely low plutonium levels in environmental samples.¹¹ The plutonium is extracted by a tertiary amine from nitrate-salted aqueous solution, then stripped into a perchloric acid solution. The excess perchloric acid is evaporated in the presence of a small amount of lithium perchlorate, and finally the plutonium is extracted in the PBBO-naphthalene HDEHP extractive scintillator for measurement of the alpha spectrum. When determination of uranium is also desired, a slight

modification of this procedure permits its coextraction and simultaneous counting, with good resolution from the plutonium in the combined alpha spectrum. Related procedures have been used for determination of alpha emitters in physiological samples and other very low-level samples.¹⁰

The use of lithium perchlorate to allow removal of the perchloric acid in the evaporation without danger of baking trace elements onto the glassware has been found an important step. Recovery of added plutonium and/or uranium from waste water samples and synthetic soil samples has been found to be quantitative, with an accuracy governed primarily by the counting statistics. Reproducibility of the complete sampling plus separation and counting for a large waste water sample (7 duplicate samples) gave a standard deviation that was 17% of the mean.

Phosphates and fluorides interfere with recovery of plutonium from soil, but not at the levels they are usually found in soil. Figure 4 shows a 15-hour count of the plutonium separated from a liter of waste water. The net count rate due to Pu is 2.5 cpm. The background under the peak is 1.0 cpm. The background under such a peak can be reduced to about 0.3 cpm if the sample tube is quartz rather than pyrex. Backgrounds can be reduced much further, to about 0.01 cpm, by electronic pulse shape discrimination, which rejects beta- and gamma-produced pulses on the basis of pulse duration.²¹

(4) One of the most interesting procedures using these techniques is currently being designed and developed to date ancient pottery by the decay of uranium and thorium, i.e., by correlation of the measured thermoluminescence of the pottery with the amount of alpha activity

present. Two 1.2 to 1.5g samples of pottery are pulverized (~ 200 mesh) and dissolved in $\text{HNO}_3 + \text{HF}$, each for the determination of two alpha emitters. One sample is taken to dryness and dissolved in 0.5M HCl . Polonium is extracted from this with a scintillator containing primary or secondary amine chloride. The aqueous raffinate from this extraction is converted to sulfate by evaporation with sulfuric acid and adjusted to 0.2N acid and 2.0N total sulfate. A scintillator containing a tertiary amine sulfate is used to extract uranium from this solution. The second sample is adjusted to 8M HCl and extracted with 0.3M tertiary amine chloride to remove iron, polonium, and uranium. The raffinate is fumed with 2-3 ml of concentrated HClO_4 , 2-3 ml concentrated HNO_3 , and 0.1g LiCl and evaporated to fused LiClO_4 , then dissolved in 5 ml of 0.5M HCl . Thorium is extracted with a scintillator containing 0.2M HDEHP. The raffinate from this extraction is evaporated to fused LiClO_4 again. This is dissolved in water, and radium is extracted with a scintillator containing 0.16M HDEHP-- 0.04M NaDEHP. The solvent extraction-liquid scintillation procedures are expected to provide a great deal more accuracy than has been obtainable by previous methods of counting the crushed pottery and correcting for self absorption.

In summary, the techniques of combined solvent extraction-liquid scintillation described above, although still relatively new, show great promise in simplifying and improving many alpha counting problems.

REFERENCES

1. H. R. Ihle, M. Karayannis, and A. P. Murrenhoff, "Liquid Scintillation Counting of Alpha Emitters," pp. 483-503 in Proceedings of a Symposium on Radioisotope Sample Measurement Techniques, IAEA, Vienna, 1965.
2. D. L. Horrocks, Rev. Sci. Instr. **35**, 334-40 (1964).
3. D. L. Horrocks, Int. J. Appl. Radiation Isotopes **17**, 441 (1966).
4. W. J. McDowell, pp. 937-50 in Organic Scintillators and Liquid Scintillation Counting, ed. by D. L. Horrocks and L. T. Peng, Academic Press, New York, 1971.
5. T. K. Kim and M. B. MacInnis, Ibid., pp. 925-35.
6. J. P. Ghysels, Ind. At. Spatiales **26**, 33-6 (1972).
7. R. F. Keough and G. J. Powers, Anal. Chem. **42**, 419 (1970).
8. L. B. Gorbushina, L. Ya. Zhiltsova, E. N. Matveeva, N. A. Surganova, V. G. Tenyaev, and V. G. Tyminsky, J. Rad. Chem. **10**, 165-72 (1972).
9. Donald C. Bogen and George A. Welford, "Applications of Liquid Scintillation Spectrometry for Total Beta and Alpha Assay," presented at International Symposium on Rapid Methods for Measuring Radioactivity in the Environment, Nuremberg, Germany (5-9 July 1971).
10. W. J. McDowell and L. C. Henley, "An Evaluation of the Possibility of Identifying Alpha Emitters in Low-Count-Rate Samples Using Some New Liquid Scintillation Counting Techniques," USAEC Report ORNL-TM-3676 (March 1972).
11. W. J. McDowell, D. T. Farrar, and M. R. Billings, "Plutonium Analysis in Environmental Samples: A Combined Solvent Extraction-Liquid Scintillation Method," manuscript in preparation.
12. W. J. McDowell and C. F. Coleman, J. Inorg. Nucl. Chem. **34**, 2831-2850 (1972).
13. H. D. Harmon, J. R. Peterson, W. J. McDowell, and C. F. Coleman, Ibid., pp. 1381-1397.
14. F. G. Seeley and D. J. Crouse, J. Chem. Eng. Data **11**, 424 (1966).
15. F. G. Seeley and D. J. Crouse, Ibid., **16**, 393 (1971).

16. C. F. Coleman, C. A. Blake, Jr., and K. B. Brown, *Talanta* 9, 297-323 (1962).
17. W. J. McDowell and C. F. Coleman, *Analytical Letters* 6, 795-799 (1973).
18. J. G. Moore, Oak Ridge National Laboratory, private communication, August 1973.
19. H. D. Harmon, J. R. Peterson, and W. J. McDowell, *Inorg. Nucl. Chem. Letters* 8, 57-63 (1972).
20. R. E. Biggers, J. T. Bell, E. C. Long, and D. W. Russ, "Mathematical Resolution of Complex Overlapping Spectra with Nonlinear Least Squares Techniques," USAEC Report ORNL-3834 (October 1971).
21. J. H. Thorngate, W. J. McDowell, and D. Christian, "An Application of Pulse Shape Discrimination to Liquid Scintillation Alpha Spectroscopy," submitted to *Health Physics*.

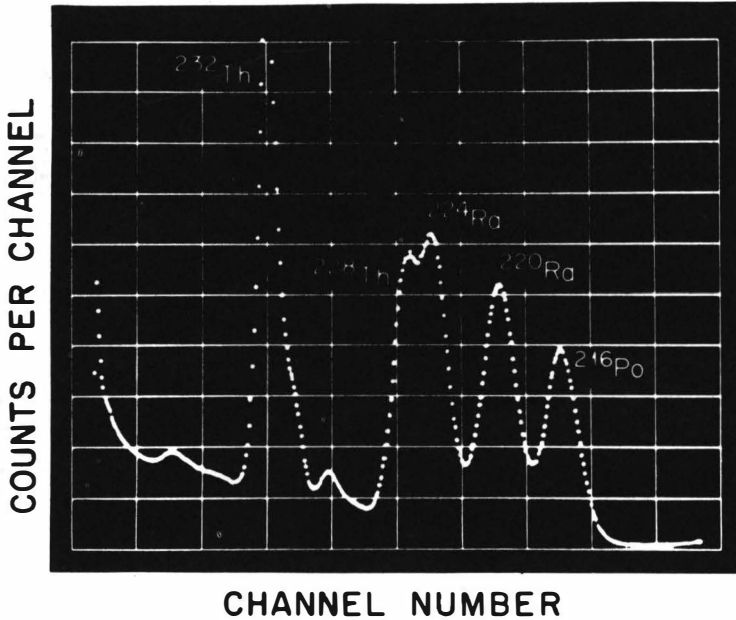


Figure 1. Spectrum of ^{232}Th and Daughters. PBBO [2-(4'-biphenyl)-6-phenylbenzoxazole] scintillator 4g/l plus 200 g/l naphthalene in toluene. The relationship between alpha energy and channel number is linear, e.g., 14.7 keV/channel in this spectrum.

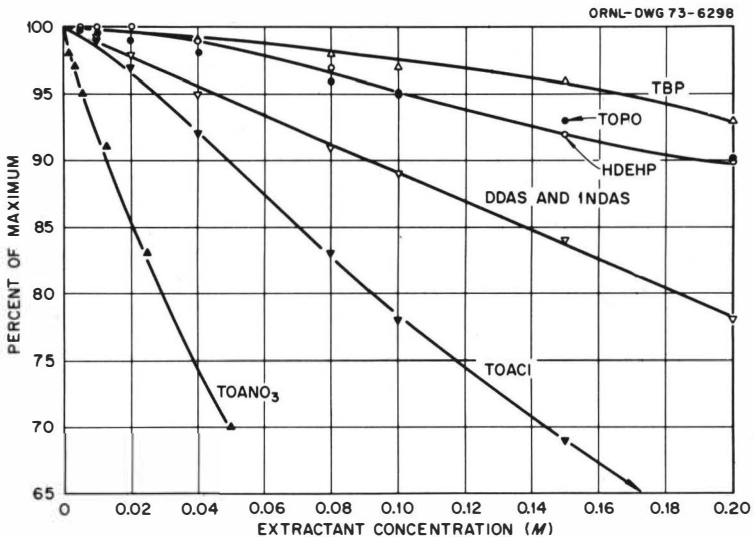


Figure 2. Percent Quenching of PBBO Scintillator, 4g/l plus 200 g/l Naphthalene in Toluene, by Several Extractants as a Function of Their Concentrations. Reprinted from Ref. 17, p. 797, by courtesy of Marcel Dekker, Inc.

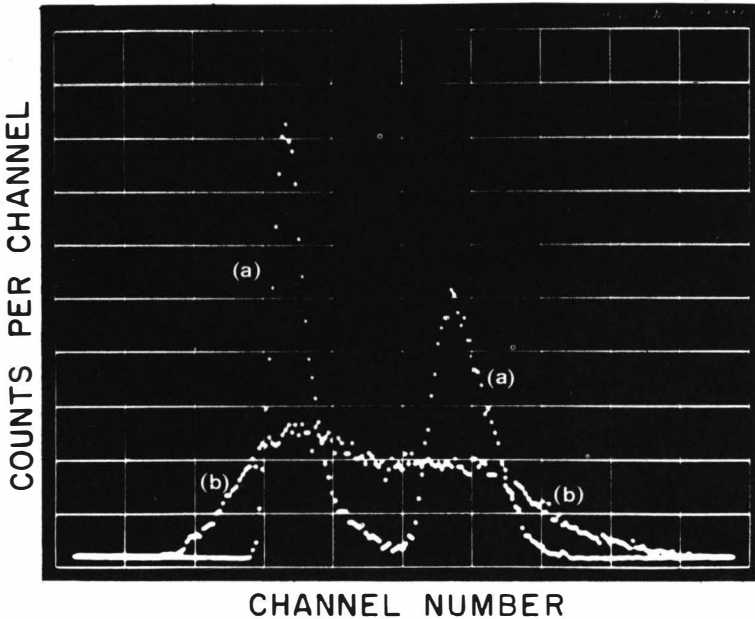


Figure 3. Direct Comparison of Spectra Obtained with PBBO Scintillator Using (a) High Resolution Detector and (b) Commercial Beta Liquid Scintillation Detector. The energy scale is the same in the two spectra.

ORNL DWG 73-8596

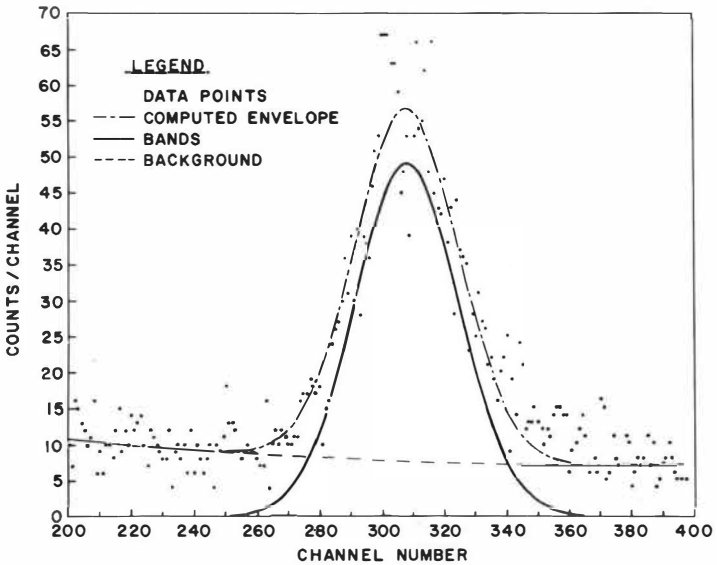


Figure 4. Example of a Spectrum from a Low Count-Rate Sample; Plutonium Separated from 1l of Waste Water, 15 hr Count, 2.4 cpm Pu, 1.0 cpm Background. The curve has been fitted and the background subtracted by a computer program (Ref. 20), a procedure most useful for spectra with overlapping bands.

DI-2-ETHYLHEXYLDITHIOPHOSPHORIC ACID
APPLICATION TO RARE AND NON-FERROUS METAL ANALYTICAL
CHEMISTRY AND HYDROMETALLURGY; CHEMISTRY OF EXTRACTION
AND EXCHANGE INTERPHASE INTERACTION OF METALS OF THE
COPPER, ZINC, GALLIUM, GERMANIUM, ARSENIC SUB-GROUPS.

I.S. Levin, V.V. Sergeeva, T.F. Rodina, V.A. Tarasova,
Yu.M. Yukhin, V.I. Varentsova, I.A. Vorsina, N.A. Balakireva,
I.A. Bykhovskaya, L.A. Novosel'tseva, L.I. Tischenko,
O.M. Frid, B.I. Kogan and G.A. Marinkina.

Application of D2EHDTPA to analytical chemistry and hydrometallurgy. Analytical studies involved elaboration of the methods for separation and determination of Tl(1), Sn(11), Au, As(111); technological studies were concerned with the purification methods of In from As and Sb; wash sulphuric acid and nickel electrolytes - from arsenic. Extraction chemistry of a series of metals and the exchange interaction have been studied. Extraction constants have been determined.

Institute for Mineral Treatment, Derzhavina 18,
Novosibirsk, USSR.

It was shown earlier that diethyl- and diphenyldithiophosphoric acids soluble in water are effective reagents in precipitation of many metals¹⁻³. The behaviour of a series of metals at extraction with dibutyldithiophosphoric acid was also studied⁴⁻⁵. However, the high solubility of the latter acid in alkalies and appreciable solubility in neutral or acid media⁶, makes it impractical for application in hydrometallurgy and limits its possibilities in analytical chemistry.

We have examined the extraction with alkylidithiophosphoric acids with long-chain radicals of elements of the copper, zinc, gallium, germanium, arsenic and iron sub-groups; and the possibilities of their separation from the accompanying metals as well as from each other in both analytical and technological aspects.

N-hexyl, n-octyl, 2-ethylhexyl-, dodecyl-, isododecyldithio-phosphoric acids and the acids synthesized from the fraction of the secondary alcohols C₈-C₁₈ have been tested.

Di-2-ethylhexyldithiophosphoric acid (D2EHDTPA) is of much promise in practical purposes, its extraction kinetics being favourable in contrast to isododecyldithiophosphoric acid. In addition, unlike the acids synthesized from alcohols C₈-C₁₂ D2EHDTPA does not form any stable emulsions.

Characteristic constants of D2EHDTPA determined by us⁷ are presented in Table 1. It is seen from the table that unlike dialkylphosphoric acids dⁿEHDTPA does not tend to dimerize and the distribution constants do not practically depend on diluents (non-polar).

Table 1. - Characteristic Constants of D2EHDTPA

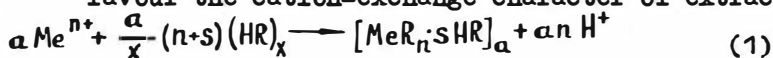
Diluent	$\lg K_a$	$\lg K_d$	$\lg K_2$
carbon tetra-chloride	-1.25 [±] 0.06	5.42 [±] 0.2	-1
Heptane		5.43 [±] 0.05	
Benzol		5.39 [±] 0.02	

D2EHDTPA is practically insoluble in acid and alkali solutions. For example, equilibration of 2 N NaOH with an equal volume of 0.3 N D2EHDTPA (106.2 g/l) results in a final concentration of the latter in water phase equal to 0.048 g/l. Specific weight of the purified acid is 0.96, refraction index - 1.478.

D2EHDTPA is sufficiently stable and without strong oxidizers

($\text{HNO}_3 \geq 6 \text{ N}$, H_2O_2 , Tl(III) , Br_2) its extractive capacity does not alter with time. D2EHDTPA extracts metals via the cation-exchange mechanism (Equation 1).

Almost complete absence of anions of mineral acids in organic phase and ratio $\frac{[\text{R}]_o}{[\text{Me}]_o}$ (found by means of the saturation method) equal to the charge of the extractive cation favour this fact. Study of dependences $\lg E - \lg [\text{HR}]_o$ and $\lg E - \lg [\text{H}^+]_{aq}$ showed that E is directly "n" power dependent on the extractant concentration in organic phase and inversely "n" power dependent on the hydrogen ion concentration in the aqueous phase ("n" - the charge of the metal cation). Besides that the absorption spectra of alkylthiophosphates within UV and IR ranges $8-12$ favour the cation-exchange character of extraction.



as $x=1$ and thus $s=0$, the extraction constant

$$K_{ex} = \frac{[\text{MeR}_n]_o [\text{H}]_{aq}^{an}}{a [\text{Me}]_{aq}^a [\text{HR}]_{aq}^{an}} \frac{\gamma_{\text{MeR}_n} \cdot \gamma_{\text{H}}^{an}}{\gamma_{\pm}^a \cdot \gamma_{\text{HR}}^{an}} \quad (2)$$

where a - polymerization degree, γ - corresponding activity coefficients. As $[\text{Me}^{n+}] = \frac{[\text{Me}]_{tot}}{\phi}$; $\phi = 1 + \sum_{i=1}^{i=K} \beta_i [\text{A}]^i$,

thus it follows from Equation 2 that if

$$\lg E - n \lg [\text{HR}]_o = \bar{K} + \frac{a-1}{a} \lg [\text{MeR}_n] \quad (3)$$

where $\bar{K} = \frac{\lg K}{a} - 2 \lg H - \lg \phi + \frac{\lg a}{a}$

is a constant, then (2) is valid only at $a=1$, i.e. in the absence of polymerization in the organic phase. It follows from the experimental data that Tl(I) , Bi , As(III) , Sn(II) , etc are extracted as monomers while Ag - as trimer.

Extraction constants of some metals are too high to be calculated by the generally accepted investigation method of dependences $\lg E_{\text{Me}} - \lg [\text{HR}]_o$ and $\lg E - \lg [\text{H}]_{aq}$ since high E values can-

not be determined accurately enough. We managed to determine by this method only the extraction constants of Co, Ni, Tl(I) and Sn(II). Very high values of the extraction constants of metals were found by means of exchange reactions following the equation

$$n \text{Me}_{II}^{m+} + m (\text{Me}_{I}R_n)_o = n (\text{Me}_{II}R_m)_o + m \text{Me}_{I}^{n+}$$

since $K_{\text{exch}} = \frac{K_{\text{Me}_{II}}^n}{K_{\text{Me}_{I}}^m C_o}$ and on the other hand $K_{\text{exch}} = \frac{E_{\text{Me}_{II}}^n}{A^m}$ where $A = \frac{C_o}{n \cdot C_{\text{Me}_{I}}}$, C_o - concentration of $\text{Me}_{I}R_n$, $C_{\text{Me}_{I}}$ - concentration of Me_{I} in the water phase, then

$$\frac{K_{\text{Me}_{II}}^n}{K_{\text{Me}_{I}}^m} = \frac{E_{\text{Me}_{II}}^n}{A^m} \quad (4)$$

The calculations are based on the value of nickel K which was determined accurately enough. In the case when constants of extraction $K_{\text{Me-H}}$ of the exchanging metals differ considerably it is impossible to determine $E_{\text{Me}_{II}}$ (the maximum E_{max} values found in the present studies were less than 10^3 - 10^4). It follows from Equation 4 that at $E_{\text{max}}=10^4$ and $A=10^{-2}$ (it is not practically possible to decrease the value of A) the constants ratio of the exchanging metals must satisfy the condition

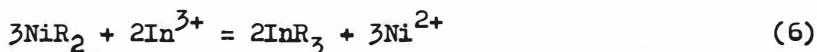
$$\frac{K_{\text{Me}_{II}}}{K_{\text{Me}_{I}}} \leq \frac{K_{\text{Me}_{I}}^{\frac{m-n}{n}} \cdot E_{\text{max}}}{A^{\frac{m}{n}}} \quad (5)$$

Analysis of Equation 5 shows

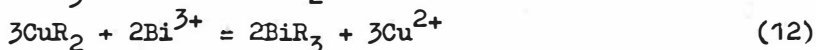
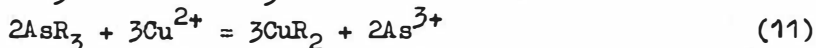
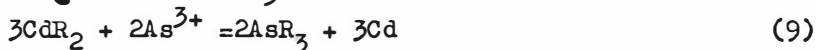
- 1) $\lg \frac{K_{\text{Me}_{II}}}{K_{\text{Me}_{I}}} \leq 6$ if the metals are of the same valency;
- 2) $\lg \frac{K_{\text{Me}_{II}}}{K_{\text{Me}_{I}}} \leq 7 + \frac{1}{2} \lg K_{\text{Me}_{I}}$ if $m=3, n=2$;
- 3) $\lg \frac{K_{\text{Me}_{II}}}{K_{\text{Me}_{I}}} \leq 5\frac{1}{3} - \frac{1}{3} \lg K_{\text{Me}_{I}}$ if $m=2, n=3$.

The Ni-In pair was chosen as an intermediate step when going from $K_{\text{Ni-H}}$ to the metal constants with higher values. The exchange was performed depending on concentration of Ni with constant $[\text{In}]_{\text{aq}}$ concentration; equilibrium pH being constant in each series of experiments. Well reproducible values of the

exchange and extraction constants for Ni-In pair have been obtained.



In a similar manner the following reactions have been studied



The obtained dependences $\lg E - \lg [n\text{C}_{\text{MeI}}]_{\text{aq}}$ at $[\text{MeI}R_n]_o = \text{const.}$ and $\lg E - \lg [\text{MeI}R_n]_o$ at $[n\text{C}_{\text{MeI}}]_{\text{aq}} = \text{const.}$ support the conclusion that exchanging reactions are described

by Equations (6-12).

It follows from Equation 4 that

$$\lg E_{\text{MeI}} = \frac{\lg K_{\text{exch}}}{n} + \frac{m}{n} \lg [\text{MeI}R_n]_o - \frac{m}{n} \lg [n\text{C}_{\text{MeI}}]_{\text{aq}} \quad (13)$$

and at constant and high concentration of the displaced MeI in water phase the inclination tangent of the dependence $\lg E - \lg [\text{MeI}R_n]_o$ is proportional to $\frac{m}{n}$. When the concentration of dithiophosphate of the displaced metal in organic phase is practically constant, i.e. at low concentrations of the displacing metal and sufficiently high concentration of $\text{MeI}R_n$ inclination tangent $\lg E - \lg [n\text{C}_{\text{MeI}}]_{\text{aq}}$ is inversely proportional to $\frac{m}{n}$. The experimental data obtained are in good agreement with Equations (6-12) - inclination tangents are equal to 3/2 for pairs Ni-In, Cd-As, Cu-Bi, and 1 for In-As, Zn-Ni, Fe-In. Besides that metals with higher extraction constant displace the stoichiometric quantity of metals with lower K_{ex} . The exchange and extraction constants are given in Table 2¹³.

Due to great differences between the extraction and exchange

constants and specific behaviour of some metals at extraction from solutions of mineral acids, alkalies and ammonia it was possible to develop the various ways of their separation. E.g. unlike other metals Tl(I) does not form any stable complex compounds with amines in water phase. This property was used for its separation from Ni, Zn, etc at the step of their stripping with diethylamines.

Table 2. - The exchange and extraction constants of metals;

Diluent - octane.

Exchange constants		Extraction constants		$\frac{1}{n} \lg K_{Me-H}$
Ni ²⁺ -In ³⁺	11.0 ± 0.3	Zn	2.25 ± 0.03	1.12
Zn-Ni	0.75 ± 0.03	Ni	3.14	1.51
		Tl(I)	2.00 ± 0.04	2.0
As-Pb	-0.67 ± 0.05	Fe(III)	8.62 ± 0.08	2.86
In-As	1.7 ± 0.1	In	10.22 ± 0.3	3.4
		Sn(II)	5.45 ± 0.1	2.72
Cd-As	2.82 ± 0.07	Cd	7.01 ± 0.7	3.5
Fe-In	1.6 ± 0.08	Pb	8.09 ± 0.05	4.04
As-Cu	12.94	As	11.93 ± 0.08	3.97
		Cu	12.3	6.15
Cu-Bi	3.3 ± 0.06	Bi	20.1 ± 0.06	6.33

Tl(I) can be separated from copper (which possesses high K_{ex} and is difficultly stripped) via the exchange reaction just with it. Thallium is completely displaced by copper which is left in organic phase. Method elaborated for determining thallium in products of lead-zinc production¹⁴ is based on these peculiarities. The universal method of tin separation has the following stages. Initially impurities are extracted from the solution which contains Sn(IV), then tin is reduced with thioglycolic acid; acidity is decreased and Sn(II) is extracted.

Tin is separated from some other elements, which hinder its determination, on the extraction as well as on stripping stages with hydrochloric acid¹⁵.

The idea of the method proposed of separating the gold is the following. Au(III) and Au(I) are extracted completely with D2EHDTPA from various media except cyanide (particularly from hydrochloric acid medium); Au is stripped with thiourea solution. The latter is destructed with aqua regia and gold is determined by the generally accepted method¹⁶.

The increase of E_{As} with acid concentration in water phase as opposed to all other metals; ready stripping with alkali and ammonia formed the basis for quantitative method of separation and determination of arsenic macro- and micro-concentrations¹⁷⁻¹⁸.

Cited peculiarities together with the high extraction constant allow to apply D2EHDTPA for high purification of solutions for hydrometallurgy, particularly of Ni-Co electrolytes and wash sulphuric acid from arsenic¹⁹. It was shown in laboratory pilot plant scale that nickel is quantitatively displaced from nickel di-2-ethylhexyldithiophosphate with arsenic according to equation $3NiR_2 + 2As^{3+} = 2AsR_3 + 3Ni^{2+}$. However the exchange kinetics depends to a considerable extent on equilibrium pH of the electrolyte. Sulphate-chloride electrolyte with arsenic concentration of 25 mg/l and pH=1 was subjected to purification. Extraction was carried out in 6-step extractor with phase ratio A:O=20:1, the rate of water phase flow being 15 l/h, organic - 0.75 l/h. It takes electrolyte 2 min to leave the mixing chamber.

After setting up the stationary conditions arsenic concentration was <0.2 mg/l. Table 3 gives the distribution of arsenic at the extraction steps.

Table 3 - Distribution of As at the extraction steps.

Step	(As) _{aq} , mg/l	(As) _o , mg/l
1	8.2	480
2	3	337
3	0.95	120
4	0.48	22
5	0.19	8
6	0.11	3

After substituting As for 25-30% of Ni, nickel is stripped with 9-10 N HCl, arsenic - with NaOH. Sodium form of the extracting agent is regenerated by contacting with electrolyte. Arsenic is extracted from wash sulphuric acid $H_2SO_4 \geq 10-100$ g/l independently of the concentration of the latter. Arsenic is concentrated on the extraction and stripping with alkali stages.

The possibility of extraction separating Bi from impurities was studied using the solutions formed in the process of hydrochloric acid leaching, particularly of tin concentrates. In spite of the fact that Bi in HCl solutions is strongly complexed, extraction constant equal to $\frac{K}{1 + \sum_{i=1}^n \beta_i [Cl^-]^i}$ where K - extraction constant from $HClO_4$ solutions in the absence of Cl^- is sufficiently high. At moderately high concentrations of chloride bismuth displaces iron and other impurities from the organic phase. It is concentrated on the stage of stripping with hydrochloric acid and is isolated from the water phase by means of electrolysis on graphite electrodes. Bismuth powder (Bi 99.7%) with 0.04% of Pb, 0.049% of As and 0.15% of Sb was obtained from solution of concentration in g/l: Bi-1.5; Sn-0.21; Pb-1.24; Fe-15.4; Zn-0.5; As-1.84; Cl-213.

The flow sheet of indium extraction with D2EHPA was applied at a series of plants. The defect of this flow sheet lies in the fact that In is separated quantitatively from all metals but antimony. It was found in practice that antimony content in hydrochloric acid strip liquors varies within the wide ranges when In concentration is from 20 to 80 g/l antimony concentration in it reaches 0.5-18 g/l (depending on the raw material). Extracting agents described in literature (TBP, butyl acetate, etc)²⁰ were found impractical for solving this problem. Strip liquors are purified from antimony either by a successive cementation on copper and iron, or by precipitation of sulphides. The first variant is tedious and is not sufficiently effective, the second one is characterized by a considerable loss of In. The method suggested for indium strip liquor purification from antimony is based on the fact that E_{In} on extraction with D2EHDTPA from HCl solutions decreases considerably faster with the increase of acid concentration in water phase than E_{Sb} that is seen from the data in Table 4 (we failed to determine the extraction constant of antimony).

Table 4 - Extraction of In and Sb(III) with D2EHDTPA in kerosine depending on the hydrochloric concentration. In=2.85 g/l; Sb=4 g/l; $\frac{D2EHDTPA}{\text{diluent}}=0.5n$; diluent - kerosine.

$[HCl]_N$	$[In]_{aq}, \frac{g}{l}$	E_{In}	$[Sb]_{aq}, \frac{g}{l}$	E_{Sb}	$[HCl]_N$	$[Sb]_{aq}, \frac{g}{l}$	E_{Sb}
3.5	0.05	56	was not	8000	8.9	0.03	1142
4	0.11	25	found		9.5	0.037	107
4.5	0.97	1.94	"		10	0.125	31
5.5	1.86	0.53	"		10.5	0.317	11.6
6.5	2.64	0.08	"		11.0	1.322	2
7.7	2.76	0.03	"	1332	11.5	2.07	0.93
					11.8	2.1	0.9

It is seen from Table 4 that from 5-8N HCl, i.e. directly from strip liquors, Sb(III) can be selectively extracted with a very high separation coefficients. We have purified indium strip liquors of the content (in g/l): In=71; Sb=8; As(V)=1.5; HCl=7.5 N. The final concentration of Sb and As (if it is preliminary reduced to As (III)) in reaffinate was not higher than U.C.5 mg/l. After the antimony stripping with concentrated hydrochloric acid the extracting agent is reusable. Up to the day this procedure was repeated many times under the laboratory conditions.

It follows from the discussion above that di-2-ethylhexyl-dithiophosphoric acid is an effective extracting agent which is of great promise in solving a series of problems for hydrometalurgy and analytical chemistry.

REFERENCES

1. Busev A.I. and Ivan'utin M.I., Vest.MGU,N5, 157 (1957).
2. Busev A.I. and Ivan'utin M.I., Zh.Analit.Khim.,13,312 (1958).
3. Busev A.I. and Ivan'utin M.I., Zh.Analit.Khim., 13, 647 (1958).
4. Handley T.A., Dean J.A. Analyt.Chem., 34, 1312 (1962).
5. Handley T.A., Nucl.Sci.Engng., 16, 440 (1963).
6. Zucal R.H., Dean J.A.and Handley T.A., Analyt.Chem., 35, 988 (1963).
7. Rodina T.F., Varentsova V.I., Levin I.S. and Kolyshev A.N., Izv. SO AN SSSR (in press).
8. Levin I.S., Sergeeva V.V., Varentsova V.I., Tarasova V.A., Rodina T.F. and Vorsina I.A., Zh.Neorg.Khim., 28, 1643 (1973).
9. Levin I.S., Varentsova V.I., Rodina T.F., Vorsina I.A. and Kolyshev A.N., Izv. SO AN SSSR (in press).
10. Levin I.S. and Tarasova V.A., Izv. SO AN SSSR (in press).
11. Levin I.S., Yukhin Yu.M., Bykhovskaya I.A. and Sergeeva V.V., Izv. SO AN SSSR, N12, 83 (1973).
12. Levin I.S., Kozlova N.E., Yukhin Yu.M. and Novosel'tseva L.A., Izv. SO AN SSSR (in press).
13. Levin I.S. and Sergeeva V.V., Izv. SO AN SSSR (in press).
14. Levin I.S., Varentsova V.I. and Rodina T.F., Zh.Analit.Khim., 28, 1086 (1973).
15. Levin I.S. and Tarasova V.A., Zh.Analit.Khim., 28, 1341 (1973).
16. Levin I.S., Novosel'tseva L.A. and Balakireva N.A., Zh. Analit.Khim., (in press).

17. Levin I.S., Sergeeva V.V. and Tischenko L.I., Zh.Analit. Khim., 28, 962 (1973).
18. Levin I.S., Sergeeva V.V., Tischenko L.I. and Dan'kova V.S. Zh.Analit.Khim., in press.
19. Levin I.S., Kheifets V.L., Gindin L.M., Maizlish R.S. and Sergeeva V.V., Izv. SO AN SSSR, N12, 117 (1973).
20. Mal'tsev V.I., Giganov G.P., Uspenskaya A.V. and Zhul'gina T.D., Sb.nauchn.trudov VNIITSVETMET. Ekstraktsiya i sorbtsiya v metallurgii tsvetnykh metallov, N12, p.38, Izdat. Metallurgia, Moscow, 1968.

ION-PAIR CHROMATOGRAPHY OF ORGANIC COMPOUNDS

S.Eksborg and G.Schill

Dep. of Analytical Pharmaceutical Chemistry

University of Uppsala, Box 574, S-751 23 Uppsala, Sweden

Liquid-liquid chromatographic systems based on ion-pair extraction have been used for the isolation of quaternary ammonium ions, amines, carboxylic acids and sulphonic acids.

The influence of counter ion, support and mobile organic phase on the chromatographic process has been investigated. The results indicate that extraction rate and diffusion in stationary or stagnant liquid phase has an important influence on the separating efficiency.

The influence of secondary processes e.g. ion-pair formation in the stationary phase, ion-pair dimerization and dissociation in the mobile phase, are discussed on the basis of equilibrium constants.

Ion-pair chromatography is based on a liquid-liquid partition technique usually called ion-pair extraction, which during the last 10 years found use in numerous procedures for the isolation and determination of organic compounds¹⁻⁴. It has been applied to widely different kinds of ionizable organic compounds such as amines, quaternary ammonium ions, amino acids, carboxylic acids, sulphonates, organic sulphates and phenols.

The general principle of the ion-pair extraction can be illustrated by the formula



The extraction of the cation, Q^{+} , can be expressed quantitatively by the distribution ratio, D_{QX} ,

$$D_{QX} = E_{QX} \cdot [X^{-}] \quad (2)$$

where E_{QX} is the extraction equilibrium constant defined by

$$E_{QX} = [QX]_{\text{org}} \cdot [Q^{+}]^{-1} \cdot [X^{-}]^{-1} \quad (3)$$

The magnitude of the extraction equilibrium constant depends on the nature of the components of the ion-pair and of the properties of the organic phase as illustrated in Tables 1, 2 and 3. Extraction equilibrium constants of ion-pairs between tetrabutylammonium and different anions are given in Table 1 and between picrate and different organic ammonium ions in Table 2. The organic phases are chloroform and methylene chloride respectively.

The addition of one alkyl or aryl carbon usually gives an increase in $\log E_{QX}$ of 0.5 - 0.6 units. Hydrophilic substituents such as hydroxyl or carboxyl decrease the extraction constant but the size of the change depends on the properties of the organic phase as illustrated in Table 3 (cf. ethyltrimethylammonium and its 2-hydroxy derivative).

The extraction equilibrium constant increases with increasing polarity of the organic phase (Table 3), and hydrogen bonding solvents

have a particularly high extracting power for ion-pairs with hydrophilic substituents.

Further discussions of the principles and applications of ion-pair extraction are given in a recent review¹ which also includes numerous extraction equilibrium constants of compounds with widely different structures.

Ion-pair extraction in liquid chromatography.

The ion-pair systems have several properties that make them particularly useful in separations based on liquid-liquid chromatography. They are very versatile and can easily be adapted to different kinds of samples by a proper choice of kind and concentration of counter ion. The extraction can usually be made with a solvent of low or moderate solvating power which makes the separation system highly selective as illustrated in Table 3.

A high sample capacity and a selective and sensitive detection of the sample components are other advantages that can be achieved in liquid chromatographic systems based on ion-pair extraction.

Experimental

Apparatus and material

Detector: Chromatronix 200-L photometer that measures the eluate absorbance at 253.7 nm in a 8 μ l cell with a path length of 10 mm.

Pump: Chromatronix Metering Pump giving flow rates of 2.4 - 120 ml/hour

Columns: Separations columns with i.d. 2.7 mm and length 300 mm. Precolumns with i.d. 9 mm and length 300 mm.

Supports: Cellulose, ethanolised (Munktell 410), extracted with ethanol to remove traces of pyridine. (mean diameter 30-65 μ for 80% of the particles). Celite, purified by boiling with acid and water. Particles with diameter 37-74 μ isolated by sieving.

Chromatographic technique

The columns were packed with a rod by use of slurry technique. The same fillings were used in precolumn and separation column. The whole chromatographic system including the detector was carefully thermostated at the experimental temperature, $25.0^{\circ} \pm 0.1^{\circ}$ C. The samples were injected as ion-pairs in the mobile phase.

Results and discussion

Construction of systems for ion-pair chromatography

The chromatographic isolation of a compound depends on its retention, usually expressed by the retention volume, V_R , and the separating efficiency of the system, H (height of a theoretical plate). The fundamental retention equation

$$V_R = V_m (1 + k') \quad (4)$$

shows that the retention volume is controlled by the capacity factor, k' , which by straight phase chromatography (mobile organic phase) is defined as

$$k = \frac{V_s}{V_m \cdot D} \quad (5)$$

V_s and V_m are the volumes of stationary and mobile phase while D is the distribution ratio.

When the compound is an ion that migrates as an ion-pair with the mobile organic phase, its distribution ratio is defined by eq. (2). D and V_R is then controlled by the concentration of the counter ion in the aqueous stationary phase and by the extraction equilibrium constant, E_{QX} , whose magnitude changes with the nature of the counter ion.

The choice of counter ion for an ion-pair chromatographic isolation can often be based on estimations from published extraction equilibrium constants (cf. Tables 1-2 and ref.1). Since the chromatographic procedure

may require modifications of the properties of the mobile organic phase, e.g. by addition of higher alcohols or other polar components, it is sometimes necessary to supplement the estimation with a constant determination ². The final adjustment of D to a suitable magnitude is made by changing the concentration of the counter ion in the aqueous phase and by minor adjustments of the composition of the mobile phase which will affect E_{QX} (cf. Table 3 and ref. ^{1,10,11}).

Support

The specific properties of the ion-pair systems cannot be fully utilized unless the composition of the phases is well known, and the support is so inert that it only has a minor or negligible influence on the migration rate of the sample. Results obtained with two supports with low adsorptive properties, diatomaceous earth (Celite) and a brand of cellulose (Munktell 410) are presented in Tables 4 and 5. The Tables give found distribution ratios, D_{found} , calculated from the found capacity factors and the measured phase volumes. The peak symmetry is illustrated by the asymmetry factor, A_s , that expresses the area ratio between the back and the front part of the peak. Table 5 also give some calculated distribution ratios, D_{calc} , computed from the extraction equilibrium constants given in Table 7.

The Tables give the following general picture of the influence of the support:

1. the peak symmetry is better (A_s is lower) on cellulose than on Celite
2. D_{found} is in most cases lower on cellulose than on Celite where it is equal or lower than D_{calc} (a lower D is equivalent to a lower migration rate).

The lower migration rate on cellulose may be due to the fact that it has a higher capacity than Celite to bind the components of the ion-pair by hydrogen bonding. The ion-pair between trimethylethylammo-

nium and picrate (Table 5:No.10) which both have little tendency to hydrogen bonding, is not retarded by cellulose ($D_{\text{found}} = D_{\text{calc}}$), while most of the ion-pairs containing naphthalenesulphonate and primary or secondary ammonium ions with a stronger hydrogen bonding capacity are significantly affected by the cellulose support.

The nature of the stationary phase has also a considerable influence on the migration rate of the ion-pair. Pentylammonium-naphthalenesulphonate has a higher D_{found} on a stationary phase of sulphonate (Tab. 5:1) than on pentylamine (Tab. 4:5) in spite of the fact that the concentration of the counter ion is the same. Similar results are obtained with di-isopropylamine (Tab. 5:6 and Tab.4:9) and triethylamine (Tab.5:8 and Tab.4:10). It is probable that these deviations depend on secondary reactions in the liquid phases, and processes of this kind will be discussed below.

The peak asymmetry is higher on Celite than on cellulose but it is hardly disturbing in most cases. The tailing tendency may be due to the porous structure of the support which can give rise to large differences in the thickness of the stationary or stagnant liquid phase layers with large variations in the diffusion time as a consequence. The strong tailing that appears with samples of quaternary ammonium ions (Table 5: No. 9-10) and benzoic acid (Table 4: No. 1) indicates more specific effects.

Cellulose columns that contain anions of benzoic acid, phenylbutyric acid or salicylic acid as stationary phase give tailing and abnormally retarded peaks with dimethylprotriptyline as sample (cf. Table 4).

Separating efficiency

A further illustration of the influence of the counter ion and the support can be obtained from studies of the separating efficiency. The height of a theoretical plate, H , can by liquid-liquid chromatography

according to Giddings¹² and Karger¹³ be expressed by:

$$H = C_S v + C_k v + C_M^* v + (A^{-1} + C_M^{-1} v^{-1})^{-1} \quad (6)$$

where

$$C_S = k'(1+k')^{-2} \cdot q d^2 D_S^{-1} \text{ (mass transfer in stationary phase)} \quad (7)$$

$$C_k = k'(1+k')^{-2} \cdot 2k_d^{-1} \text{ (extraction kinetics)}$$

$$C_M^* = 0.033 (b+k')^2 (1+k')^{-2} b^{-1} \omega^{-1} d_p^2 D_M^{-1} \text{ (mass transfer in stagnant mobile phase)} \quad (8)$$

$$C_M = \omega d_p^2 D_M^{-1} \text{ (mass transfer in mobile phase)} \quad (9)$$

$$A = 2d_p \lambda \text{ (Eddy diffusion)} \quad (10)$$

v is the linear flow rate, D_S and D_M the diffusion coefficients in mobile and stationary phase, d the diffusion path length in stationary phase, d_p the particle diameter of the support, k_d the rate constant for the extraction from the stationary into the mobile phase, b the intraparticle fraction of mobile phase, q, ω, λ constants.

The relative importance of the terms in eq. (6) can be illustrated by the relation between H and mobile phase speed at different k' .

Results obtained with some of the systems from Tables 4 and 5 are presented in Figs. 1-3.

A comparison of the chromatographic behaviour of ammonium ion-pairs of picrate and naphthalene-2-sulphonate can be based on Figs. 1 and 3. Both have been obtained with cellulose as support and it has been shown¹⁴ that the influence of stagnant mobile phase on that support is insignificant. For compounds with very low k' , eq. (6) then can be simplified to:

$$H_C = (A^{-1} + C_M^{-1} v^{-1}) \quad (11)$$

The curves are obtained with different cations, but calculations based on estimated molecular volumes¹⁵ indicate that the differences in diffusion coefficients are rather small (< 20%). It can then be assumed that C_M is the same all the compounds that are presented in the same Fig. Eqs. (6) and (11) can then be combined which gives:

$$\Delta H (1+k')^2 k'^{-1} = (qd^2 D_S^{-1} + 2k_d^{-1})v \quad (12)$$

where $\Delta H = H - H_0$. A plot of $\Delta H(1+k')^2 k'^{-1}$ versus v will give a straight line

Fig. 4 presents plots of this kind based on data from Figs. 1 and 3. Eq. (2) seems to be valid, approximately anyway; the lines are straight but there is a small intercept which possibly depends on the difficulty to determine H with good precision when the peaks are slightly asymmetric.

The lines for the picrate ion-pairs coincide almost completely. This indicates that $2k_d^{-1} \ll qd^2 D_S^{-1}$ for all the ion pairs i.e. the extraction rate is so large that it is without influence on H . The slope of the line gives $qd^2 D_S^{-1} = 0.6$.

The sulphonate ion-pairs have considerably larger slopes and the slope seems to increase with increasing k' (i.e. with decreasing E_{OX} of the ion-pair). Both facts indicate that the extraction rate has a significant influence. The slope gives $(qd^2 D_S + 2k_d^{-1}) = 1.4 - 3.3$.

It is obvious that the counter ion can have a large influence on the separating efficiency of a chromatographic system and the conclusion that this is due to the extraction rate constant has been supported by recent studies of the kinetics by ion pair extraction¹⁶.

The results obtained with cellulose as support show that H has a maximum at $k' = 1$ and decrease with with increasing k' . This is characteristic for systems where C_S and/or C_k dominate. The curves obtained with Celite as support (Fig. 2) give a quite different picture: H increases with k' until a limiting value is obtained. This indicates that stagnant mobile phase (C_M^* , eq. (8)) has a considerable influence on H , and it will be quite dominating at high k' and high mobile phase velocity, when C_S , C_k and $C_M^{-1} v^{-1}$ are insignificant. The H/v curve has under these conditions a slope of about 0.5. A decrease of the particle diameter will decrease the path length for stagnant

Selectivity

The separation factor, α , for two compounds, A^+ and B^+ , in a chromatographic system containing X^- as counter ion in the stationary aqueous phase is given by:

$$\alpha = D_A \cdot D_B^{-1} = E_{AX} \cdot E_{BX}^{-1} \quad (13)$$

(cf. eq. (2)). The equation is valid under the pre-requisite that all side-reactions except the main ion-pair extraction process (formula (1)) are negligible.

The properties of the organic phase has a great influence on the magnitude of the separation factor, and α will as a rule decrease with increasing solvating capacity of organic phase (cf. ref. ¹). An illustration is given in Table 3: $\log \alpha$ for picrate ion-pairs of ethyltrimethylammonium and its hydroxy derivative is about 1 with weakly hydrogen bonding solvents such as methylene chloride and chloroform but decreases to 0.05 when pentanol is used as organic phase.

The separation factor in a chromatographic system can as a rule only be approximated by eq. (13), since different kinds of side-reaction may have influence on distribution ratio of the sample components. Secondary reactions in the liquid phases and adsorption to the support are often the main reason to the deviations, but there are effects that cannot be explained in that way. An example is given in Table 6 which presents results from chromatography of primary ammonium ions on a column with 0.1 M naphthalenesulphonate as stationary phase on a cellulose support.

The Table shows that the deviation between D_{found} and D_{calc} increase with increasing hydrophobic character of the primary amine and with decreasing content of pentanol in the mobile phase. The ion-pairs were completely retained on the column when chloroform was

used as the mobile phase , and a pentanol content of > 10% was required to obtain distribution ratios of about the calculated magnitude.

It is not likely that the decrease of the distribution ratio is due to adsorption to the hydrophilic support since the deviation from D_{calc} increases with increasing number of alkyl carbons in the ammonium ion i.e. with increasing hydrophobicity of the ion-pair. A phenomenon of this kind may on the other hand also be the result of an adsorption of the ion-pair to the interface between stationary and mobile phase (cf. ref.^{17,18}). This can also explain the favourable effect of pentanol in the mobile phase: it reduces the interfacial adsorption due to a higher capacity than chloroform to solvate the hydrogen bonding primary ammonium ion of the ion-pair. An effect similar to interfacial adsorption has been observed by Borg¹¹ by extraction of perchlorate ion-pairs.

Side-reactions

The influence of side-reactions on an ion-pair extraction can be included in the calculations without any change of the general principle by the introduction of a conditional constant, E_{QX}^{x} , which by chromatographic experiments is defined by:

$$E_{\text{QX}}^{\text{x}} = E_{\text{QX}} \cdot \alpha_{\text{QX}} \cdot (\alpha_{\text{Q}} \cdot \alpha_{\text{X}})^{-1} \quad (14)$$

(cf. ref.^{3,14}). The α -coefficients include the effect of all side-reactions within each of the phases that interfere with the main reaction.

Association or dissociation processes that solely comprise the ion-pair or its components can give serious chromatographic disturbances , since the effect of such side-reactions will vary with the concentration of the migrating sample. Side-reaction of this kind must be avoided or suppressed in chromatographic systems , since they will give rise to asymmetric peaks or other deviations from a

normal chromatographic behaviour. Constants for the extraction equilibrium and some of the main side-reactions occurring in the chromatographic systems of Tables 4 and 6 are given in Table 7.

Ion-pair formation in the aqueous phase will increase α_Q or/and α_X which results in a decrease of the distribution ratio. The constants (k_p) found in the picrate system are of such magnitudes that significant effects can be expected when the concentrations of one or both components of the ion-pair exceed 10^{-2} M.

The dimerization of the ion-pairs in the organic phase will increase α_{QX} and the distribution ratio. The dimerization constants (k_{dim}) have in a low polarity solvent like chloroform such magnitudes that significant effects may appear when the ion-pair concentration in the organic phase is $> 10^{-4}$ M. Since the concentration of the sample decreases during the migration of the column, a dimerization will give rise to to a tailing peak.

Dissociation of the ion-pair in the organic phase will also increase α_{QX} and the distribution ratio. The effect increases with decreasing concentration of the ion-pair and a dissociation process will therefore in a chromatographic system give rise to a peak with a leading front. The dissociation constant (k_{diss}) increases with the polarity of the organic phase, and it has also been observed that quaternary ammonium ions give higher dissociation constants than primary, -secondary or tertiary. The constants in Table 7 indicate that significant dissociation effects can be expected when the concentration of the ion-pair in the injected sample is $< 10^{-5}$ M.

The dissociation can give very severe disturbances by ion-pair chromatography in the low concentration range, but its effect can be completely suppressed if another ion-pair containing the counter ion of the stationary phase is present in the mobile phase during the chromatographic procedure.¹⁴

Counter ion

The choice of counter ion for an ion-pair chromatographic process is of importance not only for the migration rate of the sample but also for the sample capacity of the system and for the detection sensitivity.

A high sample capacity, i.e. power to take up large amounts of samples without loss of separating efficiency is a property that is of great importance e.g. by separations in a preparative scale. A stable chromatographic system with a high sample capacity can be achieved if the ion-pair system has a high counter-ion buffer capacity, and it is obtained by using a stationary phase with a high counter-ion concentration¹⁴. In order to obtain a suitable distribution ratio, the extraction constant must be low, and it is in practice suitable to use a counter ion that gives $E_{OX} < 10$ with the most hydrophobic component of the sample.

Ion-pair chromatography can also be used to achieve a high detection sensitivity e.g. with a UV detector: any sample, irrespective of its UV absorbance, will give a high response if a counter ion with high molar absorptivity is used as stationary phase. Picrate which gives ion-pairs with a molar absorptivity of 10^4 (254 nm), can be used as counter ion for non-absorbing quaternary alkylammonium samples. Aromatic sulphonates (e.g. naphthalene-2-sulphonate with a molar absorptivity of $3 \cdot 10^3$ at 254 nm) can be used by the separation of both aprotic and protolytic cations.

Anions can usually be separated with quaternary ammonium compounds as counter ions. A suitable compound can usually be obtained by alkylation of one of the numerous amines with widely different hydrophobic character and molar absorptivity that are commercially available within the pharmaceutical field.²²

References

1. Schill, G., Advances in Ion Exchange and Solvent Extraction, 1973, 6. In press.
2. Modin, R. and Schill, G., Acta Pharm.Suecica, 1967, 4, 301
3. Modin, R., Persson, B.-A. and Schill, G. , Proceeding International Solvent Extraction Conference 1971, 1971, Vol. II, 1211 (London, Society of Chemical Industry)
4. Eksborg, S. and Persson, B.-A., Acta Pharm.Suecica, 1971, 8, 205
5. Gustavii, K., Acta Pharm.Suecica, 1967, 4, 233
6. Modin, R. and Tilly, A., Acta Pharm.Suecica, 1968, 5, 311
7. Borg, K.O. and Westerlund, D., Z.Anal.Chem., 1970, 252, 275
8. Fransson, B., Acta Pharm.Suecica. In press.
9. Modin, R. and Bäck, S., Acta Pharm.Suecica, 1971, 8, 585
10. Persson, B.-A., Acta Pharm.Suecica, 1968, 5, 343
11. Borg, K.O., Acta Pharm.Suecica, 1969, 6, 425
12. Giddings, J.C., Dynamics of Chromatography, 1965, Part 1, 190-193 (Marcel Dekker, New York, N.Y.)
13. Karger, B.L., Modern Practice of Liquid Chromatography, 1971, 3. J.J.Kirkland Ed.(Wiley-Interscience, New York, N.Y.)
14. Eksborg, S. and Schill, G., Anal.Chem., 1973, 45, 2092
15. Wilke, C.R. and Chang, P., A.I.Ch.E.Journal, 1955, 1, 264
16. Jansson, S.O. and Nordgren, T., Acta Pharm.Suecica. In press.
17. Duin, H. van, Nature, 1957, 180, 1473
18. Locke, D.C., J.Gas Chromatog., 1967, 5, 202
19. Gustavii, K. and Schill, G., Acta Pharm.Suecica, 1966, 3, 241
20. Modin, R. and Schill, G., Acta Pharm.Suecica, 1970, 7, 585
21. Schröder-Nielsen, M., Acta Pharm.Suecica. In press.
22. Borg, K.O. and Schill, G., Acta Pharm.Suecica, 1968, 5, 323

Table 1

Extraction equilibrium constants of tetrabutylammonium ion-pairs

Organic phase: chloroform

Class	Anionic component	$\log E_{QX}$	Ref.
Inorganic anion	Cl^-	-0.11	5
	Br^-	-1.29	5
	I^-	3.01	5
Carboxylic acid	phenylacetic acid	0.27	6
	benzoic acid	0.39	6
	salicylic acid	2.42	6
Phenol	phenol	-0.03	6
	picric acid	5.91	5
Sulphonic acid	toluene-4-sulphonic acid	2.33	2
	naphthalene-2-sulphonic acid	3.45	2
	anthracene-2-sulphonic acid	5.11	7
Sulphate	phenylpropyl-1-sulphate	4.20	8
	naphthyl-2-sulphate	4.90	8

Table 2Extraction equilibrium constants of picrate ion-pairs

Organic phase: methylene chloride

Class	Cationic components	log E_{QX}	Ref.
Primary amine	propylamine	-0.57	5
	hexylamine	1.45	5
Secondary amine	dipropylamine	2.33	5
	dibutylamine	3.54	5
Tertiary amine	tripropylamine	4.92	5
	tributylamine	6.51	5
Quaternary ammonium ion	tetrapropylammonium	4.46	5
	tetrabutylammonium	6.68	5
	trimethylethylammonium	0.77	9

Table 3

Extraction equilibrium constants of picrate ions-pairs

Cations: tetrabutylammonium (TBA)

ethyltrimethylammonium (ETMA)

2-hydroxyethyltrimethylammonium (HO-ETMA)

Organic phase	$\log E_{OX}$		
	TBA	ETMA	HO-ETMA
1-Pentanol	-	1.24	1.19
Methyl isobutyl ketone	-	0.64	0.98
Ethyl acetate	-	0.45	0.69
Methylene chloride	6.68	0.77	-0.19
Chloroform	5.91	-0.32	-1.45
Benzene	3.59	-	-
Carbon tetrachloride	1.94	-	-

Table 4

Ion-pair chromatography of organic anionsSample: 5.10^{-5} M (20 μ l) Stat. phase loading: 25% of support weight Speed : 2 mm/sec

Mobile phase: I - cyclohexane + chloroform + 1-pentanol (75+20+5)

II - chloroform + 1-pentanol (9+1)

III - chloroform + 1-pentanol (19+1)

IV - chloroform

No	Sample*	Stationary phase	Mobile phase	Cellulose		Celite	
				D _{found}	As	D _{found}	As
1	Benzilic acid	N,N-dimethylprotriptyline 0.036 M, pH 9.0	I	0.23	1.4	0.27	>5
2	Phenylbutyric acid	- " -	I	0.095	1.2	0.095	1.3
3	Salicylic acid	- " -	I	0.053	1.1	0.067	1.7
4	Naphthalene-2-sulphonic acid	propylamine 0.10 M, pH 2.4	II	0.033	1.2	0.070	1.4
5	- " -	pentylamine -"- -"-	III	0.062	1.4	0.115	1.6
6	- " -	diethylamine -"- -"-	III	0.033	1.3	0.051	1.3
7	- " -	trimethylamine -"- -"-	III	0.014	2.6	0.019	1.5
8	- " -	tetraethylammonium bromide -"- -"-	III	0.019	1.3	0.024	1.9

(continued)

Table 4 (continued)

No	Sample *	Stationary phase	Mobile phase	Cellulose		Celite	
				D _{found}	As	D _{found}	As
9	Naphhtalene-2-sulphonic acid	di-isopropylamine 0.10 M, pH 2.4	IV	0.014	4.5	0.025	4.2
10	- " -	triethylamine - " - " -	IV	0.088	1.4	0.105	2.2
11	- " -	tetrapropylammo- nium bromide - " - " -	IV	0.116	1.4	0.210	1.3

* Injected as ion-pair with the ammonium ion present in the stationary phase

$$D_{\text{found}} = V_s \cdot (V_m \cdot k'_{\text{found}})^{-1}$$

$$As = \text{asymmetry factor} = \frac{\text{back part of } w_b}{\text{front part of } w_b} \quad (w_b = \text{peak width at the base})$$

Table 5

Ion-pair chromatography of organic ammonium ionsSample: 8.10^{-5} M (20 μ l) Stat.phase loading: 25% of support weight

Speed: 2 mm/sec

Mobile phase: I - chloroform + 1-pentanol (19+1) ; II - chloroform

No	Sample *	Stationary phase	Mobile phase	D _{calc} **	Cellulose		Celite	
					D _{found}	As	D _{found}	As
1	Pentylamine	naphthalene-2-sulphonat 0.10 M , pH 2.4	I	0.16	0.09	1.2	0.16	1.3
2	Hexylamine	- " -	I	0.55	0.16	1.2	0.35	1.0
3	Di-isopropylamine	- " -	I	0.29	0.29	1.0	0.35	1.1
4	Trimethylamine	- " -	I	0.013	0.013	1.1	0.016	1.2
5	Tetraethylammonium	- " -	I	0.022	0.025	0.87	0.022	3.2
6	Di-isopropylamine	- " -	II	0.044	0.035	1.1	0.050	1.1
7	Dibutylamine	- " -	II	0.87	0.19	1.1	0.43	1.5
8	Triethylamine	- " -	II	0.23	0.16	0.93	0.18	1.2
9	Tetrapropylammonium	- " -	II	0.87	0.065	2.2	0.084	>9
10	Trimethyletylammonium	picrate 0.06 M pH 11.2	I	0.034	0.034	1.0	0.021	7.5

* Injected as ion-pair with the anion present in the stationary phase ** Calculated from E_{QX}^x in Table 7

Table 6

Distribution ratio of naphthalene-2-sulphonate ion-pairs
of primary alkylamines

Stationary phase: 0.1 M naphthalene-2-sulphonate , pH 2.4

Support: cellulose

Sample	Mobile phase	log D	
		calc.	found
Nonylamine	chloroform	+ 0.5	< -2.3
Hexylamine	chloroform- 1-pentanol (19:1)	- 0.26	-0.80
Pentylamine	- " -	-0.80	-1.05
Butylamine	chloroform- 1-pentanol (9:1)	-0.88	-0.98
Propylamine	- " -	-1.57	-1.53

D_{calc} calculated from E_{QX}^X given in Table 7

Table 7

Ion-pair constants

Constant determinations according to principles given in ref. 2,19,20

Anion	Cation	Org. * phase	log E_{QX}	log k_{diss}	log k_{dim}	log k_f
Picrate	tetramethylammonium	II	-0.51	-	-	1.2
	trimethylethylammon.	II	0.05	-	-	1.2
	trimethylpropylammon.	II	0.72	-	-	1.2
	hydroxyethyltrime- thylammonium	IV	0.00	-5.6	-	-
Naphthalene- 2-sulphonate **	di-isopropylammon.	I	-0.08	-	3.6	-
	dibutylammonium	I	1.22	-	3.7	-
	triethylammonium	I	0.63	-	-	-
	tetrapropylammon.	I	1.22	-	-	-
	pentylammonium	II	0.48	-	2.6	-
	hexylammonium	II	1.02	-	2.9	-
	di-isopropylammonium	II	0.74	-	-	-
	trimethylammonium	II	-0.63	-	-	-
	tetraethylammonium	II	-0.39	-4.8	-	-
	butylammonium	III	0.40	-	-	-
propylammonium	III	-0.29	-	-	-	

$$k_{diss} = [Q^+]_{org} \cdot [X^-]_{org} \cdot [QX]_{org}^{-1}$$

$$k_{dim} = [Q_2X_2]_{org} \cdot [QX]_{org}^{-1}$$

$$k_f = [QX] \cdot [Q^+]^{-1} \cdot [X^-]^{-1}$$

* Organic phase:

- I - chloroform
- II - chloroform + pentanol (19+1)
- III - chloroform + pentanol (9+1)
- IV - methylene chloride +
pentanol (49+1)

**

Naphthalene-2-sulphonate can form dimers and tetramers in the aqueous phase²¹. Log E_{QX} is calculated with the assumption that $\log \alpha_Q \cdot \alpha_X = 0.28$ in 0.10 M naphthalene-2-sulphonate when $C_{amina} < 10^{-3}$.

Fig. 1 Picrate as stationary phase on a cellulose support:
influence of mobile phase speed and capacity factor (k')
on the height of a theoretical plate (H).

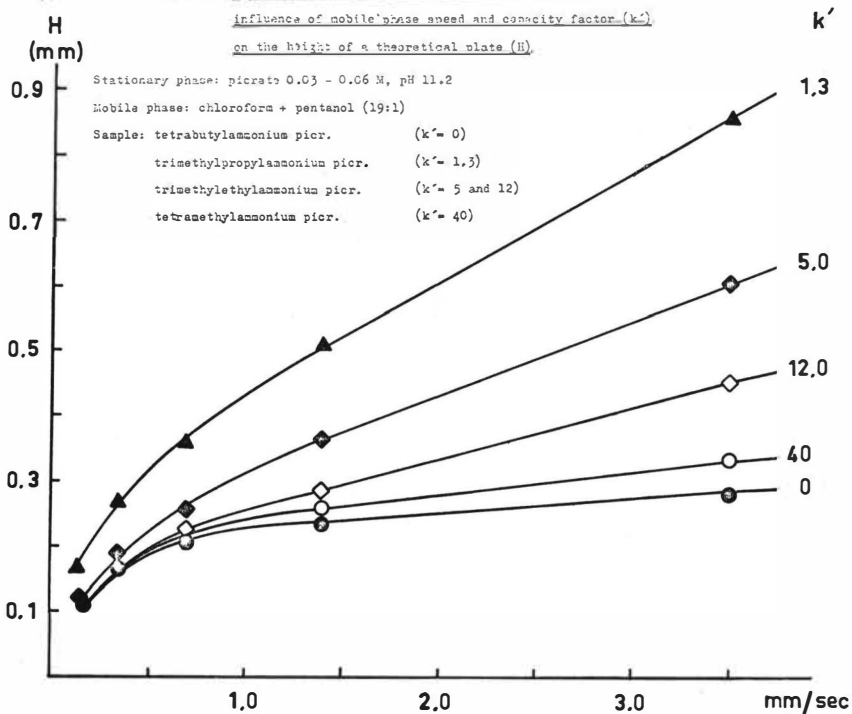
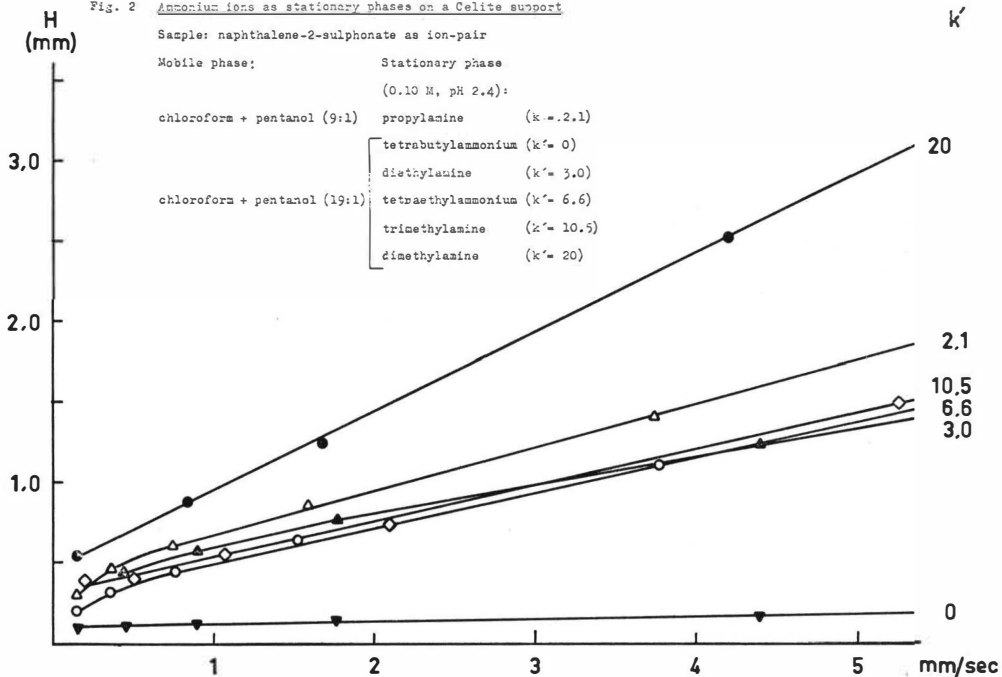


Fig. 2 Ammonium ions as stationary phases on a Celite support



H Fig. 3 Ammonium ions as stationary phases on a cellulose support

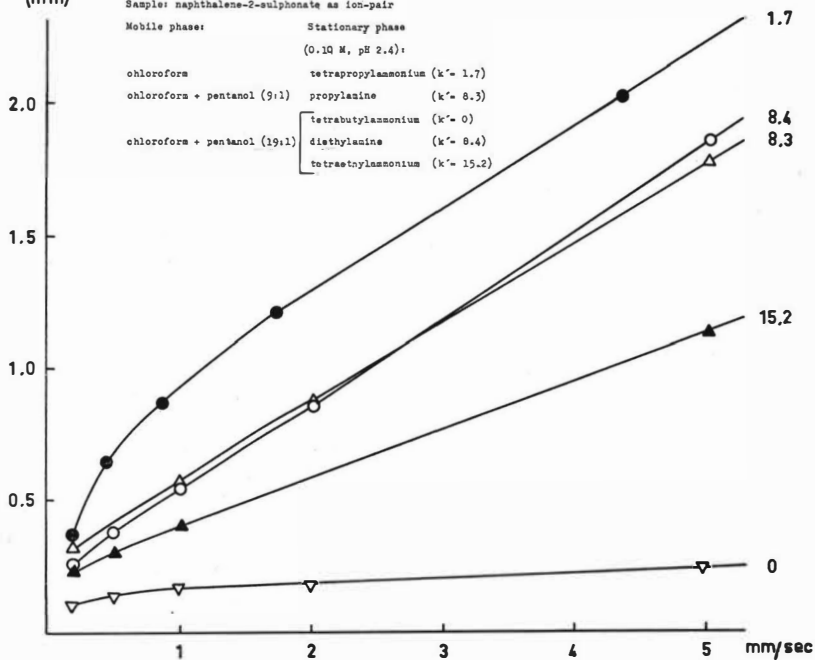
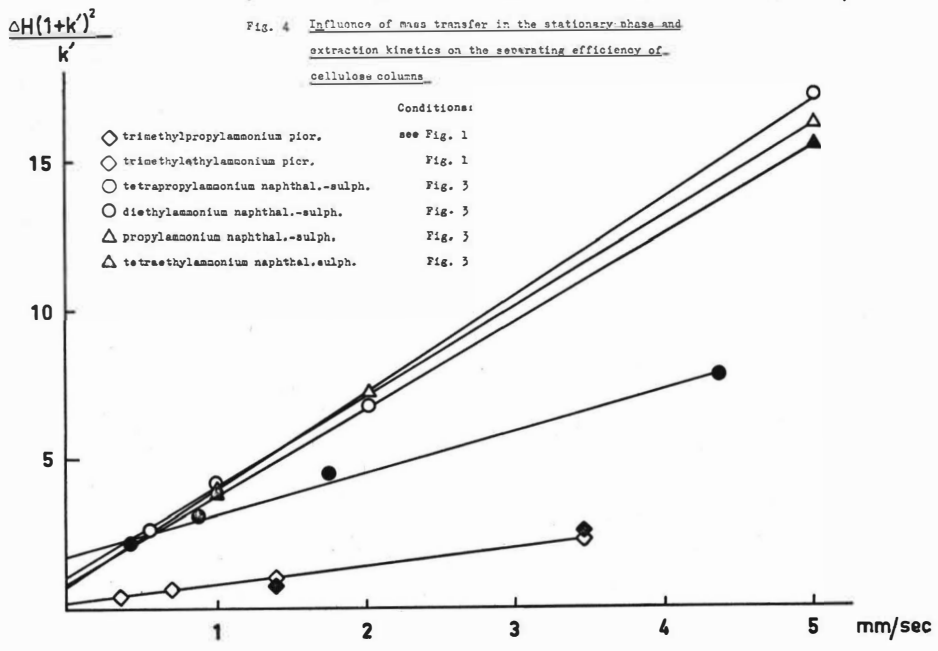


Fig. 4 Influence of mass transfer in the stationary phase and extraction kinetics on the separating efficiency of cellulose columns



ION PAIR PARTITION CHROMATOGRAPHY APPLIED TO SEPARATIONS IN THE
BIOANALYTICAL FIELD.

K.O. Borg, M Gabrielsson and T-E. Jönsson

Research Laboratories, AB Hässle, Fack, S-431 20 MÖLNDAL, Sweden.

Abstract

The separation of drugs and drug metabolites by ion pair partition chromatography was studied. The chromatographic conditions were calculated from the ion pair extraction constants determined by batch-extraction. The selectivity of the separation system was demonstrated by separation of positional isomers of hydroxylated alprenolol, two geometrical isomers and a tertiary amine from its corresponding demethylated secondary amine. A u.v. detection of the eluate was used with such a high amplification that the concentration range of interest in analysis of drugs in biological samples could be studied. A stepwise gradient-elution technique was briefly demonstrated.

In studies on pharmacological chemistry the analytical problem is in many cases to determine a low concentration (p.p.b.) of a drug or a drug metabolite in a complex biological sample. For many years ion pair extraction has been used in such analysis but with a traditional batch-extraction procedure it is in many applications not possible to obtain a sufficient selectivity and sensitivity. Recently Schill and co-workers presented a chromatographic system based on liquid-liquid partition of ion pairs (1, 2). In the present paper this technique called ion pair partition chromatography has been applied to separation problems of importance in the analysis of drugs and drug metabolites in biological material.

EXPERIMENTAL

Apparatus

The liquid chromatograph was built up from a Pye pulse free constant pressure pump, borosilicate glass chromatography columns and a Cecil u.v. spectrophotometer (CE 212) with a 8 μ l fluid cell. The separation column had an i.d. of 2.8 mm and a length of 300 mm and the pre-column an i.d. of 10 mm and a length of 100 mm. The columns were silanized before use. Injection port and column end fittings were modified Swagelok connections. Radioactivity measurements were made by liquid scintillation counting on a Packard Tri-carb 3375 instrument.

Chemicals

Manalyzed cellulose, Munktell 410, used as support was purified from pyridine traces by washing with ethanol and methylene chloride.

Organic solvents were of Fisher Certified A.C.S. quality.

The drug substances were synthesized at the chemical departments at AB Astra and AB Hässle and used without further purification.

Chromatographic technique

The chromatographic experiments were performed as given by Eksborg and Schill (1) but at a temperature of $23 \pm 1^{\circ}$ C. Photometric measurements were based on the u.v. absorption of the amine components.

THEORY

A theoretical discussion on ion pair partition in chromatographic separations was presented by Eksborg and Schill (1). The relation between the retention volume of a component, V_R , and the capacity factor, k' , is given by equation (1),

$$V_R = V_m \times (1 + k') \quad (1)$$

and the capacity factor by equation (2).

$$k' = V_s \times (V_m \times E_{QX}^x \times C_X)^{-1} \quad (2)$$

V_s is the volume of the stationary phase and V_m the interstitial volume.

The extraction constant of the ion pair, E_{QX}^x , is defined by

$$E_{QX}^x = C_{QX \text{ org}} \times C_Q^{-1} \times C_X^{-1} \quad (3)$$

$C_{QX \text{ org}}$ being the total concentration of the cationic component, Q, extracted with the anion, X, to the organic phase as ion pair, QX. C_Q and C_X are the total concentrations of Q^+ and X^- in the aqueous phase. According to equations (2) and (3) the retention volume of a certain cation can be regulated by the concentration of the anion in the stationary aqueous phase and the magnitude of the extraction constant which depends on the kind of anion component and the composition of the organic phase.

RESULTS AND DISCUSSION

Separation of tertiary and secondary amine

Many drugs are in the body transformed to more polar compounds, metabolites, prior to excretion. One of the most common routes of metabolism is dealkylation of a tertiary aliphatic aminogroup to the corresponding secondary amine. In such cases it is usually of interest from a pharmacological point of view to determine both the tertiary and the secondary

amine in biological material. A separation of a tertiary amine and its corresponding demethylated secondary amine is demonstrated in Fig. 1. The extraction constant of the chloride ion pair (1+1) with the tertiary amine, H 102/09, is given in Table 1. The retention volume of H 102/09 is close to the calculated value according to equations 1, 2 and 3. The chromatographic migration is based on the partition of the 1+1 ion pair at a pH of the stationary phase where the influence of the 1+2 ion pair could be assumed to be negligible (3). The secondary amine was only available in small quantities and batch-extraction studies could not be made. The difference in magnitude of the conditional extraction constant of the chloride ion pairs of the tertiary and secondary amine as calculated from their retention volumes was about 0.3 log units. In other studies (4, 5) it has been demonstrated that the difference in extraction constants for a tertiary amine and its corresponding dimethylated secondary amine depends very much on the organic solvent. As an example the extraction constant of imipramine (tertiary amine) is about 100 times that of desmethylinipramine when methylene chloride is used as an organic solvent while in pentanol the extraction constant of desmethylinipramine is about twice that of imipramine. The found difference between the compounds in Fig. 1 is about the expected one. It can be concluded that ethylene chloride with 20 % of 1-pentanol is not the most selective system but it has the advantage of giving a sufficient separation within acceptable time.

Separation of positional isomers of aromatic hydroxylated alprenolol

Drug molecules containing a benzene-ring are very often metabolized by aromatic hydroxylation. The position of the hydroxy-group is of interest and also the quantitative relation between different positional isomers. The separation of 4-, 5- and 6-hydroxyalprenolol by partition chromatography as ion pairs with perchlorate as counter ion is demonstrated in Fig. 2. The extraction constant of the perchlorate ion pair of 4-hydroxyalprenolol is given in Table 1. From the retention volumes it can be concluded that 6-hydroxyalprenolol is considerably more lipophilic than the 4- and 5-substituted compounds. There is a possibility for an intramolecular hydrogen bonding in 6-hydroxyalprenolol which is the probably reason for the difference in hydrophobic nature. The difference between

the 4- and 5-isomers is in agreement with observations by Schill (6). 4-hydroxyalprenolol was found to be the compound present in biological material as a metabolite of alprenolol and the chromatographic technique was also applied to quantitative determinations in biological samples (7).

Separation of geometrical isomers.

The cis and trans isomer of a compound have mostly quite different pharmacological profiles. The tertiary amine, H 102/09 mentioned above, have two geometrical isomers which can be separated by ion pair partition chromatography as given in Fig. 3. The chromatographic migration is based on the 1:1 ion pairs with chloride. The separation factor i.e. the ratio between the conditional extraction constant of the cis and the trans isomers is 1.9. The basis for the separation is probably a difference in acid dissociation constant of the pyridyl group which will influence the conditional extraction constant.

Gradient elution

The high separation factors that is obtained by ion pair partition chromatography can sometimes give rise to long separation times. A system for gradient elution can be of great interest to increase the analytical capacity. The chromatographic system consists of a pre-column that is considerably larger than the separation column which makes a continuous gradient of the mobile phase difficult. On Fig. 4 a separation of alprenolol and two of its metabolites is made by using two mobile phases with different amounts of 1-pentanol. Two pumps and two pre-columns were used and just before the separation column a valve system permitted a change of mobile phase. The time of separation with a non-gradient system was in this case five times longer.

References

1. Eksborg, S., and Schill, G., *Analyt. Chem.* 1973, 45, 2092
2. Eksborg, S., Lagerström, P-O., Modin, R., and Schill, G., *J. Chromat.* 1973, 83, 99
3. Modin, R., and Schill, G., *Acta pharm. suec.*, 1970, 7, 585
4. Persson, B-A., *Acta pharm, suecica* 1968, 5, 335
5. Persson, B-A., *Acta pharm. suecica* 1968, 5, 343
6. Schill, G., *Acta pharm. suec.*, 1965, 2, 13
7. Borg, K.O., Gabrielsson, M., and Jönsson, T-E., 1974, to be published.

Table 1.

Extraction constants of ion pairs.

Amine(Q)	pK _a	Counter ion(X)	Organic solvent	log E _{QX}
H 1o2/o9	3.3 , 8.7	Chloride	Ethylene dichloride + 1-pentanol (80+20)	0.47
4-hydroxy- alprenolol	9.7 , 10.5	Perchlorate	Cyclohexane + 1-pentanol (85+15)	-1.46

Fig.1. Separation of a tertiary amine and its corresponding demethylated secondary amine.
 Stationary phase: 1.0 M Cl⁻, pH = 2.2
 Mobile phase: Ethylene dichloride + 1-pentanol (80+20)
 Flow rate: 0.18 ml/min Sample: I= 38 ng II= 130 ng

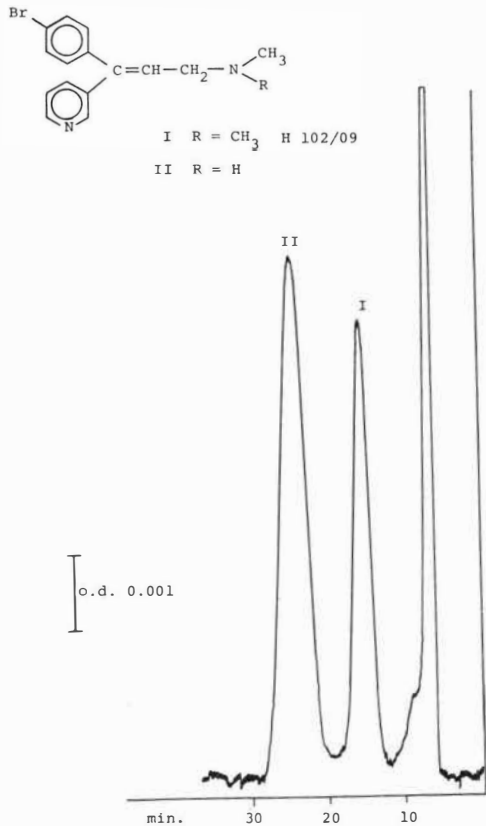


Fig.2. Separation of positional isomers of hydroxyalprenolol.
 Stationary phase: 0.9 M NaClO₄ + 0.1 M HClO₄
 Mobile phase: Cyclohexane + 1-pentanol (85 + 15)
 Flow rate: 0.39 ml/min Sample: I= 4.3 ug II= 19.4 ug III= 9.0 ug

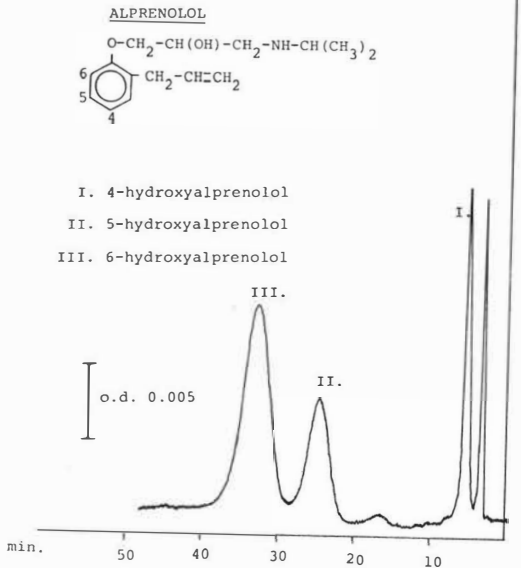


Fig.3. Separation of geometrical isomers of a divalent amine, H 102/09.
 Stationary phase: 1.0 M Cl⁻, pH = 2.2
 Mobile phase: Ethylene dichloride + 1-pentanol (85+15)
 Flow rate: 0.33 ml/min Sample: trans = 146 ng cis= 315 ng

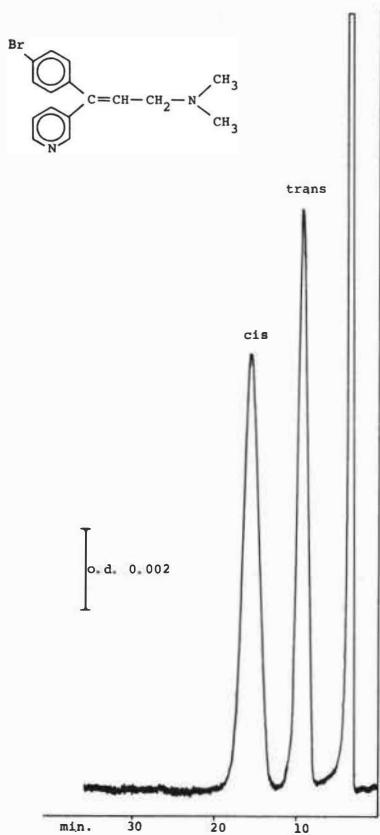
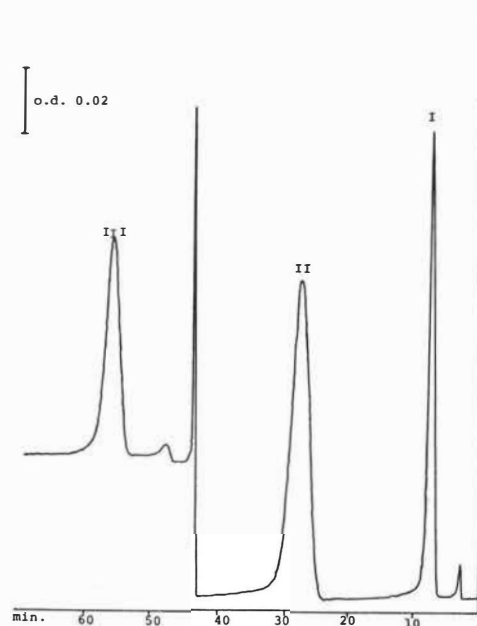


Fig.4. Stepwise gradient elution of alprenolol(I), desisopropylalprenolol(II) and 4-hydroxyalprenolol. Mobile phase: Cyclohexane + 1-pentanol. 0-40 min. (93+7), 40-70 min. (80+20) For chemical structures see Fig.2.



SESSION 21

Thursday 12th September: 14.00 hrs

C H E M I S T R Y O F E X T R A C T I O N

(Rare Metals)

Chairman:

Professor A.C. Pappas

Secretaries:

Dr. M.A. Hughes

Mr. J.C. Leroy

SEPARATION OF NIOBIUM AND TANTALUM BY SOLVENT EXTRACTION
WITH TERTIARY AMINES FROM SULPHURIC ACID SOLUTIONS

by S.Aa. Markland

Chemistry Department, Research Establishment Risø,
DK-4000 Roskilde, Denmark.

A new solvent extraction system for the separation of niobium and tantalum has been developed based on extraction by tertiary amines from sulphuric acid solutions containing hydrogen peroxide and only stoichiometric amounts of fluoride. Separation factors of the order of several hundred have been found. Metal complexes of the form $TaO(H_2O_2)F_4^-$ and $NbO(H_2O_2)F_4^-$ appear to be the extractable species involved.

INTRODUCTION

Niobium and tantalum are substances with very similar properties and consequently they are very difficult to separate from each other by chemical means.

The two elements exist together in a number of minerals of industrial importance for the production of niobium and tantalum compounds as well as metals. The most important of these minerals are columbite, tantalite, pyrochlore, micro-lite and loparite.

In the chemical processing of these minerals a solvent extraction step is usually applied resulting in a separation of niobium and tantalum. In fact only one solvent extraction system has been successfully developed into an industrial process⁽¹⁾, and it is now being used throughout the world⁽²⁾.

In this solvent extraction system tantalum and niobium are separated and purified by extraction with methyl-isobutyl-ketone from strong hydrofluoric-sulphuric acid solutions. The resulting tantalum and niobium products are of high purity, but there are a number of drawbacks associated with this system:

- 1) serious corrosion problems due to the strong hydrofluoric-sulphuric acid solutions
- 2) extensive safety precautions for the protection of operating personnel
- 3) relatively high solubility of methyl-isobutyl-ketone in water.

We have developed a new solvent extraction system that overcomes these difficulties, i.e. it contains no free hydrofluoric acid, it needs little safety precautions and the organic phase has a very low solubility in the aqueous phase.

Experiments

Hydrated oxides of niobium and tantalum were used throughout this investigation. This feed material were prepared by caustic fusion of niobium and tantalum pentoxides followed by washing with water to remove excess caustic and sodium silicate which was present. The precipitates were neutralised with sulphuric acid and filtered. The hydrated oxides were used in the wet condition.

Feed solutions for solvent extraction were prepared by dissolution of hydrated oxides in a mixture of sulphuric acid and hydrogen peroxide while slowly heating to about 50°C. A small amount of fluoride was added before extraction.

These solutions were stable for weeks and even months without any precipitations of hydrolysed niobium and tantalum compounds.

Concentrations of niobium and tantalum were determined by spectrophotometric methods. For niobium the thiocyanate-acetone method was used and tantalum was determined by means of a Nilblau A complex (3).

Experiments

A solution of 7,5 vol% Alamine 336 (tricaprylamin, General Mills Inc, USA) in Solvesso 100 (a mixture of trialkylbenzene isomers, Esso Chemicals, Denmark) was used for most of our experiments with phase ratios of 1:1. The extractant was equilibrated with sulphuric acid of the desired acidity before metal extraction.

We first studied the dependence of sulphuric acid concentration on the distribution coefficients of niobium and tantalum and the results are plotted in figure 1. It is interesting to see that for sulphuric acid concentrations of about 0,6M a separation factor of the order of 500 is to be expected.

In figure 2 the distribution coefficients for different hydrogen peroxide concentrations are presented showing that a minimum of peroxide is required for maximum extraction of both metal ions. For the preparation of feed solution a minimum of peroxide is needed corresponding to a molar ratio of 1:1 of Nb:H₂O₂ and Ta:H₂O₂. This concentration corresponds to 0,1M hydrogen peroxide in figure 2.

Fluoride has a very big influence on the extraction of the two metals as can be seen from figure 3. For high concentrations of fluoride there is a high degree of extraction of both niobium and tantalum, but virtually no separation. On the other hand there is hardly any extraction at all in the fluoride free system. This is due to the existence of heteropolyacid compounds of niobium and tantalum in fluoride free systems (4). The extraction of heteropolyacid-amine compounds is very low due to a very low solubility of these high molecular species in the organic phase.

Fortunately the heteropolyacids are broken down by the addition of fluoride and for low fluoride concentrations tantalum is preferentially extracted having a considerably higher affinity towards fluoride than niobium. Keeping the fluoride concentration at a minimum for maximum extraction of tantalum will result in an even higher separation factor than stated above.

Figure 4 presents the influence of amine concentration on metal extraction and as can be seen the tantalum extraction is directly proportional to the amine concentration while this is not the case for niobium.

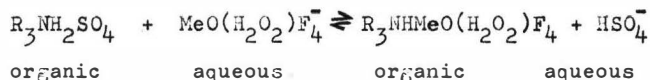
In figure 5 the equilibrium curves for both tantalum and niobium are plotted showing an approximately linear relationship.

Discussion

From the distribution data presented in fig.3 can be calculated that maximum extraction of both tantalum and niobium is reached after addition of approximately 4 moles of fluoride per mole of tantalum or per mole of niobium. Further, from figure 2 we can see that only 1 mole of hydrogen peroxide is needed for maximum extraction of 1 mole of tantalum and niobium. These facts points to the existence of complex metal species in the aqueous phase of the form: $TaO(H_2O_2)F_4^-$ and $NbO(H_2O_2)F_4^-$, leaving no room for any sulphate in the complex. Recently, species of this kind have in fact been shown to exist in sulphuric acid systems (5).

At higher hydrogen peroxide concentrations species with more than one peroxide molecule in the complex are likely to be formed. This could lead to lower solubility in the organic phase, as figure 2 shows. As can be seen from figure 1 maximum extraction of the metal complexes are obtained at low sulphuric acid concentrations. At high acid concentrations metal extraction drops to negligible amounts due to competition between HSO_4^- and $MO(H_2O_2)F_4^-$ for the tertiary amine, tricaprlyamine in the organic phase.

Summing up, the extraction mechanism can probably be represented by the following equation:



where R = Octyl and Me = Nb, Ta.

Stripping the loaded organic phase with a 5% potassium hydroxide solution was very effective and was used throughout this investigation.

The low extraction of niobium for high amine concentrations as presented in figure 4 is probably due to a high extraction of HSO_4^- resulting in hydrolysis of niobium.

Conclusion

The extraction and separation of niobium and tantalum by tertiary amines from sulphuric acid solutions containing hydrogen peroxide and stoichiometric amounts of fluoride appear to be a promising alternative to existing industrial methods. Tantalum is preferentially extracted at low fluoride concentrations resulting in separation factors of the order of several hundred.

The new method is likely to give a high degree of purification of the extracted metal compounds since very few elements are extracted by tertiary amines from sulphuric acid solutions.

A further study is under way in which mineral concentrates are used for the preparation of feed solutions of industrial relevance.

Acknowledgements

The author wish to thank Miss Lis Vinther Kristensen for her skilful technical assistance and pleasant co-operation.

References

- (1) Higbie, K.B., & Werning, J.R., US Bureau of Mines, Report of Investigations 5239
- (2) Rosenbaum, J.B., George, D.R., & May, J.T., US Bureau of Mines, Information Circular 8502
- (3) Gagliardi, E., & Wolf, E., Mikrochimica Acta (Wien), 1969, 4, 888
- (4) Gibalo, I.M., Analytical Chemistry of Niobium and Tantalum, 1970, p. 17 (London: Ann Arbor)
- (5) Latysh, G.N., Chernyak, A.S., & Khomutnikov, V.A., Nauch. Tr. Irtutsk, Nauch.-Issled. Inst. Redk. Tsvet. Metal, 1972, 27, 146

Fig. 1. Influence of sulphuric acid concentration on the extraction of niobium and tantalum by a 7,5 vol% Alamine 336 in Solvesso 100.

0,08M Nb, 0,0045M Ta, 0,081M F⁻, 0,16M H₂O₂.

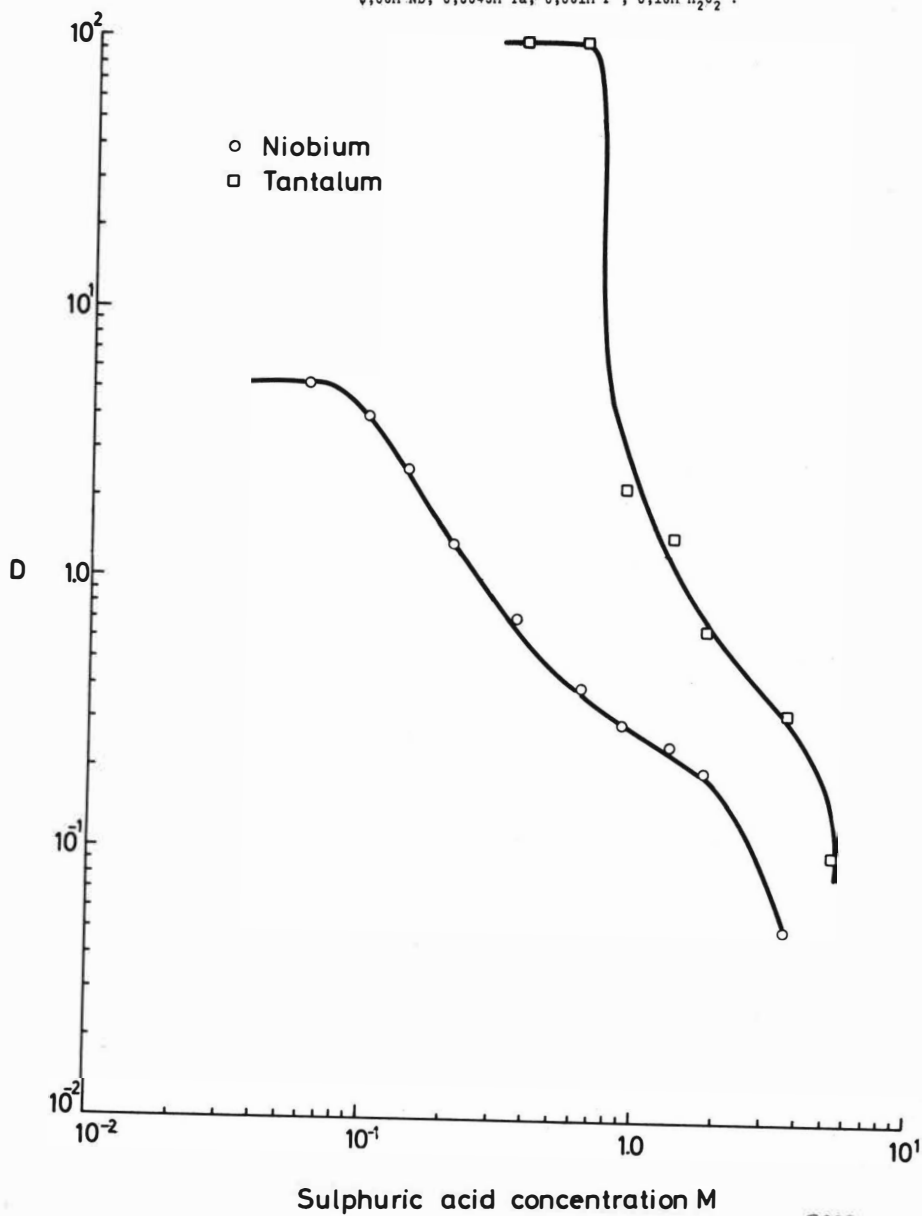


Fig. 2. Influence of hydrogen peroxide on the extraction of niobium and tantalum by a 7,5 vol% Alamine 336 in Solvesso 100.

0,081M Nb, 0,0045 Ta, 0,081M F⁻, 1,8M H₂SO₄ .

○ Niobium

□ Tantalum

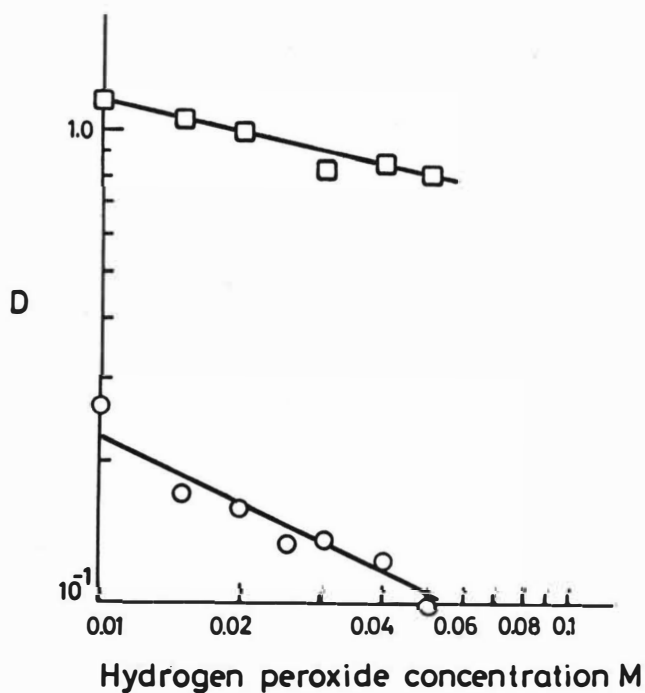


Fig. 3. Influence of fluoride concentration on the extraction of niobium and tantalum by a 7,5 vol% Alamine 336 in Solvesso 100.

0,081M Nb, 0,0045M Ta, 0,16M H_2O_2 , 1,8M H_2SO_4 .

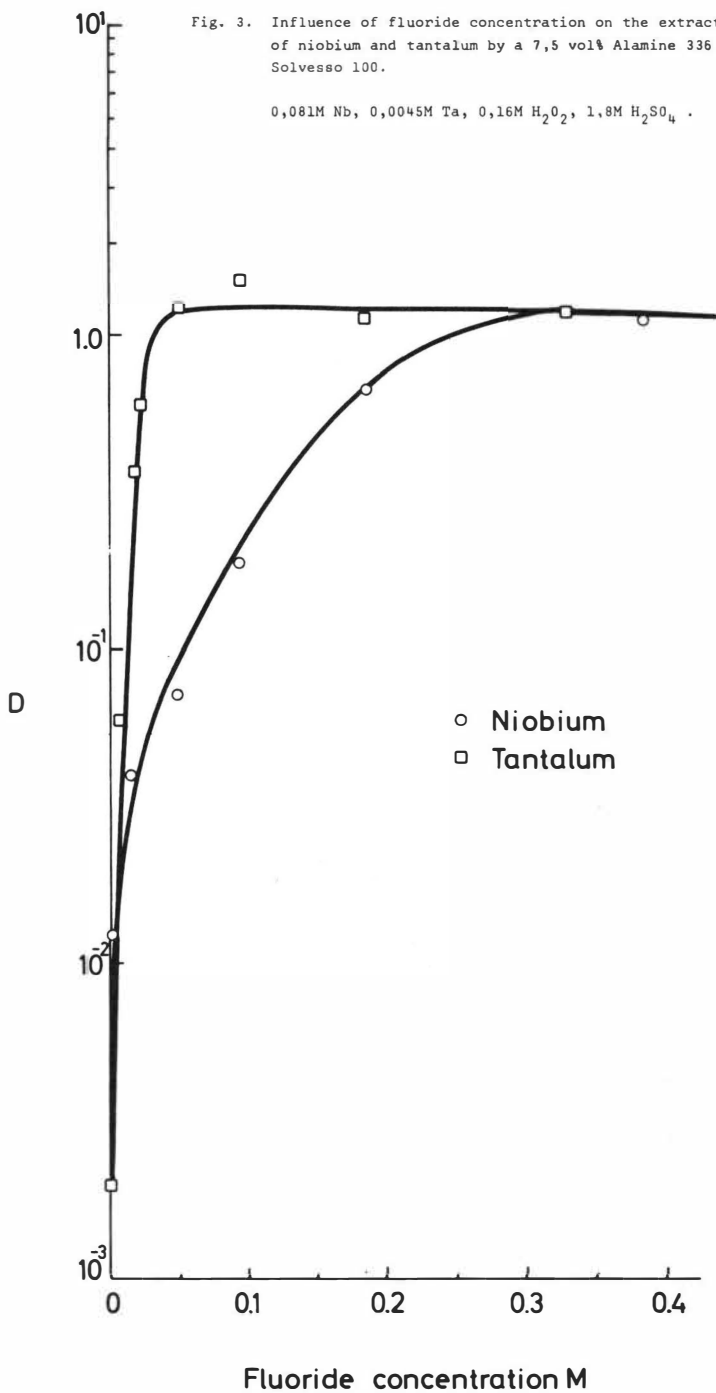


Fig. 4. Influence of amine concentration on the extraction of niobium and tantalum by a Alamine 336 solution in Solvesso 100.

0,081M Nb, 0,0045M Ta, 0,16M H_2O_2 , 0,081M F^- , 1,8M H_2SO_4

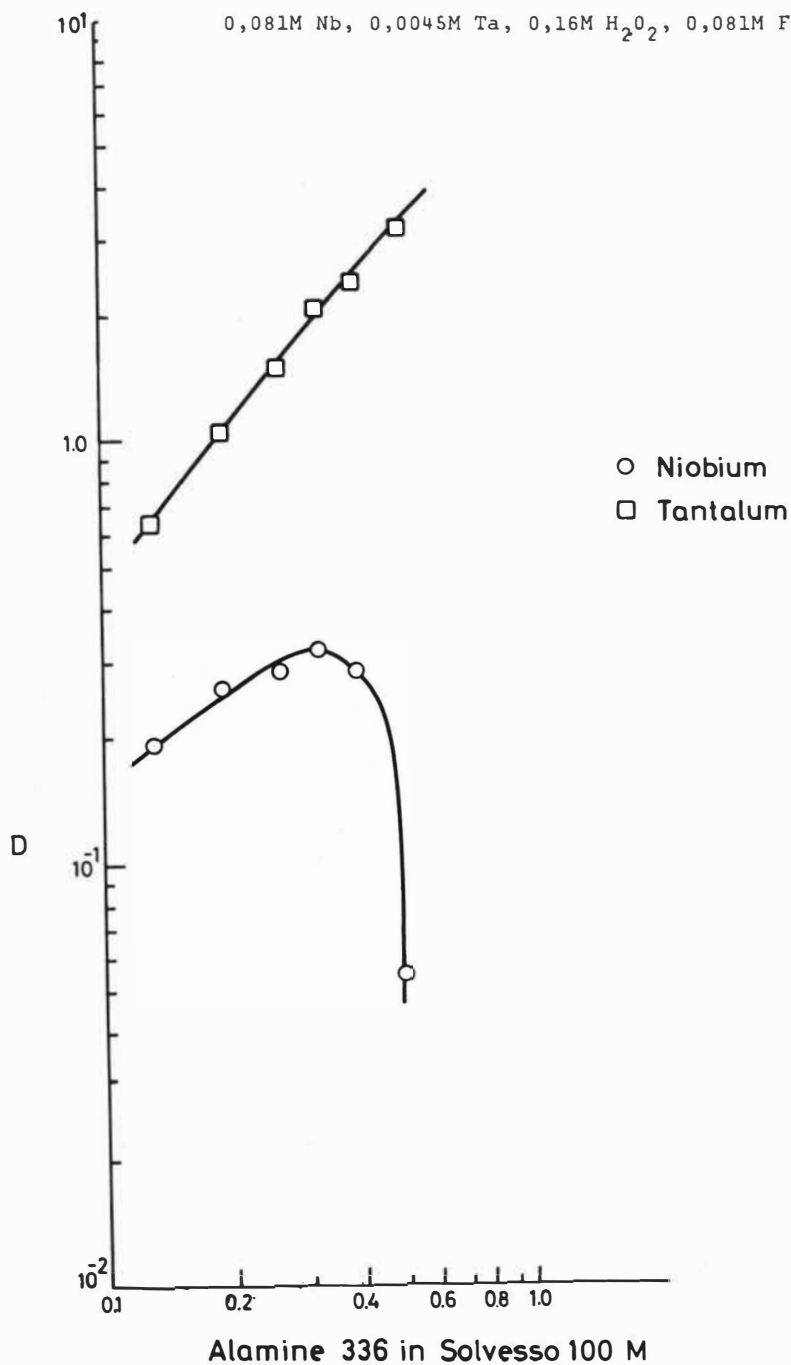
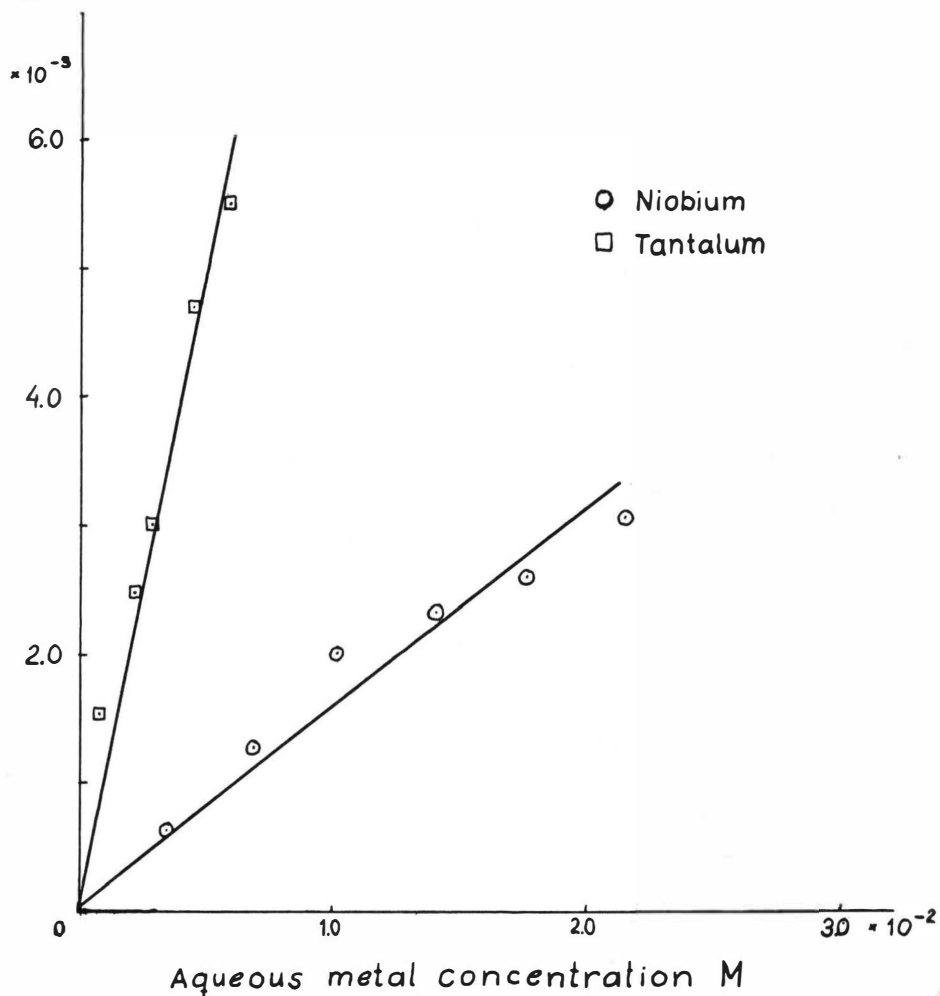


Fig. 5. Influence of metal concentration on the extraction of niobium and tantalum by a 7,5 vol% Alamime 336 in Solvesso 100.

0,081M F^- , 0,16M H_2O_2 , 1,8M H_2SO_4

Organic metal concentration M



THE STATE OF NIOBIUM WHEN EXTRACTED FROM SOLUTIONS
OF SULPHURIC AND HYDROCHLORIC ACIDS.

Yu.G. Frolov, A.F. Morgunov, N.A. Soldatenkova
(D.I. Mendeleev Institute of Chemical Technology, Moscow, USSR)

The state of niobium in organic extracts (diisoamyl methylphosphonate and TBP) and in solutions of sulphuric and hydrochloric acids in equilibrium with them is investigated.

It is ascertained that in solutions in the course of time a state of equilibrium is established between extractable monomeric and highly associated nonextractable forms of niobium. It has been found that there exists a quantitative dependence of the concentration of the monomeric form on the composition of an aqueous solution,

The extraction from solutions of sulphuric acid is shown by means of extracting, electrometric and spectroscopic methods and with the help of chemical analysis to be accounted for by the formation of solvated complex acids $H[NbO(OH)_2SO_4]$ and from solutions of hydrochloric acid - by the formation of $H[NbO(OH)Cl_3]$ and $H[NbOCl_4]$.

The state of niobium in solutions of inorganic acids largely determines the behaviour of this element in the extraction processes. It is found by the method of dialyses¹ that niobium in solutions of sulphuric and hydrochloric acids has a tendency to give polymeric forms. As a result of this process the decrease in the distribution coefficient of niobium with the increase of its concentration in solutions of sulphur² and hydrochloric³ acids was observed and the deterioration of the extractability of niobium from solutions of hydrochloric acid depending on the ageing of the aqueous phase was also noted⁴. In the absence of polymerization, niobium in solutions of sulphuric acid existed in different forms^{5,6}: $NbO(OH)_3$,

$\text{NbO}(\text{OH})_2^+$, $\text{NbO}(\text{OH})_2\text{SO}_4^-$, $\text{NbO}(\text{SO}_4)_2^-$. The state of niobium in an organic phase produced by extraction from solutions of sulphuric acid has not been sufficiently investigated. On the basis of the dependence of the distribution coefficient on the concentration of sulphuric acid and on the concentration of the extracting agent, the compound $\text{H}_5\text{Nb}(\text{SO}_4)_5$. TBP is supposed to be extracted from 4 - 7M H_2SO_4 and at a higher acidity - the compound $[\text{TBP H}][\text{NbO}_2\text{SO}_4 \cdot \text{TBP}]$. In another work² the compound $\text{HNbO}(\text{SO}_4)_2$. TBP is supposed to exist in an organic phase. Trioctylamine is found to extract $\text{NbO}(\text{SO}_4)_2^-$.

The extraction of niobium from solutions of hydrochloric acid has been investigated in greater details. There are, however, contradictory data concerning the composition of compounds in an organic phase even while extracting by such a widely used reagent as TBP. According to some authors^{8,9} complex acids HNbOC_4 , $\text{H}_2\text{NbO}(\text{OH})\text{C}_4$, H_2NbOC_5 are extracted, other authors¹⁰ believe compounds NbOC_3 , $\text{NbO}(\text{OH})\text{C}_2$ to exist in an organic phase.

In the present work the authors have investigated the state of niobium in solutions of sulphuric and hydrochloric acids by the method of extraction. The state and the composition of compounds formed in organic solutions have also been investigated.

Solutions of niobium in sulphuric acid labelled with isotope ^{95}Nb were prepared by dissolving a definite amount of Nb_2O_5 when heated in the mixture of hydrofluoric and concentrated sulphuric acids followed by the removal of HF by evaporation. The resulting solution of niobium in concentrated sulphuric acid was diluted with water and cooled with ice up to the formation of the desired concentration of H_2SO_4 and after that, the time required for preparing the solution was recorded.

Solutions in hydrochloric acid were prepared by dissolving freshly precipitated niobium hydroxide containing ^{95}Nb in concentrated hydrochloric acid then heated on a water bath, periodically cooling and saturating the solution with gaseous HCl . A portion of the resulting solution was mixed with dilute hydrochloric acid to give the desired concentrations of HCl and niobium and after that, the time required for preparing the solution was also recorded. In some experiments solutions of HbCl_5 in hydrochloric acid were used. When the isotope ^{95}Nb was used carrier-free- the concentration of niobium in solutions amounted to about 10^{-9} g-at/1. Distribution coefficients (α) were determined in terms of γ -activity of organic and aqueous phases. In some solutions the niobium content was found by the gravimetric method. Diisobutyl methylphosphonate (DiAM'P and TBP had been preliminary purified and the admixtures of alkylphosphoric acids had been removed. After that, DiAM'P and TBP were distilled in vacuum.

The formation of polynuclear compounds of niobium affects in a considerable degree its extraction with such neutral phosphoorganic compounds as DiAM'P and TBP.

Fig.1 shows the dependencies of the distribution coefficients of niobium on the time (t) for which the solutions containing $6\text{M H}_2\text{SO}_4$ were allowed to stand and different initial amounts of niobium.

When the niobium content in solutions is low - from 10^{-9} to 10^{-3} g-at/1 the distribution coefficient does not depend either on the time the solutions were allowed to stand or on the time of shaking the phases which varied from 5 seconds to 5 minutes (the time of separation in the process of centrifugation amounted to about 5 seconds). The values of α in the case of extraction coincide with the values found on re-extracting niobium from the organic phase 6M with the solution of H_2SO_4 ($\alpha=40$). This is evidence for the monomeric state of niobium in these solutions and of practically an immediate establishment of equilibrium (a few seconds of shaking are sufficient).

At a higher concentration of niobium the decrease of α with the increase of the initial concentration of Nb and of the time the solution was allowed to stand is observed, this indicates the formation of a nonextractable polymeric form of niobium. During the time of extracting (1 min), an equilibrium distribution of the monomeric form is established, but the polymeric form does not undergo any appreciable destruction. Thus for a solution, containing $3 \cdot 10^{-2}$ g/at/1 of Nb and allowed to stand for 3 days, the distribution coefficient changed from 0.42 to 0.54 on increasing the time of extraction from 1 to 15 minutes.

In organic solutions the extracted compound of niobium is in a monomeric state when the concentration of Nb_o is from 10^{-9} to 0.13 g-at/1. The distribution coefficient on re-extracting in 6M H_2SO_4 for the above mentioned concentrations is constant ($\alpha = 40$) and does not change when these organic solutions are allowed to stand for several days.

It is possible to calculate the concentration of the monomeric form of niobium in the initial aqueous solution - Nb_M from the values of distribution coefficient of the monomeric form of niobium α_o and from the distribution coefficient in the presence of polymeric forms - α .

For $V_o = V_w$ we have

$$\alpha = [Nb_o] / ([Nb] - [Nb_o]) \quad \text{and} \quad \alpha_o = [Nb]_o / ([Nb]_M - [Nb]_o),$$

where

Nb - total initial concentration of niobium in an aqueous solution

Nb_o - equilibrium concentration in an organic phase,

After transformation we get:

$$[Nb]_M = [Nb] \left[\frac{\alpha(1 + \alpha_o)}{\alpha_o(1 + \alpha)} \right]$$

If we assume that the niobium in the concentrated sulphuric acid to be in a monomeric state, an abrupt decrease of α and consequently of $[\text{Nb}]_M$ occurs both in the process of preparing dilute H_2SO_4 solution and during the first minutes of the time for which the solutions is allowed to stand. After 3 hours the concentration of the monomeric form amounts to (I.I-I.2). 10^{-2} g-at/1 with the total content of niobium from $2 \cdot 10^{-2}$ to $6 \cdot 10^{-2}$ g-at/1 in 6M H_2SO_4 . With the further increase of t the value of $[\text{Nb}]_M$ does not depend on the total concentration of Nb and asymptotically approaches $7.7 \cdot 10^{-3}$ g-at/1 (t=65 days).

The concentration of the monomeric form of niobium established in the course of time in the solution in the presence of the polymeric form increases with the increase of the concentration of sulphuric acid (table 1).

Table 1 The concentration of the monomeric form of niobium in solutions of sulphuric acid.

(extraction with 50% DiAM'P in C_6H_6 ;
extraction with 30% DiAM'P - *)

(H_2SO_4) , M	(Nb) , g-at/1	t, days	α	$(\text{Nb})_M$, g-at/1
3.0	10^{-9}	50	14.0 (α_0)	
	$1.0 \cdot 10^{-3}$		1.42	$6.2 \cdot 10^{-4}$
	$2.8 \cdot 10^{-3}$		0.22	$5.4 \cdot 10^{-4}$
	$9.2 \cdot 10^{-3}$		0.055	$5.1 \cdot 10^{-4}$
	$2.7 \cdot 10^{-2}$		0.022	$5.3 \cdot 10^{-4}$
4.0	10^{-9} - 10^{-3}	50	32 (α_0)	
	$3.0 \cdot 10^{-3}$		0.90	$1.46 \cdot 10^{-3}$
	$9.6 \cdot 10^{-3}$		0.153	$1.31 \cdot 10^{-3}$
	$1.9 \cdot 10^{-2}$		0.063	$1.25 \cdot 10^{-3}$
	$3.6 \cdot 10^{-2}$		0.038	$1.36 \cdot 10^{-3}$
5.0	10^{-9} - 10^{-3}	65	40 (α_0)	
	0.02		0.59	$7.61 \cdot 10^{-3}$
	0.03		0.324	$7.53 \cdot 10^{-3}$
	0.04		0.237	$7.86 \cdot 10^{-3}$
	0.06		0.146	$7.85 \cdot 10^{-3}$
6.0	10^{-9}	20	14 (α_0)*	
	0.05		1.58	$3.3 \cdot 10^{-2}$
	0.07		0.66	$3.0 \cdot 10^{-2}$
	0.10		0.41	$3.1 \cdot 10^{-2}$
9.0	10^{-9}	10	70 (α_0)*	
	0.135		1.54	0.082

The increase of acidity of an aqueous solution results in the destruction of the polymeric forms. Fig. 2 shows the dependence of $[Nb]_M$ on t in a solution, containing 4M H_2SO_4 and $3 \cdot 10^{-2}$ g-at/1 of niobium (curve 1). The acidification of the solution after two hours (curve 2) and after 22 hours (curve 3) to 6M H_2SO_4 (total concentration of niobium changing from $2 \cdot 10^{-2}$ g-at/1) results in the increase of the concentration of the monomeric form. In the course of several days $[Nb]_M$ was equal to $7.4 \cdot 10^{-3}$ g-at/1, which approaches the value, found before. It is obvious that in solutions of sulphuric acid an equilibrium state is gradually established between monomeric and polymeric forms.

Similarly the state of niobium in solutions of hydrochloric acid has been investigated by the extraction method. Microamounts of niobium (10^{-9} g-at/1) in a wide range of acidity ($[HCl] = 3 - 11.3$ M) of aqueous solution, are found to be in the monomeric state and the equilibrium in the process of extraction is established during several seconds when diheptyl-sulphoxide (DHSO), DiAM'P and TBP are used as extracting agents. In the case of macroamounts of niobium a decrease of the distribution coefficient with increasing the initial concentration of niobium and the time allowed the initial aqueous solutions to stand is observed. The results of the experiments on the extraction of niobium with solutions of DHSO and DiAM'P from solutions of hydrochloric acid allowed to stand for 10 days are given in Table 2. The time of shaking the phases was 1 minute. During this time the monomeric form of niobium is practically completely extracted into the organic phase from 7-9 M HCl, but the polymeric form does not undergo any appreciable destruction. The values of Nb_M , calculated according to the formula $[Nb]_M = [Nb] \frac{\alpha}{(1+\alpha)}$ at the constant concentration of HCl only increase up to a certain value with increasing the total content of niobium.

Thus in solutions of sulphuric and hydrochloric acids allowed to stand for a certain time the dependence of $[Nb]_M$ on the total concentration of the metal is absent.

Table 2. Concentration of the monomeric form of niobium in solutions of hydrochloric acid.

t = 10 days

(extraction with 0.1M DMSO in benzene;

extraction with 0.04 M DiAM'P in CS_2)

$[HCl], M$	$Nb \cdot 10^3, g-at/1$	α	$Nb_{II} \cdot 10^4, g-at/1$
7.0	0.2	1.70	1.3
	1.0	0.14	1.3
	2.0	0.065	1.2
	5.0	0.038*	1.8
8.0	0.2	76	2.0
	0.5	3.34	4.0
	4.0	0.098	5.6
	10.0	0.043*	4.6
8.7	0.2	300	2.0
	4.0	0.195	6.6
	5.0	0.162*	7.0
	10.0	0.100*	9.0
9.5	1.0	500	10
	3.0	2.27	21
	4.0	1.14	21
	5.2	0.63	23

This does not permit one to calculate polymerization constants and is an evidence of the formation of the large associations, the large aggregates are colloidal particles which are nonextractable.

As has already been mentioned the niobium compound extracted with benzene solutions of DiAM'P is mononuclear. By means of a chemical analysis it has been found that in the organic phase, in equilibrium with 3.9M H_2SO_4 , about 1.5 mole of SO_4^{2-} is bound with 1g-at of Nb. Hence it is possible to suggest the presence of two niobium compounds, containing in their composition, one and two SO_4^{2-} groups respectively.

Organic extracts, in which dichloroethane was used as a diluent, are electroconductive. Conductivity increases with the increase of Nb_0 , which indicates the dissociation of the extracted compound. The increase of the amount of separately extracted sulphuric acid results in the decrease of the dissociation of the concentration of the total hydrogen ion. A study of electromigration of niobium in organic solutions using the method described in work¹¹, showed niobium to enter into the composition of the negatively charged ions. Thus, it is probable, that complex acids $H [NbO(OH)_2SO_4]$ and $H [NbO(SO_4)_2]$ are extracted into the organic phase from solutions of sulphuric acid. The extent of their solvation, found from the dependences of the distribution coefficient of microamounts of niobium on the concentration of DiAM'P is equal to 4.

In order to investigate the mechanism of niobium extraction from solutions of hydrochloric acid the spectrophotometric method was used. Absorption spectra of organic solutions containing niobium ($[Nb] = 10^{-2}$ g-at/1) in equilibrium with solutions of hydrochloric acid of different concentrations are given in Fig.3. An absorption band with the maximum of about 280nm which can be attributed to $NbOC1_4$ ion¹² is observed in the spectra of solutions produced by the extraction with undiluted TBP. To determine from the analytical data the ratio Cl:Nb in the compound in the process of extraction with TBP is rather difficult because of a large amount of coextracted hydrochloric acid. When TBP is saturated with niobium with the aid of a solution, containing 0.4 g-at/1 of Nb in 11.6M HCl the given ratio is 2.4 and there is a band with the maximum about 265 nm in the spectrum. Extracts containing 0.1M of TBP and 10^{-2} g-at/1 of niobium are also characterized by the absorption band 265 nm due to the presence of a compound with the number of chlorine ions coordinated with niobium less than four.

Both saturation of TBP with niobium and dilution of the former with CCl_4 results in the decrease of the amount of the extracted HCl in the organic phase. The compound $HNbOC1_4$ exists probably in the organic phase in the presence of a considerable excessive amount of hydrochloric acid. This is confirmed by the fact that diluting the extract containing 0.4 g-at/1 Nb with pure TBP 100 times results in the appearance of the absorption band 265 nm.

The presence of a sharp absorption band with the maximum 951 cm^{-1} in the infra-red spectra, which can be attributed to the NbO group,^{13,14} is an evidence of its presence in the extracted compounds.

When solutions containing 1 M TBP in dichloroethane and the extracted niobium from the concentrated HCl are allowed to stand in a closed vessel over solid $NaOH$ the ratio $C1:Nb$ in them reaches a constant value approaching 3 and there is an absorption band at 265 nm in the spectra. The conductivity in these solutions increases with the increase of the content of niobium and the latter migrates to the anode in the process of electrolysis. This gives us the grounds to assume the compound with the composition $C1:Nb=3$ to be a complex acid H
 $[NbO(OH)C1_3]$.

REFERENCES

1. Gridchina, G.I., Zh.neorg.Khim., 8, 634 (1963); II, 299 (1966)
2. Kusnetsova, N.N., Zh.analit.Khim., 23, 1435 (1968).
3. Mymrik N.A., Gibalo I.M., Westn. mosk.gosud. Univ., II, Khim., 12, 738 (1971).
4. Burkin A.R., Gidrometallurgia (Hydrometallurgy), Izd. "Metalurgia", Moscow, 243 (1971).
5. Babko A.K., Nabivanets B.I., Problemy sovremennoj khimii koordinatsionnykh soedinenij (Problems of modern chemistry coordination compounds), issue 2, Izd, Leningr.gosud.Univ., Leningrad (1968).
6. Masurenko L.M., Nabivanets B.I., Zh.neorg.Khim., 14, 3286 (1969).
7. Sobinkajeva N.M., Soinova N.A., Zh.Prinkl.Khim., 41, 1173 (1968)
8. Startsev V.N., Krylov E.I., Zh.neorg.Khim., 12, 526 (1967).
9. Startsev V.N., Sannikov Yu.I., Stroganov S.S., Krylov E.I., Zh.neorg.Khim., 13 1608 (1968).
10. Koltsov Yu.I., Korovin S.S., Petrov K.I. Zh.neorg.Khim., 14 1065 (1969).
11. Morgunov A.F., Fomin V.V., Zh.neorg.Khim., II, 223 (1965).
12. Kanzelmeyer I., Ryan I., Freund J., J.An.Chem.Soc., 78 3020 (1956).
13. Selbin J., J. Chem., Education 41, 86 (1964).
14. Clark R.J.H., Kepert D.L., Whisla R.S., J. Chem.Soc., 2077 (1955).

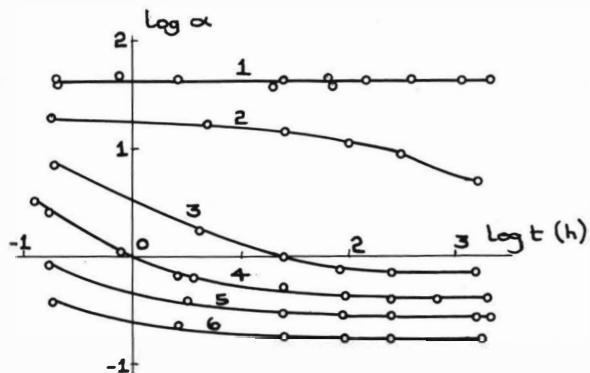


Fig. 1 The extraction of niobium from 6M H_2SO_4 with a mixture of DiAM'P and benzene (50%) depending on the time the solutions were allowed to stand. (Time of extracting 1 min., $V_0 = V_W$).

The initial concentration of niobium, g-at/l:

1 - 10^{-9} - 10^{-3} ; 2 - $1 \cdot 10^{-2}$; 3 - $2 \cdot 10^{-2}$;

4 - $3 \cdot 10^{-2}$; 5 - $4 \cdot 10^{-2}$; 6 - $6 \cdot 10^{-2}$.

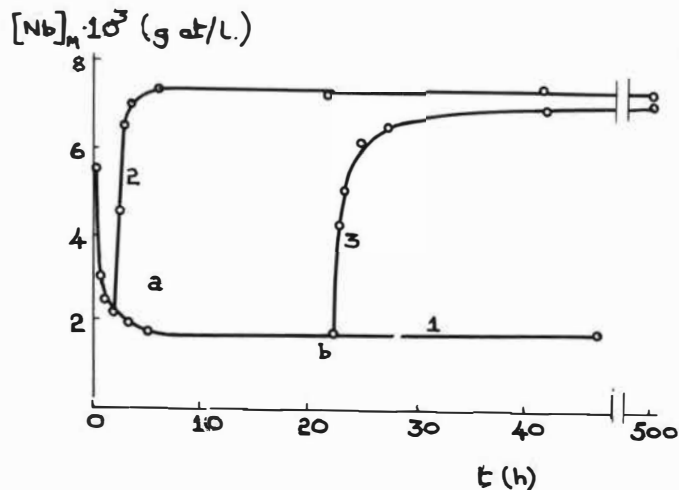


Fig. 2 The dependence of the concentration of the monomeric form of niobium on the time the solutions were allowed to stand.

1 - $[H_2SO_4] = 4M$, $[Nb] = 0.03$ g-at/l;

2,3 - the solution after acidification to $[H_2SO_4] = 6M$.
 $[Nb] = 0.02$ g-at/l; "a" and "b" acidification points.

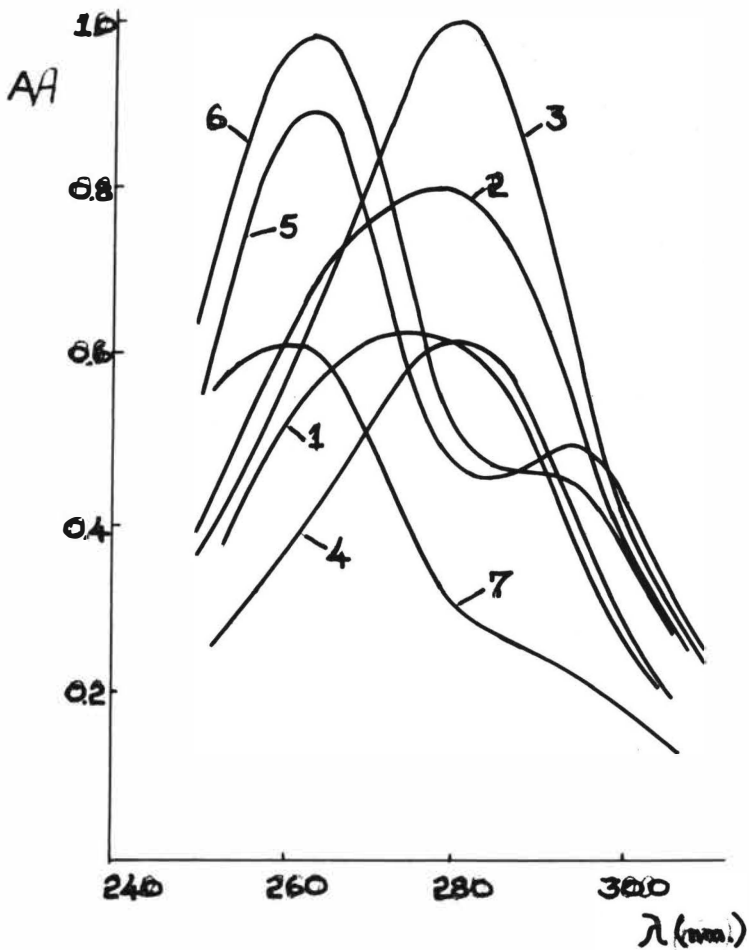


Fig.3 Absorption spectra of niobium extracts.
 ($[\text{Nb}]_0 = 10^{-2}$ g-at/l)
 100% TBP; $[\text{HCl}]$, M; 1 - 11.6; 2 - 9.8;
 3 - 8.1; 4 - 6.7.
 0.1 M TBP in CCl_4 , $[\text{HCl}]$, M;
 5 - 11.3; 6 - 9.0; 7 - 7.0.

THE EFFECT OF THE POLYMERIZATION OF ZIRCONIUM AND HAFNIUM
ON THEIR EXTRACTION BY DIFFERENT CLASSES OF ORGANIC COMPOUNDS

BY, G.A. YAGODIN, SINEFRIBOVA O.A. CHEKMAREV A.M.

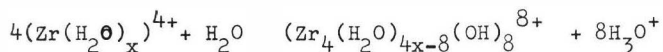
The Mendeleev Institute of Chemical Technology, Moscow, USSR.

Both monomer and polynuclear compounds of zirconium and hafnium are extracted by certain organic solvents. The nature of the extracted species depends on the nature of the extractant and the polynuclear compound formed. Under certain conditions, stable polynuclear compounds of zirconium and hafnium are formed and these are very stable under extremely severe conditions (acid high concentration, heating). When polynuclear compounds are extracted into the organic phase, the zirconium and hafnium separation factor decreases.

The existence of polynuclear compounds largely determines the chemical behaviour of zirconium and hafnium in aqueous and organic phases. In fact, many anions may serve as bridges in polynuclear associates, however, these bridges are preferentially formed by hydroxyl, oxygen and polydentate anions.

Polymerization of zirconium and hafnium hydrolyzed ions is explained by "o1" - compounds, i.e. complex compounds where metal atoms are linked with each other through OH^- bridging groups.

The appearance of o1 - bridges is assumed to be due to those water molecules that transfer directly into the first coordination sphere of the hydrolyzed ions, e.g. according to the reaction of the tetramer formation -



Increased temperature or prolonged storage of solutions results in changing "o1" groups into bridging oxi groups followed by water molecules abstraction from each pair of "o1" groups (an almost irreversible reaction).

In solutions of sulphates the zirconium and hafnium species are complicated by polynuclear compounds formation which are linked through sulphate bridges. These polynuclear compounds are formed in solutions of nonhydrolyzed zirconium and hafnium at H_2SO_4 concentrations higher than 2M. Dimer formation begins in solution with concentration $\approx 10^{-2}$ M.Me⁺⁴.

Polynuclear compound formation in solution is indicated by numerous phenomena observed in solvent extraction, ion exchange, electrometric titration, colorimetry, dialysis, etc. (Table 1 and 2).

The extraction behaviour is dependent on the nature of the polynuclear species and the extractant, thus:

1. A nonextractable polynuclear compound can transform into an extractable polynuclear compound resulting from equilibrium shift when monomer transfers into organic phase,
or
2. A Polynuclear compound is not extracted and is not transformed into monomer compound,
or
3. A polynuclear compound is extracted.

The existence of polynuclear compounds depends on their nature influences the separation of hafnium and zirconium during extraction.

Table 1

Concentration of Beginning of Polymerization and Zirconium Polymerization Factor in Mineral Acid Solutions

Acid	$[H^+]$ g-ion/l	ion strength, μ	Zirconium concentration M	Concentration of begin. polym	Polymer. factor	Research method	Reference
HNO ₃	5.5 - 7	-	6.8×10^{-5}	8.0×10^{-7}	2.0 - 3.0	coagulation	(1)
	0.002 - 6	-	$10^{-4} - 10^{-3}$	-	6.0	diffusion	(2)
	0.1	-	$10^{-3} - 10^{-2}$	-	2.5 - 7.0	comparative dialysis	(3)
	0.4	-	$10^{-3} - 2.5 \times 10^{-1}$	-	9.1	crioscopy	(4)
	0.7 - 1.0	-	$10^{-1} - 2.5 \times 10^{-1}$	-	7.7	crioscopy	(4)
	1.0	-	$10^{-3} - 10^{-2}$	5.0×10^{-4}	-	comparative dialysis	(3)
	1.0 - 2.0	2.0	10^{-1}	-	2.0	diffusion	(5)
	2.0	-	-	1.5×10^{-3}	-	comparative dialysis	(3)
	2.0	-	$10^{-3} - 10^{-1}$	-	1.0 - 7.0	comparative dialysis	(3)
HCl	0.08	2.0	5×10^{-2}	-	6.9 - 11.6	ultracentrifuging	(6)
	0.1	-	$10^{-3} - 10^{-2}$	-	2.5 - 7.0	dialysis	(3)
	0.1	2.0	5×10^{-2}	-	4.0 - 5.4	ultracentrifuging	(6)
	0.2	2.0	5×10^{-2}	-	4.2 - 5.5	- " -	(6,7)
	0.2 - 1.0	2.0	5×10^{-2}	-	3.0 - 4.0	- " -	(6,7)
	1.0	2.0	5×10^{-2}	-	3.5	- " -	(6)
	1.0 - 2.0	-	$10^{-4} - 10^{-3}$	10^{-3}	10	colorimetry	(3)
	2.0	-	$10^{-3} - 10^{-2}$	-	10 - 7.0	dialysis	(3)
	2.0	-	-	5×10^{-4}	-	electrometric titration	(5)
3.0	-	5×10^{-2}	-	2.1 - 2.7	ultracentrifuging	(6)	
2.0	-	$10^{-3} - 10^{-1}$	10^{-2}	2	extraction	(8)	
H ₂ SO ₄	pH=1	-	$10^{-4} - 10^{-2}$	10^{-3}	-	paper chromatography	(9)

Table 2

Hafnium Polymerization Factor in Mineral Acid Solutions

Acid	$[H^+]$ g-ion/l	ion strength, μ	Hafnium concentration M	Polym factor	Research Method	Reference
HNO ₃	0.11	2.0	10^{-3} - 10^{-1}	1.8 - 8.9	comparative dialysis	(10)
	1.0	2.0	10^{-3} - 10^{-1}	1.34 - 4.42	- " -	(10)
	2.0	2.0	10^{-3} - 10^{-1}	1.0 - 4.0	- " -	(10)
	2.0	2.0	10^{-1} - 2×10^{-1}	8.0 - 10.0	extraction	(11)
	6.3	-	10^{-1} - 2×10^{-1}	2.0	extraction	(11)
HCl	0.08	2.0	5×10^{-2}	5.7 - 7.1	Ultracentrifuging	(12)
	0.11	2.0	10^{-3} - 10^{-1}	1.8 - 8.9	Comp. dialysis	(10)
	0.2 - 2.0	2.0	5×10^{-2}	3.0	Ultracentrifuging	(12)
	1.0	-	7.5×10^{-3} - 10^{-1}	3.0 - 4.0	Ultracentrifuging	(13)
	3.0	-	5×10^{-2}	2.0 - 2.4	Ultracentrifuging	(12)
	5.0	-	5×10^{-2}	1.2 - 1.8	Ultracentrifuging	(12)

In the case where the polynuclear state is not extracted but is in the state of equilibrium with monomer extractable forms formation of polynuclear species in the aqueous phase results in metal-ion distribution constants which decrease as their concentration increase (resulting from an activity decrease).

This phenomenon is observed in hafnium and zirconium extraction from solutions of nitric acid with HNO_3 concentration 1M (fig.1 and 2). Polymer monomer equilibrium in these solutions is established quickly and exerts no influence on the time of the establishment of the extraction equilibrium.

The decrease of the distribution coefficient of one element in the presence of another one indicates hafnium and zirconium copolymerization in solution. (Table 3).

TABLE 3

Mutual zirconium and hafnium influence on the extraction of these elements. $\text{HNO}_3 = 2\text{M}$; extractant 0.8 M DAMP

Zr g/1 init.	Hf g/1 init.	D_{Zr}	D_{Hf}	D_{Zr} without Hf	D_{Hf} without Zr
10.91	7.14	0.197	0.008	0.472	0.050
7.32	14.25	0.222	0.007	0.620	0.041
3.64	21.42	0.305	0.006	1.120	0.032

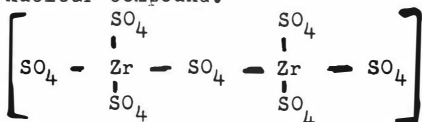
The decrease of free extractant concentration in this experiment, due to the extraction of one element, should not effect the distribution coefficient of the second element only a small quantity of metal transfers into the organic phase as compared to extractant concentration.

Hydrolytic polymerisation will influence zirconium and hafnium separation only in the case where one of the elements has a greater tendency to polymerization than the other one.

At the same time estimation of the monomer content of solutions of zirconium and hafnium at 1M and 2M HNO_3 in the concentration range of 10^{-4} - 10^{-3} M showed zirconium and hafnium to be equally polymerised (fig.3).. Monomer content in solution was estimated from metal content in organic phase and the monomer distribution coefficient was found under the metal concentration lower than concentration at the beginning of the polymerisation.

Therefore polymerisation should not affect zirconium and hafnium separation when extracted from nitric acid media into neutral phosphorganic compounds and hence metal concentration change will not considerably affect the separation factor which is confirmed by experiments¹⁴. Sulphato polynuclear compounds of unhydrolyzed zirconium, when extracted by amine, undergo rapid destruction and exert practically no influence on extraction kinetics.

Successive extraction by portions of amine solutions with little phase contact time results in practically complete metal exhaustion from the aqueous phase. For the extraction from a solution containing 1-1.5 M Zr^{4+} in the form of the following polynuclear compound.



the $\text{Zr} : \text{SO}_4$: amine ratio in the metal saturated organic phase ought to be 1 : 3, 5 : 3. Actually this ratio is equal to 1 : 4 : 4. This indicates the extraction of only monomer anions e.g. $\text{Zr}(\text{SO}_4)^{4-}$.

Under certain conditions zirconium and hafnium may form extremely stable polynuclear compounds that are not in the state of equilibrium with monomer forms¹⁵. These compounds are formed in solutions of nitric acid with high Zr and Hf concentration, (or ageing under low acidity conditions). After such a treatment of solutions it is impossible to extract part of the metal into TBP under any conditions. Subsequent acidity increase with long keeping does not result in noticeable extraction change (Table 4).

TABLE 4

Extraction dependence on (HNO_3) and time of solution keeping

(HNO_3) original	$(\text{Zr}) \text{ M}$ original	τ month	Amount of metal transferred into organic phase	Extractibility
2.0	1.18	0	0.698	59%
	1.17	3	0.644	55%
	1.17	6	0.644	55%
	0.42	9	0.244	58%
	0.42	12	0.252	58%
4.0	1.18	0	0.701	59%
	1.22	3	0.696	57%
	1.22	6	0.732	60%
	0.31	9	0.195	63%
	0.31	12	0.199	64%
	0.9 ^{x)}	0	0.480	53.2%
6.0	0.95	0	0.574	58.5%
	1.05	3	0.630	60%
	1.05	6	0.673	63%
	0.25	9	0.170	68%
	0.25	12	0.175	70%

x) hafnium

Extraction was carried on with three contact periods with 100% TBP at $V_{org} : V_{aq} = 3 : 1$.

The isotherm obtained in the experiment with extractable zirconium exhaustion from the solution containing stable polynuclear compounds is shown on fig.4.

Zirconium compounds which are not extracted by TBP are not extracted into much stronger neutral phosphorus organic compounds (DAMP, TBPO, TOPO). Stable polynuclear compounds have also been prepared under similar conditions in solutions of hydrochloric acid (Table 5).

TABLE 5

Metal Concentration and Hydrochloric acid Influence on the Polynuclear Stable Compounds Formation during Evaporations

Element	HCl initial M before vaporizing	Me initial before extraction	Content of non-extractable compounds	Note Extraction Conditions
Zr	0.5	0.242	52.5	Extraction from 6M HCl in 100 % TBP n = 3 $V_{org} : V_{aq} = 3 : 1$
	1.2	0.265	32.8	
	2.5	0.317	12.0	
	3.5	0.214	2.7	
Hf	0.65	0.253	39.5	

The resulting polynuclear compounds do not react to colorimetric indicators, nor are they sorbed by cation exchange (fig.5). They do not participate in isotope exchange reaction.

The presence of these compounds in the solution can be detected by the precipitate formation with sulfuric acid.

Infrared spectra of these compounds indicate no zirconyl groups but a Zr - O - Zr bond. Titration methods, in the presence of F-ion¹⁶⁻¹⁷, showed no OH - groups.

The polymerization factor of polynuclear stable compounds determined by dialysis through cellophane membranes proved to be the multiple 4.

Polynuclear stable compounds exert a salting-out action on zirconium monomer extraction (fig.6). At the same time Zr and Hf when extracted have separation factors which are not affected by the presence of polynuclear stable compounds since synthesis of these compounds with tracer¹⁸¹ Hf show zirconium and hafnium to have equal tendency to form these compounds.

DISCUSSION

For years zirconium and hafnium have been recognised to be extracted by various extracting agents but only in the form of monomer compounds. However, later investigations showed that under specific conditions polynuclear compounds bound by both hydroxyl and sulphate bridges may transfer into organic phase.

For example, Korovin, Apraksin et al¹⁸ found that when aqueous solution has little acid and a large amount of lithium nitrate and repeated contacts are made with new portions of 100% TBP with $V_{org} : V_{aq} = 1 : 10$ polynuclear zirconium, compounds with OH : Zr ratio = 1:2 transfer into the organic phase. The authors have used α -oxychloride $ZrOC1_2 \cdot 8H_2O$ as an initial compound. Chlorine-ion is extracted in a small extent.

Zirconium and hafnium possessing relatively equal tendency for hydrolytic polymerization, one should not expect Zr and Hf separation to take place in case of polymer compounds extraction. Experiments conducted in our laboratory have confirmed this assumption. (Table 6).

TABLE 6

Distribution of Zr and Hf between 7 M LiNO_3 solution and 100% TBP. $V_{\text{org}} : V_{\text{aq}} = 1 : 3$. Initial substance $\text{ZrOC1}_2 \cdot 8\text{H}_2\text{O}$ with 1.5% Hf.

NN contact	(Me)aq.	(Me)org.	D_{Zr}	D_{Hf}	S
1	174.1	171.7	0.99	1.00	0.99
2	145.1	177.1	1.22	1.08	1.13
3	126.9	182.5	1.44	1.14	1.35
4	102.3	188.3	1.84	1.61	1.14
5	83.5	208.6	2.47	1.83	1.35
6	70.3	131.2	1.86	2.52	0.74
7	60.5	78.3	1.29	1.24	1.04
8	58.7	59.7	1.01	0.86	1.17

The presence of polymer compounds in organic phase may be expected in the extraction of Zr and Hf thiocyanate complexes into neutral phosphorus - organic compounds since thiocyanate complex extraction is performed as a rule from weak acid solutions, hydrolyzed compounds transferring into the organic phase.

This research ¹⁹ shows that in case of counter-current extraction of Zr and Hf thiocyanate complexes the stage by stage separation factor sharply falls and thus is likely to be due to copolymer extraction.

Table 7

Zr and Hf Extraction in TBP from various solutions. $[\text{HSCN}]_{\text{org.}} = 3.2\text{M}$,

$V_{\text{org.}} : V_{\text{aq.}} = 1 : 1$

Substance dissolved in HSCN	$[\text{MeO}_2]$ initial g/l	Organic phase analysis									D_{Hf}	D_{Zr}	S
		Concentration g-ion/l				Ratio							
		Zr	NCS	OH	$\sum (\text{OH} + \text{O})$	NCS:Zr	$\sum (\text{O} + \text{OH}):Zr$	OH:Zr	O:Zr	-			
$\text{ZrOCl}_2 \cdot 8\text{H}_2\text{O}$	44.8	0.233	0.460	0.457	0.457	1.97	1.96	1.96	-	2.80	1.84	1.52	
$\text{ZrO}_{0.5}(\text{OH})_3$	55.0	0.408	0.820	0.400	0.812	2.05	2.0	0.98	0.5	2.57	2.77	0.93	
$\text{ZrO}(\text{OH})_2$	44.8	0.318	0.640	0.063	0.622	3.02	1.96	0.20	0.88	2.70	2.15	1.28	
$\text{ZrO}_{1.5}(\text{OH})$	49.0	0.358	0.700	0.206	0.750	1.96	2.10	0.58	0.76	1.87	1.54	1.22	

Table 7 lists extraction results of thiocyanate compounds from solutions of different origin. The following substances dissolved in HSCN have been used as starting compounds: zirconium oxychloride (as a material where zirconium atoms are bound by hydroxyl groups);

β - $ZrO_{0.5}(OH)_3$ hydroxide (zirconium atoms are bound by both hydroxyl and oxogroups). γ - hydroxide $ZrO(OH)_2$ and δ - hydroxide $ZrO_{1.5}(OH)$ (zirconium atoms are bound mainly by oxogroups). After extraction the organic solution was analysed for Zr, SCH^- - and O content^{16,17}. The hafnium content in the zirconium compounds was the natural isotopic ratio. The hafnium distribution coefficient was determined radiometrically. The data listed in table 7 show Zr (Hf) thiocyanate complexes to be extracted both with hydroxyl and oxogroups only in the case of oxocompounds of these elements being present in the aqueous phase. Infrared spectra of extracts indicate Zr = O group in the organic phase which makes one suppose oxogroups to be present in the zirconium extractable complexes to form a bridging bond between two metal atoms.

Zirconium and hafnium separation in case of polynuclear compounds extraction should be only slight since along with Hf-O-Hf and Zr-O-Zr compounds there will also be Hf-O-Zr compounds among the extracted species.

In fact in the case of oxocompounds extraction, the Hf distribution coefficient (Hf is more easily extracted than Zr in this system) is observed to be somewhat lower and vice versa where the Zr distribution coefficient sharply increases at first and falls only when there is a great number of bridge - O - groups, because oxocompounds are extracted with more difficulty than are hydroxocompounds.

Presence of unhydrolyzed compounds with sulphate bridges in the aqueous phases decreases the separation factor (S) for amine extracted because of the greater tendency of zirconium to polymerize¹⁴, the zirconium sulphate activity coefficient decreases more rapidly than that of hafnium sulphate also resulting in the S value decrease. Under these conditions the proper selection of a compound preferentially extracting monomer hafnium will result in better separation.

However, polymerization is accompanied by S value decrease¹⁴ when nonhydrolyzed sulphates are extracted by di-2-ethyl-hexyl phosphoric acid. (HDEHP). This phenomenon may be explained by transfer of the dimer molecules into the organic phase without their destruction. Under these conditions it is only reasonable to suppose that the extraction constants for dimers of various compositions to change in the following order: $(\text{Hf})_2 > \text{Hf} - \text{Zr} > (\text{Zr})_2$.

Hafnium dimer, $(\text{Hf})_2$, formation is unlikely to be due to small hafnium concentration² in the mixture and Hf-Zr dimer transfer into organic phase will make separation poorer than that observed in monomer conditions.

Transfer of dimers with sulphate bridges is supported by the direct measurement of sulphate-ion distribution. In the extraction from sulphate solutions with tracer radioactive isotope³⁵S, organic phase activity depends on the zirconium concentration in the aqueous phase.

As one can see from table 8, SO_4 - group transfers into the organic phase when $(\text{Zr}^{4+})_{\text{aq}}$ equals $5 \cdot 10^{-3}$ M which coincides with the dimer formation boundary.

In the infrared spectrum of the extract obtained under conditions of zirconium dimerization bands appear at wavelengths in the range of 580-680 cm^{-1} . These bands may be related to valent ν_4 vibrations of SO_4 - group (fig. 7).

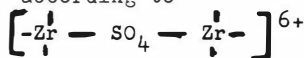
In this case, free HDEHP and monomer zirconium extract spectra practically coincide. Unfortunately in the region of SO_4 - group valent the vibrations in the wavelength range of 1000-1200 cm^{-1} are masked by HDEHP absorption bands.

TABLE 8.

Zirconium Extraction from solutions of Sulfuric acid with HDEHP in octane

initial (Zr)M solution H_2SO_4	(Zr)org.M	SO_4 org.M	$V_{\text{org.}} : V_{\text{aq.}}$
5.8×10^{-3}	1.12×10^{-1}	0	1 : 20
1.19×10^{-1}	1.16×10^{-1}	8×10^{-3}	1 : 1
2.74×10^{-1}	1.96×10^{-1}	8.8×10^{-2}	1 : 1
5.48×10^{-1}	2.32×10^{-1}	1.2×10^{-1}	1 : 1

Extraction from solutions containing dimerized metal ions results in the ratio $\text{Zr:HDEHP} = 1 : 3$ for the organic phase saturated with metal. This ratio may be determined by dimer complexes transfer into organic phase and this may be expressed according to



Besides this ratio realization in conditions of simultaneous monomer concentration growth makes it possible to suppose preferential dimer transfer into the organic phase. This preferential dimer transfer is related to their lower capacity (compared to monomer) to form anion complexes. Such an explanation of the observed regularities is in good agreement with the factor of preferential monomer complexes extraction with amines.

This explanation of the dependence of S on $(Me)_{aq}$ concentration for amine and HDEHP extraction makes one understand the cause of the sharp fall in the case of HDEHP extraction (fig.8). Indeed, in amine extraction, the initial dimers which are formed and which do not transfer into the organic phase should exert less effect on the S-value than in the case of the preferential dimer extraction with acidic phosphate.

Zirconium sulphate hydrolysis ceases in 2 M H_2SO_4 solution. When using solutions containing less than 2M H_2SO_4 there is possibility of hydrolyzed complexes extraction.

To solve the question of preferential extraction of hydrolyzed or unhydrolyzed ions we have studied the amine: zirconium ratio in the organic phase dependence on the amine salt concentration.

A typical extraction curve is given in fig.9. Amine concentration increases result in amine: zirconium ratio decreases which may be explained by the assumption about organic phase saturation with highly charged unhydrolyzed anions when extractant concentration is small. Organic phase saturation with unhydrolyzed anions is known to follow metal: amine ratio = 1:4. Saturation with hydrolyzed complexes leads to the decrease of this compound. Taking these data into account, the curves in fig.9 are explained by the assumption of better extraction of unhydrolyzed complexes. This also accounts for zirconium concentration dependence in organic phase on concentration in aqueous phase for weakly acidic solutions (fig.10). An increase in the total metal concentration results in increased equilibrium concentration of unhydrolyzed zirconium which is present here in sufficient amount to saturate all the extractant. A total concentration decrease does not provide sufficient concentration of unhydrolyzed complexes for complete amine saturation, the excess amount is then saturated with hydrolyzed anions, and the amine : Me ratio being decreased.

Bearing in mind one may state the organic phase to be saturated at all points of the descending branch of the curve in Fig.9, the minimum on the curve corresponds to maximum extractant concentration which is saturated under these conditions. It should be noted that the curve characterized in fig.10 depends on the ageing of the solution after dilution or after extraction of the first portion of the metal ion, since preferential removal of unhydrolyzed ions from the system requires some definite time, for equilibrium establishment in new conditions. The increased time of equilibrium establishment is connected with slow process of the destruction of hydrolyzed polynuclear zirconium complexes. Thus, presence of hydrolyzed polynuclear complexes in solution increases the time to reach equilibrium

So far the question of possible transfer of hydrolyzed anion complexes into organic phase when amine extracted has not been investigated. To study the possibility of hydrolyzed polymer anion complexes extraction we have conducted cryoscopic measurements; freezing temperature decrease of benzene solutions of tri-n-octylamine sulphates saturated with zirconium sulphate has been studied in different conditions. True molal concentration of the solution and the Vant-Hoff (N_{Cr}) coefficient has been calculated according to freezing temperature depression of the solutions.

$$N_{Cr} = \frac{M \text{ analytical}}{M \text{ true}}$$

where M analytical is amine analytical molal concentration and M true is molal concentration defined from freezing point of the solution. Zirconium concentration determination in the organic phase has been carried out by gravimetric method. On the basis of these data we have estimated N_{Zr} value equal to the number of amine moles per 1 mole of zirconium in organic phase.

Table 9

Extract Cryoscopy. Extraction Conditions: Solution of amine sulphate
in Benzene, $V_{\text{org.}} : V_{\text{aq.}} = 1 : 1$

Experimental run	TOA concentration volume %	Initial Aqueous Phase	N_{Cr}	N_{Zr}
A	2.5	0.225 M Zr^{4+} , 1 M H_2SO_4	4.31	3.75
	5.0		2.91	4.25
	7.5		2.81	4.01
B	2.5	0.786 M $\text{Zr}(\text{SO}_4)_2 \cdot 4\text{H}_2\text{O}$	3.58	3.62
	5.0	in water, 40 days keeping	3.11	3.82
	7.5	after dissolving	2.81	3.99
C	2.5	0.315 M $\text{Zr}(\text{SO}_4)_2 \cdot 4\text{H}_2\text{O}$	4.49	3.40
	5.0	in water, 46 days keeping	3.66	3.82
	7.5	hydrolyzed precipitate filtrated	3.24	3.17
D	2.5	solution 2.5 M $\text{Zr}(\text{SO}_4)_2 \cdot 4\text{H}_2\text{O}$	11.24	1.81
	5.0	in water (keeping for more	7.42	1.25
	7.5	than 40 days) is diluted before extraction with water up to 0.11M	4.07	1.56

For approximate consideration of dissolved water contribution we have determined benzene freezing point depression after contacting with 1M solution of H_2SO_4 . This acid solution has been chosen as the solution with approximately average water activity for all experiments. Naturally, this selection introduces some error in determining true solvate concentration.

The data obtained (considering dissolved water) are listed in Table 9.

The data in table 9 show N_{Cr} and N_{Zr} to be in good agreement in the three series A,B,C, i.e. in all cases where zirconium solutions may be considered in equilibrium. This fact proves the monomer nature of extractable compounds. It should be noted that in series A, zirconium sulphate is not hydrolyzed, in series B and C there are hydrolyzed complexes (and hydrolyzed polynuclear compounds as well, because the concentration at the beginning of the polymerization of hydrolyzed sulphate complexes may be taken equal to $10^{-3} - 10^{-4}$ M Zr). Quite different results have been obtained only for series D solutions where non equilibrium zirconium sulphate hydrolyzed solutions have been used. In this case N_{Zr} drops sharply (which agrees with the proposed extraction of the low charged hydrolyzed complexes, N_{Cr} being sharply increased. Bisulphate solutions in water are attended to by hydrolyzed polynuclear compound formation which do not stay permanently in the solution due to their unsaturated coordination. An example of such compound may be $Zr_3(OH)_4(SO_4)_6^{4-}$.

It is clear that the organic phase saturation with anions of this type according to anion exchange mechanism should give the following values.

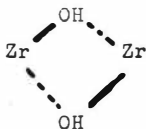
$$N_{Cr} = 4 \quad N_{Zr} = 1,33$$

As one can see from the investigation ²⁰ these anions exist in the solution for a short time and then become larger resulting fromolation process and sulphate bridges formation.

Large (equilibrium) polynuclear compounds possibly do not transfer into organic phase (or their extraction constant is small).

The fact that one equilibrium hydrolyzed polymers transfer into the organic phase is supported by the sharp increase of Fe^{3+} coextracted under conditions similar to those used in D series. When extracted from zirconium equilibrated sulphate solutions, Fe^{3+} does not practically transfer into the organic phase.

Infrared spectra of extracts obtained under conditions of equilibrated zirconium solutions do not show absorption bands usually attributed to Zr-O-Zr chains or



Thus, one may suppose polynuclear compounds of nonhydralyzed zirconium (hafnium) to be rapidly broken during the extraction process or to transfer into organic phase without being destroyed and this does not exert appreciable influence on the extraction kinetics. Their influence on separation is mainly determined by the extraction of one element or other in the system in question and is clearly manifested in the case of associates transferred into the organic phase.

Hydrolysed polymers of intermediate stability with ol-bridges as a rule, also tend to be quickly destroyed in the monomer forms extraction in sulphate systems is then somewhat slower.

Hydrolysed compounds transferred into organic phase also sharply decreases the separation factor.

Polynuclear complexes with oxobridges are not actually broken in the extraction process nor are they extracted; they exert no noticeable influence on the separation because both Zr and Hf are equal components of these polymers.

REFERENCES

1. Matijevic E, Mathal A, Kerrer M.J. Phys Chem. 66 (1962), 1799 .
2. Lister B., Mc.Donald L.J. Am. Chem. Soc. 74 (1952), 4315.
3. Babko A.E., Gridchina T.J. G. Neorg. him. 6 № 6, (1961), 1336
7 № 4 (1962), 889
4. Komarov E.V., Krilov V.N., Pushlenkov M.F.
J. Neorg. Him. 13 № 2 (1968), 467
5. Solovkin A.S., Tsvetkova Z.N. Uspehi himii, 31 № 11 (1962), 1394
6. Johnson T.S., Kraus K.A. J. Am. Chem. Soc. 78 (1956), 3937
7. Johnson T.S., Kraus K.A. Inorg. Synthesis 2 (1946)
8. G.A. Yagodin, A.M. Chekmarev, L.M. Vladimirova
Jurn. Neorg. him. 15, № 7 (1970), 1834
9. A.M. Chekmarev, G.A. Yagodin, L.M. Vladimirova
Dokladi AH SSSR, 183 № 1 (1970), 1968
10. Savenko N.F., Sheka I.A.
Ukrainsk. him. j. 34 , № 4 (1968), 309
11. Lebedeva E.N., Korovin S.S., Rozen A.M.
J. Neorg. him., № 7 (1964), 1744
12. Kraus K.A., Johnson I.S., J. Am. Soc. 75 (1953), 5769
13. Johnson I.S., Kraus K.A., Helmberg R.W. J. Am. Chem. Soc. 78 (1956), 26
14. Yagodin G.A., Sinegribova O.A., Checkmarev A.M.,
Proceedings of ISEC-71, p. 1124.
15. Kazak V.G., Sinegribova O.A., Yagodin G.A.
Trudi MXTI im. D.I. Mendeleev, 48, M (1968), 68
16. Zaitsev L.M., Bochkarev G.C.
Jurn. Neorg. himii, 7 (1962), 795
17. Zaitsev L.M., Pospelova L.A.
Jurn. Neorg. himii, 11 (1966), 1863
18. Kluchnikov V.M., Zaitsev L.M., Korovin S.S.,
Apraksin I.A.
Jurn. Neorg. himii, 17 (1972), 3030.
19. Pepelyaeva E.A., Sinegribova O.A., Shostenko N.A., Yagodin G.A.
Jurn. prikl. himii, 46, № 6 (1973), 1301.
20. Clearfield A. Rev. of Pure and Appl. Chem., 14 (1964), 91.

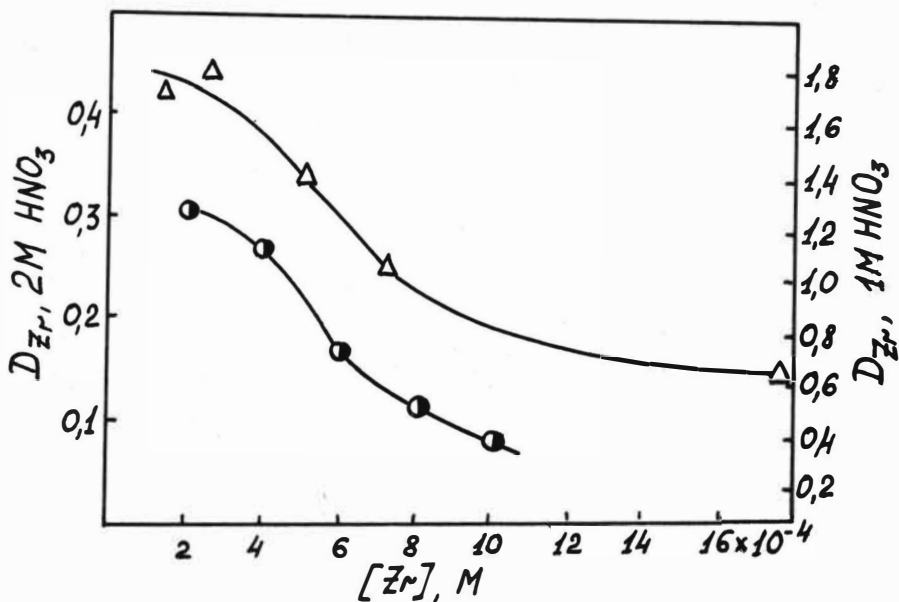


Fig.1 Zirconium distribution coefficient dependence on zirconium concentration in initial aqueous solution.

-○- 1 M HNO_3 ; extractant 20% DDAMP

-△- 2 M HNO_3 ; extractant 5% DAMP

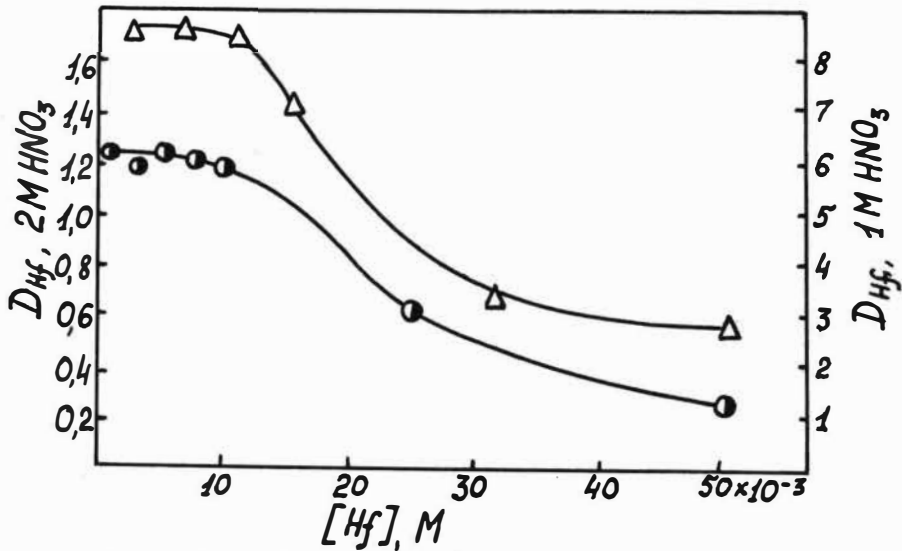


Fig.2 Hafnium distribution coefficient dependence on hafnium concentration in initial aqueous solution.

-○- 1 M HNO_3 ; extractant 20% DAMP

-△- 2 M HNO_3 ; extractant 15% DAMP

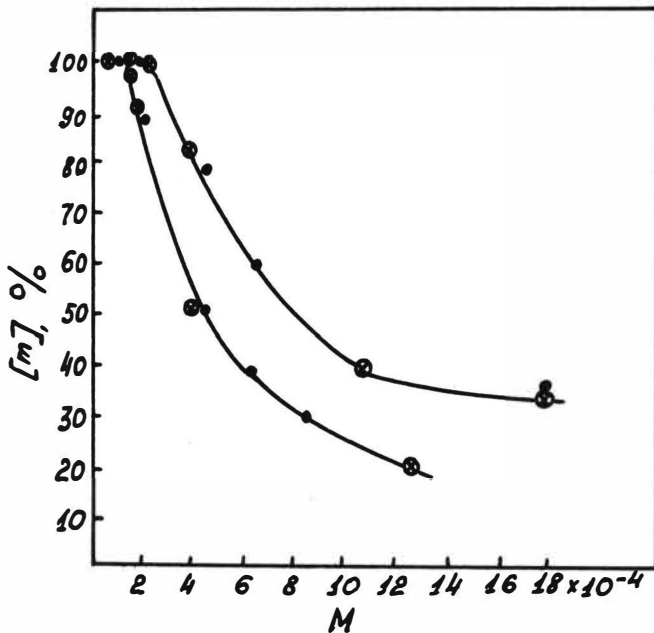


Fig.3 Monomer forms content in aqueous solution with different metal concentration.

●- zirconium

○- hafnium

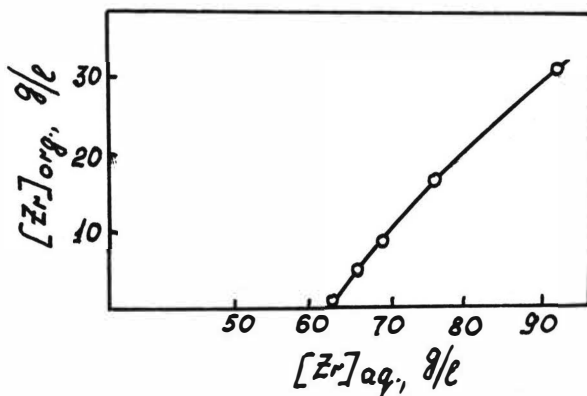


Fig.4 Extractable forms exhaustion from solution with 123 g/l zirconium concentration in 4 M.HNO₃
Extraction conditions: 100% TBP, V_{org.}: V_{aq.} = 3 : 1

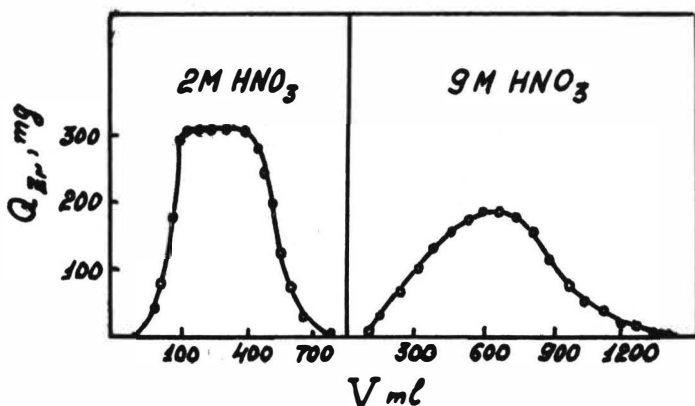


Fig.5 Separation chromatogram of extractable and nonextractable zirconium.

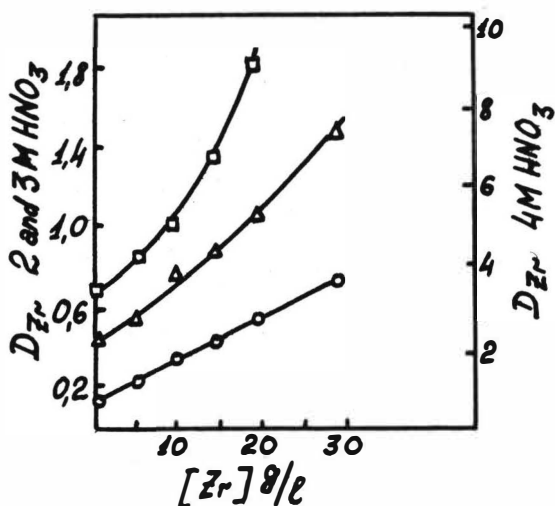


Fig.6 Stable polynuclear compounds influence on distribution coefficient of extractable zirconium

-○- 2 M HNO_3

-△- 3 M HNO_3

-□- 4 M HNO_3

Initial concentration of extractable zirconium 10 g/l.

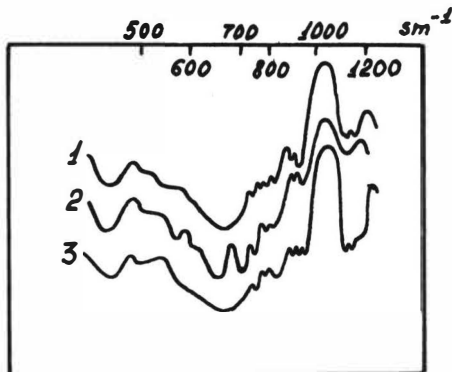


Fig. 7 Infra-red spectra of organic solutions absorption.

- 1 - HDEHP + Zr (Zr extraction from solution in 1 M . H₂SO₄ ; initial conc. Me⁺⁴ 0,005 M; V_{org.} : V_{aq} = 1 : 50)
- 2 - HDEHP + Zr (Zr extraction from solution in 1 M . H₂SO₄ ; initial conc. Me⁺⁴ 1,14 M V_{org.} : V_{aq.} 1 : 1)
- 3 - Pure HDEHP

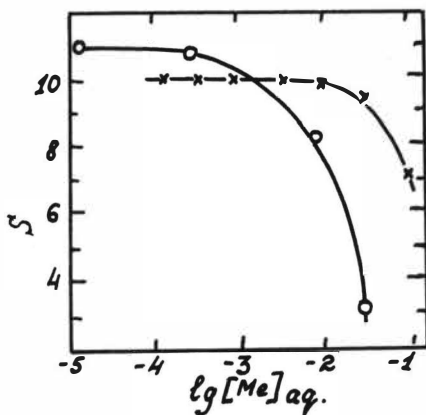


Fig. 8 Distribution coefficient dependence on metal concentration in aqueous phase during extraction.

- O - - HDEHP, H₂SO₄ = 1 M

S = D_{Hf}/D_{Zr}

- x - - tri-n-octylamine, H₂SO₄ = 1.5 M.

S = D_{Zr}/D_{Hf}

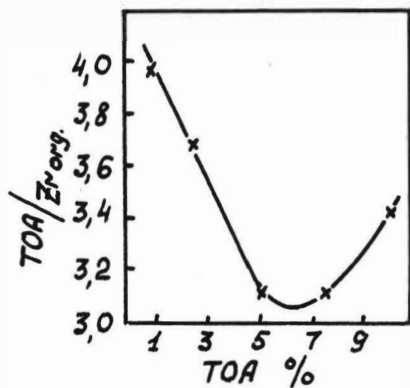


Fig. 9 Zirconium extraction by tri-n-octylamine in benzene from solution of Zr basic sulphate.

MeO₂ initial = 150 g/l in water

Zr : SO₄ ratio = 1 : 1,2

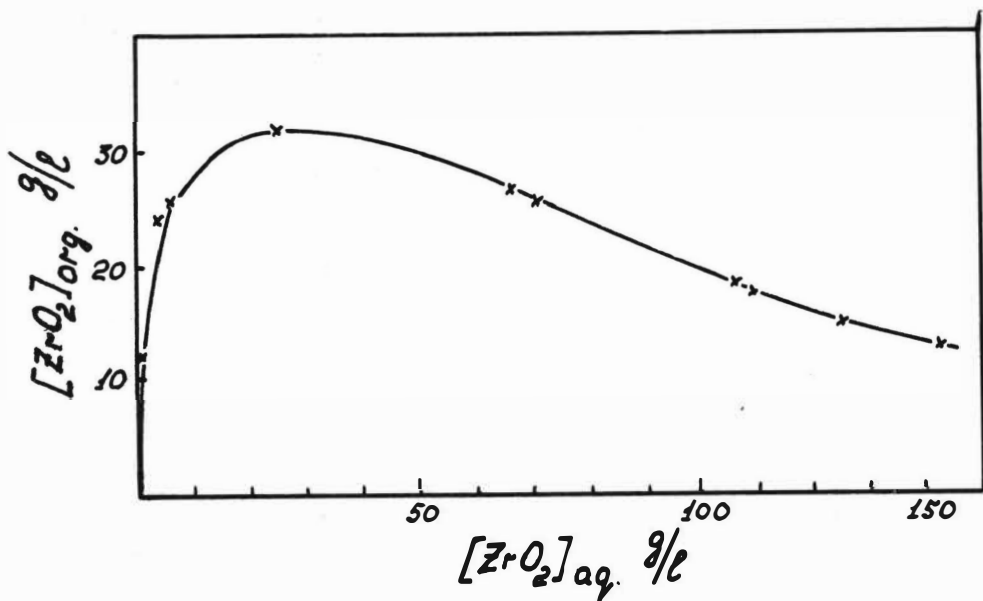


Fig. 10 Typical "isotherm" of Zr⁺⁴ extraction by tri-n-octylamine sulphate in benzene (30% volume) from Zr (SO₄)₂ · 4 H₂O solution in water.

SOLVENT EXTRACTION OF ZIRCONIUM AND HAFNIUM
WITH SOME TRIFUNCTIONAL PHOSPHINE OXIDES

P. Bronzan and H. Meider-Gorican, Institute Rudjer
Boskovic, Zagreb, Yugoslavia

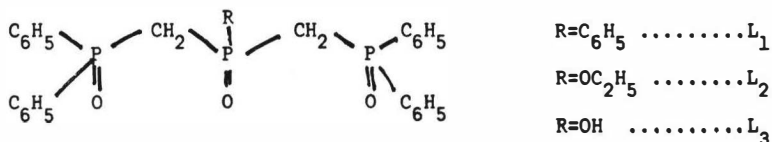
SYNOPSIS

The extraction of zirconium and hafnium from hydrochloric, perchloric and sulphuric acid solutions with $/(C_6H_5)_2(O)PCH_2/2$, $P(O)C_6H_5(L_1)$, $/(C_6H_5)_2(O)PCH_2/2P(O)OC_2H_5(L_2)$ and $/C_6H_5)_2(O)PCH_2/2P(O)OH(L_3)$ has been studied. The properties of the ligands and the formation of the complexes with zirconium and hafnium as well as with perchloric acid have been investigated. The influence of the electronegativity of the substituent, bound to the central phosphorus atom, on the extraction of zirconium and hafnium has been discussed. From alcoholic solutions of metal tetrachlorides adducts with the phosphine oxides corresponding to the formula $MeCl_n \cdot L_n$ ($Me = Zr$ or Hf , $L_n =$ ligand) have been isolated and characterized.

INTRODUCTION

In recent years the coordination properties of bifunctional phosphine oxides have been extensively studied¹⁻⁶. Contradictory conclusions regarding their properties and complex formation with different metals were derived³⁻⁷. Studies of the reaction of alkali metal and cupric halides with bisphosphine oxides showed that the substituent bound to the phosphorus atom has an inductive and mesomeric effect on the arrangement of the electron density on the oxygen from the $P=O$ group, which results in the ligands having different donor properties^{6,8,9}. The extraction and complex formation with transition metals has also been studied. Most often, the chelate formation through two oxygens has been proposed for these ligands¹⁰. The formation of ionic and nonionic species has been established^{1,2,11}.

Trifunctional phosphine oxides and their mono and dialkali metal salts have been synthesized recently¹². However there are reports on the behaviour of these compounds in solutions or their complex formation. In our investigations we used three different trifunctional phosphine oxides with different substituent groups bound to the central phosphorus atom:



The purpose was to determine the influence of the substituent on the extraction behaviour of the phosphine oxides and to determine the possible structure of zirconium and hafnium complexes in solutions and in the solid state.

EXPERIMENTAL

Reagents

Bis (diphenylphosphinyl)methyl/phenylphosphine oxide (L₁) bis (diphenylphosphinyl)methyl/phosphonic acid (L₃) and bis (diphenylphosphinyl)methyl/phosphinate (L₂) were prepared by the method described by Kabachnik et al¹². Radioactive ³²P labelled phosphine oxides were prepared by the same method using ³²PCL₃ (R.C.C., Amersham).

Chloroform (Merck p.a.) has been used in all extraction experiments as solvent without further purification. HCl, HClO₄ and H₂SO₄ (Merck p.a.) were used. Ethanol (Merck p.a.) was dried before use.

Stock solutions, distribution measurements and the separation of extracting species were carried out as described before¹³.

⁹⁵Zr solutions were prepared immediately before using, separating ⁹⁵Zr from ⁹⁵Nb with DOMPA¹⁵.

I.r. spectra were recorded in KBr and in chloroform solutions on a Perkin-Elmer spectrophotometer Model 257 in the region 6000 cm⁻¹-4000 cm⁻¹. Chloroform was used in the reference cell.

Molecular weights were determined by osmometric measurements with a Mehrolab Vapour Pressure Osmometer.

The concentration of the perchloric acid in the organic phase was determined by twophase titration.

RESULTS

Ligand properties

The distribution of the phosphine oxides between chloroform and 0.1M H⁺, /Na,H,ClO₄/= 1M and 4M HClO₄ aqueous solutions has been studied with special reference to the influence of the aqueous phase concentrations. The degree of extraction does not depend on the L₁ and L₂ concentration when 0.1M H⁺, /Na,H,ClO₄/=1M solutions are used but D values of L₃ increase with increasing concentration of the ligand. When the extraction was carried out from 4M HClO₄ solutions, a small increase of the D value with an increase of ligand concentration for all three ligands was observed. Osmometric measurements showed that the compounds L₁ and L₂ are monomeric in chloroform. A dimeric form of L₃ in chloroform solutions has been established. HCl and H₂SO₄ do not react with the phosphine oxides. The extraction data of HClO₄ into 4.10⁻²M L₁ chloroform solutions are given in Table 1. Similar results have been obtained for L₃ as a ligand. Because of the third phase formation and precipitation of a perchlorate complex of L₂, the extraction of HClO₄ with this ligand could not be investigated. The dependence of the ligand extraction on hydrogenion concentration has been studied.

The H^+ ion concentration was adjusted with a sodium acetate buffer. For L_1 no dependence on hydrogen ion concentration has been observed. The results obtained for L_2 and L_3 as ligands are given in Table 2.

Infrared spectra of the phosphine oxides in the solid state and in the chloroform solutions, and the spectra of the chloroform solutions of the ligands equilibrated with $HClO_4$, have been investigated. Spectra of L_3 in solid state, chloroform solutions of L_1 and L_3 , and chloroform solutions of L_1 and L_3 equilibrated with $HClO_4$ are shown in Fig.1. Spectra of L_1 in solid state and in chloroform solutions are the same. Absorption bands which appear at 1190 cm^{-1} and 1250 cm^{-1} in the spectra of L_1 and L_2 respectively, corresponding to the $P=O$ stretching of the central $P=O$ group, are absent in the spectra of the perchlorate complexes and L_3 chloroform solutions. A new absorption band at about 1160 cm^{-1} is due to the protonation of the oxygen of the central $P=O$ group. The absorption band corresponding to the $P=O$ stretching of the terminal $P=O$ groups remains unchanged at 1120 cm^{-1} . In the perchlorate complexes of the ligands the absorption band at 1090 cm^{-1} corresponding to the perchlorate group vibration is clearly resolved.

Zirconium and hafnium extraction studies.

The extraction of zirconium and hafnium has been studied from perchloric, hydrochloric and sulphuric acid solutions. Metal solutions (10^{-6} M) were used in all experiments, higher concentrated solutions have a tendency to hydrolyze with the formation of polynuclear species.

In Fig.2 the dependence of the Zr and Hf extraction from $4\text{ M } HClO_4$ and $4\text{ M } HCl$ aqueous solutions on the L_1 and L_2 concentration is represented. Extraction experiments carried out with L_3 as a ligand gave analogous results. High D values between 10^2 and 10^3 have been observed.

The extraction behaviour observed with 0.1M H_2SO_4 and 3M H_2SO_4 aqueous solutions, is given in Fig.3. Because of the low D values obtained for the extraction of Zr and Hf from 3M H_2SO_4 solutions with L_1 and L_2 , only the extraction studies with L_3 as ligand at high acid concentration are given. Depending on the ligand and the composition of the aqueous phase, the slopes of the curves, (given in Fig.2 and 3.) vary from one to three, but are mostly near to two. The initial ligand concentration in the organic phase is always plotted in the graphs. The deviation from the linearity present in the curves, obtained upon studying the extraction from perchlorate solutions, is due to the complex formation between perchloric acid and the ligands. The dependence of the Zr and Hf extraction on the H^+ ion concentration has been examined from perchlorate and sulphate solutions. No dependence of the extraction of Zr and Hf from perchlorate solutions on the H^+ ion concentration has been observed. Results obtained for the Zr and Hf extraction from sulphate solutions are given in Fig.4. When identical results have been obtained for Zr and Hf, only the results for one of the metals are shown. Fig.5. shows the dependence of the Zr and Hf extraction on the HSO_4^- ion concentration. In the experiments represented in Fig.4 and 5., $5.10^{-3} M L_1$, $1.10^{-2} M L_2$ and $1.10^{-4} M L_3$ chloroform solutions have been used. A decrease of D with an increase of H^+ and HSO_4^- ions has been observed.

Extracting species and chloride adducts.

Extracting species have been isolated from 4M $HClO_4$ and 4M HCl solutions. The extracting species were characterized by chemical analysis and i.r. spectra. In the species isolated from 4M HCl solutions, an excess of the free ligand was always present. I.r. spectra of the species isolated from 4M $HClO_4$ solutions show that in addition to the ligand metal complexes formed, complexes formed between perchloric acid and the phosphine oxides are also present.

Adducts of Zr and Hf tetrachlorides and ligands obtained from alcoholic solutions have also been isolated in form of white crystals. On the basis of elemental analysis and i.r. spectra their composition is $\text{MeCl}_4 \cdot L_n$ where Me-Zr and Hf and $L_n = L_1, L_2$ and L_3 . Calculated and (experimental) percentage for $\text{ZrCl}_4 / (\text{C}_6\text{H}_5)_2(\text{O})\text{PCH}_2/2\text{P}(\text{O})\text{C}_6\text{H}_5$: Zr:11.59 (12.07), P:11.80 (10.42); Cl:18.02 (18.20); C:48.83 (47.15); H:3.71 (4.16). Two characteristic P=O stretching bands at 1125 cm^{-1} and 1085^{-1} are present in the spectra of all compounds. The P-OC₂H₅ stretching vibration present in the spectra of L_2 at 1030 cm^{-1} remains unchanged in the spectra of the corresponding Zr and Hf complexes. Bands attributable to the M=O stretching mode or M-O-M vibrational mode were not found. Therefore formation of polynuclear species has to be excluded.

DISCUSSION

Molecular weight measurements in chloroform solutions show that L_1 and L_2 ($R = \text{C}_6\text{H}_5$ and OC_2H_5) are monomeric while L_3 ($R = \text{OH}$) is dimeric. One can assume that intermolecular bridges between OH and P=O groups are formed.

Hydrochloric and sulphuric acid do not react with the phosphine oxides, but one molecule of perchloric acid is usually bound to one molecule of the ligand. Oxygen from the central P=O group becomes protonated. Owing to their similarity, zirconium and hafnium phosphine oxides, complexes of identical type. The results show that zirconium compounds are more stable than the corresponding hafnium compounds. The lower stability of hafnium complexes is apparently connected with the somewhat greater size of the Hf^{4+} ion. Data reported in the literature suggest the presence of $\text{Me}(\text{OH})_3^+$, $\text{Me}(\text{OH})_2^{2+}$ and $\text{Me}(\text{OH})^{3+}$ hydroxocomplexes in perchloric acid solutions¹⁴. Based on the assumption that the solvation number is given by the slope of logarithmic plot of distribution ratio versus ligand concentration, solvation numbers two or three are more less always acceptable. Depending on the perchloric acid concentration $\text{Me}(\text{OH})_2(L_n)_m$ and $/\text{Me}(L_n)_m / (\text{ClO}_4)_4$ Me=Zr, Hf; $L_n = L_1, L_2$ or L_3 ; $m=2$ or 3) complex species are probably extracted into the organic phase.

Since the ν_3 vibration mode of the perchlorate ion is not split and appears as a single band at 1090 cm^{-1} in the spectra of the perchlorate extracting species it can be concluded that the ClO_4^- ion is not coordinated to the metal atom. From 4M HCl solutions $\text{MeCl}_4 \cdot 2\text{L}_1$, $\text{MeCl}_4 \cdot \text{L}_2$ and $\text{MeCl}_4 \cdot 2\text{L}_3$ adducts are extracted into chloroform. Curves obtained during the zirconium and hafnium sulphuric acid extraction studies indicate, that in chloroform, complexes are formed where one or two H^+ and HSO_4^- ions are released. At low acid concentration the formation of $\text{Me}(\text{OH})_2(\text{L}_n)_2$ and $\text{Me}(\text{SO}_4)(\text{L}_n)_2$ complex compounds can be proposed. The fact that L_3 reacts with the metals also at a high acid concentration is because of its relatively high dissociation constant ($\text{pK}=2.64$). The formation of complexes from 3M H_2SO_4 solutions can be shown from the equilibrium:



In all the systems studied, it has been found that independent of the composition of the aqueous phase, the distribution ratio decreases in order $D_{\text{L}_3} > S_{\text{L}_1} > D_{\text{L}_2}$. With an increase of the electronegativity of the substituent bound to the phosphorus atom, the stability of the complexes decreases. If the substituent is an OH group, the metal salt formation accounts for the higher D values. In nonaqueous solutions neither OC_2H_5 nor OH group are involved in the complex formation. The decrease of the P=O stretching frequencies to the same wave numbers independent of the different P=O stretching frequencies present in the spectra of the ligands, indicates that identical types of complexes are formed and that all three oxygens from P=O groups are coordinated to the metal. Therefore seven coordinated MeCl_4L_n complex compounds are probably formed.

LITERATURE

1. Sandhu S. S. and Sandhu R. S. ,
Inorg. Chim. Acta, 1972, 6, 383
2. Mani F. and Bacci M. ,
Inorg. Chim. Acta, 1972, 6, 487
3. O'Laughlin J. W. , Jensen D. F. , Ferguson J. W. , Richard J. J. ,
and Banks C. V. ,
Anal. Chem. , 1968, 40, 1931
4. Goffart J. and Duyckaerts G. ,
Anal. Chim. Acta, 1965, 36, 499
5. Medved T. Ya. , Karolev B. A. , Judina K. S. , Stepanov B. I. and
Kabachnik M. I. ,
Teor. eksp. khim. , 1968, 4, 116
6. Jacimirskij K. B. , Kabachnik M. I. and Sheka Z. A. ,
Teor. eksp. khim. , 1968, 4, 446
7. Kabachnik M. I. , Sheka Z. A. , Medved T. Ya. , Sinjavskaja E. I. ,
Kulumbetova K. Zh. and Konstantinovskaja M. A.
Zhur. neorg. khim. , 1973, 18, 2042
8. Sinjavskaja E. I. , Sheka Z. A. , Medved T. Ya. , Pisareva S. A.
and Kabachnik M. I. ,
Zhur. neorg. khim. , 1973, 18, 2427

9. Kabachnik M. I. , Sheka Z. A. , Medved T. Ya. , Sinjavskaja K. Zh.
and Konstantinovskaja M. A. ,
Zhur. neorg. Khim. ,1973,18,2042
10. Mrochek J. E. , O'Laughlin J. W. and Banks C. V. ,
J. Inorg. Nucl. Chem. ,1965,27,603
11. Bridson B. J. ,
J. Chem. Soc. Dalton Trans. ,1972,20,2247
12. Medved T. Ya. , Polikarpov Yu. M. , Pisareva S. A. , Matrosov E. I.
and Kabachnik M. I. ,
Izv. Akad. Nauk. SSSR Ser. khim. ,1968,2062
13. Meider-Goričan H. ,
J. Inorg. Nucl. Chem. ,1971,6,487
14. Ryabchikov D. I. , Marov I. N. , Ermakov A. N. and Belyaeva V. K. ,
J. Inorg. Nucl. Chem. ,1964,26,965
15. Goričan H. and Djordjević C. ,
Croat. chem. Acta,1965,37,265

Table 1.

Extraction of HClO_4 into $4 \cdot 10^{-2} \text{M} / (\text{C}_6\text{H}_5)_2(\text{O})\text{PCH}_2/2 \text{P}(\text{O})\text{C}_6\text{H}_5$ (L_1)
chloroform solutions

HClO_4 aq(in)	$^a\text{HClO}_4$	HClO_4 org.
0.50	1.4×10^{-3}	7.3×10^{-4}
0.25	3.6×10^{-4}	2.1×10^{-4}
0.10	6.5×10^{-5}	5.6×10^{-5}
0.06	2.3×10^{-5}	3.7×10^{-5}

$^a\text{HClO}_4$ = activity of HClO_4 in aqueous phase

Table 2.

Extraction of $/(\text{C}_6\text{H}_5)_2(\text{O})\text{PCH}_2/2 \text{P}(\text{O})\text{OC}_2\text{H}_5$ (L_2) and $/(\text{C}_6\text{H}_5)_2(\text{O})\text{PCH}_2/2 \text{P}(\text{O})\text{OH}$ (L_3)
into chloroform

H^+ aq	D_{L_3}	D_{L_2}
7.08×10^{-3}	20.4	194.0
6.46×10^{-4}	15.1	108.4
5.89×10^{-5}	10.8	91.0
8.91×10^{-6}	7.72	80.2
8.51×10^{-7}	2.44	72.0
2.40×10^{-9}	1.36	63.6

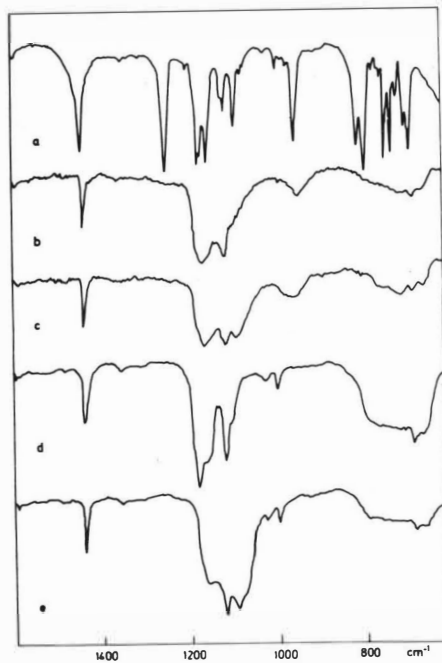


Fig. 1. I.r. spectra of a) L_3 in KBr. b) L_3 chloroform solution, c) L_3 chloroform solution equilibrated with 4M $HClO_4$, d) L_1 chloroform solution and L_1 chloroform solution equilibrated with 4M $HClO_4$.

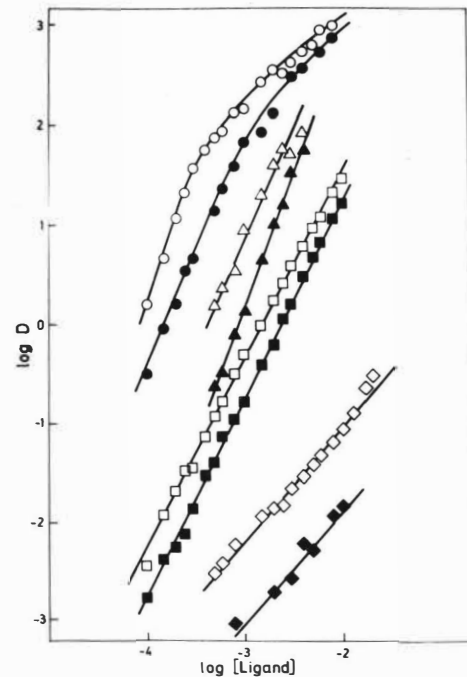


Fig. 2. Extractant dependence of the extraction of $\circ, \Delta, \square, \diamond$, Zr and $\bullet, \blacktriangle, \blacksquare, \blacklozenge$ Hf from $\circ, \bullet, \Delta, \blacktriangle$ 4M $HClO_4$ and $\square, \blacksquare, \diamond, \blacklozenge$ 4M HCl aqueous solutions with $\circ, \bullet, \square, \blacksquare$ L_1 and $\Delta, \blacktriangle, \diamond, \blacklozenge$ L_2 into chloroform.

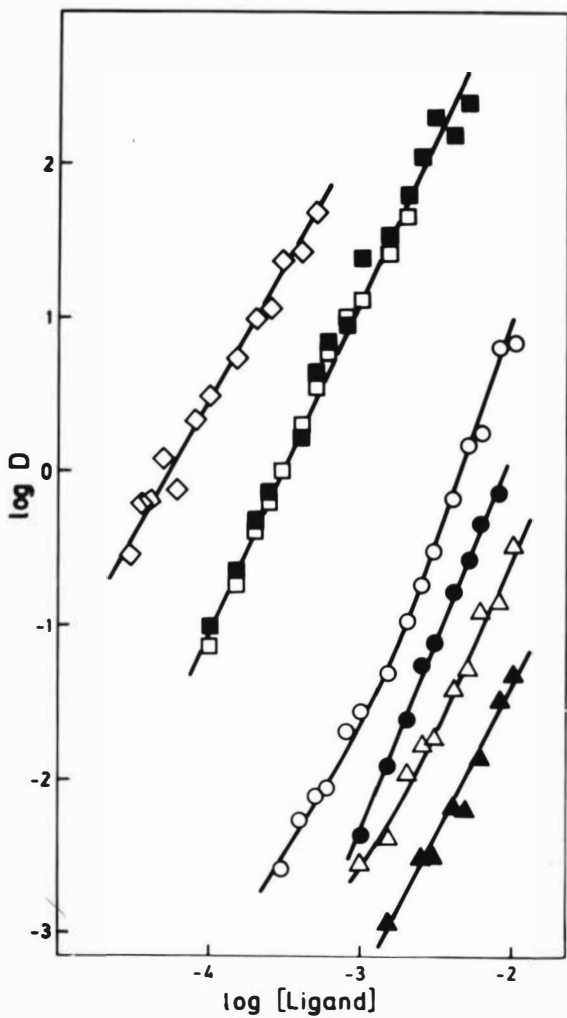


Fig. 3. Extractant dependence of the extraction of
 ◇ , □ , ○ , △ Zr and ■ , ● , ▲ , Hf from
 ◇ , ○ , ● , △ , ▲ 0.1M H₂SO₄ and □ , ■ 3M
 H₂SO₄ aqueous solutions with ○ , ● L₁, △ , ▲ ,
 L₂ and □ , ■ , ◇ , L₃ into chloroform.

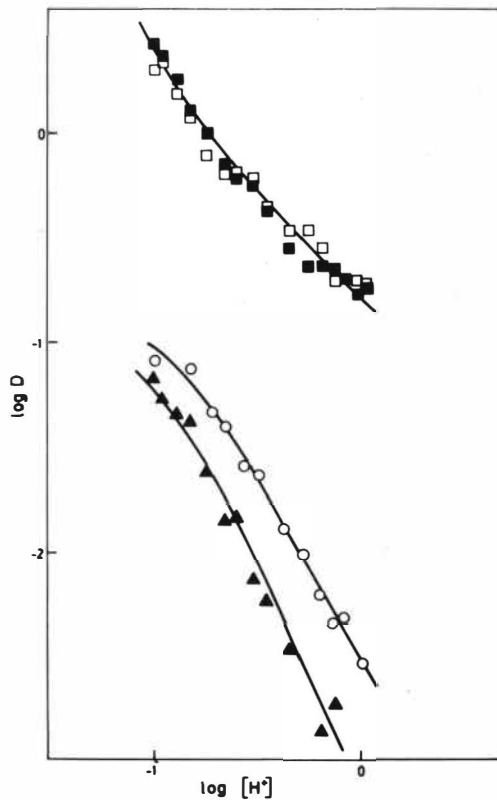


Fig. 4. Hydrogen ion dependence of the extraction of \square , \circ Zr and \blacksquare , \blacktriangle Hf with \circ L_1 , Δ L_2 and \square , \blacksquare L_3 into chloroform from $0.1\text{M } \text{H}^+ / \text{Na, H, HSO}_4^- = 1\text{M}$ aqueous solutions

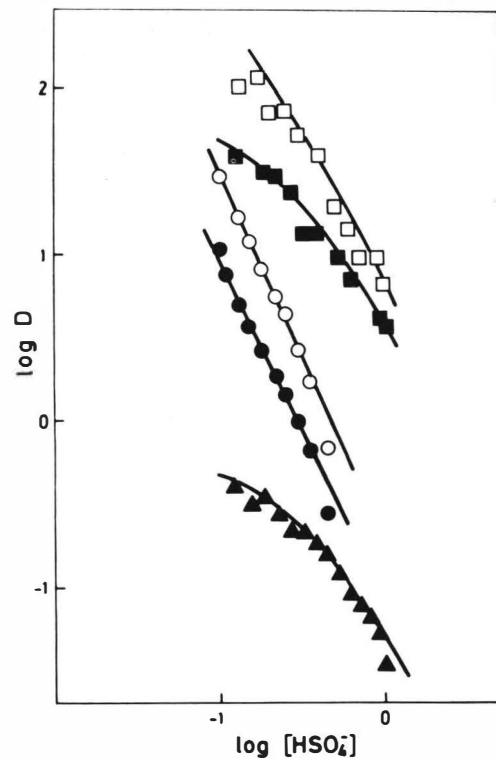


Fig. 5. HSO_4^- ion dependence of the extraction of \square , \circ Zr and \blacksquare , \bullet , \blacktriangle Hf with \circ , \bullet L_1 Δ L_2 and \square , \blacksquare L_3 from $\text{H, HSO}_4^-, \text{ClO}_4^- = 1\text{M}$ aqueous solutions

THE EXTRACTION OF ANIONIC VANADIUM (IV) - THIOCYANATO
COMPLEX FROM AQUEOUS SOLUTIONS BY LONG CHAIN ALKYL
QUATERNARY AMMONIUM COMPOUND

Taichi SATO, Shiegeo KOTANI and Osamu Terao
(Department of Applied Chemistry, Faculty of Engineering,
Shizuoka University, Hamamatsu, Japan).

ABSTRACT

The extraction of the vanadium (IV) - thiocyanato complex anionic species from aqueous solutions by long chain quaternary ammonium salt in benzene has been investigated under different conditions. Both the aqueous and organic phases have been examined by spectrophotometry. Infrared and electron spin resonance spectral studies have been carried out for the complex formed in the organic phase. As a result, it is concluded that the extracted species is transformed from $(VO(NCS)_5)^{3-}$ to $(VO(NCS)_4)^{2-}$ with increasing vanadium concentration in the organic phase. The mechanism of extraction is discussed on the basis of the results obtained.

INTRODUCTION

The utilization of tricaprilmethylammonium thiocyanate as a selective extraction agent in the spectrophotometric determination of cobalt (II) has been studied by Wilson et al¹. The present authors have also investigated the distributions of thorium (IV)² and uranium (VI)³ between aqueous solution containing hydrochloric acid in the presence of potassium thiocyanate and benzene solution of the quaternary salt. This paper extends the work to the extraction of vanadium (IV)

EXPERIMENTAL

Reagents

Tricaprylmethylammonium chloride (from General Mills as Aliquot-336, $R_3R'NC1$), used as the quaternary compound, was purified as described previously⁴. The stock solution of vanadyl chloride was obtained by dissolving vanadyl chloride ($VOCl_2$) in a hydrochloric acid solution of the selected concentration. The other chemicals were analytical reagent grade.

EXTRACTION AND ANALYTICAL PROCEDURES

The procedure for obtaining distribution coefficient (the ratio of the equilibrium concentration of vanadium in the organic phase to that in the aqueous phase) was as follows: Equal volumes (15 ml) of the quaternary compound in benzene and the aqueous vanadyl chloride solution containing hydrochloric acid in the presence of potassium thiocyanate were shaken for 10 min in 50 ml stoppered conical flasks in a water-bath thermostatted at the required temperature; after the separation of the aqueous and organic phases by centrifugation, vanadium in the organic phase was stripped with 1 M hydrochloric acid, and then the distribution coefficient was determined.

Vanadium was determined by back-titration of the aqueous solution adding an excess of EDTA with thorium nitrate solution using xylenol orange as indicator at pH 3⁵. The concentrations of chloride and thiocyanate in the organic phase were determined as follows: the precipitate from the organic solution with silver nitrate was decomposed by boiling for 1 hr in the presence of concentrated nitric acid, and the residue was weighed as silver chloride⁶, accordingly the loss in weight from the initial precipitate was equivalent to the concentration of thiocyanate.

Spectrophotometry and E S R

The absorption spectra were obtained using a Hitachi Model EU-2 recording spectrophotometer and a Shimadzu Model QV - 50 spectrophotometer, using matched 1.00 cm fused silica cells.

The infrared spectra of the samples prepared by the evaporation of diluent in the organic phases were determined on a Japan Spectroscopic Co. Ltd. Model IR - S, equipped with potassium chloride prisms for measurement at $4000-550\text{ cm}^{-1}$, and IR - F, a grating model for measurement at $700-200\text{ cm}^{-1}$, as a capillary film between thallium halide plates.

ESR spectrum was determined on a high-sensitivity ESR spectrometer, designed in the Research Institute of Electronics, Shizuoka University and made by Shimada Rikakogyo Co. Ltd. Measurements were made in the solid state by using a super-heterodyne detection⁷; the wave-guide units in the spectrometer are standard X-band components at the response of 1 sec., and the amplitude of the modulating field being 3 gauss, at room temperature. The calculation of ESR derivative line shape of the sample was made using a HIPAC 103 computer.

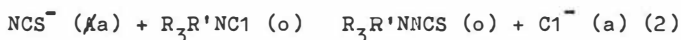
RESULTS AND DISCUSSIONS

Extraction isotherm

The extraction of vanadium (IV) from its solution (1 g/1 as VOCl_2) containing hydrochloric acid in the presence of potassium thiocyanate by quaternary compound in benzene at 20°C gave the results illustrated in Fig. 1. The distribution coefficient for vanadium at first rises with aqueous thiocyanate concentration, and passes through a maximum at initial concentration in 0.15 M and then falls again. For the variation of the distribution coefficient, it may be interpreted that the formation of the vanadium (IV)-thiocyanate complex accounts for the rise in the curve, while the competition between vanadium and thiocyanate for association with the quaternary compound provides a check on this rise. From Fig. 1 it is also seen that the extraction efficiency of vanadium is lowered as the initial aqueous hydrochloric acid concentration increases. In the extraction of vanadium (IV) from the solution (1 g/1) containing 0.3M hydrochloric acid and lithium chloride at various concentrations in the presence of 1.0M potassium thiocyanate by 0.02 M quaternary compound in benzene at 20°C , the distribution coefficient was not appreciably influenced by the chloride concentration.

Additionally, the value of log (distribution coefficient) decreased linearly with log (initial aqueous hydrochloric acid concentration) at a fixed total chloride concentration ((HCl) + (LiCl)=1.0 M), analogous to the curve for hydrochloric acid alone. It is thus presumed that the species containing chloride ion is inextractable, and when the hydrochloric acid in the aqueous phase is partly replaced by lithium chloride the decrease in the distribution coefficient is checked owing to the removal of the competition for vanadium (IV) - thiocyanato complex between hydrochloric acid and quaternary salt.

If we assume that the extraction of vanadium^{IV} from aqueous solutions in the presence of thiocyanate is carried out by an ionexchange reaction similar to that for thorium (IV)²⁺, viz.

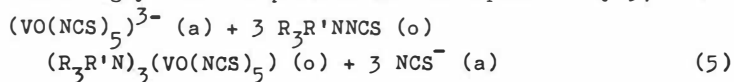


in which (a) and (o) represent aqueous and organic phases respectively, the following relationship would be expected:

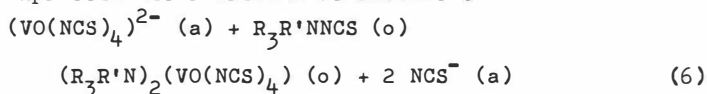
$$\log E_a = \log K + m \log (C_A - m C_V) / C_{\text{NCS}} \quad (4)$$

where E_a is the distribution coefficient, K the equilibrium constant, C_A the total quaternary compound concentration, C_V the vanadium concentration of the organic phase and C_{NCS} the aqueous thiocyanate concentration and in addition $m=n-2$.

In the extraction of vanadium (IV) from the solution (1 g/l) containing hydrochloric acid in the presence of 1.0 M potassium thiocyanate at 20°C, log-log plots of E_a vs. $(C_A - m C_V) / C_{\text{NCS}}$ reveal that Equation (4) is satisfied for $m=3$ at initial $(\text{R}_3\text{R}'\text{NC1})$ 0.015 M, and for $m=2$ at initial $(\text{R}_3\text{R}'\text{NC1})$ 0.015 M. It is therefore thought that each vanadium (IV) - thiocyanate complex ion is associated with three molecules of quaternary compound in the extraction at low vanadium concentration, and accordingly $n-2$ in Equation (3) is expressed by 3, i.e.



In the extraction at higher vanadium concentration, since two molecules of quaternary compound are associated with each vanadium (IV) - thiocyanato complex ion, the equilibrium expression is rewritten as follows :



indicating $n=4$ in Equation (3) equals 2.

This is also supported by the fact that, the molar ratios of the concentrations of vanadium and thiocyanate in the organic phase to the concentration of quaternary compound as a function of initial aqueous vanadium concentration (at 0.5 M hydrochloric acid in the presence of 1.0 M potassium thiocyanate with 0.02 M quaternary compound in benzene at 20°C), are expected to approach the limiting values of 0.5 and 2 respectively. The plot in Fig.2, implies that the vanadium (IV) - thiocyanate complex formed in the organic phase contains vanadium : thiocyanate : quaternary compound in the molar ratio 1 : 4 : 2 indicating the stoichiometry $(\text{R}_3\text{R}'\text{N})_2\text{VO}(\text{NCS})_4$.

Temperature effect

The extraction of vanadium (IV) from the solution (1 g/l) containing 0.5 or 0.9 M hydrochloric acid, in the presence of 1.0 M potassium thiocyanate, by 0.03 M quaternary compound in benzene, at temperature between 5 and 40°C, gave the result shown in Fig.3. The observation that distribution coefficient decreases with rising temperature is similar to the result for the extraction of thorium (IV)². The heat of reaction (change in enthalpy, kJ/mole) in Equation (5) is estimated to be 14.35 in 0.5 M HCl and 9.57 in 0.9 M HCl.

Electronic, infrared and ESR spectra

The absorption spectra of both the aqueous and organic phases from the extraction of vanadyl chloride solutions containing 0.5 M hydrochloric acid in the presence of potassium thiocyanate with 0.02 M quaternary compound in benzene at 20°C are illustrated in Figs. 4-5. The spectrum of the aqueous solution of vanadyl chloride at 1 g/l in the presence of 0.5 M hydrochloric acid and 0.5 M potassium thiocyanate exhibits the characteristic absorption bands at 610 and 765 m μ , whose absorptions shift to shorter and longer wavelengths respectively, as the

thiocyanate concentration increases⁸, (Fig.4). This perhaps corresponds to the transformation from penta- to hexa-coordination of thiocyanato group for vanadium. For the spectrum of the organic solution from the extraction of vanadyl chloride solution (1 g/l) containing 0.5 M hydrochloric acid in the presence of 1.0 M potassium thiocyanate, the absorptions at 575 and 775 m are accompanied by the charge-transfer band at 465 m due to the transition (Fig.5) With increase the vanadium concentration, these absorptions show a progressive increase in intensity and slightly shift to 480, 575 and 750 m respectively, and simultaneously the organic phase changes in colour from blue to brown. The spectral results probably confirm that the extracted species is transformed from $(VO(NCS)_5)^{3-}$ to $(VO(NCS)_4)^{2-}$ with increasing the vanadium concentration in the organic phase, as indicated in Equations (5) and (6).

When the water content of the brown complex prepared by the evaporation of benzene in the brown organic solution was examined, it was calculated that the complex contained one molecule of water. By drying in vacuo at above 60°C, this complex dehydrates and changes in colour from brown to green. However, since the V-O stretching band⁹⁻¹² in the infrared spectrum of the anhydrous (green) complex is little different from that of the hydrous (brown) complex, it is considered that the water molecule in the hydrous complex does not coordinate directly to vanadyl ion. This is also supported by the electronic spectra result. In the spectrum of the hydrous complex, if we presume that the species $(VO(NCS)_5)^{2-}$ is in a point group C_{4v} symmetry, the absorption bands at 575 and 750 m (17400 and 13300 cm^{-1}), which appear in addition to the charge-transfer band at 480 m (20800 cm^{-1}), are assigned to the transitions 2B_2 , 2B_1 and 2B_2 , 2E respectively¹³. In the contrast, the spectrum of anhydrous complex shows the transitions from the ground state 2B_2 to the states 2B_1 and 2E_2 at 585 and 750 m (17100 and 13300 cm^{-1}) respectively, although the absorption due to the charge-transfer shifts toward shorter wavelength. If it is assumed that the transformation from pento hexa-coordinated structure is caused by the bonding of a water molecule to vanadyl ion, the lowering in the e level should be observed as the shift to a lower frequency in the electronic spectrum¹⁰.

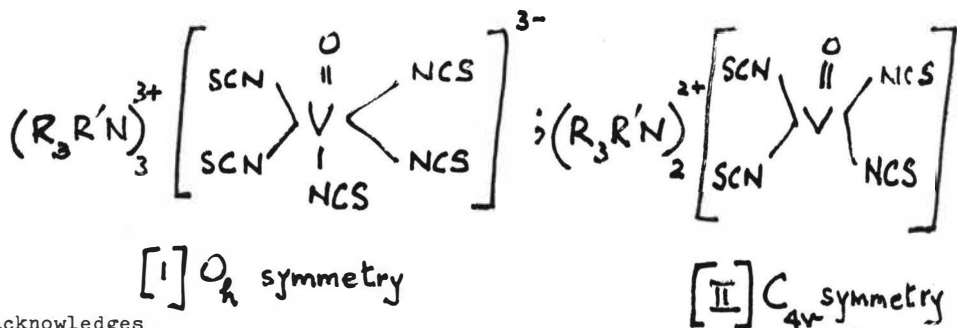
As the spectra of the both complexes exhibit no change in the absorption band due to the transition ${}^2B_2 \rightarrow {}^2E$, it is postulated that the symmetrical configuration of the hydrous complex is similar to that of the anhydrous complex.

The organic extracts from the extraction of vanadium (IV) from aqueous solutions at initial vanadyl chloride concentrations of 5, 10 and 20 g/l containing 0.5 M hydrochloric acid in the presence of 1.0 M potassium thiocyanate with 0.094 M quaternary compound in benzene at 20°C were examined by infra red spectroscopy. As a representative spectrum, the frequencies and probably band assignments for the anhydrous complex, prepared by drying the vanadium-saturated organic solution, are given in Table 1, compared with those for the organic extract from the extraction of aqueous potassium thiocyanate solution in the absence of vanadium². The spectrum of the organic extract without vanadium shows the OH stretching and bending bands, and in addition the CN stretching band at 2092 cm^{-1} and the NCS bending frequency at 468 cm^{-1} , implying that the compound $R_3R'NCS \cdot H_2O^2$ is formed according to the reaction in Equation (2). In the presence of vanadium, the absorptions due to the asymmetric and symmetric stretching vibrations of the vanadyl group⁹⁻¹² appear at 1003 and 952 cm^{-1} respectively, and the intensities of the OH bands decrease in accordance with the result of the Karl Fischer titrations and at the same time the CN stretching band appears at 2088 cm^{-1} , the NCS bending band at 479 cm^{-1} and the V-N stretching bands at 380 and 346 cm^{-1} , implying that the thiocyanate ion coordinates to vanadium through the nitrogen atom¹⁴ as well as the complexes in the other instances^{2,3}). As similar result is obtained in the spectrum of the hydrous complex, and also shows that the absorptions are similar to those of the anhydrous complex, except for the presence of the OH bands.

The ESR spectrum of the anhydrous complex is illustrated in Fig.6 compared with the spectrum obtained by the calculation assuming as the line shape arising from randomly oriented sample in a tetragonal pyramidal symmetry^{15,16}).

The experimental spectrum reveals a pattern due to the hyper-fine structure and consists with the calculated curve. The calculated g values^{15,26} are $g_{11}=1.951$ and $g = 1.991$, expecting to be isotropic in the thiocyanato group coordinated to vanadyl ion.

From the results mentioned above, the following structures, (I) and (II), are proposed for the species extracted at low and higher vanadium concentrations, respectively :



Acknowledges

We wish to thank Professor I, Takao of the Research Institute of Electronics, Shizuoka University for the ESR spectral experiment and Messrs. T. Nakamura and T. Kato for assistance with part of the experimental work.

References

1. Wilson, A.W., and McFarland, O.K. *Analyt. Chem.*, 1963, 35, 302
2. Sato, T., Kotani, S., and Good, M.L., *J. inorg. nucl. Chem.*, 1973, 35, 2547

- 3) Sato, T., Kotani, S., and Good, M.L., J. inorg. nucl. Chem.,
(in press)
- 4) Sato, T., and Watanabe, H., Analy. Chim. Acta, 1970, 49, 463
- 5) Kinnunen, J., and Wennerstrand, B., Chemist-Analyst, 1957,
46, 92
- 6) de Sousa, A., Talanta, 1961, 8, 782
- 7) Mirshon, J.M., and Fraenkel, G.K., Rev. Sci. Instr., 1955,
26, 34 ; Misra, H., ibid., 1958, 29, 590
- 8) Selbin, J., Maus, G., and Johnson, D.L., J. inorg. nucl.
Chem., 1967, 29, 1735
- 9) Kiltz, P.A., and Nicholls, D., J. chem. Soc. (A), 1966, p.1175
- 10) Selbin, J., Holmes, L.H., Jr., and McGlynn, S.P., J. inorg.
nucl. Chem., 1965, 25, 1359
- 11) Sathyanarayana, D.N., and Patel, C.Y.C., J. inorg. nucl.
Chem., 1968, 30, 207
- 12) Sato, T., and Takeda, T., J. inorg. nucl. Chem., 1970, 32,
3387
- 13) Ballhausen, C.J., and G^uay, H.B., Inorg. Chem., 1962,
1, 111
- 14) Nakamoto, K., 'Infrared Spectra of Inorganic and Coordi-
nation Compounds', 1970, p.152 (New York : Wiley-
Interscience)
- 15) Kneubüher, F.K., J. chem. Phys., 1960, 33, 1074
- 16) Vanngard, T., and Aasa, R., 'Proc. 1 st. Int. Conf. Para-
magnetic Resonance, Jerusalem, 1962' (Edited by Low, W.),
Vol.2, 1963, p.509 (New York : Academic Press)
- 17) Abragam, A., and Pryce, M.H.L., Proc. Roy. Soc., 1951,
A 205, 135 ; ibid., 1955, A 230, 169
- 18) Bloch, F., Phys. Rev. 1946, 70, 460

- 19) Bleaney, B., *Phil. Mag.*, 1951, 42, 441 ; *Proc. phys. Soc.*, 1950, A 75, 621
- 20) O'Reilly, D.E., *J. chem. Phys.*, 1958, 29, 1138
- 21) Gaughey, W.S., *J. chem. Phys.*, 1961, 34, 591
- 22) Bernal, I., and Riger, P.H., *Inorg. Chem.*, 1963, 2, 256
- 23) Kivelson, D., and Lee, S.K., *J. chem. Phys.*, 1964, 41, 1896
- 24) Hecht, H.G., *J. chem. Phys.*, 1967, 46, 23
- 25) Figgis, B.N., 'Introduction to Ligand Fields', 1962, p.293 (New York : Interscience)
- 26) Ballhausen, C.J., 'Introduction to Ligand Field Theory', 1962 (New York : McGraw-Hill)

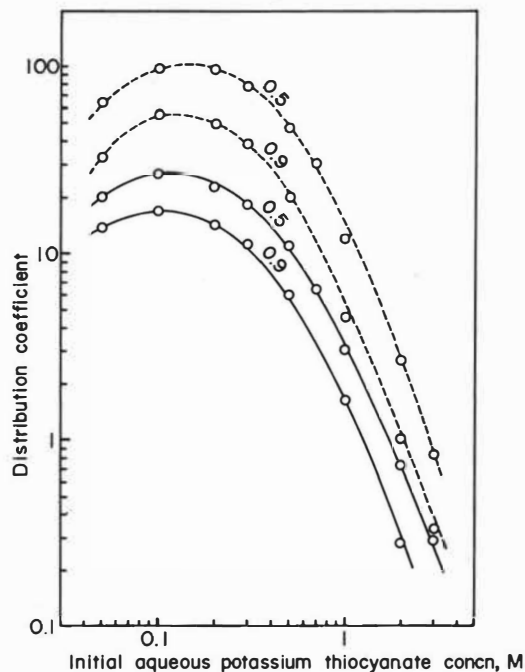


Fig. 1. Extraction of vanadium (IV)-thiocyanato complex from hydrochloric acid solutions in the presence of potassium thiocyanate at different concentrations by quaternary compound in benzene (continuous and broken lines represent the extractions by quaternary compound in 0.02 and 0.03 M, respectively; numerals on curves are initial aqueous hydrochloric acid concentrations, M).

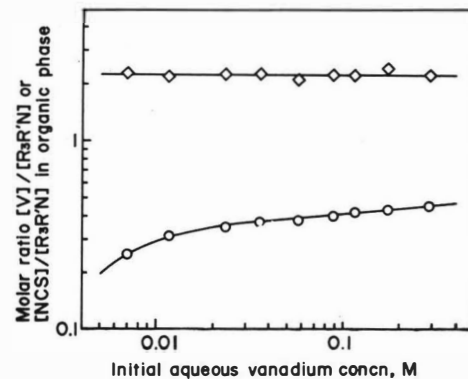


Fig. 2. Variation in the concentrations of vanadium and thiocyanate in the organic phase with initial aqueous vanadium concentration for the extraction of vanadium (IV)-thiocyanato complex from 0.5 M hydrochloric acid solution in the presence of potassium thiocyanate at 1.0 M by 0.02 M quaternary compound in benzene (○ and ◇ denote the molar ratios of $[V]/[R_3R'N]$ and $[NCS]/[R_3R'N]$, respectively, in the organic phase).

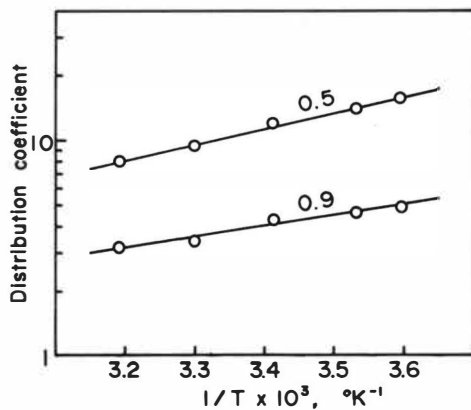


Fig. 3. Temperature dependence of distribution coefficient for the extraction of vanadium (IV)-thiocyanato complex from hydrochloric acid solutions in the presence of potassium thiocyanate at 1.0M by 0.03M quaternary compound in benzene (numerals on curves are initial aqueous hydrochloric acid concentrations, M).

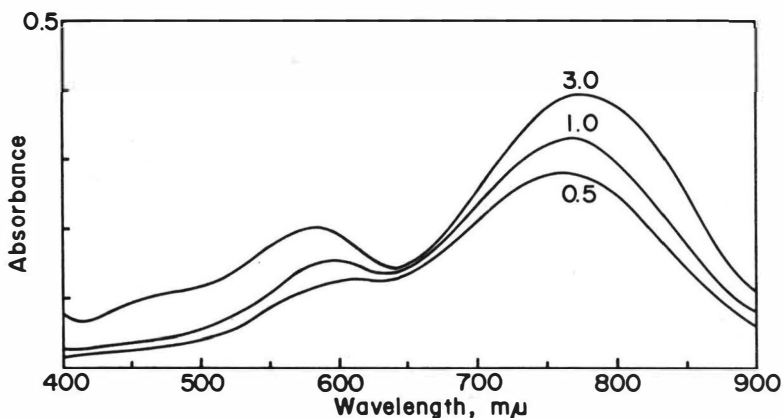


Fig. 4. Absorption spectra of the aqueous solutions of vanadyl chloride at 1 g/l in the presence of 0.5 M hydrochloric acid and potassium thiocyanate at different concentrations (numerals on curves are initial potassium thiocyanate concentrations, M; thickness of cell, 1.00 cm).

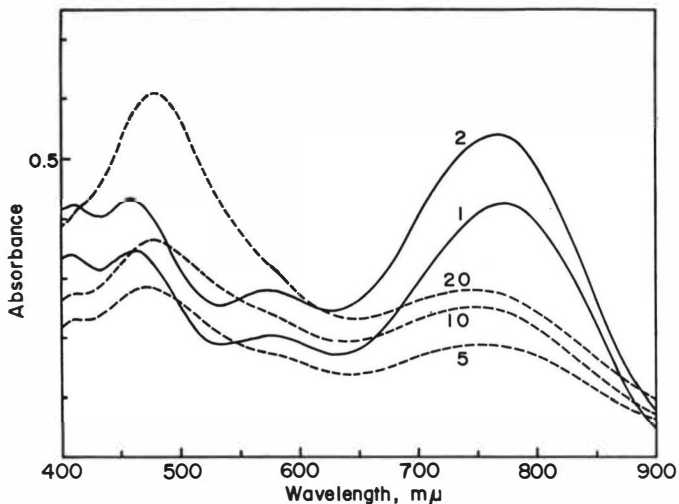


Fig. 5. Absorption spectra of the organic solutions from the extraction of vanadyl chloride solutions containing 0.5M hydrochloric acid in the presence of potassium thiocyanate at 1.0M with 0.02 M quaternary compound in benzene (numerals on curves are initial aqueous vanadyl chloride concentrations, g/l; dilution, X1 and X5 in continuous and broken lines, respectively; thickness of cell, 1.00 cm).

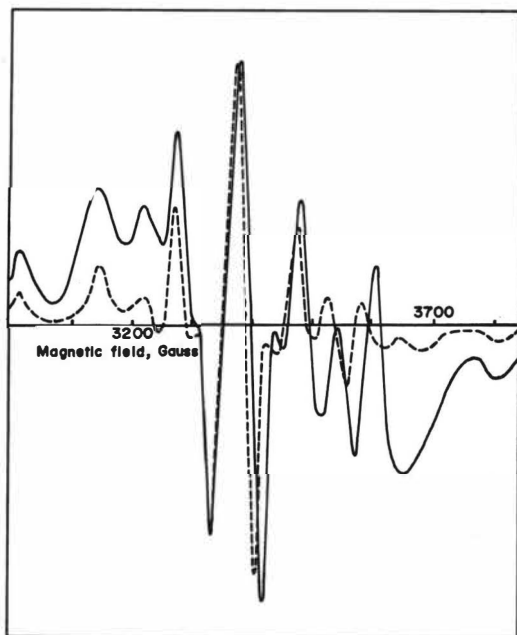


Fig. 6. ESR spectrum of vanadium (IV)-thiocyanate complex (continuous and broken lines represent the observed and calculated spectra, respectively).

Table I Infrared spectral data for the vanadium(IV)-thiocyanato complex

Frequency, cm ⁻¹		Probable assignment
R ₃ R'NNCS·H ₂ O	(R ₃ R'N) ₂ [VO(NCS) ₄]	
3400 (wb)*		} OH stretching
3200 (sh)		
2920 (s)	2920 (s)	} CH stretching (sym. and asym.)
2820 (ms)	2860 (ms)	
2092 (s)	2088 (s)	CN stretching
1710 (vw)		} OH bending
1620 (wb)		
1465 (m)	1465 (m)	CH ₃ degenerate bending CH ₂ scissoring
1375 (w)	1375 (w)	CH ₃ sym. bending
	1003 (m)	} M-O stretching (sym. and asym.)
	956 (w)	
	786 (vw)	CS stretching
720 (w)	720 (w)	CH ₂ rocking
468 (w)	479 (w)	NCS bending
	380 (s)	} V-N stretching
	346 (ms)	

* s = strong, ms = medium strong, m = medium, w = weak, vw = very weak, b = broad, sh = shoulder

MECHANISM OF SOLVENT EXTRACTION OF PERRHENATE IONS
BY CYCLOHEXANONE

by - N. Jordanov, + M. Pavlova, + D. Boikova++
+ Institute of General and Inorganic Chemistry,
Bulgarian Academy of Sciences, Sofia 13, Bulgaria
++ High Institute of Chemical Technology, Sofia 56,
Bulgaria

ABSTRACT

The mechanism of solvent extraction of ReO_4^- by cyclohexanone is studied for various media - acids, bases and salts. In an acid medium the mechanism involves hydration-solvation and the salting-out effect of the acids decreases in the series: $\text{H}_3\text{PO}_4 > \text{H}_2\text{SO}_4 > \text{HCl} > \text{HNO}_3$. In a medium obtained from the corresponding salts and a base, the mechanism involves only solvation and the salting-out effect decreases in the series: $\text{Na}_2\text{CO}_3 > \text{Na}_2\text{SO}_4 > \text{NaCl} > \text{NaOH} > \text{NaNO}_3$. The corresponding solvation and hydration numbers were found. For the stripping of ReO_4^- , a dilution of the organic phase by chloroform is recommended.

INTRODUCTION

It is known that ketones can extract perrhenate ions from acidic, neutral and alkaline media. A great number of investigations has been devoted to this solvent extraction reaction.¹⁻¹⁵ Ryabchikov et al.⁵ have studied the mechanism of solvent extraction of ReO_4^- in ketones from neutral and alkaline media. They have found that the solvates are hydrated in the organic phase. Gerlit et al.⁴ have studied the effect of the cationic and anionic compositions of the aqueous phase on the solvent extraction of ReO_4^- by ketones. The prevailing opinion is that the mechanism of solvent extraction of perrhenate ions is still insufficiently studied.

In the present paper we are presenting the results of a detailed study on the solvent extraction of ReO_4^- by cyclohexanone. Among the ketones used so far, cyclohexanone is the best extracting reagent being produced in large quantities at a low price. The purpose of our investigation is to elucidate the solvent extraction mechanism and thus to reveal new possibilities for its analytical and technological applications.

EXPERIMENTAL

Reagents with qualification p.a. from Merck were used with the exception of KReO_4 (supplied by Fluka) and cyclohexanone (Bulgarian product). Cyclohexanone was rectified and the collected fraction has a b.p. $155-6^\circ\text{C}$. The purity of cyclohexanone was checked by gas chromatography.

The distribution coefficients were determined both radio-metrically (^{186}Re), by tracing the activity of the two phases, and photometrically, by the rhodanide method.¹⁶ Sodium was determined by atomic absorption using a Pye-Unicam SP 90B spectrophotometer. In all experiments the volume of the aqueous and organic phases were equal to 5 ml. The contacting lasted for five minutes. Preliminary experiments showed that the equilibrium between the two phases is attained within five minutes.

RESULTS AND DISCUSSION

Extraction of ReO_4^- from various media

The extraction curves for the solvent extraction of ReO_4^- by cyclohexanone from aqueous solutions of H_3PO_4 , H_2SO_4 , HCl , HNO_3 , are shown in Figure 1. The extraction curves for the solvent extraction of ReO_4^- from aqueous solutions of NaOH , NaCl , Na_2SO_4 , Na_2CO_3 , and NaNO_3 are shown in Figure 2. It is seen from these curves that both the anionic and cationic components of the aqueous phase play an important role for the solvent extraction of ReO_4^- . The various ions interact with water in a different way and thus differently affect the structure and activity of water.

In this case both the electric charge and the size of the ions are of decisive nature. The nitrate ion is more strongly negatively hydrated than the chloride ion and this favourably affects its extraction; further, due to competition, the extraction of perrhenate is then lowered. As seen from Figure 1, if the concentration of the acids is increased above a certain value the distribution coefficient starts to decrease. This could be connected both with the competitive and the dehydrating actions of some of the acids. Depending on the nature of the salting-out reagent, the mutual solubility of the phases is altered to a different extent, thus the dielectric permeability of the phases and, thereby, the distribution coefficients are also changed.¹⁷ When comparing the values of D for an equal anionic and differing cationic compositions, the importance of the cationic composition is easily seen (Fig.3)

Choice of diluent

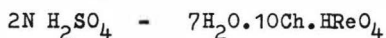
Among the great number of tested "inert" diluents the best diluents were found to be benzene and chloroform. For these two diluents the distribution coefficients for ReO_4^- using 50% cyclohexanone as extractant are 0.17 for 2N H_2SO_4 and less than 0.004 for 2N Na_2SO_4 and 2N NaOH. It is seen that perrhenate ions are practically not extracted from these solutions. This permits the stripping extraction of ReO_4^- in a pure water phase by diluting the organic phase with some of these diluents.

Determination of the solvation and hydration numbers

The solvation numbers were determined graphically from the double logarithmic plot, $\log D/\log (Ch)$ (where (Ch) denotes cyclohexanone concentration. Various concentrations of the studied media and various diluents of cyclohexanone were used in these experiments. A mean solvation number $\bar{S} \approx 10$ was found for the solvent extraction of ReO_4^- from the following media: H_2SO_4 , Na_2SO_4 , NaOH, and Li_2SO_4 . However $\bar{S} \approx 6$ was found for the solvent extraction of ReO_4^- from K_2SO_4 .

It is therefore seen that regardless of the nature and concentration of the salting-out reagent, if the cation is positively hydrated, the extraction process proceeds via solvation of the corresponding electroneutral species involving on the average 10 molecules of cyclohexanone. The potassium ion, which is considered to be negatively hydrated,¹⁸ is more weakly solvated.

The hydration numbers were determined by the Karl Fischer method in a modified version which requires the addition of small amounts of methanol and a large amount of pyridine in the course of titration¹⁹. We have determined the water content of the organic phase after an extraction of 0.02 M ReO_4^- in the appropriate media. If the extraction is carried out from solutions of K_2SO_4 , Na_2SO_4 , NaCl , the solvated species are not hydrated. If ReO_4^- is extracted from 2 N H_2SO_4 using 100% cyclohexanone, the hydration number is approximately 7. Hence the composition of the solvates is:



After the solvent extraction of ReO_4^- from the media containing Na_2SO_4 and NaOH , cyclohexanone was evaporated and the dry residue was analysed for Na and Re. The concentrations which were found correspond to the stoichiometric concentrations of these elements in NaReO_4 . The fact that anhydrous NaReO_4 may be dissolved in cyclohexanone supports the proposed solvation mechanism for the extraction of ReO_4^- from neutral and alkaline media.

GENERAL CONCLUSIONS

The results obtained show that ReO_4^- could be successfully extracted by cyclohexanone from acidic, neutral and alkaline solutions. The salting-out action of the acids decreases in the series: $\text{H}_3\text{PO}_4 > \text{H}_2\text{SO}_4 > \text{HCl} > \text{HNO}_3$. From acidic media the proposed solvent extraction mechanism involves hydration-solvation. In neutral and alkaline media, obtained by the appropriate salts and bases, the salting-out effect, decreases in the series: $\text{Na}_2\text{CO}_3 > \text{Na}_2\text{SO}_4 > \text{NaCl} > \text{NaOH} > \text{NaNO}_3$. In this case the mechanism involves only solvation.

On the bases of the investigation carried out so far we could predict the behaviour of cyclohexanone by the solvent extraction of ReO_4^- from media of other acids, bases and salts, as well as the extractive properties of other extractants of the same type, which extract perrhenate ions by the same mechanism.

The considerably higher basicity of cyclohexanone, in comparison to the corresponding hydrocarbon with a straight chain²⁰, and the greater steric accessibility of the herero-atom, could, in this case, be the cause of the observed high distribution coefficients.

The sharp decrease in the extraction power of cyclohexanone on diluting with CHCl_3 and C_6H_6 is probably due to the intermolecular interactions between the extractants and the diluent. This last result suggests the method for the stripping of perrhenate ions.

REFERENCES

1. Gerlit, Yu. B., Report of the Soviet Delegation at the International Conference on Peaceful Use of Atomic Energy; Published in "Investigations in the Field of Geology, Chemistry, and Metallurgy", 1955 (Moscow: Publ. House Acad. Sci. USSR).
2. Gerlit, Yu. B., in "Chemistry and Geology of the Nuclear Fuel", 1956 (Moscow)
3. Gerlit, Yu. B., Solomatina, G. S., Report at the All-Union Meeting on Radiochemistry, 1957 (Leningrad)
4. Gerlit, Yu. B., Ryabchikov, D. I., "Contemporary Methods of Analysis", 1965 (Moscow: Publ. House Nauka)
5. Ryabchikov, D. I., Gerlit, Yu. B., Karyakin, A. V., Zarinskii V. A., Zubrilina, M. E., Doklady Akad. Nauk, U.S.S.R., 1962, 144, 585

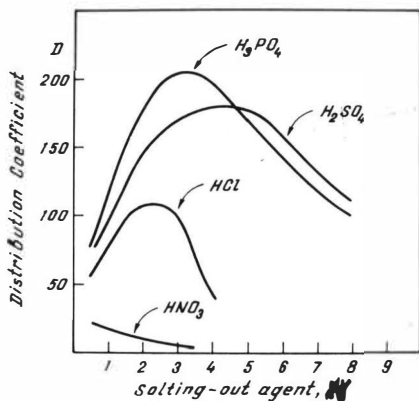


Fig. 1. The dependence of the distribution coefficients of ReO_4^- on the concentration of the acids: H_3PO_4 , H_2SO_4 , HCl , and HNO_3 .

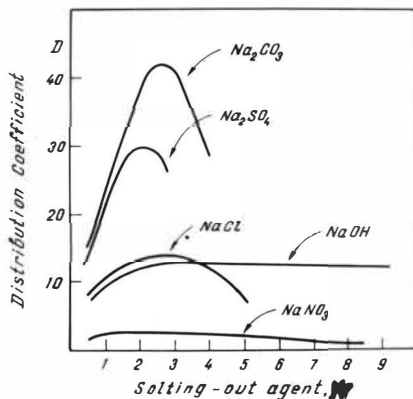


Fig. 2. The dependence of the distribution coefficients of ReO_4^- on the concentrations of Na_2CO_3 , Na_2SO_4 , NaCl , NaOH , and NaNO_3 .

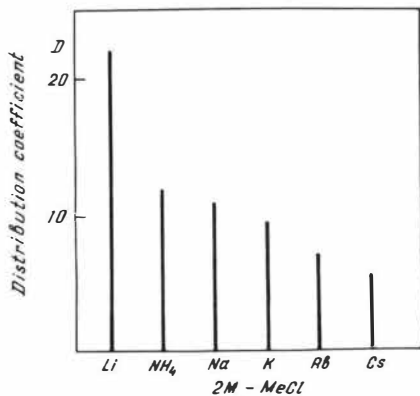


Fig. 3. The dependence of the distribution coefficients of ReO_4^- on the nature of the cation.

SESSION 22

Thursday 12th September: 14.00 hrs

E Q U I P M E N T

(Contractor Performance)

Chairman:

Mr. J. Dolfus

Secretaries:

Dr. W.J. Korchiński

Mr. Euzen

METAL EXTRACTION BY DI-N-HEPTYLSULPHOXIDE (DHpSO);
APPLICATION IN A PULSED COLUMN

LAURENCE, G. * , CHAIEB, M.T. ** , HABSIEGER, D. *
MICHEL, P. *** and TALBOT, J. *

Having recalled the characteristics of molar solutions of di-n-heptylsulphoxide (DHpSO) in 112-tri-chloroethane (TCE) the authors recapitulate the properties of this solvent for metals extraction (U, Th, Mo, Ce, Zr, Hf, Fe, Co, Ni, Mn, Cu, Al, ...)/.

Two examples of application in a pulsed column are given. They deal with zirconium-hafnium separation in nitric acid medium, and iron purification in hydrochloric acid medium. The main characteristics of the column are : height 4m, diameter 4cm, perforated plates made of "teflon". The results show perfect behaviour of the solvent in the pulsed column.



- * Laboratoire de Genie chimique; ENSCP; 11 rue P-et-M Curie, 75005 Paris, France.
- ** Ecole Nationale d'Ingenieurs de Tunis; Campus Universitaire, Tunis, Tunisie.
- *** Centre d'Etudes Nucleaires de Fontenay-aux-Roses, B.P. no.6 92 Fontenay-aux-Roses, France.

The works concerning the use of aliphatic sulphoxides - general formula R_2SO - in liquid-liquid extraction dating back to about ten years. The possibilities of these solvents, for a great number of separations have been generally considered. Several bibliographical details have recently been published on this subject^{1,2}.

We have already shown that the 1,1,2-trichloroethane (TCE) may be used as a diluent for di-n-heptylsulphoxide³ (DHpSO). This compound can dissolve up to 2 moles/liter of DHpSO. The purpose of this article is to summarise the principle extractive properties of molar solutions of DHpSO in TCE, and secondly to study its behaviour in a continuous pulsed extraction column, in order to separate metals.

1. Physical chemical properties of molar solutions of DHpSO in the TCE.

The DHpSO is a white crystallised solid, melting at the temperature of 70°C. It can be prepared starting by easy synthesis^{1,3}.

The TCE is a chlorinated solvent, chemically stable with a specific gravity equivalent to 1,431. Its boiling point is 113°C under 760 torrs. It can dissolve up to 2 moles/liter of DHpSO.

The molar solutions of DHpSO in the TCE have the following properties:

specific gravity : 1,280
viscosity : 1,775 centipoises
interfacial tension with water: 17.5 dynes/cm.

The stability of the solutions have been checked following prolonged usage. No production of $C1^-$ ions starting from the diluent was observed even when very acid solutions were used.⁴

2. Extraction of metals in nitric medium

We have already shown that the DHpSO extracts nitric acid, with formation of a complex of the type $\text{HNO}_3 \cdot \text{DHpSO}^{1,3}$. DHpSO extracts also a great number of metals, principally those of very high valency. During the extraction of these metals, there is always a competition with the extraction of HNO_3 . It is therefore to study the influence of HNO_3 for each metallic cation.

2.1. Experimental

The measurements of the distribution coefficients were all made at a temperature of 20°C . The metal concentrations were determined by the following methods: U (VI) : cerimetry of uranium IV^3 ; Th : colormetry of the thorin complex³ ; Ce : colormetry of the EDTA complex⁵. All the other metal concentrations were determined by atomic-absorption spectroscopy (Fe, Co, Ni, Mo, Mn) or by flame-emission spectroscopy (Zr, Hf, Al).

2.2. Results

Figure 1 shows the distribution coefficients for the following metals : U (VI), Th, Zr, Hf, Ce (III), Mo, and Fe (III), for aqueous concentrations of 1 g/1 metal in relation to the aqueous acidity.

It has been stated that the elements best extracted are uranium, thorium and zirconium.

The extraction of U (VI) is at its maximum point for an aqueous acidity of about 5N ; for the thorium, this maximum is at 2N. The zirconium is practically non-extracted for acidities less than 4N. With higher acidities, the distribution coefficient for zirconium becomes greater than 1.

The distribution coefficients of iron increases regularly with increasing acidity, but remains however at low values.

Among the non extracted metals (distribution coefficient $K_D \cdot 10^{-2}$), : Co, Ni, Mn, Cu, Al, alkaline and alkaline earths.

2.3. Discussion

It is immediately noticeable that there is a resemblance between these results, and those obtained with molar solutions of TBP in kerosene. It thus appears that the fields of application of DHpSO in solution in TCE should be the same as those of TBP. The conditions of separation for U-Th have already been discussed³.

DHpSO, when compared to TBP also has the advantage of not being subject to any degradation. It is known that the degradation of TBP is catalysed by zirconium ions, making its use impossible for zirconium hafnium separation. Thus we decided to study the possibilities of DHpSO applied to this particular separation.

3. Zirconium-hafnium separation in a pulsed-column

This separation was chosen in order to test molar solutions of DHpSO-TCE in nitric acid medium using a continuous liquid-liquid extraction column. Before reporting these results, it is necessary to consider the extraction characteristics of zirconium and hafnium.

3.1. Extraction of zirconium in nitric medium

The solutions of zirconium used were obtained by dissolving, in nitric acid media, hydrated zirconia, $ZrO_2 \cdot xH_2O$, which itself was obtained through the attack on the pure metal by fluorhydric acid, and precipitation in neutral medium.

Distribution isotherms have been drawn for varying aqueous normalities. There are shown in figure 2, while the distribution coefficients, $K_D \text{ Zr}$, for various aqueous concentrations in metal are shown in figure 3.

It has been stated that the extraction of Zr begins to be detected only for acidities greater than 2N and is measurable for acidities greater than 3N. The form of the isotherms shows that the extraction is rather important for low concentrations of metal. No saturation appears. The distribution coefficient increases regularly in proportion with the aqueous acidity, without however reaching the values 10 in the most favourable case.

3.2. Extraction of hafnium in nitric medium

Solutions of hafnium were prepared in a similar manner to that for zirconium, i.e. attack of the metallic Hf by HF, precipitation of the hydroxide and nitric dissolution. The distribution isotherms are shown in figure 4, the corresponding distribution coefficients in figure 5.

These curves show that the extraction of the hafnium begins to be detectable only at aqueous acidities greater than 4,6N. The distribution coefficient remains very low, whatever the acidity may be. In particular the distribution coefficient is less than $3 \cdot 10^{-2}$ for an aqueous acidity less than 3,5N. The ratio $K_D \text{ Zr} / K_D \text{ Hf}$ is always superior to 10.

The results show that the separation Zr-Hf is possible using DH_2SO_4 .

3.3. Characteristics of the pulsed column

Since the purpose of our study was chiefly to study the behaviour of DHP₂SO-TCE solutions in a column apparatus a complete equipment (with extraction and scruvving sections), was not prepared but only a simple extraction section.

The arrangement of the column is shown in figure 6. The main characteristics are as follows :

- the plate section, in "Pyrex" glass, was 3.75 meters long with inside diameter 3.7 cm,
- the pulsations were obtained using a compressed air-electrovalve, system,
- the feed was achieved with a pump, of glass and teflon construction, with adjustable flow ranging from 0 to 30 liters/hour.

The principal feature of this column was its fabrication with perforated plates made of "teflon". The choice of this material was dictated by the necessity of employing the column in hydrochloric acid medium, which is incompatible with the use of stainless steel. The perforated plates had a fractional free perforated opening of 40%, and they were separated from one another by a distance of 5 cm.

The use of the original material for the plates, and the utilisation of a new solvent necessitated previously reported work in order to determine optimal working conditions, in particular flooding curves and the variation of efficiency of extraction in relation to the pulsing conditions^{4,6}.

It was noticed that the highly hydrophobic nature of the teflon plates did not allow any working of the column in continuous aqueous phase.

3.4. Research of optimal conditions of working

In order to fix the working conditions, it was necessary to have two precise sets of data : the limiting throughout of the column and the optimal efficiency in relation to the pulsation frequency. All these parameters have been determined for a constant amplitude of pulsation equal to 4 cm (this value was chosen after a number of experiments).

3.4.1. Flooding

The flooding at an amplitude of 3 cm, has been determined in the absence of material transfer. We have shown in figure 7, the flooding points, in relation with the velocity of the two phases, and with the product amplitude x frequency. We can see that the flooding conditions are of the same value as those observed in a pulsed column with plates made of stainless steel with TBP-kerosen.

3.4.2. Efficiency

We have studied the optimal pulsing frequency for mass transfer at an amplitude of 4 cm. The height equivalent to theoretical stage (HETS) of the column was determined for the extraction of HNO_3 using two flow rate values, 9 and 13 liters/hour. The results are shown in figure 8.

The parts of the curves shown in dotted lines correspond to the flooding. It has been stated that optimal conditions are to be found at the limit of flooding, but one notice that it is better to work at low flow rates; the minimal HETS amounting to 50cm for 9 l/h and 60 cycles/mn, and 60 cm for 13 l/h and 55 cycles/mn. The results obtained in this particular example for the mixture DH_2SO_4 -TCE and a teflon plate are comparable to those observed with the TBP.

Figures 7 and 8 enable the choice of conditions suitable for the study of the extraction.

3.5. Zr-Hf separation in column

It was chosen to purify a zirconium feed containing 4.7% of hafnium. For the experimental results given in the preceding paragraphs, the following conditions were adopted:

- aqueous acidity; 8.5N
- flow rate of the aqueous phase: 5.5 l/h
- flow rate of the organic phase: 5.0 l/h
- amplitude of the pulsation: 4 cm
- frequency of the pulsation: 40 cycles/min

The aqueous solution to be extracted was prepared as previously described.

After dissolution and adjustment to the acidity of 8.5N, the concentrations were 20.15 g/l Zr and 0.95 g/l Hf. The determination of the concentration of Zr / Hf were made by gravimetry. The ratio Zr/Hf was determined by neutronic activation. The solvent to be supplied to the column was previously acidified by HNO_3 , at the concentration of 1 N.

The compositions of the phases were measured at steady state giving the results shown in the following Table:

TABLE 1

	concentration in	
	Zr g/l	Hf g/l
loaded solvent	22.2	0.2
extraction raffinate	traces	0.7

3.6. Discussion

The results of the obtained separation are in conformity with that which could be expected from the distribution isotherms: almost all the zirconium has been recuperated in the solvent, while the ratio Zr/Hf decreases from 4.7% in the aqueous feed, to 0.9% in the loaded solvent, corresponding to about 4 theoretical stages.

The most important point concerns the behaviour of the solvent in the column. As could be expected according to the physical-chemical properties, no irregularity in the working of the column was observed. The dispersion appeared to be normal and coalescence in the end stages gave no problem.

The experiment confirms that molar solutions of DHpSO in the TCE may perfectly well be used in a pulsed column. The chosen example - separation Zr-Hf also confirms the possibilities of the solvent for this separation.

4. Extraction of metals in hydrochloric acid medium

Practically all the extracted metals in the form of nitrate are extracted in the form of chloride.

We will be contented with giving the results concerning the purification of iron in the pulsed column, to check the behaviour of the solvent in the case of an extraction in hydrochloric acid medium. Before reporting the results of the separation, it is necessary to consider the equilibrium results concerning the extraction of pure iron, cobalt and nickel.

4.1. Extraction of Fe, Co and Ni

NiCl_2 is not extracted by DHpSO , but CoCl_2 is extracted. The corresponding isotherms are shown on figure 9. The extraction of CoCl_2 becomes appreciable only for aqueous acidities equal or greater than 4 N. Its distribution coefficient however never reaches very high values (always < 1).

Also FeCl_2 is practically not extracted.

The distribution isotherms of FeCl_2 are shown on figure 10.

There we can see that FeCl_3 is extracted by the DHpSO with excellent distribution coefficients, which increase with increasing aqueous acidity.

These extractions results for the pure metals show that a separation is theoretically possible. A study of the simultaneous extraction of these compounds also confirmed that nickel and cobalt salt out the iron⁷.

4.2. Purification of iron in pulsed column

In the column previously described, a solution of ferric chloride obtained from a commercial metallic iron, dissolved in HCl and oxidized at the ferric state by hydrogen peroxide was extracted. The characteristics of the solutions were as follows :

- aqueous solution : 73.5 g/l in iron, acidity 2.35 N, flow rate 3 l/h;
- organic solution: DHpSO (M) in TCE, flow rate 7.5 l/h.
- stirring: amplitude 4 cm, frequency 50 cycles/mn.

The iron solutions were determined by neutronic activation, before and after extraction. The results are shown in Table 2.

4.3. Discussion

As far as the observed decontamination factors are concerned, they are quite favourable. If we except some metals for which their estimations do not allow us to give precise results, (Cr, Zr, Mo, Ag, Au), we can see that the purification is good, sometimes even excellent for some impurities (Mn, As, Sb, W).

Table 2

impurity	concentration, in 10^{-6} (weight)	
	before extraction	after extraction
Mn	220	1.5
Ni	8	3
As	7.6	0.4
Na	7	2.4
Cu	2.8	2.16
Cr	~ 2	< 2
Co	2	0.2
Sb	1.5	0.09
W	0.5	0.03
Zn	< 0.5	< 0.5
Mo	0.1	< 0.1
Ag	< 0.1	< 0.1
Au	< 0.01	< 0.01
P	600	16

Fig. 1 : Extraction of metals by DHPsD (1M) in TCE ; distribution coefficients of several metals as a function of aqueous acidity. Concentration of metals in aqueous phase : 1 g/l.

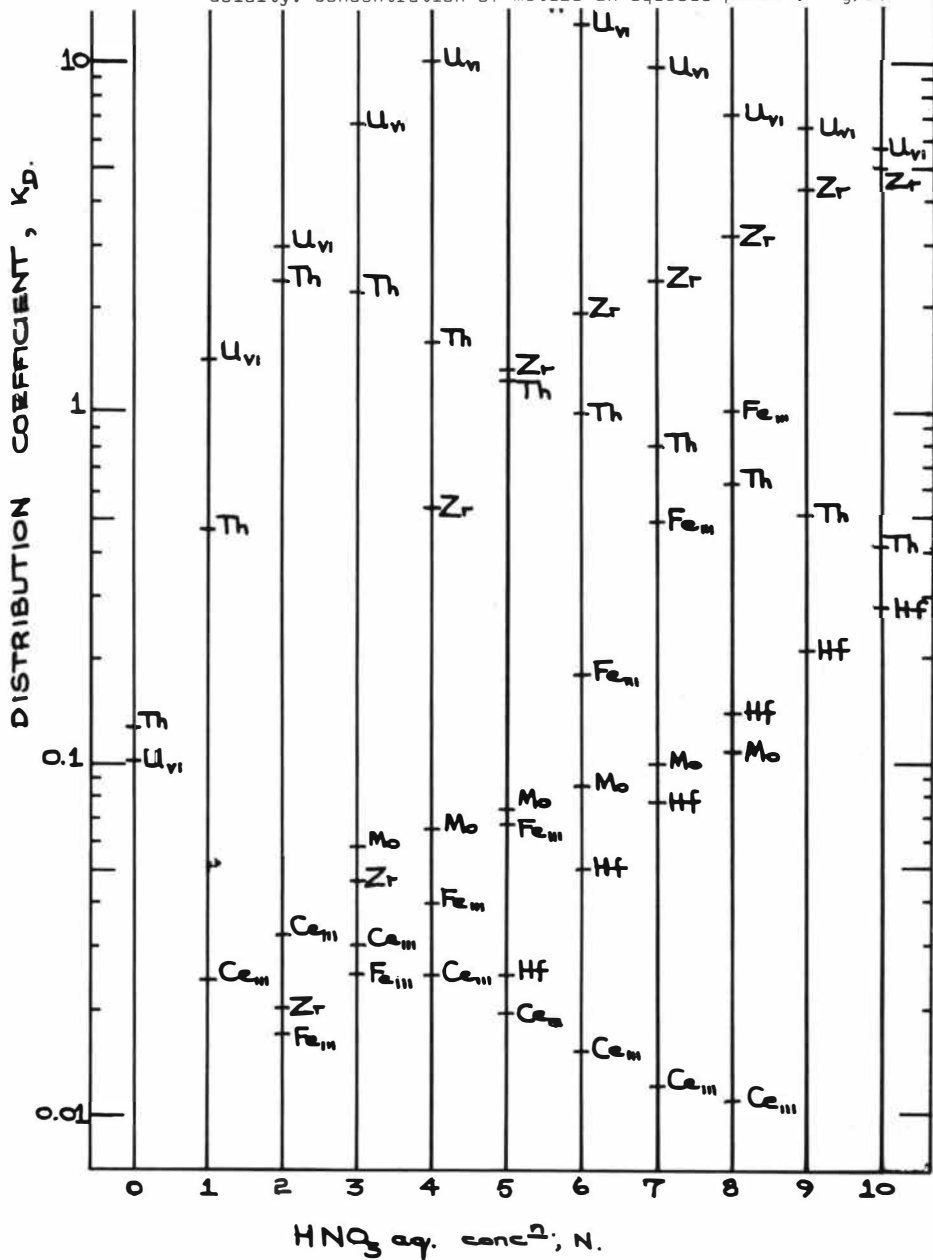


Fig. 2 : Zirconium extraction by DHP50 (1M) ; distribution isotherms for several aqueous acidities.

Curve 1, 8,80N ; 2, 7,68N ; 3, 6,30N ; 4, 4,88N ; 5, 4,12N ; 6, 3,12N ; 7, 2,17N.

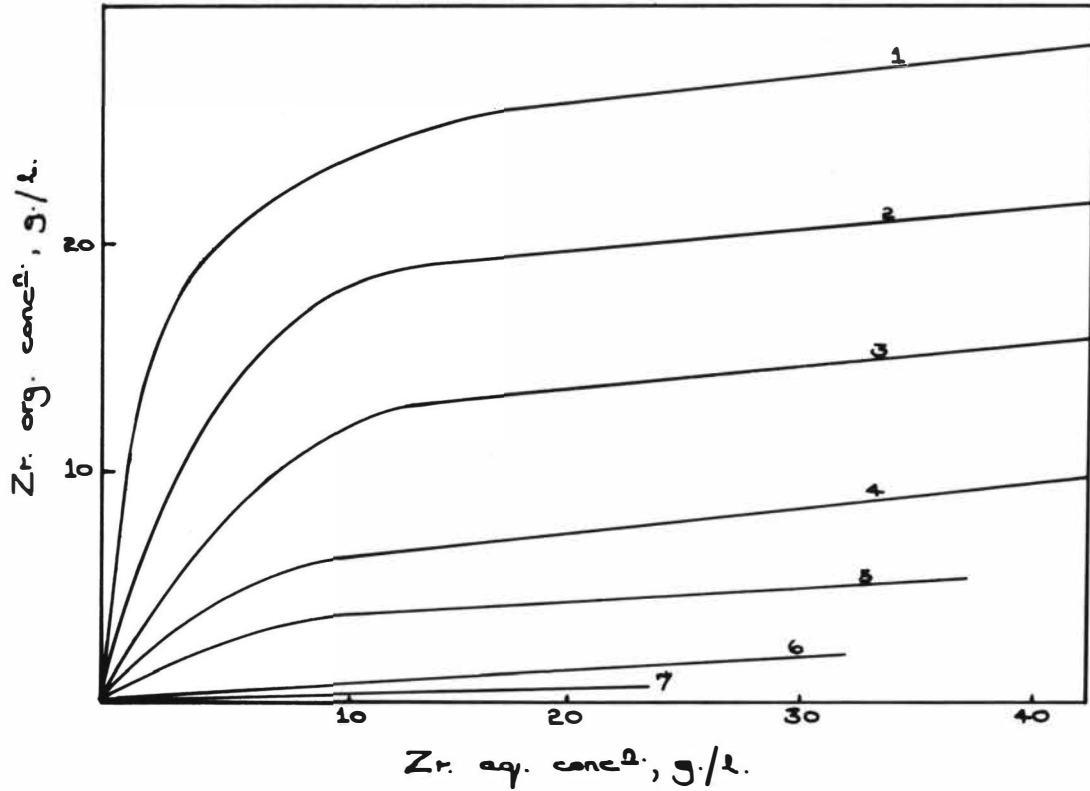


Fig. 3 : Zirconium extraction by DHpSO (1M) ; distribution coefficient for several concentrations of metal.in aqueous phase.

Curve 1, 1 g/l Zr ; 2, 10 g/l Zr ; 3, 20g/l Zr.

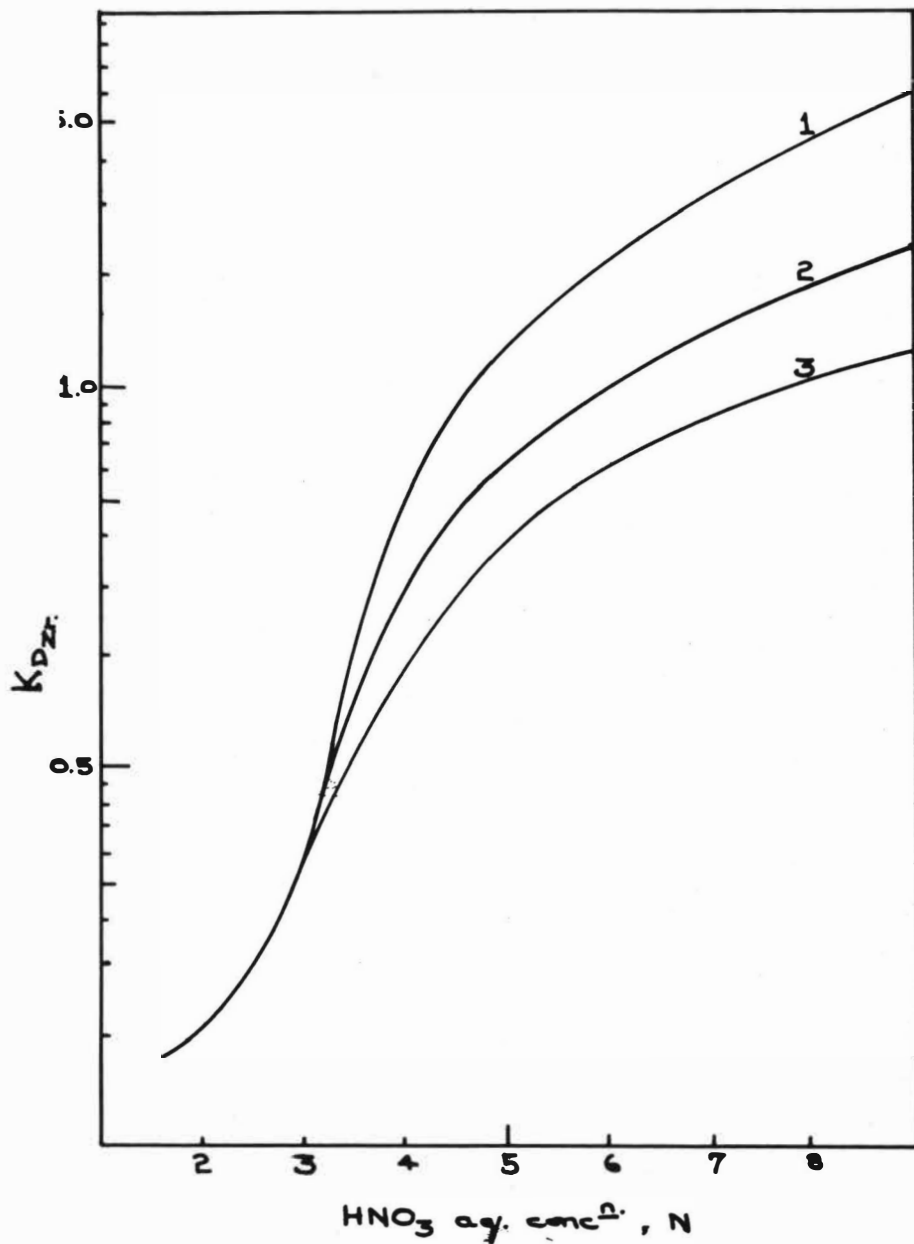


Fig. 4 : Hafnium extraction by DHP50 (1M) ; distribution isotherms for several aqueous acidities.
 Curve 1, 9,67N ; 2, 8,64N ; 3, 7,67N ; 4, 5,75N ; 5, 4,61N.

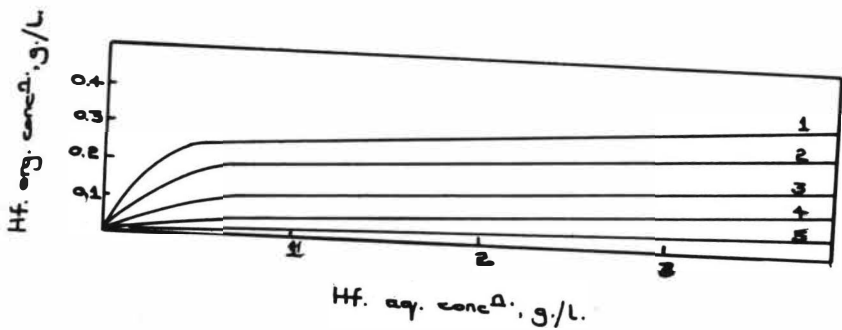
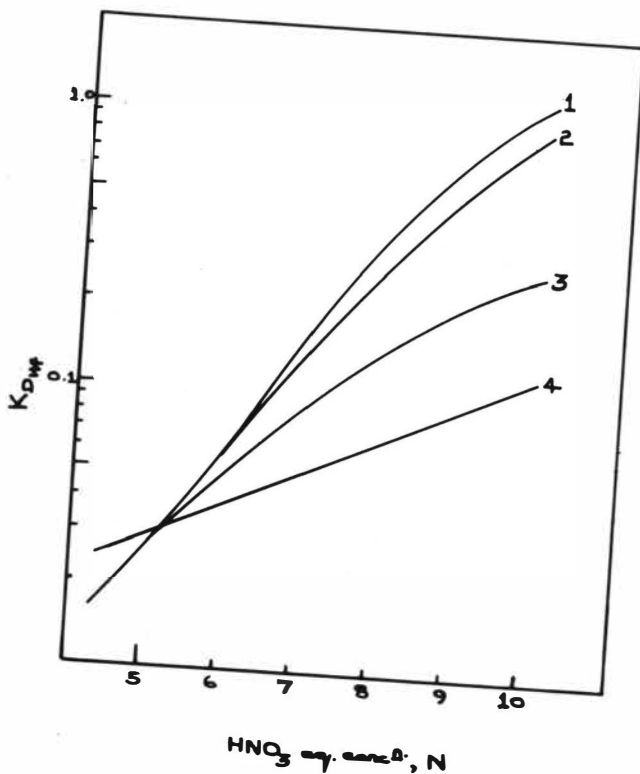


Fig. 5 : Hafnium extraction by DHP50 (1M) ; distribution coefficients for several aqueous concentrations of metal.
 Curve 1, 0.1 g/l ; 2, 0.2 g/l ; 3, 1g/l ; 4, 3 g/l



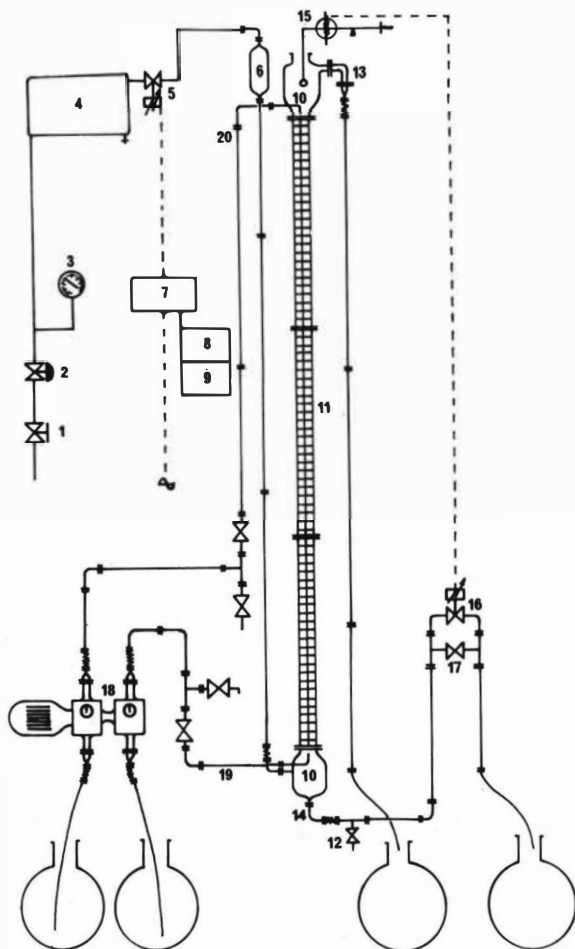


Fig. 6 : Pulsed column ; 1 : air cock ; 2 : reducing valve ;
 3 : manometer ; 4 : air container ; 5 : electrovalve ;
 6 : security pipe ; 7 : timer ; 8 and 9 : counting-
 mechanisms for seconds and impulses ; 10 : phase
 disengaging section ; 11 : plate section ; 12 :
 empty device ; 13 : light phase out ; 14 : heavy phase
 out ; 15 : interface measurement ; 16 : taflon electro-
 valve ; 17 : hand-valve ; 18 : pump ; 19 : light
 phase in ; 20 : heavy phase in.

Fig. 7 : Flooding volume vs. ωf product, for an amplitude of 4 cm.

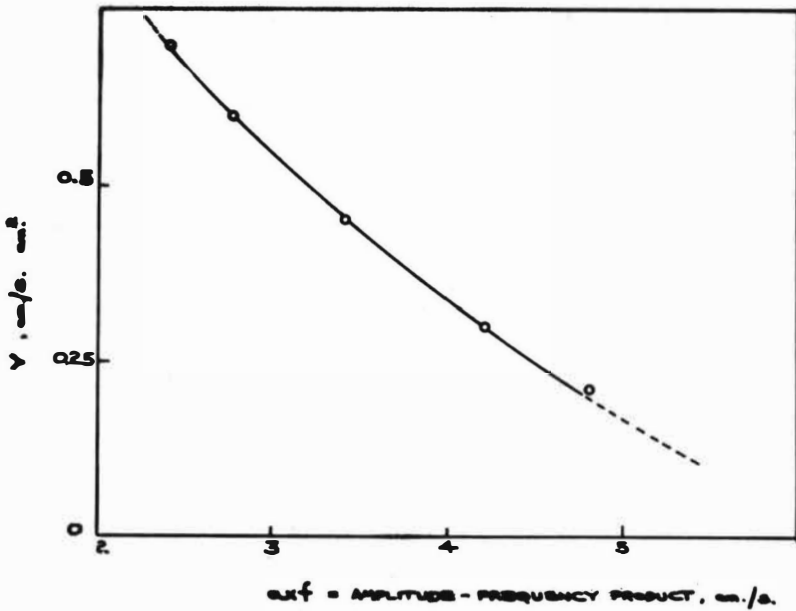
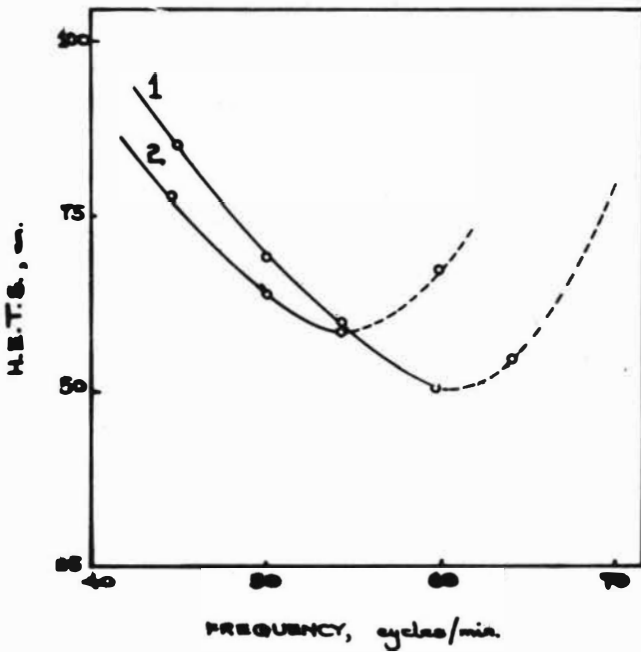


Fig. 8 : H.E.T.S. as a function of ωf .



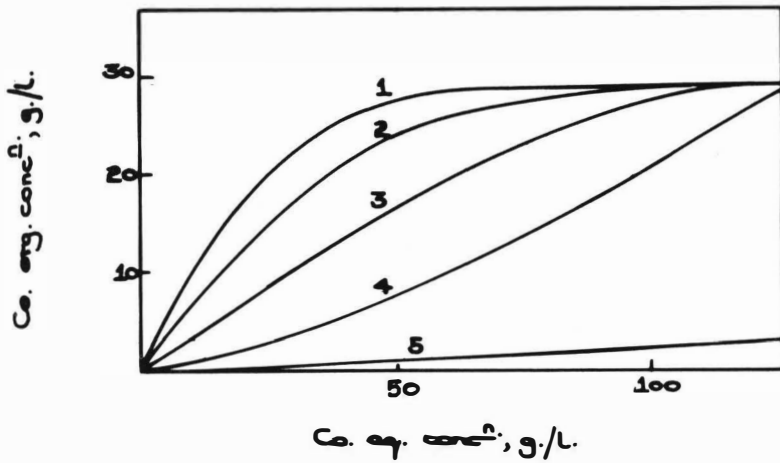
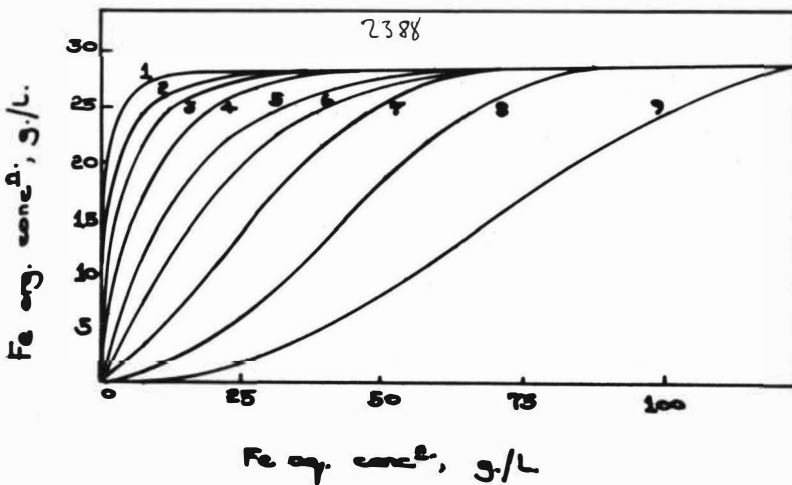


Fig. 9 : Extraction of CoCl_2 by DHP80 (1M) ; distribution isotherms for several aqueous acidities. :
 Curve 1, 10N ; 2, 8N ; 3, 6N ; 4, 4N ; 5, 2N.

Fig. 10: Extraction of FeCl_3 by DHP50 (1M) ; distribution isotherms for several aqueous acidities.
 Curve 1, 10N ; 2, 8N ; 3, 6N ; 4, 4N ; 5, 2N ; 6, 1M ; 7, 0.5N ; 8, 0.5N ; 9, 0.1N.



CALCULATION OF MASS TRANSFER COEFFICIENTS IN EXTRACTION
COLUMNS UNDER NON-IDEAL-FLOW CONDITIONS.

L. Steiner and S. Hartland

Because of complicated flow pattern the scale-up of extraction columns is difficult. In this paper the effect of backmixing is considered using digital simulation and mass transfer coefficients are calculated from the response to an impulse of soluble tracer. The results are tested on computer-simulated data to establish the accuracy which is necessary for evaluation of actual experiments.

Department of Industrial and Engineering Chemistry
Swiss Federal Institute of Technology, Zurich, Switzerland

December 1973

1. Introduction

The theory of liquid-liquid extraction has improved considerably in recent years. In particular mass transfer rates may be predicted now that nonideal flow is better described. Earlier, heights of transfer units and heights equivalent to a theoretical stage, based on entry and exit concentrations, were commonly used. These parameters were introduced when plug flow was considered a reasonable assumption for flow patterns inside a counter current column. Later, the nonideality of this flow was correctly recognised, and the fact that the mass transfer coefficients are strongly dependent on the column construction has been explained this way. However, mass transfer rates are often still quoted together with column size and a warning against scaling-up.

To improve this situation, a more detailed approach than a correlation of the end concentrations against physical properties of the phases, dimensions of the column and flow rates, is necessary. The mass transfer coefficients should be calculated from actual concentrations inside the column, and the nonideality of the flow should not be involved, but expressed by some other means. A true mass transfer coefficient, based on a proper description of flows inside a column, will not be dependent on column dimensions. Scaling-up should be considerably improved as soon as the calculation formulae realistically represent the processes involved. It will be shown in this paper, that even simple backmixing models may contribute considerably to this aim.

2. Backmixing models and digital simulation of column performance

Out of three models, listed by Widmer (1), the stagewise one with backflows in both phases has been found to be the most convenient for our purposes. The stagewise model without backflows does not express the conditions inside the column properly, as it does not allow material to move against the main stream along the length of the column, and at present the differential model is limited to constant flow rates and perfectly immiscible solvents.

The stagewise model with backflows, if used for unsteady state operation, gives a set of ordinary differential equations which may be directly solved on a computer, using a digital simulation language, such as MIMIC, developed for CDC computers.

In this case there is no restriction, apart from the computer capacity, to the number of variables. The number of the stages must be selected so that the backflows are always positive, which is an disadvantage if the backmixing is very low, as too many stages are then needed.

The model has been introduced by Schleicher (2) and developed by many other authors, such as Miyachi and Vermeulen (3) or Hartland and Mecklenburgh (4), so that only a short description will be given here. The translation into MIMIC has been made by Dunn and Ingham (5) for perfectly immiscible solvents. A typical section of a countercurrent column is shown in Fig. 1, together with both end-stages. The heavy phase flows from the top, and it is contacted with the light phase which rises from the bottom. In addition to the main flows, two hypothetical flows in the opposite direction are considered, which represent the backmixing. It is assumed here that these flows

are proportional to the flow rates of the main stream of the same phase in the same cross-section of the column. This assumption, introduced by Mecklenburgh and Hartland (6), is the most restrictive one, as the flow rates and physical properties of the phases may change from one stage to another. The stages are hypothetical, perfectly mixed sections of the column, the concentration inside each being equal to its exit concentration. For the purpose of the model it may be assumed that the mixed stages fill all the volume of the column with step changes in concentration between them. The volume of the stages is shared by both phases, the volumetric fraction of the light one being denoted by ϵ and the interfacial area per unit of the stage volume by a . As long as the stages have finite volumes, there is some mixing even if the backflows do not exist. It is, therefore, necessary to have the number of stages sufficiently large, so that the minimum backmixing considered for the column in question would be greater than that for the stagewise model without the backflows. It is possible to write the balances quite generally, varying any of the parameters involved. However, it is desirable to simplify the relations as much as possible, as the computer capacity is not infinite, and each variable requires a new differential equation for each stage. Only the case with perfectly immiscible solvents, assuming constant densities and volumetric fractions of the phases along the column, will be discussed here. However, the programs for partially miscible solvents, as well as for the dispersion model, have also been prepared and published elsewhere. (9)

If the solvents are immiscible, the flows do not change along the column, and relative mass fractions are the best means of expressing the concentrations of the solute. Following Fig. 1, the unsteady-state balances for a typical stage n may be written:

$$(1+f)\dot{H}_s X_{n+1} + f\dot{H}_s X_{n-1} - (1+f)\dot{H}_s X_n - f\dot{H}_s X_n + r_n A \delta = \rho_x (1-\epsilon) A \delta \frac{dX_n}{dt} \quad (2.1)$$

and

$$(1+g)\dot{L}_s Y_{n-1} + g\dot{L}_s Y_{n+1} - (1+g)\dot{L}_s Y_n - g\dot{L}_s Y_n - r_n A \delta = \rho_y \epsilon A \delta \frac{dY_n}{dt}$$

Introducing the actual velocities of both solvents;

$$u_s = \dot{H}_s / [A \rho_x (1-\epsilon)] \quad \text{and} \quad v_s = \dot{L}_s / (A \rho_y \epsilon) \quad (2.2)$$

the balances may be rewritten;

$$\frac{dX_n}{dt} = \frac{u_s}{\delta} [(1+f)(X_{n+1} - X_n) - f(X_n - X_{n-1})] + \frac{r_n}{\rho_x (1-\epsilon)} \quad (2.3)$$

and

$$\frac{dY_n}{dt} = \frac{v_s}{\delta} [(1+g)(Y_{n-1} - Y_n) - g(Y_n - Y_{n+1})] - \frac{r_n}{\rho_y \epsilon} \quad (2.4)$$

where

$$r_n = K_x a (X_n^* - X_n) = K_y a (Y_n - Y_n^*) \quad (2.5)$$

The balances for the first and the last stages differ from equation (2.3) and (2.4), as no backflows leave the column. The corresponding equations, written directly in terms of u_s and v_s are for the first stage;

$$\frac{dX_1}{dt} = \frac{u_s}{\delta} (1+f)(X_2 - X_1) + \frac{r_1}{\rho_x (1-\epsilon)} \quad (2.6)$$

$$\frac{dY_1}{dt} = \frac{v_s}{\delta} [Y_1 + gY_2 - (1+g)Y_1] - \frac{r_1}{\rho_y \epsilon} \quad (2.7)$$

and for the last one;

$$\frac{dX_N}{dt} = \frac{u_s}{\delta} [X_i + fX_{N-1} - (1+f)X_N] + \frac{r_N}{\rho_x (1-\epsilon)} \quad (2.8)$$

$$\frac{dY_N}{dt} = \frac{v_s}{\delta} (1+g)(Y_{N-1} - Y_N) - \frac{r_N}{\rho_y \epsilon} \quad (2.9)$$

Equations (2.4) to (2.9) were directly converted into a MIMIC program, as shown in Fig. 2. Two examples of its use will now be described.

- a) Steady state profiles: Fig. 3a shows the concentration, dependence on time at different positions in the column for a feed of constant composition starting at zero time. If the integration is carried out till all the curves are horizontal, all dX/dt and dY/dt become zero, and the profile is the steady state one. Plotting all the X and Y's against the length of the column gives the concentration profile shown in Fig. 3b.
- b) Response to a single rectangular impulse: Constant flows of pure solvents are maintained throughout the column, and in a given time, an impulse of the solute is added to one of the phases. The concentration profiles in different parts of the column are shown in Fig. 4. This technique may be used to measure the mass transfer and the backmixing coefficients.

3. Determination of mass transfer and backmixing coefficients by the impulse technique for perfectly immiscible solvents

At the beginning of the measurement, pure solvents are passed through the column countercurrently with constant flow rates. When the steady-state has been established, a given amount of solute is introduced at the inlet of one of the phases and the concentration dependence with time is recorded at different positions along the column height as shown in Fig. 4. The area under the curves corresponds to the total amount of solute that still remains in the original phase, or that has been transferred to the other one and the mass transfer coefficient may be evaluated from the changes of this area by the following procedure.

3.1 Evaluation of the mass transfer coefficients

3.1.1. Stagewise model

If there are n stages between the control planes, where the concentrations are measured, the total mass transfer is the sum of the transfers in all the stages involved. Assuming that the impulse has been added to the y -phase, the mass transfer in a stage j may be written using equation (2.4) as

$$K_y a \delta \int_0^T (Y_j - Y_j^*) dt = \rho_y \epsilon v_s \int_0^T [(1+g)(Y_{j-1} - Y_j) - g(Y_j - Y_{j+1})] dt - \rho_y \epsilon \delta \int_{Y_0}^{Y_T} dY_j \quad (3.1)$$

The last integral at the right-hand side of the equation (3.1) is equal to zero if the time interval is so selected that $Y_j = 0$ both at $t = 0$ and at $t = T$. The transfer in all the stages may then be added together, and the mass transfer coefficient may be expressed explicitly:

$$K_y = \frac{\rho_y \epsilon v_s}{a \delta} \frac{(1+g) \int_0^T (Y_0 - Y_n) dt - g \int_0^T (Y_1 - Y_{n+1}) dt}{\sum_{j=1}^n \left(\int_0^T Y_j dt - m \int_0^T X_j dt \right)} \quad (3.2)$$

To use this formula, the concentrations between all respective stages must be known. As this is not possible in practice, they must be estimated from the end concentrations. The simplest way to do this is to assume a linear variation in concentration between the control planes at any time, which, as may be seen from Fig. 4, is possible, if the control planes are sufficiently close to each other.

Following the situation given in Fig. 5, the final approximate formula for the mass transfer coefficient may be rewritten as

$$K_y = \frac{2\rho_y \epsilon v_s}{a \Delta z} \frac{\int_0^T Y_0 dt - \int_0^T Y_n dt}{\left(1 + \frac{1}{n}\right) \int_0^T Y_n dt + \left(1 - \frac{1}{n}\right) \int_0^T Y_0 dt - m \left[\left(1 + \frac{1}{n}\right) \int_0^T X_{n+1} dt + \left(1 - \frac{1}{n}\right) \int_0^T X_1 dt \right]} \quad (3.3)$$

where $\Delta z = n \delta$. If the accuracy of the straight-line approximation is not sufficient, a parabolic approximation may be tried. In this case the section must contain an even number of stages, and the concentrations in the middle must be known in addition to those at the ends. To express the concentrations between the respective stages, Taylor's series may be used starting from the middle of the section. Referring again to Fig. 5, the final formula for the mass transfer coefficient, assuming the parabolic dependence of the concentration on the position in the column, is

$$K_y = \frac{6N_0 y_e v_s}{a \Delta z} \frac{(N+4g) \int_0^T Y_o dt - 8g \int_0^T Y_M dt - (N-4g) \int_0^T Y_N dt}{A + B + C} \quad (3.4)$$

$$\text{where } A = (N^2 - 3N + 2) \left(\int_0^T Y_o dt - m \int_0^T X_{n+1} dt \right)$$

$$B = 4(N^2 - 1) \left(\int_0^T Y_M dt - m \int_0^T X_M dt \right)$$

$$C = (N^2 + 3N + 2) \left(\int_0^T Y_N dt - m \int_0^T X_1 dt \right)$$

Formulas (3.3) and (3.4) are tested with data delivered by the computer in the following sections.

3.1.2 Continuous change of concentration

Equations (3.3) and (3.4) enable data calculated by the computer to be evaluated using the model described in Section 2. To use these equations for experimental data obtained from actual columns they should be extrapolated for an infinite number of stages when the straight-line and parabolic approximations become respectively:

$$K_y = \frac{2\rho_y \epsilon v_s}{a \Delta z} \frac{\int_0^T Y_o dt - \int_0^T Y_n dt}{\int_0^T Y_o dt + \int_0^T Y_n dt - m \left(\int_0^T X_1 dt + \int_0^T X_{N+1} dt \right)} \quad (3.5)$$

$$K_y = \frac{6\rho_y \epsilon v_s}{a \Delta z} \frac{\int_0^T Y_o dt - \int_0^T Y_N dt}{\int_0^T Y_o dt + \int_0^T Y_N dt + 4 \int_0^T Y_M dt - m \left(\int_0^T X_1 dt + \int_0^T X_{N+1} dt + 4 \int_0^T X_M dt \right)} \quad (3.6)$$

It may be seen from these equations that the backmixing coefficients disappear completely, and the mass transfer coefficient may thus be calculated independently.

3.2 Evaluation of the backmixing coefficient

The backmixing coefficients may be calculated from the changes of the shape of an originally rectangular concentration impulse if no mass transfer occurs. The simplest way to describe this change is to calculate the variance of the concentration curve and use the formulae derived by Levenspiel and Smith (7) for recalculation. The variance is defined

by;

$$\sigma_t^2 = \frac{\int_0^\infty t^2 Y dt}{\int_0^\infty Y dt} - \left(\frac{\int_0^\infty t Y dt}{\int_0^\infty Y dt} \right)^2 \quad (3.7)$$

and according to Levenspiel (8) is related to the dispersion coefficient, for open and half closed systems respectively, by

$$\sigma_t^2 = \frac{1}{v^4} (8 D^2 + 2 D v z) \quad (3.8)$$

and

$$\sigma_t^2 = \frac{1}{v^4} (3 D^2 + 2 D v z) \quad (3.9)$$

These formulae have been derived for the dispersion model assuming there is no mass transfer and that all the solute was introduced into the column in the same time. As it is difficult to realise such an impulse, it is better to record the concentration curve at different points along the height of the column using an ordinary rectangular impulse and calculate the dispersion coefficient from the increase of the

variance along the column height. For this purpose the formula (3.8) or (3.9) may be differentiated with respect to the height z to obtain;

$$\frac{d \sigma_t^2}{a z} = \frac{2 D}{v^3} \quad (3.10)$$

This formula shows that the variance should be proportional to the height z and that the dispersion coefficient D may easily be calculated from the slope, if σ_t^2 is plotted against z . For recalculation of the dispersion coefficients D_y and D_x to the parameters f or g for use with the stage-wise models, Miyauchi and Vermeulen, (3) recommend an empirical formula;

$$\frac{D_y}{v z} = \frac{N}{(N-1)(2N+1)} + \frac{2g}{2N-1} \quad (3.11)$$

Combining (3.10) with (3.11) we have

$$\frac{d \sigma_t^2}{a z} = \frac{2 z}{v^2} \left[\frac{N}{(N-1)(2N+1)} + \frac{2g}{2N-1} \right] \quad (3.12)$$

from which g may be calculated.

4. Recalculation of mass transfer and backmixing coefficients from simulated concentration profiles.

For practical use with actual data it is necessary to know how the approximate formulae represent the actual situation and how accurate the concentration measurements must be for evaluation of the coefficients. These problems were solved by recalculation of the coefficients from concentration profiles delivered by the computer. In this case the actual values are known and all influences may easily be separated. To evaluate the demands on accuracy, the values of X and Y were artificially scattered.

4.1 Mass transfer coefficients

The model described in Section 2 was used to generate the concentration profiles as a response to a single rectangular impulse at the entrance of the y-phase. The X and Y values from all 15 stages used were punched into cards in very short time intervals (1.5 sec) and evaluated by special Fortran programs. In the same time integrals of both concentrations at exit of each of the stages were directly generated by MIMIC. The results of the recalculations may be summarised as follows:

4.1.1 Recalculation of mass transfer coefficients from integrals generated by MIMIC: The direct integration by MIMIC gives the most accurate results available, as the integration step is variable and may be as short as 3×10^{-9} if necessary to achieve the prescribed accuracy of 5×10^{-6} . In this way, comparison of formulae (3.3) and (3.4) with the exact formula (3.2) was done with very accurate integrated values so that the deviations between the formulae may only have been caused by the approximation itself. The mass transfer coefficients were calculated from sections of 4 stages so that 11 values were obtained from 15 stages.

The arithmetic mean and standard deviations were also calculated, the results of a sample series being given in Table 1. It may be seen that the values calculated from the exact formula itself are not perfectly in agreement with the actual value of the coefficient used for the generation of profile, which may be explained by accumulation of very small errors during the successive integrations. Values calculated according to the parabolic approximation, formula (3.4) are very close to those calculated from formula (3.2), both for the mean value and standard deviation, thus proving that this approximation is very accurate. The linear approximation formula (3.3) differs slightly from the exact values, giving consistently lower results. As may be seen from the table, the differences may be as high as 7%, however usually they were smaller than 3%. The differences between the parabolic and linear approximation decrease if artificially scattered data are used, so that the use of the more complicated formula (3.4) is justified only if the measured concentration profiles are very accurate (Standard deviation of the measurements less than 0.2%).

4.1.2 Recalculation of the coefficients with numerical integration from discrete values of X and Y: The same calculation has been performed from the values of X and Y generated in preset time intervals. Simpson's rule was used for the integration and the integration step was changed by removal of some cards. In this way steps of 1.5, 3 and 6 sec. were obtained. It was found that the respective values of the coefficients, calculated from all three formulae, were much more scattered, while the mean of the total 11 points remained nearly the same. As an average from some 30 profiles it may be claimed that for the standard deviations to be not worse than about twice the values given in Table 1.

the integration steps must be very short. They are dependent of the velocity of the corresponding phase in the column and they should not be greater than $0.02 Z/v_s$.

4.1.3 Evaluation from artificially scattered values: The previous paragraph shows that even if the values of X and Y are exact, the final result may be considerably scattered if the numerical integration is not sufficiently accurate. The time-intervals for sampling may be close to 1 sec. if the flow rate approaches 10^{-1} m/s, which would make the practical sampling and analysis very difficult. Fortunately, the integrals used in the formulae may be obtained directly, recognising that $\int_{t_1}^{t_2} Y dt = \bar{Y} (t_2 - t_1)$. The mean value of \bar{Y} may be obtained if small amounts of liquid are continuously removed from the column into a mixed vessel, and analysed after a preset time interval. The values obtained this way should be as accurate as the analytical method itself. To see how accurate the method must be, a calculation with artificially scattered values of the MIMIC integrals was performed. The procedure was the same as described here under 4.1.1, but the values of the original integrals were multiplied by random numbers with Gaussian distribution, the mean value being always equal to unity and the standard deviation being varied from zero to 5%. The results of a sample series are given in Table 2. As in the case of numerical integration the means remain very close to the exact ones but the individual values are much more scattered. To keep the standard deviation of the result under 10%, it was necessary to have all the original integrals with standard deviations less than 0.5%. This is also the accuracy to which the analysis should be performed.

4.2 Backmixing coefficients

Working with zero mass transfer, a few profiles were generated to check equation (3.10). The variances were calculated both by integration and by summation of discrete values in preset time intervals and the best straight lines were found by the method of least squares. The coefficients of regression were calculated in the same time and used as a criterion for fitting the points to the line. Plotting the variances against the column height gave good straight lines except for some cases with very high backmixing when the last few stages did not agree with the other points. Neglecting systematically the values from the last three stages, the straight lines were practically perfect with coefficients of regression better than 0.995. As in the previous calculation, the variances calculated from discrete values gave a little worse results with coefficients of regression between 0.97 and 0.99. It was found that the summation may be done in intervals equal to about $0.1 Z/v_s$ and still have variances with acceptable accuracy. The method of calculation of the backmixing from a series of measurements along the column should not therefore cause difficulties and the result should be better than from other methods which use the variation in concentration with time at one point only. At the same time it was established by comparison that mass transfer changes the shape of the peaks so that simultaneous measurement of the mass transfer and backmixing coefficients is difficult. However, good results may be obtained if a mixture of two solutes, one of them soluble in the other phase, is injected and the concentration profiles evaluated by two different analytical methods.

5. Conclusions

The use of the digital simulation for generating concentration profiles in extraction columns makes it possible to consider the influence of backmixing in any routine calculation. The mass transfer coefficients necessary for such a calculation may be measured by the unsteady-state technique in a column of any size without consuming large volumes of solvents. Computer tests show that the only condition necessary for such a measurement is a good analytical method giving results accurate to 0.5%.

Literature:

1. Widmer F.: Vermischungseffekte bei Gegenstromverfahren,
Chemische Rundschau 1973, Nr. 14
2. Schleicher C.A.: Entrainment and extraction efficiency of mixers-settlers.
AICHE J. 1960, 6, 529.
3. Miyauchi T., Vermeulen T.: Diffusion and back-flow models for two-phase axial dispersion.
I & EC Fundamentals 1963, vol. 2, 304
4. Hartland S., Mecklenburgh J.C.: A comparison of differential and stagewise countercurrent extraction with backmixing. Chem. Eng. Sci. 1966, 21, 1209.
5. Dunn I.J., Ingham J.: Modelling of continous process systems: an introduction to digital simulation programming.
Verfahrenstechnik 1972, 6, 399.
6. Mecklenburgh J.C., Hartland S.: Design methods for countercurrent flow with backmixing - II. Solvent extraction with partialy miscible solvents.
Chem. Eng. Sci. 1969, 24 1063.
7. Levenspiel O., Smith W.K.: Notes on the diffusion type model for the longitudinal mixing of fluids in flow.
Chem. Eng. Sci. 1957, 6 227.

8. Levenspiel O. Chemical Reaction Engineering, J. Wiley & Sons, New York, 1966.
9. Steiner L., Hartland S.: Paper presented in the SIA congress, Zürich, February 1974.

List of symbols

a	Interfacial area per unit volume	$[\text{m}^2/\text{m}^3]$
A	Cross-sectional area of column	$[\text{m}^2]$
D	Eddy diffusion coefficient	$[\text{m}^2/\text{s}]$
f	Backmixing coefficient, heavy phase	
g	Backmixing coefficient, light phase	
\dot{H}	Mass flux, heavy phase	$[\text{kg}/\text{s}]$
K	Mass transfer coefficient	$[\text{kg}/\text{m}^2\text{s}]$
\dot{L}	Mass flux, light phase	$[\text{kg}/\text{s}]$
m	Equilibrium distribution coefficient	
M	Middle plane	
n	Number of typical stage	
N	Total number of stages	
r	Rate of mass transfer	$[\text{kg}/\text{s}]$
t	Time	$[\text{s}]$
v	Actual velocity, light phase	$[\text{m}/\text{s}]$
u	Actual velocity, heavy phase	$[\text{m}/\text{s}]$
X	Relative mass fraction, heavy phase	$[\text{kg solute}/\text{kg solvent}]$
Y	Relative mass fraction, light phase	
z	Height	$[\text{m}]$
Z	Total height of column	$[\text{m}]$

Greek symbols

ϵ	Volumetric fraction of light phase	
δ	Height of a stage	
ρ	Density	$[\text{kg}/\text{m}^3]$
σ_t^2	Variance based on real time	

Indices

i	Column inlet
j	Number of a stage
M	Middle plane
n	Number of typical stage
N	Last stage
s	Solvent
x	Heavy phase
y	Light phase
*	Equilibrium value

Table 1

Comparison of approximation formulae using integrals
generated by MIMIC

g	K_{act}	mean value			standard deviation %		
		K_{ex}	K_{par}	K_{lin}	K_{ex}	K_{par}	K_{lin}
0	1.5	1.5014	1.5014	1.4815	0.051	0.051	0.049
0.5	1.5	1.5031	1.4981	1.4632	0.082	0.67	1.15
0	0.5	0.5021	0.5021	0.4922	1.27	1.28	1.44
0	1.0	1.0056	1.0065	0.9662	2.8	2.97	3.03
0	2.0	2.0075	2.0083	1.8573	6.18	6.32	6.28
1	0.5	0.5041	0.4993	0.4878	1.0	2.1	4.09
1	1.0	1.0130	1.0028	0.9706	2.27	3.06	4.49
1	2.0	2.0290	2.0093	1.9041	4.83	5.52	5.73

Table 2

Calculation of mass transfer coefficient K_{ex} from artificially scattered values, exact formula only, $K_{act} = 1.5$, $\sigma_n =$ standard deviation of scattering random numbers, $\sigma_K =$ standard deviation of result, $K_{ex} =$

ε	σ_n [%]	K_{ex}	σ_K [%]
0	0	1.503	0.12
	0.5	1.511	8.07
	1	1.492	13.7
	2	1.499	28.3
	5	1.470	78.1
0.5	0	1.501	0.08
	0.5	1.482	11.0
	1	1.457	15.6
	2	1.661	37.7
	5	1.473	144.3

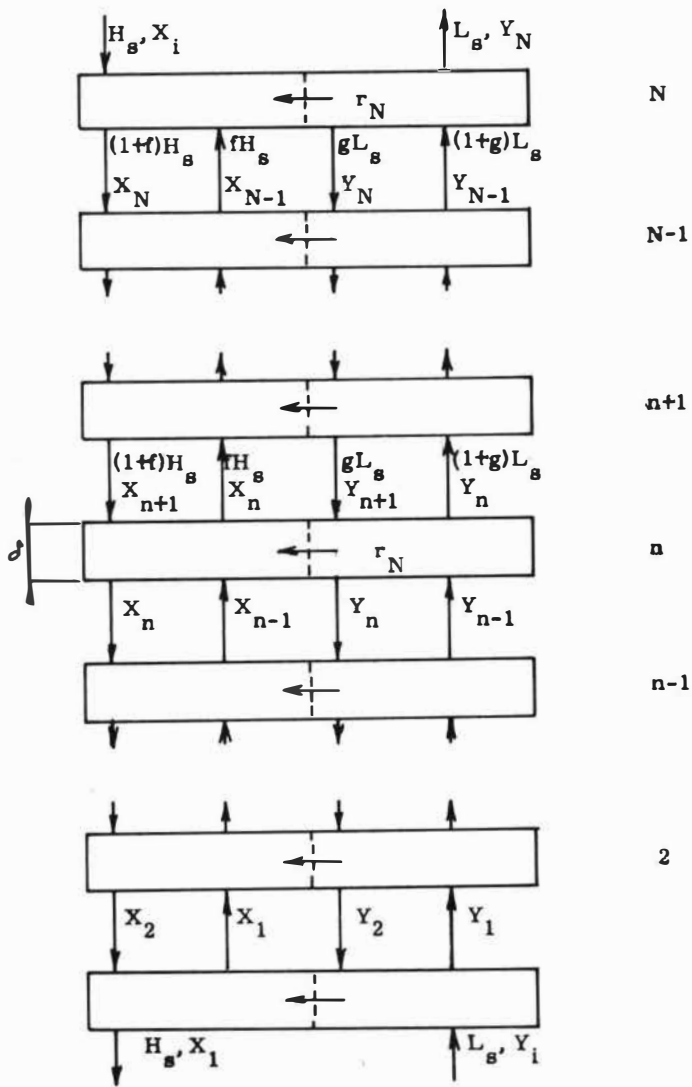


Fig.1 Derivation of Stagewise Model

*** MIMIC SOURCE-LANGUAGE PROGRAM ***

```

CON(DT,N)
CON(M,UI,VI,XI,YI)
CON(RX,RY,E,A)
PAR(F,G,K)
FSW(T,TRUE,TRUE,FALSE)
ST      KX      K*A/((1.-E)*RX)
ST      KY      K*A*M/(E*RY)
*INLET CONCENTRATION
      YI      YII
*SECTION 1
D1X1    UI*(1.+F)*(X2-X1)/N+KX*(XP1-X1)
D1Y1    VI*(YI-(1.+G)*Y1+G*Y2)/N-KY*(Y1-YP1)
XP1     Y1/M
YP1     M*X1
*SECTION 2
EQX     CSP(X3,X2,X1,Y3,Y2,Y1)
        RSP(D1X2,D1Y2)
        .
        .
*SECTION 14
EQX     CSP(X15,X14,X13,Y15,Y14,Y13)
        RSP(D1X14,D1Y14)
*SECTION 15
D1X15   UI*(XI-(1.+F)*X15+F*X14)/N+KX*(XP15-X15)
D1Y15   VI*(1.+G)*(Y14-Y15)/N-KY*(Y15-YP15)
XP15    Y15/M
YP15    X15*M
*INTEGRATION
X1      INT(D1X1,0.)
Y1      INT(D1Y1,0.)
        .
        .
X15     INT(D1X15,0.)
Y15     INT(D1Y15,0.)
*SUBPROGRAM
EQX     BSP(XA,XB,X,YA,Y,YB)
XP      Y/M
YP      M*X
D1X     UI*((1.+F)*(XA-X)-F*(X-XB))/N+KX*(XP-X)
D1Y     VI*((1.+G)*(YB-Y)-G*(Y-YA))/N-KY*(Y-YP)
EQX     ESP(D1X,D1Y)
*RESULTS
        FIN(T,3.)
        OUT(X1,X2,X3,X4,X5)
        OUT(X6,X7,X8,X9,X10)
        OUT(X11,X12,X13,X14,X15)
        OUT(Y1,Y2,Y3,Y4,Y5)
        OUT(Y6,Y7,Y8,Y9,Y10)
        OUT(Y11,Y12,Y13,Y14,Y15)
        END

```

Fig. 2 MIMIC Program for Stagewise Model, Steady State Operation, Immiscible Solvents

Fig. 2

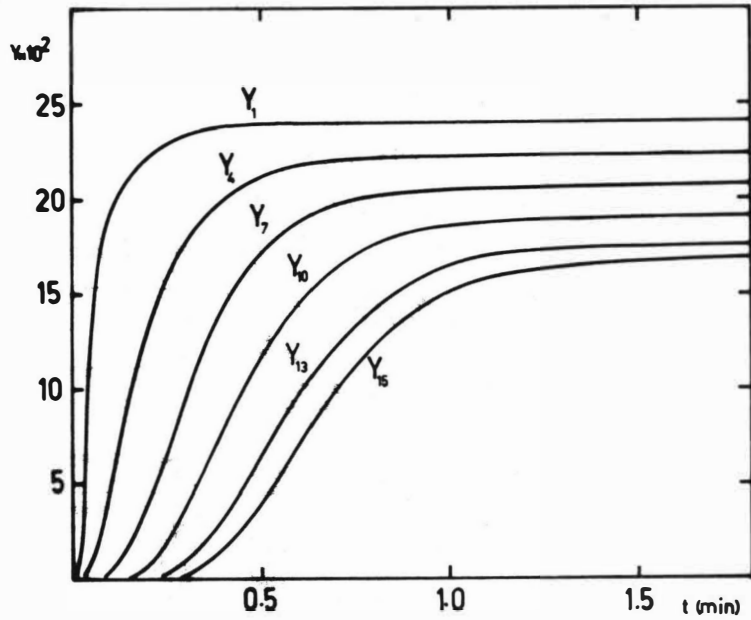


Fig. 3a Results Obtained from Program Given in Fig. 2

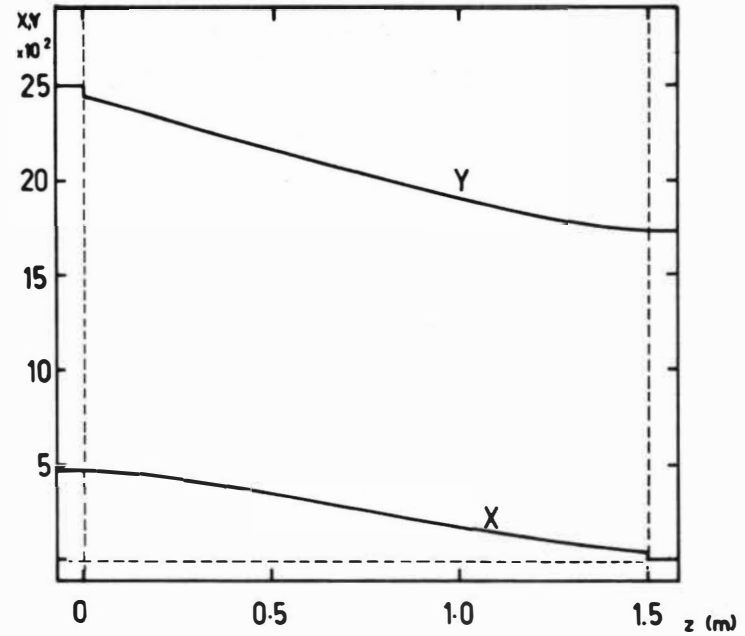


Fig. 3b Steady State Concentration Profile Obtained from Fig. 3a

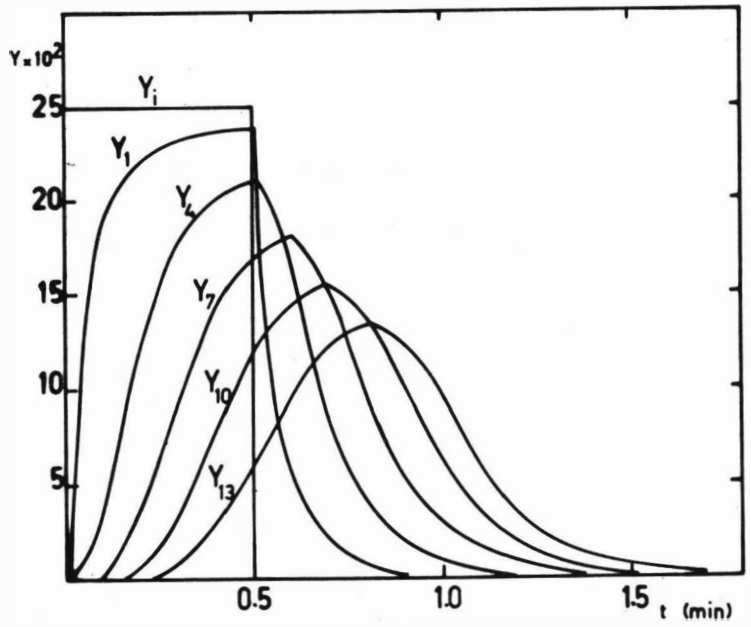


Fig. 4 Response of Column to Single Impulse of Solute, Stagewise Model

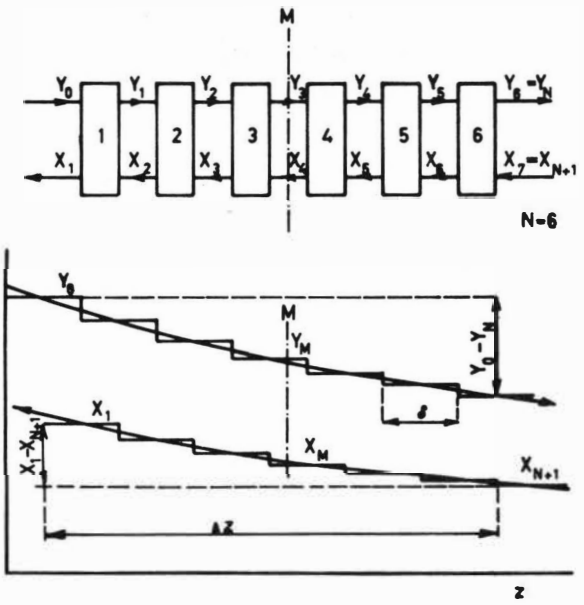


Fig. 5 Derivation of Approximative Formulae

HYDROMATIC BEHAVIOUR AND MASS TRANSFER OF EXTRACTION
COLUMNS WITH VARIOUS ROTATING PARTS

S. Weiss, W. Spathe, R. Wurfel, D. Mohring

ABSTRACT

Different rotating parts are examined under the same conditions in an extractor of 200 mm diameter and an operating height of 1m, with the system water/phenol/butyl acetate (water in continuous phase, butyl acetate in dispersed phase). For rotary disc extractors, results concerning the mean drop diameter, the hold up, and the flow rate at the flooding point for different dimensions of the rotor discs and stator rings are reported, and propositions are presented for modelling of the drop diameter and the velocity at the flooding point.

A rotary disc extractor with favourable dimensions for mass transfer and flow rate is compared with other rotating parts: Stator rings and impellers of round bar steel; radial baffle plates (at least 9/10 of the cross sectional area of the column remains free), and impellers of round bar steel and flat steel, respectively. The drop diameter dependence on the stirrer speed and HTU-value dependence on the hold up and the mass transfer area are shown for the different rotating parts. Taking into consideration the mass transfer and flow rate, differences up to 50% between the different rotating parts are found.

INTRODUCTION

In the last decade, extraction columns with rotating parts gained an increasing importance in liquid-liquid extraction. One of the designs first introduced into industry is the rotary disc contactor which even now is very often utilized.

The hydromatic behaviour and mass transfer are influenced decisively by the droplet size distribution, the hold up, and the axial mixing. The efficiency of the extractor can be estimated by the specific flow rate, e.g. in m^3 liquid/ m^2 cross-sectional area/hour, and the quality of the mass transfer, e.g. by the H_{OR} value. It is the aim of this work to examine the droplet size distribution, hold up, mass transfer, and flow rate for different rotating parts under comparable conditions.

EXPERIMENTAL

The experimental investigations were conducted with the system water/phenol/butyl acetate in an extraction column with a diameter of 200 mm and a height containing the rotating parts of ca. 1 m. The scheme of the experimental arrangement is shown in fig.1. Glass was chosen as material for the walls of the extractor column so that the flow could be observed. The butyl acetate was dispersed. The ratio of the volume of the dispersed phase to the volume of the continuous phase was 1:3,5. In all experiments with mass transfer the phenol concentration of the water at the inlet was adjusted to ca. 5 kg/m^3 . With this small portion of phenol, we can count upon constant quantities of raffinate and extract within the extractor. The following values were measured in the experiments.

CONCENTRATION of the water containing phenol and that of butyl acetate were measured at the inlet and at the outlet. This was done by sampling (places of sampling see figure 1) and subsequent determination of the phenol concentration in the laboratory by the universal spectrophotometer VSU of VEB Carl Zeiss, Jena.

The volume flows of water containing phenol and those of butyl acetate which entered the extractor, were measured by rotameters. For determination of the hold up, various measuring methods were used. For the most part, the method of separation by switching off the extractor was used. This method is very exact. Greater hold up values were corrected in order to take into account the volume outside the operating space.

The Droplet size distribution was measured through the wall of the extractor by photography with a camera Exacta Varex VX 1000 with an objective 1,4/75 and a stroboscope with a flash-light time of 10^{-6} sec. The advantage of this method was the fact that the flow in the extractor was not influenced. The curved wall of the extractor was equalized by an appropriate arrangement according to fig.2. It is supposed that the droplet size distribution near the wall of the extractor is the same as that near the rotating disc, see also fig.1. The measurements of the droplet size distribution were conducted at 5 different sections throughout the height of the column: at the second, fifth, eighth, eleventh, and fourteenth section, counted from below. In the experimental results described here, the drop diameter was determined in the fifth, eighth, and eleventh section, and from these values, an average value was calculated. For every measuring point, ca.1500 drops were evaluated. The difference of the average drop diameter in the fifth, eighth, and eleventh section reached 25%. The necessary data for the evaluation - phase equilibrium, density, viscosity of both phases, and interfacial tension - were measured in the laboratory. For values see Table 1.

TABLE 1 Data in the experiments

	aqueous phase continuous	butyl acetate dispersed
ρ , kg/m ³	998	878
$10^3 \mu$, kg/(m s)	1,04...1,06	0,74...0,77
$10^2 \gamma$, N/m		1,13...1,41

various rotating parts were examined under the same conditions (see fig.3). Uniform for all experiments were the following values: Diameter of the extractor . 200 mm; 15 sections, height of sections 64 and 60 mm, respectively; ratio of dispersed phase to continuous phase 1:3,5.

The following combinations of column internals were tested:

1. Rotary disc contactor, see fig.3a. The different dimensions of the rotating parts are listed in table.2, the height of a section measuring constantly 64 mm.

TABLE 2 RDC with different dimensions of stator rings and rotor discs

d_{st}, mm	148	148	148	148	148	154
d_r, mm	100	110	120	130	140	130
designation in) measuring points figures 4 to 7) curve	□	▽	○	▷	•	×
	2	3	4	5	6	1

2. Extractor with stator rings and impellers made of round bar steel, see fig.3b.

3. Extractor with radial stationary baffle plates and impeller made of round bar steel with four blades, see fig. 3c [3].

4. Extractor with radial stationary baffle plates and impeller made of flat steel with four blades, see fig. 3d [3].

The experiments with different rotating parts were conducted according to the following experimental scheme:

Constant flow rate at varying stirrer speed and increase up to the flooding point.

Constant stirrer speed at varying flow rate and increase up to the flooding point.

Better informations about the different rotating parts are given by the experiments at varying stirrer speed. Therefore, only experiments with constant flow rate of 0,280 m³/h water and 0,060 m³/h butyl acetate corresponding to 0,340 m³ total flow rate are described in this paper.

The flow rate was varied only in the experiments on the flooding point in figures 6 and 7, according to the given statements.

RESULTS

At first, the results of an RDC with different geometrical dimensions are discussed. Thereupon, the RDC with dimensions favourable for hydrodynamics and mass transfer will be compared with those of the other rotating parts (figures 3b, c and d)

RDC with different geometrical dimensions

It is supposed that the efficiency of the RDC with different geometrical dimensions is characterized in a sufficiently exact way by the droplet size distribution, the hold up, and the flow rate. Therefore, the experiments were conducted only with water/butyl acetate without mass transfer. By comparing experiments with mass transfer it was observed that the differences in experiments with and without mass transfer are small under the conditions chosen here. The other conditions being the same, the flow rate at the flooding point, e.g., was influenced by mass transfer to less than 5%.

Of the different definitions of the mean drop diameter, the Sauter diameter

$$d_{32} = \frac{\sum_i n_i d_i^3}{\sum_i n_i d_i^2}$$

will be used below. The drops are counted according to classes, 0,1 mm is used as class interval. Figure 4 shows the Sauter diameter in dependence on the stirrer speed for the RDC with different geometric dimensions according to Table 2. With increasing diameter of the rotor discs and constant diameter of the stator more energy is introduced, and therefore the drop diameter becomes smaller at constant stirrer speed. Deviations are found only at low stirrer speed below 190 rotations/min at a diameter ratio of $d_{st}/d_r = 1,14$. Figure 4 confirms the fact known from other experiments that different drop diameters caused by different geometrical dimensions are widely compensated by choosing an appropriate stirrer speed.

In the plot of the drop diameter dependence on the hold up (after sauter), the measuring points for different dimensions at the same hold up move closer together since the hold up gives a better reflection of the introduced energy necessary for the dispersion than does the stirrer speed. At hold up values of $> 10\%$ for rotor radius of 100 to 130 ($d_{st} = 148$ mm) corresponding to $d_{st}/d_r = 1,14$ to $1,48$ approximately the same Sauter diameter is obtained at the same hold up values. On the other hand, the drop diameter at the same hold up is clearly greater for $d_r = 140$ mm corresponding to $d_r/d = 0,70$ and $d_{st}/d_r = 1,057$ although the introduced energy is comparably greatest at a rotor diameter of 140 mm. Obviously, the cause of this fact is the unfavourable formation of the cross-sectional areas manifesting itself also by a decreased flow rate at the flooding point (see fig.7) and presumably leading to an increased coalescence. The slightly different behaviour of the Sauter diameter for an RDC with $d_{st} = 154$ mm and $d_r = 130$ mm can be ascribed, apart from the changed stator diameter, to the influence of the mass transfer since contrary to all other series of experiments this one was conducted with mass transfer, according to Table 2.

The number of the measuring points for hold up $> 20\%$ is relatively small since the RDC has operating characteristics according to which the hold up increases rapidly at higher hold up values (in this case $> 20\%$) at a slight increase of the stirrer speed, and the flooding point is reached at a slightly higher stirrer speed. Further special investigations revealed the fact that the Sauter diameter again increases slightly near the flooding point at high hold up values.

Modelling of the droplet size distribution in the RDC

As to this point, further experiments were conducted on rotary disc extractors with a diameter of 100 mm with different dimensions, see (2), as well as additional experiments with the mixture perchlorethylene/water (6). Investigations and equations for calculation of the droplet size distribution in RDC were published recently by Kagan (4), Misek (5) and Fischer (1).

A check of our own experimental results using the equations of these publications only partially yielded satisfactory results with deviations smaller than 20%. For different geometrical dimensions, the deviations were greater than 50%. For the modelling, the distribution function used by Misek (5) with the volume distribution density

$$H(d_i) = \frac{d_i^3}{6\alpha} \exp\left(-\frac{d_i}{\alpha}\right) \quad (2)$$

is used. From the distribution parameter α , we can obtain the approximate Sauter diameter from $d_{32} = 3\alpha$. In order to describe the distribution parameter throughout the whole range of stirrer speed, the following equation is chosen (6).

$$\alpha = \alpha_0 (1 + CC) \exp(-CC) \quad (3)$$

Physical considerations for the partial processes and the regression analysis for determination of the constants with our own experimental data yield

$$\alpha_0 = C_1 \left(\frac{\gamma}{\Delta \rho g}\right)^{0,5}$$

α_0 upper limit value of distribution parameter corresponding to the maximum drop diameter)

$$CC = We^3 / C_4 + (We/Re)^{C_6} \cdot \frac{1}{C_7}$$

$$We = \frac{[n d_r - C_2 (\Delta \rho g / \gamma)^2]^{C_3} d_r}{\gamma} ; \frac{We}{Re} = \frac{(n d_r - C_5 \Delta \rho g / \gamma)^{C_4}}{\gamma}$$

If $C_2 (\Delta \rho g / \gamma)^2 > n d_r$ and $C_5 \Delta \rho g / \gamma > n d_r$, respectively, we can put $we = 0$.

The constants can be taken from Tab. 3.

Table 3: Constants for equations (3)

Constant	without mass transfer	with mass transfer	measuring unit
C_1	0,445	0,442	-
C_2	$25,2 \cdot 10^{-12}$	$23,86 \cdot 10^{-12}$	m^5/s
C_3	0,5	0,5	-
C_4	24,5	24,0	-
C_5	$1,555 \cdot 10^{-6}$	$2,30 \cdot 10^{-6}$	m^3/s
C_6	0,5	0,5	-
C_7	0,125	0,15	-

In equation (3) the following range was covered for extractors with diameters of 100 and 200 mm: $d_r/d = 0,5$ to $0,7$; $d_{st}/d = 0,68$ to $0,77$; $h/d = 0,325$ to $0,40$; $\Delta p = 108$ to 565 kg/m^3 ; $\rho = (10 \text{ to } 21) \cdot 10^{-3} \text{ N/m}$; $\rho_a = 1000 \text{ kg/m}^3$; $\eta_c = 0,00106 \text{ kg/m s}$; $\eta_d = (7,4 \text{ to } 8,8) \cdot 10^{-4} \text{ kg/m s}$.

In the values calculated according to equation (3), the deviation was in most cases less than 10% as compared to the experimental values. At hold up values above 15% the distribution parameter is also influenced. This can be taken into account by a coalescence factor C_8X in the following way:

$$\alpha = \alpha_0 (1 + CC) \exp(C_8X - CC) \quad (4)$$

In our experiments, the constant C_8 in equation (4) varied between 0,1 and 3,1.

Flow rate at the flooding point in the RDC

In the RDC of 200 mm diameter, the flow rate at the flooding point was measured without mass transfer at different stirrer speed at $d_{st} = 148 \text{ mm}$ and different $d_r = 120, 130, \text{ and } 140 \text{ mm}$. The results in fig.6 demonstrate clearly that the flow rate at the flooding point increases at constant stirrer speed with increasing differences $d_{st} - d_r$.

An equation published by Kagan and co-workers (8) for the calculation of the stirrer speed at the flooding point with V_{cf} and V_{df} could be used for description of our own experimental results after adapting to a constant to the experimental results. According to a model of Salzer (which was developed in the RDC with $d = 65$ and 100 mm on the base of the energy balance at the drops (assuming the drops to be of the same size), the following correlation is found:

$$V_{cf} = V_{df} + K + y - 2 \left[K (V_{df} + y) \right] \quad (5)$$

$$K = 0,321 \delta^{-0,337} (\Delta\rho \cdot \eta_c)^{-0,117} \rho_a^{-0,101} d_r^{-0,458} g^{0,68} n^{-0,933}$$

$$\text{for } \eta_c \leq 0,00735 \text{ kg/m s and } \delta \leq 0,010 \text{ N/m}$$

$$y = 0,04195 (n^2 d_r / g)^{-0,36} \cdot G$$

Salzer did not change the geometry of the rotating parts. On the base of the experimental results shown in Fig.6, G is determined by;

$$G = 0,628 \left[\frac{(d^2 - d_r^2) + (d_{st}^2 - d_w^2)}{2d^2} \right]^{-0,8}$$

Hereby the speed at the flooding point can be calculated according to equation (5) with a maximum error of 4,5% as compared to the measured values. However, a check of the results of other authors as to the flow rate at the flooding point partially yielded remarkable deviations.

Fig.7. shows the flow rate at the flooding point in dependence on the energy dissipation per volume unit formed by analogy to mixers. Logarithmic division of the coordinates yields a straight line which agrees with the results of other authors.

In further experimental series which are not shown here, the flow rate up to the flooding point in the RDC at constant stirrer speed was determined. The analysis of all investigations shows that an RDC with $d_{st}/d = 0,72$ to $0,77$ and $d_{st}/d_r = 1,14$ to $1,19$ yields favourable conditions for mass transfer and flow rate. For further comparing investigations with different rotating parts an RDC with the dimensions $d = 200$ mm, $d_{st} = 154$ mm, $d_r = 130$ mm, $h_s = 64$ mm was used.

Comparison of extractors with different rotating parts

Under the same conditions, the following values for different rotating parts were measured at a flow rate of 280 l/h continuous phase (water with 5 kg phenol/m³ at the inlet) and 80 l/h dispersed phase:

Drop size distribution, hold up and the concentration at the inlet and outlet. The following rotating parts were involved into the investigations: See table 4.

TABLE 4 - Experiments with different rotating parts with mass transfer in an extractor of 200 mm diameter, 15 sections

	RDC $d_{st}=154$ mm	Extractor according to fig.3b	Extractor according to fig.3c	Extractor according to fig.3d
	$d_r = 130$ mm,			
	$h_s = 64$ mm,			
	see fig. 3a			
designations in) measuring figures 9 to 12) points	\times	\circ	Δ	∇
curve	1	2	3	4

For characterization of the mass transfer, the height of the transfer unit is used. It was determined from the experimental results in the following way:

$$H_{OR} = h/N_{OR} \quad (6)$$

No back mixing
for
Since the equilibrium line and the operating line are straight lines (see also fig.8), the following equations be current for the number of transfer units based on raffinate phase:

$$N_{OR} = (x_K - x_T) / \Delta x_m; \Delta x_m = (\Delta x_K - \Delta x_T) / \ln (\Delta x_K / \Delta x_T) \quad (7)$$

By means of the measured concentrations x_K and x_T and the appertaining equilibrium compositions, the value of a transfer unit is determined by equations (6) and (7). The results for the different rotating parts according to Table 4 are shown in figures 9 to 12. The dispersion is influenced essentially by the rotating parts. This behaviour can be estimated better by a plot $d_{32} = f(\Sigma)$ according to fig.10 than by $d_{32} = f(n)$ according to figure 9.

At hold up values up to 10%, the RDC yields relatively great mean drop diameters as compared to the other rotating parts. In the RDC under the present conditions, hold up values between 20 and 45 % are out of the question for continuous operation since the flooding point is reached already by relatively small changes, and the RDC does not work steadily any longer. At high hold up values, the extractor with stator rings and impeller according to fig. 3b shows the same behaviour. The energy dissipation by the impeller is greater than that by a disc, so that relatively small Sauter diameters are reached already at a hold up from 3% upwards. These characteristics of the extractor according to fig. 3b will not be of advantage for the use in industry.

Extractors with radial baffle plates and impellers made of round bar steel (figure 3 c) or flat steel (fig. 3d) show an essentially different behaviour. Already at relatively small values of the hold up, a relatively small drop diameter is obtained. Values of 20 to 40 % for the hold up are obtained in a higher range of stirrer speed so that the operation of the extractor remains stable even at values of the hold up between 20 and 40%. The different behaviour can be observed very well by observation of the hold up in the ranges of 4 to 17% and of 17 to 40% and the appertaining range of stirrer speed, see Table 5.

Table 5 Range of stirrer speed n (rotations/min in dependence on the hold up

	RDC	extractor according to fig. 3c	extractor according to fig. 3d
Δn for $X=4$ to 40%	183 = 100%	214 = 100%	537 = 100%
Δn for $X=4$ to 17%	136 = 74,3%	87 = 40,7%	157 = 29,2%
Δn for $X=17$ to 40%	47 = 25,7%	127 = 59,3%	380 = 70,8%

In rotating parts with radial baffle plates and impellers, the droplet size distribution is much more like that of monodisperse distribution than is the case in the RDC. As was stated by Fischer (1), the impeller requires much less energy (partially only 1/3) for the same dispersion than do the discs in the RDC. It is also remarkable that the strongly different characteristics $d_{32} = f(n)$ in figure 9 for both extractors with radial baffle plates and impellers from round bar steel (curve 3) and impellers from flat steel (curve 4) in a plot $d_{32} = f(x)$ in figure 10 can be practically represented by one curve.

In the plot $H_{OR} = f(x)$ in figure 11, the rotating parts with impellers instead of discs clearly yield a better H_{OH} value for $x < 10\%$. For $x < 10\%$, the H_{OH} values of all rotating parts of the extractor show an approximate agreement. The measuring points for the H_{OR} values in dependence on the mass transfer existing in the extractor can be approximately characterized by the marked curve, see fig. 12. This indicates that the stirrers with the different parts there are roughly the same conditions for the axial mixing.

CONCLUSIONS

1. Different rotating parts with different characteristics for the Sauter diameter; the behaviour of the mixer speed is only partially possible.
2. On calculating the better operation taking into account the mass transfer and the H_{OR} value difference up to 50% for the differences are found.
3. Rotating parts with radial baffle plates and impellers show a favourable behaviour under different phase conditions and good mass transfer over a great range of load. This is due to their characteristics (steady behaviour also at high hold

REFERENCES

1. Fischer, A. Verfahrenstechnik, 5, 360
2. Spathe, W., Weiss, S., Wissenschaftl. Zeitschrift Techn. Hochsch. Chemie Leuna-Merseburg 1972, 14, 66
3. Wirtschaftspatent DDR 101296, 1973
4. Kagan, S.Z., Aerov, M.E., Volkova, T.S. Truchanov, V.G. J.of Appl.Chem. USSR 1964, 37, 67
5. Misek, T. Development and applications of the ARD extractor (lecture summary), Research Institute of chemical equipment, Prague, 1970
6. Spathe, W. Dissertation Merseburg 1973
7. Salzer, G. Dissertation Merseburg, 1969
8. Kagan, S.Z., Truchanov, V.G., Ogai, J.A. Chemical Industry USSR, 1971, 620

NOMENCLATURE

A	Area of mass transfer	m^2
d	Extractor diameter	m
d_i	drop diameter	m
d_r	Diameter of rotor disc	m
d_{st}	Inside diameter of stator ring	m
d_w	Wave diameter	m
d_{32}	Mean Sauter diameter	m
g	Gravitational acceleration	m/s^2
h	Operating height of extractor	m
h_s	Height of a section in extractor	m
H_{OR}	Overall height of a transfer unit based on raffinate phase	m
n	Stirrer speed	1/s
N_{OR}	Number of transfer units based on raffinate phase	
v	Velocity	m/s
V_{tot}	Total volume flow of continuous and dispersed phases	m^3/s
V	Volume flow	m^3/s
x	Concentration of phenol in raffinate	
X	Hold up at dispersed phase	
y	Concentration of phenol in extract	
α	Distribution parameter	
Δn	Range of stirrer speed	1/min
Δx_m	Mean logarithmic driving force	
$\Delta \rho$	Difference of density between both phases	kg/m^3
γ	Surface tension	N/m
η	Viscosity	$kg/m \cdot s$
ρ	Density	kg/m^3
Subscripts		
c	Continuous phase	
d	Dispersed phase	
f	Flooding point	
K	Extractor, top	
T	Extractor, bottom	

FIGURES

Fig.1: Scheme of experimental arrangement

- 1: extractor
- 2: gear
- 3: motor
- 4: rotameter
- 5: container water/phenol
- 6: container butylacetate
- 7: container extract
- 8: raffinate
- 9: butylacetate/phenol for distillation

Fig.2: Arrangement for photographic measurement of droplet size distribution

- 1: camera
- 2: optical flat
- 3: packing
- 4: filling of fluid
- 5: wall of extractor

Fig.3: Examined rotating parts in extractor, in all experiments

- d) = 200 mm
- a) RDC, $h = 64$ mm
- b) extractor with stator rings and impellers, $h_s = 64$ mm
- c) extractor with radial stationary baffle plates and impellers of round bar steel
- d) extractor with radial stationary baffle plates and impellers of flat steel

Fig.4: Sauter diameter for drops in dependence on stirrer speed for RDC 200 mm diameter without mass transfer (with exception of 1) symbols see table 2.

Fig.5: Sauter diameter in dependence on hold up for RDC of 200mm diameter without mass transfer (with exception of 1) symbols see table 2.

Fig.6. Flow rate at flooding point in dependence on stirrer speed

for κDC of 200 mm diameter. Symbols see Table 2.

Fig.7: Flow rate at flooding point in dependence on specific energy per volume unit for experimental points according to Fig.6.

Fig.8: Schematic diagram of equilibrium line and operating line in xy diagram

1: equilibrium line

2: operating line

Fig.9: Sauter diameter in dependence on stirrer speed, see also Table 4.

Fig.10. Sauter diameter in dependence on hold up. See also Tab.4.

Fig.11. Height of a transfer unit in dependence on hold up.
See also Tab.4.

Fig.12. Height of a transfer unit in dependence on mass transfer area in extractor. See also Tab.4.

Legend

1-extractor, 2-gear, 3-motor, 4-rotameter,
5-water/phenol, 6-butylacetate,
7-extract, 8-raffinate, 9-to distillation

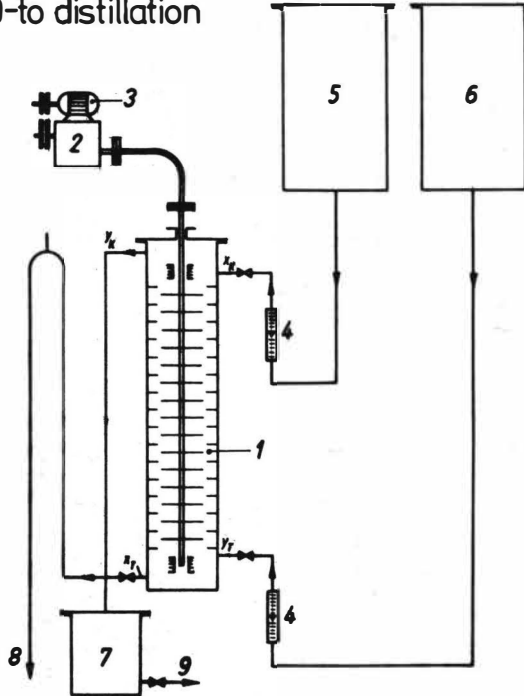


Fig.1 Scheme of Experimental Arrangement

Legend

1-camera, 2-optical flat,
3-packing, 4-filling of fluid,
5-wall of extractor

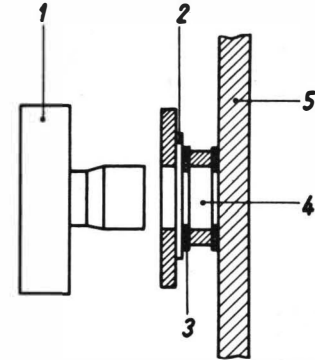


Fig.2 Arrangement for Photographic Measurement of Droplet Size Distribution

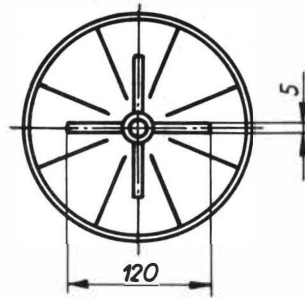
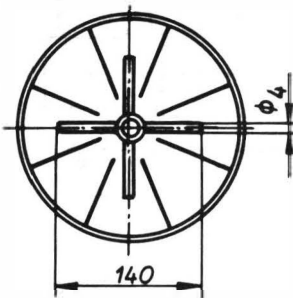
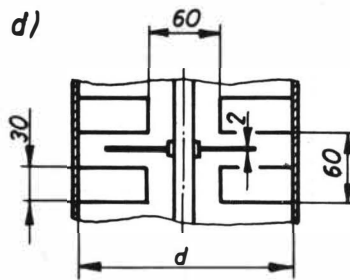
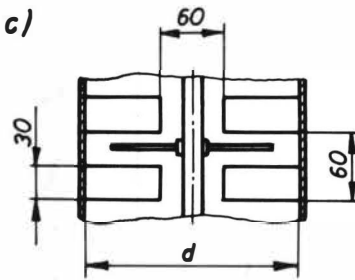
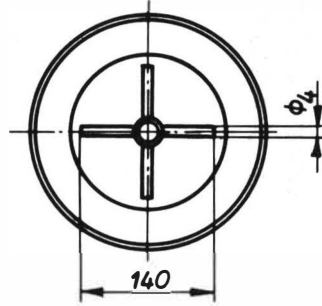
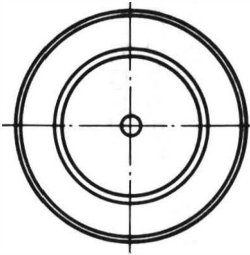
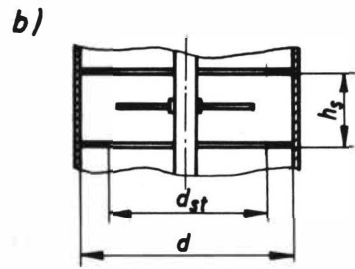
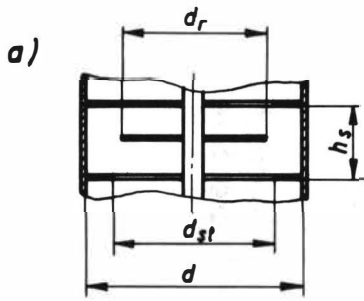
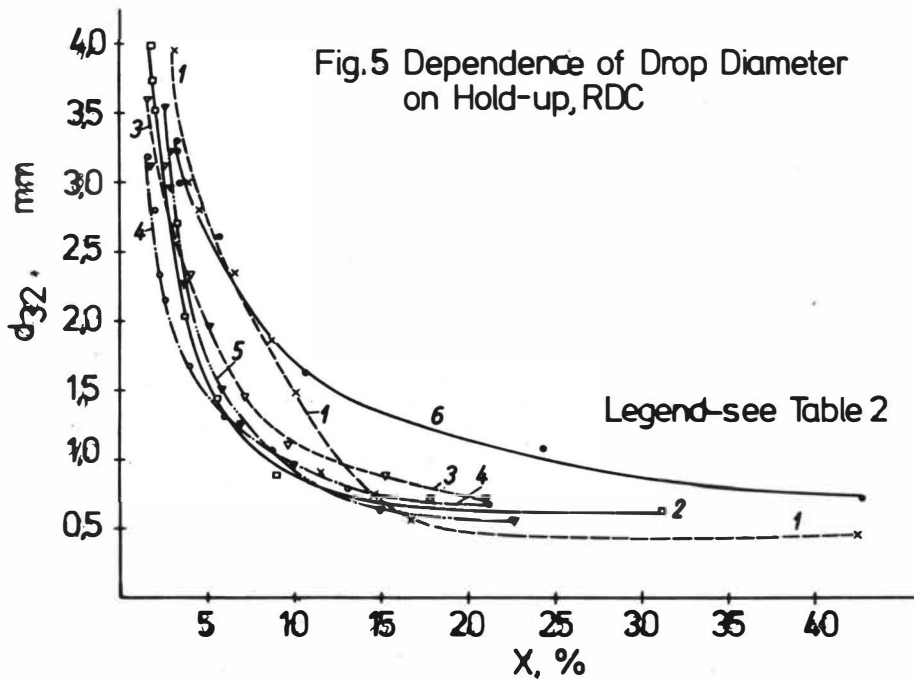
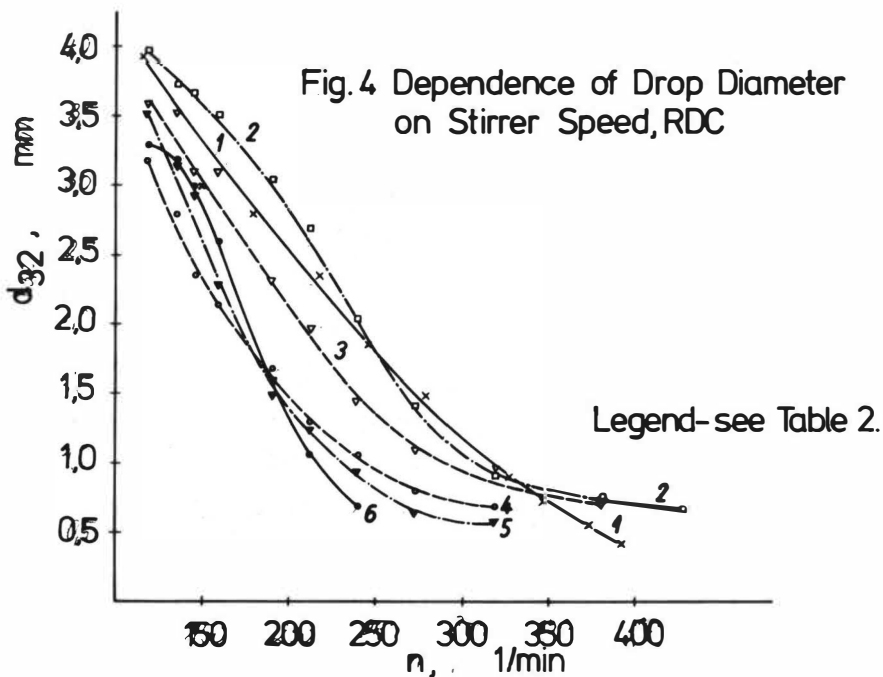


Fig. 3 Examined Rotating Parts($d=200\text{mm}$)



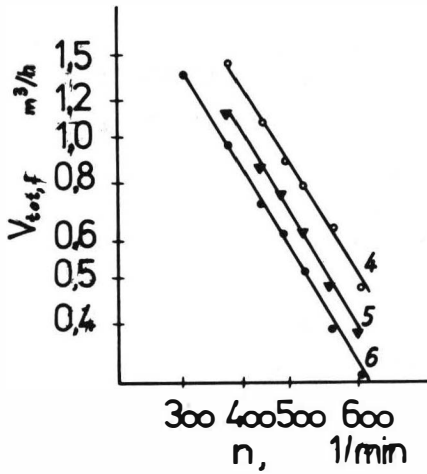


Fig.6 Dependence of Flow Rate at Flooding on Stirrer Speed, RDC

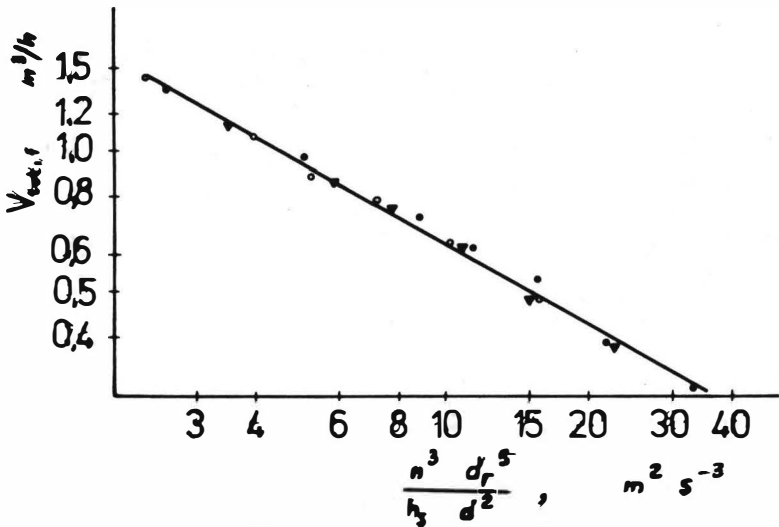


Fig.7 Dependence of Flow Rate at Flooding on Specific Energy per unit Volume

1-equilibrium line
2-operating line

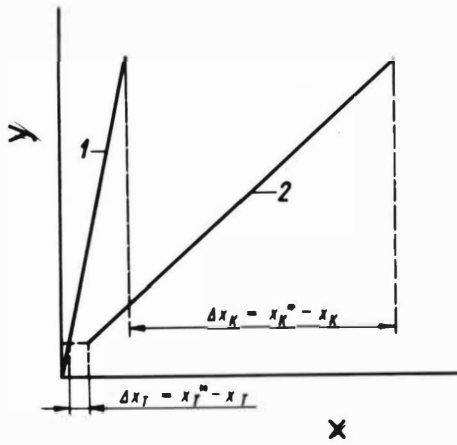
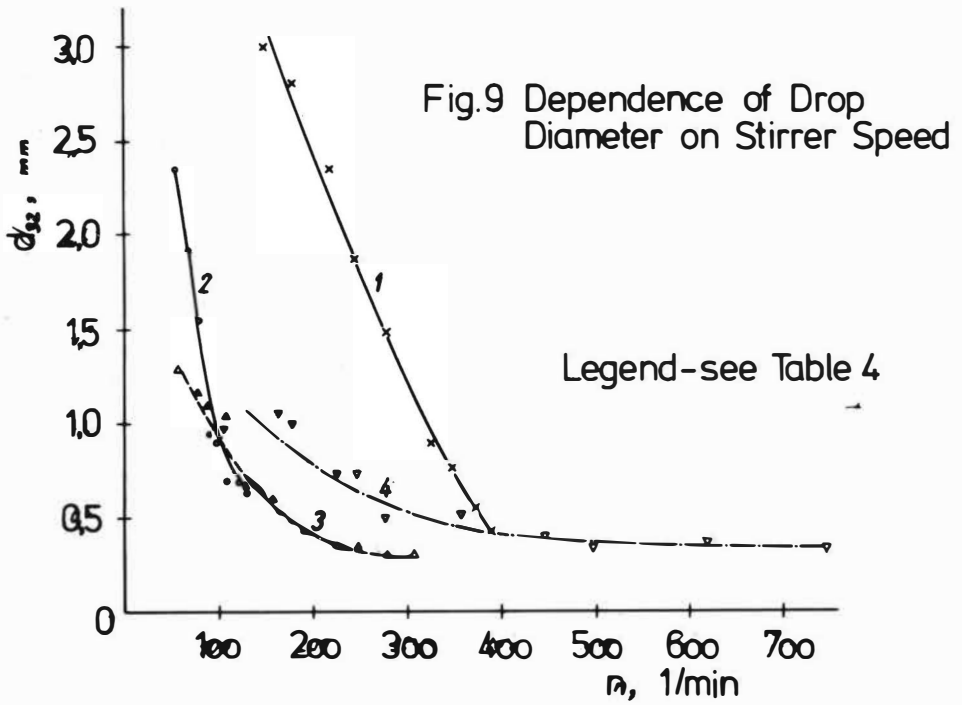


Fig.8 Schematic x-y Diagram



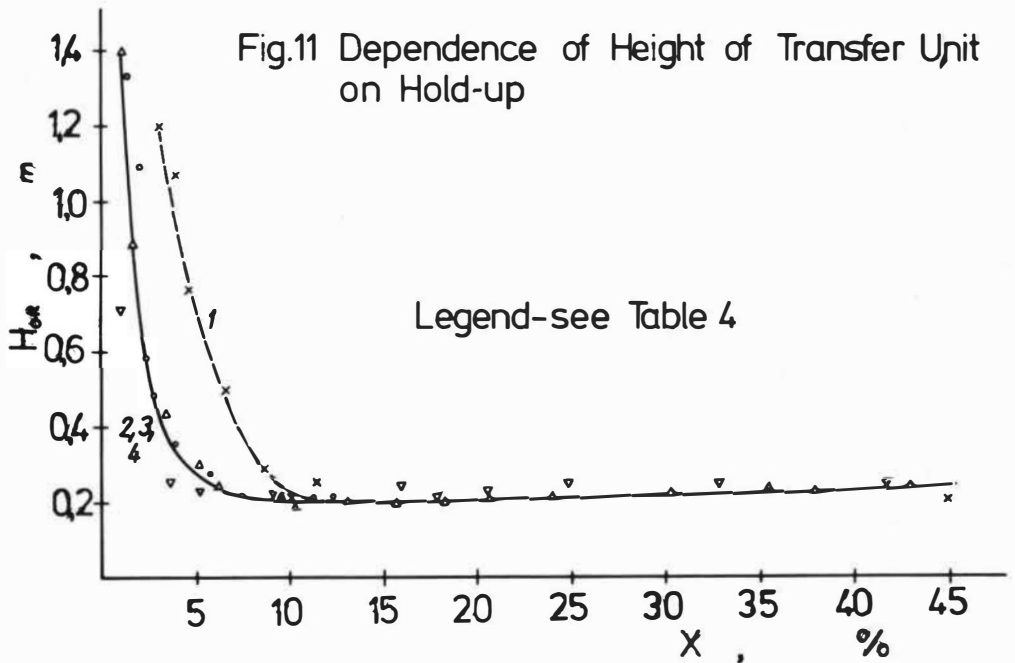
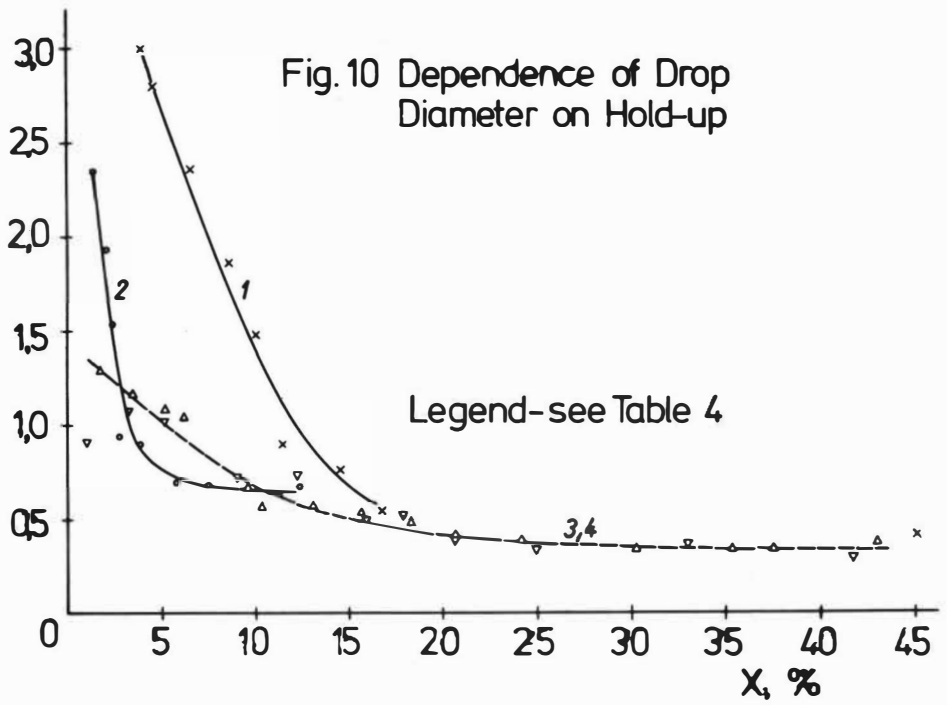
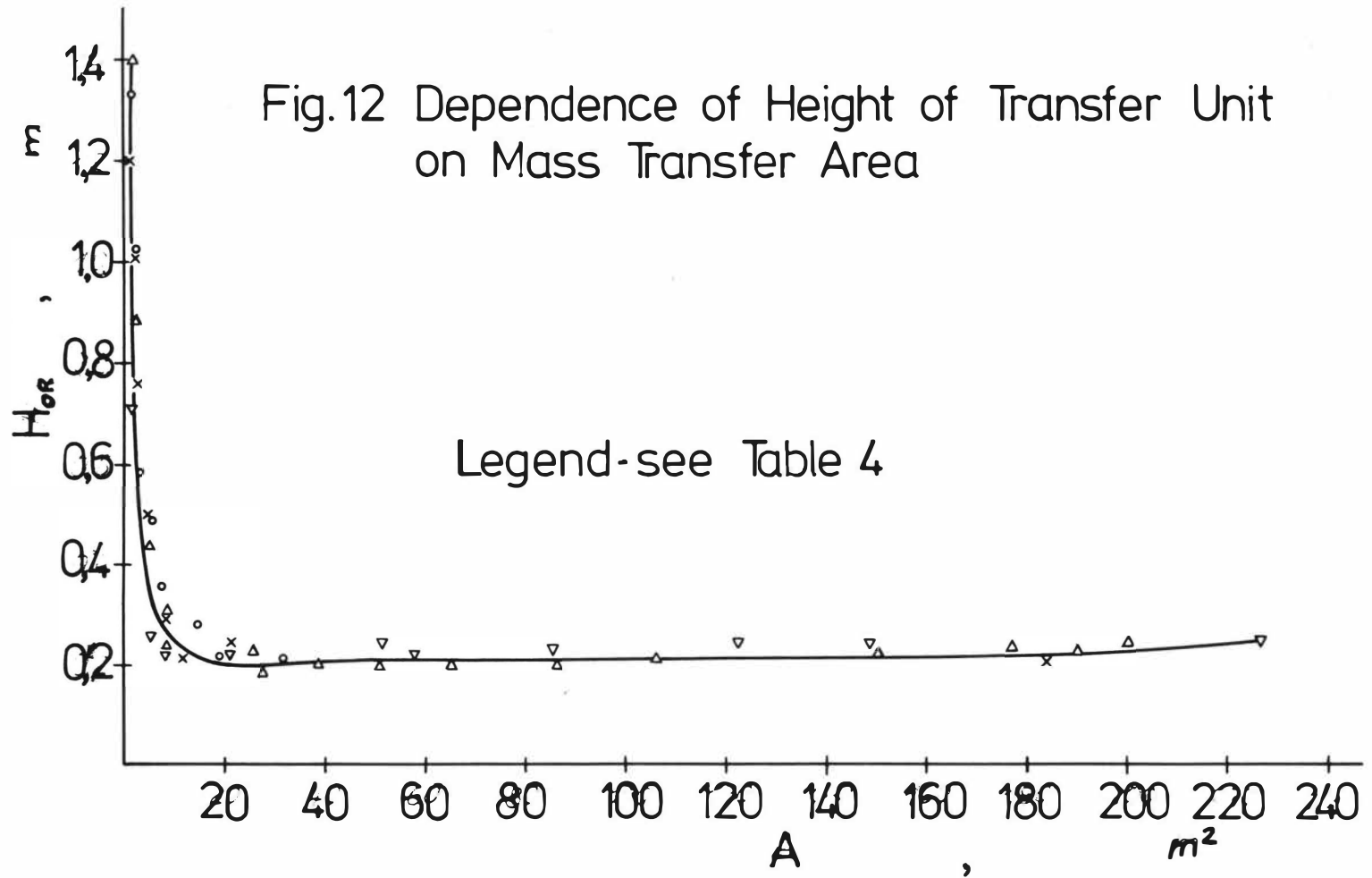


Fig.12 Dependence of Height of Transfer Unit on Mass Transfer Area

2337



PRESENT STUDY AND DEVELOPMENT
OF EXTRACTION PULSED COLUMNS

H. ROUYER - J. LEBOUHELLEC - E. HENRY - P. MICHEL

Commissariat à l'Energie Atomique
Département de Génie Radioactif
B. P. n° 6
92260 FONTENAY-AUX-ROSES
FRANCE

INTRODUCTION

Since the 50's, pulsed column development has been connected with, on the one hand, nuclear applications for processing uranium ores and, on the other hand, for processing of irradiated reactor fuels. For the latter application, production outputs which were needed during these last ten years have hardly forced to improve existing contactors which were satisfactory.

Large throughout liquid-liquid extraction columns were developed outside of the nuclear field, mainly in the petroleum field. Thus agitated columns appeared consisting of mechanically moving parts, and they attained the industrial stage as we know it.

Presently, the nuclear industry has new future perspectives for accelerating reactor construction programs and correlatively increasing the output of processing plants for irradiated fuels. These circumstances have pointed once again to the pulsed column and its advantages in this field : operating simplicity, high reliability, good efficiency, and small volume.

Moreover, the development of hydrometallurgical processes induces searches for high capacity and good efficiency extractors. Critical constraints in the nuclear field are also oriented toward increasing specific flows. These converging considerations led to study more closely hydraulics of pulsed columns, on the one hand, and the possibilities of extrapolating the diameters of these devices, on the other hand.

.../...

The pulsed column consists of a vertical column partly equipped with regularly spaced plates. Two liquid phases, one of which is in drop form, are flowing countercurrently through the device. At the top or at the bottom of the column the dispersed phase coalesces to an interphase. A pulsing device at the base of the column causes a periodic two-phase up-down motion and maintains the dispersion.

The aim of this first part of the study was to know the characteristics of this dispersion as a function of different variables which come into play in the system : type of plates, spacing, perforated surface ratio, hole diameter, pulse intensity, and magnitude of flowrates.

The operating field of the pulsed column is normally represented on the Sege and Woodfield diagram where the sum of specific flows of the two phases = $V_c + V_d$ is given as a function of the product of the amplitude "a" multiplied by the frequency "f" of the pulse motion. Different types of operation have to be considered according to the different diagram areas, but only the emulsion operating area is used in practice and this is the area that measurements were limited to. (Fig. 1).

I - 1 - Experimental method

It consisted of setting in dynamic equilibrium (most of the time without mass transfer) approximately thirty 100 mm diameter columns presenting different geometric characteristics as well as three 300 mm diameter columns and a 600 mm diameter column. Once these columns were in equilibrium, the emulsion was sampled at different levels by means of valves especially designed for small diameter columns and by means of high throughput taps for large diameter columns. For these last, radial samples were also taken. In most cases, a mean phase ratio was calculated along the column and considered as characteristic of the column, the used phases, the flows, and the af product.

To analyze these results and interpret them, they had to be connected to a simple mathematical scheme drawn from many works in the literature.

I - 2 - Hydrodynamic model for a pulsed column

The aim was to have a mathematical model which would allow to describe the variation in phase volume ratio in the column throughout the emulsion operating area of the column.

The first hydrodynamic studies on pulsed columns were made by D.H. Logsdail and J.D. Thornton in 1957.² They proposed correlating specific flow to phase volume ratio by the following equation :

$$(1) \quad \frac{V_d}{\varphi} + \frac{V_c}{1 - \varphi} = \bar{V}_0 (1 - \varphi)$$

where \bar{V}_0 is called the "drops' characteristic velocity".

By assuming this equation valid up to column flooding and by successively deriving with respect to V_c and V_d to obtain the maximums V_{ce} and V_{de} of V_c and V_d , it becomes :

$$(2) \quad V_{de} = - 2 \bar{V}_0 \varphi e^2 (1 - \varphi e)$$

$$(3) \quad V_{ce} = \bar{V}_0 (1 - \varphi e)^2 (1 - 2 \varphi e)$$

By setting $LR = \frac{V_{ce}}{V_{de}}$, equations (2) and (3) give the values of retention at flooding.

$$(4) \quad \varphi e = \frac{- 3 + (1 + 8LR)^{1/2}}{4 (LR - 1)}$$

.../...

Note that this theory leads to the conclusion that the phase ratio at flooding is only a function of flow ratios. It would then vary approximately 25 % for a ratio approximately 3 to 40 % for a ratio of 0.33.

not clear?

The expression thus established has the advantage of making the flow ratio disappear and connecting flows at flooding to a single variable V_0 , which depends then only on agitation energy, the physical-chemical system, and the column geometry if the calculated value is given to e . This theory was used with success in correlation studies for flooding curves of pulsed columns ² & ³. Also note that the correlation formulas can be used only in a limited sense since the authors themselves of the previous mathematical model underline that the equations which they established are valid only when there is no coalescence between the drops and the drop size distribution is independent of flowrates up to the flooding point.

opposed to

Proposed model

After examining the experimental results of phase volume ratio throughout the emulsion operating domain of several pulsed columns, it seems that the relative drop velocity with respect to the continuous phase with flow rate and "axf" constant was a linear phase ratio function at least in an interval that is practically the usage area of the column. Moreover, the angular coefficient of the straight lines thus defined is fairly constant in the considered field. Thus it was logical to adopt equations similar to the previous ones for correlating experimental phase ratio data, that is :

$$\frac{V_d}{\psi} + \frac{V_c}{1-\psi} = U_{g_e} - A (\psi - \psi_e) = U_g$$

$$V_{d_e} + V_{c_e} = \frac{B}{af + C}$$

Note that U_g is the relative drop velocity with respect to the continuous phase, a speed that is usually called slip velocity.

.../...

An identification computer program was written in Fortran. This program permits finding the best values of A, B and C which determine the model for each series of experimental results. Table 1 on which calculated and measured retention results can be read for a special case shows good agreement.

I - 3 - Results for the 100 mm diameter columns

1) Slip velocity variation direction

Table 2 summarizes a part of the obtained results and indicates through coefficient A how the slip velocity of drops varies as a function of the phase ratio ; when A is positive, the slip velocity diminishes with phase ratio ; when A is negative, the slip velocity increases.

- a - Influence of the type of plates

Table 2 shows that, in general, when the continuous phase wets the plates, that is, in a continuous aqueous phase, with stainless steel plates and in a continuous organic phase with plastic plates, A is positive and the slip velocity diminishes with phase ratio as assumed in the usual equations ; however, when the continuous phase does not wet the plates, the slip velocity increases with phase ratio and most of the correlation equations are not convenient.

This result leads one to think that coefficient A reflects in some way the tendency for coalescence within the column. In fact, the more drops have a tendency to coalesce with the increase in phase ratio, the more their mean diameter increases and their relative speed with respect to the continuous phase tends to increase with phase ratio. A liquid ^{drop} particle is ^{normally} subjected to a higher dispersion power for an axf product constant when flows increase in a column. Drops become then smaller and their relative

.../...

velocity diminishes. Depending on whether the coalescence increases faster or slower with phase ratio, the main phenomenon is dispersion or coalescence, and slip velocity increases or decreases.

In the tests corresponding to the first part of the table (tests 1 to 10) for columns which will be called type I to simplify the expression, the main phenomenon is dispersion ; for columns of type II (tests 11 to 18), the main phenomenon is coalescence.

- b - Effect of other variables.

- Plate spacing : in columns of the first type, plate spacing has no effect upon the value of A (tests 1, 2, and 3) while it has a strong effect in the second case (tests 11 and 12) where coalescence increases more especially as the plate spacing is increasing.

- Void ratio and hole diameter

In columns of the first type it must be noted that the void ratio and the hole diameter play a role on A only from a certain value (tests 3, 4, 5, 6 and 7). "A" then increases very much which indicates a large dispersion increase. This effect can be explained in so much as the increase in hole diameter as well as in the void ratio increases the liquid jet interference across the holes, and, as a result, increases the local agitation energy between the holes.

- c - Flow ratios.

In the column of the first type, when the ratio V_c/V_d is close to or less than 1, "A" does not vary very much. On the other hand, it varies very much and becomes even negative when the continuous phase flow becomes large

.../...

compared to the discontinuous phase flow. Note that the absolute velocity of the continuous phase is then large ; back mixing is becoming important under these conditions and the presence of many small drops in the continuous phase can enhance the coalescence of larger drops (tests 8, 9 and 10).

In columns of the second type, the smaller the discontinuous phase flow rate is; the smaller the influence of coalescence becomes (tests 16, 17 and 18).

2) Variation of column throughput as a function of various parameters

- Type of plates

Among the columns of the first type, although, according to what was said before, coalescence is not the main parameter ; the type of plates plays a very important part. It was observed throughput variations up to 50 % between columns of which one was fitted with PTFE plates and the other with very hydrophobic plastic plates, everything else being identical.

Columns of the second type allow generally throughput almost twice the one of the first type, all geometric parameters remaining identical. Thus flowrates greater than $6.2 \text{ l.h}^{-1} \text{ cm}^{-2}$ can be obtained using a system consisting of aqueous solution of acetic acid and 30 % TBP with mass transfer.

- Plate spacing and perforations

With a mean void ratio and mean diameter holes, the throughput in the column increases regularly with plate spacing but when hole diameter and void ratio exceed a certain value, flowrate variation cannot be maintained ;

.../...

it reaches a minimum value. This is, no doubt, to be correlated with the variation of coefficient A previously mentioned. Likewise, for a constant hole diameter, the flowrate reaches a maximum depending on the free area of the plates.

- Flow ratio

As the correlation equations in the literature predict, the flowrate is growing in columns of type I with the flow ratio V_c/V_d . For columns of type II, flowrate variation with the flow ratio is lower.

Figure 2 shows typical experimental results.

I - 4 - Large diameter column hydraulics

Scaling up columns in diameter may cause a certain anisotropy in the emulsion which could lead progressively to channeling phenomena. It seems that for pulsed columns, at least up to a diameter of 600 mm, this anisotropy does not appear. Figures 3, 4, and 5 show how the phase volume ratio vary radially at different levels in 300 and 600 mm diameter columns. For the 300 mm column, there is no significant variation along a radius. It is not the same for the 600 mm column ; but the phase ratio increase at the center and the lower part of the column can be undoubtedly attributed to the opening of the pulse leg as represented on figure 6. This is also confirmed by the difference which can be noted between figures 4 and 5, and which is only in connection with pulsation energy. It must be stated that, instead of being emphasized, this variation is attenuated progressively when going up and becomes negligible at a height of 4 m. This phenomenon shows that the agitation mode in the pulsed column is clearly leading to suppress radial heterogeneity.

.../...

Flowrates in large column

The flooding curves obtained with 100, 300 and 600 mm diameter columns, everything else being equal, are practically the same. Specific flows are thus independent of the size at least up to a 600 mm diameter and probably above.

II - EFFICIENCY VARIATION IN PULSED COLUMNS

II - 1 - Influence of the type of plates

The efficiency of pulsed columns is measured generally by the height equivalent to a theoretical stage or the height of a transfer unit for a given physical-chemical system.

It is well known that these heights vary appreciably depending on the operating point chosen in the Sege and Woodfield diagram. When specific flow rates are constant, they pass generally through a minimum when product α increases, and they vary greatly in percentages with the specific flow. In a general way, what is looked for in an extractor is the best compromise between the throughput and the efficiency ; this compromise can be expressed from a purely technical point of view by the volumic efficiency or residence time per theoretical stage or transfer unit.

$$\Theta = \frac{H E T S}{V_c + V_d}$$

Under these conditions, experiments have shown that for columns of type I fitted with stainless steel plates and columns of type II

.../...

fitted with PTFE plates having the same geometric features, the residence times/per theoretical stage are equal. This result was obtained for the stripping of uranium in a nitric solution with a flow ratio close to 1. Time Θ was about 50 sec.

II - 2 - Influence of void ratio and plate spacing

For equal specific flowrate, the void ratio has not a great influence on the efficiency which is more sensitive to plate spacing. Nevertheless, equal minimum residence times can be obtained for two columns having for this operating condition different specific flowrates residence time of 27 sec. per theoretical stage was obtained for a total specific flowrate of 1.34 cm sec.⁻¹ and a 5 cm spacing, and the same residence time for a total specific flow of 1.83 cm sec.⁻¹ and a 10 cm spacing for columns of type II. The system used was acetic acid and 30 % TBP -dodecane.

II - 3 - Efficiency of a 300 mm diameter column

The column used for the experiment is a column of type II in which uranium is extracted from a nitric medium by 30 % TBP. The solvent is saturated at 80 %, and the total specific flowrate is 1 cm sec.⁻¹.

The H. T. U. measured is 60 cm which is strictly identical to that found with a 100 or even 50 mm diameter column under the same operating conditions.

II - 3.1 - Efficiency variation along the column's axis

To measure the concentration profile in the column, it was proceeded as before by drawing off the emulsion at different levels. To take into account the transfer which could have taken place after sampling, a simulated profile was calculated by balancing the concentrations of two phases with phase ratio as shown on table 4.

Moreover, a computer program was perfected to calculate concentration profiles for uranium and nitric acid using some assumptions on the HTU and its variation along the column.

Results

Table 3 shows that by considering the column on different heights from the introduction, the mean HTU varies considerably. In the upper part of the column, this variation is not easily explained only with phase ratio modifications. That can be seen on figure 7. Table 4 shows the results which are obtained by assuming that the HTU is a function either of the density variation between two phases or the density gradient along the column's axis. This assumption seems to be valid and it can be considered that axial mixing contributes largely to the efficiency variation.

II - 3.2 - Efficiency improvement

Figure 7 shows how the phase ratio profile was modified by modulating the plate's hole diameter. This allowed increasing column throughput of 25 % and increasing in the same time the efficiency in the lower part of the column.

II - 4 - Axial mixing in pulsed columns

Since the work of Miyauchi and Vermeulen ⁴, many workers were interested in the problem of axial mixing in extraction columns and particularly in pulsed packed columns. ^{5,6} Few results were published concerning pulsed columns with perforated plates.

.../...

The mathematical model proposed by Miyauchi is the following :

- Let E_i : a convection diffusion coefficient in phase i
 K_i : mass transfer coefficient
 C_i : solute concentration in phase i
 U_i : velocity of phase i

The model corresponds to the following system of equations :

$$E_1 \frac{d^2 C_1}{dz^2} - U_1 \frac{dC_1}{dz} - K_1 / C_1 - (mC_2 + q) / = 0$$

$$E_2 \frac{d^2 C_2}{dz^2} + U_2 \frac{dC_2}{dz} + K_1 / C_1 - (mC_2 + q) / = 0$$

where m and q are parameters of the equilibrium curve considered as a straight line.

Replacing z by the variable $\frac{Z}{h_c} = z/h_c$, where h_c is the column length, it becomes :

$$\frac{E_1}{h_c U_1} \frac{d^2 C_1}{dZ^2} - \frac{dC_1}{dZ} - \frac{K_1 h_c}{U_1} / C_1 - (mC_2 + q) / = 0$$

$$\frac{E_2}{h_c U_2} \frac{d^2 C_2}{dZ^2} - \frac{dC_2}{dZ} + \frac{K_1 h_c}{U_2} / C_1 - (mC_2 + q) / = 0$$

The expression $\frac{h_c U_1}{E_1}$ is currently called the Peclet number.

II - 4.1 - Experimental method

This number was measured using the colored tracer method. A colored tracer soluble only in the continuous phase is injected into a column in the form of an injection during a time as short as possible and of negligible value compared to the flow rate of the considered phase. This

.../...

phase is drawn off continuously at two points of the column and its coloration is continuously measured with two identical colorimeters. The response curves of the colorimeters are processed with the Laplace transform and a linear regression allows to obtain the convective diffusion coefficient E_1 ⁷. The dye used was the ferrous orthophenanthroline and the phases were nitric acid and 30 % TBP dodecane.

II - 4.2 - Results

Figure 8 shows the results obtained for a 45 mm diameter column and a 600 mm diameter column fitted with plates having the same hole diameter, the same free area and spaced in the same way. It can be noted that convective diffusion coefficients obtained in a 600 mm diameter column show that there is up to this diameter no tendency for axial mixing increase in large columns.

Figure 9 shows that the Peclet number decreases with the plates spacing which is in agreement with observations previously made on the efficiency decrease.

III - COMPARATIVE COST EQUIPMENT ESTIMATE FOR AN INDUSTRIAL INSTALLATION

Figures given in tables' 5 and 6 are related to a liquid-liquid extraction process characterized, on the one hand, by a low transfer kinetic and, on the other hand, by a large emulsification tendency. It includes an extraction unit including an extraction section - 4 theoretical stages - a scrubbing section - one stage - and a stripping section consisting of 3 theoretical stages. To operate this process on an industrial scale, studies were made with mixers-settlers and pulsed columns. Experiment has shown that the HETS amounts about to 1 m. Moreover using pulsed column allows to

.../...

suppress scrub section which is necessary with mixer-settlers mainly because of the products carried away. These conditions show for plastic devices a clear advantage in favour of pulsed columns.

CONCLUSION

The few elements which were developed in this paper show that the pulsed column is an extractor which can be easily scaled up to a limit which is still not defined but probably at least 1 m diameter without efficiency decreasing. Experiments are presently planned on such columns at CEA.

Studies have still to be carried out on the theoretical level, particularly to establish models where the wettability of materials could be considered, which would allow to establish some new and more universal correlation equations for throughput. Nevertheless, qualitative knowledge acquired already allows to direct column optimization studies for which the type of materials can have great importance, in particular, in connection with flow ratios required by the processes. It can be noticed particularly that the behavior of certain columns could be changed considerably by modifying the type of plates and their geometry.

On a practical level, an effort has still to be made concerning large column technology. However, up to a 600 mm diameter, specific flowrates can be high - 2 to 6 $\text{lh}^{-1} \text{cm}^{-2}$ and pulsed columns can be sized only after technical criteria and not practical ones as, for example, making maintenance in the column easier, which an advantage with respect to agitated columns.

On the economic level, the comparison was limited to the simple example of equipment cost. Obviously many other elements must be considered, but the high volumic efficiency of pulsed columns represents undoubtedly an important advantage in most cases.

BIBLIOGRAPHY

- 1 - SEGE G. - WOODFIELD F.W.
Chem. Eng. Prog. 50, p 396-402 (1954)
- 2 - LOGSDAIL D. H. - THORNTON J.D.
Trans. Inst. Chem. Engng 1957, 35, 316
- 3 - GROENIER W.S. - & al.
ORNL 3890 (1966)
- 4 - MIYAUCHI T. - VERMEULEN Th.
Ind. Engn Chem. fundamentals, 1963, 2, 113
- 5 - ROZEN A.M. - RUBEZHNYI Y.G. - MARTYNOV B.V.
Chem. Ind. [Khim. Prom] 1970, 66
- 6 - SPAAY N.M. - SIMONS A.J.F. - ten BRINK G.P.
Proceeding ISEC 1971 - 281 - Society of Chemical
Industry London
- 7 - OSTERGAARD R. - MICHELSEN M.L. - CANO J.
Chem. Eng. 1969, 47, 107

$af \text{ cm s}^{-1}$	1,37	1,50	1,62	1,75	1,87	2,00	2,25	2,50	1,50	1,75	2,00	1,25	1,37
$Vc \text{ cm s}^{-1}$	0,093	0,093	0,093	0,094	0,094	0,094	0,094	0,094	0,118	0,118	0,141	0,141	0,141
$Vd \text{ cm s}^{-1}$	0,495	0,495	0,495	0,495	0,495	0,495	0,495	0,495	0,618	0,618	0,618	0,743	0,743
$\psi_{\text{experimental}}$ in %	14,3	15,3	15,4	15,9	17,2	19,1	22,7	31	18,2	22,9	36,2	23,2	25,7
ψ calculated in %	13,9	15,1	16,4	17,8	19,2	20,8	24,8	32,8	20,3	24,8	32,3	20,9	23,6

TABLE 1

Comparison between the experimental and calculated valeurs of the phase volume ratio for a 100 mm diameter column in the emulsion operating region. Aqueous phase is 25.5 g. l^{-1} uranium, 2.92 N HNO_3 ;
Organic phase is 90.3 g. l^{-1} uranium, 0.15 N HNO_3

PLATES				SYSTEM					A	N° Test
Material	∅ holes cm	voidage %	spacing cm	continuous phase	Vc/Vd	mas's transfer	aqueous phase	organic phase		
inox	0,3	23	5	Aq	1,0	S	HNO ₃ 1N	TBP 30 %	3,97	1
inox	0,3	23	10	Aq	1,0	S	HNO ₃ 1N	TBP 30 %	3,98	2
inox	0,3	23	20	Aq	1,0	S	HNO ₃ 1N	TBP 30 %	3,92	3
inox	0,3	35	20	Aq	1,0	S	HNO ₃ 1N	TBP 30 %	3,87	4
inox	0,3	50	20	Aq	1,0	S	HNO ₃ 1N	TBP 30 %	4,48	5
inox	0,3	35	10	Aq	1,0	S	HNO ₃ 1N	TBP 30 %	4,00	6
inox	0,6	35	10	Aq	1,0	S	HNO ₃ 1N	TBP 30 %	5,49	7
plastic	0,35	45	8	Or	0,25	S	HNO ₃ 2N	TBP 30 %	2,33	8
plastic	0,35	45	8	Or	1,0	S	HNO ₃ 2N	TBP 30 %	2,45	9
plastic	0,35	45	8	or	4,0	S	HNO ₃ 2N	TBP 30 %	2,5	10
téflon	0,35	23	5	Aq	0,455	A	CH ₃ COOH	TBP 30 %	-2	11
téflon	0,35	23	10	Aq	0,455	A	CH ₃ COOH	TBP 30 %	-4,54	12
téflon	0,35	23	10	Aq	0,455	S	CH ₃ COOH	TBP 30 %	-4,52	13
inox	0,35	18	5	Or	0,25	S	HNO ₃ 2N	TBP 30 %	-2,5	14
inox	0,35	18	5	Or	1	S	HNO ₃ 2N	TBP 30 %	-2	15
inox	0,35	18	5	Or	4	S	HNO ₃ 2N	TBP 30 %	-1,5	16
téflon	0,35	18	5	Aq	0,33	S	HNO ₃ 2N	TBP 30 %	-3	17
téflon	0,35	18	5	Aq	1,0	S	HNO ₃ 2N	TBP 30 %	-2,80	18

TABLE 2

Variation of the A coefficient of the hydrodynamic model for 100 mm diameter columns.

Average HTU between aqueous feed and the considered level	27,5 cm	45 cm	60 cm	48 cm	45 cm	60 cm
Distance between aqueous feed and the considered level	0,50 m	1 m	1,50 m	2 m	2,5 m	4 m

TABLE 3

Variation of HTU in a 300 mm diameter column

Height of the sample point	$\varphi CA + (1-\varphi) Co$ Experimental value uranium	$\varphi CA + (1-\varphi) Co$ calculated value * uranium concentration	$\varphi CA + (1-\varphi) Co$ calculated value ** uranium concentration
4 m			
3,5 m	98,3 g l ⁻¹	115,4 g l ⁻¹	112,0 g l ⁻¹
3 m	77,1 g l ⁻¹	95,2 g l ⁻¹	72,8 g l ⁻¹
2,5 m	66,6 g l ⁻¹	69,6 g l ⁻¹	35,2 g l ⁻¹
2 m	9,93 g l ⁻¹	12,7 g l ⁻¹	10,4 g l ⁻¹
1,5 m	0,219 g l ⁻¹		0,18 g l ⁻¹
1,0 m			
0,5 m			

TABLE 4

Identification of experimental concentration profile in a 300 mm diameter column. Two different models are used for the HTU variation along the axis

$$* \text{ HTU} = \text{HTU}_0 + \frac{K}{(\Delta d)^2}$$

$$\Delta d = da(Z) - do(Z)$$

$$** \text{ HTU} = \text{HTU}_0 + K \frac{\Delta d}{\Delta Z}$$

$$\Delta d = da(Z) - da(Z + dZ)$$

	Real number of stages	Unit-price KF	Total price KF
Extraction	5	55	275
Scrubbing	1	55	55
Stripping	4	55	220
Total			<u>550</u>

TABLE 5

Extraction equipment cost for an extraction and stripping cycle =
plastic mixer settler

	Column height	Column price KF	pulse + annexes appliance	Total KF
Extraction	6 m	100	50	150
Scrubbing	0			
Stripping	6 m	100	50	150
Compressor				5
Total				305

TABLE 6

Extraction equipment cost for an extraction and stripping cycle =
plastic pulsed columns

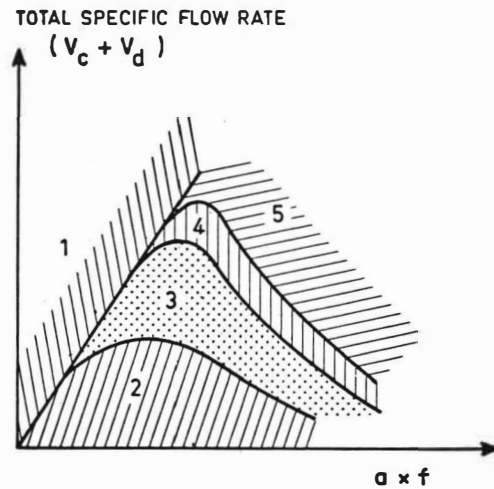


FIGURE 1 : SEGE & WOODFIELD DIAGRAM

- 1) Flooding region
- 2) Mixer settler operating region
- 3) Emulsion operating region
- 4) Instable operating region
- 5) Flooding region

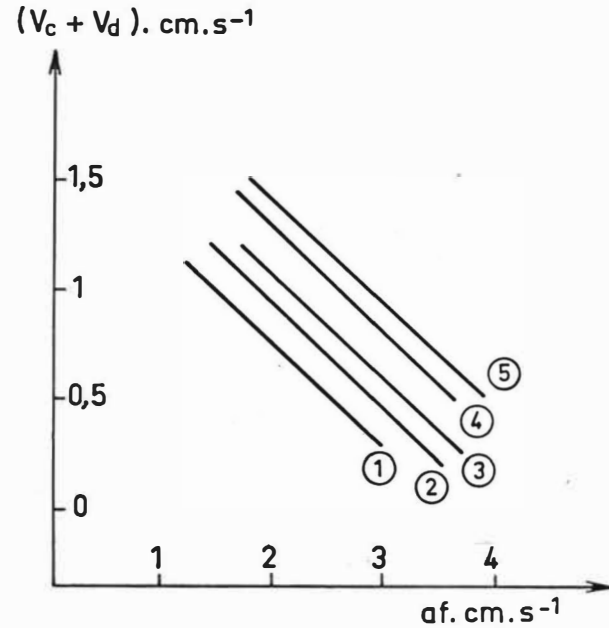


FIGURE 2 : FLOODING CURVES ACCORDING TO GEOMETRICAL PARAMETER

- 1) 5 cm pulse plate spacing, 23 % free area
- 2) 10 cm pulse plate spacing, 23 % free area
- 3) 20 cm pulse plate spacing, 23 % free area
- 4) 20 cm pulse plate spacing, 50 % free area
- 5) 20 cm pulse plate spacing, 35 % free area

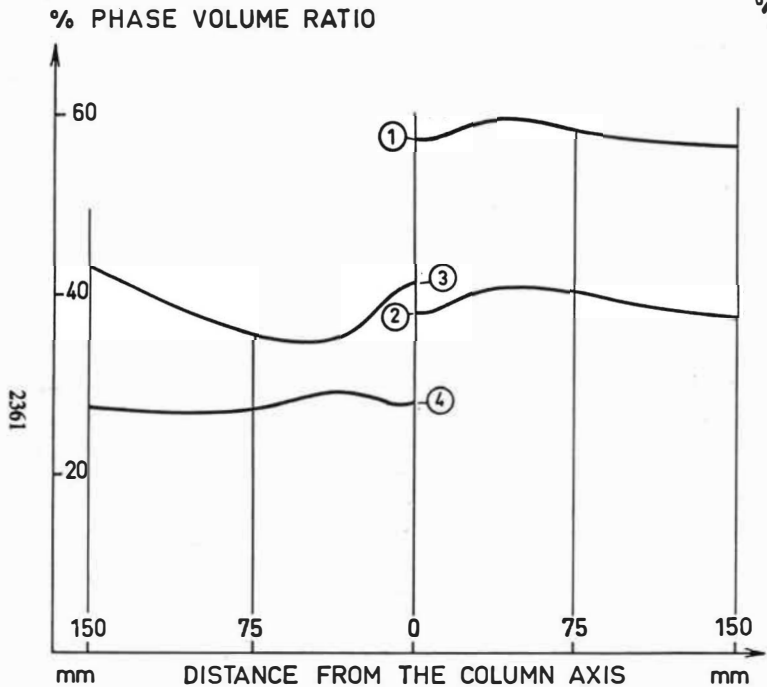


FIGURE 3 : VARIATION OF PHASE VOLUME RATIO ALONG THE RADIUS OF A 300 mm DIAMETER COLUMN AT DIFFERENT HEIGHTS

1) 0,5 m ; 2) 1,5 m ; 3) 2,5 m ; 4) 3,5 m
 Total flowrate is $2 \text{ m}^3 \text{ h}^{-1}$, $a_f = 2.55 \text{ cm s}^{-1}$

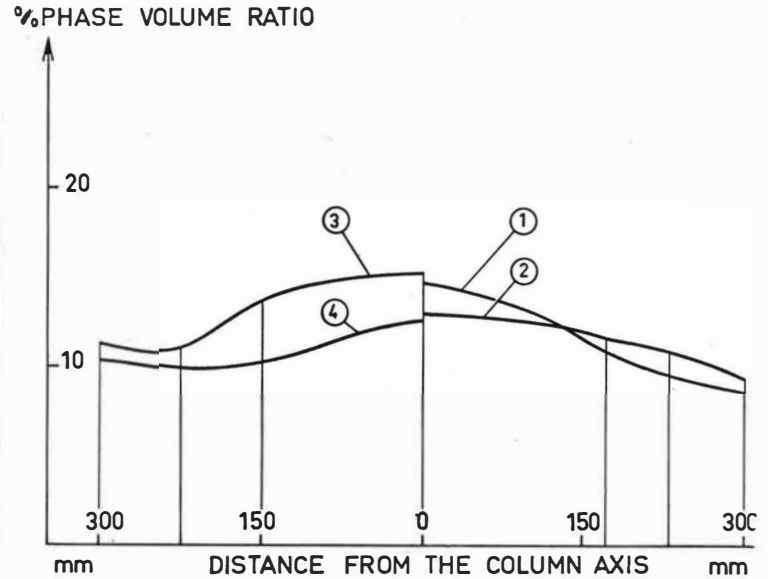


FIGURE 4 : VARIATION OF PHASE VOLUME RATIO ALONG THE RADIUS OF A 600 mm DIAMETER COLUMN AT DIFFERENT HEIGHTS

1) 0,5 m ; 2) 2,5 m ; 3) 3 m ; 4) 3,5 m
 Total flowrate is $9 \text{ m}^3 \text{ h}^{-1}$, $a_f = 1.2 \text{ cm s}^{-1}$

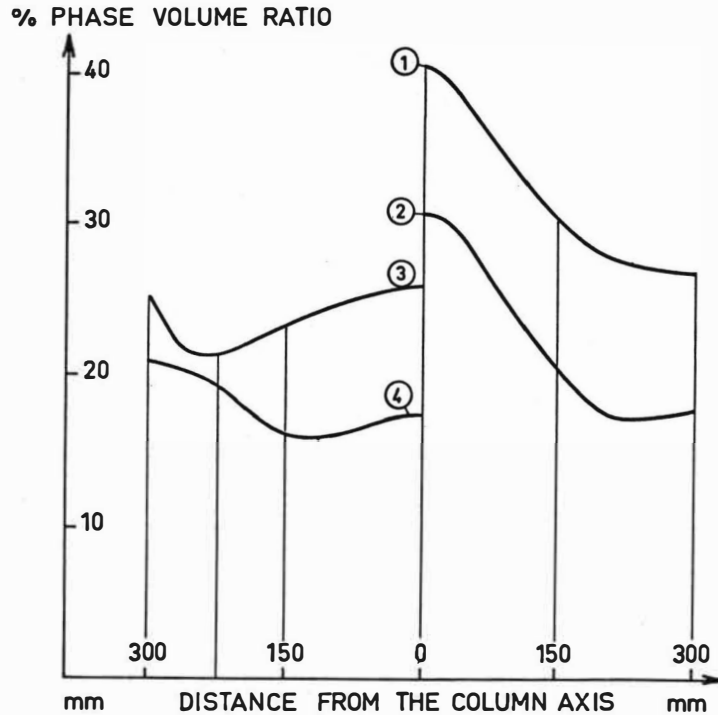


FIGURE 5: VARIATION OF PHASE VOLUME RATIO ALONG THE RADIUS OF A 600 mm DIAMETER COLUMN AT DIFFERENT HEIGHTS

1) 0.5 m ; 2) 2.5 m ; 3) 3 m ; 4) 3.5 m
 Total flowrate is $9 \text{ m}^3 \text{ h}^{-1}$, $af = 2.2 \text{ cm s}^{-1}$

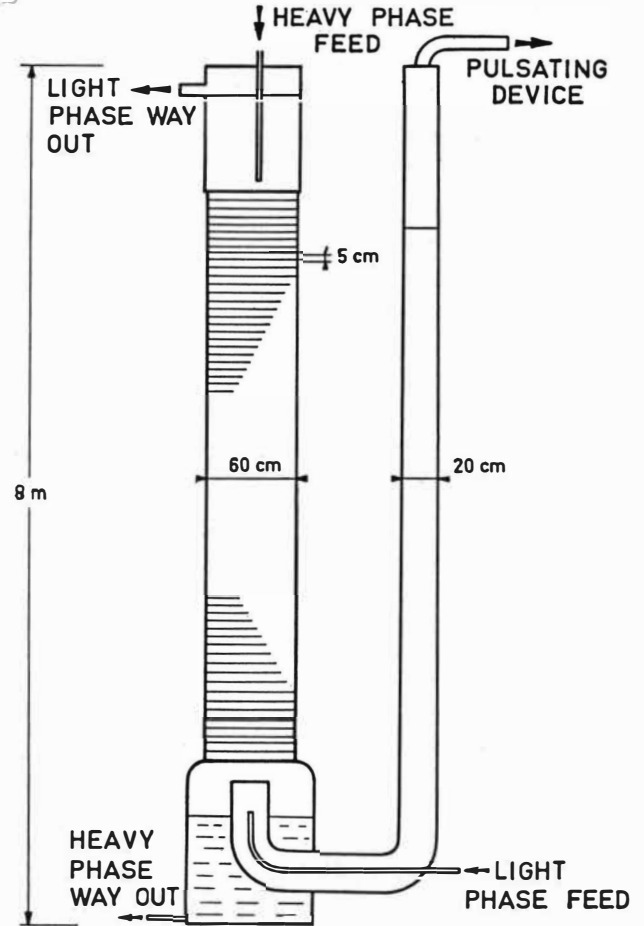


FIGURE 6: 600 mm DIAMETER COLUMN

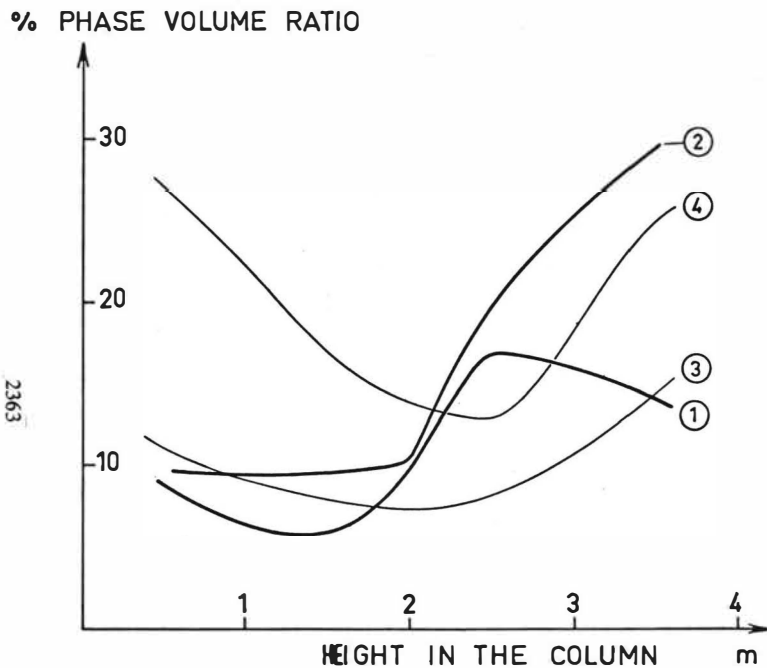


FIGURE 7 : VARIATION OF PHASE VOLUME RATIO OF A 300 mm DIAMETER COLUMN WITH MASS TRANSFER OF URANIUM IN NITRIC SOLUTION

- 1) $af = 1.68 \text{ cm s}^{-1}$, every plate is identical all through the column.
- 2) $af = 2 \text{ cm s}^{-1}$, every plate is identical all through the column.
- 3) $af = 1.8 \text{ cm s}^{-1}$, the plates at the upper part of the column have larger holes.
- 4) $af = 2.47 \text{ cm s}^{-1}$, the plates at the upper part of the column have larger holes.

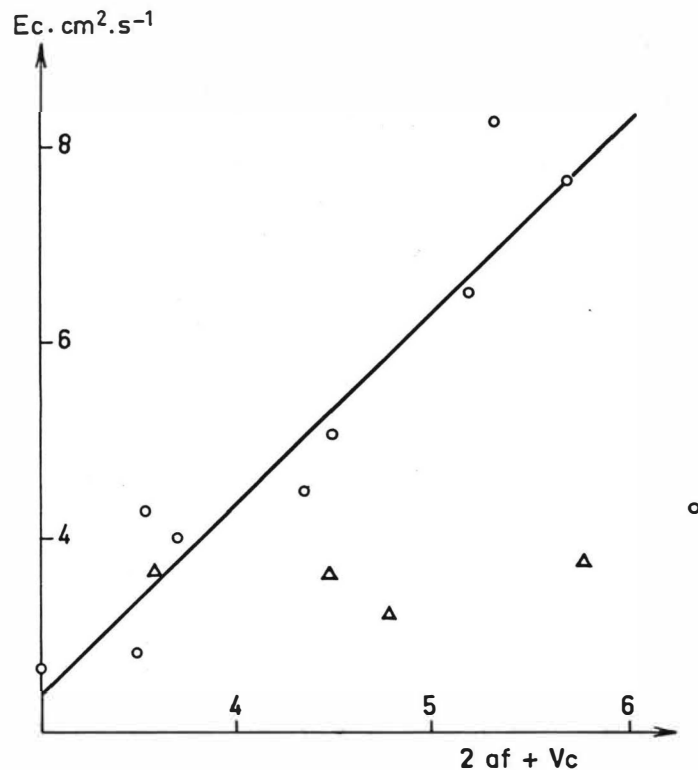


FIGURE 8 : VARIATION OF THE SUPERFICIAL AXIAL MIXING COEFFICIENT ACCORDING TO OPERATING PARAMETER

- 45 mm diameter column
- △ 600 mm diameter column

PECLET NUMBER

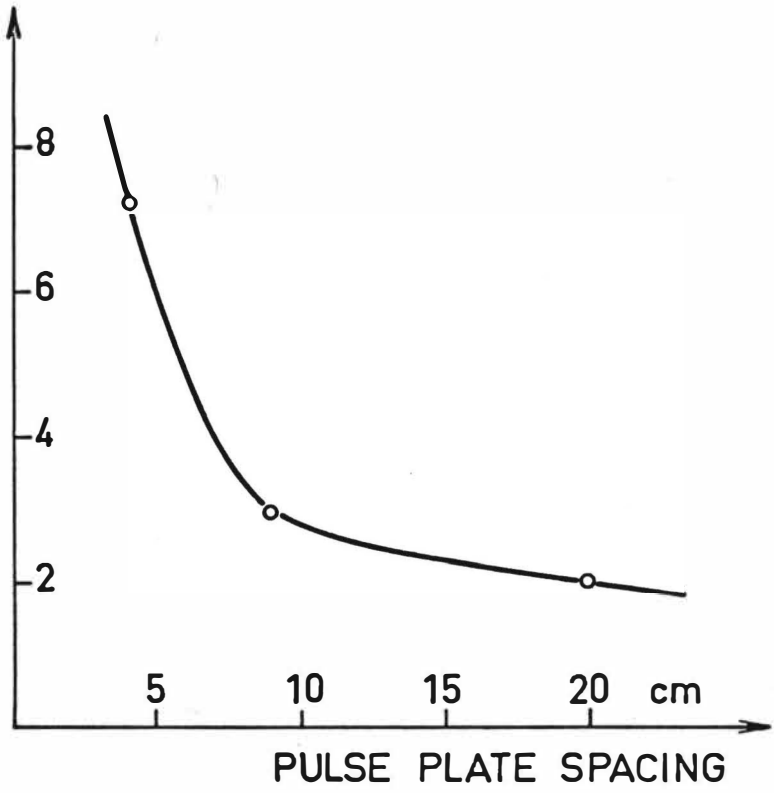


FIGURE 9 : VARIATION OF THE PECLET NUMBER ACCORDING TO PULSE PLATE SPACING AT CONSTANT PHASE VOLUME RATIO AND α_f PRODUCT

**Liquid Flow Study in
the Cross-Section of ARD Extractor**

**B. Seidlová
T. Mišek**

The cross components of liquid movement in ARD extractor are responsible for the transport of liquids from the mixing zone to the separating zone, for the cross mixing and the residence time in both zones. The distribution of the velocities over the cross-section influences deeply the longitudinal mixing effects and other important characteristics of the apparatus.

The measurement of the velocity distribution has been performed using an indicating particle. The diameter of the equipment used was 250, 2 290, 2 800 and 4 000 mm. Important conclusions have been drawn, enabling to evaluate the critical equipment size, the mixing conditions in the compartment and the settling conditions.

**Research Institute
of Chemical Equipment**

Prague, Czechoslovakia

In the past time many papers have been published describing various aspects of operational behaviour of Asymmetrical Rotating Disc Extractors (ARD), e. g. the motion, the breaking-up and the coalescence of droplets, longitudinal mixing and mass transfer. An insufficient attention has been paid to the rotary motion of the dispersion in the individual extractor compartments, although this motion is highly important both for the mass transfer and for the throughput of liquids in the extractor. A similar situation arises with other types of agitated liquid extractors e. g. the RDC, Oldshue-Rushton, Kühni and other types.

The importance of the investigation of rotational velocities of liquids and their distribution increases especially with large diameter extractors, and it may be presumed that in large extractors the drop of the rotational speed can be the limiting factor for the extractor size. These facts - along with the necessity to obtain data for design of large diameter extractors - have initiated the present work.

Rotational speeds have been studied on models of the mixing compartment of an ARD Extractor in diameters ranging from 250 through 4 000 mm, the geometry of which can be seen in Fig. 1. The models were closed from the upper side with a transparent cover, enabling the respective measurements.

The speed of the circulating liquid in the model can be followed in different ways, the most of which being able however recording only some of the mean velocities, but not the whole velocity distribution range. As a suitable solution therefore the method of an indicating particle was used, based on the following presumptions:

- a) an indicating particle of suitable design has a small mass, the same specific gravity as the ambient liquid and a high hydraulic drag factor;
- b) such a particle is drifted nearly completely along with the ambient liquid
- c) the influence of the turbulent liquid pulsations, which are smaller than the particle - is negligibly small in comparison with the circulation time of the particle;
- d) the transitions of a particle from one possible path onto another, are of a stochastic character and with a large number of runs, their distribution expresses also the distribution of volumetric throughputs.

The design of a suitable indicating particle is shown in Fig. 2. The particle is made of polyethylene and is balanced with a high accuracy by pressing a sealing plastic compound into the cavity in its center. The balancing is performed in a liquid at the measuring temperature so that the particle features a slight ascending velocity in the first half of the measurements and a slight descending velocity in the second half. The velocities are checked at the start and at the stop of each test series. It has been found that the balance accurateness of the particle exerts a considerable influence on the measuring result and that this value should be anxiously followed.

In the orientation test runs it has been investigated, whether the presumption c) had really been met. Particles of 5, 10 and 20 mm diameter were tested and it has been found that the size of the particles exerted no systematic influence on the circulating time and that the particles could be therefore held for equivalent. Valid measurements

have been performed with the 5 mm particle in the 250 mm diameter model and with the 10 mm particle in all other models.

In the next orientation test series the method of the indicating particle has been compared with the measurements performed by means of a propeller-type tachometer. Here an exact coincidence of results could hardly be expected, but the velocity values obtained in both methods did not controverse with each other and presented no significant differences.

The tests have been performed in the following way:

The indicating particle has been inserted into the model in which a mixing disc rotated at a constant speed and the circulation times of the particles were measured as the time difference between two consequent crossings of a suitably selected model radius, whilst records were made whether the particle passed along the inner path - through the mixing compartment - or along the outer path - through the settling compartment. A large number of such measurements has been undertaken.

The main measurement result are the circulation times τ divided into two groups: τ_{in} are the circulation times of particles along the inner path

τ_{out} are the circulation times of particles along the outer path

Results of a large number of measurement have been statistically evaluated as the mean circulation time

$$\left(\bar{\tau} = \frac{\sum \tau}{n} \right)_{in, out}$$

and the variance of the circulation time

$$\left(\overline{\sigma^2}(\tau) = \frac{\xi \tau^2}{n} - \bar{\tau}^2 \right)_{in, out}$$

The circulation times of the particles depend mainly from the peripheral speed of the disc mixer $\pi n D$. It is therefore of advantage, to use these values, for definition of the so-called slip:

$$\alpha = \frac{n_R D \tau}{D_k}$$

The published theoretical solutions of the liquid flow caused by a smooth rotating disc in an infinite predict only a slight correlation of this slip on the modified Reynolds number for mixing

$$\alpha \sim \left(\frac{\eta_m^2 n_R \varphi}{\mu} \right)^a$$

the exponent a being in the range from 0 to 0.1. When testing the results it has been proved that the exponent value was 0.085 and that its statistical significance was so low, that it could be neglected and the slip considered as independent from the Reynolds number, i. e. also from the viscosity, RPM and the specific gravity. This makes possible summing-up the results obtained with different rotational speeds of individual models and expressing them by the mean slip value

$$\left(\bar{\alpha} = \frac{\xi \alpha}{n} \right)_{in, out}$$

and by the slip variance

$$\left(\sigma^2(\alpha) = \frac{\sum \alpha^2}{n} - \bar{\alpha}^2 \right)_{in, out}$$

The measured data have been summed-up in Table 1. The data show clearly, that the mean slip values for individual models differ not quite expressive and unsystematically from each other. If we want to judge on the extent of the influence of individual models on the slip mean value, the joint variance of all the results measured and the weighted mean variance of individual models may be used. It appears that a combination of the inner path slip values in one single value is feasible, but on the outer path brings about a higher variance which proves a considerable influence of the column diameter on this value. The results are accordingly correlated with the diameter in the Fig. 3.

The data thus obtained help us to formulate answers to several questions put forward frequently when designing agitated extractors:

- 1) Does the flow pattern in the column vary with the diameter?

For treating this question, we use the assumption d) of the measuring method according to which

$$\frac{n_{in}}{n_{out}} = \frac{Q_{in}}{Q_{out}}$$

and as according to Danckwerts the mean residence time in the mixer does not depend on its distribution, then also

$$\frac{v_{out}}{v_{in}} = \frac{n_{out}}{n_{in}} \cdot \frac{\bar{\tau}_{out}}{\bar{\tau}_{in}}$$

It may be assumed, that the formation of dead water zone adjacent to the periphery of the mixed compartment the effective volume ratio of the outer V_{out} and of the inner V_{in} path will decrease. This really occurs as it can be seen from the data in the Table 1 and from the informative courses in Fig. 4. In models up to 2 800 mm of diameter a plain glass disc has been used. This however, was impossible with the model 4 000 mm of diameter, where a braced disc welded up from three sections had to be used.

The data indicate, that the dead water zone arises when using a plain disc, in an extractor of about 2 800 mm in diameter and with a braced welded disc in diameter over 3 600 mm. This size can be probably considered as the upper limit in the design of extractors of this geometry.

2) The second question: Is an ideal mixer achievable in one single compartment of an ARD Extractor ?

According to the results of our measurements the residence time distribution of particles arising during one cycle in the compartment can be calculated for any constant RPM. This distribution is

$$\sigma^2(\tau) = \frac{\sigma^2(\sigma_{\tau})}{\bar{\sigma}_{\tau}^2} \equiv \frac{\sigma^2(\mathcal{R})}{\bar{\mathcal{R}}^2}$$

and by comparing with a flow model through a cascade of ideal mixers the equivalent number of ideal mixers for one circulation cycle can be calculated:

$$\frac{1}{n_{IM}} = \sigma^2(\tau)$$

Here a joint slip variance must be taken into account

$$\sigma^2(\bar{x}) = \frac{\sigma^2(\bar{x})_{in} + \frac{n_{out}}{n_{in}} \sigma^2(\bar{x})_{out}}{1 + n_{in}/n_{out}} + \frac{\bar{\sigma}_{in}^2 + \bar{\sigma}_{out}^2 \frac{n_{out}}{n_{in}}}{1 + n_{in}/n_{out}} - \bar{\sigma}^2$$

and so the joint mean slip value

$$\bar{\sigma} = \frac{\bar{\sigma}_{in} + \bar{\sigma}_{out} \frac{n_{out}}{n_{in}}}{1 + n_{out}/n_{in}}$$

The mean residence time of the particle in one compartment

$$t = \frac{h_m}{u_i} \quad ; \quad u_i = \frac{U_i}{x_i} \quad ; \quad i = c, d$$

is, however, longer than the circulation time, which means that several circulation cycles are performed during the mean residence time of the particle in the compartment.

Owing to these circulations the variance of the residence time is increased as follows:

$$\sigma^2(\tau) = \frac{m \sigma^2(\bar{x})}{\bar{\sigma}^2}$$

The number of circulations m can be calculated from the circulation time and from the mean residence time of the particle in the compartment and for the condition of the realisation of an ideal mixer the following inequality can be written

$$m = \frac{t}{\tau} = \frac{h_m x_i n_R D}{U_i \bar{\sigma} D_K} \geq \frac{\bar{\sigma}^2}{\sigma^2(\bar{x})}$$

For typical parameters of the ARD it can be inserted and obtained:

$$n_R \geq 107 \frac{U_i}{x_i h_m}$$

In individual cases it can be concluded whether the inequality has been met and whether the compartment has been thoroughly mixed. With a dispersed liquid it cannot be pre-

sumed that the inequality will be fulfilled in the normal operational range of the extractor whereas for a continuous liquid, on the contrary, the mixing under standard operational conditions veritably approaches an ideal mixer.

3) The third question: What are the conditions for the settling of a dispersion in the settling section ?

For an efficient settling (separation) of a dispersed and a continuous liquid in the settling section it is of a considerable advantage that the tangential flow in this zone approaches the piston flow (10 ideal mixers are effected here during one circulation) and that the flow velocity is low. For a complete settling of a dispersion, having a settling velocity u_{st} , a simple condition

$$\frac{u_{st}}{u_{out}} \geq \frac{h_m}{L} \quad ; \quad u_{st} \geq \frac{h_m}{L} \cdot \frac{\pi n_R D}{\bar{d}_{out}}$$

is valid, into which numerical values of a typical geometry can be inserted.

$$u_{st} \geq 0,227 \cdot h_m \cdot n_R$$

In large extractors even-small droplets having a small settling velocity will settle practically completely. Thereby the transport of the dispersed liquid in the vertical direction is stimulated and the extractor capacity is considerably increased. Large ARD extractors operate practically in the conditions of a mixer-settler.

In general it may be concluded, that the indicating particle method proved to be a suitable aid for the investigation of the flow pattern in agitated extractors. The conclusions obtained from the application of this method made possible to clear a number of important problems of large diameter extractor design.

Symbols

D	disc diameter	cm
D_K	compartment diameter	cm
h_m	height of the compartment	cm
m	number of circulations	l
n	number of runs	l
n_M	equivalent number of ideal mixers	l
q	volume throughput	cm^3/s
T	dimensionless time	l
t	residence time in the compartment	s
U	superficial velocity	cm/s
u_{st}	settling velocity	cm/s
v	effective volume	cm^3
X	hold- up	l
\mathcal{H}	the slip	l
μ	viscosity	P
ρ	specific gravity	g/cm^3
τ	circulation time	s

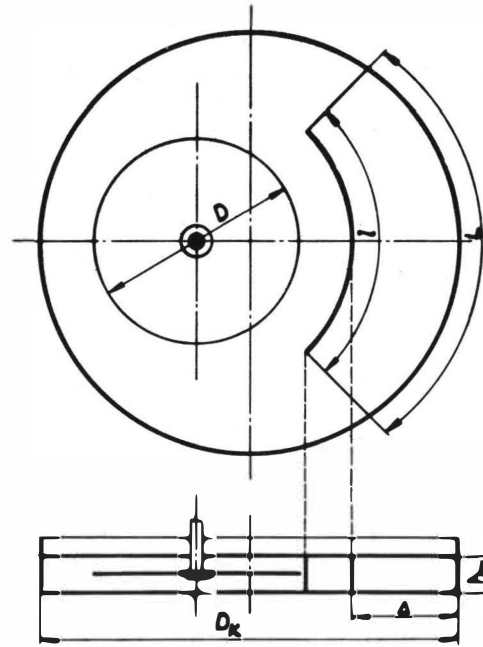
Indices

in	inner path
out	outer path
c	continuous liquid
d	dispersed liquid

Table I.

Results

D_K mm	250	2 290	2 800	4 000	Composed Value
n_{in}	354	510	783	60	1 707
n_{out}	672	993	559	54	2 278
\bar{x}_{in}	3.97	6.11	4.10	6.88	4.77
\bar{x}_{out}	6.85	12.48	10.16	9.79	10.19
$\sigma^2(x)_{in}$	2.10	3.39	1.15	6.39	3.23
$\sigma^2(x)_{out}$	4.35	6.98	2.43	7.23	10.66
n_{in}/n_{out}	0.53	0.51	1.4	1.1	-
$\bar{x}_{out}/\bar{x}_{in}$	1.72	2.04	2.48	1.43	2.13
v_{out}/v_{in}	3.25	3.99	1.76	1.29	-



[mm]					
D_k	D	h_m	L	l	Δ
250	122	50	196,2	146,7	63
2200	1120	230	1797,6	1342,3	580
2800	1370	258	2198	1640,6	710
4000	1960	350	3140	2342,4	1016

Fig.1 Lay-out of the ARD
Extractor Compartments



Fig.2 Construction of the
Indicating Particle

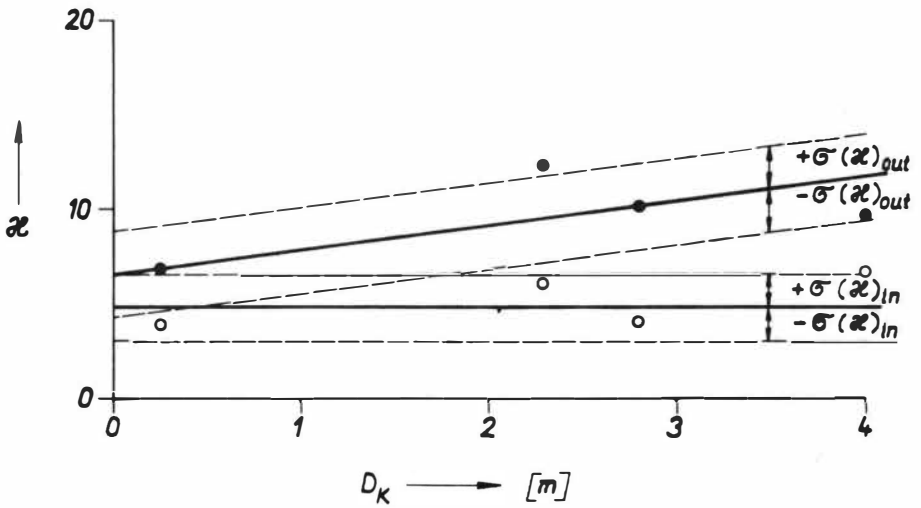


Fig.3 Correlation of the Slip with the Compartment Diameter

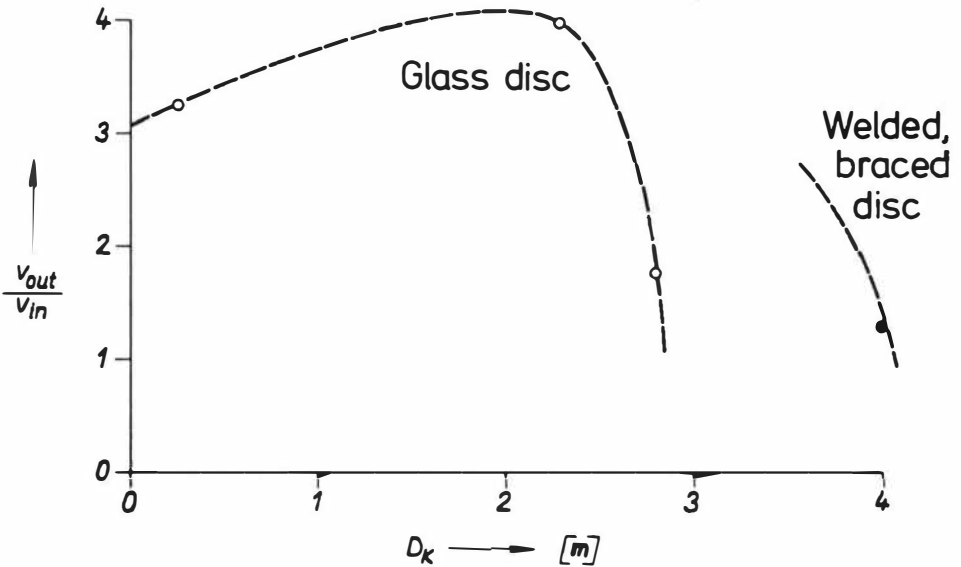


Fig.4 Dependence of the Effective Volumes Ratio on the Compartment Diameter

PERFORMANCE OF CENTRIFUGAL EXTRACTORS

David B. Todd and Gordon R. Davies
Baker Perkins Inc.
Saginaw, Michigan, USA 48601

ABSTRACT

The design and operation of Podbielniak® type centrifugal liquid-liquid extractors are described. Performance data on extraction efficiency, capacity, and residence time distribution are presented on a new more compact, more portable, and more versatile pilot extractor, which is capable of operation with centrifugal forces up to 10 000 G's. These data are compared with similar information on commercial centrifugal extractors, covering the combined throughput range from 0.1 to 100 m³/hr.

PERFORMANCE OF CENTRIFUGAL EXTRACTORS

David B. Todd and Gordon R. Davies
Baker Perkins Inc.
Saginaw, Michigan 48601

INTRODUCTION

Centrifugal extractors, although widely used, are probably equally widely poorly understood. Some of the mystery about their operation stems from a lack of visibility. It is not possible to make a glass or plastic centrifugal extractor that will operate with the centrifugal forces commercially encountered. Nor is it convenient to obtain intermediate samples required for study of discrete stage phenomena. Thus, as may be common with many chemical reactors, conclusions are drawn about what is happening internally by the observation of output responses to input changes.

The very compactness of centrifugal extractors has posed some challenging questions for both the manufacturer and the user. Relatively high capacities are achieved in a small geometric space. The short residence time (usually less than one minute) makes it possible to study many process variables, since steady state is so rapidly approached. In commercial operation, an upset in the inlet conditions is reflected so rapidly in the extract and raffinate that corrective actions can be initiated equally rapidly without jeopardizing production or producing a sizeable inventory of off-spec product.

Although centrifugal extractors exist in which the axis of rotation is vertical (1), this discussion is confined to the horizontal axis species, generally known as the Podbielniak® type contactor.

DESIGN AND OPERATION

The centrifugal extractor is a perforated plate extraction tower (without downcomers) that has been wrapped around a shaft, which in turn is rotated to create a centrifugal force field that allows a great reduction in the height and time required to achieve a countercurrent contacting process result. The typical features of the commercial size continuous countercurrent centrifugal extractor are illustrated in Figure 1. All fluids enter and leave the rotor via mechanical seals and shaft passageways. Radial conduits connect the shaft passageways to the appropriate collection or distribution points within the rotor.

The extraction process may be described by assuming a typical extraction of a solute from an aqueous feed with a less dense organic solvent. The organic solvent is introduced into the rotor through distributors located near the periphery. Aqueous feed is introduced similarly through distributors located nearer the shaft. The heavier liquid is centrifuged outward, causing a displacement of the lighter phase inward. The countercurrent flow of the two phases through the compartments effects a series of intimate contacts. Clarification zones are provided inboard of the feed inlet and outboard of the solvent inlet. The extract collects at the shaft. The raffinate collects at the periphery, and then is led back through conduits to the shaft passageway.

Mechanical features provided include access ports to the rotor interior (ASCO tubes) which can be used for inspection or cleaning. Disassembly is not required for cleaning, although one rotor end plate can be removed. The internal contacting trays are now made with such precision that an existing centrifugal extractor can be retrayed in the field should the intended service be changed. The radial position of the feed ports may be altered, without disassembly, by reworking or replacing the appropriate radial conduits. The rotor is driven via a belt connected to a fluid coupling variable speed drive. Power requirements are low since the fluids enter and leave at the same axial "ground-stage," and only windage and friction must be overcome.

The comparison with the perforated plate tower is more readily visualized by looking at the radial section in Figure 2. The centrifugal force accelerates the separation process, and allows greatly reduced plate spacings (in the order of 6 mm), with the resultant compaction of tower height and greatly reduced settling times.

The positioning of the principal interface between the two phases is accomplished by imposing a back pressure on the light liquid effluent. That is, the selection of the predominantly dispersed and the predominantly continuous phase may be accomplished in a manner similar to that used for liquid level control in a tower. Although the "height" may be very small, and the specific gravity difference may be slight, the product of these two terms multiplied by the G-forces yields a satisfactory pressure differential. The inlet and outlet pressures can be interpreted in terms of legs of a manometer, and the position and nature of the principal interface within the centrifugal extractor can be deduced from the pressure interrelationships (2).

A head of coalesced dispersed phase accumulates above or below each tray depending on which phase is continuous (i.e. a head of heavy liquid exists inboard of the tray for light liquid continuous). The depth of this phase (h), or the depth of continuous phase displaced, and the associated centrifugal force, provide the pressure drop for the liquids through the orifices. In the most simplistic of terms, this may be represented by:

$$2(\rho_H - \rho_L)RW^2h = \rho_C(Q_C/A_C)^2 + \rho_D(Q_D/A_D)^2$$

where R is the radius, W is the angular velocity, ρ_H , ρ_L , ρ_C and ρ_D are the densities of the heavy, light, continuous (light or heavy) phase and dispersed phase respectively, Q_C and Q_D is the volumetric flow rate of each phase and A_C and A_D , the flow cross-sectional area, may be related to the actual open area by orifice coefficients.

PILOT CENTRIFUGAL EXTRACTORS

The early pilot centrifugal extractor was the Podbielniak Pup. Most of the extraction performance data which have been published (3, 4, 5, 6) have been obtained on these units. The construction consisted of a series of milled annular grooves, as compartments, with two milled slots between each pair of grooves, as schematically illustrated in Figure 3. The two 430 mm diameter end plates were held together with 72 bolts, many of which passed through the extraction zone. The rotor interior was only about 6 mm wide. The machined design, as well as the small internal dimensions, precluded the study of geometric variables, such as tray spacing, hole size (which may be as large as 12 mm in commercial units), hole shape, and hole patterns. The maximum speed was 5000 RPM, and a typical maximum capacity was about 0.5 liters per minute. Although only a pilot device, the rotor and base weighed about 95 kg. The heavy weight, coupled with the complications of the closing bolts, made this pilot equipment not readily serviceable by laboratory personnel.

Recently, a new pilot centrifugal extractor, the Model A-1 as shown in Figures 4 and 5, has been developed which is even more compact, and yet has features much more in common with the commercial counterparts. The 216 mm outside and 178 mm inside diameter rotor is constructed with a removable end plate, and fourteen removable trays, spaced at 4 mm. This offers the adaptability to investigate various tray designs, and to a limited extent, the effect of tray spacing. The trays are gasketed in each end plate. This positive seal eliminates possible leaks around the trays, and the possible misinterpretation of data where end effects might be accounting for a large portion of the capacity. The internal width is 25 mm, and the total internal volume is about 0.5 liter.

Both heavy and light fluids enter and leave via three radial distributors. Typically, the heavy liquid enters at a radius of 40 mm, and the lighter liquid at a radius of 88 mm, with ten cylindrical contacting trays in between. Two coalescing trays are provided outboard of the countercurrent contacting zone for clarification of the heavy phase. Similarly, two coalescing trays are provided inboard of the contacting zone for clarification of the light phase. The ratio of contacting to clarifying trays may be varied. Rim plugs at each of the radial inlet and exit channels, as well as around the tray section may be removed to allow cleaning and inspection.

The stainless steel rotor and aluminum housing weigh only 46 kg., and are mounted with a variable speed drive on a 70 cm by 110 cm aluminum base plate, permitting desk top operation. The light weight, coupled with the ease of disassembly, including a simple split key at the shaft to accomplish end-plate closure, facilitates the retraying of the unit to study alternate designs. Depending upon the internal tray design, maximum capacity ranges from 0.5-5 liters per minute. The maximum operating speed is 10 000 RPM, at which speed 10 000 G's (multiples of gravity) are developed at the rim. With only a fraction-of-a-minute holdup time, steady state is rapidly approached, and a multitude of process conditions can be tested in a very short period.

PILOT PLANT PERFORMANCE

Extraction. The pilot plant centrifugal contactor was installed in the test loop as schematically illustrated in [Figure 6](#). Temperature and pressure gauges were installed at each of the inlets and outlets. Spring loaded, diaphragm type pressure control regulators were located in both the light liquid (methyl isobutyl ketone) and heavy liquid (deionized water) effluent lines. The feed system for each phase consisted of a feed pump, back pressure regulator (by-pass valve) water cooled heat exchanger, calibrated rotameter, and needle flow control valve. The pump by-pass valves served to divert the unused portion of the feed capacity, as well as adjust the pressure such that a small pressure drop existed over the rotameter and needle valve flow regulating combination. This leads to more stable operations with minimal drift of rotameter float. Distribution coefficients for acetic acid partitioned between methyl isobutyl ketone (MIBK) and water were determined for three concentration levels over the range of 26 to 38°C, employing standard titration techniques. The data proved to be linear and quite insensitive to temperature over the region of interest. The equilibrium curve is shown in [Figure 7](#). A feed solution containing approximately 5% acetic acid in the methyl isobutyl ketone was prepared. Typical performance data are shown in [Table 1](#) for three different internal designs. For this system, both speed of rotation and location of principal interface are important. Maximum efficiency was obtained at the maximum operating speed. Performance was also better when the entire countercurrent contact zone was filled with the low flow aqueous phase, in agreement with the general rule that the liquid with the greater flow rate should be selected as the dispersed phase. The McCabe-Thiele plot for the best run is illustrated in [Figure 7](#), with 5.4 theoretical stages.

The model system of methyl isobutyl ketone-acetic acid-water with extraction from the organic to the aqueous phase has been used to illustrate the applicability of general extraction rules, for column extractors, to the centrifugal contactor. Both the choice of the continuous phase, and the approach to flooding conditions, each of which relate to the available interfacial area for mass transfer, have indicated a marked difference in extraction efficiency. An overall extraction efficiency of 60% per compartment has been demonstrated for this system. In actual practice, other circumstances may influence the preference for the continuous phase, and extraction efficiency may be sacrificed. An undesirable density gradient caused by solute transfer may preclude choice of the low flow liquid as the continuous phase. The tendency toward emulsification is usually greater at the feed-extract end than at the solvent- raffinate end. Emulsification difficulties are often altered by entering one of the liquids into a large body of the other. In general, interfacial emulsions or the formation of a steady-state interfacial "rag" are more readily accommodated at the rotor light-liquid-in port where a higher centrifugal force exists. In the case of explosive or radioactive materials, minimizing the inventory of one of the phases, may be predominant in the selection of the dispersed phase.

Capacity. The flooding of the centrifugal contactor is similar to columns in that three types are possible. Light liquid (or shaft) flooding, observed by entrainment of heavy liquid into the light liquid effluent, may occur, even at low capacities, by moving the major interface through the light liquid clarifying zone, and out of the equipment. At higher capacities this type of flooding may occur, even with the major interface positioned in the contacting zone, when the clarifying section residence time and settling forces are insufficient to achieve coalescence and disengagement of droplets generated in the contacting zone. Heavy liquid (or rim) flooding, observed by entrainment of light liquid into the heavy liquid effluent, may occur in an analogous manner at the other extreme of the column or centrifugal contactor. Capacity flooding is observed by simultaneous flooding (entrainment) at both ends of the unit. This flooding is initiated in the contact zone, and occurs when an excessive head (h) of coalesced dispersed phase is required to generate the pressure drop for flow of the liquids through the orifices. The tray design in the contacting section should be selected such that flooding occurs in each compartment at approximately the same capacity for maximum extraction efficiency, and the avoidance of a capacity bottleneck in a portion of the section. The pilot centrifugal contactor was operated in the test loop ([Figure 6](#)) on the system kerosene (specific gravity approximately 0.8)-water. Typical flooding envelope capacity curves, for two internal designs, at three speeds and two phase ratios are presented in [Figures 8 and 9](#). The ordinate P_{LLO} (= $P_{LLO} - P_{HLO}$) represents the range of back pressures on the exiting light phase (LLO) over which the extractor may be operated. The 3x set of internals was specifically designed to provide a threefold increase in capacity.

The approach to capacity flooding, as distinct from shaft or rim flooding, is extremely rapid, and definition of the curve at these points is difficult. The maximum abscissa lines represent inoperable capacity flooding for the respective conditions, whereas the plotted points represent a full range of operable major interface positions from light liquid flooding to heavy liquid flooding. The approximate flood point capacity, for each of the curves, is shown in Table 2.

The data are in general agreement with Equation 1; namely, that the combined flow is proportional to the first power of speed. This test also confirmed the attainment of the threefold capacity increase. The total capacity appears to be higher when the ratio of light-to-heavy phases is increased.

Residence Time Distribution. The distribution of residence times for the flow of water alone was determined by injection of a pulse of concentrated NaNO_3 solution, and measuring the cumulative amount collected in the effluent at a function of time. The tracer was charged to a small injection loop. A quarter turn of a 4-way valve permitted injection of the tracer without any interruption in flow. The amount of NaNO_3 in sequential samples was determined by measuring the electrical conductivity. The cumulative distributions for five different flow rates are shown in Figure 10, compared with the theoretical curve for 13 well-mixed stages in series. Except for the 300 and 600 ml./min. rates, the data points all lie close to the theoretical curve. One can conclude from these data that each compartment is well mixed, and that there is essentially no backmixing across the trays at high net flows. The amount of backmixing can be deduced from the shape of the cumulative distribution curve (7). Where the data coincide with the theoretical curve for the same number of compartments, the amount of backmixing is negligible. For the 300 ml./min. flow, the amount of backmixing is estimated to be 175 ml./min. At 600 ml./min., this had dropped to 150 ml./min. At 1080 ml./min., no further backmixing could be detected.

COMERCIAL SCALE PERFORMANCE

Users of commercial centrifugal extractors are generally most reluctant to release their operating data. The commercial units, once installed, are generally run to meet production needs, and are not available at the investigator's whim to demonstrate performance over a wide range of variables. The manufacturer of the equipment is limited in his ability to develop the data without constructing a complete solvent recovery plant. Despite these limitations, some data have been obtained with several of the smaller commercial Model B-10 extractors (capacity about $7 \text{ m}^3/\text{h}$) and with an intermediate size Model D-18 (capacity about $23 \text{ m}^3/\text{h}$). Dimensions of these units are listed in Table 3.

Pressure Drop. The pressure drop for single phase flow is shown in Figure 11 for a Model B-10 extractor. The total pressure drop can be divided into entrance and exit losses, and a loss through the contacting zone. The data indicate a significant contribution of rotation above that at zero rpm. This additional energy dissipation is one of the factors controlling droplet size.

For centrifugal extractors, the data can generally be correlated by a power equation for zero rpm and an additive term for the effect of rotor speed. The pressure drop at zero rpm (ΔP_0) is dependent upon the geometry and flow rate Q:

$$\Delta P_0 = ZQ^a$$

The additive term for rotation depends upon both flow rate Q and rotor speed N:

$$\Delta P_N = \Delta P_0 + BQN$$

Z and B in the above equations are constants depending upon the system and extractor. The curves in Figure 11 are plotted on the basis of the constants noted.

The effect of countercurrent flow is demonstrated in Figures 12 and 13 for the water-kerosene system in the same Model B-10 contactor. The water phase pressure drop is determined under conditions wherein the principal interface is held inboard of the heavy phase inlet (contact zone filled with water). The kerosene phase pressure drop is similarly determined, with the interface held just outboard of the light phase inlet (contact zone filled with kerosene). As either flow is increased, the required pressure increases, probably due to both an increased holdup of the dispersed phase and the competition of both fluids for the available flow passageways within the rotor.

Curves similar to Figures 11, 12 and 13 have been generated for the other sizes of centrifugal extractors.

Extraction. The extraction of n-butyl amine from kerosene with water was studied in both the Model B-10 and D-18 extractors listed in Table 3. Typical extraction data for the Model B-10 extractor operating at 3000 rpm with 3.4 m³/h of kerosene and 1.7 m³/h of water are shown in Table 4 and Figure 14.

An attempt was also made to obtain direct contact heat transfer data for this extractor, as longer steady state runs could be obtained without as much testing difficulty. The number of heat transfer stages, as shown in Figure 15 parallel the data for mass transfer. For this series, there were 10 compartments between the warm kerosene and the cold water feeds.

Although the Model D-18 extractor had been designed for 23 m³/h, it was tested on the same kerosene - n-butyl amine - water system at the maximum rates obtainable with the existing pumping and metering system (≈ 11 m³/h). The observed five theoretical stages (Figure 16) compare favorably with the data from the smaller units.

Capacity. The flooding envelopes which define the capacity limits for commercial centrifugal extractors are very similar in form to those for the pilot extractors. Typical kerosene-water flooding envelopes for a Model B-10 extractor are shown in Figure 17. As was noted with the Model A-1 in Figures 8 and 9, the maximum combined flow is higher as the ratio of light-to-heavy phases is increased.

As with the pilot units, the ultimate capacity is generally approximately proportioned to rotor speed (7). Some exceptions are encountered in the very readily emulsified systems. In these, the pressure differential over which the extractor may be operated is expanded as the rotor speed is increased, but the capacity flood point is not increased proportionately. Typical flooding limits as observed in a Model E-48 centrifugal extractor operating on the extraction of aromatics from lubricating oil with phenol are shown in Figure 18.

Backmixing The residence time distributions were determined for the aqueous phase with varying amounts of countercurrent kerosene flow in a Model B-10 extractor. The operating conditions were specifically chosen to exaggerate any backmixing effect - namely, a very low continuous phase superficial velocity and high countercurrent flows. The cumulative distributions are shown in Figure 19 for four flow conditions, and are compared with the curve for 25 theoretical well mixed stages. The amount of backmixing was deduced from the deviation between the data and the theoretical curve. Table 5 shows the calculated amount of backmixing. Apparently, increasing the counter flow of kerosene does not induce or entrain increasing quantities of water. As the water rate is increased, the relative amount backmixing decreases, but the absolute quantity increases. This may reflect the increasing turbulence within the compartment.

CONCLUSIONS

Although differing in many respects from single gravity tower operation, the performance of centrifugal extractors bears a lot of similarities to conventional extraction towers. Operation close to flooding is frequently desirable to maximize mass transfer area. The ability to vary this point by varying the centrifugal force is an advantage that centrifugal extractors possess. However, the major advantages of centrifugal extractors evolve from either their compactness (I) or the use of multi-gravitational separating forces (II).

- I. Processes dependent upon compactness:
 - a. Extraction of unstable ingredients, such as penicillin from acidified broth.
 - b. Extraction where an expensive inventory of solvent would otherwise be tied up, such as in liquid ion exchange processes.
 - c. Extraction or separation where expensive alloy materials of construction are required, such as in various acid treating processes.
 - d. Extraction where space is at a premium, such as in existing buildings or on oil drilling rigs at sea.

II. Processes dependent upon superior separation:

- a. Extraction processes which involve easily emulsified systems, such as certain pharmaceutical extractions, vegetable oil refining or lube-oil refining with phenol.
- b. Extractions with very little specific gravity difference between the phases, such as plasticizer washing.
- c. Extractions where one or both phases are very viscous, such as catalyst removal from polymer solutions.
- d. Extractions where completely clarified effluent streams are mandatory.

The development of a new laboratory centrifugal extractor built along the same lines as the commercial units now permits better modeling studies and more assured scaleup.

TABLE 1

Performance of Model A-1 Laboratory Extractor
Extraction of Acetic Acid from MIBK into Water

Internal Set	Rpm	Liter/min.		Interface R/R Max.	No. of Stages
		MIBK	Water		
A	10 000	0.755	0.551	0.40	5.4
	10 000	0.755	0.551	0.55	4.5
B	10 000	0.755	0.551	0.55	4.2
	10 000	0.755	0.551	0.40	5.0
	7 000	0.635	0.525	0.40	3.9
C	10 000	0.755	0.551	0.40	3.7

TABLE 2

Maximum Capacity (Flooding Point) Kerosene-water
Model A-1 Extractor

Internal Set	<u>QK</u> <u>QW</u>	Combined Flow, liters/min., at Rotor RPM		
		<u>6000</u>	<u>7500</u>	<u>9000</u>
1X	0.5	1.14	1.50	1.75
	1.0	1.18	1.53	1.80
	2.0	1.31	1.58	2.03
3X	0.5	3.50	4.53	5.16
	1.0	3.98	4.65	5.48
	2.0	4.51	5.03	6.00

TABLE 3

Dimensions of Centrifugal Extractors

<u>Model</u>	<u>Rotor ID, mm</u>	<u>Rotor Width mm</u>	<u>Holdup Liters</u>	<u>RPM at 1.0 S.G.</u>	<u>Max. G's</u>	<u>Rated Capacity M³/H (a)</u>
A-1	180	25	0.5	10 000	10 030	0.1
B-10	580	250	57	3200	3340	7
D-18	860	450	220	2100	2130	34
D-36	860	900	440	2100	2130	68
E-48	1140	1200	980	1600	1630	136

(a) For typical multi-stage extraction.

TABLE 4

Extraction of n Butyl Amine from Kerosene with Water
 Model B-10 Extractor, 3000 RPM, 3.4 M³/H Kerosene
 1.7 M³/H Water

<u>Run</u>	<u>R R max</u>	<u>Feed</u>	<u>Conc. mm/1 Raff.</u>	<u>Solv.</u>	<u>Extr.</u>	<u>No. of Stages</u>
105	0.40	596	105	0	910	6.6
107	0.82	38	9.5	6	62	6.7
109	0.36	39	5.5	3	62	6.3
118	0.36	52	20	4	74	5.3
119	0.40	56	25	3.5	71	3.6
120	0.69	66	26	3.5	94	6.4
122	0.97	64	18	3	91	4.0
124	0.34	169	44	2	241	4.0

TABLE 5

Effect of Dispersed Kerosene Flow on Backmixing
 in a Model B-10 Extractor, 3000 RPM

<u>Flows Kerosene Q_K</u>	<u>M³/H Net Water Q_W</u>	<u>Backmixing Q_B</u>
0	2.41	0.85
1.14	1.14	0.53
2.27	1.14	0.61
3.41	1.14	0.59

NOMENCLATURE

a	exponent in pressure drop equation
A	flow cross sectional area
B	dimensional constant in pressure drop equation
h	height of dispersed phase layer
N	rotor speed
P	pressure
\bar{P}	pressure – P_{HLO}
Q	volumetric flow rate
R	radius
t	time
W	angular velocity
Z	dimensional constant in pressure drop equation
ρ	density
θ	average residence time of extractor

subscripts

C	continuous
D	dispersed
H	heavy phase
HLI	heavy phase in
HLO	heavy phase out
L	light phase
LLI	light phase in
LLO	light phase out
N	at speed N
O	at zero speed

REFERENCES

1. Todd, D. B. and Podbielniak, W. J., "Advances in Centrifugal Extraction," Chem Engr. Progr. 61, No. 5, 69 (1965).
2. Todd, D. B., "Improving Performance of Centrifugal Extractors," Chem Engr. 79, No. 16, 152 (1972).
3. Barson, N., and Beyer, G. H., "Characteristics of a Podbielniak Centrifugal Extractor," Chem Engr. Progr. 49, 243 (1953).
4. Alexandre, M., and Gentilini, P., "Détermination de L'Efficacité d'un Appareil Semi-industriel d'Extraction par Solvants, Le Super - Contacteur Podbielniak." Revue IFP II, No. 3, 389 (1956).
5. Jacobsen, F. M., and Beyer, G. H. "Operating Characteristics of a Centrifugal Extractor," AIChE Journal 2, 283 (1956).
6. Fox, J.M., "Centrifuge Compared for Phenol Extraction of Lube," Hydrocarbon Processing 42, No. 9, 133 (1963).
7. Todd, D. B., "Multiple Functions in a Centrifugal Extractor," Chem Engr. Progr. 62, No. 8, 119 (1966).

2390

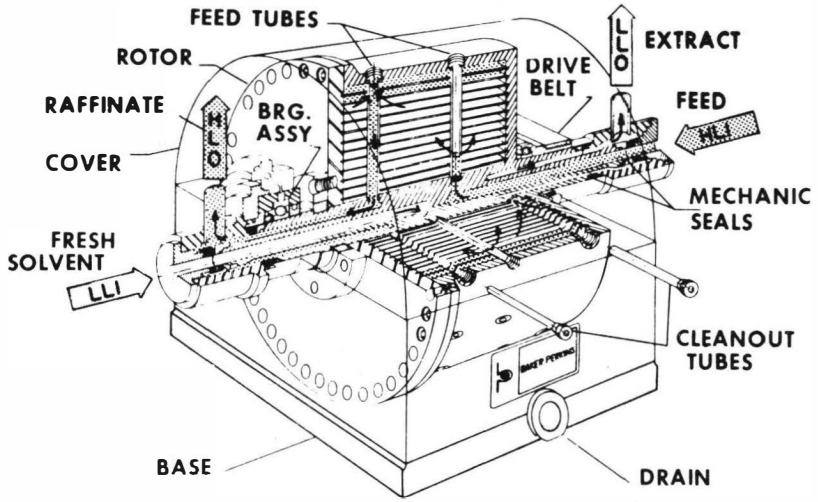


FIGURE 1. CUTAWAY OF CENTRIFUGAL EXTRACTOR

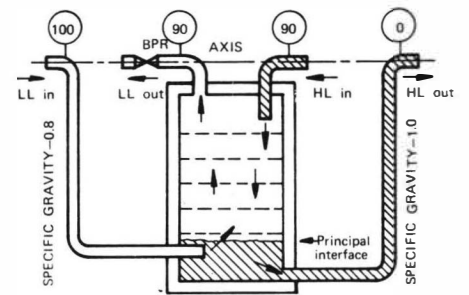


FIGURE 2. TOWER ANALOGY OF A CENTRIFUGAL EXTRACTOR

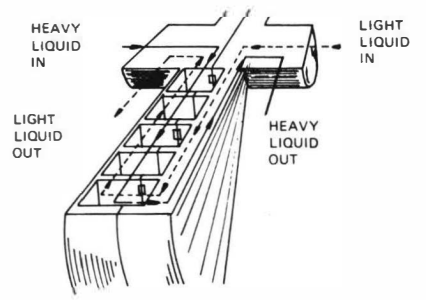


FIGURE 3. SCHEMATIC DIAGRAM OF PUP EXTRACTOR

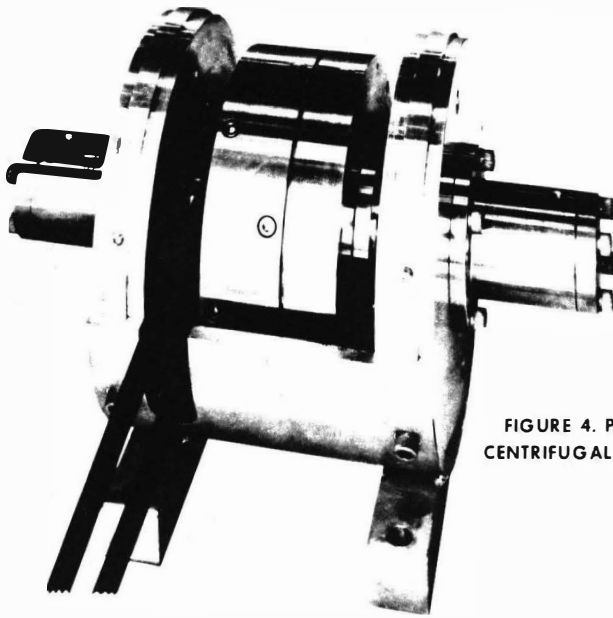


FIGURE 4. PILOT PLANT CENTRIFUGAL EXTRACTOR

BAKER PERKINS
23-1111

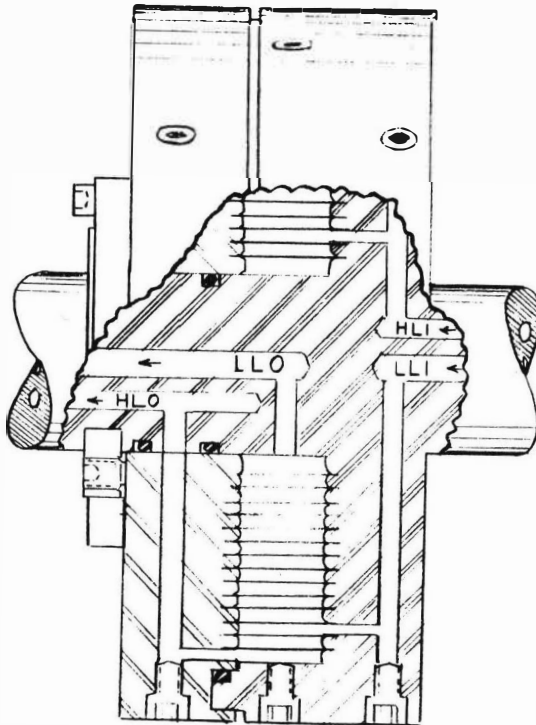


FIGURE 5. CROSS-SECTION OF PILOT EXTRACTOR

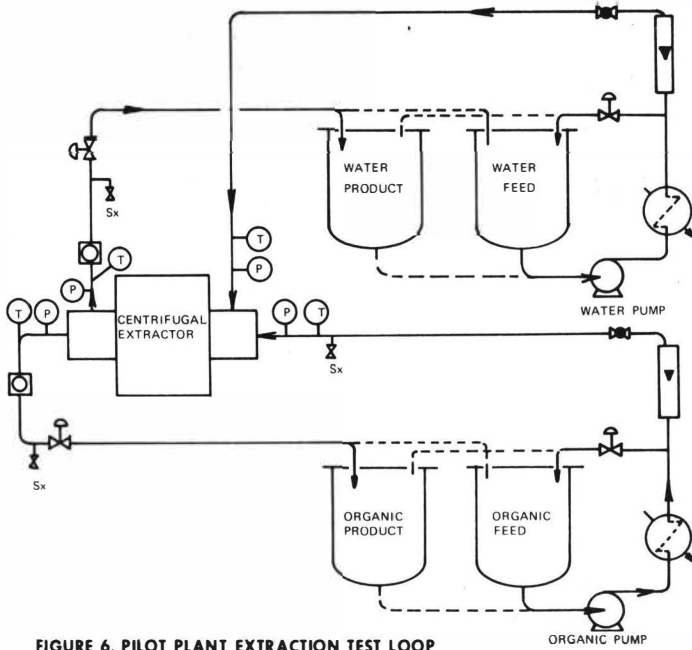


FIGURE 6. PILOT PLANT EXTRACTION TEST LOOP

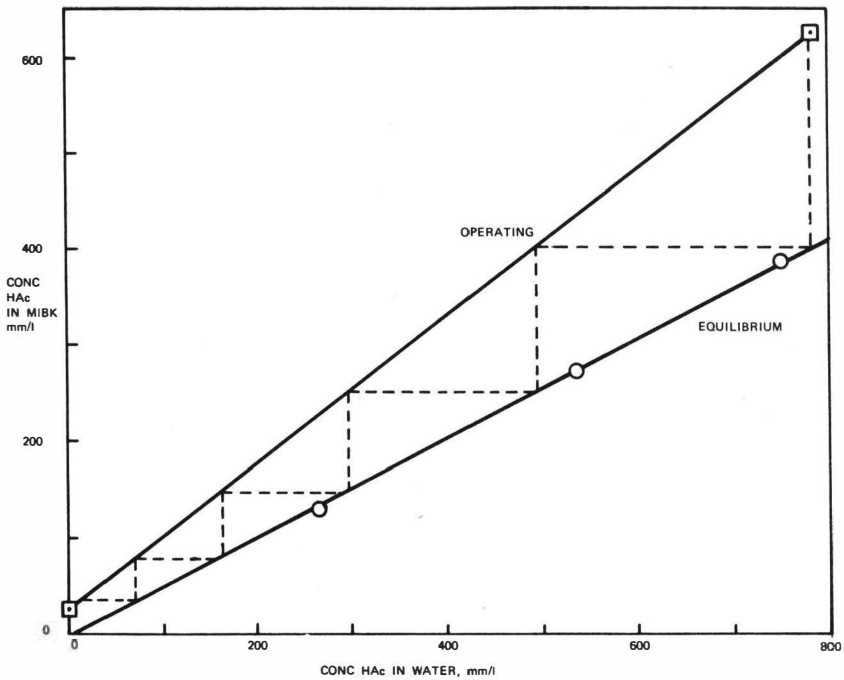


FIGURE 7. EQUILIBRIUM AND THEORETICAL STAGES, MIBK-HAC-WATER

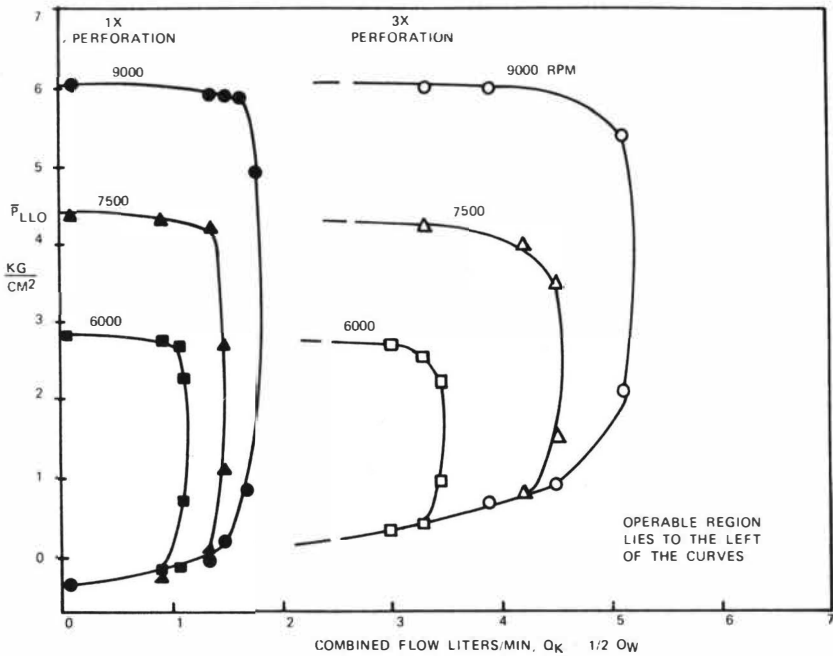


FIGURE 8. FLOODING ENVELOPES AT $Q_k=0.5 Q_w$ (KEROSENE-WATER SYSTEM)

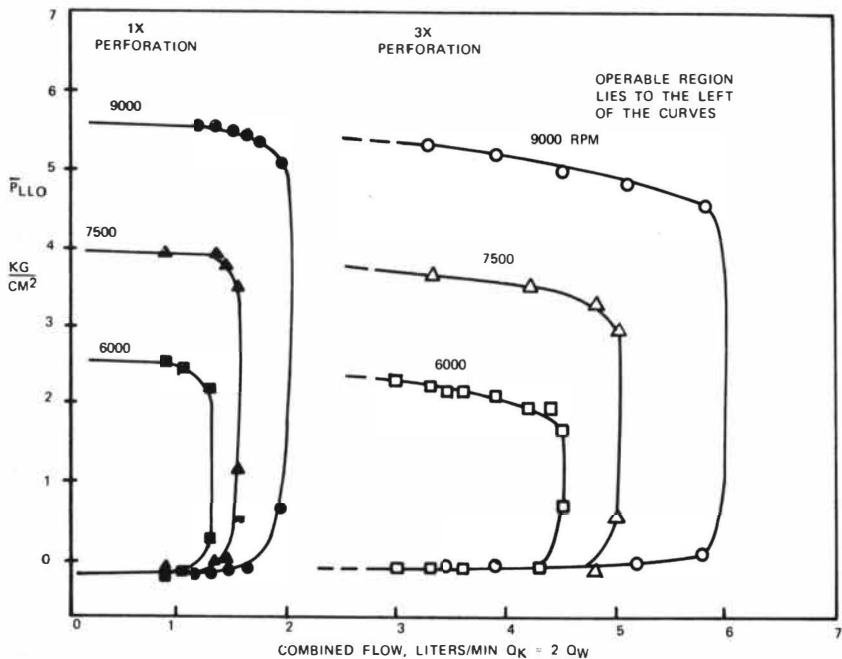


FIGURE 9. FLOODING ENVELOPES AT $Q_k= 2.0 Q_w$ (KEROSENE-WATER SYSTEM)

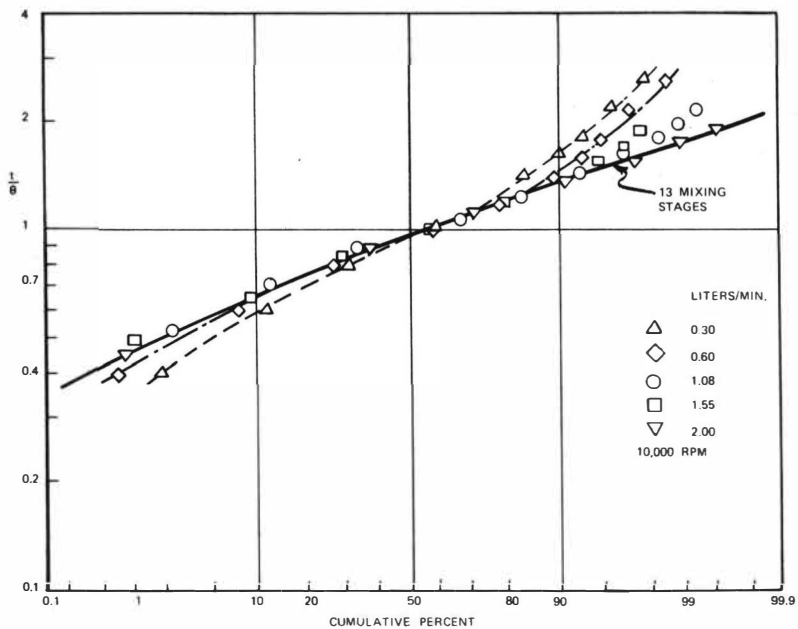


FIGURE 10. RESIDENCE TIME DISTRIBUTIONS FOR THE PILOT CENTRIFUGAL EXTRACTOR

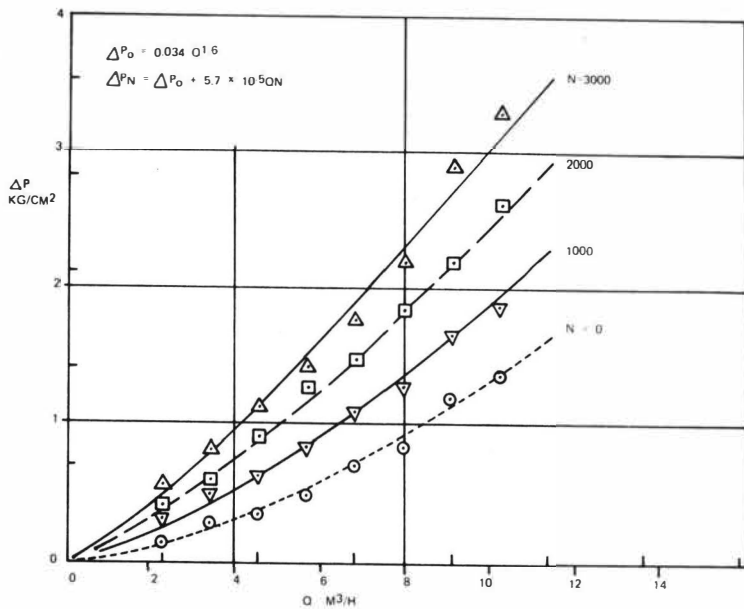


FIGURE 11. PRESSURE DROP THROUGH A MODEL B-10 CENTRIFUGAL EXTRACTOR

2395

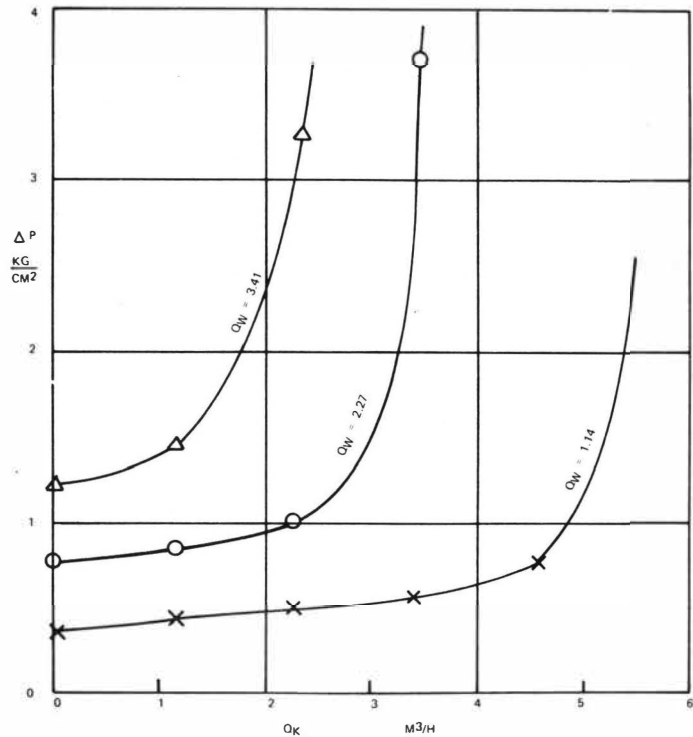


FIGURE 12. EFFECT OF KEROSENE FLOW ON WATER PHASE PRESSURE DROP (MODEL B-10 AT 3000 RPM)

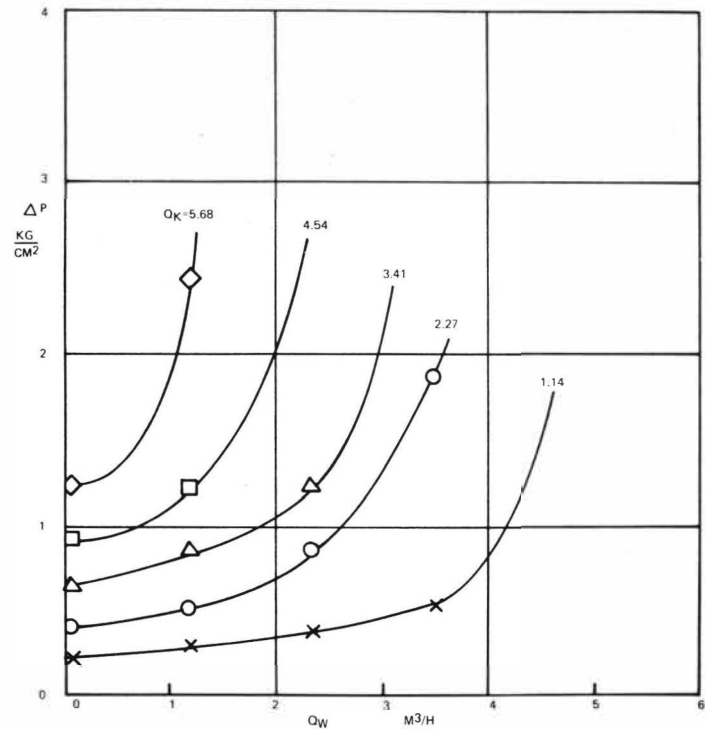


FIGURE 13. EFFECT OF WATER FLOW ON KEROSENE PHASE PRESSURE DROP (MODEL B-10 AT 3000 RPM)

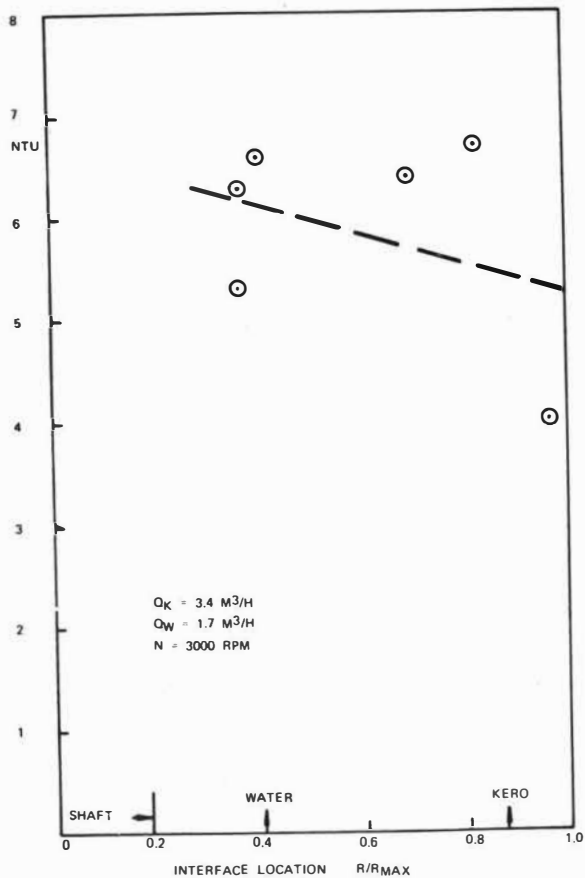


FIGURE 14. EXTRACTION STAGES STAGES FOR KEROSENE-
 n BUTYLAMINE-WATER (MODEL B-10)

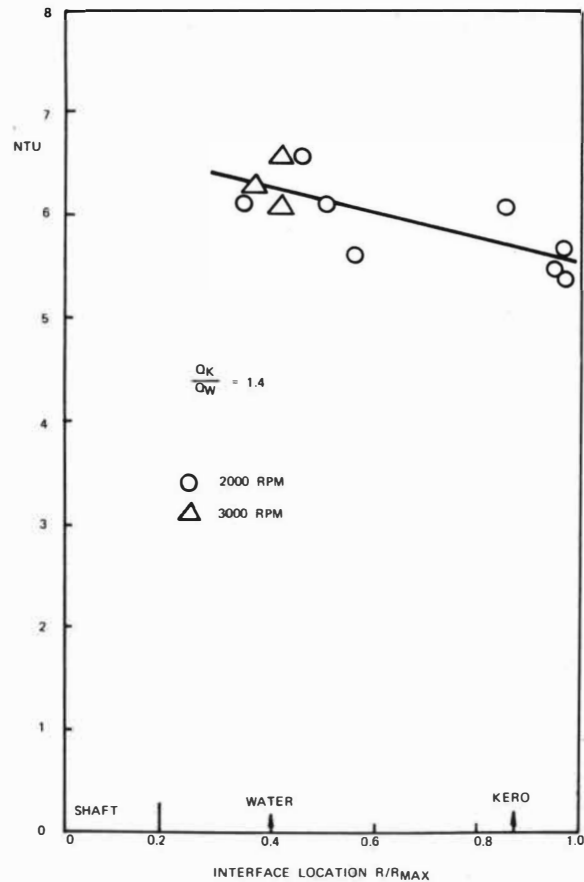


FIGURE 15. DIRECT HEAT TRANSFER STAGES
 KEROSENE-WATER (MODEL B-10)

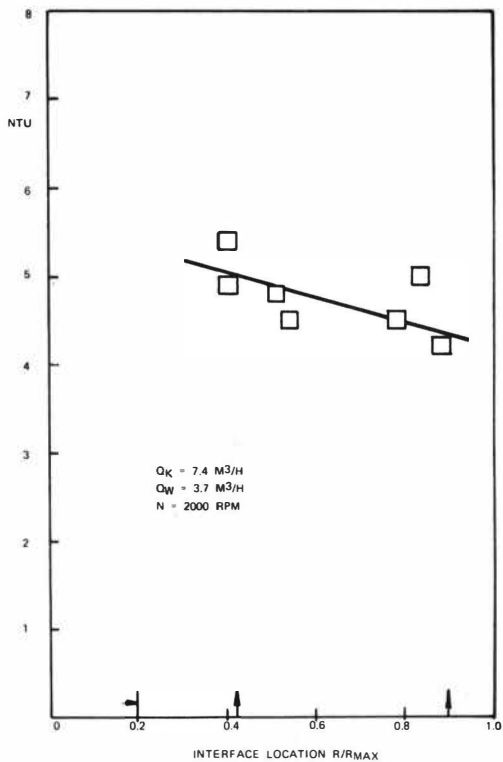


FIGURE 16. EXTRACTION STAGES FOR KEROSENE-n BUTYL AMINE-WATER (MODEL D-18)

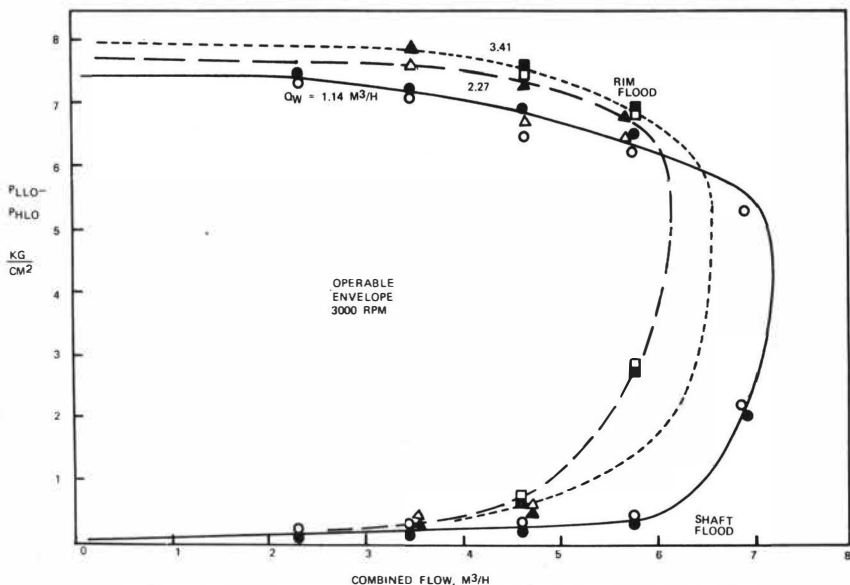


FIGURE 17. CAPACITY ENVELOPE FOR MODEL B-10 EXTRACTOR (KEROSENE-WATER)

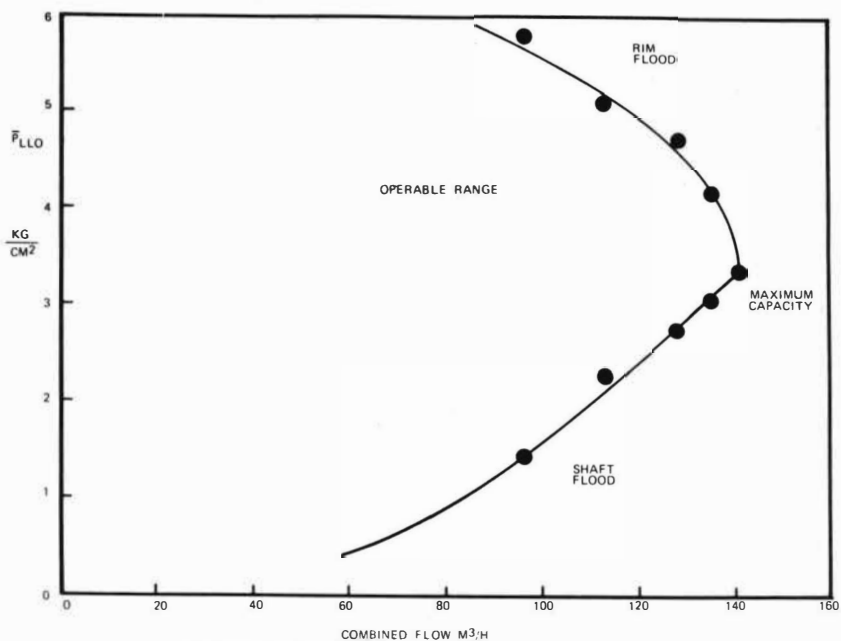


FIGURE 18. CAPACITY ENVELOPE OF MODEL E-48 EXTRACTOR, PHENOL-LUBE OIL. 1600 RPM

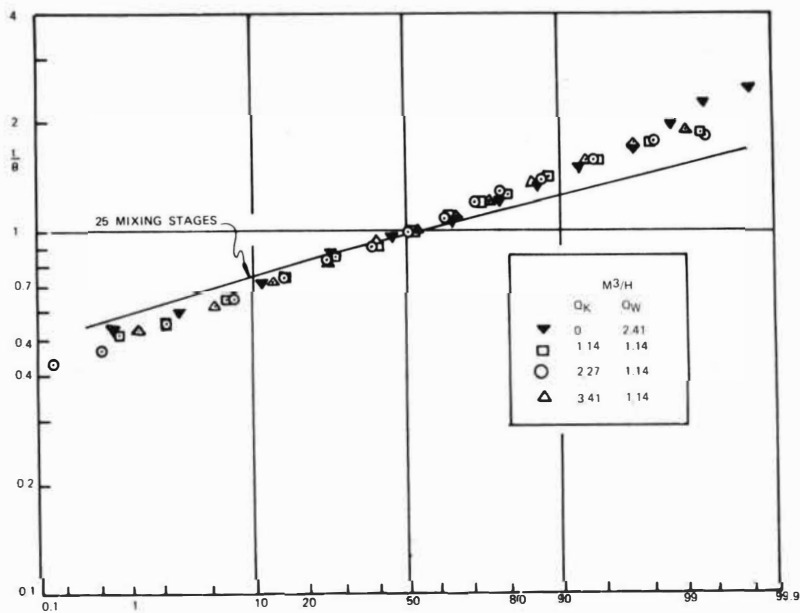


FIGURE 19. RESIDENCE TIME DISTRIBUTIONS FOR THE MODEL B-10 CENTRIFUGAL EXTRACTOR

SESSION 23

Thursday 12th September: 14.00 hrs

M A S S T R A N S F E R P H E N O M E N A

II

Chairman:

Professor J.D. Thornton

Secretaries:

Mr. J.D. Griffin

Mr. C. Lachme

C. HANSON, M.A. HUGHES and J.G. MARSLAND

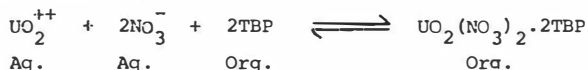
University of Bradford, U.K.

SUMMARY

Attention is drawn to the importance of chemical kinetic resistances in determining overall rates of solute transfer in some solvent extraction processes and the analogy which can be drawn with heterogeneous liquid phase reactions such as aromatic nitration. Existing work is reviewed over the whole range and the methods of study critically considered. A theoretical model is developed to describe the overall rate of transfer when the process involves a fast reaction taking place in a reaction zone in the aqueous phase adjacent to the interface. This is applicable to aromatic nitration reactions under limited conditions and it is shown that the model could explain certain aspects of the rates of different metals extraction processes.

1. INTRODUCTION

Many solvent extraction processes involve a clearly identifiable chemical interaction between the solute and an extractant present in the solvent phase. A classic example is the extraction of uranium from an aqueous solution into a solvent comprising a solution of tri-n-butyl phosphate (TBP) in a suitable diluent. For nitrate media the reaction may be represented by:



The distribution coefficient is determined by the position of this reaction equilibrium. This can be adjusted by control of the nitrate ion concentration, taking advantage of the common ion effect, thus making possible both forward and back-extraction. This type of equilibrium situation has been extensively studied and is well documented. However, being an equilibrium process, it gives no guidance as to the overall rate of the mass transfer process from one phase to the other, a factor of key importance in determining the design and performance of continuous industrial solvent extraction units. At best the chemical reaction, once identified, can only indicate those solutes which could determine the kinetics of the chemical interaction.

In most cases the overall mass transfer rate will be a function of both the kinetics of the chemical interaction and the rates of diffusion (molecular and eddy) of one or more of the species involved between the two phases. The only true exceptions to this generalisation will be when either the reaction or the mass transfer is instantaneous. On the other hand, it is reasonable to classify a process as either kinetic or mass transfer controlled if one rate virtually determines the transfer resistance.

Until recently, most solvent extraction processes have been classified as mass transfer controlled and the possible importance of chemical kinetic effects are only now being recognised. There are several reasons for the early neglect of these effects. Most flowsheets, and even plants, have been designed from the number of equilibrium stages required to effect a given separation. Design from equilibrium isotherms automatically neglects kinetic effects. Secondly, many processes involving chemical interactions have been carried out in mixer-settlers. The mixer compartments are generally over-designed and the long residence times resulting have ensured equilibrium between the phases. Processes performed in differential contactors have usually either involved no specific chemical interaction or the latter has been of a rapid type. The uranium extraction process, for example, is rapid under normal industrial conditions. However, the expanding scope of solvent extraction is introducing processes in which chemical kinetics can be important in determining plant performance. Their neglect could introduce serious errors, particularly with the design of differential contactors. In addition, differences in kinetic rates can be expected to influence the separations achieved between solutes in a finite time of contact, giving separation factors either greater or less than would be predicted from distribution coefficients measured under equilibrium conditions. Such effects could be the cause of some anomalous separation performances which have been observed with existing plants.

Solvent extraction processes involving specific chemical interactions are not restricted to the metals field but include examples of organic separations such as m- from p- cresol by dissociation extraction⁽¹⁾ and of extractive reactions such as the I.M.I. process for manufacture of potassium nitrate⁽²⁾.

While the possible importance of chemical kinetic effects in solvent extraction processes has only recently been widely recognised, the converse is equally true for many heterogeneous liquid phase reactions used in organic synthesis. Thus the rates of aromatic nitration reactions, involving interaction between an aromatic hydrocarbon and an aqueous solution of nitric and sulphuric acids, were long thought to be dependent under all conditions only on the kinetics of the reaction. This assumption is surprising in view of the fact that such reactions can be so rapid that their control is difficult. They have been the subject of extensive study over the last decade and many of the principles developed are applicable to solvent extraction.

2. RATES OF LIQUID-LIQUID REACTIONS

The earliest studies of the kinetics of liquid-liquid reactions were concerned with the process of saponification. In 1904, Nernst⁽³⁾ noted that the rate of diffusion of the molecules taking part in the chemical reactions in emulsions was limited by the overall rate of reaction. However, other workers⁽⁴⁾ assumed that the saponification reaction was truly heterogeneous or interfacial, taking place at the surface of contact between the two phases. This was in spite of the more soluble esters (acetates, propionates and even benzoates with simple alcohols) with which they worked.

Viallard⁽⁵⁾ produced a convincing set of experimental facts for the case of alkaline hydrolysis of esters which had low solubility in the aqueous phase, e.g. benzyl benzoate. He adopted experimental conditions which were favourable to a possible true surface reaction but if this reaction took place at all, it occurred to only a negligible extent compared with the homogeneous reaction in the aqueous phase.

Early work on the macrokinetics of aromatic nitration has been reviewed by Hanson and co-workers⁽⁶⁾. This group has subsequently worked on the nitration of both toluene and chlorobenzene in continuous stirred tank reactors with nitrating acid mixtures typical of those used industrially (15 mole % HNO_3 , 30 mole % H_2SO_4 , 55 mole % H_2O) and have shown that, contrary to previous opinion, diffusional resistances are important in determining the overall rate of reaction over a wide range of conversions^(7,8).

Strachan and Cox⁽⁹⁻¹¹⁾, and also Sohrabi⁽¹²⁾, have nitrated these hydrocarbons in batch reactors using a range of acid strengths. For a given degree of conversion, they were able to demonstrate that the overall rate can be described in terms of the chemical kinetics of the reaction alone at low sulphuric acid concentrations (<20 mole %), when the reaction is very slow, but that diffusional resistances begin to make a significant contribution when the reaction rate becomes greater due to increase in the sulphuric acid concentration, which increases the rate constant for this reaction. Working with a given system, they were also able to show a transition with increasing conversion (i.e. decreasing concentrations of the reactants) from a rate which was mainly dependent on diffusion to one corresponding to the chemical kinetics of the reaction.

The criterion adopted by the above workers to identify the regime was simply to ascertain whether the observed overall rate would fit a model based on the known kinetics of nitration taking place homogeneously throughout the aqueous phase. The development of any such model clearly requires a knowledge of the locale of the reaction. The question of possible models will be discussed later.

Hanson⁽¹³⁾ has described criteria which can be employed to distinguish between processes which are kinetically controlled and those which involve a diffusional resistance, and has pointed out how easily erroneous conclusions can be drawn.

Probably the classic case is the effect of agitation on apparent rate in a continuous stirred tank reactor with constant temperature and residence time, i.e. the conditions found in the mixer of a mixer-settler. The fact of apparent rate becoming constant at high agitation rates has often been taken as proof of the elimination of diffusional resistances, the limiting rate being assumed to correspond to the true chemical kinetic rate. Yet this neglects several factors. Firstly, the hold-up in such a mixer is not necessarily given by the phase ratio found in the exit stream. Below a critical degree of agitation this will not be the case and variations of rate with agitation will include a contribution from the change in hold-up, assuming reaction does not proceed at the same rate in both phases. This has been demonstrated as the cause of some of the change in rate with agitation during nitration of toluene⁽⁷⁾. Secondly, increase in agitation gives progressively smaller increases in interfacial area in the higher regions. Finally, intense agitation can inhibit dispersed phase mass transfer through suppression of internal circulation in drops and of drop interaction.

While widely employed, temperature can be a confusing parameter to use. It not only affects reaction kinetics but also the position of equilibrium for the reaction, distribution coefficients between the phases and diffusion rates.

The effects of changes in phase ratio and space time in a continuous system can give an indication but must be treated with caution because of the many parameters involved.

Perhaps the most conclusive test for the existence of a diffusional resistance under any given set of conditions is to check whether phase inversion affects the rate. It should not do so if this depends only on chemical kinetics but it will change the rate somewhat if a diffusional resistance is present because of its effect on drop size (hence interfacial area per unit volume) and mass transfer coefficients.

Ismail⁽¹⁴⁾ has recently shown that toluene nitration with industrial concentration acid mixtures can be described in terms of mass transfer with simultaneous chemical reaction. The latter basis has also been used by Jeffreys and co-workers^(15,16) to model the rate of hydrolysis of fats in a continuous column-type fat splitter. There seems little doubt that these types of approach would be applicable to some solvent extraction systems.

Amongst other two liquid-phase unit processes which have recently been shown often to have overall rates depending on mass transfer resistances are alkylation⁽¹⁷⁾ and sulphonation⁽¹⁸⁾. Both were previously thought to have overall rates depending only on the chemical kinetics of the reactions.

3. KINETIC STUDIES ON SOLVENT EXTRACTION SYSTEMS

The most detailed work to date has been that associated with the extraction of uranium and plutonium. Other data have been published on the extraction of copper by the LIX reagents and of certain transition metals by phosphorus based acids, e.g. di-2-ethylhexyl phosphoric acid, D2EHPA. The broad types of approach adopted have been (a) taking "dip samples" at time intervals from a stirred tank, (b) measurement of the rate of transfer to

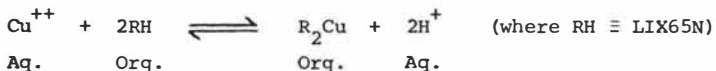
single drops of known size produced in a vertical column, end effects being eliminated by the use of different lengths of travel, (c) use of the AKUFVE mixer centrifuge, (d) measurement of the rate of transfer in a variety of stirred cells with constant interfacial areas, and (e) a wetted wall column.

The first of these techniques, which is similar to that used in most work on aromatic nitrations, is widely practised for solvent extraction at plant level where rough estimates of the rate of transfer are required. Unless the reaction is a reasonably slow one, the technique requires considerable manual dexterity and immediate centrifuging of the dip sample to separate the two phases. Ryon and Johnsson⁽¹⁹⁾ used the technique to study the stripping step, by sodium carbonate, in the DAPEX process for the recovery of uranium from leach liquors. The rate data were treated by the method of Hixon and Smith⁽²⁰⁾ to show that the rate constant is directly proportional to the excess sodium carbonate in the stripping section and to the power input to the mixing vessel. Rate constants obtained by the dip sample technique cannot give area-free mass transfer coefficients.

The single drop method is well described by Baumgärtner and Finsterwalder⁽²¹⁾. It is satisfactory provided the drops are sufficiently small for all internal circulation to be eliminated so that the overall mass transfer is governed by the chemical kinetics of the interaction and molecular diffusion in the dispersed phase. The practical problems which lead to difficulties are: (a) contamination of surfaces by surfactants, (b) wake phenomena, (c) mass transfer across the interface where the drops are collected, and (d) variable mass transfer during drop formation. (The use of large drops would require a knowledge of the hydrodynamics of the system.)

The AKUFVE apparatus⁽²²⁾ has been used by Flett et al⁽²³⁾ to study kinetic effects during copper extraction by LIX extractants. A tracer technique was employed to follow the rate of extraction and thus the apparent chemical kinetics, at or near zero mass transfer. The extraction rate was found to become constant above an agitator speed of 550 rev/min. but this is not proof that the rate is then independent of the surface area generated, as would be necessary to obtain true chemical kinetics. In this apparatus further interfacial area is generated in the centrifuge quite separate from the mixer. It has also been shown in the previous section that a high degree of agitation does not necessarily eliminate all diffusional resistances. A further experimental difficulty is to ensure that the high rates of shear introduced do not establish a temperature gradient.

It is of interest to note that these workers established that for extraction by LIX65N the reaction is first order with respect to the copper concentration and that increasing pH increases the rate of extraction. For the reaction:



these observations suggest a bulk phase process.

Constant interfacial area cells have been widely employed. The cell designed by Lewis has been used in several investigations^(24,25,26) into the extraction of uranyl nitrate and organic solutes. Interfacial turbulence was observed in the case of uranyl nitrate, giving transfer rates higher than predicted. Observed rates tend to diminish with time due to building up of an interfacial barrier. This is associated with the rates of association of

the $(\text{UO}_2)^{++}$ and $(\text{NO}_3)^-$ ions to give $\{\text{UO}_2(\text{NO}_3)_2\}$ which then reacts with the extractant molecule, i.e. TBP. Thus the reaction appears to be at the interface.

The rate of supply of materials to the interface can often be a limiting factor in such equipment due to the effect of slow agitation coupled with a low interfacial area-volume ratio (giving long diffusion paths). Typically, the interfacial area in such cells is of the order of 30cm^2 and the volume of each phase is of the order of 300cm^3 . Keisch⁽²⁷⁾ developed a cell having both a much higher interface-volume ratio and high speed stirring. These modifications minimise the mass transfer resistance in the bulk phase, maintaining a uniform bulk concentration and greatly shortening the distance material must travel to reach the phase boundary. In this cell, because a tracer technique was used, the concentration of the reactants were kept constant during individual rate measurements and the system was otherwise at equilibrium. The rate law was found to be:

$$\text{rate} = k [\text{UO}_2^{++}]_{\text{Aq.}} [\text{NO}_3^-]_{\text{Aq.}}^{1.2} [\text{TBP}]_{\text{Org.}}^{1.8}$$

and interfacial mechanisms were proposed to fit this law.

It is of interest to note that whether the reaction is truly heterogeneous or not, the diffusion rates of the species in both phases are key parameters and measurement of self diffusion coefficients of the species becomes important. Only in the case of the extraction of uranium by TBP has this been attempted. Thus, Hahn⁽²⁸⁾ reports interesting results of diffusion measurements for uranium in aqueous uranyl nitrate and the (uranium - 2TBP) complex in TBP.

Constant interface cells have been used in other studies on metals extraction. Two workers^(29,30) have criticised the use of circumferential wall baffles in the Lewis cell where, because of the unknown contact angle of the phases at the baffles, the interfacial area cannot be measured accurately. McManamey⁽³¹⁾ has used an unbaffled cell to measure mass transfer of cobalt, copper and nickel nitrates from water into n-butanol and has shown that, like the uranium system, the mass transfer process is influenced by an interfacial resistance due to reaction at the water - n-butanol phase boundary, as well as diffusional resistances in each of the phases. Htaik⁽³²⁾ used the same type of cell to study the extraction of uranyl sulphate by naphthenic acid but here the reaction is controlled by a chemical reaction taking place in the main liquid phases near to the interface.

Roddy and co-workers⁽³³⁾ have used small stirred cells, with constant interface, to study the extraction of iron (III) by D2EHPA and suggest that the rate controlling reactions are at the interface.

Thus the constant interface cell has been widely used and both types of mass transfer control noted, i.e. reaction at the interface or in the bulk phase.

Further evidence for the bulk phase site of the reaction in many practical situations is that noted⁽²³⁾ for chelate systems where the extraction of zinc, cobalt and nickel as dithiozates; aluminium and indium as trifluoroacetates; and iron, cobalt and nickel as acetylacetonates show dependency on both the pH and the chelating agent concentration.

A wetted wall column⁽³⁴⁾ has been used for a study of the distribution of uranyl nitrate between water and the solvents dibutyl carbitol and methyl isobutylketone. It has the advantage that the hydrodynamics of the system can be defined. However, the method is limited for practical reasons since, for instance, low interfacial tension and large density difference between the phases can result in instability in the water phase film on the wall.

4. MODELS FOR MASS TRANSFER WITH CHEMICAL REACTION IN LIQUID-LIQUID SYSTEMS

4.1 Introduction

Theories of mass transfer with chemical reaction in heterogeneous systems have been reviewed by Danckwerts⁽³⁵⁾.

The two extreme cases of a chemical kinetically controlled process and one dependent only on mass transfer rate can be modelled quite easily. When both rate steps are important in determining the overall rate, the situation is more difficult. Firstly, it is necessary to know the locale of the reaction and its kinetics under homogeneous conditions. Then a knowledge is required of the factors governing mass transfer (interfacial area per unit volume, diffusivities, etc.).

If the two phases are completely immiscible or the reactants do not distribute at all between the two phases, then reaction can only take place at the interface. Interfacial reactions are quite common in heterogeneous systems where one of the phases is a solid but the necessary criteria are unlikely to be entirely met in liquid-liquid systems, although interfacial reactions have been considered for a metal extraction system⁽³²⁾. Nevertheless, as has already been seen, some systems may approximate sufficiently closely for their rates to be described adequately by a model which assumes all reaction to take place at the interface.

A more probable situation is of reaction taking place in a zone in the aqueous phase adjacent to the interface. This would picture a certain amount of extractant dissolving in the aqueous phase at the interface and then diffusing into the bulk phase, reacting on the way with the solute. The solute-extractant complex would then diffuse back into the solvent phase. This situation is more likely in the case of metals extraction than that of a reaction zone in the solvent as the latter would assume free cations transferring into an organic phase.

4.2 Reaction Zone in Aqueous Phase

As described in the previous section, the reaction could take place in a reaction zone within the aqueous phase (in agreement with Abramzon and Kogan's postulation⁽³⁶⁾ that a liquid-liquid reaction involving ionic and non-ionic reactants would proceed in the aqueous phase). This implies that the chemical reaction itself is fast. Sharma⁽³⁷⁾ showed that, in the case of a second order irreversible reaction, a very slow reaction could completely control the rate of the overall process and that the rate of transfer would be that predicted by the chemical rate equation. A slightly faster reaction rate will lead still to a reaction occurring uniformly throughout the aqueous phase, although the overall rate will be controlled by the mass transfer process across the interface. A fast reaction will be confined within a reaction zone adjacent to the interface.

Astarita⁽³⁸⁾ has developed a general model (based on the Whitman two-film model) for a fast, diffusion controlled reaction -

$$\bar{R} = \sqrt{2D_A \int_{[A]_b}^{[A]_i} r(A) d[A]} \quad (1)$$

where \bar{R} is the transfer rate per unit interfacial area

$[A]_b$ is the bulk concentration of A in the phase in which the reaction takes place

$[A]_i$ is the interfacial concentration of A in that phase

D_A is the diffusion coefficient of A through the phase

$r(A)$ is the rate of the reaction with respect to A

Solutions have been obtained for various cases of irreversible reaction^(14,38, 39,40). However, metals extraction processes must be reversible to permit extraction and stripping.

Consider an extraction process in which an extractant, HR, transfers into the aqueous phase where it reacts with a solute, M^{n+} , according to the reaction:



(This equation is typical of many commercial metals extraction systems.) k_1 and k_2 are the rate constants for the forward and reverse reactions.

For an elementary reaction, the rate equation will be:

$$r = k_1 [M^{n+}] [HR]^n - k_2 [MR_n] [H^+]^n \quad (3)$$

The complex, MR_n , then diffuses to the interface and transfers into the organic phase. The extractant and the complex will be in chemical equilibrium in the bulk of the aqueous phase and each will be in individual mass transfer equilibrium at the interface. The situation is illustrated in Fig.1. A relationship between $[HR]$ and $[MR_n]$ within the reaction zone can be obtained by recalling that the model is based on the two-film theory, and hence that the system is time-invariant. Thus the quantity of extractant entering the aqueous phase must be equivalent to the complex leaving, since there is no accumulation in the steady state. A balance on the extractant anion shows that for every mole of HR entering, then $1/n$ moles of MR_n must leave. A similar equivalence exists at every plane parallel to the interface within the reaction zone, i.e. the rate of transfer of the complex will be $1/n$ times the rate of transfer of the extractant and will be in the opposite direction.

$$\bar{R}_{MR_n} = -\frac{1}{n} \bar{R}_{HR} \quad (4)$$

The diffusion rates will be given by Fick's Law and substitution in equation(4) leads to:

$$-D_{MR_n} \frac{d}{dx} [MR_n] = \frac{D_{HR}}{n} \frac{d}{dx} [HR] \quad (5)$$

whence:

$$[MR_n] - [MR_n]_i = \frac{1}{n} \frac{D_{HR}}{D_{MR_n}} ([HR]_i - [HR]) \quad (6)$$

Since the solubilities in the aqueous phase of both the extractant and the complex are likely to be very low, then the solute and the hydrogen ions will be present in the reaction zone in great excess relative to the other reactants. Thus any change in their concentrations will be very small and the effective concentrations of solute and hydrogen ions throughout the zone may be considered constant and equal to their concentrations in the bulk of the liquid. (It is readily seen that this is true for the solute; since electrical

neutrality must be maintained then it must also hold for the hydrogen ions.)

The chemical rate equation for the reaction at a plane in the reaction zone parallel to the interface may now be written as:

$$r(\text{HR}) = k_1 [M^{n+}]_b [\text{HR}]^n - k_2 [H^+]_b^n [MR_n] \quad (7)$$

and from (4):

$$r(\text{HR}) = k_1 [M^{n+}]_b [\text{HR}]^n - k_2 [H^+]_b^n \left([MR_n]_i + \frac{\delta}{n} [\text{HR}]_i - \frac{\delta}{n} [\text{HR}] \right) \quad (8)$$

where $\delta = D_{\text{HR}}/D_{MR_n}$. (In many cases, the diffusivities of the extractant and the complex will be of the same order i.e. $\delta \rightarrow 1$).

Substitution in (1) yields (after integrating with respect to [HR]):

$$\bar{R}_{\text{HR}} = \sqrt{\frac{2D_{\text{HR}} \{ k_1 [M^{n+}]_b ([\text{HR}]_i^{n+1} - [\text{HR}]_b^{n+1}) - k_2 [H^+]_b^n \left(\frac{\delta}{n} [\text{HR}]_i^2 + [MR_n]_i [\text{HR}]_i \right) + k_2 [H^+]_b^n \left(\frac{\delta}{n} [\text{HR}]_i + [MR_n]_i \right) [\text{HR}]_b + \frac{k_2 \delta [H^+]_b^n ([\text{HR}]_i^2 - [\text{HR}]_b^2) \}}{n+1}} \quad (9)$$

In many cases, the bulk concentration of the extractant in the aqueous phase will be very small, and as $[\text{HR}]_b \rightarrow 0$, then $[\text{HR}]_i \gg [\text{HR}]_b$.

Equation (9) then reduces to:

$$\bar{R}_{\text{HR}} = \sqrt{\frac{2D_{\text{HR}} \{ k_1 [M^{n+}]_b [\text{HR}]_i^{n+1} - k_2 [H^+]_b^n ([MR_n]_i + \delta [\text{HR}]_i) [\text{HR}]_i \}}{n+1}} \quad (10)$$

This can be further simplified by assuming that the effect of the reverse reaction is negligible in the extraction stage. This is justifiable because the conditions are selected, as far as possible, to minimise this reverse reaction. We then obtain:

$$\bar{R}_{\text{HR}} = \sqrt{\frac{2D_{\text{HR}} k_1 [M^{n+}]_b [\text{HR}]_i^{n+1}}{n+1}} \quad (11)$$

Equation (11) is, in fact, the equation for a pseudo n -th order irreversible reaction derived by Danckwerts⁽⁴⁰⁾. It can be rewritten as:

$$\bar{R}_{\text{HR}} = [\text{HR}]_i^{\frac{n+1}{2}} \sqrt{\frac{2D_{\text{HR}} k_1 [M^{n+}]_b}{n+1}} \quad (12)$$

Since we have assumed that the extractant is in phase equilibrium at the interface, and also that all resistance to mass transfer lies in the aqueous phase, we can write $\frac{[\text{HR}]_{\text{org}}}{[\text{HR}]_i} = \phi_{\text{HR}}$, where $[\text{HR}]_{\text{org}}$ is the extractant concentration in the bulk organic phase and ϕ_{HR} is the partition coefficient for the extractant.

$$\text{Then } \bar{R}_{\text{HR}} = \left(\frac{[\text{HR}]_{\text{org}}}{\phi} \right)^{\frac{n+1}{2}} \sqrt{\frac{2D_{\text{HR}} k_1 [M^{n+}]_b}{n+1}} \quad (13)$$

and from equation (4):

$$\bar{R}_{MR_n} = \frac{-1}{n} \left(\frac{[\text{HR}]_{\text{org}}}{\phi} \right)^{\frac{n+1}{2}} \sqrt{\frac{2D_{\text{HR}} k_1 [M^{n+}]_b}{n+1}} \quad (14)$$

$$= -\left(\frac{[\text{HR}]_{\text{org}}}{\phi}\right)^{\frac{n+1}{2}} \sqrt{\frac{2}{n^2(n+1)} D_{\text{HR}} k_1 [\text{M}^{n+}]_b} \quad (15)$$

The rate of extraction will still be a function of $[\text{HR}]_{\text{org}}$ even for those cases where the reverse reaction cannot be ignored. ϕ_{HR}

A corresponding expression can be obtained for the stripping process. Here we are concerned with the rate of transfer of the complex, MR_n , back into the aqueous phase and its subsequent reaction:



For a simple reaction, the chemical rate equation will be:

$$r(\text{MR}_n) = k_2 [\text{MR}_n] [\text{H}^+]^n - k_1 [\text{M}^{n+}] [\text{HR}]^n \quad (16)$$

By equation (6) and the assumption that solute and hydrogen ion concentrations again remain constant:

$$r(\text{MR}_n) = k_2 [\text{MR}_n] [\text{H}^+]_b^n - k_1 [\text{M}^{n+}]_b \left([\text{HR}]_i + \frac{n}{\delta} [\text{MR}_n]_i - \frac{n}{\delta} [\text{MR}_n] \right)^n \quad (17)$$

Equation (1) now becomes:

$$\bar{R}_{\text{MR}_n} = \sqrt{2D_{\text{MR}_n}} \int_{[\text{MR}_n]_b}^{[\text{MR}_n]_i} r(\text{MR}_n) d[\text{MR}_n] \quad (18)$$

Substituting for $r(\text{MR}_n)$ and integrating, leads to:

$$\bar{R}_{\text{MR}_n} = \sqrt{2D_{\text{MR}_n}} \left\{ k_2 \frac{[\text{H}^+]_b^n}{2} ([\text{MR}_n]_i^2 - [\text{MR}_n]_b^2) + \frac{\delta}{n(n+1)} k_1 [\text{M}^{n+}]_b [\text{HR}]_i^{n+1} - \frac{\delta}{n(n+1)} k_1 [\text{M}^{n+}]_b \left([\text{HR}]_i + \frac{n}{\delta} [\text{MR}_n]_i - \frac{n}{\delta} [\text{MR}_n]_b \right)^{n+1} \right\} \quad (19)$$

and for negligible bulk phase concentration of MR_n and negligible back reaction, this reduces to:

$$\bar{R}_{\text{MR}_n} = \sqrt{D_{\text{MR}_n} k_2 [\text{H}^+]_b^n [\text{MR}_n]_i^2} \quad (20)$$

$$= \frac{[\text{MR}_n]_{\text{org}}}{\phi_{\text{MR}_n}} \sqrt{D_{\text{MR}_n} k_2 [\text{H}^+]_b^n} \quad (21)$$

Equation (20) is again in agreement with Danckwerts' equation for an irreversible reaction⁽⁴⁰⁾.

4.3 Discussion of models

For the reasons discussed in section 4.1, it is felt that true interfacial reactions will be relatively uncommon in liquid-liquid systems, although sufficient evidence has been presented to show that their occurrence cannot be completely ignored.

An examination of equation (15), which predicts the rate of extraction, assuming reaction takes place in the aqueous phase in a zone adjacent to the interface, reveals that the partition coefficient of the extractant is an important parameter. The greater the solubility of the extractant in the

aqueous phase, the greater should be the rate of extraction, if this model holds good. It must be emphasised that the model is not presented as being the most likely but as a hypothesis still to be tested rigorously. Nevertheless, it is interesting to note that both KELEX 100 and LIX 70 which have greater solubilities in the aqueous phase than LIX 65N, also extract copper at an appreciably greater rate. The forward rate constants, k_1 , for the respective homogeneous reactions are probably high and of the same order, since chelations are known to be fast reactions; and hence it is difficult to explain the difference in extraction rates by a chemical mechanism. On the other hand, the rate of the strip process is governed, according to equation (21), by the partition coefficients of the complexes. If these are more nearly equal, this presents a possible explanation for the fact that the three extractants strip at comparable rates.

If we substitute values of n into the equations we can predict the apparent orders of the rate process,

e.g. $n = 1$ (monovalent solute):

$$\bar{R}_{MR} = - \left(\frac{[HR]_{org}}{\phi_{HR}} \right) \sqrt{D_{HR} k_1 [M^+]} \quad \text{for extraction}$$

$$n = 2 \quad \bar{R}_{MR_2} = - \left(\frac{[HR]_{org}}{\phi_{HR_2}} \right)^{3/2} \sqrt{\frac{1}{6} D_{HR} k_1 [M^{2+}]} \quad \text{for extraction}$$

$$\text{and} \quad \frac{[MR_2]_{org} [H^+]}{\phi_{MR_2}} \sqrt{D_{MR_2} k_2} \quad \text{for stripping}$$

It will be seen that this model, based on mass transfer with a simultaneous fast chemical reaction, predicts overall rates which appear of fractional order even though the actual chemical reactions are simple. Hence the explanation of some fractional overall orders which have been reported may lie in the existence of a mass transfer resistance rather than in a complex reaction mechanism.

The equations are considerably simplified if the reaction is not reversible, as in the case of some important unit processes such as aromatic nitration. For the nitration of toluene, assuming a second order irreversible reaction in the aqueous phase with nitric acid concentration uniform to the interface, the model simplifies to:

$$\bar{R} = \frac{[Tol]_{org}}{\phi_{Tol}} \sqrt{Dk [HNO_3]_{aq}}$$

This model, proposed by Giles (39), has been verified by Ismail (14) under conditions where (a) the sulphuric acid concentration in the aqueous phase is sufficiently high to give a fast reaction, and (b) the diffusion process is by molecular diffusion only. For a turbulent system, D would be the sum of molecular and eddy diffusion coefficients, with the latter dominating. Uncertainty as to the eddy diffusion component will always make the use of these models difficult for quantitative predictions of transfer rates under normal industrial conditions. As noted previously, Strachan (9-11) and Sohrabi (12) have shown a transition for the rates of toluene nitration from the above model to one assuming uniform reaction throughout the aqueous phase as sulphuric acid concentration has been reduced, thus reducing the kinetic rate constant.

If a model of the type developed can be shown to hold, then if the rate constants, partition coefficients and concentrations are known, measurement of overall rate of extraction could be used to determine the diffusion coefficient.

REFERENCES

1. Anwar M.M., Hanson C. and Pratt M.W.T.: Proceedings International Solvent Extraction Conference, The Hague (Society of Chemical Industry), 911 (1971)
2. Baniel A. and Blumberg R.: Chim.Ind., 4,27(1957)
3. Nernst W.Z.: Phys.Chem., 47,55(1904)
4. Treub J.P.: J.Chim.Phys., 16,107(1918)
5. Viellard A.: Chem.Eng.Sci., 14,183(1961)
6. Hanson C., Marsland J.G. and Wilson G.: Chemy.Ind., 675(1966)
7. Hanson C., Marsland J.G. and Wilson G.: Chem.Eng.Sci., 26,1513(1971)
8. Hanson C., Marsland J.G. and Naz M.A.: Chem.Eng.Sci.(publication pending)
9. Cox P.R. and Strachan A.N.; Chem.Eng.Sci., 26, 1013(1971)
10. Cox P.R. and Strachan A.N.: Chem.Eng.Sci., 27, 457(1972)
11. Cox P.R. and Strachan A.N.: Chem.Eng.J., 4,253(1972)
12. Sohrabi M.: PhD Thesis, University of Bradford (1972)
13. Hanson C.: Chapter 12 in "Recent Advances in Liquid-Liquid Extraction", Ed. Hanson C., Pergamon Press (1971)
14. Ismail H.A.M.: PhD Thesis, University of Bradford (1973)
15. Jeffreys G.V., Jenson V.G. and Miles F.R.: Trans.Instn.Chem.Engrs., 39,389(1961)
16. Jenson V.G., Jeffreys G.V. and Edwards R.E.: Proc.36th Internat. Congr. Ind.Chem., Brussels. T32.Vol 3 (1967)
17. Albright L.F.: Chem.Engng.,Albany, 73(14)119(1966)
18. Chaudhry M.S.K.: MSc Thesis, University of Bradford (1970)
19. Ryon A.D., Johnsson K.O.: ORNL - 2213 (1956)
20. Hixon A.W., Smith M.I.: Ind.Eng.Chem., 41,973(1948)
21. Baumgärtner F., Finsterwalder L.: J.Phys.Chem., 74(1),108(1970)
22. Reinhardt H., Rydberg J.: Acta.Chem.Scand., 8,23(1969)
23. Flett D.S., Okuhura D.N., Spink D.R.: J.Inorg.Nucl.Chem.,35,2471(1973)
24. Lewis J.B.: Chem.Eng.Sci., 3,248(1954)
25. Lewis J.B.: Chem.Eng.Sci., 3,260(1954)

26. Lewis J.B.: Chem.Eng.Sci., 8,295(1958)
27. Keisch B., IDO - 14490
28. Hahn H.T., HW - 31803(1954)
29. Davis J.T., Mayers G.R.A.: Chem.Eng.Sci., 16,55(1961)
30. McManamey W.J.: PhD Thesis, University of Sydney (1959)
31. McManamey W.J.: Chem.Eng.Sci., 15,210(1961)
32. Htaik T.: PhD Thesis, University of Sydney (1965)
33. Roddy J.W. and Colman C.F.: Solvent Extraction Reviews, 1,63(1971)
34. Murdoch R., Pratt H.R.C.: Trans.Inst.Chem.Engrs., 31,307(1955)
35. Danckwerts P.V.: "Gas-Liquid reactions", McGraw Hill (1970)
36. Abramzon A.A. and Kogan N.A.: J.Appl.Chem.(USSR), 36,1949(1963)
37. Sharma M.M. and Nanda A.K.: Trans.Inst.Chem.Eng., 46,44(1968)
38. Astarita G.: "Mass Transfer with Chemical Reaction", Elsevier (1967)
39. Giles J.W.: PhD Thesis, University of Bradford (1970)
40. Sharma M.M. and Danckwerts P.V.: Brit.Chem.Eng., 15,522(1970)

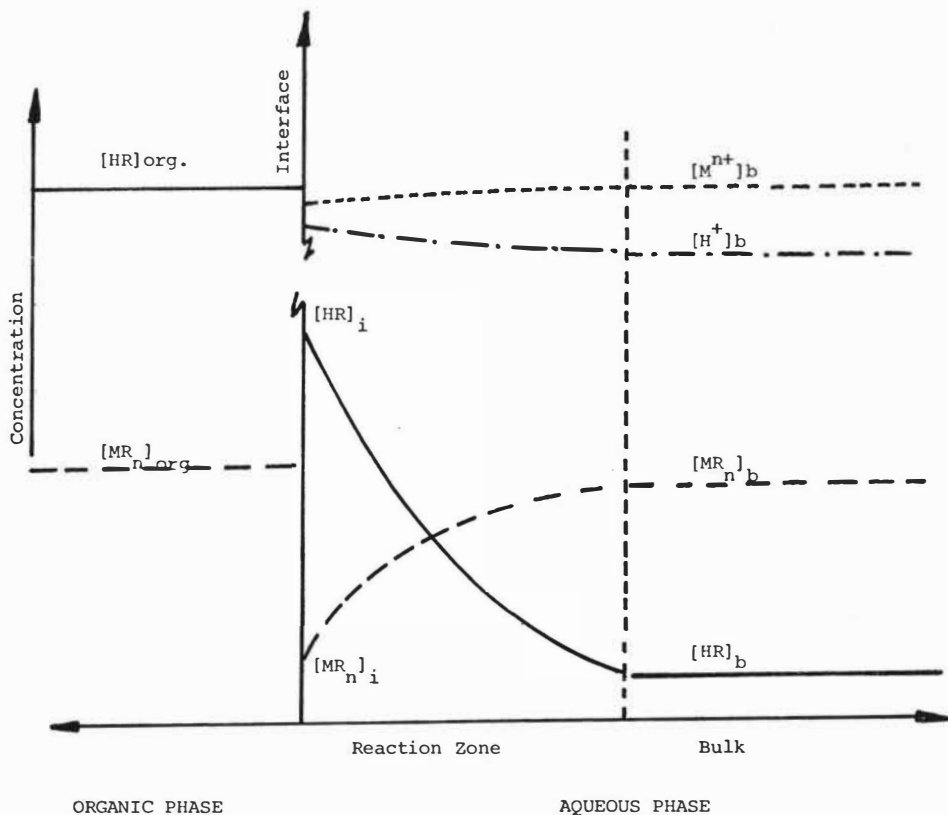


Fig. 1 Concentration Profiles for Extraction Process with a Reaction Zone in the Aqueous Phase.

(NB Concentrations of solute and hydrogen ion are drawn on a smaller scale than extractant and complex.)

THE INFLUENCE OF CHEMICAL REACTION (NITRATION) ON THE RATE OF
SURFACE RENEWAL AT A LIQUID-LIQUID INTERFACE

P.R. Cox and A.N. Strachan

Department of Chemistry, Loughborough University of Technology,
Loughborough, Leicestershire, England.

Abstract The two phase nitration of chlorobenzene has been studied under mass transfer control conditions in a stirred reactor and a stirred cell. In both cases the fast reaction diffusional regime is observed, in which the reaction rate influences the concentration gradient of chlorobenzene in the acid phase at the interface, and hence the rate at which chlorobenzene is transferred into the acid phase and nitrated. Danckwerts plots yield values for the overall mass transfer coefficient of 2.10×10^{-3} and 2.29×10^{-3} cm/sec for the stirred reactor and stirred cell respectively.

With the stirred reactor, as the reaction rate constant decreases, the transition to the slow reaction diffusional regime and then to the kinetic regime is observed. However with the stirred cell, the expected levelling off of the mass transfer rate with decreasing reaction rate, corresponding to the onset of the slow reaction diffusional regime, does not occur. Instead the mass transfer rate falls continuously. In the absence of chemical reaction, the overall mass transfer coefficient is found to have the value 1.73×10^{-4} cm/sec. The conclusion is drawn that, with the stirred cell, chemical reaction promotes good surface renewal which the agitation alone is insufficient to maintain.

INTRODUCTION

During the early stages of two phase aromatic nitration, chemical reaction occurs almost exclusively in the aqueous acid phase¹. The sequence of events is therefore

- (i) transfer of the aromatic from the organic to the acid phase,
- (ii) reaction of the aromatic in the acid phase,
- (iii) transfer of the nitroproducts from the acid to the organic phase.

The rate will be mass transfer or kinetically controlled depending upon whether (i) or (ii) is the rate controlling step. This in turn depends² upon the relative magnitudes of $a'k$ and $k_2[\text{HNO}_3]$, where a' is the interfacial area per unit volume of the acid phase, k is the overall mass transfer coefficient, k_2 is the second order nitration rate constant, and $[\text{HNO}_3]$ is the concentration of nitric acid in the acid phase.

The value of $a'k$ for a mechanically agitated liquid-liquid contactor is likely to lie in the range $3 \times 10^{-2} - 0.4 \text{ sec}^{-1}$ (ref. 3). With chlorobenzene in 70.2% H_2SO_4 , $k_2 = 1.75 \times 10^{-2} \text{ l/mol sec}$ (ref. 1), so that when $[\text{HNO}_3] = 3.2 \times 10^{-2} \text{ mol/l}$, $k_2[\text{HNO}_3] = 5.6 \times 10^{-4} \text{ sec}^{-1}$. In such circumstances $k_2[\text{HNO}_3]$ should be considerably smaller than $a'k$ and step (ii) should be rate controlling. That the rate is kinetically controlled under these conditions is verified experimentally.¹

However the value of k_2 for chlorobenzene increases by a factor of 2.49 for each 1% increase in the sulphuric acid strength⁴, so that at higher sulphuric acid strengths and higher nitric acid concentrations, $k_2[\text{HNO}_3]$ should become greater than $a'k$ and step (i) should then become rate controlling.

It was with the object of verifying this prediction and observing the nitration of chlorobenzene under mass transfer control conditions that the present investigation was undertaken. Some experiments were carried out with a stirred cell since this should have a smaller value of $a'k$ than a stirred reactor, thus favouring mass transfer control. A further advantage is that a' in a stirred cell is fixed and known.

EXPERIMENTAL

Materials Laboratory Reagent grade chlorobenzene was twice distilled, the centre cut being retained each time. The final fraction used in the experiments had a b.p. of 132-132.5°C (lit.⁵, 132.0°C). The sulphuric and nitric acids were of high purity (British Drug Houses AnalaR grade). The o-, m- and p-nitrochlorobenzenes were of B.D.H. Laboratory Reagent grade and the hexane of Spectroscopic grade. Aqueous sulphuric acid was prepared by the addition of concentrated acid to distilled water, the composition being checked by density and volumetric methods. The mixed acid was prepared by adding 12.5 ml of aqueous nitric acid ($d = 1.42 \text{ g/cm}^3$) to 350 ml of aqueous sulphuric acid to produce a solution 0.56 M in nitric acid. The addition was performed at 5°C to prevent the formation of nitrosyl sulphuric acid. With the stirred reactor the whole of this mixed acid (362.5 ml) was stirred

with 20 ml of chlorobenzene, resulting in a molar ratio of pure nitric acid to chlorobenzene of 1.03 : 1 and a volume fraction of dispersed phase of 0.052. With the stirred cell 170 ml of the mixed acid were stirred with 20 ml of chlorobenzene resulting in a molar ratio of pure nitric acid to chlorobenzene of 0.48 : 1.

Procedure The stirred reactor, stirred cell and procedure were the same as employed previously with toluene^{6,7} except that 25 μ l, instead of 20 μ l, samples of the organic phase were taken and diluted with hexane, to 25 ml with the stirred reactor, and to 10 ml with the stirred cell. In both cases the absorbances were measured at 340 nm instead of 350 nm, the wavelength used with toluene. All runs were carried out at 25°C and at constant stirring speed. This was 2500 rev/min for the stirred reactor and 65 rev/min for the stirred cell.

The value of k for the stirred cell in the absence of chemical reaction was determined by contacting 20 ml of chlorobenzene with 170 ml of 70.4% H₂SO₄ at 25°C and constant stirring speed. Periodically a 5 ml sample was withdrawn from the acid phase, its absorbance A was quickly measured at 265 nm, and the sample was then returned to the stirred cell. This return of the sample ensured that no significant change in either the volume of the acid phase or the level of the interface occurred during the run. A plot of $\ln(A_{\infty} - A)$ versus time was constructed, A_∞ being the absorbance at infinite time. This was linear. The slope was measured and equated with a 'k'. Hence knowing a', k was obtained.

Conversion factors So that absorbance measurements in the nitration runs could be converted into percentage reaction and moles of chlorobenzene nitrated, a mixture was made of nitrochlorobenzenes in the ratio in which they are formed in the nitration (35% ortho, 1% meta and 66% para). A series of solutions of this mixture and chlorobenzene in varying proportions was prepared. Each solution was then diluted with hexane and its absorbance measured in exactly the same way as during a stirred reactor run.

The absorbance was found to increase linearly with mole percentage nitrochlorobenzene (i.e. percentage reaction) up to the 20% mark at a rate of 0.0205 for each 1% increase. Since 20 ml (0.196 mol) of chlorobenzene were present at the start of each run, an absorbance of 0.0205 in a stirred reactor run corresponded to 0.00196 mol of chlorobenzene nitrated. Hence initial rates in absorbance per minute were converted into moles of

chlorobenzene nitrated per litre of the acid phase per second by multiplying by a factor of $(0.00196/0.0205) \times (1000/362.5)/60 = 4.40 \times 10^{-3}$ in the case of the stirred reactor and by a factor of $4.40 \times 10^{-3} \times (362.5/170) \times (10/25) = 3.75 \times 10^{-3}$ in the case of the stirred cell.

RESULTS

At the start of all nitrations the absorbance was found to increase linearly with time. With the stirred cell runs this linearity extended over the first 5% of the reaction, the range to which measurements were confined. With the stirred reactor runs it extended over the first 30% of the reaction. Hence in both cases initial reaction rates were readily measured.

Values of the initial nitration rate, R , for both stirred reactor and stirred cell at different strengths of sulphuric acid are listed in Table 1. In the first column of the table is the strength of sulphuric acid before the addition of the aqueous nitric acid. The second column lists the strength corrected for the water added with the nitric acid (i.e. the strength of sulphuric acid containing pure nitric acid).

Also listed in Table 1 are the solubilities of chlorobenzene, $[C]_a^S$, and values of the second order nitration rate constant, k_2 , corresponding to the different strengths of sulphuric acid employed, together with the diffusivities of chlorobenzene, D , in the more concentrated acid solutions. The solubilities were obtained by interpolation of the data of Deno and Perizzolo⁸ after absorbances had been converted into solubilities using the recently determined value for the solubility of chlorobenzene in 70.2% sulphuric acid¹. The k_2 values were interpolated from the data of Schofield and co-workers⁴ via a $\log_{10}k_2$ versus % H_2SO_4 plot which is linear. The diffusivities were calculated from a modified Wilke-Chang equation⁹ by the method adopted previously to calculate the diffusivities of toluene in mixed acid.⁶

Plots of $R/[C]_a^S$ versus % H_2SO_4 (or $\log_{10}k_2$) for both stirred reactor and stirred cell are shown in Fig. 1.

DISCUSSION

STIRRED REACTOR Three regimes, similar to those observed with toluene⁶, are discernible in the plot of the stirred reactor data shown in Fig. 1. At the highest acid strengths is the fast reaction regime, where the k_2 values are large enough for the reaction rate to influence the concentration

Table 1. Initial reaction rate R at 25°C and constant stirring speed as a function of sulphuric acid strength, with $[\text{HNO}_3] = 0.56 \text{ mol l}^{-1}$

% H ₂ SO ₄ as prepared	% H ₂ SO ₄ corrected	$R \times 10^6$ /mol l ⁻¹ sec ⁻¹	$[\text{C}]_a^S \times 10^3$ /mol l ⁻¹	k_2 /l mol ⁻¹ sec ⁻¹	$D \times 10^7$ /cm ² sec ⁻¹
Stirred Reactor (2500 rev/min)					
80.90	80.20	436	2.82	1.68×10^2	7.5
80.50	79.85	371	2.79	1.19×10^2	7.7
80.05	79.40	314	2.75	7.94×10	7.9
79.80	79.15	266	2.73	6.30×10	8.0
79.30	78.65	218	2.69	4.08×10	8.2
78.65	78.00	174	2.63	2.24×10	8.6
78.10	77.45	146	2.59	1.38×10	8.8
77.60	76.95	115	2.55	8.71	9.1
77.00	76.35	110	2.50	5.01	9.4
76.50	75.85	102	2.47	3.24	9.7
76.10	75.45	98.9	2.44	2.24	9.9
75.40	74.80	86.6	2.39	1.23	
75.20	74.60	87.9	2.38	1.02	
74.80	74.20	84.0	2.35	7.24×10^{-1}	
73.90	73.30	65.5	2.30	3.16×10^{-1}	
72.20	71.60	45.0	2.18	6.76×10^{-2}	
70.20	69.60	16.9	2.06	1.10×10^{-2}	
Stirred Cell (65 rev/min)					
81.0	80.30	5.51	2.84	1.78×10^2	7.5
80.5	79.85	4.44	2.79	1.19×10^2	7.7
80.0	79.35	3.60	2.74	7.24×10	8.0
79.1	78.45	2.57	2.67	3.35×10	8.3
78.4	77.75	1.84	2.61	1.78×10	8.7
77.0	76.35	0.900	2.50	5.01	
75.0	74.40	0.319	2.36	8.51×10^{-1}	

gradient of chlorobenzene in the acid phase at the interface, and hence the rate at which chlorobenzene is transferred into the acid phase and nitrated. As the acid strength is lowered and the value of k_2 falls, transition occurs to the slow reaction diffusional regime where the rate of mass transfer becomes independent of the value of k_2 and a plateau is reached in the plot of $R/[C]_a^S$ versus % H_2SO_4 . At still lower acid strengths the nitration rate becomes so slow that transition from mass transfer to kinetic control occurs and the kinetic regime is entered.

Transition from fast to slow reaction Over the transition from fast to slow reaction, the initial rate, according to Danckwerts' surface renewal theory¹⁰, should be given by

$$R = a' \sqrt{k^2 + Dk_2[HNO_3]} [C]_a^S \quad (1)$$

$$\text{Hence } (R/[C]_a^S)^2 = (a'k)^2 + a'^2 Dk_2[HNO_3] \quad (2)$$

A Danckwerts plot of $(R/[C]_a^S)^2$ versus $k_2[HNO_3]$ is shown in Fig. 2. The slope and intercept of the least-squares line through the points yield values of $2.43 \times 10^{-4} \text{ sec}^{-1}$ and 0.036 sec^{-1} for a'^2D and $a'k$ respectively. Over the range of sulphuric acid strengths (80.2-77.45%) covered by the points in the plot, D varies from 7.5 to $8.8 \times 10^{-7} \text{ cm}^2/\text{sec}$. Taking a mean value for D of $8.1 \times 10^{-7} \text{ cm}^2/\text{sec}$, values of $17.3 \text{ cm}^2/\text{cm}^3$ and $2.10 \times 10^{-3} \text{ cm}/\text{sec}$ are obtained for a' and k respectively. These are of the same order of magnitude as those obtained with a dilute solution of toluene in 2,2,4-trimethylpentane⁷ and contrast with the anomalous values obtained with pure toluene.⁶ The complication of the ionization of the nitric acid becoming the rate limiting kinetic step, which is the probable explanation of the pure toluene results⁷, does not arise with chlorobenzene owing to the fact that the latter is considerably less reactive towards nitronium ions than is toluene.

Transition from mass transfer to kinetic control Over the transition from mass transfer to kinetic control

$$R = a'k ([C]_a^S - [C]_a) = k_2[HNO_3][C]_a \quad (3)$$

where $[C]_a$ is the steady state concentration of chlorobenzene in the acid phase. Elimination of $[C]_a$ leads to

$$R = k_2[\text{HNO}_3] a'k[C]_a / (k_2[\text{HNO}_3] + a'k) \quad (4)$$

$$\text{Hence } 1/a'k = [C]_a^S/R - 1/k_2[\text{HNO}_3] \quad (5)$$

Values of $[C]_a^S/R$ and $1/k_2[\text{HNO}_3]$ and of the difference between them, $1/a'k$, for the five runs in the transition region are listed in Table 2. It will be seen that $1/a'k$ remains constant within experimental error. The average value of 25.6 sec leads to a value of 0.039 sec^{-1} for $a'k$ in reasonable agreement with the value of 0.036 sec^{-1} obtained from the Danckwerts plot.

Table 2. Values of various quantities over the transition from mass transfer to kinetic control

% H ₂ SO ₄ corrected	$[C]_a^S/R$ /sec	$1/k_2[\text{HNO}_3]$ /sec	$1/a'k$ /sec
74.8	27.6	1.6	26.0
74.6	27.1	1.8	25.3
74.2	28.0	2.5	25.5
73.3	35.1	5.7	29.4
71.6	48.4	26.4	22.0

STIRRED CELL

Fast reaction regime It will be seen from the plot of the stirred cell data in Fig. 1 that, at the highest acid strengths corresponding to the fast reaction regime, the rates with the stirred cell follow a similar trend to those with the stirred reactor. A Danckwerts plot of the data in this region is shown in Fig. 2. The slope and intercept of the least-squares line through the points yield values of $3.55 \times 10^{-8} \text{ sec}^{-1}$ and $4.63 \times 10^{-4} \text{ sec}^{-1}$ for a'^2D and $a'k$ respectively. The dimensions of the cell and the volume of the acid phase give a' the value $0.202 \text{ cm}^2/\text{cm}^3$. Hence D must have the value $8.7 \times 10^{-7} \text{ cm}^2/\text{sec}$, in very good agreement with the calculated values of D (Table 1) which range from 7.5 to $8.7 \times 10^{-7} \text{ cm}^2/\text{sec}$ over the range of sulphuric acid strengths (80.3-77.75%) covered by the points in the Danckwerts plot. Similarly the known value of a' means that k must have the value $2.29 \times 10^{-3} \text{ cm}^2/\text{sec}$ which agrees well with the value of $2.10 \times 10^{-3} \text{ cm}^2/\text{sec}$ obtained with the stirred reactor.

Slow reaction diffusional regime Transition from fast to slow reaction occurs when $k_2[\text{HNO}_3]$ becomes less than k^2/D . The Danckwerts plots indicate that k^2/D does not change significantly between stirred reactor and stirred cell. Since the same concentration of nitric acid was used in both systems and k_2 depends solely on the sulphuric acid strength, the transition to the slow reaction diffusional regime would be expected to occur with the stirred cell at about the same strength of sulphuric acid ($\sim 76\%$) as it does with the stirred reactor. The transition should lead to $R/[C]_a^S$ becoming constant and equal to $a'k$, which from the Danckwerts plot has the value $4.63 \times 10^{-4} \text{ sec}^{-1}$.

Furthermore this plateau in $R/[C]_a^S$ corresponding to the slow reaction diffusional regime would be expected to extend much further than with the stirred reactor since transition to the kinetic regime will not occur until $k_2[\text{HNO}_3]$ becomes less than $a'k$. Since $a'k$ for the stirred cell is some 80 times smaller than for the stirred reactor, transition to the kinetic regime is not expected until sulphuric acid strengths below the 70% mark are reached.

The broken curve in Fig. 1 shows the stirred cell behaviour which might have been expected on the basis of the data obtained from the Danckwerts plot. Figure 1 also shows quite clearly that this behaviour is not in fact followed. The value of $R/[C]_a^S$ falls continuously as the sulphuric acid strength is lowered, and no plateau is ever reached.

Since a' is fixed, the only possible explanation for this phenomenon is that the value of k falls as the rate of chemical reaction decreases. To provide confirmation of this explanation, the value of k was measured in the absence of chemical reaction and found to be $1.73 \times 10^{-4} \text{ cm/sec}$ i.e. more than 10 times lower than the value of $2.29 \times 10^{-3} \text{ cm/sec}$ obtained from the Danckwerts plot. An exactly similar behaviour is observed with toluene¹¹.

It is clear that with the stirred cell, chemical reaction promotes good surface renewal which the agitation alone ($Re \approx 500$) is insufficient to maintain. As the reaction rate falls the interface becomes increasingly stagnant and the value of k decreases.

Hence care should be exercised when values of k or $a'k$ determined by the fast chemical reaction method^{12,13} are used in the design of solvent extractors.

Acknowledgement We are grateful to Hickson and Welch Ltd., Castleford for a Research Scholarship (for P.R.C.) and for help and interest in this work. We are also indebted to Mr. J.W. Chapman who carried out the determination of k for the stirred cell in the absence of chemical reaction.

NOTATION

A	absorbance
A_{∞}	absorbance at infinite time
a^i	interfacial area per unit volume of the acid phase, cm^{-1}
$[C]_a$	steady state concentration of chlorobenzene in the acid phase, mol/l
$[C]_a^s$	saturation concentration of chlorobenzene in the acid phase, mol/l
D	diffusivity of chlorobenzene in the acid phase, cm^2/sec
d	density, g/cm^3
$[\text{HNO}_3]$	concentration of nitric acid in the acid phase, mol/l
k	overall mass transfer coefficient, cm/sec
k_2	second order nitration rate constant, $\text{l}/\text{mol sec}$
L	length (tip-to-tip) of stirrer blade, m
N	stirring speed, rev/sec
R	initial reaction rate, $\text{mol}/\text{l sec}$
Re	Reynolds number ($= L^2N/\nu$)
ν	kinematic viscosity, m^2/sec

REFERENCES

1. Cox P.R. and Strachan A.N., Chem. Engng Sci., 1971, 26, 1013.
2. Cox P.R. and Strachan A.N., Chem. Engng Sci., 1972, 27, 457.
3. Sharma M.M. and Danckwerts P.V., Br. chem. Engng, 1970, 15, 522.
4. Coombes R.G., Crout D.H.G., Hoggett J.G., Moodie R.B. and Schofield K., J. chem Soc. (B), 1970, 347.
5. Handbook of Chemistry and Physics, 1973, 54th Ed., (Cleveland, Ohio, Chemical Rubber Co. Press).
6. Cox P.R. and Strachan A.N., Chem. Engng J., 1972, 4, 253.
7. Chapman J.W., Cox P.R. and Strachan A.N., Chem. Engng Sci., In Press.
8. Deno N.C. and Perizzolo C., J. Am. chem. Soc., 1957, 79, 1345.

9. Perkins L.R. and Geankopolis C.J., Chem. Engng Sci., 1969, 24, 1035.
10. Danckwerts P.V., Trans. Faraday Soc., 1950, 46, 300.
11. Chapman J.W., Cox P.R. and Strachan A.N., Unpublished Results.
12. Nanda A.K. and Sharma M.M., Chem. Engng Sci., 1966, 21, 707.
13. Sankholker D.S. and Sharma M.M., Chem. Engng Sci., 1973, 28, 2089.

Fig. 1. Values of the initial reaction rate R divided by the saturation concentration of chlorobenzene in the acid phase $[C]_a^s$ at 25°C , for both stirred reactor and stirred cell, as a function of sulphuric acid strength.

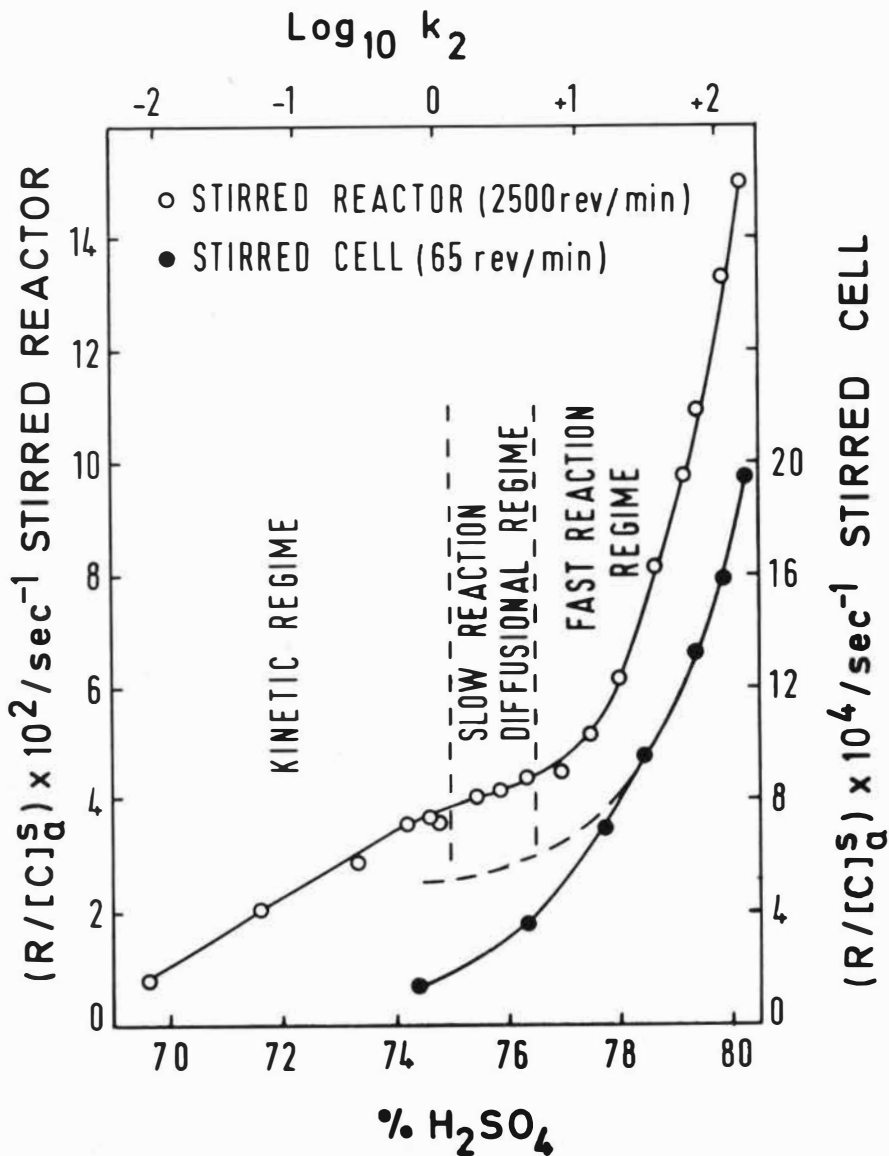
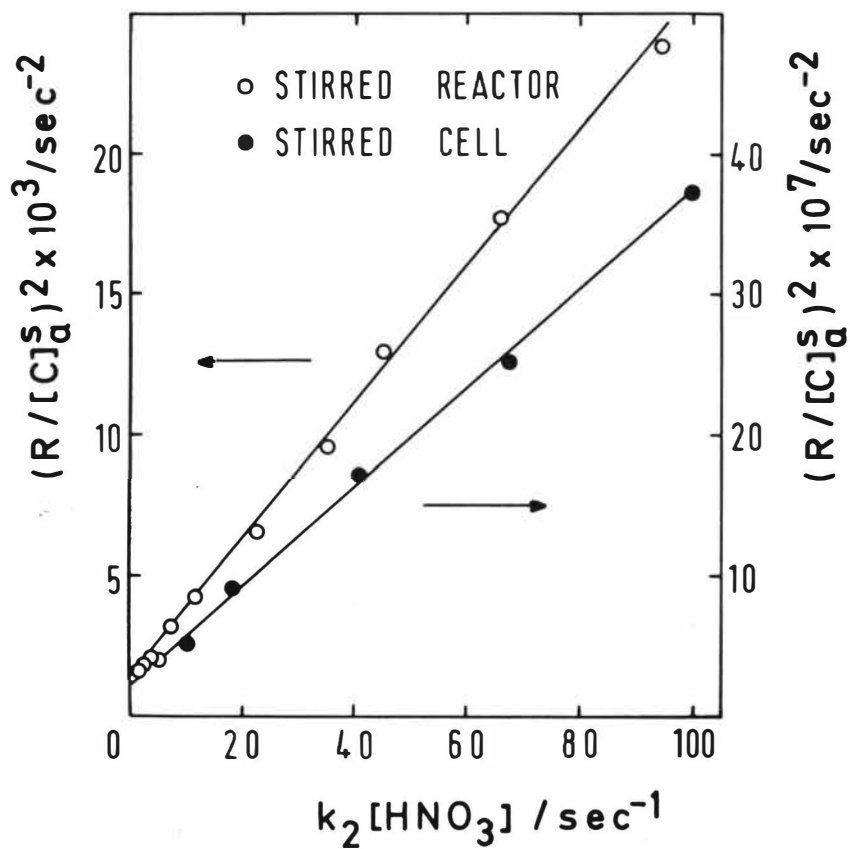


Fig. 2. Danckwerts plots of $(R/[C]_a^S)^2$ versus $k_2[\text{HNO}_3]$ for stirred reactor and stirred cell.



Transfer of Metal Nitrates
between Aqueous Nitrate Media and Neutral Organo-
phosphorus Extractants

L. Farbu*, H.A.C. McKay, A.G. Wain,
Atomic Energy Research Establishment, Harwell, U.K.

Abstract

The rate of transfer of uranyl nitrate between an aqueous continuum and rising droplets of tri-n-butyl phosphate (TBP) or tri-n-octyl phosphine oxide (TOPO) in Odourless Kerosene (OK), has been determined. Results have also been obtained for yttrium nitrate and TOPO/OK. All solutes were at low concentrations.

All the transfer rates measured were found to be of first order in the metal concentrations. In the uranyl nitrate/TBP case, the continuum \rightarrow drops rate constant (k') varied as $[TBP]^2$, while the drops \rightarrow continuum rate constant (k) was independent of $[TBP]$. The rate-determining step therefore involves formation or break-up of $UO_2(NO_3)_2 \cdot 2TBP$. In the uranyl nitrate/TOPO case there is a more complicated state of affairs, with k' varying relatively slowly with $[TOPO]$, and k also depending on $[TOPO]$; it is suggested that the transfer is diffusion-controlled. In the yttrium nitrate/TOPO case the few results obtained suggest an intermediate state of affairs.

INTRODUCTION

The purpose of this investigation was to study mass transfer between an aqueous and an organic phase under constant hydrodynamic conditions. By eliminating hydrodynamic variability it was hoped to obtain a better insight into the transfer process itself.

To this end systems consisting mainly of water and an organic solvent (diluent) were used, all solute concentrations being kept as low as practicable, so as not to modify the viscosities, interfacial tension etc. more than could be helped. The transferring species itself was at an essentially trace concentration, and all other species were at equilibrium between the phases; material flow between the phases was therefore minimal and unlikely to affect the configurations of the phases.

The systems selected consisted of an aqueous nitrate medium and either tri-n-butyl phosphate (TBP) or tri-n-octyl phosphine oxide (TOPO) in Odourless Kerosene (OK), with uranyl nitrate and, in a few experiments, yttrium nitrate, as the transferring species. The metal concentration was always low in comparison with the extractant concentration; in the transfer experiments, a maximum of 3% of the extractant was complexed with metal, and in most cases <1%.

The $UO_2(NO_3)_2/HNO_3/TBP/diluent$ system has already been studied by several authors [1-7]. TOPO was the initial choice in the present work because it is a very powerful extractant and can therefore be used at very low concentrations in the diluent, but in view of the unexpected results obtained, TBP was later included for comparison.

The rising-drop technique was employed essentially as described in [1,7] and elsewhere. Droplets of organic phase emerge from a jet, travel upwards through a column of aqueous phase and are collected in a capillary at the top of the column. Either phase may be loaded with metal (uranium or yttrium),

* Present address, Department of Chemistry, University of Oslo, Oslo 3, Norway.

the other phase being barren initially, so that metal transfer can be observed in either direction. The aim is to determine the transfer to or from a freely and steadily rising drop, so effects occurring in the early stages of a drop's career (end-effects) must be eliminated. This can be done straightforwardly by varying the length of column; the alternative variable throughput method used in [7] seems to us of doubtful validity, for reasons given below.

An essential feature of the rising-drop method, not hitherto emphasised, is a sensibly constant concentration of the transferring species in the continuous phase, as the experiment proceeds. If transfer to or from the droplets were to cause appreciable concentration changes in the continuous phase, these would vary in an uncertain manner along the length of the column (which is not stirred) with incalculable effects on the results.

The results so far obtained are limited in scope, but very suggestive. A full interpretation must await more extensive data.

EXPERIMENTAL

Materials

TBP obtained from Albright and Wilson was purified as described by Alcock et al. [8]. TOPO (Société Nationale de Poudres et Explosives, Paris) was purified by multistage acid (6M HCl at 40°C) and alkaline (5% Na₂CO₃) washes of a 0.1M TOPO solution in benzene [9]. Finally the TOPO solution was successively treated with charcoal and activated alumina and the benzene evaporated off under reduced pressure. Odourless Kerosene (Shell Chemicals Ltd.) was washed several times with 5% sodium carbonate and with distilled water before use.

Nitric acid, sodium nitrate and uranyl nitrate were of AnalaR grade.

²³²U, produced by irradiating ²³¹Pa, was purified from daughter products by anion exchange in hydrochloric acid solution. The radiochemical purity was verified by alpha pulse analysis. ⁹⁰Y was obtained from the Radiochemical Centre, Amersham.

Distribution Measurements

Equilibrium distribution measurements were made by stirring together equal volumes of organic and aqueous phases in a centrifuge tube for 5 minutes at 21°C. The phases were then centrifuged, separated and analysed.

Rate of Transfer Measurements

The apparatus used for the rising-drop studies was similar to those described in the literature, e.g. in [1,7]. A stainless steel jet (hypodermic needle) was used in place of a glass capillary. The capacity of the column was large enough (1.8 cm diam.) to maintain the concentration of the continuous phase essentially constant during an experiment. Provision was made for varying the length of the column by changing the central section. Six lengths between 15 cm and 130 cm were normally used.

The drop size was obtained from the number of drops and the volume of liquid passed. The mean drop sizes were 0.007 ± 0.001 ml and 0.009 ± 0.001 ml for the TBP and TOPO experiments respectively. The area for mass transfer was calculated from the drop volume, assuming the drops to be perfect spheres. Time of contact between the drop and the continuous phase was determined by means of a stopwatch.

The procedure for eliminating end-effects is discussed below. Essentially it consists in relying on differences between measurements at different column lengths.

No temperature control was attempted; the ambient temperature varied between 20 and 23°C.

Analysis

Uranium concentrations in drop samples were measured colorimetrically using dibenzoylmethane [10]. ⁹⁰Y was determined by gamma scintillation counting of 1 ml liquid samples and ²³²U by alpha scintillation counting after evaporating a suitable aliquot on a stainless steel planchet.

TREATMENT OF THE RESULTS

Pseudo-first-order Rate Theory

Let V = volume of phase, C = concentration of transferring metal, A = area of contact between phases, and let a prime distinguish one of the phases. Treating the net transfer as the difference between transfer at a rate kAC from the unprimed phase and k'AC' from the primed phase (pseudo-first-order kinetics), we obtain

$$kACdt - k'AC'dt = -VdC = V'dC'. \quad (1)$$

Here it has been tacitly assumed that the bulk phases are of uniform composition, i.e. well mixed, so that there is no ambiguity in the meaning of C and C'.

In the rising drop method we shall assume that eq. (1) applies throughout the life of a drop, except for the initial stages. The measurements give C (droplet phase) as a function of t, and since C is measured after mixing, VdC gives a true measure of the net transfer, as required in eq. (1). C' (continuous phase) is maintained sensibly constant, as already noted, so there is no ambiguity about the k'AC'dt term, while the V'dC' term, which is subject to ambiguity, is not required for the subsequent argument. There remains the kACdt term, which assumes good mixing throughout the drop as it rises through the column. We may treat this as a hypothesis to be tested.

Eq. (1) without the V'dC' term integrates to

$$\ln(kC - k'C') = \text{constant} - kAt/V. \quad (2)$$

In the particular case of loaded drops and a barren continuum (C' = 0) it becomes

$$\ln C = \text{constant} - kAt/V. \quad (3)$$

Ultimately, with an indefinitely long column, C will reach an equilibrium value, C_e, equal to DC', where D is the distribution coefficient. Provided eq. (1) still holds, with no change in the value of k, we have

$$D = C_e/C' = k'/k. \quad (4)$$

This enables us to calculate k from k' and vice versa, and to express eq. (2) in the form

$$\ln(C_e - C) = \text{constant} - kAt/V. \quad (5)$$

Eq. (5) can be used when barren drops are passed into a loaded continuum. The validity of (4) and (5) may depend on C_e, as well as all the C's, being low in comparison with the extractant concentration; in fact the highest value of C_e used corresponded to combination with only 10% of the extractant.

Examples of the application of eq. (3) and (5) to the experimental results are given in Fig. 1. The results for each run were interpolated so as to refer to constant throughput of the droplet phase, but this introduced very little uncertainty. It will be seen that satisfactory straight lines were obtained, from whose slopes k -values could be calculated. This tends to confirm the assumptions on which the equations are based, in particular pseudo-first-order kinetics and good mixing in the organic phase. (Further confirmation of the kinetics is given below.)

Elimination of End-Effects

There are end-effects at the bottom of the column in the formation of the drops, and at the top of the column where the drops are collected. The former should be essentially independent of column length, and their effects can therefore be eliminated by comparing different column lengths. All that is necessary is to use eq. (3) or (5), as the case may be, without attempting to extrapolate to $t = 0$. (In Fig. 1 it will indeed be noted that the intercepts of the lines on the vertical axis at $t = 0$ differ from $\log C_{\text{feed}} = -3.73$ in the case of eq. (3), and from $\log C_e = -3.55$ in the case of eq. (5). The deviations are measures of the end-effects.)

At the top end of the column there will be some additional transfer of material at the interface where the drops are collected. The effect is most simply regarded as an additional but unknown period of contact between the drops and the continuum. It therefore involves a displacement of the lines in Fig. 1 along the t -axis, but does not effect the slopes, from which the k -values are calculated.

We conclude that the use of eq. (3) or (5), avoiding the vicinity of $t = 0$, eliminates end-effects.

A further complication is a slight variation in the C -values when the throughput of the droplet phase, i.e. the number of drops per unit time, is varied. However, we found that, provided eq. (3) or (5) was applied under conditions of constant throughput, the k -values were essentially independent of throughput.

Nitsch [11] attempted to eliminate end-effects in the continuum \rightarrow drops case by plotting his C -values against $1/\text{throughput}$ and extrapolating to zero throughput. The extrapolated values are quite well-defined in this procedure, because the plots are nearly linear and of low slope. The argument is that at high throughputs the formation and removal times of the drops at the ends of the column tend towards zero, so end-effects become vanishingly small. Against this it can be contended that the amount of turbulence and other disturbances increase with throughput, which vitiates the argument. In our experiments insertion of the extrapolated C -values into eq. (5) still did not give lines with the expected intercepts at $t = 0$, indicating that end-effects were still present.

Baumgärtner and Finsterwalder [7] followed Nitsch's procedure in their study of the $\text{UO}_2(\text{NO}_3)_2/\text{HNO}_3/\text{TBP}/\text{diluent}$ system, ascribing the observed curvature of the $C_{\text{extrapolated}}, t$ -curves in the vicinity of $t = 0$ to the kinetics of the transfer process, rather than to end-effects. They therefore took the initial slope at $t = 0$ as a measure of k' . In our experience the initial slopes cannot be determined with any certainty from the data, and in any case we believe they are considerably affected by end-effects.

Unfortunately Baumgärtner and Finsterwalder give insufficient information to assess the errors that might have been introduced by their, in our view, faulty method of interpretation. We attempted to estimate the errors by

measurements on a system similar to one of theirs, viz. a 0.01M $UO_2(NO_3)_2$ /3M HNO_3 aqueous continuum and 20% TBP/OK droplets pre-equilibrated with 3M HNO_3 . From eq. (5) we obtained $k' = 68 \mu\text{m}/\text{sec}$, whereas the initial slope corresponded to roughly $k' = 130 \mu\text{m}/\text{sec}$, compared with $k' = 110 \mu\text{m}/\text{sec}$ in ref. [7] (with dodecane diluent). While there is approximate agreement, it appears that the values in ref. [7] may be about double the true values. Moreover the errors may well differ according to the conditions.

RESULTS AND DISCUSSION

Transfer of Uranyl Nitrate using TBP

The variation of D and k' with [TBP] for a constant aqueous phase is shown in Fig. 2. Attention is drawn to the following features:

(1) The k' -values refer to different uranium concentrations, and for 0.2M TBP a direct comparison was made between 0.39mM U ($k' = 9.6 \mu\text{m}/\text{sec}$) and 2.1mM U ($k' = 8.8 \mu\text{m}/\text{sec}$). The fact that all the points lie on the same line confirms the assumption of a first-order variation of rate with uranium concentration.

(2) The k' -values calculated from k -values (i.e. from rate constants for the reverse transfer) by means of eq. (4) fall on the same lines as those determined directly. This demonstrates that the pseudo-first-order rate equations provide a consistent interpretation of the experimental results.

(3) D and k' both vary as $[TBP]^2$, while k is independent of [TBP]. So far as the D-values are concerned, this result is expected from the well-known fact that a di-solvate, $UO_2(NO_3)_2 \cdot 2TBP$, is formed. The laws for k' and k indicate that the rate-determining step in the transfer process is the formation or break-up of the di-solvate.

The absolute values of k' are of the same order of magnitude as those published by other authors. Exact comparisons are not generally possible, owing to differences in conditions. Nevertheless there is a remarkable measure of agreement, even when quite different methods have been used. The following values all refer to ca. 20% TBP/diluent and a 0.1 - 3M HNO_3 aqueous phase at ambient temperature:

k' ($\mu\text{m}/\text{sec}$)	Method	Ref
ca. 30*	Rising organic drops	[1]
60-120 ⁺	Stirred cell	[4]
55	U exchange in stirred cell	[5]
58-69	Falling aqueous drops	[6]
110 ⁺	Rising organic drops	[7]
68	Rising organic drops	This work

* Early, rough figure

+ Depending on stirring speed etc.

✓ Overestimated from results, see text.

Hahn's technique [3] with unstirred bulk phases, on the other hand, led in effect to a study of self-diffusion, and his transfer rates are not comparable.

Transfer of Uranyl Nitrate using TOPO

The variation of D and k' with [TOPO] for two constant aqueous phases is shown in Fig. 3. The following table gives k' -values for 0.01 M HNO_3 /0.99M $NaNO_3$ /0.05M TOPO, and demonstrates that the transfer is of first order in the uranium concentration:

$[\text{UO}_2(\text{NO}_3)_2]$	(mM)	0.042	0.082	0.164
k'	($\mu\text{m}/\text{sec}$)	49	53	55

Direct measurements of k were not possible in this system on account of the high D -values.

Fig. 3 presents a marked contrast to Fig. 2:

(1) The D -values vary approximately as $[\text{TOPO}]^{2.7}$, suggesting a tri-solvate as the principal species. Indications of a higher solvate than the di-solvate were obtained by Heyn and Soman [12], who found $D \propto [\text{TOPO}]^{2.2}$.

(2) The k' -values vary much more slowly with [extractant] than in the TBP case. If eq. (4) is applicable, this implies that k , so far from being independent of $[\text{TOPO}]$, varies more rapidly than does k' .

(3) A comparison between TOPO and TBP for 0.01M $\text{HNO}_3/0.99\text{M NaNO}_3/0.01\text{M}$ extractant is given in the table at the end of the paper, from which it can be seen that the powerful extraction by TOPO compared with TBP is due to a combination of faster transfer into the solvent and slower transfer out of the solvent.

It seems clear from the k' -curves in Fig. 3, that formation and break-up of solvate(s) cannot be the rate-determining step in the transfer under the conditions in question. It may be speculated that some diffusion process is involved.

Fig. 3 gives results at two nitrate ion concentrations, and the effect of varying $[\text{NO}_3^-]$ on D and k' at constant $[\text{TOPO}]$ is shown in Fig. 4. If the activity coefficient results in [13] are introduced, it can be shown that the residual variation of D in Fig. 4 is roughly as $[\text{NO}_3^-]^2$, as expected. The k' -values, however, vary approximately as $[\text{NO}_3^-]^{0.6}$ (without introduction of activity coefficients). Attention is also drawn to the fact that the ratio between the k' -values at the two nitrate concentrations varies with the TOPO concentration.

Transfer of Yttrium Nitrate using TOPO

The variation of D and k' with $[\text{TOPO}]$ with a constant aqueous phase is given in Fig. 5, with values for k' for the uranium case from Fig. 3 for comparison. D varies as $[\text{TOPO}]^{2.7}$ indicating predominantly a tri-solvate, as expected, while k' varies as $[\text{TOPO}]^2$. The situation thus appears to be intermediate between those for the two uranium systems, and the intermediate value of k' agrees with this view. It may be supposed that both the chemical reaction rate and diffusion affect the transfer rate.

System	U/TBP (1)	U/TOPO (2)	Y/TOPO (3)	Ratio	
				(2):(1)	(2):(3)
D	0.0013	3100	0.13	1.4×10^6	2.5×10^4
k' ($\mu\text{m}/\text{sec}$)	0.026	33	1.7	1.3×10^3	19
k'/D ($\mu\text{m}/\text{sec}$) [*]	20	0.0106	13	5.3×10^{-4}	8.1×10^{-4}

*If eq. (4) holds, $k'/D = k$

REFERENCES

- [1] H.A.C. McKay and D. Rees, AERE-C/R-1199 (1953).
- [2] J.B. Lewis, AERE CE/R-1366 (1956) and Nature, 178, 274 (1956).
- [3] H.T. Hahn, J. Amer. Chem. Soc., 79, 4625 (1957).
- [4] L.L. Burger, HW-62087 (1959).
- [5] B. Keisch, IDO-14490 (1959).
- [6] W. Knoch and R. Lindner, Z. Elektrochem., 64, 1020 (1960).
- [7] F. Baumgärtner and L. Finsterwalder, J. Phys. Chem., 74, 108 (1970).
- [8] K. Alcock, S.S. Grimley, T.V. Healy, J. Kennedy and H.A.C. McKay, Trans. Faraday Soc. 52, 39 (1956).
- [9] G.W. Mason, S. McCarty and D.F. Peppard, J. Inorg. Nucl. Chem. 24, 967 (1962).
- [10] C.A. Horton and J.C. White, Anal. Chem., 30, 1779 (1958).
- [11] W. Nitsch, Dechema Monograph. 55, 143 (1965).
- [12] A.H.A. Heyn and Y.D. Soman, J. Inorg. Nucl. Chem., 26, 287 (1964).
- [13] I.L. Jenkins and H.A.C. McKay, Trans. Faraday Soc., 50, 107 (1954).

ACKNOWLEDGEMENTS

We would like to thank F.J.G. Rogers for the alpha pulse analysis measurements, and Dr. J.H. Miles, D. Scargill and R.J.W. Streeton for helpful discussions.

One of us (L.F.) is indebted to the Royal Norwegian Council for Scientific and Industrial Research for a Research Fellowship enabling this work to be carried out in England.

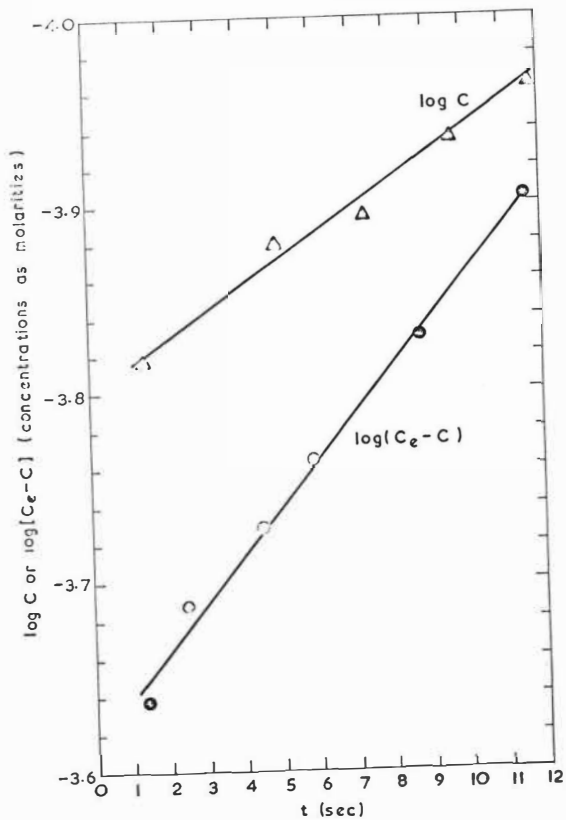


FIG. 1. TYPICAL FIRST-ORDER PLOTS:
 Δ drops → continuum, eq. (3)
 ○ continuum → drops, eq. (5)

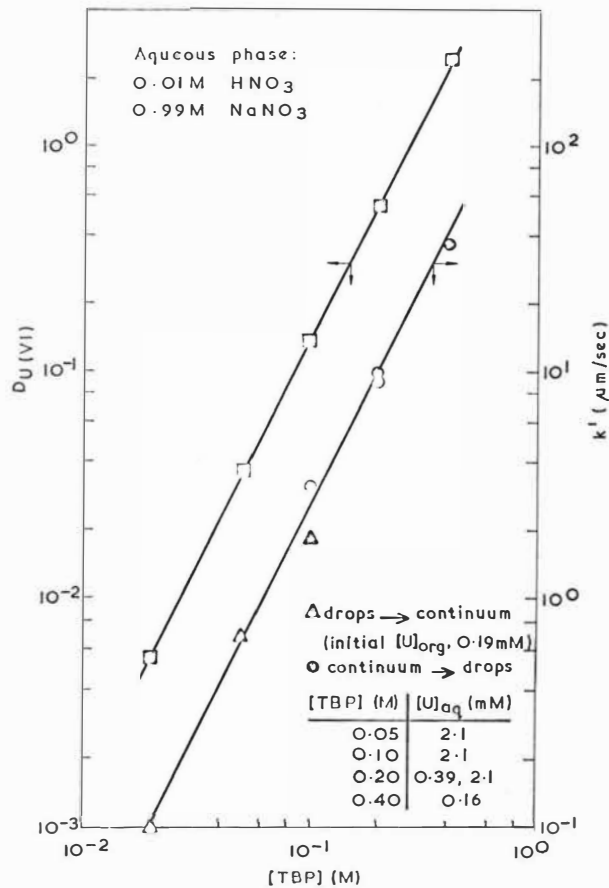


FIG. 2. RESULTS FOR THE U/TBP SYSTEM.

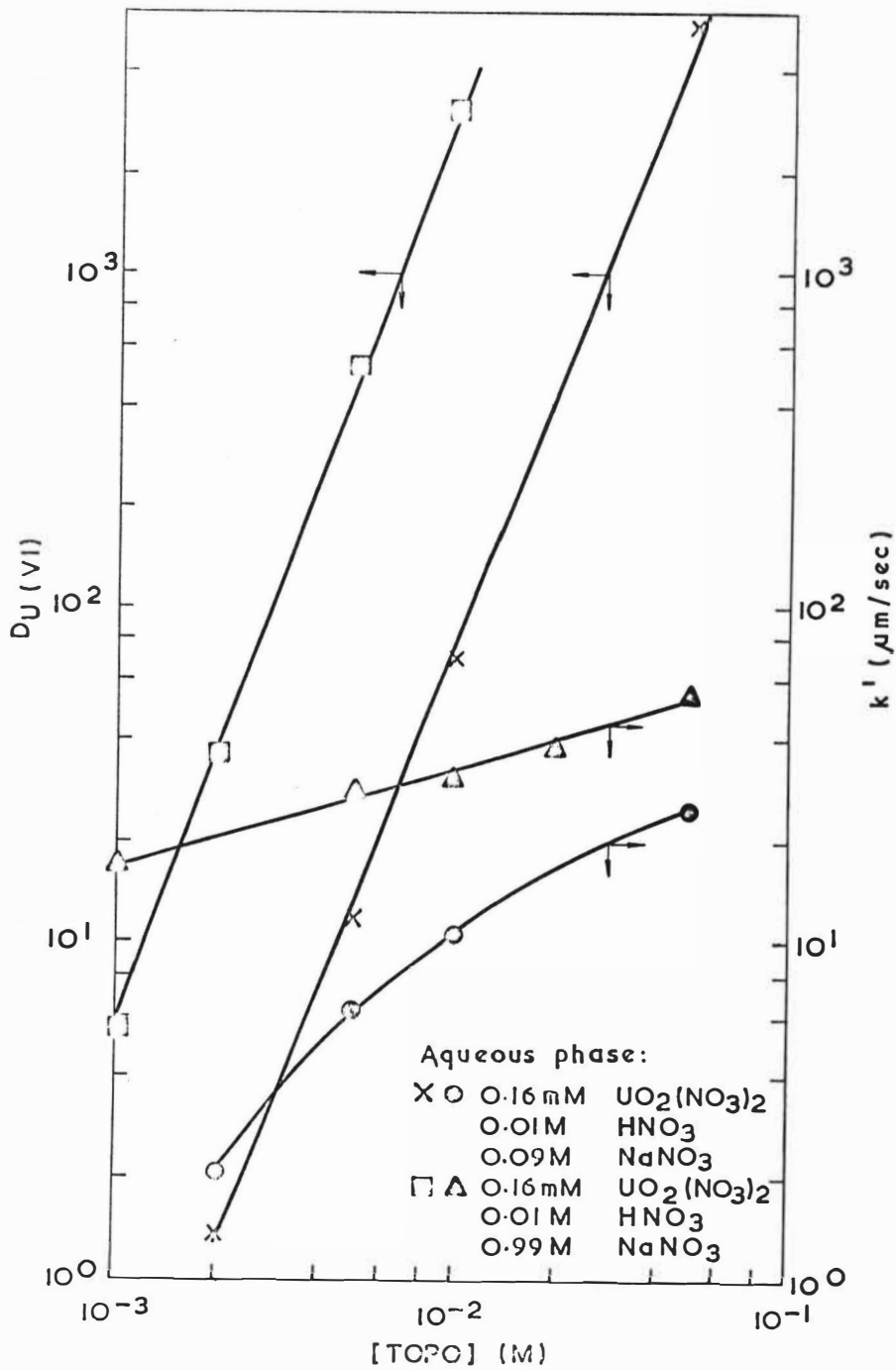


FIG. 3. RESULTS FOR THE U/TOPO SYSTEM

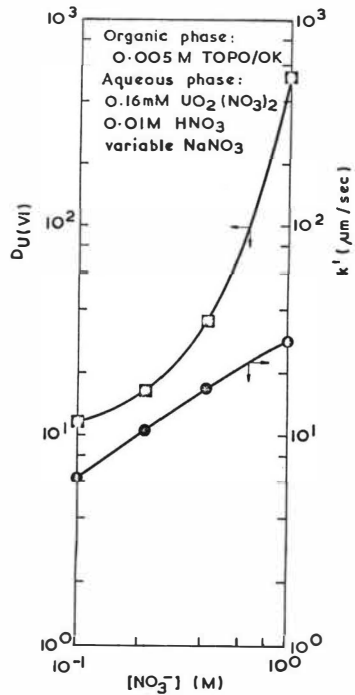


FIG. 4. RESULTS FOR THE U/TOPO SYSTEM.

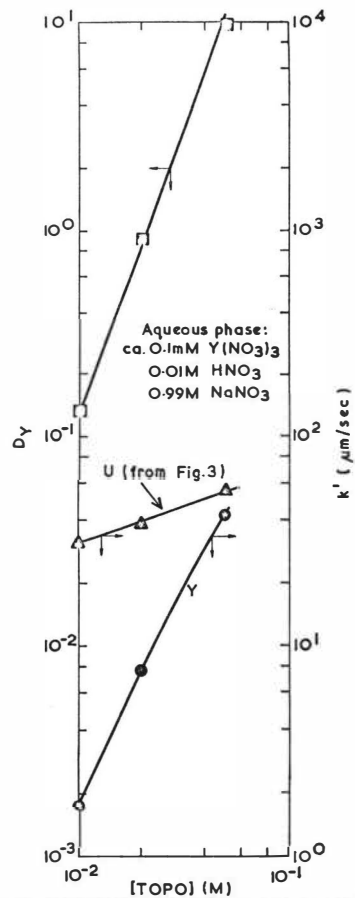


FIG. 5. RESULTS FOR THE Y/TOPO SYSTEM.

by

G.M. Ritcey* and B.H. Lucas**

ABSTRACT

The diluents as well as the modifiers chosen for mixing with the extractant can have an important bearing on the solvent mixture. The physical properties of the system with regard to dispersion and coalescence, as well as the extraction and separation of metals can often be related to the selection of the diluent and modifier. Properties such as dielectric constant, polarity, aromaticity, and solubility parameters of diluents are discussed. Increase in polarity or dielectric constant are shown to adversely affect extractability. Also the concentration of aromatics, paraffins, or naphthenes in the diluent, as well as the solubility parameter, influence the extractability and separation of metals more in some systems than in other systems. The influence of the modifier in the process does not appear to follow any defined pattern, and therefore evaluation is required before a choice is made. Proper selection of the diluent and modifier can affect the kinetics and equilibrium, and therefore equipment type, stages required and the capital cost of equipment and solvent inventory.

*Research Scientist, and Head, Solution Treatment Section, Extraction Metallurgy Division, Mines Branch, Ottawa.

**Research Scientist, Solution Treatment Section, Extraction Metallurgy Division, Mines Branch, Ottawa.

INTRODUCTION

Although there have been numerous articles written, and numerous researches undertaken on evaluation of the most suitable extractant for a particular process, comparatively very little attention has been directed towards optimizing the solvent extraction process with respect to the diluent and modifier. Proper selection of the diluent and modifier can be almost as important as selecting the extractant, and, because of the effects on phase disengagement the diluent and modifier can exhibit, the economics of a process can be seriously affected. Early plants for the extraction of uranium assumed a local supply of kerosene was satisfactory. In the case of the Eldorado Nuclear operation at Port Radium, N.W.T., the initial diluent was a local kerosene from Norman Wells, known as Arctic Diesel.⁽¹⁾ Later the diluent was changed to JP4 jet fuel in order to improve phase disengagement, but this diluent had a low flash point and was not used in succeeding plants because of the possible fire hazard. The diluent was also usually considered to have no effect on the extraction characteristics, and was therefore "inert" to the process. This was also the case with the modifiers. With the development of the copper plants also came a new diluent, Napoleum 470, produced by Kerr McGee, an aliphatic, high, narrow boiling range fraction which was put to use in both copper and uranium plants. Since then, with the more critical evaluation of diluents as related to performance and the consequent economics, much information is available, as well as possible diluents for the solvent extraction process. Investigators have found that not only are diluents and modifiers

not "inert" to the solvent extraction process, but that they can play a very substantial role in determining the success of an operation.

Several ideas have been advanced to correlate extraction coefficients and physical properties of diluents. For example, the solvation ability of the diluent has been suggested as the reason for increasing positive deviations from the ideal partition law with aliphatic diluents rather than with aromatic diluents.⁽²⁾ Another approach is that taken by Taube,⁽³⁾ who suggests that the complex-solvent dipole interaction is the cause. Thus since non-polar hydrocarbons do not have a particular ordered structure, extraction into these liquids takes place more readily than into a completely or more ordered structure, as is found in more polar diluents. According to Rozen, no correlation exists between the dielectric constant and extraction.⁽⁴⁾

Another particular important aspect of diluent effects is that of third-phase formation.⁽²⁾ Third phases are generally of a density intermediate between that of the aqueous phase and of the solvent phase, the results of the effect or influence of the diluent on the heterogeneous equilibria associated with the system. The phenomenon of third-phase formation has been noted, particularly in the case of the extraction of uranium,⁽⁵⁾ although it is a fairly common occurrence in liquid-liquid extraction systems.⁽⁶⁾

Formation of two organic phases is considered to be the result of the limited solubility of a metal-extractant

species in a non-polar hydrocarbon diluent. This conclusion is drawn because, in almost all cases of third-phase formation, one of the two organic phases is the pure - or almost pure - diluent. The make-up of a second organic phase is not necessarily of constant composition.

Third-phase formation is particularly evident in systems employing aliphatic amines and DEHPA. (7,8) From the many investigations into this phenomenon, several conclusions may be drawn: (i) third-phase formation is temperature dependent; increasing the temperature will usually result in the disappearance of the third phase; (ii) appearance of a second organic phase is more likely to occur when using an aliphatic diluent; (iii) for the case of amine extractants, the tendency for third-phase formation with different anions is in the order nitrate < chloride < sulphate. A similar tendency is observed with DEHPA as the extractant.

Another effect of diluent on the formation of two organic phases is illustrated by the system TBP-diluent-HCl. The TBP concentration required for formation of a third-phase decreases as the molecular weight of the diluent (aliphatic) increases for a fixed hydrochloric acid concentration. (9)

Diluents have been shown to have a synergistic effect on the extraction of metal ions. Thus, for example, the extraction coefficient of some metal ions is greater in carbon tetrachloride than in chloroform, being the result of an interaction of the chloroform (the more polar liquid) with the neutral liquid. (5,10) Further, the synergistic effect of the diluent

in the extraction of promethium and americium thenoyltri-fluoroacetone complexes with TBP has been demonstrated. (11,12)

This paper described investigations carried out in an attempt to relate a property or properties of diluents and modifiers with the extraction and separation of metals, while at the same time not forgetting the important aspect of phase separation.

DILUENTS

The term diluent refers to the organic liquid in which the active reagent (extractant) and modifier are dissolved to form the solvent. In the majority of cases, the diluent makes up the major portion of the solvent solution.

Generally, the requirements of a diluent are that it be inert with respect to the extractant, modifier and aqueous phase, and be insoluble in the aqueous phase. Naturally, the extractant and modifier must be very soluble in the diluent.

A diluent may not be necessary in the solvent make-up. This situation can occur with the use of TBP, and also in many analytical separations where the metal ion is complexed with a reagent in the aqueous phase and the complex extracted into an organic phase composed only of a suitable inert liquid such as carbon tetrachloride or toluene. Diluents are necessary when the extractant is a solid. One example of this situation is tri-octylphosphine oxide (TOPO) which is a solid, and is usually dissolved in cyclohexane or similar organic reagent.

There are many inert organic liquids available commercially for use as diluents in the solvent extraction process. These range from (essentially) completely aliphatic to completely aromatic. Some of the more common diluents that were examined in the present investigation are listed in Table 1, together with some of their physical properties.

The choice of a diluent cannot readily be predicted. Usually a diluent is selected after experimental work has been carried out on several of the more likely ones. It must be pointed out that a diluent cannot be assumed not to enter into the mechanism of solvent extraction. In some cases this is to be avoided; in others the diluent can assist in the extraction. In many cases the enhancement or otherwise of the extraction by a diluent is the result of some "impurity" in the diluent, which for one reason or another cannot be isolated. For example, a small amount of an aromatic compound in an aliphatic diluent may aid in the extraction of a particular metal species, while a sample of the pure aliphatic liquid may provide substantially lower extraction characteristics. It is preferable, therefore, in bench-scale tests to use the commercial diluent which would be used in pilot-plant test work, rather than the pure (reagent grade) diluent. This practice is suggested for all bench-scale work.

Flash Point

In considering the diluents which may be applicable to a particular process, the solubility in the aqueous solution and the flash point are important. Early work on the liquid-

TABLE 1

COMMERCIALY AVAILABLE DILUENTS USED IN REPORT

DILUENT	FLASH PT. (°F)	COMPONENT ANALYSIS			SP.GR. 20°C	B.PT. °F	KAURI BUTANOL	SOLUBILITY PARAMETER	VISCOSITY AT 25°C
		AROMATIC	PARAFFIN	NAPHTHENES					
ISOPAR L (A)	144	0.3	92.7	7.0	0.767	373	27	7.2	1.60
ISOPAR E (A)	<45	0.05	99.94	-	0.723	240	29	7.1	
ISOPAR M (A)	172	0.3	79.9	19.7	0.782	405	27	7.3	3.14
NORPAR 12 (A) *	156	0.6	97.9	1.1	0.751	384			1.68
Esso Lops (A)	152	2.7	51.8	45.4	0.796	383			2.3
DX3641 (A)	135	6.0	45	49	0.793	361	33.6	7.7	1.165
SHELL 140 (B)	141	6.0	45	49	0.785	364	32		
HAPOLEUM 470 (C)	175	11.7	48.6	39.7	0.811	410	33		2.10
ESCAID 110 (A)	168	2.4	39.9	57.7	0.808	380			2.51
SHELL-LIVESTOCK SPRAY (B)	270	15	48	37	0.819	512			
MENTOR 29 (A)	280	15	48	37	0.800	500			
SHELL PARABASE (B)	210				0.788	428			
ESCAID 100 (A)	168	20	56.6	23.4	0.790	376			1.78
NS-144 (A)	140	16	42	42					
NS-148D (A)	160	4.5	36.6	43			30.9		1.603
SOLVESSO 100 (A)	112	98.9	1.1	-	0.876	315	92	8.8	
SOLVESSO 150 (A)	151	97.0	3.0	-	0.895	370	90	8.7	1.198
XYLENE (A)	80	99.7	0.3	-	0.870	281	98	8.9	0.62
HAN (A)	105	88.5	4.1	6.8	0.933	357	105	8.9	1.975
CYCLOHEXANE (E)	-	-	-	100				8.2	
CHEVRON 40L (D)	141	78			0.886	360	76		
CHEVRON 370 (D)	127	0			0.758	346	27		
CHEVRON 44L (D)	154	69			0.893	366	73		
CHEVRON 3 (D)	145	98			0.899	360	88		
CHEVRON 425 (D)	142	2			0.787	360	26		
CHEVRON LOS (D)	130	0			0.779	350	33		
CHEVRON 25 (D)	115	99			0.875	316	94		

(A) ESSO OR EXXON (B) SHELL (C) KERR-MCGEE (D) CHEVRON (E) OTHERS * Now Escaid 200

liquid extraction of uranium using a long chain tertiary amine⁽¹⁾ employed kerosene jet fuel, such as Esso JP-4 or BA T-2, as the diluent. This had a very low flash-point (~32°F) and presented a potentially hazardous system. Today, diluents having much higher flash-points are used.

The effect of extractant and diluent on the flash point of the solvent mixture is shown below. Also included are the flash points of stripped and equilibrated solvent.

	Flash Point, °F	
	TCC*	TOC**
Shell 140 Flash Naphtha	139	153
50 vol % TBP in Shell 140 FN (fresh mixture, non equil)	146	169
50 vol % TBP in Shell 140 FN (used, stripped solvent)		168,164
50 vol % TBP in Shell 140 FN (used, equil, with HNO ₃)		176,178

* TAG closed cup test.

** TAG open cup test.

Polar Nature

In the extraction of rare earths with Aliquat 336,⁽¹³⁾ there was noted a decrease in the extraction of the metals with an increase in the polar nature of the diluent. Also the separation factor for La/Pr was decreased as the polar nature increased. These results are shown in Table 2.

TABLE 2

Influence of Polar Nature of Diluent on the Extraction of
Rare Earths using Aliquat 336

<u>Diluent</u>	<u>Polar Nature</u>	<u>Extraction, %</u>	<u>Sep. Factor, La/Pr</u>
Toluene	↓ increasing ↓	27	2.7
Xylene		24	2.8
Octane		18	2.0
Stand. Mineral Spirit		18	2.6
Ethyl ether		14	1.6
MIBK		9	1.2
Butyl acetate		4	1.4

Similar effects are shown in the extraction of americium with mixtures of 1-phenyl-3-methyl-4-benzoyl-pyrazolon-5 and TBP from nitrate solution.⁽¹⁴⁾ The extraction constants decrease with increasing polar nature of the diluent.

Influence of diluent on the extraction of molecules or anions such as H_2O ,⁽¹⁵⁾ $FeCl_4^-$,⁽¹⁶⁾ $ZnCl_4^{2-}$,⁽¹⁷⁾ HCl_2^- ,⁽¹⁶⁾ with tertiary amines indicates that the influence is similar irrespective of the species, namely

cyclohexane ~ o-xylene > toluene > benzene
 >> chlorobenzene >> carbon tetrachloride
 >>> chloroform⁽¹⁷⁾

One conclusion which may be drawn is that the diluent affects the solvation of the extractant and hence its extractive properties.

Interaction of the diluent with the extractant can result in lower extraction coefficients for metal ions. Thus the formation of an extractant-diluent species in the organic phase produces a lower concentration of the "free extractant", with a consequent decrease in extraction coefficient. (18)

Dielectric Constant Effect

Although most of the normal diluents that would be considered for use in solvent extraction processing are of the kerosene-type materials, and having a dielectric constant in the range of 2-3, nevertheless there is always the possibility of using a diluent with a higher dielectric constant.

In Table 3 is shown a comparison of the extraction coefficients, E , with various diluents in an alkylphosphoric acid extraction of uranium. Kerosene was the best of those tested, that is, the diluent with the lowest dielectric constant resulted in the highest extraction. (19) Similar effects were shown for the system TBP- HNO_3 -Am. (16)

TABLE 3

URANIUM EXTRACTION AS A FUNCTION OF THE DIELECTRIC CONSTANT⁽¹⁹⁾Aqueous phase: 0.5 M $\text{SO}_4^{=}$, pH 1.0, 0.004 M U(VI) initially

Organic phase: 0.1 M reagent in indicated diluent

Aqueous/organic phase ratio = 1/1, temperature = 25°C

Diluent	Dielectric constant D	Extraction coefficient, E		
		EHPA	DDPA	HDPA
Kerosene	2	135	650	550
Carbon tetrachloride	2.2	17	-	-
Benzene	2.3	13	-	-
Chloroform	5.1	8	-	-
2-Ethylhexanol	-	0.1	-	-

A.K. De⁽²⁰⁾ compared the dielectric constants of various diluents and the effect on the extraction of various metals with a high molecular weight carboxylic acid, SRS-100 (Shell Chemicals). The results indicated that diluents such as benzene having low dielectric constants show high extraction, whereas diluents with higher dielectric constants, such as butanol and diisopropyl ether, reduce the extraction.

However, in the work, the effect of change of the dielectric constant in the range 2-4, on the extractability was not noted for all the metals. For example, Fe^{3+} , Pb^{2+} , Ca^{2+} , Sr^{2+} , Ba^{2+} , Mg^{2+} , and Pd^{2+} were unchanged. Zn^{2+} and Hg^{2+} only decreased in extraction at the highest dielectric constant of butanol (16.1). Also the results indicated a decrease in extractability of Fe^{2+} , Co^{2+} , Ni^{2+} , and Mn^{2+} occurring with increase in the dielectric

constant to 16.1. The extraction of Cu^{2+} decreased only at the highest dielectric constant.

In Figure 1⁽²¹⁾ are shown some other results obtained by varying the dielectric constant of the diluent in the separation of cobalt and nickel. Again there was an increase in extractability of the cobalt and nickel, as well as an increase in the separation of cobalt and nickel, with a decrease in the dielectric constant, using DEHPA.

However, such effects are difficult to ascribe solely to the dielectric constants. Other effects, such as impurities, degree of aromaticity, solubility of water in the diluent, etc., may also be involved. In many cases extraction coefficients cannot be correlated with one particular physical property of a diluent.

Aromatics, Paraffins, Naphthenes

DEHPA-SO₄-Rare Earths

Work at the Mines Branch has demonstrated that the degree of aromatic or aliphatic component in the diluent can have an effect on extraction. This is illustrated in Figure 2 for rare earths. Here the amount of aromatic constituent in the diluent is seen to have a considerable effect on the distribution coefficients of several rare earths when using DEHPA to extract from a sulphate leach solution. Such dramatic increases in distribution coefficients are not, however, too common. It is most likely that the diluent becomes less inert towards the metal ion as the aromatic character is increased. That is, the diluent may be incorporated in some way in the extractable species.

The aromatic content of the diluent was thus shown for the rare earth system to have a pronounced effect on the extraction characteristics of the metals, although not having any significant effect on the separation of adjacent rare earth pairs.

DEHPA-SO₄-Co-Ni

Having found such a good correlation between extraction and aromaticity in the rare earths system, other systems were then examined.

In subsequent work, also from a sulphate leach solution, cobalt and nickel were extracted and separated in one-stage using the DEHPA process⁽²²⁾ at an equilibrium of pH 6.0; with 20% DEHPA. The results of variation in the aromatic content of the diluents did not show the same well defined correlation as was demonstrated with the rare earth system. In fact no correlation could be drawn between aromaticity and the Co/Ni ratio; and for total metal loading there was a parabolic relationship with the lowest loading occurring in the range of 40 to 70% aromaticity. Variation of the diluent type resulted in a total metal loading ranging between 17.6 and 18.6g/l, and a Co/Ni separation factor (SF) ranging between 1.95 and 2.84 (Table 4).

Although no real relationship was found between the properties of the diluent and extractability, the results did show that not only the loading could be affected by diluent choice, but also the separation factor of two metals (Co/Ni). A one-stage contact of the loaded solvent with fresh feed (10g Co/l, 10g Ni/l), at an A/O ratio of 5, resulted in an increase from the extraction SF of 1.95 to 2.84 to scrubbing SF of 5.5 to

TABLE 4

Single Stage Extraction with DEHPA
 Diluent Effect on Separation of Cobalt and Nickel
 20% DEHPA, 10g Co/l + 10g Ni/l, Equil. pH 6.0

Diluent	Extraction Coeff. (E)		SF
	Co	Ni	
Chevron 40 L	1.93	0.99	1.95
Chevron 44 L	2.06	0.98	2.10
Chevron 370	2.06	0.96	2.14
Chevron 25	2.17	1.00	2.17
Varsol DX3641	2.27	0.99	2.29
Isopar L	2.20	0.91	2.42
Chevron LOS	2.20	0.87	2.53
Solvesso 150	2.39	0.94	2.54
Chevron 3	2.35	0.90	2.61
Napoleum 470	2.35	0.85	2.76
Chevron 425	2.46	0.89	2.76
Shell 140	2.27	0.80	2.84

16.0. The increase in purity, defined by the Co/Ni ratio in the loaded solvent, indicates again a parabolic relationship with either the paraffinic, or aromatic diluents being the most effective in scrubbing. The results are summarized in Table 5.

TABLE 5
Diluent and Effect on Scrubbing

Diluent	Aromatic %	Co/Ni Ratio in Solvent		Purity Factor Increase Scrub Ratio Extn
		Extn	Scrub	
Shell 140	5	1.79	7.43	4.15
Isopar L	0	1.51	8.62	5.71
Chevron 40 L	78	1.43	6.12	4.28
Chevron 44 L	69	1.49	5.46	3.66
Solvesso 150	97	1.65	9.24	5.60
Chevron 3	98	1.68	16.0	9.52

The scrubbing effectiveness on diluents was continued, with a three-stage scrub on the loaded solvent, using feed solution containing 10 g/l each of Co and Ni. The summary of the three-stage loading (with scrubbing), using other diluents than shown in previous Tables 4 and 5, is shown in Table 6. Phase separations in loading, as well as stripping, were satisfactory in all tests. Cyclohexane gave the highest metal loading, while Isopar L resulted in the best Co/Ni ratio in the loaded solvent.

TABLE 6

Three-Stage Loading and Diluent Effect
 on Extraction and Separation of Cobalt and Nickel
 20% DEHPA, Equil. pH 6.0, 10g Co/l, 10g Ni/l

Diluent	Total Metal g/l	Ext'd	Co/Ni Ratio
HAN	18.00		4.96
Napoleum 470	18.30		5.5
Shell Parabase	16.94		5.5
Solvesso 100	16.90		5.65
Isopar M	16.96		5.7
Isopar E	17.82		5.8
Shell Livestock Spray	16.66		6.1
Esso LOPS	13.30		6.6
DX3641	18.06		6.7
Xylene	17.32		6.7
Mentor 29	16.42		6.8
Solvesso 150	16.72		7.36
Cyclohexane	18.76		7.68
NS-144	16.54		8.00
Isopar L	16.44		8.55
Isopar L + Solvesso 150 1/1	17.20		7.18
Isopar L + Solvesso 150 2/1	17.20		7.18
Isopar L + Solvesso 150 1/2	16.78		7.56

Graphical correlations between either the diluent constituents of aromatics, paraffins, or naphthenes, with total metal loading or Co/Ni ratio in the loaded solvent, were impossible to obtain.

Because there appeared to be better results from the aromatic or paraffinic diluents, in the next series of tests mixtures of Esso's Isopar L and Solvesso 150 were used. The results of these diluent blending tests, performed in identical manner as the previous Co-Ni-DEHPA tests, using three stages of extraction at equilibrium pH 6.0, are shown in Figure 3 indicating a decrease in the Co/Ni ratio with increase in aromatic content.

Mixtures of Isopar L, Solvesso 150, and a naphthene diluent, cyclohexane, were used in another series of tests to determine the effect of the naphthene content on extraction and separation. In Figure 4 are shown the results of these tests, indicating a decrease in the separation of cobalt and nickel, with an increase in the amount of naphthenic content in such a mixture. The highest metal loading was achieved where the diluent consisted of only cyclohexene.

LIX64N and Kelex 100-SO₄-Cu

Investigation of the aromatic content of the diluent and the effect on the extraction of copper from acidic solution with either LIX64N or Kelex 100 has been reported(23), and indicated a trend towards decreased extraction with increased aromaticity. Also by proper choice of the diluent in this system the settling time could be reduced by 50%. In addition, the kinetics of extraction and stripping with LIX64N decreased generally with increase in aromaticity.

By contrast, the rate of settling in the Kelex system, either in extraction or stripping, increased with increase in aromatic content of the diluent⁽²³⁾. No change in extractability was noted with change in diluent composition. In stripping, the highest aromatic content resulted in the poorest efficiency.

Work at the Mines Branch, using a feed containing 5g Cu/l, in contact with 20% LIX64N, at an equilibrium pH 1.80 showed a tendency for decrease in extractability with increase in aromaticity, as shown in Table 7. Also, extraction appears to increase and become constant with increase in the naphthenic or paraffinic content (Figure 5). This is similar to results shown in Figure 4. The loading varied from 2.14 to 3.03 g Cu/l with variation of diluent.

With some of the same diluents as used for the LIX64N system, similar tests were performed with 0.5 M Kelex 100 (containing 10% isodecanol modifier), in contact with 15 g Cu/l. Again, the results indicated that an increase in aromaticity decreased extractability, E ranging from 7.2 to 2.5 in the range 0 to 100% aromatic content. Even with a modifier present, diluents such as Isopar E, L, M, Norpar 12, DX3641, NS148D, and Mentor 29 solidified in the extraction stage on contact with the feed solution.

Mixtures of Isopar L and Solvesso 150, covering the range 100% Isopar L to 100% Solvesso 150 and containing 0.5 M Kelex 100, were contacted with 5 g Cu/l, at an equilibrium pH 1.8. Figure 6 shows a decrease in extractability, as well as a decrease in the phase separation time, with increase in aromaticity.

TABLE 7

Diluent Effect on LIX64N
Extraction of Copper

20% LIX64N 5g Cu/l pH 1.80 equil

Diluent	Loading g Cu/l	Phase Disengagement Time (Sec)
Xylene	2.14	19.5
Solvesso 150	2.34	24
HAN	2.38	28
Solvesso 100	2.44	23
Isopar E	2.76	25
Escaid 100	2.77	20
Isopar L	2.84	23
DX3641	2.88	35
Cyclohexane	2.90	38
Isopar M	2.90	23
Mentor 29	3.02	25
Norpar 12	3.03	21.5

Similar tests, as for the cobalt nickel system, using Isopar L, Solvesso 150, and cyclohexene were performed. However the data did not indicate any influence of the cyclohexene content on extractability as was demonstrated in Figure 4 for cobalt and nickel separation.

Tertiary Amine - SO_4 -U

In the uranium-amine-sulphuric acid system using 0.1 M Alamine 336 containing 5% isodecanol in contact with an aqueous solution containing 2.5g U/l, the same series of diluents was evaluated as shown in the LIX64N and Kelex 100 systems. The loading in one stage of extraction at A/O of 2 varied between 3.85 and 4.29g U/l, for the diluents tested. Although there were trends towards lower extraction with increasing aromatic and naphthenic content, and higher extraction with increasing paraffinic content, there was also a scatter of data. Mixtures of Isopar L and Solvesso 150 indicated an increase in extractability with increase in aromatic content.

Tertiary Amine - HCl-Cu

Using mixtures of Solvesso 150 and Isopar L, in the copper-amine-hydrochloric acid system, there was again an increase in extractability with an increase in aromatic content, as was demonstrated in the amine-U- SO_4 system. The feed solutions, at 2g Cu/l and 165g HCl/l, were contacted at a phase ratio of A/O of 2, with a solvent consisting of 0.1M Alamine 336 containing 5% isodecanol in the diluent mixture.

TBP - NO₃-U

The influence of aromaticity was investigated in a solvating system , using a feed solution containing 5g U/l and 3M free HNO₃, in contact with 25% TBP in an Isopar L - Solvesso 150 diluent mixture, at A/O ratio of 5. Again, as with the amine extraction processes, there was a slight increase in extractability with increase in aromaticity.

TBP - HCl-Fe-Cu

Similar tests, as above, were performed for the chloride system, containing 5g Fe/l and 2.5g Cu/l, and containing 50 g/l free HCl. Fifty percent (50%) TBP was dissolved in the Isopar L -Solvesso 150 diluent mixture. Extractability again increased with increase in aromaticity.

The results of extractability and aromaticity are summarized in Figure 7, showing a percentage change in loading with increase in aromaticity. It is evident that the solvating systems and the anion-exchange systems are enhanced, while the cation systems are depressed, by increase in aromaticity.

Conclusions that might be drawn from the attempt to correlate the components of the diluent with extractability are:

- 1) There appears to be a slight relationship between the aromatic, paraffin, and naphthene content of commercial diluents and extractability. However, with a blend of paraffinic (Isopar L) and aromatic (Solvesso 150), there is a definite correlation with extraction.

- 2) Because the pure blends result in good correlation with extraction, can we then postulate that impurities such as naphthenes or olefins are detrimental factors in making a diluent choice?
- 3) There appears to be a difference in the diluent influence on extractability dependent upon whether the mechanism of extraction is by solvation or cation or anion exchange. With DEHPA, LIX, and Kelex, a decrease in extraction resulted with an increase in aromatic content above 25%, while for the amine and tributyl phosphate systems, the reverse was true.

Kauri Butanol Number

One other parameter that was examined for a possible correlation with extractability was the Kauri Butanol Number of the diluent. This number is some measure of the solvency properties of the diluent. These numbers, provided in the manufacturers' data sheet, were therefore plotted against the metal extraction using the several diluents listed previously for DEHPA, LIX 64N, Kelex 100, and Alamine 336. The four results, shown in Figure 8 (a,b,c,d), indicate a general trend towards decreasing extractability with increasing Kauri Butanol Number. The LIX 64N system falls rapidly after 20, compared to 80 for the amine system, and 92 for the Kelex system. The DEHPA system shows a scatter of results for loading and for the Co/Ni separation.

Solubility Parameter

With the relative success of employing the composition of the diluents and the Kauri Butanol value as correlations with extractability, it was decided that the choice of a diluent must lie in its solvency ability. That is, the solubility is a measure of the extent to which molecules of a diluent will form a stable, homogeneous mixture with the molecules of the other components of the solvent mixture. The measure of solubility, the Solubility Parameter (δ) can be calculated from the following formulae: (24)

From the heat of vaporization:

$$\delta = \left(\frac{\Delta H_v - RT}{M/D} \right)^{1/2}$$

From surface tension:

$$\delta = 3.75 \left[\frac{P}{(M/D)^{1/3}} \right]^{1/2}$$

where ΔH_v = latent heat of vaporization, cal/mole

R = gas constant, 1.987 cal/(Mole) ($^{\circ}$ K)

T = temperature, $^{\circ}$ K

M = molecular weight

D = density, g/cc

P = surface tension, dynes/cm

The solubility parameter values used in the present investigation were obtained from the manufacturers' diluent data sheets. These parameters were plotted against the extraction results already noted earlier in this paper. For the LIX64N and Kelex 100 systems, increase in the solubility

parameter decreased extractability, as is shown in Figure 9.

Again, as in the examination of the component effect of the diluent on extraction, blends of diluents were examined. In general, the solubility parameter of a blend is equivalent to the volume weighted average of the components. The blend of Solvesso 150 with Isopar L was again examined with respect to the solubility parameter. Again, there was a trend towards decreasing extractability with increasing solubility parameter in the Kelex 100 system. With DEHPA, the total loading, as well as the separation of cobalt and nickel also decreased with increase in solubility parameter. However, with the amine and TBP systems, the opposite was true, with increase in solubility parameter resulting in an increase in extractability. The results are summarized in Figure 10.

Conclusions that might be made regarding the solubility parameter and its effect on extractability, are therefore:

- 1) there appears to be a relationship between solubility parameter and the aromatic content and their correlation with extractability;
- 2) an increase in the solubility parameter can affect a metal separation process, such as the Co/Ni separation using DEHPA;
- 3) as in the case of aromatic correlation with extractability, the solubility parameter also appears to show one relationship with cation exchange systems (DEHPA, Kelex, LIX), and a different relationship with anion exchange and solvating processes.

MODIFIERS

The formation of third-phase, or two organic phases, which present problems in solvent extraction processes is generally overcome by the addition of what are generally termed modifiers. In almost all cases, modifiers are alcohols. These are insoluble in water but mutually soluble in the extractant and in the diluent. The most popular alcohols used are isodecanol and 2-ethylhexanol. Another fairly common modifier is TBP.

Modifiers presumably increase the solubility of the extracted species in the solvent phase by changing some of the physical and chemical properties of the solvent. These additives also serve to inhibit the formation of stable emulsions during contacting of the aqueous and organic phases.

The choice of a modifier will depend on the system, not only in respect of the above points, but also in the degree to which it enters into the chemistry of the extraction process.

In any particular solvent system the concentration of modifier required cannot be determined except by experiment. Usually the amount required is between 2 and 5 vol %. Some solvents, such as Versatic 911 in kerosene when used to extract cobalt from nickel in ammonium sulphate solutions at pH 7.5 - 8.0⁽²⁵⁾ do not require the addition of modifiers. The following will attempt to show the effect of the modifier on the extraction, scrubbing, and stripping of the metal, as well as how the modifier choice may also affect phase disengagement.

Extraction, Scrubbing, Stripping, and Phase Disengagement

DEHPA-SO₄-Rare Earth

Modifiers present in a solvent can affect the solvent's extractive properties. This is illustrated in Figure 11 where the effect of TBP, isodecanol and 2-ethylhexanol (all at 5 vol%) is shown on the extraction of rare earths with DEHPA. All three modifiers have a depressant (antagonistic) effect on the extraction, the order being 2-ethylhexanol>isodecanol>TBP. Differences between extraction coefficients, with and without modifier, can be as great as one order of magnitude.

Similar effects of these modifiers are shown on the stripping of rare earths from a solvent containing DEHPA plus modifier with 25 vol % sulphuric acid, as shown in Figure 12. In these cases, the effects of modifier on stripping occurs in the order TBP>2-ethylhexanol>isodecanol. The inability of the acid to strip the rare earths from a solvent containing isodecanol would indicate that this modifier interacts with the extractant and rare earths to produce a complex which is not very soluble in sulphuric acid. Although the isodecanol was suitable for extraction, in stripping it would have been most unsatisfactory. So the conclusion in this system, of the modifiers tested, would be to use TBP if a modifier was required.

DEHPA-SO₄-Co-Ni

Modifiers are also seen to influence the ability of a salt (scrub) solution to remove unwanted metals from a loaded solvent. An example of this is the use of isodecanol or TBP as

modifiers in the separation of cobalt and nickel using DEHPA as the extractant with kerosene as diluent.⁽²⁶⁾ The loaded solvent, containing cobalt and nickel, was scrubbed with fairly strong solutions of cobalt salts to remove nickel. The results of these tests, given in Table 8 show that isodecanol allows a higher loading of cobalt and nickel (23 g/l total) but a poor Co/Ni ratio, whereas TBP gives a significantly lower total loading (16 g/l) but a much higher Co/Ni ratio.

Kelex 100-SO₄-Cu-Co-Ni

Work has been previously reported by one of the authors on the evaluation of various modifiers, at different concentrations, on the extractive and stripping characteristics of Kelex 100. Various concentrations of nonylphenol, isodecanol, tributyl phosphate, as well as a mixture of isodecanol and nonylphenol, were used with 20% Kelex 100 in Solvesso 150 diluent.⁽²⁷⁾ The various solvent mixtures were contacted with a leach solution containing in g/l: 14.6 Cu, 13.2 Ni, 1.0 Co, and 2.6 Fe, at 50°C in one stage of extraction at O/A 1.2/1. Based on phase disengagement rates shown in Figure 13(a), for the extraction stage, although 5% isodecanol had the shortest separation time, 10% isodecanol or 10% isodecanol plus 10% nonylphenol mixture were better because of minimum secondary haze. Figure 13(b) shows an effect on extraction efficiency due to modifier type and varying concentrations. Although 10% nonylphenol was the best, there was a two-minute time for secondary haze clearing. Similarly, in Figure 13(c), are shown the disengagement rates when the loaded

TABLE 8

Effect of Modifier on the
Scrubbing of a 15 Vol % DEHPA Solvent
Containing Cobalt and Nickel

Scrub Solution	Modifier	Extract		No. of Contacts
		Co g/l	Ni g/l	
			A	
Co(NO ₃) ₂	isodecanol	20.8	2.0	1
20 g/l Co	5 vol %	21.6	1.5	2
		22.4	1.4	3
			B	
CoSO ₄	TBP	16.0	0.1	1
27 g/l Co	5 vol %	16.1	0.04	2
		16.0	0.03	3
			C	
Co(NO ₃) ₂	TBP	16.2	0.2	1
26 g/l Co	5 vol %	16.3	0.1	2
		16.2	0.08	3

A/O = 5/1

A: Original extract contained 8.4 and
4.5 g/l Co and Ni resp.

B;C: Original extract contained 12.9 and
3.8 g/l Co and Ni resp.

solvents were stripped with 15% H_2SO_4 , O/A 4/1. Although 5% nonylphenol and 20% isodecanol gave the best phase separation rates in stripping, the 5% nonylphenol had a secondary haze. Use of 20% isodecanol although satisfactory for stripping, was not the best for extraction. Again, 10% isodecanol was the preferred modifier, since both the 10% nonylphenol and mixture had secondary hazes in the extraction stage. In Figure 13(d) are shown the comparison of the modifier for selectivity of copper over iron, cobalt and nickel. From the results in Figure 13(a,b,c,d) it was concluded that of the modifiers and concentrations tested, 10% isodecanol with Kelex 100 was the best combination. Any slight lack in selectivity of copper over cobalt or nickel would be overcome in stagewise extraction. Thus, while isodecanol, in the proper concentration, enhances extraction, nonylphenol improves stripping and coalescence.

Alamine 336-SO₄-U

In the systems described above, on the modifier effects on extraction and phase separation, the diluent was constant, with the modifier being changed. Tests were then performed on the amine system for extraction of uranium from a sulphuric acid leach liquor, where two diluents were used in the evaluation of nonylphenol, 2-ethylhexanol isodecanol, and TBP. Isopar L and DX3641, essentially paraffinic and mixture of paraffinic and naphthenic respectively, were the diluents used in the investigation. Feed solution at pH 1.8, and containing 2.5 g U/l, was contacted with the mixed solvent containing 0.1 M Alamine 336, a modifier, and the diluent, at an A/O of 2/1.

Figure 14(a,b) show the effect of the modifier and of the diluent on the extraction of uranium and on the phase separation rates. In extraction, the two diluents for the same modifier gave values of extraction which were within 0.5 g U/l. Of the modifiers evaluated, 2-ethylhexanol resulted in the highest loading, with isodecanol slightly lower (Figure 14a). However, as regards primary phase disengagement time, the isodecanol was the fastest, with nonylphenol taking slightly longer (Figure 14b). TBP would obviously not be used in such a system, because of its long separation time as well as low loading that resulted. In Figure 14c are shown the relative rates for the secondary phase separation during extraction. Again, isodecanol is exceptionally fast compared to the other modifiers. Although TBP was unsuitable because of the long primary break time, it was better than the other two modifiers for the secondary break time. All modifiers were about equal at about 20-30 seconds for the primary and secondary break times on stripping. These examples illustrate the fact that a modifier cannot be selected indiscriminately.

DISCUSSION AND CONCLUSIONS

The object in this paper has not been to solve the problem of diluent and modifier selections, but rather to at least provide sufficient data to show that the choice of the diluent or modifier should not be arbitrary. A complete understanding of the mechanism of the reactions involved in the use of the diluent and modifier is not known. However, by means of a minimum number of tests, one may select the best diluent or modifier

in that particular process, based on the chemical components of the diluent, or the physical characteristics such as the dielectric constant, polar nature of the diluent, and solubility parameter. The effect of the modifier and diluent in the extraction process can differ greatly from that found in the scrubbing and stripping operations, both from the standpoint of mass transfer and kinetics, and also from the aspect of phase disengagement and solvent entrainment tendency. The rate of phase disengagement may, in the final analysis, be the determining factor in the selection of the diluent and modifier for that particular system.

The choice cannot be made on the basis of physical parameters of the diluent or modifier. Because of the nature of the aqueous feed solution, as well as the extractant being used, and the extracted species, it may be necessary therefore to conduct a limited number of tests before the diluent and modifier are chosen. Obviously cost of the reagents, together with their physical properties of flash point, density, viscosity, and the effect on extraction, scrubbing and stripping characteristics and phase disengagement properties will need to be considered. Also, occasionally metal selectivity can be improved by the proper choice of the diluent and modifier.

The influence of the polar nature of the diluent can affect extractability, in that increase in polarity results in a decrease in extraction. The influence of the dielectric constant on the extractability of metals, or the separation of one metal from one another, would appear to be minimal if the extractant is in a diluent of the commercial kerosene type. However, with

other possible diluents having higher dielectric constants, such as cyclohexane, MIBK, cumene, butanol, etc., then with an increase in the dielectric constant a decrease in the extractability results. The proper selection of the diluent with respect to its composition of aromatics, paraffins, or naphthenes can greatly influence extractability and separation of metals, more in some systems than in other systems. With the cation exchange systems, an increase in aromaticity results in a decrease in extractability while for the anion exchange and solvating processes, an increase in aromaticity results in an increase in metal extraction. The same is also true for the solubility parameter correlation with extractability.

Although modifiers are not as numerous as diluents, they nevertheless can be as difficult to select, because they do not appear to follow a definite pattern, compared to the diluents. The modifier evaluation therefore has to be done by testing in systems containing the actual feed solution, and making the choice based on this evaluation of its effects on extraction, scrubbing, stripping, metals separation, and phase disengagement.

The proper selection of the diluent and modifier can therefore affect:

- the size or choice of the contactor, as the kinetics of the extraction may be improved by the diluent and/or modifier choice.
- settler area, and therefore cost of solvent inventory for the extraction, scrubbing, and stripping sections

- equilibrium, and therefore efficiency of the system, resulting in more or less stages of extraction, scrubbing, and stripping.

One can't generalize on the selection of diluents and modifiers for all systems, and each particular process may have to be evaluated by testing actual leach solutions at the desired conditions of extraction, and using established criteria such as we have discussed for limiting the number of tests and therefore optimizing the diluent or modifier choice. Ideally, if the solvent system can be optimized early in the investigation, then proper choice of the equipment and subsequent design of the most economical plant can be facilitated.

ACKNOWLEDGEMENTS

The authors gratefully acknowledge the assistance of K. T. Price and J. B. Kearns of the Solution Treatment Section in the investigation, and J. B. Zimmerman, V. Reynolds, D. Sheldrick and R. Pugliese of the Chemical Analysis Section for the analyses.

REFERENCES

1. Tremblay, R., and Bramwell, P., *Trans. C.I.M.M.*, 62, No. 44, 44-53 (1959).
2. Kertes, A.S., "Solvent Extraction Chemistry of Metals" Ed. McKay, p. 377.
3. Taube, M., *J. Inorg. Nucl. Chem.*, 12, 174 (1959).
4. Rozen, A.M., "Solvent Extraction Chemistry", Proceedings of the International Conference, Goteborg, 1966, pp. 195-235, North-Holland Pub. Co., 1967.
5. Siddall, T.H., *J. Inorg. Nucl. Chem.*, 13, 151 (1960)
6. Mills, A.L., Logan W.R., "Solvent Extraction Chemistry", Eds., Dyrssen, D., Liljenzin, J.O., and Rydberg, J., North-Holland, Amsterdam, 1967, p. 322.
7. Coleman, C.F., Brown, K.B., Moore, J.G., and Crouse, D.J., *Ind. Eng. Chem.* 50, p. 1756 (1958).
8. Coleman, C.F., *Atomic Energy Rev.* 2, 3 (1964).
9. Indikov, E.M., Solovkin, A.S., Teterin, E.G., and Shesterikov, N.N., *Zh. Neorg. Khim.*, 8, 2187 (1963).
10. Sekine, T., and Dyrssen, D., *J. Inorg. Nucl. Chem.*, 29, 1489 (1967).
11. Healy, T.V., *Nucl. Sci. Eng.*, 16, 413 (1963).
12. Healy, T.V., *J. Inorg. Nucl. Chem.*, 19, 328 (1961).
13. Bauer, D.J., and Linstrom, R.E., USBM RI-7524, June 1971.
14. Myasoedov, B.F., Chmutova, M.K., and Lebedev, I.A., Proceedings of the International Solvent Extraction Conf., The Hague, April, 1971, pp. 815-819, Pub Society of Chemical Industry, London, 1971.
15. Muller, W., and Diamond, R.M., *J. Phys. Chem.*, 70, 3469 (1966).
16. Muller, W., and Duyckaerts, G., *Eurtom Rep EUR-2246* (1965).
17. Desreux, J.F., Proceedings of the Int. Solvent Extraction Conf., The Hague, April, 1971, pp. 1328-1332. Pub Society of Chemical Industry, London, 1971.
18. Ferraro, J.R., *Appl. Spectrosc.*, 17, 12 (1963).

19. Blake, C.A., from Peaceful Uses of Atomic Energy, United Nations, Sen. Conf., 1958, 28/289, pg. 188.
20. De, Anil K., and Ray, Uday Sankari, Separation Science, 6, pp. 443-450, June 1971.
21. Ashbrook, A.W., and Ritcey, G.M., Eldorado Nuclear Ltd., Ottawa. Report TB 65-10 (1965).
22. Ritcey, G.M., and Ashbrook, A.W., U.S. Patent 3,399,055 (Aug. 1968), Presented at Annual Meeting, AIME, San Francisco Feb 1972.
23. Murry, K.J., and Bouboulis, C.J., E/MJ, pp 74-77, July 1973.
24. "Parameters of Solubility", Esso Chemicals Publication.
25. Ritcey, G.M., and Lucas, B.H., Proceedings of the International Solvent Extraction Conference, The Hague, 1971, pp. 463-475, Pub. Society of Chemical Industry, London, 1971.
26. Ashbrook, A.W., and Ritcey, G.M., "The Eldorado Process for the Separation of Cobalt and Nickel by Liquid-Liquid Extraction from Acid Solution", Presented at the Fifth Conference of Metallurgists, Aug. 29-31, 1966, Toronto.
27. Ritcey, G.M., Canadian Institute of Metallurgy, CIMM Trans. LXXVI, pp. 71-79, 1973.

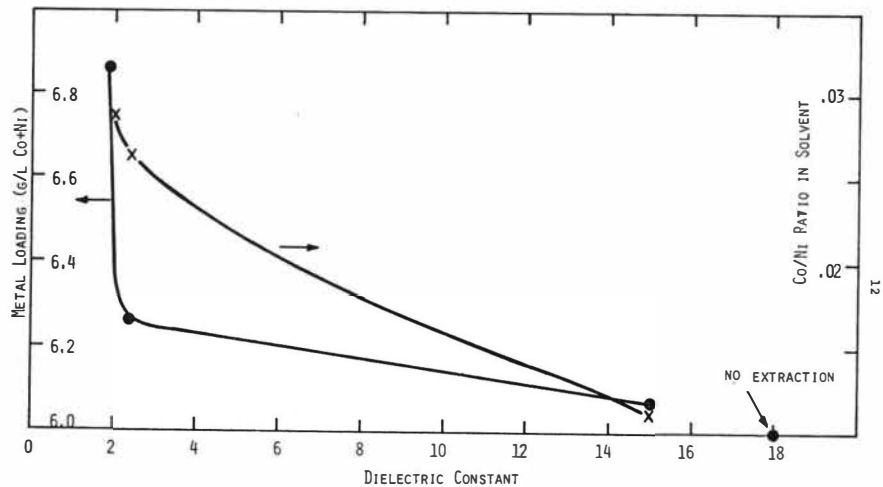


FIG. 1 DIELECTRIC CONSTANT AND EXTRACTION OF COBALT AND NICKEL FROM ALKALINE SOLUTION WITH DEHPA

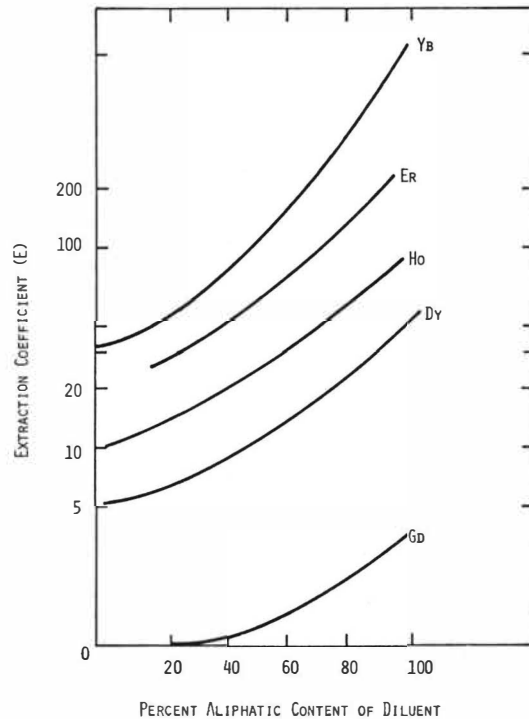


FIG. 2 EFFECT OF ALIPHATIC CONTENT OF DILUENT ON THE EXTRACTION OF RARE EARTHS WITH DEHPA

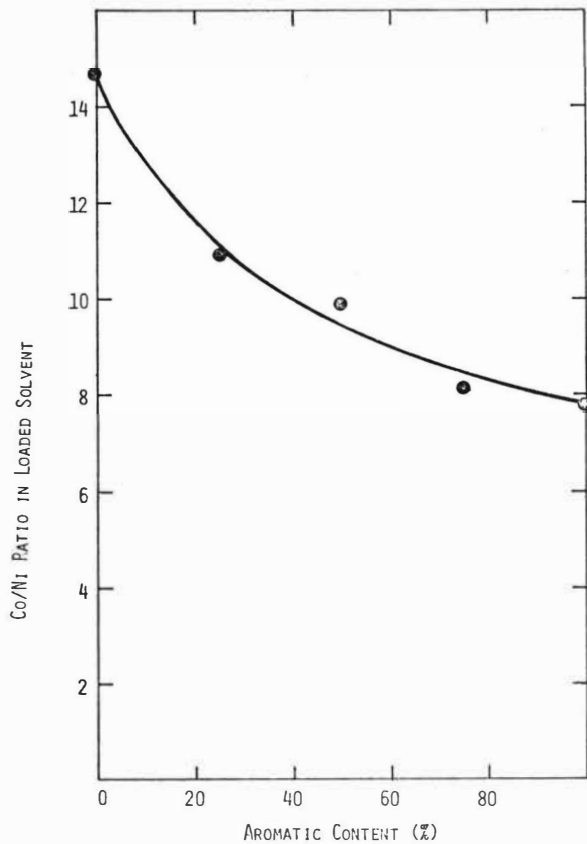


FIG. 3 EFFECT OF AROMATIC CONTENT ON SEPARATION OF COBALT FROM NICKEL WITH DEHPA

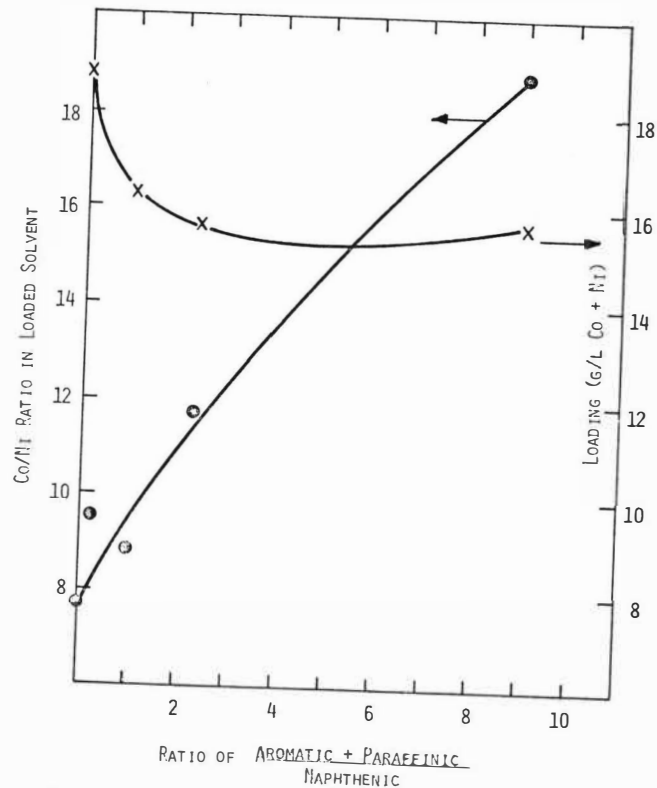


FIG. 4 INFLUENCE OF COMPONENTS OF DILUENT ON THE Co/Ni SEPARATION

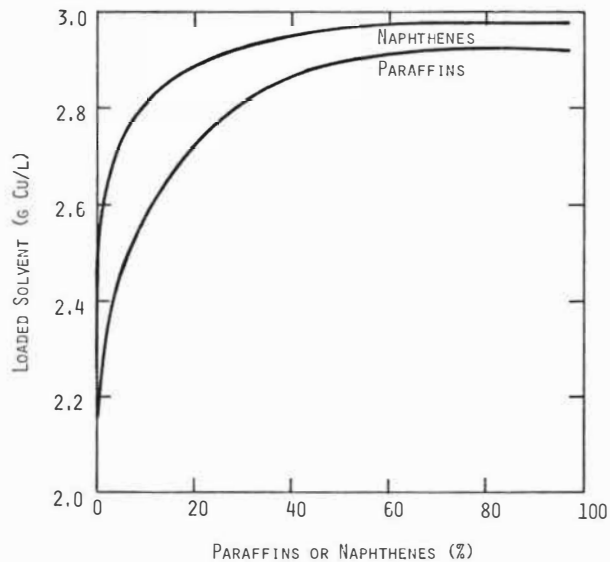


FIG. 5 EFFECT OF NAPHTHENES AND PARAFFINS ON EXTRACTION OF COPPER WITH LIX64N

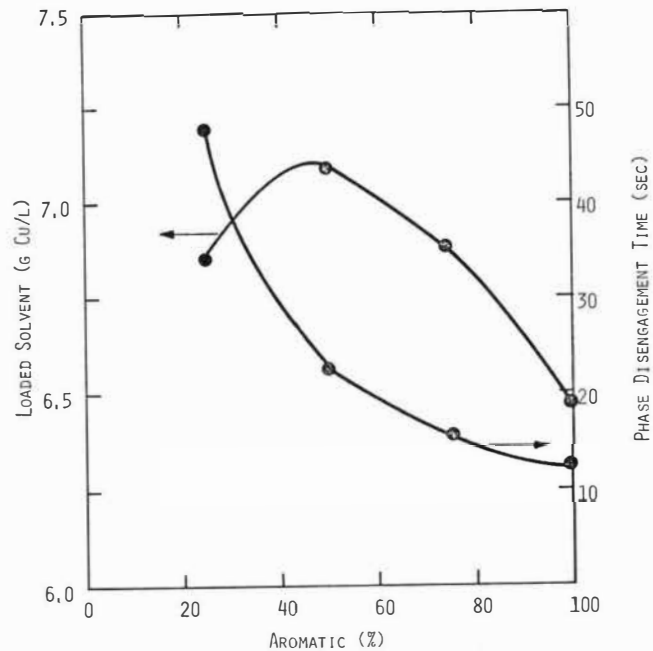


FIG. 6 EFFECT OF AROMATICITY ON EXTRACTION OF COPPER AND PHASE SEPARATION RATE USING KEXEL 100

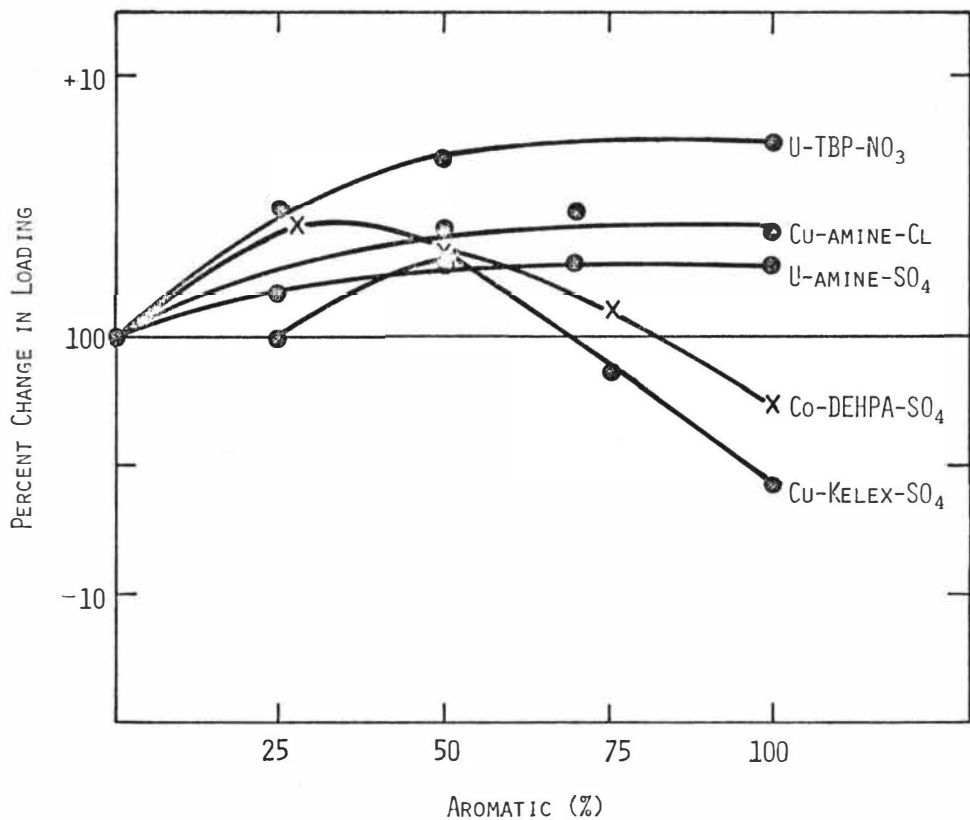


FIG. 7 EFFECT OF MECHANISM OF EXTRACTION AND AROMATICITY ON EXTRACTABILITY

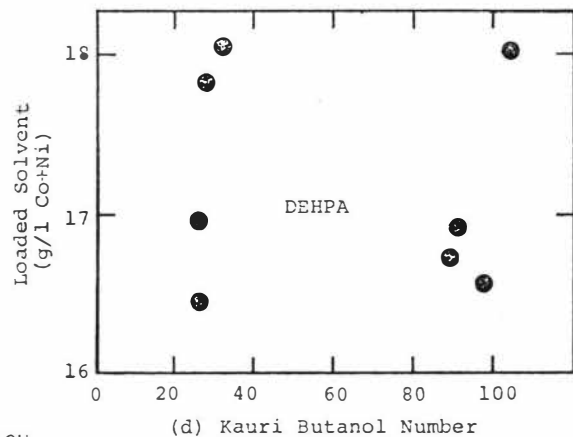
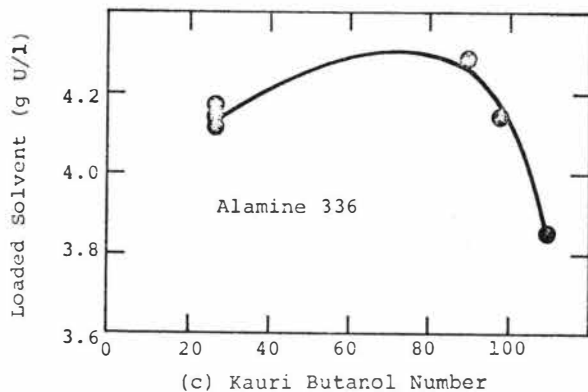
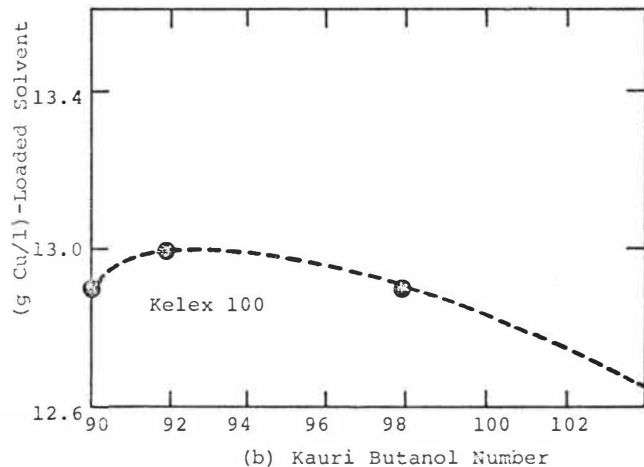
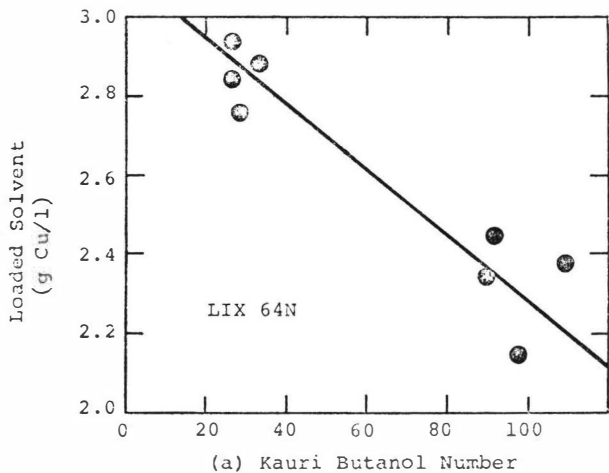


FIG. 8 EFFECT OF KAURI BUTANOL NUMBER ON EXTRACTION

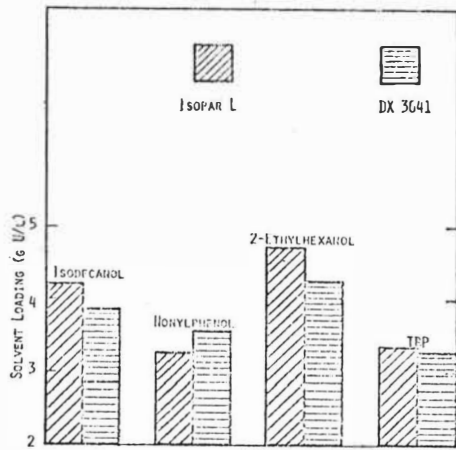


Fig. 14(a) Effect of Modifier and Diluent on Extraction of Uranium with Alamine 336

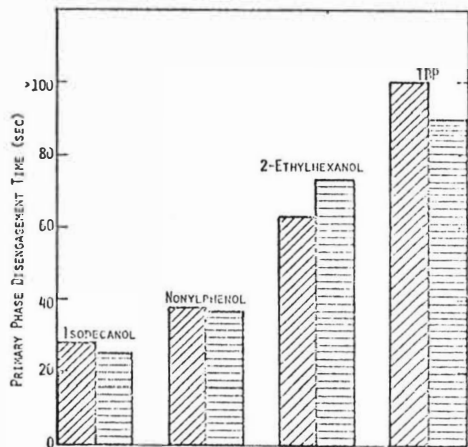


Fig. 14(b) Effect of Modifier and Diluent on Primary Phase Separation in Extraction

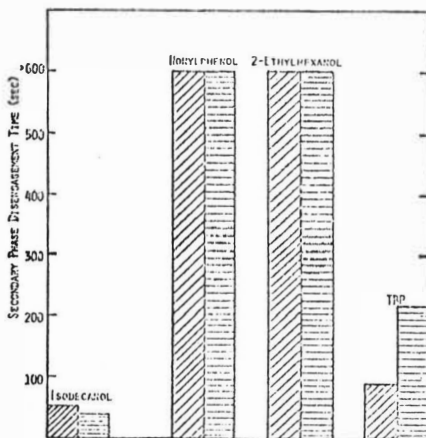


Fig. 14(c) Effect of Modifier and Diluent on Secondary Phase Separation in Extraction

FIGURE 14

MASS TRANSFER OF WATER FROM SINGLE AQUEOUS SOL DROPLETS
FLUIDIZED IN A PARTIALLY MISCIBLE ALCOHOL*

S. D. Clinton
Oak Ridge National Laboratory
Oak Ridge, Tennessee 37830

ABSTRACT

During the preparation of sol-gel microspheres, droplets of the aqueous sol must be suspended or fluidized in an organic phase until enough water is extracted from the sol to cause gelation. The rate of mass transfer was investigated by fluidizing single water or thoria sol droplets in a partially miscible alcohol and measuring their diameters as a function of time. Three alcohols were studied: 2-ethyl-1-hexanol, 2 methyl-1-pentanol, and n-hexanol. The first alcohol was studied at 25, 40, and 50°C, whereas the remaining two were studied at 25°C only. The Schmidt numbers for these systems ranged between 5,000 and 36,000, and the sphere Reynolds number varied from 0.2 to 30.

A surface-active agent, Ethomeen S/15, was added to the organic phase to produce a rigid liquid drop with no induced circulation. By relating the tangential velocity at the drop interface to the sphere drag coefficient, an expression for the Sherwood number was derived and then confirmed experimentally for both water and sol drop data.

*Research sponsored by the U. S. Atomic Energy Commission under contract with the Union Carbide Corporation.

An explicit relationship for the mass transfer coefficient was shown to be independent of the drop diameter, and an expression was obtained to predict the gelation times of thoria sol droplets from known sol and solvent properties.

INTRODUCTION

The sol-gel process which was developed at the Oak Ridge National Laboratory is a method for preparing a wide variety of ceramic fuel materials for use in nuclear reactors. As compared with conventional preparation procedures, the sol-gel process has the distinct advantage of low calcination temperature for obtaining particles of near-theoretical density.¹

The original objective of the sol-gel process was to produce thorium-uranium fragments suitable for vibratory compaction in metal tubes; however, during the past ten years, emphasis has been shifted toward the preparation of spherical particles, or microspheres. Pyrolytic-carbon-coated microspheres of thorium and uranium oxides, 200 to 400 microns in diameter, are the proposed fuel materials for certain high-temperature, gas-cooled reactor designs. These microspheres are prepared by dispersing uniformly sized drops of the appropriate sol into a partially miscible alcohol such as 2-ethyl-1-hexanol (2EH). The sol droplets must be fluidized in the organic phase until enough water is extracted from the aqueous sol to cause gelation. After drying, the gelled microspheres are calcined at 1150°C to produce an oxide product having a density within 1% of theoretical.²

The transfer of mass from systems of spheres to a surrounding fluid has been investigated rather extensively by studying single spheres suspended in a controlled flow of liquid or gas. Mass transport between a suspended fluid sphere and its surroundings can usually be separated into three categories: (1) transfer within the sphere, (2) transfer through the interface, and (3) transfer

outside the sphere. The aim of this study is to characterize mass transfer from a fluidized liquid drop in which the rate limiting resistance is located outside the sphere.

Many experimental data on forced-convection mass transfer from solid spheres have been correlated by a relationship for the Sherwood number involving the product of $N_{Re}^{1/2}$ and $N_{Sc}^{1/3}$.³⁻⁶ Although the exponent for the Reynolds number can be assumed to be constant and equal to 1/2, there is an accumulation of evidence to indicate that the exponent for the sphere Reynolds number varies with N_{Re} , increasing from 1/3 in the Stokes' law regime to 2/3 in the fully turbulent region.⁷ Despite the extensive investigations with single spheres, the available information is inadequate to establish a universal relationship for the mass transfer coefficients.^{8,9}

As compared with solid spheres, forced-convection mass transfer from liquid drops is complicated because conditions at the interface can induce internal circulation of the drop. Although numerous relationships are available for varying degrees of mobility of the drop surface,¹⁰ the actual mass transfer process can be very complex and may involve effects of interfacial turbulence varying from mild circulation near the interface to spontaneous emulsification.¹¹ In the past, some investigators have tried to attribute unexpected mass transfer results to a significant interfacial resistance caused by the accumulation of high-molecular-weight materials at the interface.¹² From later studies with liquid-liquid systems, however, it has become increasingly evident that, instead of acting as interfacial barriers, surface-active agents merely modify the drop hydrodynamics.¹³

In contrast with the situation for gases, the theory of the liquid state is only partly developed; and the existing theories do not provide as good a basis for the prediction of diffusion coefficients as the available empirical equations. Sherwood and Reid¹⁴ have recommended that the diffusivity of water in organic solvents be estimated by calculating a value from the Wilke-Chang relationship¹⁵ and then dividing the results by 2.3. Previously, the comparison of calculated and experimental values for the diffusivity of water in different organic solvents had led Olander¹⁶ to suggest this factor of 2.3. Olander concluded that, as a diffusing species in an organic solvent, water has a molar volume four times larger than expected due to polymerization of the molecules.

In the present study,¹⁷ single water or thoria sol drops were fluidized in three different alcohols: 2EH, 2-methyl-1-pentanol (2MP), and n-hexanol (nH). The droplet diameter and the fluidizing flow rate were measured as a function of time. The controllable variables in each run were initial drop diameter, initial sol molarity, organic-phase temperature, and water concentration in the organic phase. A surface active agent was added to the organic phase to produce a rigid aqueous drop. The objectives of this study were to determine mass transfer coefficients for the transport of water into the organic phase and to develop a correlation to predict drop gelation times from known sol and organic-phase properties.

At 25°C the controlling mass transfer resistance for a thoria sol droplet fluidized in 2EH was shown to be in the organic-phase film surrounding the drop.¹⁸ With this model, the mass transfer coefficients for a water drop and a sol drop will be equal under identical hydrodynamic conditions. The amount of solvent that can be transferred into the aqueous drop is inconsequential; therefore, the change in drop diameter is a direct measure of the amount of water transferred into the organic phase. The mass flux can be related to the measured change in drop diameter with time, as follows:

$$N = - \frac{\rho_w}{\pi D_p^2} \left(\frac{\pi}{6} \right) \frac{d(D_p^3)}{dt} = - \frac{\rho_w dD_p}{2dt} = K(C_s - C_o) \quad (1)$$

During gelation the mass transfer resistance within a thoria sol drop will be negligible if water can be supplied to the interface rapidly enough to maintain C_s at saturation.

When the controlling mass transfer resistance is in a thin continuous-phase film surrounding the drop, the steady-state, convective-diffusion equation for the solute in natural curvilinear coordinates (see Figure 1) is:

$$u \frac{\partial C}{\partial x} + v \frac{\partial C}{\partial y} = D_v \frac{\partial^2 C}{\partial y^2} \quad (2)$$

In Equation (2), tangential diffusion is assumed to be negligible. In the immediate vicinity of the drop, the continuity equation for the continuous phase is:

$$\frac{\partial(ur)}{\partial x} + \frac{\partial(vr)}{\partial y} = 0 \quad . \quad (3)$$

Friedlander¹⁹ has suggested that the thin concentration boundary layer approximation is valid for Peclet numbers greater than 10^2 . Since the Schmidt numbers in this study are greater than 5,000, the approximation should apply for Reynolds number values greater than 0.02.

Because of the large Schmidt numbers, the concentration boundary layer thickness should be an order of magnitude thinner than the corresponding momentum boundary layer. Consequently, the entire concentration gradient will occur in the immediate vicinity of the drop surface, and for a rigid interface, the tangential velocity can be represented approximately by:

$$u = u_i' y \quad . \quad (4)$$

After substituting Equation (4) into (3) and integrating with respect to y , the following relationship is obtained for the radial velocity component:

$$v = -\frac{1}{r} \frac{\partial}{\partial x} \left(r u_i' \frac{y^2}{2} \right) \quad . \quad (5)$$

Using Equations (4) and (5) for the tangential and radial velocity components, Equation (2) can be integrated to obtain the solute concentration profile in the thin continuous-phase film. By the application

of Fick's law, the resulting concentration gradient at the drop interface can be related to the Sherwood number as follows:^{20,21}

$$N_{Sh} = 0.641 N_{Pe}^{1/3} \left[\int_0^\pi \left(\frac{D_p u'_i}{2U} \right)^{1/2} (\sin \theta)^{3/2} d\theta \right]^{2/3} \quad (6)$$

By defining an average value of u'_i which can be treated as a constant, Equation (6) can be integrated to give:

$$N_{Sh} = 0.738 N_{Pe}^{1/3} \left[\left(\frac{D_p}{U} \right)^{1/2} (u'_i)_{avg}^{1/2} \right]^{2/3} \quad (7)$$

For the Reynolds number range of interest in this study (0.2 to 30), an expression for $(u'_i)_{avg}$ can be approximated from basic fluid-flow data. The drag coefficient for flow around a sphere is defined by the following relationship:

$$F = \frac{f_D}{g_c} \left(\frac{\rho_s U^2}{2} \right) \left(\frac{\pi}{4} D_p^2 \right) \quad (8)$$

Since the drag coefficient for a sphere, f_D , is a function of Reynolds number only, the following expression can be used to describe the drag coefficient for a limited Reynolds number range:

$$f_D = A N_{Re}^a \quad (9)$$

where A is a constant (24 for the Stokes' law region) and the exponent, a , varies from -1 for $N_{Re} < 0.1$ to 0 for $N_{Re} > 1000$. The force exerted on the sphere by the flowing fluid can be separated into two categories: form drag and frictional drag. By summing the tangential shear stress over the drop surface in the direction of flow, the drag force due to friction for a Newtonian fluid is:

$$F_{\text{friction}} = \frac{\pi \mu_s}{2g_c} D_p^2 \int_0^\pi u_i' \sin^2 \theta \, d\theta \quad (10)$$

By defining a second average value of u_i' , Equation (10) can be integrated to give:

$$F_{\text{friction}} = \frac{\pi^2 \mu_s}{4g_c} D_p^2 (u_i')_{\text{AVG}} \quad (11)$$

For the Stokes' law region, the ratio of friction drag to the total drag force is $2/3$. Jenson²² has calculated this ratio to be 0.66, 0.64, 0.63, and 0.60 for sphere Reynolds numbers of 5, 10, 20, and 40, respectively. Assuming $F_{\text{friction}} = (2/3)F$, Equations (8), (9), and (11) can be combined to give:

$$(u_i')_{\text{AVG}} = \frac{A N_{Re}^a \rho_s U^2}{3 \pi \mu_s} \quad (12)$$

For the Stokes' law region where $u_i' = (3 U/D_p) \sin \theta$, it can be shown that $(u_i')_{\text{AVG}} = 1.05 (u_i')_{\text{avg}}$. Assuming that the averaging techniques

can be extrapolated to larger Reynolds numbers, the combination of Equation (7) and (12) gives:

$$N_{Sh} = 0.344 A^{1/3} N_{Re}^{(2+a)/3} N_{Sc}^{1/3} \quad (13)$$

Since the numerical coefficient in Equation (13) has been calculated using two assumptions from the Stokes' law region, it would appear logical to let $A = 24$; then Equation (13) would become:

$$N_{Sh} = 0.99 N_{Re}^{(2+a)/3} N_{Sc}^{1/3} \quad (14)$$

where the value of a must be determined from experimental drag coefficient data.

A simplified expression can be obtained for the mass transfer coefficient by eliminating the fluidizing velocity from Equation (13). With F equal to the weight of the aqueous drop in the continuous phase, the following expression is obtained from Equation (8) for the solvent fluidizing velocity:

$$U^2 = \frac{4g D_p (\rho_p - \rho_s)}{3 f_D \rho_s} \quad (15)$$

Substituting Equation (9) into Equation (15) for the drag coefficient, an explicit relationship can be obtained for the fluidizing velocity. Using this result in Equation (13) gives:

$$K = 3.76 \frac{D^{2/3}}{\mu_s^{1/3}} (\rho_p - \rho_s)^{1/3} \quad (16)$$

For a given system and temperature, Equation (16) predicts that the mass transfer coefficient for a fluidized rigid sphere is dependent only on the density difference of the drop and the continuous phase.

By expressing the drop diameter and density as a function of the sol molarity, an expression can be derived from Equations (1) and (16) to predict the gelation time of any sol drop when the controlling mass transfer resistance is in the continuous phase. For a temperature range of 25 to 50°C, the density difference of the thoria sol drop and the solvent for the alcohol systems in this study is:

$$\rho_p - \rho_s = 0.238 M_p + 0.175 \quad (17)$$

The diameter of a sol drop can be related to the molarity of the thoria sol by the following equation:

$$D_p = \left(\frac{M_c}{M_p} \right)^{1/3} D_c \quad (18)$$

where the calculated value of M_c is 37.9. By using Equations (16), (17), and (18), Equation (1) can be integrated to give the following expression for gelation time (in minutes):

$$\theta_G = 2.5 \times 10^{-3} \frac{\mu_s^{1/3} D_c}{D_v^{2/3} (C_s - C_o)} \int_{M_I}^{M_G} \frac{d M_p}{M_p^{4/3} (0.238 M_p + 0.175)^{1/3}} \quad (19)$$

The sol molarity integral function in Equation (19) was evaluated, and values of the integral are tabulated in Table 1. For a desired theoretically dense sphere size, Equation (19) can be used to determine the required fluidization time for a given initial sol molarity and concentration of water in the bulk solvent. Since the value of the integral function is relatively small for the variation in molarity from 12 to 20, the exact gel molarity for a particular system is not necessary in order to obtain a reasonable estimate of the gelation time.

EXPERIMENTAL DATA

The primary purpose of the experimental equipment used in this study was to measure the diameter of a fluidized aqueous drop as a function of time. Basically, the equipment consisted of a tapered Plexiglas column, a light source, a photomacro lens positioned to magnify the drop by a factor of 20 on a ground-glass viewing screen, a Polaroid attachment, a timer, a centrifugal pump to circulate the alcohol, a rotameter, a heat exchanger, and a constant-temperature circulating water system.

The 8-in.-long tapered column was machined from a block of Plexiglas with a convergent-divergent flow channel. A vertical, laminar velocity profile was developed in the convergent section so that each aqueous drop could be fluidized along the central axis of the divergent column

with no horizontal motion. The vertical position of the fluidized drop was controlled by the alcohol flow rate, and all measurements were obtained at an inside column diameter of 0.635 cm.

The general procedure for each experimental run was to form and fluidize a single aqueous sol drop in the desired alcohol and then to measure the alcohol flow rate and drop diameter (to within ± 10 microns) until shrinkage no longer occurred. The independent variables in each experimental run were: initial drop diameter, 0.08 to 0.22 cm; initial sol molarity, 0 to 2.5 M thoria; solvent, 2EH, 2MP, or nH; solvent temperature, 25 to 50°C; and water concentration in the bulk solvent, 0 to 50% of saturation. A surface-active agent, Ethomeen S/15 (a tertiary amine marketed by Armour Industrial Chemical Company), was added to the organic phase in sufficient concentration (0.01 to 1.0 vol %) to produce a rigid liquid drop having no induced circulation.

The diameters of fluidized drops of water and thoria sol were measured, as a function of time, in a series of 131 runs. Typical data obtained for single water drops fluidized in nH at 25°C are shown in Figure 2. The concentration of water in the nH was 27 mg/cc, and the surfactant concentration was 1.0 vol %. The constant slope of the water-drop-diameter data with time indicates a constant mass flux of water from the drop.

Typical diameter data for single thoria sol drops fluidized in 2EH at 50°C are shown in Figure 3. The initial molarity of the thoria sol was 1.1, the concentration of water in the 2EH was 11 mg/cc, and the surfactant concentration was 0.01 vol %. The slope of the diameter data, which is proportional to the mass flux or the mass transfer coefficient, increases with increasing sol molarity. At the gelation

time, the apparent mass transfer rate becomes zero. The thoria gelation concentration varied from 13 to 18 \underline{M} and was a function of the particular alcohol system and surfactant concentration.

For each diameter measurement, a characteristic fluidizing velocity was calculated by the following equation:

$$U = \frac{8 Q}{\pi(D^2 - D_p^2)} \quad (20)$$

The diffusion coefficients of water in the different alcohols were calculated by using the recommendation of Reid and Sherwood.¹⁴ Values of mass diffusivity, Schmidt number, and water solubility for the alcohol systems are given in Table 2.

RESULTS

The mass transfer data for the water and sol drop runs were correlated by plotting the logarithm of the Sherwood number divided by the Schmidt number raised to the 1/3 power against the logarithm of the Reynolds number (see Figure 4). The sphere Reynolds number varied from 0.2 to 30, and the Schmidt numbers for the different alcohol systems ranged between 5,000 and 36,000. A least-squares line was calculated for each of the 43 water drop runs (1785 data points), and the solid line in Figure 4 was obtained by averaging all of the least-squares constants. The equation for the solid line is:

$$N_{Sh} = 0.980 N_{Re}^{0.417} N_{Sc}^{0.333} \quad (21)$$

and the standard deviations in the coefficient and the Reynolds number exponent are 0.043 and 0.015, respectively. In Figure 4, all of the water

Figure 4 shows the data points with two parallel dashed lines which indicate a ± 10 percent variation from Equation (21). The data points in Figure 4 represent all of the sol drop runs at thoria molarities from 0.85 to 18. Despite the increased scatter in the thoria data, the mass transfer coefficients for both sol and water drops appear to be equal at a particular value of the sphere Reynolds number.

To test the validity of Equation (16), which is an explicit expression for the fluidized-drop mass transfer coefficient, the experimental rigid-drop data are shown in Figure 5. The ordinate is the product of the mass transfer coefficient and the solvent viscosity raised to the 1/3 power, divided by the mass diffusivity to the 2/3 power; the abscissa is the density difference for the aqueous drop and the solvent. The 43 water drop runs are located within a density difference of 0.17 to 0.18 g/cc, and the 408 sol drop data points are located within a density difference range of 0.4 to 4 g/cc. The equation of the least-squares line through all of the mass transfer data is:

$$K = 3.48 \frac{D_v^{2/3}}{\mu_s} (\rho_p - \rho_s)^{0.347} \quad (22)$$

In Figure 5, the solid line is Equation (22) and the two parallel dashed lines indicate a ± 10 percent variation. The single dotted line in Figure 5 is the theoretical prediction of Equation (16).

As predicted by Equation (19), the experimentally determined gelation times for the sol drop runs were plotted against the proposed function of sol and solvent properties (see Figure 6). The solid line in Figure 6 was determined by applying the method of least squares to the 88 data points. The slope and the intercept of the least-squares line are

2.72×10^{-3} and -0.06 min, respectively. The average error between the least-squares line and the experimental gelation times for the sol drop runs is ± 4.5 percent.

DISCUSSION OF RESULTS

The hydrodynamic data for the fluidized rigid water drop runs were correlated to determine the coefficient and exponent in Equation (9). A least-squares line was calculated for each run, and the following equation is the result of averaging the least-squares constants for all 43 runs:

$$f_D = 33.7 N_{Re}^{-0.749} \quad (23)$$

The standard deviations in the coefficient and the exponent of Equation (23) are 4.3 and 0.046, respectively. In this study, the ratio of the drop diameter to the column diameter ranged from 0.06 to 0.35. The flow restriction imposed by the column wall effectively decreases the infinite medium fluidizing velocity, resulting in an increased drag coefficient for a given sphere Reynolds number.

By applying the experimental data of Equation (23) to Equation (13), the predicted Reynolds number exponent for mass transfer is $(2 + a)/3 = 0.417 \pm 0.015$, which agrees precisely with the average measured result [see Equation (21)]. In general, the measured Reynolds number exponent for mass transfer is greater than the average value for the N_{Re} range of 2 to 30 and less than the average value for N_{Re} between 0.2 and 3. These results support the theory that the Reynolds number exponent for mass transfer varies with N_{Re} , increasing from $1/3$ where Stokes' law is applicable to $2/3$ for N_{Re} greater than 1,000.

With Equation (13) the value of the coefficient predicted from hydrodynamic data is $0.344 A^{1/3} = 1.11 \pm 0.05$, whereas the average measured value is 0.980 ± 0.048 [see Equation (21)]. From Equation (14) with $A = 24$ (Stokes' law region with unbounded flow), the value of the predicted coefficient is 0.99. Since the coefficient in Equation (13) is based on a constant fraction, $2/3$, of the total drag for unbounded flow, then the fraction of total drag due to friction should be reduced for flow restricted by a column wall. Consequently, the use of $A = 24$ in deriving Equation (14) is more justifiable than using an experimentally determined value with bounded flow (i.e., $A = 33.7$).

The preceding reasoning is also consistent with the theoretical and experimental mass transfer coefficient expressions, Equations (16) and (22). If the fluidizing velocity of a drop is reduced by 20 percent as the result of the effects of a column wall, then Equation (14) predicts that the mass transfer coefficient will be reduced by 8 percent ($1.20^{0.417} = 1.08$) independent of the value of the equation coefficient. Conversely, the functional variables in Equations (16) and (22) are independent of the fluidizing velocity, and the effect of the column wall must appear in the equation coefficients. Equation (16) theoretically predicts the mass transfer coefficient for a fluidized drop in an unbounded flow field, whereas Equation (22) is the experimental mass transfer coefficient correlation for a drop fluidized within a column wall. Consequently, the experimentally determined equation coefficient of 3.48 is 8 percent lower than the theoretical value of 3.76. Comparison of Equations (16) and (22) over the experimental density difference range (0.17 to 4 g/cc) shows that the 4 percent variation in the density different exponent contributes a maximum variation of only 2 percent in the predicted and measured mass transfer coefficient values.

The greater variation in the sol drop data for mass transfer can be attributed, for the most part, to the nonspherical shape achieved by the drops during some stage of the gelation process. Shape distortion was most apparent in runs where a large sol drop diameter and a high concentration of surfactant in the alcohol were used. As compared with 2EH, 2MP and nH required a higher concentration of Ethomeen S/15 to prevent drop circulation. Although a higher Ethomeen S/15 concentration has little apparent effect on the water-alcohol interface, the interfacial tension at the sol-alcohol interface is significantly lowered. With increased surfactant concentration, the resulting decrease in interfacial tension permitted a fluidized sol drop to become somewhat ellipsoidal during gelation. The higher Ethomeen S/15 concentration in the alcohol has no effect on the observed mass transfer rate; however, the molarity of the gelled product is apparently decreased.

In spite of the sphericity problem associated with sol drops, about 90 percent of the sol drop mass transfer data lies within the limits of the water drop data (see Figure 4). The agreement of sol and water drop Sherwood numbers for identical Reynolds numbers confirms that the limiting mass transfer resistances for fluidized-rigid sol and water drops are equal.

The gelation times of sol drops can be predicted from sol and solvent properties with sufficient accuracy to justify any engineering design calculations. The increased slope, 2.7×10^{-3} , in Figure 6 as compared with the predicted value of 2.5×10^{-3} in Equation (19) can be attributed directly to the 8 percent variation between the theoretical and experimental expressions for the mass transfer coefficient, Equations (16) and (22). Theoretically, the time intercept should approach zero as the value of D_c becomes infinitesimally small. Since the experimental

gelation times were determined to the nearest even tenth of a minute, the calculated intercept of -0.06 min for the data in Figure 6 can be neglected.

CONCLUSIONS

The following conclusions can be drawn from this study with regard to the mass transfer of water from aqueous droplets fluidized in a partially miscible alcohol:

1. The addition of a surface-active agent to the organic phase can produce a rigid aqueous drop with no induced circulation.
2. During the process of gelation, the controlling mass transfer resistance for a thorium sol drop is located in the organic phase surrounding the drop.
3. The forced convection mass transfer correlation for a fluidized drop can be predicted from theoretical considerations and hydrodynamic data.
4. The mass transfer coefficient for a rigid fluidized drop is a function of the mass diffusivity, the solvent viscosity, and the drop and solvent density difference.
5. The required gelation time for a fluidized rigid sol drop can be predicted from the properties of the aqueous sol and the solvent.

LIST OF REFERENCES

1. Ferguson, D. E., Dean, O. C., and Douglas, D. A., "The Sol-Gel Process for the Remote Preparation and Fabrication of Recycle Fuels," A/Conf. 28/P/237, presented at the Third International Conference on the Peaceful Uses of Atomic Energy, held in Geneva, Switzerland, Aug. 31-Sept. 9, 1964.
2. Haas, P. A., and Clinton, S. D., "Preparation of Thoria and Mixed-Oxide Microspheres," Ind. Eng. Chem., Prod. Res. Develop. (1966), 5, 236.
3. Garner, F. H., and Grafton, R. W., "Mass Transfer in Fluid Flow from a Solid Sphere," Proc. Roy. Soc. (London) (1954), A224, 64.
4. Garner, F. H., and Kee, R. B., "Mass Transfer from Single Solid Spheres," Chem. Eng. Sci. (1958), 9, 119.
5. Garner, F. H., and Suckling, R. D., "Mass Transfer from a Soluble Solid Sphere," A.I.Ch.E.J. (1958), 4, 114.
6. Linton, M., and Sutherland, K. L., "Transfer from a Sphere into a Fluid in Laminar Flow," Chem. Eng. Sci. (1960), 12, 214.
7. Rowe, P. N., and Claxton, K. T., "Heat and Mass Transfer from a Single Sphere to Fluid Flowing Through an Array," Trans. Inst. Chem. Engr. (London) (1965), 43, T321.
8. Pritchard, C. L., and Biswas, S. K., "Mass Transfer from Drops in Forced Convection," Brit. Chem. Eng. (1967), 12, 879.
9. Rowe, P. N., Claxton, K. T., and Lewis, J. B., "Heat and Mass Transfer from a Single Sphere in an Extensive Flowing Fluid," Trans. Inst. Chem. Engrs. (London) (1965), 43, T14.
10. Griffith, R. M., "Mass Transfer from Drops and Bubbles," Chem. Eng. Sci. 12, 198.
11. Acrivos, A., Modern Chemical Engineering, 1963, Vol. 1, p. 89 [New York, Reinhold].
12. Sherwood, T. K., "Mass Transfer Between Phases," Thirty-Third Annual Priestly Lectures, 1959, pp. 72-80 [University Park, Pa., The Pennsylvania State University].
13. Chester, C. V., An Investigation of the Transfer of Uranyl Nitrate Across the Water-Tributyl Phosphate Interface by the Method of Photographic Photometry, ORNL-3109, Oak Ridge National Laboratory, Oak Ridge, Tennessee (1961).
14. Reid, R. C., and Sherwood, T. L., The Properties of Gases and Liquids, 1966, p. 543 [New York, McGraw-Hill].

15. Wilke, C. R., and Chand, P., "Correlation of Diffusion Coefficients in Dilute Solutions," A.I.Ch.E.J. (1955), 1, 264.
16. Olander, D. B., "The Diffusivity of Water in Organic Solvents," A.I.Ch.E.J. (1961), 7, 175.
17. Clinton, S. D., Mass Transfer of Water from Single Aqueous Sol Droplets Fluidized in a Partially Miscible Alcohol (Thesis), ORNL-TM-3771, Oak Ridge National Laboratory, Oak Ridge, Tennessee (1972).
18. Clinton, S. D., and Whatley, M. E., "Mass Transfer of Water from Single Thoria Sol Droplets Fluidized in 2-Ethyl-1-hexanol," A.I.Ch.E.J. (1972), 18, 486.
19. Friedlander, S. K., "A Note on Transport to Spheres in Stokes' Flow," A.I.Ch.E.J. (1961), 7, 347.
20. Baird, M. H. I., and Hamielec, A. E., "Forced Convection Transfer Around Spheres at Intermediate Reynolds Numbers," Can. J. Chem. Eng. (1962), 40, 119.
21. Lochiel, A. C., and Calderbank, P. H., "Mass Transfer in the Continuous Phase Around Axisymmetric Bodies of Revolution," Chem. Eng. Sci. (1964), 19, 471.
22. Jenson, V. G., "Viscous Flow Around a Sphere at Low Reynolds Numbers (<40)," Proc. Roy. Soc. (London) (1959), A249, 346.

LIST OF SYMBOLS

a	exponent in drag coefficient equation, dimensionless,
A	coefficient in drag coefficient equation, dimensionless,
C	local concentration of water in solvent, g/cc,
C ₀	concentration of water in bulk solvent stream, g/cc,
C _S	concentration of water in solvent at drop interface, g/cc,
D	column diameter, cm,
D _C	diameter of theoretically dense thoria sphere, cm,
D _P	diameter of aqueous drop, cm,
D _V	diffusion coefficient, cm ² /sec,
f _D	drag coefficient for flow around a sphere, dimensionless,
F	force exerted by fluid on sphere, dynes,
g	acceleration of gravity, cm/sec ² ,
g _C	dimensional constant, 1 g-cm/dyne-sec ² ,
K	mass transfer film coefficient, cm/sec,
<u>M_C</u>	molarity of theoretically dense thoria, moles/liter,
<u>M_G</u>	thoria molarity of gelled sphere, moles/liter,
<u>M_I</u>	initial thoria molarity of sol drop, moles/liter,
<u>M_P</u>	thoria molarity of sol drop, moles/liter,
N	mass flux of water from drop, g/cm ² -sec,
N _{Pe}	Peclet number, $\frac{D_P U}{D_V}$,
N _{Re}	sphere Reynolds number, $\frac{D_P \rho_S U}{\mu_S}$,
N _{Sc}	Schmidt number, $\frac{\mu_S}{\rho_S D_V}$,

N_{Sh}	Sherwood number, $\frac{KD}{D_v}$,
Q	volumetric alcohol flow rate, cc/sec,
r	radial distance from axis of symmetry to drop interface, cm,
r_p	radius of drop, cm,
t	time, sec,
u	tangential velocity component in x-direction, cm/sec,
u'_i	derivative of interfacial velocity with respect to y, 1/sec,
U	fluidizing velocity, cm/sec,
v	radial velocity component in the y-direction, cm/sec,
x	distance along drop from forward stagnation point, cm,
y	distance normal to interface in continuous phase, cm,
θ	polar angle measured from forward stagnation point, radians,
θ_G	gelation time, min,
μ_s	viscosity of solvent, g/cm-sec,
ρ_p	density of aqueous drop, g/cc,
ρ_s	density of bulk solvent, g/cc,
ρ_w	density of water, g/cc.

TABLE 1
 VALUES OF THE SOL MOLARITY INTEGRAL FUNCTION
 FOR THORIA MOLARITIES FROM 0.1 TO 20

M (moles/liter)	$\int_M^{20} \frac{dM_p}{M_p^{4/3} (0.238 M_p + 0.175)^{1/3}}$
0.1	7.42
0.2	5.17
0.3	4.11
0.4	3.47
0.5	3.02
0.6	2.69
0.8	2.23
1.0	1.91
1.2	1.68
1.4	1.50
1.6	1.35
1.8	1.23
2.0	1.13
2.2	1.05
2.4	0.974
2.6	0.910
2.8	0.853
3.0	0.802
3.5	0.696
4.0	0.612
4.5	0.543
5.0	0.486
6.0	0.395
7.0	0.326
8.0	0.271
9.0	0.227
10.0	0.190
12.0	0.131
14.0	0.087
16.0	0.052
18.0	0.024
20.0	0.000

TABLE 2
 PHYSICAL AND CHEMICAL DATA FOR THE ALCOHOLS

Alcohol	Temperature (°C)	D_v (cm ² /sec)	N_{Sc} ($\mu_s/\rho_s D_v$)	C_s (g/cc)
2EH	25	0.25×10^{-5}	35,700	0.020
2EH	40	0.47×10^{-5}	10,900	0.023
2EH	50	0.68×10^{-5}	5,450	0.025
2MP	25	0.33×10^{-5}	18,500	0.043
nH	25	0.39×10^{-5}	13,400	0.054

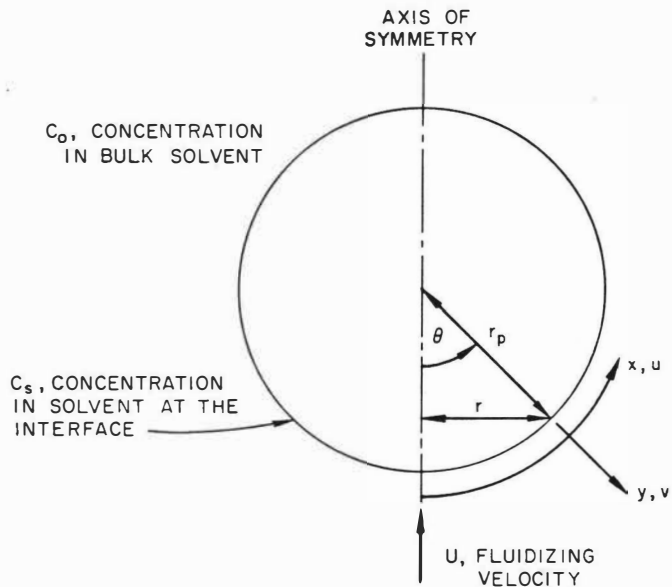


Figure 1. Natural Curvilinear Coordinates for a Thin Region at the Surface of the Drop.

2508

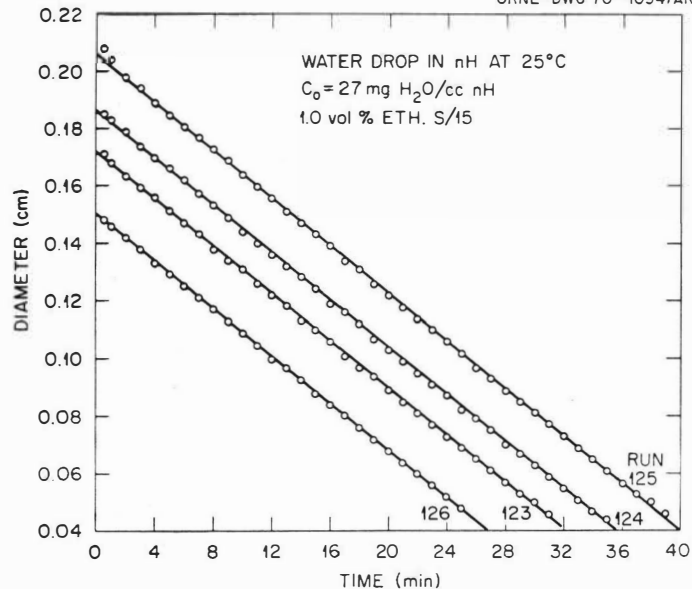
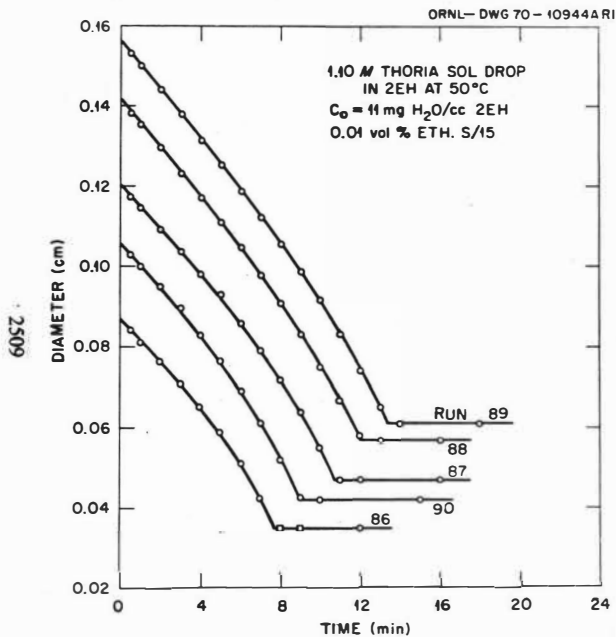


Figure 2. Diameter-Time Relationship for Water Drop Fluidized at 25°C in n-Hexanol Containing 27 mg of Water per cc.



3. Diameter-Time Relationship for 1.10 M Thoria Sol Drop in 2-Ethyl-1-hexanol Containing 11 mg of water per cc.

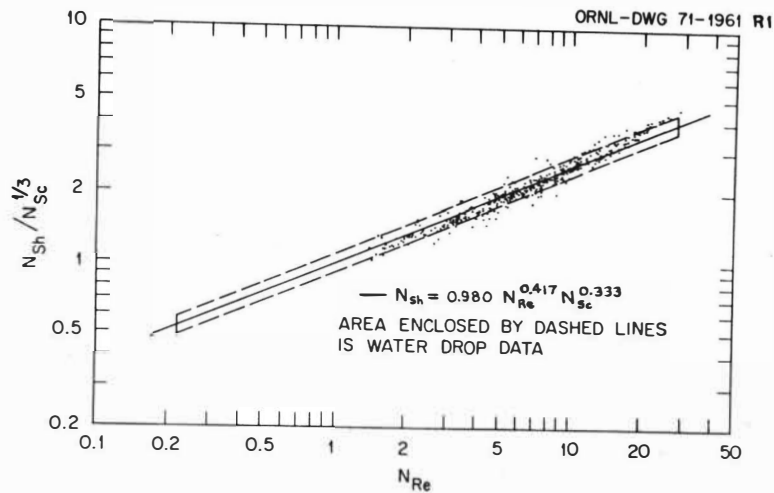


Figure 4. Mass Transfer Correlation for Fluidized Rigid Thoria Sol Drops.

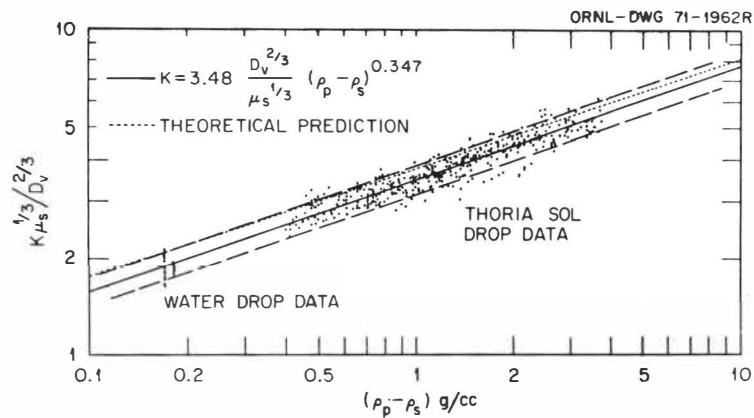


Figure 5. Correlation of Mass Transfer Coefficient for Fluidized Rigid Drops.

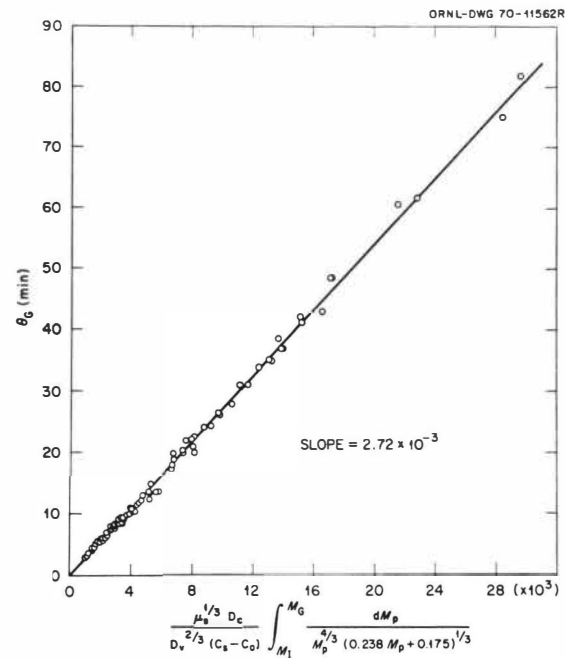


Figure 6. Correlation of Gelation Time for Fluidized Rigid Thoria Sol Drops.

SESSION 24

Friday 13th September: 9.00 hrs

C H E M I S T R Y O F E X T R A C T I O N

(Synergism & Kinetics)

Chairman:

Dr. H.A.C. McKay

Secretaries:

Mr. T.V. Healy

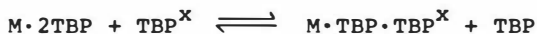
Mr. P. Claudy

¹H- AND ³¹P-NMR STUDY OF LIGAND EXCHANGE KINETICS IN THE
SYSTEMS UO₂(NO₃)₂ - TBP AND Pu(NO₃)₄ - TBP

Reinhard von Ammon

ABSTRACT

The kinetics of the ligand exchange reaction

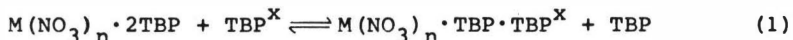


were studied by ¹H- and ³¹P-NMR line shape analysis. The free energy of activation (ΔG^\ddagger) of this first order reaction depends strongly on i) the metal ion (UO₂⁺² and Pu⁺⁴, resp.), ii) the presence of HNO₃, and iii) the solvent. TBP exchanges much faster with the plutonium than with the uranium complex; the exchange is slowed down by the presence of hydrogen-bonded HNO₃ and by polar solvents. The results indicate that the metal-TBP complexes interact with TBP by dipolar forces. The activated state presumably is an associate of the type M·3TBP. Evidence for this and against a dissociative mechanism is provided by rather high, negative values of the free entropy of activation (ΔS^\ddagger) suggesting a highly ordered activated state.

Kernforschungszentrum Karlsruhe, Institut für Heisse
Chemie, Karlsruhe, Federal Republic of Germany

In the Purex process for the recovery of spent nuclear fuels the ions UO_2^{+2} and Pu^{+4} are extracted from an aqueous nitrate medium into an organic phase containing TBP (tri-n-butyl-phosphate). It is well known that the transfer rates of various metal ions between these phases differ tremendously. Baumgärtner and Finsterwalder¹⁾ showed that the extraction of UO_2^{+2} and Pu^{+4} is controlled by the reaction rates of an interfacial metal species with both TBP from the organic and nitrate ions from the aqueous phase. A whole series of mechanisms - of associative and dissociative type, in the forward and backward direction - are thus involved in the overall reaction.

It is experimentally difficult to study most of these partial processes separately. One of them, however, can be conveniently observed by conventional NMR techniques: the exchange of the organic ligand TBP with the metal complex in the organic phase (equation 1):



The rate of this reaction being determined by the activation barrier of the ligand exchange should be indicative of the strength of the metal-TBP bond.

In this study, the TBP ligand exchange was investigated with the metal ions UO_2^{+2} and Pu^{+4} in various solvents.

METHOD OF MEASUREMENT

Determination of the rate of an exchange process by NMR line shape analysis is a well established method²⁾. At higher temperatures, where the exchange rate is fast on the NMR time scale, i.e. much larger than the difference of the resonance frequencies $\Delta\nu$ of the ligand nucleus in the free and the complexed state, respectively, only a single, averaged signal can be observed. At lower temperatures, however, where the exchange rate has been slowed down appreciably, the spectra of the ligand in the two environments can be observed separately. The exchange broadened spectra in the intermediate temperature region, if evaluated by complete line shape analysis, render the rate

constants at various temperatures and thus the Arrhenius activation energy E_a of the exchange reaction.

This method is inherently prone to a series of errors³⁾, especially in paramagnetic systems, where the line widths and line positions are strongly temperature dependent.

An alternative, approximate method⁴⁾ which gives quite reliable results, is to determine the free energy of activation ΔG^\ddagger from the rate constant k_c at the coalescence temperature T_c with equation (2) and (3)⁵⁾.

$$\Delta G^\ddagger = 4.57 T_c [10.32 + \log k_c/T_c] \quad (2)$$

$$k_c = \pi \cdot \Delta\nu / \sqrt{2} \quad (3)$$

In eq. (3) $\Delta\nu$ is the difference of the resonance frequencies in Hz in the exchange free region extrapolated to T_c . This method can be applied safely only, if $\Delta\nu \gg w_{1/2}$, the half-width of the two signals, i.e. in the absence of any signal overlap.

We used a combination of both methods in this study: generally we applied the approximate method but, for a check, we used the complete line shape analysis in the case of the ^{31}P spectra. Agreement was satisfactory. Since we evaluated only spectra at the coalescence temperature, we obtained the more reliable ΔG^\ddagger -values instead of E_a -values.

Siddall⁶⁾ had shown for the first time that the ligand exchange of excess TBP with $\text{UO}_2(\text{NO}_3)_2 \cdot 2\text{TBP}$ has favourable rates on the NMR time scale by observing separate $\alpha\text{-CH}_2\text{-}^1\text{H}$ -signals at -50°C in CDCl_3 . From the coalescence temperature he determined the free activation energy as "approximately 10 kcal/mole". More recently, Egozy and Weiss⁷⁾ carried out a complete line shape analysis of the ^1H -NMR spectra of this and similar systems in three solvents. For the system $\text{UO}_2(\text{NO}_3)_2 - \text{TBP}$ they determined E_a -values between 7.0 and 8.4 kcal/mole. They also confirmed the first order nature of the TBP ligand exchange.

EXPERIMENTAL

Samples were prepared by mixing appropriate amounts of $\text{UO}_2(\text{NO}_3)_2 \cdot 2\text{TBP}$ with excess TBP and by extraction of nitric acid (4 N) solutions of UO_2^{+2} and Pu^{+4} , respectively, with TBP dissolved in either chloroform, n-hexane or toluene. The final solutions contained about 20 vol.-% TBP.

TBP (Fluka) was used as received. The complex $\text{UO}_2(\text{NO}_3)_2 \cdot 2\text{TBP}$ was prepared by evaporating a solution of stoichiometric amounts of $\text{UO}_2(\text{NO}_3)_2 \cdot 6\text{H}_2\text{O}$ and TBP in ethanol.

The metal content of the solutions was determined by x-ray fluorescence (U^{81}) and α -counting (Pu), the HNO_3 concentration by titration, and the H_2O content by the Karl-Fischer method.

^1H -NMR spectra were recorded at 90 MHz, ^{31}P -NMR spectra at 36.46 MHz (10 mm tubes) on a Bruker spectrometer model HFX 90/60. A proton solvent signal was internal stabilization signal in both cases. Temperatures were calibrated with a thermocouple after each measurement. Coalescence temperatures are estimated to be accurate within $\pm 2^\circ\text{C}$. The concentration ratio of free and complexed TBP was kept near unity and was determined from the low temperature spectra by intensity measurements of the signals. The computer program used to fit the experimental spectra was a modified version of SHAPE 4 with the subroutine LADDAB, kindly supplied by Professor Dr. R.S. Drago, University of Illinois. In the computer simulation of the ^{31}P spectra, spin-spin splitting due to the $^{31}\text{P} - ^1\text{H}$ coupling was neglected, as it was not resolved in the experimental spectra (fig. 1).

RESULTS

1. System $\text{UO}_2(\text{NO}_3)_2 \cdot 2\text{TBP} - \text{TBP}$

In tables 1 and 2 the observed coalescence temperatures and $\Delta\nu$ -values as well as the corresponding rate constants and ΔG^\ddagger -values are listed. ^1H - and ^{31}P -data are compared for the case of "synthetic" (dry) samples and for extracted samples, i.e. samples containing HNO_3 and H_2O . The $\Delta\nu$ - and $w_{1/2}$ -values were read from spectra at temperatures between 190 and 230°K. Both values are rather temperature independent in this region.

The $\Delta\nu$ -values from the "synthetic" and the extracted samples differ appreciably in the ^{31}P -spectra. The reason is the noticeable high-field shift of $\text{TBP} \cdot \text{HNO}_3$ compared to "free" TBP (2 ppm⁹). The exchange of TBP with $\text{TBP} \cdot \text{HNO}_3$ is so fast, however, that no exchange broadening of this signal can be observed.

The absolute error of the ΔG^\ddagger -values is estimated to be ± 1 kcal/mole; the relative error, however, as determined from the accuracy of the temperature and resonance frequency measurements, is ca. ± 0.2 kcal/mole.

The agreement of the corresponding ^1H - and ^{31}P -data is quite good. Unfortunately, ^1H - and ^{31}P -coalescence temperatures of a particular sample are so close together that a $\log k_c$ -vs- $1/T$ plot from these two data points to obtain an E_a -value is not accurate enough. In order to estimate the activation enthalpies and entropies, ΔH^\ddagger and ΔS^\ddagger , the E_a -values of Egozy and Weiss were taken from the literature⁷⁾ and used for our "synthetic" samples which are comparable to theirs. The resulting ΔH^\ddagger and ΔS^\ddagger numbers are also given in table 1. For the extracted samples this method cannot be applied. The additional assumption was made, that the entropy change, ΔS^\ddagger , in the two systems is identical. Thus, E_a and ΔH^\ddagger could be calculated for the HNO_3 -containing system, using relations (4) and (5).

$$\Delta G^\ddagger = \Delta H^\ddagger - T \cdot \Delta S^\ddagger \quad (4)$$

$$\Delta H^\ddagger = E_a - R \cdot T \quad (5)$$

2. System $\text{Pu}(\text{NO}_3)_4 \cdot 2\text{TBP} - \text{TBP}$

For this system only ^1H -NMR data are presented (fig. 2 and table 3), because the ^{31}P -spectra obtained from these samples, sealed in 5 mm tubes, suffer from poor signal/noise ratio.

Pu^{+4} is a paramagnetic ion (electron configuration $5f^4$). The NMR shifts of its complexes are therefore strongly temperature dependent. Thus, $\Delta\nu$ has to be extrapolated from the low temperature, non-exchange region to T_c . In fig. 3 the line positions of the free and complexed TBP- $\alpha\text{-CH}_2$ signals are plotted vs. $1/T$. The linear Curie-Weiss dependence of the complexed TBP signal permits the fairly accurate extrapolation to $T_c = 203^\circ\text{K}$.

It is interesting to compare these low temperature data of the complex $\text{Pu}(\text{NO}_3)_4 \cdot 2\text{TBP}$ with data obtained earlier with a different technique¹⁰⁾ at 30°C : in a series of extraction experiments with increasing plutonium content the organic phase shows a linear shift dependence up to 0.12M, the limiting Pu concentration because of the development of three phases in n-dodecane as diluent (fig. 3). Extrapolation to 0.354M, the Pu-concentration of the complex $\text{Pu}(\text{NO}_3)_4 \cdot 2\text{TBP}$, if it is formed stoichiometrically in 20 vol.-% TBP, yields $\delta_{\text{TMS}} = 3.60$ ppm. This δ -value coincides fairly well with $\delta_{\text{TMS}} = 3.75$ ppm, obtained at $T = 303^\circ\text{K}$ in fig. 3. ΔH^\ddagger and E_a were estimated again (table 3) by assuming that the entropy change, ΔS^\ddagger is identical to the UO_2^{+2} case (synthetic samples).

The following conclusions can be drawn from the results:

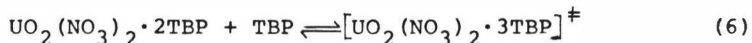
1. Influence of metal ion

The activation barrier of the TBP exchange is much lower in the plutonium than in the uranium complex. In toluene and in the presence of HNO_3 the decrease in ΔG^\ddagger amounts to 4 kcal/mole (from 13.7 kcal/mole (table 2) to 9.6 kcal/mole (table 3)). This result is in accord with the well known effect that the UO_2^{+2} -complex with TBP¹¹⁾ is more stable than the Pu^{+4} complex¹²⁾ and therefore more easily extracted¹⁾. Thus, the TBP ligand exchange, although certainly not the rate determining step in the extraction of metal ions is a measure of the complex stability in the organic phase.

2. Influence of diluent

The exchange is definitely enhanced in n-hexane as solvent compared to toluene and, particularly, chloroform. This phenomenon is apparent only in the "synthetic" samples (table 1), i.e. in the absence of nitric acid and water. The lowering of T_c in hexane was observed already by Siddall⁶⁾, who made hydrogen bonding between chloroform and TBP responsible for the rise of the activation energy. The effect does not show up in the E_a -data of Egozy and Weiss⁷⁾ who, on the contrary, reported a minimum E_a -value for the toluene solutions. They attributed the difference in their measured exchange rates to different frequency factors.

Our results suggest a competition between the polar solvent and TBP about the complex $\text{UO}_2(\text{NO}_3)_2 \cdot 2\text{TBP}$ via dipole-dipole interactions. In addition, this model favours the assumption of an associative mechanism with equation (6) as the limiting step for the formation of the activated complex.

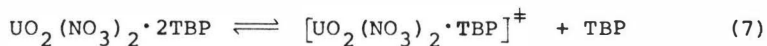


3. Influence of hydrogen bonds at the phosphoryl group

In the presence of strong hydrogen bonds at the P = O group of TBP the increase of the activation barriers is even more pronounced. The extracted samples (table 2) show ΔG^\ddagger -values about 1 - 1.5 kcal/mole higher than the corresponding "synthetic" samples. Since the former contain appreciable amounts of coextracted HNO_3 and H_2O (ca. 0.2M HNO_3 and 0.1M H_2O compared to 0.17M uranium) and since the hydrogen bonding between these proton donating substances and TBP is well established by IR- and NMR-methods⁹⁾, it must be concluded that the coordination of the metal ion with TBP is inhibited by these hydrogen bonds.

4. The free entropy of activation

The ΔS^\ddagger -values given in tables 1 - 3 offer rather direct evidence as to the nature of the activated complex. Although the magnitude of these data has to be considered *cum grano salis*, because they were obtained by combining our results with data from the literature⁷⁾, their negative sign is unambiguous. Thus, a dissociative mechanism for the formation of the activated complex according to equation (7) is definitely ruled out,



because such a mechanism would require a positive ΔS^\ddagger . The negative sign implies an activated state more ordered than the sum of the components at the start of the reaction. This requirement is fulfilled by the associative mechanism (eqn.6) discussed before.

ACKNOWLEDGEMENTS

The help of Professor Dr.R.S. Drago, University of Illinois, USA and Dr.Y. Egozy, Nuclear Research Center, Beer-Sheva, Israel, who made their computer programs available to us, is gratefully acknowledged. Dr.H.-R. Mache and DI.J.L. Krug, Kernforschungszentrum Karlsruhe, adapted the programs, and Mrs. S. Netzer assisted in the experiments and NMR-measurements.

LITERATURE

1. F. Baumgärtner and L. Finsterwalder, *J.phys.Chem.* 74, 108 (1970).
2. a) H.S. Gutowsky and C.H. Holm, *J.chem.Phys.* 25, 1228 (1956);
b) A. Allerhand, H.S. Gutowsky, J. Jonas and R.A. Meinzer, *J.Amer.Chem.Soc.* 88, 3185 (1966);
c) G. Binsch, *J.Amer.Chem.Soc.* 91, 1304 (1969).
3. a) R.R. Shoup, E.D. Becker and M.L. McNeel, *J.phys.Chem.* 76, 71 (1972);
b) K.C. Ramey, D.J. Louick, P.W. Whitehurst, W.B. Wise, R. Mukherjee and R.M. Moriarty, *Org.Magn.Resonance* 3, 201 (1971).
4. D. Kost, E.H. Carlson and M. Raban, *J.Chem.Soc., Chem.Commun.* 1971, 656.
5. H. Kessler, *Angew.Chem.* 82, 237 (1970); *Angew.Chem.Internat. Edit.* 9, 219 (1970).
6. T.H. Siddall, III and W.E. Stewart, *Inorg.Nucl.Chem.Letters*, 3, 279 (1967).
7. Y. Egozy and S. Weiss, *J.inorg.nucl.Chem.* 33, 1451 (1971).
8. D. Ertel and W. Wettstein, Kernforschungszentrum Karlsruhe, Report KfK 747 (1968).
9. R.v. Ammon and G. Baumgärtel, Kernforschungszentrum Karlsruhe, Report KfK 867 (1968).

10. R.v. Ammon, unpublished results.
11. A.M. Rozen and L.P. Khorkhorina, Zhur.neorg.Khim. 2, 1956 (1957).
12. E.I. Moiseenko and A.M. Rozen, Radiokhimiya 2, 274 (1960).

CAPTIONS OF FIGURES

- Fig. 1: ^{31}P -NMR spectra of a solution of 0.195M UO_2^{+2} , 0.215M HNO_3 and 0.15M H_2O in 20 vol.-% TBP-n-hexane at various temperatures; the spectrum at the coalescence temperature (center) was computer simulated: 1 = experimental spectrum; 2 = simulated spectrum; 3 = deviation.
- Fig. 2: ^1H -NMR spectra of a solution of 0.186M Pu^{+4} in 20 vol.-% TBP-toluene at various temperatures; the sample was obtained by extraction from an aqueous solution 0.2M in Pu^{+4} and 4M in HNO_3 .
- Fig. 3: The chemical shift difference $\Delta(\text{ppm}) = \delta_{\text{ops.}} - \delta_0$ ($\delta_0 = 3.98$ ppm from TMS) of the $\alpha\text{-CH}_2\text{-}^1\text{H}$ -signal of TBP in the spectra of a Pu-containing solution (composition same as in the caption of fig. 2) as a function of the reciprocal absolute temperature.
- Fig. 4: The chemical shift of the $\alpha\text{-CH}_2\text{-}^1\text{H}$ -signal of TBP in the spectra of solutions of $\text{Pu}(\text{NO}_3)_4$ in 20 vol.-% TBP-n-dodecane as a function of the plutonium concentration at 30°C; the solutions were obtained by extraction from 4M HNO_3 solutions.

Table 1:

Solvent	NMR nucleus	Spectral data			ΔG^\ddagger [kcal/mole]	$E_a^{x)}$ [kcal/mole]	ΔH^\ddagger [kcal/mole]	ΔS^\ddagger [cal/deg.mole]
		$\Delta\nu$ [Hz]	T_C [K]	k_c [sec ⁻¹]				
toluene	¹ H	38	248.0	84	12.2	7.0	6.5	-23
	³¹ P	61	254.0	135	12.3		6.5	-22
chloroform	¹ H	39.5	252.0	88	12.4	8.4	7.9	-18
	³¹ P	55	254.0	122	12.4		7.9	-18
n-hexane	¹ H	44	236.0	98	11.5	8.2	7.7	-16
	³¹ P	75	238.0	166	11.4		7.7	-16

2522

¹H- and ³¹P-NMR spectral data and kinetic parameters of the TBP-ligand exchange in the system $UO_2(NO_3)_2 \cdot 2TBP - TBP$, "Synthetic" samples.

x) Data taken from lit. 7.

Table 2:

Solvent	NMR nucleus	Spectral data			ΔG^\ddagger [kcal/mole]	$\Delta S^\ddagger(x)$ [cal/deg.mole]	ΔH^\ddagger [kcal/mole]	Ea [kcal/mole]
		$\Delta\nu$ [Hz]	T_c [K]	k_c [sec ⁻¹]				
toluene	¹ H	49.5	279.0	110	13.7	-22.5	7.4	7.9
	³¹ P	119	288.5	264	13.7		7.3	7.9
chloroform	¹ H	37.5	271.5	83	13.4	-18	8.5	9.0
	³¹ P	79.0	274.5	175	13.2		8.3	8.8
n-hexane	¹ H	41.5	265.0	92	13.1	-16	8.9	9.4
	³¹ P	123	274.5	273	12.9		8.5	9.0

¹H- and ³¹P-NMR spectral data and kinetic parameters of the TBP ligand exchange in the system UO₂(NO₃)₂·2TBP - TBP, "extracted" samples.

x) Data taken from table 1

Table 3:

Solvent	NMR nucleus	Spectral data			ΔG^\ddagger [kcal/mole]	ΔS^\ddagger [cal/deg.mole]	ΔH^\ddagger [kcal/mole]	Ea [kcal/mole]
		$\Delta\nu$ [Hz]	T_c [K]	k_c [sec ⁻¹]				
toluene	¹ H	83.5	203	186	9.6	-23	5.0	5.4

2524

¹H-NMR spectral data and kinetic parameters of the TBP ligand exchange in the system Pu(NO₃)₄·2TBP - TBP, "extracted" sample.

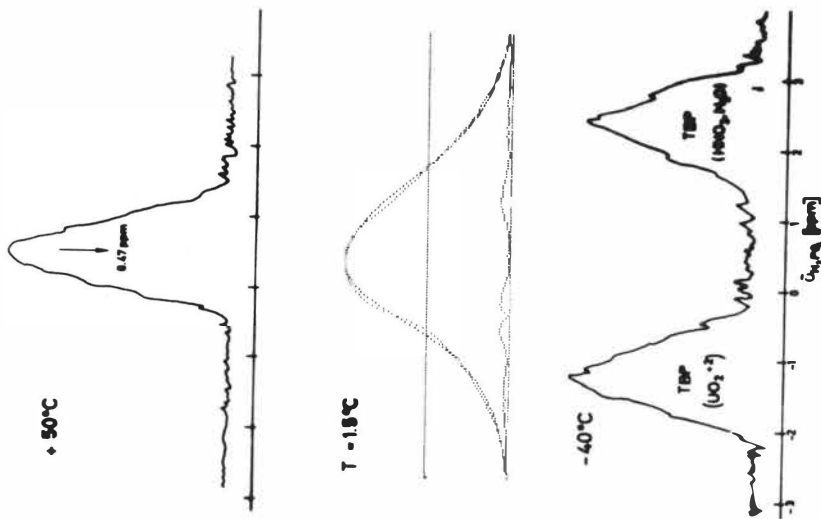


Fig. 1: ^{31}P -NMR spectra of a solution of 0.166 M UO_2^{2+} , 0.276 M HNO_3 , and $0.15\text{ M H}_2\text{O}$ in $20\text{ vol.}\% \text{ TBP-n-hexane}$ at various temperatures; the spectrum at the coexistence temperature (center) was computer simulated; 1 - experimental spectrum, 2 - simulated spectrum, 3 - doublet.

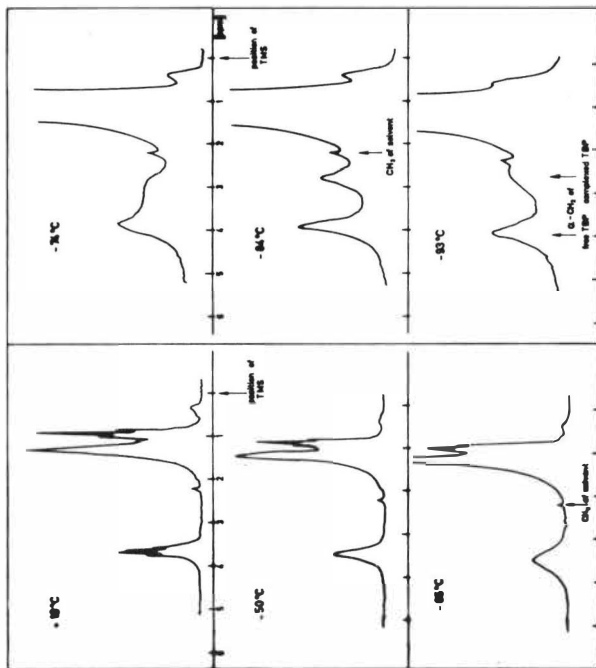


Fig. 2: ^1H -NMR spectra of a solution of 0.166 M Pu^{4+} in $20\text{ vol.}\% \text{ TBP-toluene}$ at various temperatures; the sample was obtained by extraction from an aqueous solution 0.2 M in Pu^{4+} and 4 N in HNO_3 .

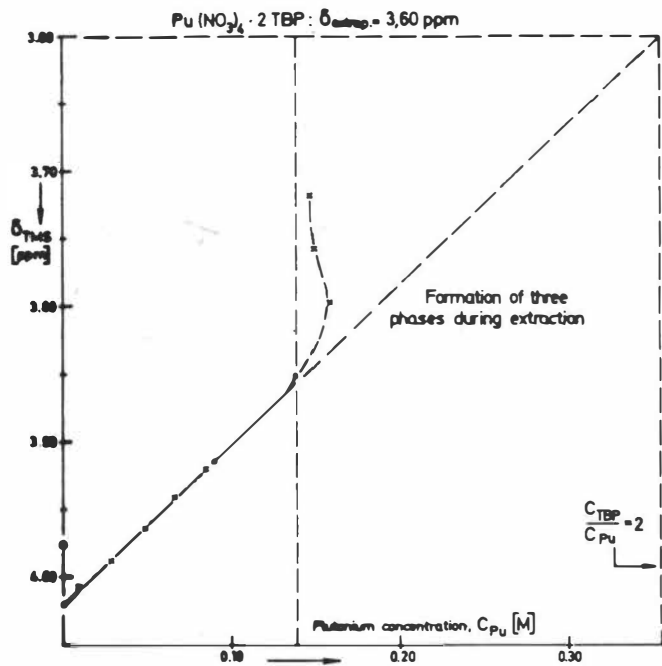


Fig. 4: The chemical shift of the α - CH_2 - ^1H -signal of TBP in the spectra of solutions of $\text{Pu}(\text{NO}_3)_4$ in 20 vol.-% TBP-n-dodecane as a function of the plutonium concentration at 30°C ; the solutions were obtained by extraction from 4 N HNO_3 solutions.

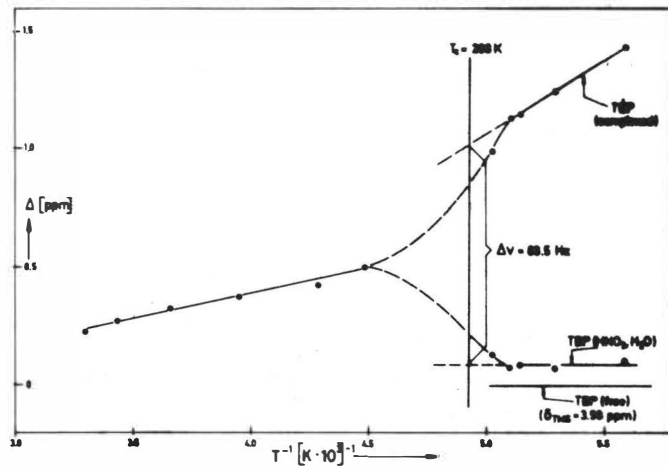


Fig. 3: The chemical shift difference $\Delta(\text{ppm}) = \delta_{\text{obs}} - \delta_0$ ($\delta_0 = 3.90$ ppm from TMS) of the α - CH_2 - ^1H -signal of TBP in the spectra of a Pu-containing solution (Composition same as in the caption of fig. 2) as a function of the reciprocal absolute temperature.

THE EFFECT OF DILUENTS ON THE EXTRACTION OF TRACER LEVEL COPPER

BY AN ALKYL HYDROXY QUINOLINE (KELEX 100^{*})

D.R. Spink and D.N. Okuhara

Department of Chemical Engineering

University of Waterloo

Waterloo, Ontario

CANADA

ABSTRACT

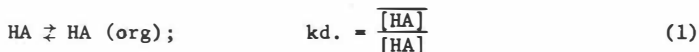
The effect of diluents on the solvent extraction equilibrium of tracer level copper by a proprietary alkyl β hydroxy quinoline (Kelex 100^{*}) was studied using an AKUFVE. An equilibrium scheme in which complexes of the type CuA_2 and CuA_2HA are both extracted is proposed and fitted to the experimental data. The extraction constants are correlated with the solubility parameters of the diluent on a qualitative basis.

INTRODUCTION

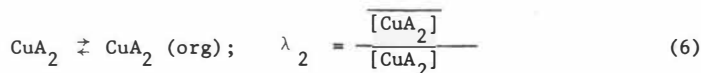
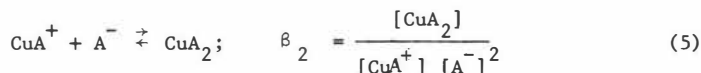
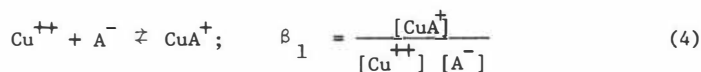
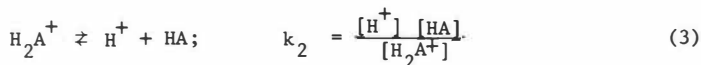
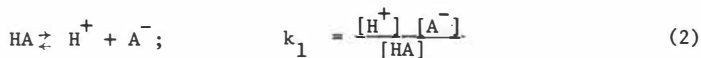
The distribution of metal oxinates between organic solvents and water have been studied by various investigators^(1,2). J. Sary⁽³⁾ studied the extraction of 32 metals with solutions of oxine in chloroform. Mottola and Frieser⁽⁴⁾ studied the distribution of copper (II) chelates of oxine, and 2 and 4 methyl oxine between a series of organic solvents and water. They interpreted their work in terms of solubility parameters.

The purpose of this work was to investigate the distribution of copper using an alkyl β hydroxy quinoline (Kelex 100^{*}) in various diluents and to attempt to correlate the extraction constants with the solubility parameters of the organic diluents used.

On the assumption that only neutral species are extracted, the distribution of copper by a solution of oxine, HA, can be described by the following equilibrium reactions:

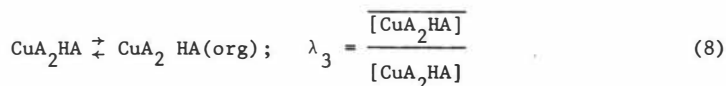
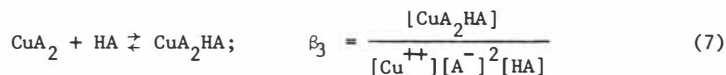


* Kelex 100 is a registered trade mark product of Ashland Chemical Co.



where bars indicate concentration in the organic phase and k_d and λ_2 are partition constants of the extractant and metal chelate respectively, k_1 and k_2 are the first and second acid dissociation constant of the chelating extractant and β_1 and β_2 are the formation constants for the complexes CuA^+ and CuA_2 in the aqueous phase respectively.

J. Stary⁽⁴⁾ supports this simple approach by reporting that the complex extracted by oxine in chloroform is CuA_2 . It is proposed here that both CuA_2 and CuA_2HA are formed and extracted with the Kelex 100. The degree of extraction of each species depends on the diluent, i.e.



where β_3 is the formation constant for the adduct complex, CuA_2HA , and λ_3 is the partition constant. The distribution ratio of copper oxinate, D , is therefore defined as:

$$D = \frac{\lambda_2\beta_2' [\overline{\text{HA}}]^2 [\text{H}]^{-2} + \lambda_3\beta_3' [\overline{\text{HA}}]^3 [\text{H}]^{-2}}{1 + \beta_1' [\overline{\text{HA}}] [\text{H}]^{-1} + \beta_2' [\overline{\text{HA}}]^2 [\text{H}]^{-2} + \beta_3' [\overline{\text{HA}}]^3 [\text{H}]^{-2}} \quad (9)$$

where the stability constants are defined as follows:

$$\beta_1' = \beta_1 k_1/kd \quad \beta_2' = \beta_2 (k_1/kd)^2 \quad \beta_3' = \beta_3 k_1^2/kd^3$$

To obtain the partition and stability constants for the extraction of copper, the distribution ratio was measured as a function of pH and Kelex 100 concentration.

EXPERIMENTAL

The AKUFVE apparatus as described previously^(5,6) was used to determine the distribution of tracer level copper as a function of pH for various Kelex 100 concentrations. Temperature was held at $25 \pm 0.5^\circ\text{C}$.

Kelex 100 was used as received from Ashland Chemical Co. Sodium sulfate, sulfuric acid and sodium hydroxide were of reagent grade. Radioactive copper, ^{64}Cu , produced in the reactor at McMaster University was used throughout as a tracer in these studies.

The solvents used as diluents were reagent grade except Escaid 100, NS148A and Solvesso 150, industrial solvents produced by Imperial Oil Co. Ltd.

The ionic strength in the aqueous phase was kept constant with $1M \text{Na}_2\text{SO}_4$.

Table 1 lists the solvents used as diluents with their solubility parameter.

TABLE 1

DILUENTS AND THEIR SOLUBILITY PARAMETERS

	DILUENT	SOLUBILITY PARAMETER
1	Isooctane	6.9
2	n-Heptane	7.4
3	Benzene	9.2
4	Toluene	8.9
5	Xylene	8.8
6	Methylcyclohexane	7.8
7	Perchloroethylene	9.3
8	50/50 vol % Heptane - Toluene	8.2
9	NS14 8A Imperial**	8.2
10	Solvesso 150*	8.7
11	Escaid 100†	7.9

** 20% paraffins, 34% naphthenes, 6% aromatic

* 98% aromatic

† 80% naphthenes & paraffins, 20% aromatic

RESULTS AND DISCUSSION

The Distribution ratio as a Function of pH

The log D vs pH data for several of the diluents studied are shown in Figures 1 through 4. If the Cu^{++} ion is the predominant species in the aqueous phase, equation 9 would predict a slope of 2. Examination of the log D vs pH plots at low pH shows a family of lines with a slope of about 1.70 for all of the diluents studied. This would indicate that in the pH range involved, the formation of intermediate complexes is significant thus resulting in a lowering of the slope. The effect of the diluent on the slope is shown in Figure 5. As equation 9 indicates, the concentration of the intermediate species in the aqueous phase is a function of the stability constants, β_1' , β_2' , β_3' . Since the stability constants are dependent on the diluent through k_d , the slope of log D vs pH should be a function of the solubility parameter of the organic phase.

Since for each diluent the family of lines plateaus at approximately the same value, (Figure 1 through 4) one would infer that only one species is being extracted, i.e. CuA_2 . However, there is the possibility that the partition constants for CuA_2 and CuA_2HA are approximately equal which would result in very little change in the plateau value.

The Distribution Ratio as a Function of The Kelex 100 Concentration

To determine the Kelex 100 concentration in the organic phase, it was equated to the initial organic concentration with the following assumptions. (1) the solubility of the oxine in the aqueous phase was low, (2) the concentration of the dissociated oxine, $[\text{A}^-]$ was insignificant at low pH values, and (3) the formation and distribution of the protonated oxine in the organic phase would not be too significant. This last assumption may warrant criticism; however the loss of the extractant by protonation did not seem to be significant at the experimental conditions used since the slopes of log D vs pH curves was not greater than 2.0.

Plots of log D vs log $[\text{Kelex 100}]_o$ at pH 1.5 are shown in Figure 6.

Examination of the slopes shows a dependence of about 2 for all the diluents except n-heptane (2.23) and isooctane (2.56). As Equation 9 predicts, a slope between 2 and 3 is expected depending on the relative concentration of CuA_2 and CuA_2HA in the organic phase. Formation of intermediate species would lower the slope of the $\log D/\log [\text{Kelex } 100]_o$ plots; we can probably assume that the concentration of the intermediate species is not significant over the experimental Kelex 100 concentration range.

Partition and Stability Constants

Table 2 gives the partition and stability constants obtained through a least square fit of the model described by equation 9 to the data. The error square sum, U , is also given for the fit. For a few of the diluents the error square sum, U_2 , is also shown for the fit of the model in which only CuA_2 is extracted. In all cases the error square sum is less for the model involving extraction of both species.

PARTITION AND STABILITY CONSTANTS FOR THE EXTRACTION OF

TABLE 2

TRACER LEVEL Cu BY KELEX 100 IN VARIOUS DILUENTS

	DILUENT	$\log \beta_1'$	$\log \beta_2'$	$\log \beta_3'$	$\log \lambda_2$	$\log \lambda_3$	U^\dagger	δ_o	U_2^\dagger	$\log \lambda_2 \beta_2'$	$\log \lambda_3 \beta_3'$
1	Isooctane	-0.791	-2.988	-0.567	3.428	3.115	2.2×10^2	6.9		.440	2.548
2	n-Heptane	-1.122	-2.245	-0.611	3.001	2.819	1.7×10^{-2}	7.4	8.5×10^{-2}	.756	2.208
3	Benzene	-1.122	-2.410	-1.112	3.188	2.811	2.3×10^{-2}	9.2		.778	1.699
4	Toluene	-1.233	-2.141	-1.721	2.790	2.932	2.5×10^{-2}	8.9	6.2×10^{-2}	.649	1.211
5	Xylene	-1.017	-1.996	-1.326	2.906	2.853	2.2×10^{-2}	8.8		.910	1.527
6	Methylcyclohexane	-1.189	-2.652	-1.127	3.390	2.653	1.3×10^{-2}	7.8	3.8×10^{-2}	.738	1.526
7	Perchloroethylene	-0.889	-1.832	-1.534	2.650	3.118	1.3×10^{-2}	9.3	2.7×10^{-2}	.818	1.584
8	50/50 vol % Toluene-Heptane	-1.216	-1.769	-1.517	2.517	3.055	3.1×10^{-2}	8.2		.748	1.438
9	NS148A	-1.192	-2.078	-2.386	3.035	3.710	0.8×10^{-2}	8.2*	1.3×10^{-2}	.957	1.324
10	Solvesso 150	-1.017	-2.618	-1.317	3.081	2.483	4.0×10^{-2}	8.7		1.063	1.166
11	Escaid 100	-1.148	-2.210	-1.136	3.075	2.733	1.2×10^{-2}	7.9*		.865	1.597

Temp = 25.0 °C [NaSO₄] = 1.0M

† U, U₂ Error Square sums.

* Estimated from typical values for paraffins, naphthenes and aromatics.

The partition constants of the copper (II) chelate in Table 2 are of the same order of magnitude as found by Mottola and Freiser⁽³⁾ for various alkylated oxines although the ionic strength of their aqueous system was lower than employed in this study.

To determine the relative extraction of the two complexes it is necessary to combine the partition and stability constant of each to form the extraction constant i.e. $\log \lambda_2 \beta_2'$ and $\log \lambda_3 \beta_3'$. (Table 2). The adduct complex is extracted to a greater extent, (especially in isooctane and n-heptane) primarily due to the larger stability constant for the adduct complex, i.e. $\beta_3' > \beta_2'$.

Several investigators^(7,8) have obtained various degrees of success in correlating the partition constant with solubility parameters. The approach we have taken is purely qualitative. From regular solution theory⁽⁹⁾, an expression developed for the partition constant is as follows:

$$2.3 RT \log \lambda^x = Vc [(\delta_c - \delta_{aq})^2 - (\delta_c - \delta_o)^2]$$

where λ^x represents the partition constant expressed as mole fraction ratio, δ_c and Vc the solubility parameter and molar volume of the distributing species respectively and δ_{aq} and δ_o the solubility parameters of the aqueous and organic phase.

Figure 7 shows the partition constant λ_2 as a function of the solubility parameter of the pure diluent. The increase in $\log \lambda_2$ with decrease in solubility parameter is as expected. Figure 8 shows λ_3 as a function of the δ_o .

To correlate the extraction of the CuA_2 and CuA_2HA complexes, $\log \lambda_2 \beta_2'$ and $\log \lambda_3 \beta_3'$ are plotted against the solubility parameter, δ_o , of the pure organic phase (Figure 9). As can be seen, preferential extraction of the adduct complex occurs at low solubility parameter, δ_o , decreasing with increase in δ_o until a minimum value is reached at about 8.75 after which point preferential extraction increases again. Conversely, the extraction constant for the CuA_2 complex is smallest at low values of the solubility parameter and goes through a maximum.

To test the usefulness of this correlation the extraction constants for the mixed diluents (Points 8,9,10,11) are also plotted in Figure 9. The agreement is only qualitative.

CONCLUSION

At tracer level copper, the alkyl β hydroxy quinoline forms and extracts both CuA_2 and CuA_2HA complexes and the extent of the adduct complex being extracted greatly depends on the diluent. Their respective extraction constants correlated reasonably with the solubility parameter, δ_0 , of the pure organic.

ACKNOWLEDGEMENT

The authors gratefully acknowledge the financial support from Ashland Oil Canada Limited and Imperial Oil Limited.

REFERENCES

1. Dyrssen, D., and Dahlberg, V., Acta Chem. Scand., 1953, 7, 1186.
2. Schweitzer, G.K., and Bramlitt, E.L., Anal. Chem. Acta, 1961, 24, 311.
3. Stary, J., Anal. Chem. Acta, 1963, 28, 132.
4. Mottola, A.H., and Freiser, H., Talanta, 1963, 13, 55.
5. Andersson, S.O., and Spink, D.R., Can. Res. Dev., 1971, 4, 16.
6. Flett, D.S., Okuhara, D.N., and Spink, D.R., J. Inorg Nucl. Chem., 1973, 35, 2471.
7. Omori, T, Wakhayashi, T., Oki, S, and Suzuki, N., J. Inorg Nucl. Chem., 1964, 26, 2255.
8. Siekierski, S., J. Inorg, Nucl. Chem., 1962, 24, 205.
9. Hildebrand, J.H., and Scott, R.L., Solubility of Nonelectrolyte, 1950, 3rd ed., (New York, Reinhold).

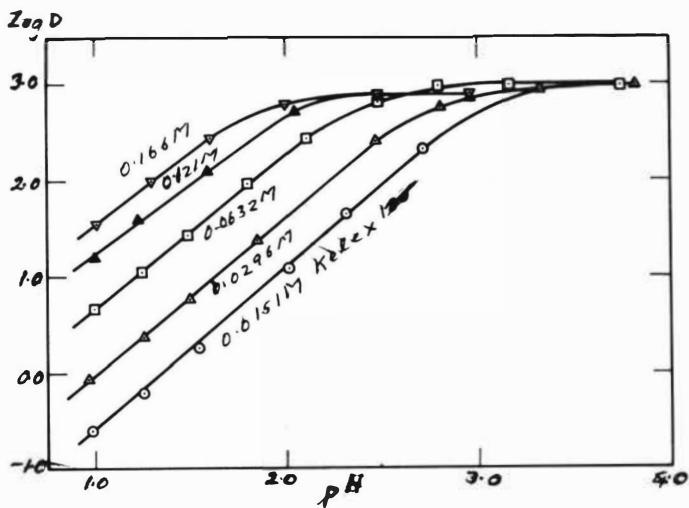


Fig. 1. The Distribution of Tracer Level Copper as a Function of the pH for Various [Kelex 100]₀ Concentrations. [Na₂SO₄]_a = 1.0.M. Temp = 25°C. [Cu]_a = 2.4 × 10⁻⁴M Diluent: Benzene.

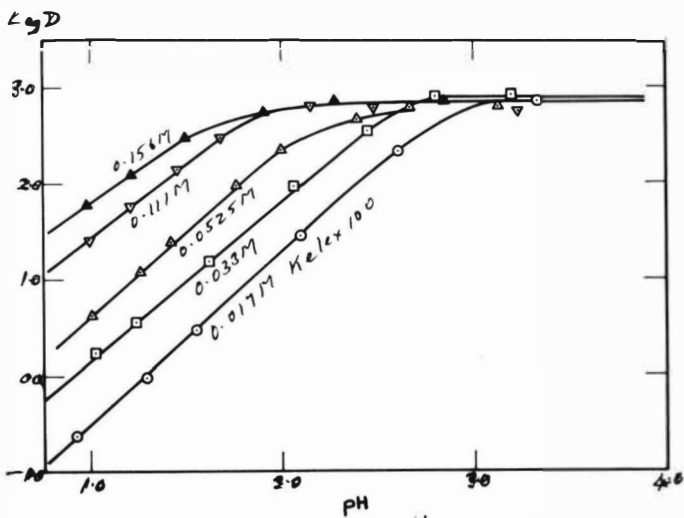


Fig. 2. The Distribution of Tracer Level Copper as a Function of the pH for Various [Kelex 100]₀ Concentrations. [Na₂SO₄]_a = 1.0.M. Temp = 25°C. [Cu]_a = 9.0 × 10⁻⁵M Diluent: n-Heptane

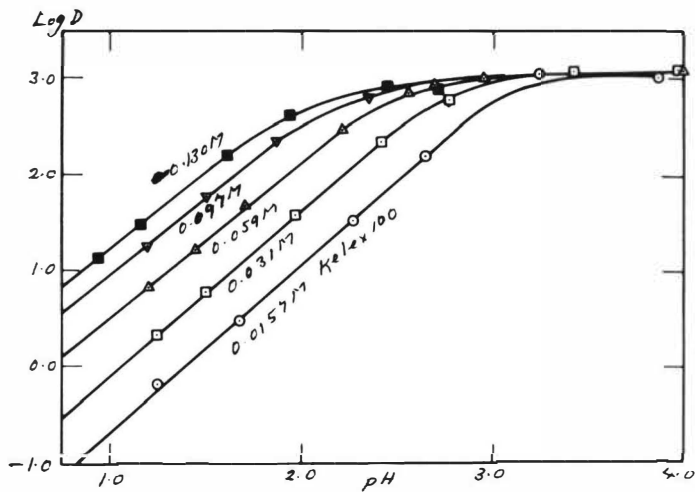


Fig. 3. The Distribution of Tracer Level Copper as a Function of the pH for Various $[\text{Kelex } 100]_0$ Concentrations. $[\text{Na}_2\text{SO}_4]_a = 1.0\text{M}$. Temp. 25°C . $[\text{Cu}]_a = 9.0 \times 10^{-5}\text{M}$ Diluent: Methylcyclohexane

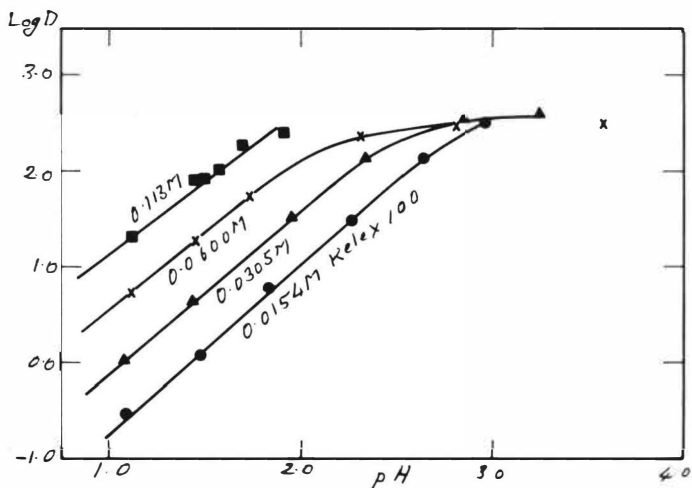


Fig. 4. The Distribution of Tracer Level Copper as a Function of the pH for Various $[\text{Kelex } 100]_0$ Concentrations. $[\text{Na}_2\text{SO}_4]_a = 1.0\text{M}$. Temp = 25°C . $[\text{Cu}]_a = 8.0 \times 10^{-5}\text{M}$ Diluent: 50/50 vol.% n-Heptane Toluene

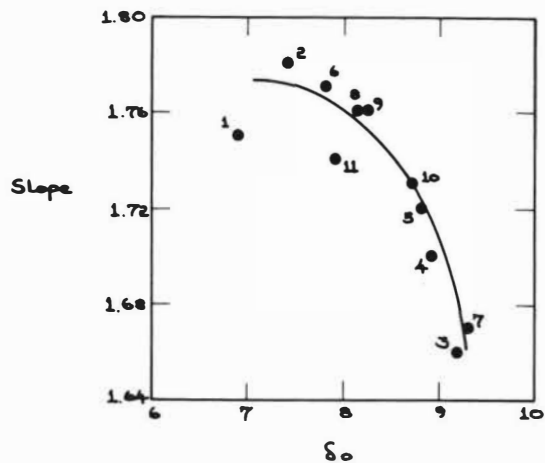


Fig. 5. The slope $\text{Log } D/pH$, as a Function of the Solubility Parameter of the Diluent.

Temp = 25°C. $[\text{Na}_2\text{SO}_4]_a = 1.0\text{M}$. $[\text{Kelex } 100]_o \approx 5.0 \text{ g/l}$.

Numbers correspond to diluents in Table 1.

Fig. 6. The Distribution of Tracer Level Copper as a Function of the Kelex1000 Concentration at pH 1.5 for various Diluents. ● Isooctane ■ n-Heptane ○ 50/50 Vol.% n-Heptane, Toluene △ Methylcyclohexane ▲ Toluene

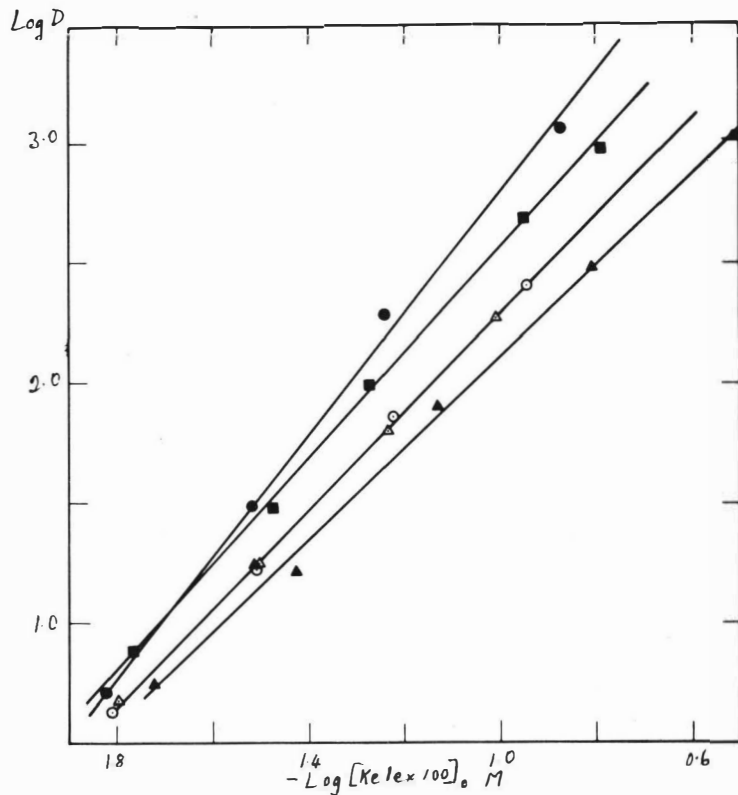


Fig. 7. The Partition Constant, λ_2 , as a Function of the Solubility Parameter of the Pure Diluent. Numbers correspond to diluents in Table 1.

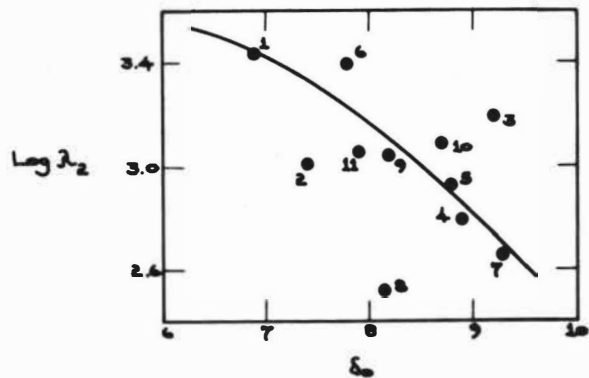


Fig. 8. The Partition Constant, λ_3 , as a Function of the Solubility Parameter of the Pure Diluent. Numbers correspond to diluents in Table 1.

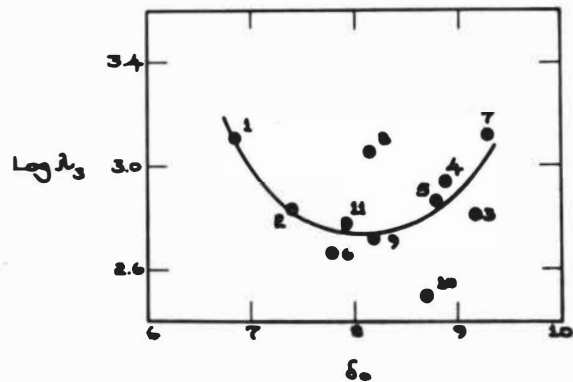
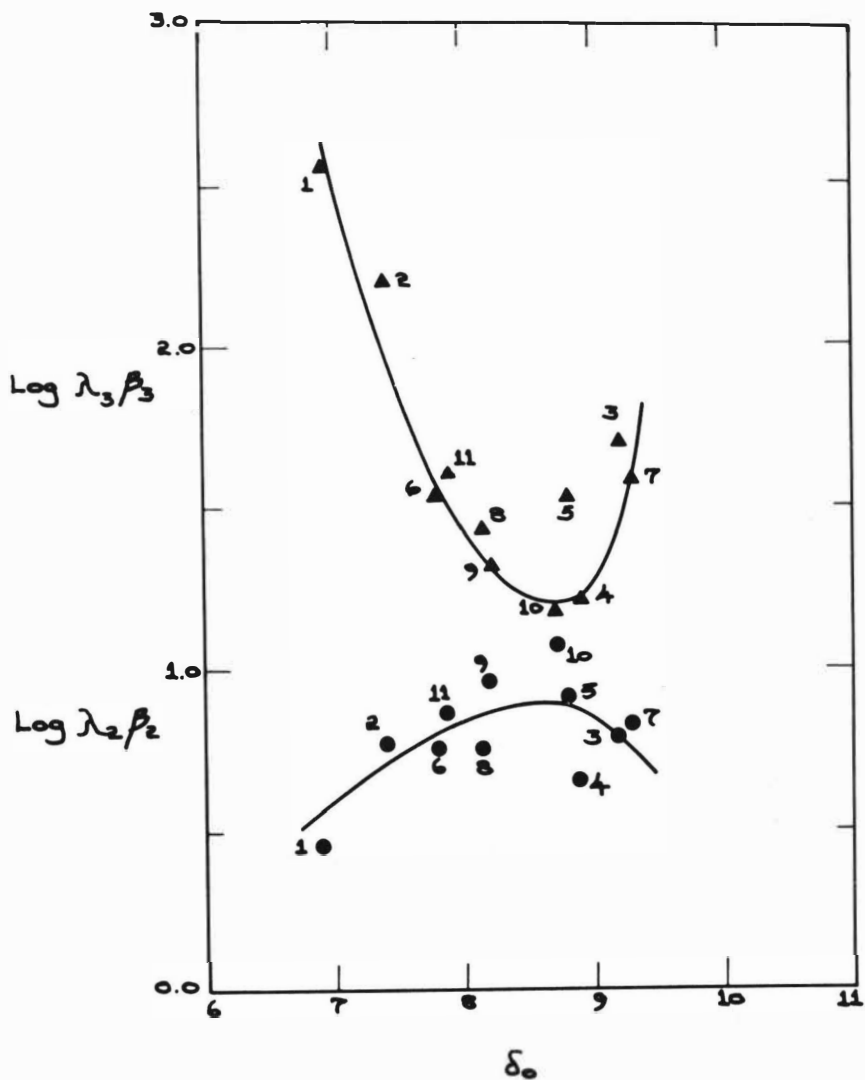


Fig. 9. The Extraction Constants as a Function of the Solubility Parameter of the Pure Diluent. Numbers correspond to diluents in Table 1.



The State of Substances in the Organic Phase
and Stripping Microkinetics

G. A. Yagodin, V. V. Tarasov and N. F. Kizim

The Mendeleev Institute of Chemical Technology,
Moscow, U.S.S.R.

Mathematical diffusion models with heterogeneous chemical reactions have been worked out and their analysis is given. It has been shown that the transient time value (t_t) calculated from the plots $m(t) = f(t^{\frac{1}{2}})$ is the measure of the chemical resistance of a heterogeneous reaction (R_s). In some cases the analytical expressions for R_s have been found. The values t_t of the stripping of mineral acids from neutral organophosphorus extractants have been determined using two variants of the short-time phase contacting method.

Assuming an irreversible reaction of the first order takes place at the interface, the values R_s have been calculated. It has been found that R_s correlates with the water content in the organic phase. This confirms that the slow stage is a heterogeneous hydration reaction.

The high sensitivity of the mass flux to the composition of the organic phase leads to the conclusion that the short-time phase contacting method may be used to get information on the state of substances in non-aqueous solutions.

Heterogeneous reactions in the formation of extracted complexes are typified in the extraction of inorganic materials by the most frequently used extractants: amines, acids, neutral compounds.^(1,2) In spite of the fact that the most convincing evidence of the existence of such reactions has been provided by slow processes⁽³⁻⁶⁾ there is no doubt that rapid heterogeneous reactions also exist. To prove this, special methods have been developed to study the kinetics of extraction. One of them is the short-time phase contacting method.^(7,8) It was used to study the kinetics of the stripping of mineral acids from tributylphosphate (TBP) and trioctylphosphin oxide (TOPO).^(7,9) The interfacial resistance detected was said to be identical with the chemical resistance of the heterogeneous solvates hydration reaction. Though the dependencies described in published papers⁽⁷⁻⁹⁾ were in favour of this assumption additional evidence was required. This could be obtained by increasing the number of the systems being investigated and obtaining more detailed data on the influence of all the system's components on the stripping kinetics. Such investigations were supposed to result in obtaining data sufficient for the determining of the correlation between the reactivity of extractants and interfacial resistance values. It was therefore necessary to determine the interfacial resistance values as these could exert a profound influence on the efficiency of short-time contactors, such as centrifugal extractors.

The following important task was to work out the mathematical description of diffusion processes with heterogeneous reactions with a short-time contact of phases.

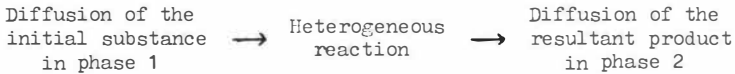
It should be mentioned that the most widely used models of mass transfer through the interface, that is the penetration and the surface renewal models,^(10,11) are based on the assumption that the non-stationary, molecular diffusion is of significant importance. However there is practically no mathematical description of such elementary processes with heterogeneous reactions in the literature. This is to be expected as the heterogeneous reaction has usually been considered only as a limit of the homogeneous reaction and not as an independent type of

reaction taking place, always in the interface, regardless of the transport and kinetic coefficients.

Mathematical models of the molecular diffusion with heterogeneous chemical reactions

The distinctive feature of the mathematical representation of the molecular diffusion in the two-phase system with a reaction in the interface is that one of the boundary conditions is based on the chemical reaction equation. This means that the mass flux into the interface is equal to the rate of reaction of the diffusing component in the production of the intermediate substances in the interface.

The following uniform scheme of consecutive processes is the basis of all the models:



The following are generally assumed for all types of models:

1. The phase contact time is infinitely short.
2. The phases length is quasi-infinite (the contact time is short).
3. There is no diffusion of the initial substance into phase 2.
4. There is no diffusion of the resultant product into phase 1.
5. The transport of the substances is described according to Fick's law.
6. The concentrations of substances in the interface equal or are proportional to the volume concentrations in the layers adjoining the interface.
7. The diffusion coefficients in the phases are not dependent on the concentration.

The solution models 1-6 are in Tables 1 and 2. The equations of models 1-6 are solved using the Laplace transformation method. Models 3-5 are solved using the approximate quasi-stationary method described by Frank-Kamenetsky.⁽¹²⁾ In models 3 and 4 the accumulation of the intermediate product B in the interface is not taken into consideration. It is assumed that the intermediate product B exists only in the interface, the thickness of which is σ . The accumulation of substance B in the interface is accounted by the following boundary condition:

$$D_1 dC_A/dx|_{x=0} = dC_B/dt + D_2 dC_C/dx|_{x=0} \quad (1)$$

Functions F_{1-6} of model 5 can be obtained in the following way:

$$F_1 = \beta_1 \beta_2 / \gamma_1 \gamma_2 + \{ [\gamma_1^2 - \gamma_1 (\beta_1 + \beta_2 + K_2) + \beta_1 \beta_2] / \gamma_1 (\gamma_1 - \gamma_2) \} \exp(-\gamma_1 t) + \{ [\gamma_2^2 - \gamma_2 (\beta_1 + \beta_2 + K_2) + \beta_1 \beta_2] / \gamma_2 (\gamma_2 - \gamma_1) \} \exp(-\gamma_2 t) \quad (2)$$

$$F_2 = \beta_2 / \gamma_1 \gamma_2 + (\beta_2 - \gamma_1) \exp(-\gamma_2 t) / \gamma_1 (\gamma_1 - \gamma_2) + (\beta_2 - \gamma_2) \exp(-\gamma_2 t) / \gamma_2 (\gamma_2 - \gamma_1) \quad (3)$$

$$F_3 = 1 / \gamma_1 \gamma_2 + \exp(-\gamma_1 t) / \gamma_1 (\gamma_1 - \gamma_2) + \exp(-\gamma_2 t) / \gamma_2 (\gamma_2 - \gamma_1) \quad (4)$$

$$F_4 = \beta_2 F_3 / F_2 \quad (5)$$

$$F_5 = \beta_1 F_2 / F_1 \quad (6)$$

where γ_1 and γ_2 are the roots of the square equation:

$$\gamma^2 + \gamma(\beta_1 + \beta_2 + K_1 + K_2) + K_1 K_2 + K_1 \beta_1 + \beta_1 \beta_2 = 0 \quad (7)$$

taken with opposite signs.

It should be mentioned that the equations of model 1 are identical with those known from ref. 12 at $\alpha = 1$, and the equations of model 2 are described in ref. 14. The special solutions of the equations of model 2 are published in refs. 13 and 15.

The Analysis of the mathematical models

We are interested in the behaviour of the functions (table 1) at large and short contact time. It should be noted that $F(\lambda_1) \rightarrow 0$, when $t \rightarrow \infty$ and $F(\lambda_1) \rightarrow 1$, when $t \rightarrow 0$.

At sufficiently large t , all the models lead to the linear equation:

$$m_2(t) = \bar{A} t^{\frac{1}{2}} - \bar{B} \quad (8)$$

When extrapolating this dependence into the region of short time we note that it does not pass through the origin but cuts off the intercept ($-\bar{B}$) on the axis of ordinates and the intercept $t_0^{\frac{1}{2}}$ on the axis of abscissae. In some cases the value of the latter can be connected with the interfacial resistance value R_S . The \bar{A} values $t_0^{\frac{1}{2}}$ and R_S are given in table 3 for different models. The coefficients A_1 , A_2 and A_3 are in no way connected with the heterogeneous reaction kinetics. It means that at sufficiently large t the process takes place in the diffusion region. The coefficient A_2 (model 2) is dependent on the equilibrium constant K_e . In this case, A_2 may vary from zero to the value characteristic of the irreversible reaction, passing the value A for the homogeneous diffusion.⁽¹⁵⁾

The coefficients A_4 and A_6 depend to some extent on the reaction rate though such conclusions seem to be rather unexpected. It should be mentioned that at $\Psi^2 \ll K_2$ the value A_6 equals A_1 .

The analysis of equations for models 1-6 in the region of short time leads to the general conclusion that the chemical kinetics play an important role. In all cases at $t = 0$, we have a kinetic region and the mass flux to the interface depends only on the chemical reaction rate. Fig. 1 represents the dependence of the dimensionless mass $k_1 m(t) / D_1 C_1^0$ of the substance transferred into the second phase on the square root of the dimensionless time $(k_1 t^{\frac{1}{2}} / D_1^{\frac{1}{2}})$ (curve 1). The calculation is according to model 1. The dependence for the case of the rapid irreversible first order reaction in the extracting phase is shown in the same figure. The calculation was according to Danckverts' equation,⁽¹¹⁾

$$m_2(t) = C_2^0 (D/k)^{1/2} \left[(kt + 1/2) \operatorname{erf}(kt)^{1/2} + (kt/\pi)^{1/2} \exp(-kt) \right] \quad (9)$$

which in the dimensionless form is as follows:

$$m_2(t) k^{1/2} / C_1^0 D^{1/2} = (kt + 1/2) \operatorname{erf}(kt)^{1/2} + (kt/\pi)^{1/2} \exp(-kt) \quad (10)$$

It can be easily seen that the influence of the homogeneous reaction increases at t unlike the heterogeneous reaction the influence of which is the most significant at $t = 0$. Also, curve 2 (Fig. 1) is above the square's diagonal reflecting the mass-transfer without a chemical reaction, and curve 1 is below it. This means that the homogeneous reaction accelerates the mass transfer and the heterogeneous reaction inhibits it.

The analysis of the behaviour of functions $j_1(0,t)$, $j_2(0,t)$ and $m_2(t)$ of model 6, in the region of short time, is of particular interest (Fig. 2). Note that the function $m_2(t) = f(t^{\frac{1}{2}})$ has two inflections with the coordinates

$$t_{1,2}^{1/2} = \pi^{1/2} (\kappa_2 + \psi^2) / 4\psi^3 \pm [\pi(\psi^2 + \kappa_2)^2 + 8\psi^2 \kappa_2]^{1/2} / 4\psi^3 \quad (11)$$

Function $j_2(0,t)$ comes above the maximum. The time corresponding to the extreme point is:

$$t_{max} = (\psi^2 + \kappa_2)^2 \pi / 2 \psi^6 \quad (12)$$

Experimental

In this work neutral organophosphorus compounds were used as extractants. Their list, chemical composition and some physico-chemical properties are given in table 4.

Method of investigation

This work has been carried out using the short-time phase contacting method.⁽⁷⁻⁹⁾ Some results were obtained with the help of a modified method without using paper samples,⁽¹⁾ in order to be sure that R_s is not dependent on the way it is measured. It is essential that the change of electrical conductivity of the aqueous phase layers adjoining the interface is proportional to the change of the electrolyte concentration in them. The proportional coefficients for all the monobasic acids are practically equal. The results can then be analysed on the basis of the dependence of Δx on t .

Discussion

Previous results,⁽⁷⁻⁹⁾ obtained while studying the stripping kinetics of the acids, lead us to assume that stripping is mass transfer via a heterogeneous reaction:

1. The dependencies $\Delta x = f(t^{\frac{1}{2}})$ are linear at sufficiently long-time phase contacting ($t > 0.1$ sec).
2. The coefficients \bar{A} are proportional to the solvate concentration in the organic phase.
3. The dependencies $\Delta x = f(t^{\frac{1}{2}})$ are non-linear at short-time phase contacting. In all cases, except the case of HClO_4 stripping, the transient time t_t occurs. The value of t_t considerably depends on the system but not on the concentration of "free" extractant.
4. The coefficients \bar{A} depend on the properties of the organic phase and in particular on its viscosity ($\bar{A} \sim 1/\eta^{\frac{1}{2}}$).

The extension of the number of systems investigated and the range of measurements made allow us to make more accurate modifications of some of the above conclusions. Conclusions 1-4 are now discussed in the light of the new results.

First of all it appears that the linear character of the dependencies $\Delta x = f(t^{\frac{1}{2}})$ at sufficiently large t is confirmed by the study of the stripping of acids from the majority of the extractants used. The exceptions are found under certain conditions whilst stripping HClO_4 from TBF solutions and HNO_3 from TNP solutions (Fig. 3). We consider that the shapes of the curves (Fig. 3) indicate either that some forms of transferred component exists in the organic phase or that they are formed while stripping (e.g. during diffusion of water into the organic phase). It should be mentioned that, in multicomponent mass

transfer, the curves often have a shape as in Fig. 4. This takes place each time two substances are transferred, one of which has a low interfacial resistance and the other a high one (e.g. during simultaneous stripping of HNO_3 and metal nitrates). However in the majority of cases rather a good correlation between Δx and t^2 is observed. For example, on stripping HNO_3 from 0.1M TBP/decane, the analysis of 20 kinetic curves according to the least squares method provides the coefficients A and B and the correlation coefficient r .

$$\Delta x = 6.088 \times 10^{-5} t^2 - 8.168 \times 10^{-6}$$

It appears that $r = 0.991$ indicating good correlation.

The second conclusion, that the coefficient \bar{A} is proportional to the organic phase solvate concentration (following from the models), is not however correct for all systems. As a rule in the measurement range of solvate concentration from 0.05 to 0.3M the dependence between \bar{A} and C_1^0 is practically linear (Fig. 5). However at higher concentrations considerable deviations from linearity are observed, which are probably connected with increasing non-ideality in the organic phase. In some cases (e.g. on stripping HNO_3 from TBPO solutions) the dependence between \bar{A} and C_1^0 is rather complicated even at low concentrations (Fig. 6). The cause of such deviations will be discussed below. The influence of the concentration of the "free" extractant on the coefficient \bar{A} for different systems is not identical. For example, in the system TBP- HNO_3 -decane, the dilution effect on the coefficient \bar{A} is the same, whether the dilution is by TBP solutions or by decane (Fig. 7). The same is true for the systems with TOP, TFP and TOPO. However in other cases (e.g. the system with TBPO) the "free" extractant concentration plays an important role.

Our work confirms that the transient time is considerably dependent on the extraction system (conclusion 3). The acids being extracted according to the hydroxonium mechanism (e.g. HClO_4), have practically no transient time ($t_t=0$). The value t_t generally appears to be a complicated function of the organic phase composition, so that even for the same system t_t is not constant. This is a consequence of the multicomponent character of the complexes so no satisfactory correlation of t_t and R_s with values of the extracting ability has been found. The experimental values of t_t and R_s are given in Table 5.

In some cases in Table 5, the values of t_t and R_s are obtained from results at various time intervals. This means that they are considerably dependent on the organic phase. It is also known that the mineral acid complexes in this phase will change with the conditions of extraction.

Similar acid content of the organic phase may be obtained on contacting different concentrations of extractant with different aqueous solutions, the water also being coextracted to a different degree. The water content of the organic phase has a large effect both on the transient time t_t (or R_s) and on the coefficient \bar{A} . On stripping HNO_3 and HSCN from TBP solutions the \bar{A} , t_t and R_s values are lower, corresponding to the higher water content of the organic phase. The data in Table 6 confirm this.

It was mentioned earlier that the dependence $\bar{A} = f(C_1^0)$ for the system TBPO- HNO_3 - H_2O is complicated. In the concentration region of HNO_3 in the organic phase (0.05-0.15M) inflexions are observed (Fig. 6). Our data show that the organic phase water content changes irregularly in the same region. We consider this phenomenon takes place due to the formation and further destruction of intermediates while the organic phase composition changes. Note that the intermediate formation in the system TBPO- H_2O is described in detail in ref. 16. Though the influence of water content in the organic phase

on the stripping kinetics is not clear, the results may be explained in the following way. The water content increase in the organic phase causes a displacement of the equilibrium:



in the direction of the formation of the latter. Thus if the heterogeneous reaction slow stage is the process of hydration, the hydroxonium formation in the organic phase must cause a decrease of the interfacial resistance. This explanation is quite reasonable as there is no resistance while stripping HClO_4 . This acid exists in the organic phase usually in the hydroxonium form. The decrease of the A value with increase in water content during stripping of HNO_3 and HSCN , can be explained either by the decrease of the diffusing substance activity or by the decrease of its diffusion coefficient.

Thus some of the above results can be explained in terms of model 2 (or of its special case - model 1). Application of more complicated models (3-6) at present would be unreasonable due to there being additional parameters, the selection of which might lead to an accidental coincidence of the experimental results with the model. Such a conclusion seems reasonable, as at present we have no information on the diffusion coefficients of the solvates in the organic phase and on their concentration dependence. As all the equations have been obtained only in the concentration form, they give only an approximate description of the process.

At the same time, some results indicate that processes involving the accumulation of complexes in the interface may be of considerable importance under certain conditions. Thus the factors affecting the stripping of HClO_4 from dilute TBP (where non-aqueous solvates exist⁽¹⁷⁾) favour model 6 (Fig. 8). If this is proved in the future we may speak about the impossibility of describing the mineral acids stripping process by a single model.

Nomenclature

\bar{A} - coefficient of equation 8

B - intercept on the axis of ordinates

A, B and C - compounds

C_1^0 - initial concentration of diffusion compound in the raffinate phase (phase 1), M/cm^3

D_1 and D_2 - diffusion coefficients of compounds in phases 1 and 2 respectively

$F(\lambda_1)$ - function, $F(\lambda_1) = \exp(\lambda_1^2) \operatorname{erfc}(\lambda_1)$

\bar{F}_{1-6} - functions, are given in the text

$j_1(0_1, t)$ and $j_2(0_1, t)$ - mass fluxes from the phase 1 on the interface and from the interface into phase 2 respectively, $\text{M/cm}^2\text{sec}$.

k_1 - rate constant of the direct stage of the heterogeneous reaction, cm/sec .

$K = K_i/a$ - effective rate constant, cm/sec

k - rate constant of the homogeneous irreversible reaction, $1/\text{sec}$.

K_e - reaction equilibrium constant

$m_2(t)$ - mass of the compound transferred into extract phase, M/cm^2 .

R_s - interfacial resistance, sec/cm .

t - diffusion time, sec.

a - reactive activity coefficient

β - reverse stage rate constant of the heterogeneous reaction, cm/sec .

γ - roots of equation 7

δ - thickness of the interface (adsorption region), cm

$\lambda_{1,6} = \bar{k}_{1,6} t^{1/2} / D_1^{1/2}$ - dimensionless parameter (models 1, 6)

$\lambda_2 = (\bar{k}_{2,1} / D_1^{1/2} + \beta_2 / D_2^{1/2}) t^{1/2}$ - dimensionless parameter (model 2)

$\lambda_3 = [\delta \bar{k}_{2i} k_2 / (k_2 + \beta_1) D_1^{1/2}]$ - dimensionless parameter (model 3)

$\lambda_4 = [\delta \bar{k}_{2i} k_2 / (k_2 + \beta_1) D_1^{1/2} + \delta \beta_1 \beta_2 / (k_2 + \beta_1) D_2^{1/2}] t^{1/2}$ - dimensionless parameter (model 4)

$\Delta \kappa$ - change of electrical conductivity of boundary layer of the water phase,
l/cm

$\Psi = \bar{k} / D_1^{1/2}$ - parameter, $\text{sec}^{-1/2}$

References

1. Tarasov V.V., Yagodin G.A., "Kinetika ekstratsii" 1974 (Moscow: VINITI).
2. Tarasov V.V., Yagodin G.A., "Poslednie dostizheniya v oblasti ekstraktsii" 1974 (Moscow: Khimiya).
3. Kletenick Yu.B., Navrotskaya V.A., Zurn. neorgan. Khim., 1967 (12), 3114.
4. Navrotskaya V.A., Kletenick Yu.B., Zurn. neorgan. Khim., 1969 (14), 1900.
5. Roddy J.B., Coleman C.F., Arai S., J. Inorg. Nucl. Chem. 1971, 33, 1899.
6. Karpatcheva S.M., Ilozeva A.V., Radiochimiya, 1969 (11), 37.
7. Tarasov V.V., Yagodin G.A., Kizim N.F., Dokl. Akad. Nauk. SSSR, 1970 (194) 6.
8. Tarasov V.V., Kizim N.F., Yagodin G.A., Z. phys. khimii, 1971 (45), 2517.
9. Tarasov V.V., Kizim N.F., Yagodin G.A., Z. phys. khimii, 1972 (46), 899.
10. Astatita G., Massoperedacha S Khimicheskoi reaktivnoy (1971), (Leningrad: Khimiya).
11. Danckwerts P.V., Trans. Faraday Soc., 1950, 43, 1460.
12. Frank-Kamenetsky D.A., "Diffuziya i teploperedacha v khimicheskoy kinetike", 1967.
13. Jost W., Diffusion in solids, liquids, gases, New York Academic Press, 1960.
14. Delahay P., "Novie pribori i metodi v elektrokhemii" 1957 (Moscow: Inostr. literat.).
15. Yurtov E.V., Tarasov V.V., Z. phys. khimii, 1972 (46), 2262.
16. Nikolaev A.V., Yakovlev I.I., Dyadin Yu.A., Kolesnikov A.A., Aphanasev Yu.A., Torgov V.G., Michilov V.A., Gribanova I.N., Rogatirev V.L., Ryabinin A.I., "Ekstraktsiya neorganicheskikh veshchestv", 1970 (Novosibirsk: Nauka).
17. J.J. Bucher, R.M. Diamond, J. Inorg. Nucl. Chem., 1972, 34, 3531.

Table 1

The mathematical models of molecular diffusion with heterogeneous reactions

Model	Reaction type	Mass flux expressions
1	A $\xrightarrow{k_{1i}}$ B	$j_1(0,t) = \bar{k}_{1i} C_1^0 F(\lambda_1)$; $j_2(0,t) = j_2(0,t)$
2	A $\xrightleftharpoons[\beta_1]{k_{1i}}$ B	$j_1(0,t) = (\bar{k}_{1i} C_1^0 - \beta_1 C_2^0) F(\lambda_2)$; $j_1(0,t) = j_2(0,t)$
3	A $\xrightleftharpoons[\beta_1]{k_{1i}}$ B $\xrightarrow{k_2}$ C	$j_1(0,t) = \lambda_3 C_1^0 F(\lambda_3) D_1^{1/2} / t^{1/2}$; $j_1(0,t) = j_2(0,t)$
4	A $\xrightleftharpoons[\beta_1]{k_{1i}}$ B $\xrightleftharpoons[\beta_2]{k_2}$ C	$j_1(0,t) = \delta k_{1i} k_2 C_1^0 F(\lambda_4) / (k_2 + \beta_1)$; $j_1(0,t) = j_2(0,t)$
5	A $\xrightleftharpoons[\beta_1]{k_{1i}}$ B $\xrightleftharpoons[\beta_2]{k_2}$ C plus B accumulation	$\left\{ \begin{aligned} j_1(0,t) &= k_{1i} C_1^0 (1 - F_5) / (\pi t)^{1/2} [k_{1i} (1 + F_5) + D_1^{1/2} / (\pi t)^{1/2}] \\ j_2(0,t) &= (k_2 - \beta_2) C_1^0 / \{1 - \beta_2 (1 - F_2 / \beta_2 F_3) (\pi t / D_1)^{1/2}\} \end{aligned} \right.$
6	A $\xrightarrow{k_{1i}}$ B $\xrightarrow{k_2}$ C plus B accumulation	$\left\{ \begin{aligned} j_1(0,t) &= k_{1i} C_1^0 F(\lambda_6) \\ j_2(0,t) &= k_{1i} k_2 C_1^0 F(\lambda_6) / (\psi^2 + k_2) - k_{1i} k_2 C_1^0 \exp(-k_2 t) / (\psi^2 + k_2) + \\ &+ [k_{1i} k_2 C_1^0 \exp(-k_2 t) \int_0^t (\exp(k_2 \tau) d\tau / \tau^{1/2})] / (\psi^2 + k_2) \pi^{1/2} \end{aligned} \right.$

The mathematical models of molecular
diffusion with heterogeneous reaction

Model	Reaction type	The quantity of the substance transferred into phase 2
I	A $\xrightarrow{k_{xi}}$ B	$m_2(t) = 2 c_1^0 (D_1 t / \pi)^{1/2} - c_1^0 D_1 [1 - F(\lambda_1)] / \bar{k}_{xi}$
2	A $\xrightleftharpoons[\beta_1]{k_{xi}}$ B	$m_2(t) = 2 (\bar{k}_{xi} c_1^0 - \beta_1 c_2^0) t / \lambda_2 \pi^{1/2} - (\bar{k}_{xi} c_1^0 - \beta_1 c_2^0) t^{3/2} [1 - F(\lambda_2)] / \lambda_2^2$
3	A $\xrightleftharpoons[\beta_1]{k_{xi}}$ B $\xrightarrow{k_2}$ C	$m_2(t) = 2 c_1^0 (D_1 t / \pi)^{1/2} - c_1^0 D_1^{1/2} t^{3/2} [1 - F(\lambda_3)] / \lambda_3$
4	A $\xrightleftharpoons[\beta_1]{k_{xi}}$ B $\xrightleftharpoons[\beta_2]{k_2}$ C	$m_2(t) = 2 \delta k_{xi} k_2 c_1^0 (k_2 + \beta_1) (D_1 D_2)^{1/2} t^{3/2} / (\delta k_{xi} k_2 D_2^{1/2} + \delta \beta_1 \beta_2 D_1^{1/2}) \pi^{1/2} - c_1^0 (D_1 t)^{1/2} [1 - F(\lambda_4)] / \lambda_4$
5	A $\xrightleftharpoons[\beta_1]{k_{xi}}$ B $\xrightleftharpoons[\beta_2]{k_2}$ C plus B accumulation	—
6	A $\xrightarrow{k_{xi}}$ B $\xrightarrow{k_2}$ C plus B accumulation	$m_2(t) = k_{xi} k_2 c_1^0 \left\{ [2 \exp(-k_2 t) \int_0^t \tau^{1/2} \exp(k_2 \tau) d\tau] / \psi \pi^{1/2} + F(\lambda_6) / \psi^2 (\psi^2 + k_2) + \exp(-k_2 t) \int_0^t (\exp(k_2 \tau) d\tau / c^{1/2}) / \pi^{1/2} \psi (\psi^2 + k_2) + \exp(-k_2 t) / k_2 (\psi^2 + k_2) - 1 / \psi^2 k_2 \right.$

Table 3

The coefficients \bar{A} , the transients time t_t and interfacial resistances R_s according to the models mentioned

Model	\bar{A}	$t_t^{1/2}$	R_s
1	$2C_1^0(D_1/\pi)^{1/2}$	$\alpha(\pi D_1)^{1/2}/2K_{1i}$	$2t_t^{1/2}/(\pi D_1)^{1/2}$
2	$2[(C_1^0 - \alpha K_e C_2^0)(D_1/\pi)^{1/2}]/[1 + \alpha K_e(D_1/D_2)^{1/2}]$	$\alpha(\pi D_1)^{1/2}/2K_{1i}[1 + \alpha K_e(D_1/D_2)^{1/2}]$	—
3	$2C_1^0(D_1/\pi)^{1/2}$	$(\pi D_1)^{1/2}(K_2 + \beta_1)/2\delta K_{1i}K_2$	$2t_t^{1/2}/(\pi D_1)^{1/2}$
4	$2\delta K_{1i}K_2C_1^0(K_2 + \beta_1)(D_1D_2)^{1/2}/(\delta K_{1i}K_2D_2^{1/2} + \delta\beta_1\beta_2D_1^{1/2})\pi^{1/2}$	—	αt $K_2 > \beta_1$ $2t_t^{1/2}/(\pi D_1)^{1/2}$
6	$2K_2C_1^0D_1^{1/2}/(\psi^2 + K_2)\pi^{1/2}$	$\pi^{1/2}(\psi^2 + K_2)/2K_2\psi$	—

Table 4

The extractants and their properties

Extractants	Chem. formula	Physico-Chemical properties			
		n ₂₅	d ²⁵	content of P, % found	theory
Tripropylphosphate (TPP)	(C ₃ H ₇ O) ₃ PO	1.418	1.012	13.9 ± 0.2	13.8
Tributylphosphate (TBP)	(C ₄ H ₉ O) ₃ PO	1.424	0.977	11.8 ± 0.2	11.6
Trioctylphosphate (TOP)	(C ₈ H ₁₇ O) ₃ PO	1.434	0.915	7.2 ± 0.2	7.15
Trinonylphosphate (TNP)	(C ₉ H ₁₉ O) ₃ PO	1.436	0.915	6.6 ± 0.2	6.51
Triphenylphosphate (TPHP)	(C ₆ H ₅ O) ₃ PO	-	-	9.6 ± 0.2	9.51
Tributylphosphineoxide (TBPO)	(C ₄ H ₉) ₃ PO	-	-	14.4 ± 0.3	14.6
Trioctylphosphineoxide (TOPO)	(C ₈ H ₁₇) ₃ PO	-	-	8.1 ± 0.2	8.09
Triphenylphosphineoxide (TPhPO)	(C ₆ H ₅) ₃ PO	-	-	11.2 ± 0.2	11.2
1,4-bis-di-octylphosphinylbutan (1,4-bis-DOPB)	(C ₈ H ₁₇) ₄ (PO) ₂ (CH ₂) ₄	-	-	10.7 ± 0.2	10.6

Table 5

The R_s values for the stripping of some
acids and metal nitrates

S y s t e m s	t sec	R_s sec/cm
$\text{HClO}_4 - \text{H}_2\text{O} - \text{TBP} - \text{C}_6\text{H}_6$	0	0
$\text{HClO}_4 - \text{H}_2\text{O} - \text{TOPO} - \text{C}_6\text{H}_6$	0	0
$\text{HNO}_3 - \text{H}_2\text{O} - \text{TPP} - \text{C}_6\text{H}_6$	0.032	77
$\text{HNO}_3 - \text{H}_2\text{O} - \text{TBP} - \text{C}_6\text{H}_6$	0.025	68
$\text{HNO}_3 - \text{H}_2\text{O} - \text{TOP} - \text{C}_6\text{H}_6$	0.005-0.06	30-110
$\text{HNO}_3 - \text{H}_2\text{O} - \text{TNP} - \text{C}_6\text{H}_6$	0.006-0.025	34-70
$\text{HNO}_3 - \text{H}_2\text{O} - \text{TBPO} - \text{C}_6\text{H}_6$	0-0.014	0-52
$\text{HNO}_3 - \text{H}_2\text{O} - \text{TPhPO} - \text{C}_6\text{H}_6$	0.025	69
$\text{HNO}_3 - \text{H}_2\text{O} - \text{TOPO} - \text{C}_6\text{H}_6$	0.062	110
$\text{HNO}_3 - \text{H}_2\text{O} - 1,4\text{-bis-DOPB} - \text{C}_6\text{H}_6$	0.032	77
$\text{HSCN} - \text{H}_2\text{O} - \text{TBP} - \text{C}_6\text{H}_6$	0.09	120
$\text{Ce}(\text{NO}_3)_4 - \text{H}_2\text{O} - \text{TBP} - \text{C}_6\text{H}_6$	0.005	60
$\text{La}(\text{NO}_3)_3 - \text{H}_2\text{O} - \text{TBP} - \text{C}_6\text{H}_6$	0.017	105
$\text{Cu}(\text{NO}_3)_2 - \text{H}_2\text{O} - \text{TBP} - \text{C}_6\text{H}_6$	0.11	270
$\text{Ni}(\text{NO}_3)_2 - \text{H}_2\text{O} - \text{TBP} - \text{C}_6\text{H}_6$	0.13	290
$\text{Co}(\text{NO}_3)_2 - \text{H}_2\text{O} - \text{TBP} - \text{C}_6\text{H}_6$	0.3-1.5	440-1000
$\text{Zr}(\text{NO}_3)_4 - \text{H}_2\text{O} - \text{TOPO} - \text{C}_{10}\text{H}_{22}$	8.0	2500

Table 6
 Dependence of R_s , $t_t^{1/2}$ and \bar{A} on the water
 content of the organic phase

S y s t e m	Water concentration	$t_t^{1/2}$, sec 1/2	R_s , sec/cm	$\bar{A} \times 10^5$
HNO ₃ - TBP -	0.225	0.03	12.0	5.2
C ₁₀ H ₂₂ - H ₂ O	0.063	0.075	32.4	7.1
	0.016	0.158	68.0	7.9
HSCN - TBP -	0.37	0.02	4.3	5.5
C ₁₀ H ₂₂ - H ₂ O	0.122	0.06	28.5	6.4
	0.0158	0.13	47.5	6.9

Note that satisfactory linear correlations are found between $t_t^{1/2}$ and C_{H_2O} . The \bar{A} values also correlate with C_{H_2O} .

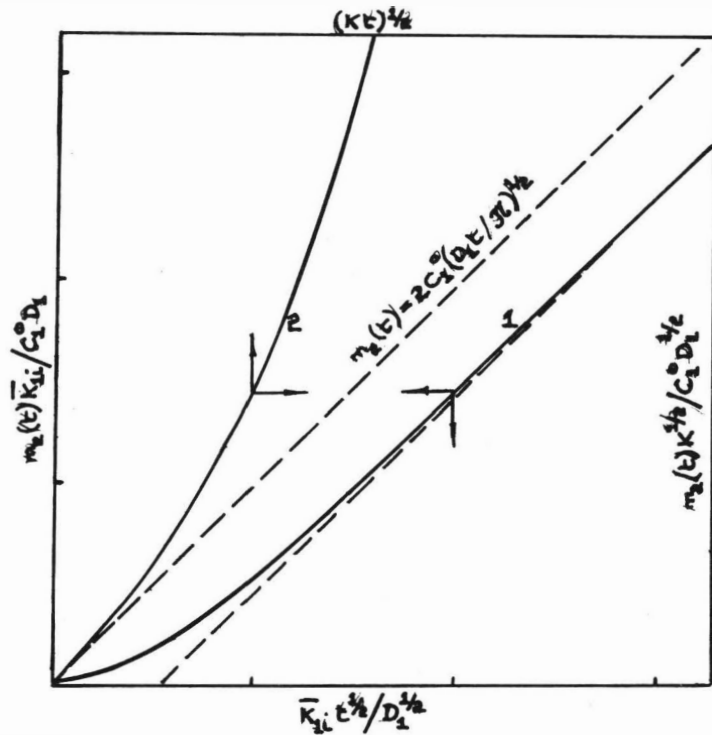


Fig. 1 Dimensionless mass dependence on dimensionless time

1. According to model 1
2. According to Danckwerts' model

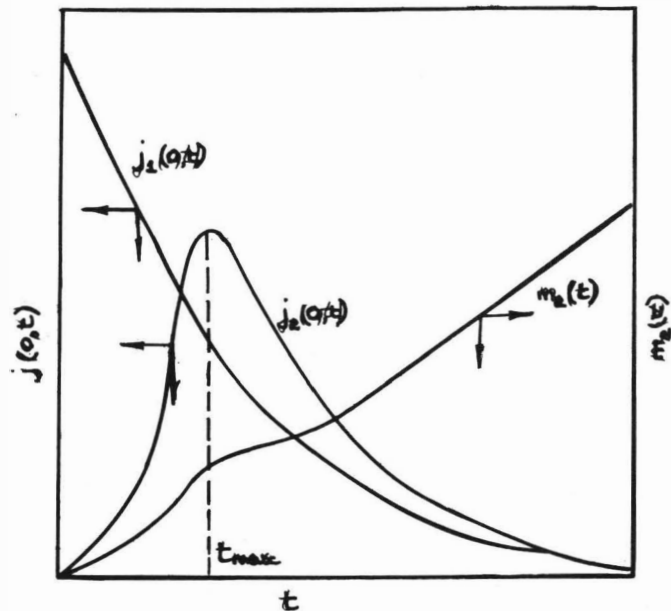


Fig. 2 Kinetics of mass transfer according to model 6.

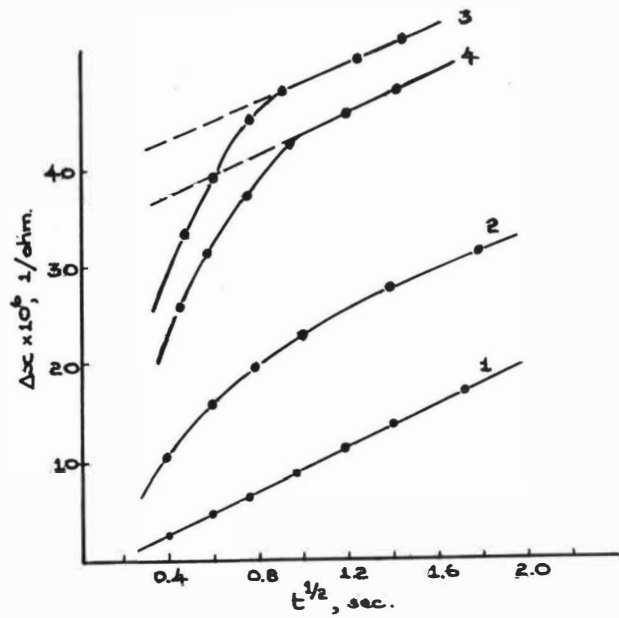


Fig. 3 Kinetics of stripping of HNO_3 from TNP solutions
1, 2, 3, 4 - consecutive contact numbers.

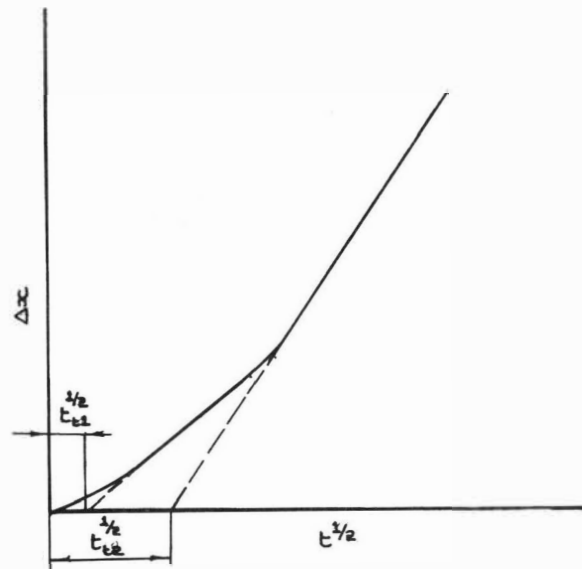


Fig. 4 Kinetics of stripping in case two component mass transfer ($R_{s1} \ll R_{s2}$)

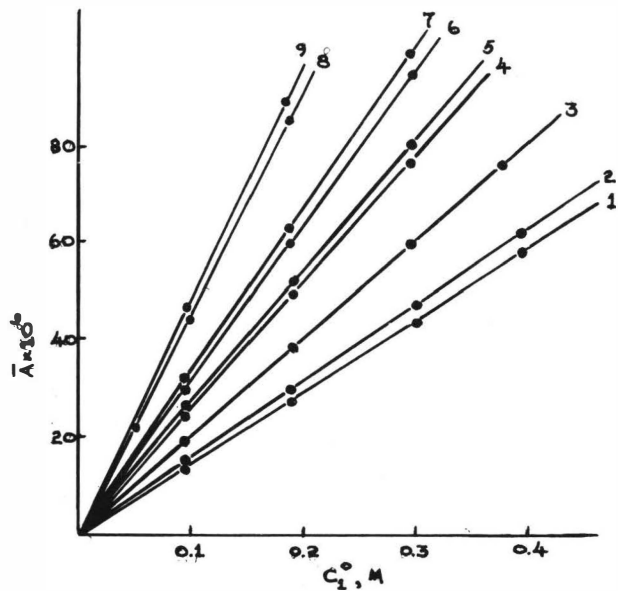


Fig. 5 Coefficients \bar{A} dependence on the HNO_3 solvate concentration.

1 - TOPO, 2 - TPhP, 3 - TNE, 4 - 1,4 bis DOBP, 5 - TPhPO, 7 - TOP,
8 - TBP, 9 - TFP

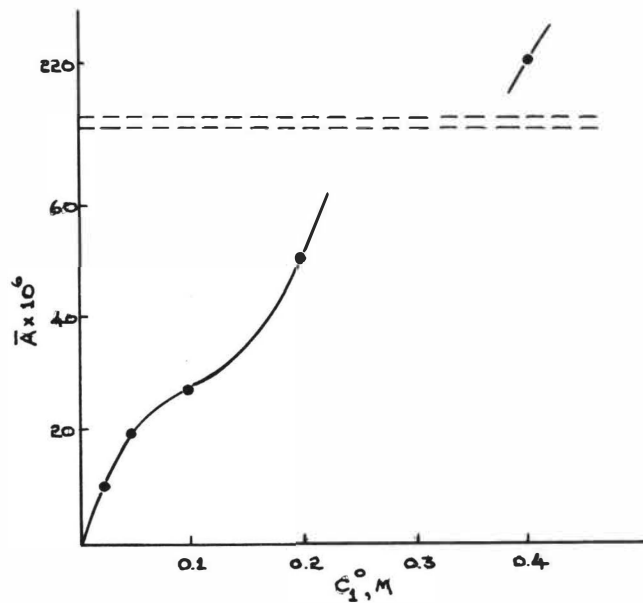


Fig. 6 Coefficients \bar{A} dependence on the HNO_3 solvate concentration, system
TBPO- HNO_3 - H_2O - C_6H_6 .

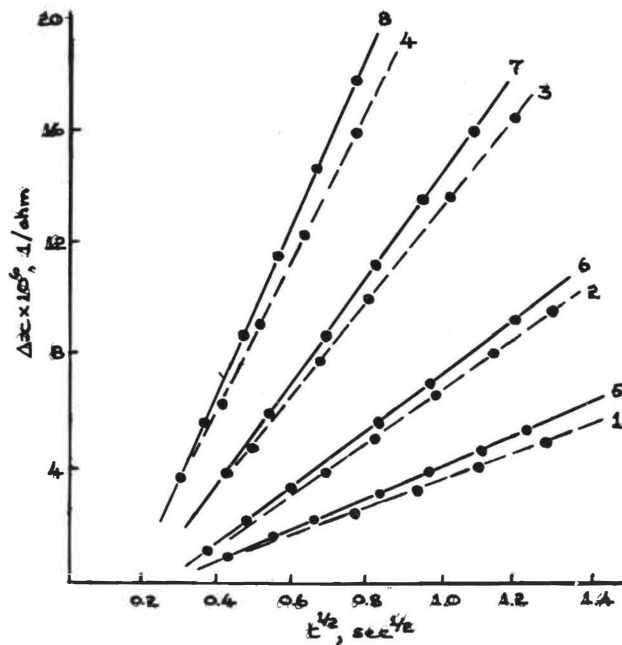


Fig. 7 Influence of "free" extractant concentration on the coefficient $\bar{\lambda}$. Stripping of HNO_3 from 0.1M TBP in a decane.

1, 2, 3, 4 - dilution of initial solution by 0.1M TBP in decane.
5, 6, 7, 8 - dilution of initial solution by decane.

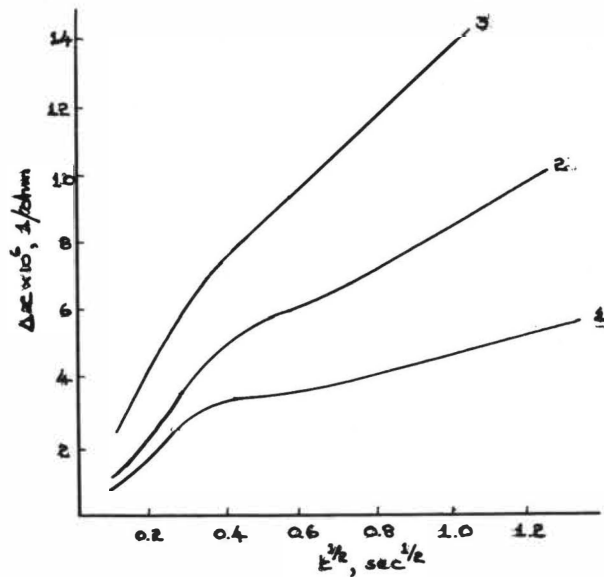


Fig. 8 Kinetics of stripping HClO_4 from diluted solutions of extractants.

1 - TPP (0.0125M), 2 - TBP (0.0145M), 3 - TOPO (0.083M)

PAPER NO. 91EXTRACTION OF NICKEL BY α HYDROXY OXIME /
CARBOXYLIC ACID MIXTURES

D.S. FLETT

M. COX

J.D. HEELS

Paper to be presented to ISEC 74 Conference

Lyon, France, 8-14 September 1974

(International Solvent Extraction Conference 1974)

Sponsored by The Society of Chemical Industry

Proofs to:A.J. Sharp Esq
Publications Office
Warren Spring Laboratory
P.O. Box 20
Gunnels Wood Road
Stevenage
Hertfordshire
SG1 2BXSent to:Dr. A. Naylor
British Nuclear Fuels Limited
Windscale and Calder Works
Seascale
Cumberland
CA20 1PG

* D.S. Flett
Ø M. Cox
Ø J.D. Heels

SYNOPSIS

The stoichiometry of the mixed complex formed on the extraction of nickel with α hydroxy oxime/lauric acid mixtures has been determined. The anomalously slow rate of extraction of nickel by the mixed extractants has been shown to be due to specific interfacial effects caused by the interaction between the nickel and the lauric acid.

INTRODUCTION

Studies of the extraction of several metal ions with various α hydroxy oxime/carboxylic acid mixtures showed that appreciable synergism occurred, particularly in the extraction of divalent metal ions and the degree of synergism varied with the type of carboxylic acid. Of particular interest were the selectivity reversals that were observed for copper over ferric iron and nickel over ferric iron when the chosen carboxylic acid was α bromolauric acid⁽¹⁾. Stoichiometric studies with copper have indicated that the complex contains copper/ α hydroxy oxime/ α bromolauric acid in the ratio of 1:2:4⁽²⁾. Development work with this system has shown that there is no justification for considering either α hydroxy oxime/di(2-ethylhexyl) phosphoric acid (DEHPA) or α hydroxy oxime/carboxylic acid mixtures as satisfactory alternatives to existing commercial copper extraction reagents⁽³⁾.

The extraction of nickel with α hydroxy oxime/carboxylic acid mixtures is of considerable potential commercial interest. Separation factors of up to 50 have been found for nickel from cobalt in sulphate solutions when the carboxylic acid is naphthenic acid, while the ability to extract nickel in preference to ferric iron with α hydroxy oxime/ α bromolauric acid mixtures is unmatched by any existing commercial solvent extraction reagents or reagent combinations. Thus considerable incentive exists for further

* Warren Spring Laboratory, Stevenage, Hertfordshire, England.

Ø The Hatfield Polytechnic, Hatfield, Hertfordshire, England.

development work but the rate of extraction is particularly slow, taking about three hours to reach equilibrium at room temperature⁽¹⁾. This is surprising because the rate of extraction of nickel by the individual extractants is such that, at the very most, ten minutes only are required to reach equilibrium.

The kinetics of solvent extraction systems involving extraction of metal chelates has not received much attention and consequently almost nothing has been reported on the kinetics of metal extraction where two or more extractants are employed to achieve equilibrium synergism. However, from data available on single extractant systems, (see Alimarin et al⁽⁴⁾ and Flett et al⁽⁵⁾ for critical reviews of published data) there seems to be a divergence of opinion about whether chelating extraction reaction should be discussed in terms of the kinetics of complex formation in homogeneous aqueous solution or in terms of the heterogeneous kinetics concerning species adsorbed at the aqueous organic interface. While it is obviously not possible at present to reconcile these divergent viewpoints it is perhaps appropriate to note that, with the extractants used or proposed for use commercially, the aqueous solubility is such that the molarity of the extractant in the aqueous phase, and in particular the molarity of the extractant anion, is so low that homogeneous aqueous rate-controlling complexing reactions are unlikely. Thus the rate-controlling step for the extraction of iron with DEHPA⁽⁶⁾ has been shown to occur at the aqueous organic interface and a similar conclusion has been drawn to explain rate data for the extraction of copper by α hydroxy oxime/ β hydroxybenzophenone oxime mixtures⁽⁵⁾ (i.e. LIX63, LIX65N and LIX64N). Therefore, in the present case, it would seem a reasonable assumption that the anomalous rate effects observed in the extraction of nickel with α hydroxy oxime/carboxylic acid mixtures are interfacial in origin. Study of the interfacial properties of the nickel system should show differences when compared with the properties of systems containing, for example, copper and cobalt. One of the most easily measured interfacial properties is the interfacial tension and it is well known that changes in interfacial tension result in changes in mass transfer rates and vice versa. To attempt to discover the cause of the anomalously slow rate of extraction of nickel by α hydroxy oxime/carboxylic acid mixtures, the stoichiometry of the mixed complex has been determined, and a study of the interfacial tension of α hydroxy oxime/carboxylic acid system has been undertaken. The results of this study are presented in this paper.

MATERIALS

The α hydroxy oxime used was prepared from 2-ethylhexanoic acid by the method described by Swanson⁽⁷⁾. Laboratory reagent grade lauric acid, (Hopkins and Williams) . was used without further purification. Metal nitrate solutions were prepared from BDH Analar grade chemicals and pH adjustments were made with AR nitric acid and sodium hydroxide solution prepared from BDH standard solutions. Hexane, AR grade, was selected as the diluent.

COMPLEX STOICHIOMETRY

Distribution studies were carried out as described by Flett and West⁽¹⁾. The extraction of nickel with α hydroxy oxime (HOx), lauric acid, (RH) and the extractant mixture is shown as log D/pH plots in Fig. 1. The slope of these plots correspond to 2.0 except for the extraction of nickel with the α hydroxyoxime which shows a slope of 1.6.

Preliminary work revealed that the addition of lauric acid to the nickel α hydroxy oximate in hexane caused a near instantaneous colour change from red to green and the UV and visible spectra of both complexes are shown in Fig. 2. The UV and visible spectrum of this green complex was identical with that for the complex formed by solvent extraction of nickel with the mixed extractants.

The spectrum of the nickel α hydroxy oximate in hexane (Fig. 2) is typical of nickel square planar complexes and thus it may be inferred that the stoichiometry of the nickel oximate is $\text{Ni}(\text{Ox})_2$. This stoichiometry was confirmed by means of the method of continuous variation (Job's method) wherein the optical density of the organic extract was plotted against the composition of the aqueous phase, Fig. 3. Experimentally the desired result was achieved by keeping the total molarity of the nickel and α hydroxy oxime constant while varying the individual concentrations from 0 to 0.1 mol. The figure shows clearly that the stoichiometry is $\text{Ni}(\text{Ox})_2$.

Because, as can be seen in Fig. 2, there is clearly no contribution from the spectrum of the mixed complex to the colour peak of the nickel α hydroxy oximate, a spectrophotometric titration technique could be employed to determine the number of lauric acid molecules associated with this complex. Various amounts of lauric acid were added to aliquots of the nickel α hydroxy oximate in hexane and the change in optical density of the red oximate peak (415 nm)

plotted against the amount of carboxylic acid added. A typical spectrophotometric titration plot is shown in Fig. 4.

From this spectrophotometric titration the ratio of lauric acid to nickel in the mixed complex is seen to be 2:1. The spectrum of the mixed complex (Fig. 2) is typical of six-coordinate nickel and thus it seems that the carboxylic acid molecules interact directly with the central metal atom to achieve a coordination number of six. The existence of only one mixed complex is indicated by the presence of the isosbestic points when a series of spectra are recorded for varying molar ratios of nickel laurate and nickel α hydroxy oximate, Fig. 5. Thus the molar ratios in the mixed complex are Ni/lauric acid/ α hydroxy oxime; 1:2:2 and the monomeric formula $\text{Ni}(\text{Ox})_2(\text{RH})_2$ is proposed for the mixed complex.

INTERFACIAL TENSION MEASUREMENTS

Interfacial tension measurements were carried out with a Du Nuoy ring tensiometer. The following procedure was adopted. The aqueous and organic phases were first equilibrated for 15 min, the phases were separated and the pH values measured. Equal volumes of the aqueous and organic phases were then placed together in the measuring dish and the interfacial tension recorded. The final pH value of the aqueous phase was varied by the addition of sodium hydroxide or nitric acid. Metal ion concentrations of 0.1 mol were adopted for these studies and the sodium ion concentration was kept constant at 0.04 mol by the addition of sodium nitrate except where indicated.

Preliminary testwork showed that, of the two reagents, the carboxylic acid was much more surface-active than the α hydroxy oxime. Indeed in mixtures of the α hydroxy oxime and lauric acid, the measured interfacial tension reflected the concentration of lauric acid only. Thus the effect of nickel on the interfacial tension in the system lauric acid/hexane/water was considered to correctly represent, at least qualitatively, the effects to be expected from the mixed system. The variation of interfacial tension of the system, lauric acid (0.1 mol) hexane/ $\text{Ni}(\text{NO}_3)_2$ (0.1 mol)/ H_2O is shown in Fig. 6 together with the corresponding plots for α hydroxy oxime (0.1 mol)/hexane/ $\text{Ni}(\text{NO}_3)_2$ / H_2O , lauric acid (0.1 mol)/hexane/ H_2O and α hydroxy oxime (0.1 mol)/hexane/ H_2O . The figure shows that while in the case of the α hydroxy oxime the presence of nickel increases the interfacial tension, its presence tends to decrease the interfacial tension of the lauric acid system. The curve is

seen to be in two parts which suggests that the presence of the nickel may be causing a phase change in the adsorbed molecules at the interface.

To see whether this interfacial tension variation for the lauric acid/nickel system was as anomalous as the extraction rate with the mixed reagents, interfacial tension variations with pH were measured for the lauric acid system with copper, cobalt and sodium. These data are shown graphically in Fig. 7 from which it can be clearly seen that the behaviour of nickel is anomalous.

The effect of nickel concentration on the variation of interfacial tension with pH has been studied as has the effect of lauric acid concentration. These results are shown in Figs 8 and 9.

DISCUSSION

The stoichiometry of the mixed complex formed between nickel and α hydroxy oxime/lauric acid mixtures is $\text{NiOx}_2(\text{RH})_2$. This is sufficiently different from the stoichiometry of the corresponding copper complex, where the carboxylic acid was α bromolauric acid, to question whether the spectrophotometric method used in the present study gave results which were consistent with the slope analysis method used previously. Consequently a spectrophotometric titration was carried out wherein lauric acid was added to the copper oximate. The stoichiometry obtained therefrom was $\text{CuOx}_2(\text{RH})_4$, in complete agreement with the result from slope analysis.

While the $\log D/\text{pH}$ plots for the lauric acid and the α hydroxy oxime/lauric acid mixture seem normal exhibiting a slope of ~ 2.0 , the slope for the α hydroxy oxime only is anomalously low. Low slopes can be caused by any or all of the following:

- (i) formation of intermediate aqueous soluble complexes with the extractant,
- (ii) hydrolysis of the metal ion,
- (iii) non-equilibrium conditions.

The concentration of hydrolytic species of nickel⁽⁸⁾ at pH 6 and below is insufficient to reduce the slope of the $\log D/\text{pH}$ plot and rate data for nickel extraction with the α hydroxy oxime indicate that equilibrium is probably achieved within five minutes. No direct evidence exists for the formation of intermediate aqueous soluble species between the α hydroxy oxime and nickel.

It was therefore of some interest to see whether similarly anomalous slopes occurred when $\log D/pH$ data was obtained for the stripping reaction. Such data were readily acquired by contacting aliquots of a hexane solution of the red nickel oximate complex with aqueous phases containing varying concentrations of acid. These data are shown as a $\log D/pH + \log HOx$ plot in Fig. 10, where $\log HOx$ denotes the calculated "free" α hydroxy oxime concentration in the organic phase assuming the complex to be $NiOx_2$. The slope of this plot is seen to be 1.92. The reason for the anomalously low slope of the $\log D/pH$ plot obtained for the extraction reaction remains unexplained.

Because the extraction of nickel by the α hydroxy oxime is complete in less than 5 minutes and the reaction between lauric acid and the nickel oximate is very fast, the mechanism of nickel extraction cannot follow that route. From Fig. 1 it is far from clear whether the nickel would prefer to react preferentially with the lauric acid or the α hydroxy oxime in any sequential stepwise mechanism in the formation of the mixed complex. However it is quite clear from the interfacial tension data that the combination of nickel and lauric acid yields anomalous values for the interfacial tension when compared with copper and cobalt. It would therefore seem to be more than fortuitous that the lowering in the interfacial tension found in the present study corresponds with a lowering in the extraction rate of the metal ion. It should be observed that the addition of nickel to the α hydroxy oxime/hexane/ H_2O system increases the interfacial tension and nickel is extracted relatively rapidly by that system.

Accurate physical-chemical descriptions of the cause of interfacial tension changes are not readily made. Peters^(9,10) has measured the interfacial tensions of long-chain acids at the benzene/water interface and correlated change of interfacial tension with ionization of the acids. If the lowering of interfacial tension results from the population of the interface with carboxylic acid molecules which increasingly ionize as the pH value increases, then addition of cation-like copper, cobalt and sodium must decrease this interfacial concentration of carboxylic acid. Clearly, when extraction of these cations commence the interfacial tension will fall as the extraction reaction takes place at the interface. This effect can be seen in Fig. 7. The anomalous interfacial tension-lowering in the presence of the nickel may be ascribed in two ways. Either the nickel is interacting with the carboxylic acid in some way at the interface or it is staying away from the interface altogether so that there is no barrier to the carboxylic acid molecules

collecting at the interface. In this latter case a curve similar to that for the lauric acid/water system would be expected. Because the shape of the curve for the lauric acid/nickel system is quite different to that for the lauric acid/water system (Fig. 6) it is concluded that the interfacial tension-lowering is caused by interaction between nickel and the lauric acid at the interface. The hiatus in the variation of the interfacial tension with pH merely denotes a change of state of the adsorbed species at the interface, probably from a two-dimensional liquid to a two-dimensional solid. Langmuir trough experiments will provide useful additional data.

Earlier studies⁽¹¹⁾ have shown that from mixed solutions of nickel and cobalt, the rate of cobalt extraction is still fast compared with nickel. The interfacial tension of a solution of 1 mol cobalt and nickel nitrate equilibrated with 0.1 mol lauric acid in hexane is equal to that of cobalt only. Since it has been concluded that the lowering of interfacial tension in the presence of nickel is caused by interaction between the nickel and the lauric acid at the interface then the observed effect of cobalt addition must mean that cobalt is more strongly adsorbed at the interface but without forming a solid interfacial phase. Thus, while interfacial potential measurements are unlikely to differentiate between nickel and cobalt, interfacial viscosity measurements will show considerable differences between these two metal ions.

The effect of multivalent ions on carboxylic acid monolayers has been studied by several workers⁽¹²⁻¹⁷⁾. Such cations, especially those of the alkaline earth metals, copper, lead and aluminium, alter the properties of ionized fatty acid monolayers markedly. Correlation between the pH of change to solid expanded films and the pH of hydroxide precipitation of Ca^{2+} , Zn^{2+} , Cu^{2+} , Al^{3+} , and Fe^{3+} has been reported for the spreading of stearic acid over the metal solution⁽¹²⁾. The effect of nickel seems to have been reported only once. This study does provide comparative data between nickel and copper and the amount of each metal found in the stearic acid film spread on the aqueous solution.

At pH 4.1, 70% of the amount of nickel required to form nickel stearate compared with only 6.6% of copper, is found in the film which indicates that nickel interacts more strongly than copper with the stearic acid monolayer.

Thus the problem of the rate of nickel extraction would seem to be caused by the formation of a solid interfacial phase containing nickel which acts as a barrier to mass transfer.

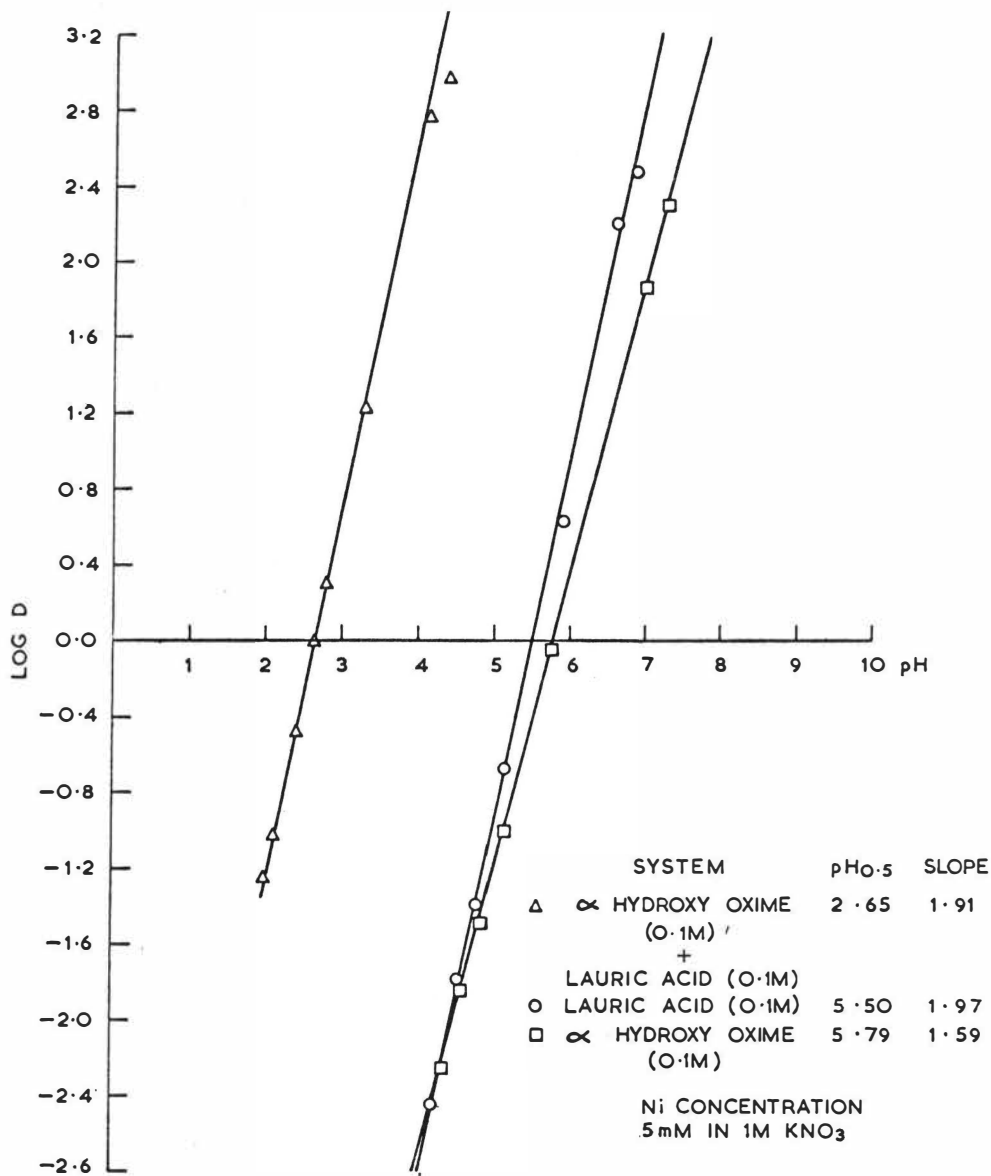
CONCLUSIONS

The stoichiometry of the mixed complex formed on the extraction of nickel with α hydroxy oxime/lauric acid mixtures is $\text{NiOx}_2(\text{RH})_2$. The anomalously slow rate of extraction of nickel by the mixed extractants has been shown to be due to specific interfacial effects. Rather than attempt to explain solvent extraction kinetics in terms of homogeneous aqueous complexing reaction, attention should be given to the physical chemistry of the interfacial region.

References

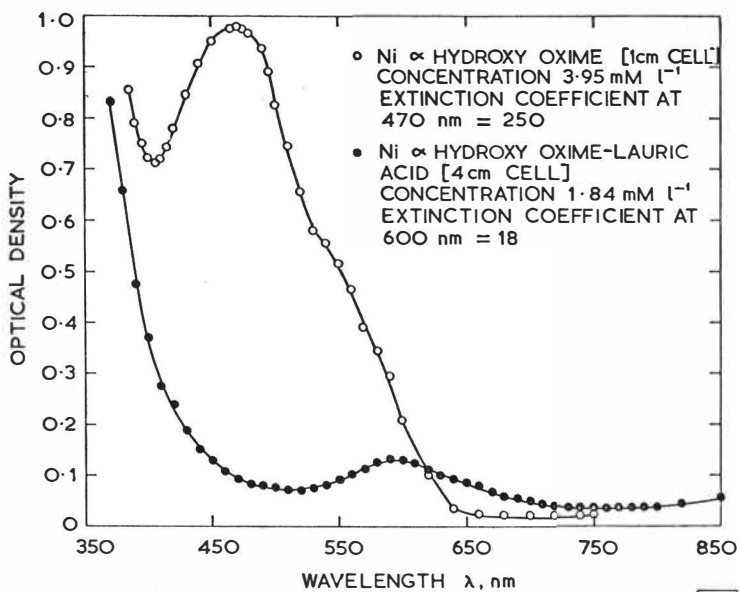
- 1 Flett, D.S. and West, D.W. in Proceedings ISEC 71 (1971) p. 214 (London, S.C.I.).
- 2 Cox, M. and Flett, D.S. in Proceedings ISEC 71 (1971) p. 204 (London, S.C.I.).
- 3 Flett, D.S. and West, D.W. Trans. Instn Min. Metall. 1973, 82 C 107.
- 4 Alimarin, I.P.; Zolotov, Y.A. and Bodnya, V.A. Pure Appl. Chem. 1971, 25 (4), 667.
- 5 Flett, D.S.; Okuhara, D.N. and Spink, D.R. J. inorg. nucl. Chem. (1973) 35, 2471.
- 6 Roddy, J.W.; Coleman, C.F. and Arai, S. J. inorg. nucl. Chem. (1971) 33, 1099.
- 7 Swanson, R.R. U.S. Pat. 3,224,873, (1969).
- 8 Perrin, D.D. J. Chem. Soc. (1964) 3644.
- 9 Peters, R.A. Trans. Faraday Soc. (1930), 26, 197.
- 10 Peters, R.A. Proc. R. Soc. (1931), A 133, 147.
- 11 Flett, D.S. Unpublished data.
- 12 Spink, J.A. and Sanders, J.V. Trans. Faraday Soc. 1955, 51, 1154.
- 13 Betts, J.J. and Pethica, B.A. Trans. Faraday Soc. (1956), 52, 1581.
- 14 Spink, J.A. J. Colloid Sci. 1963, 18, 512.
- 15 Goddard, E.D. and Ackilli, J.A. J. Colloid Sci. 1963, 18, 585.

- 16 Stickland, F.G.W. J. Colloid Sci. 1972, 40, 142.
17 Stickland, F.G.W. J. Colloid Sci. 1973, 42, 96.



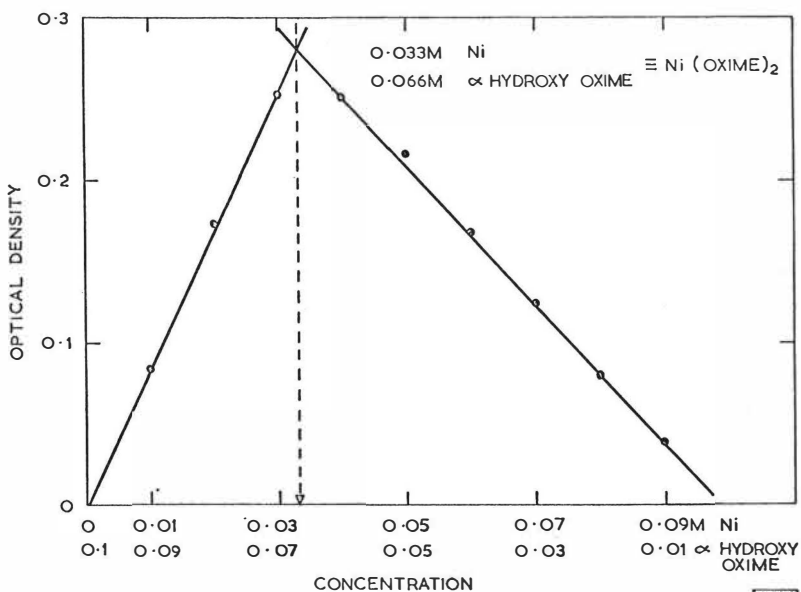
5762

FIG.1 EXTRACTION OF Ni. WITH AN α HYDROXY OXIME AND LAURIC ACID; VARIATION OF LOG D WITH pH



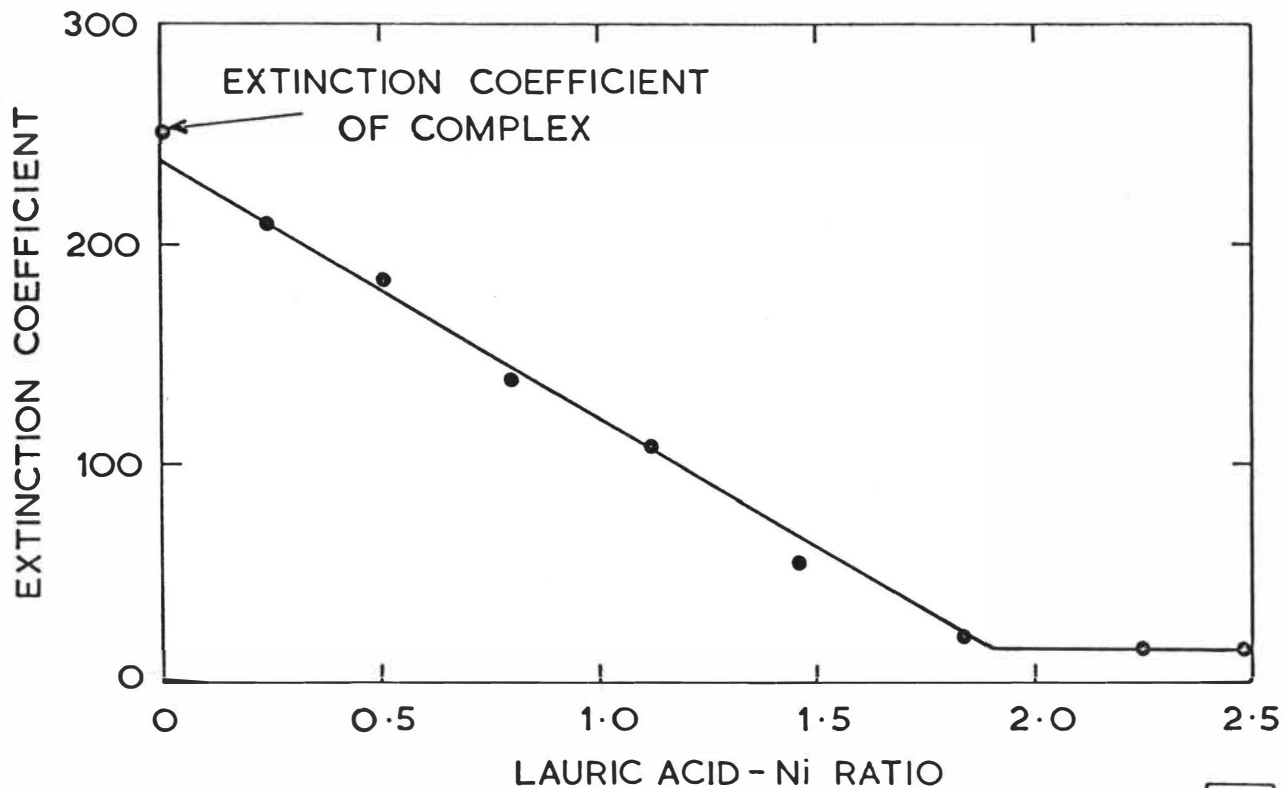
5763

FIG. 2 UV AND VISIBLE SPECTRA OF Ni α HYDROXY OXIME AND Ni α HYDROXY OXIME LAURIC ACID COMPLEXES



5764

FIG. 3 ISOMOLAR SERIES PLOT FOR THE EXTRACTION OF Ni WITH α HYDROXY OXIME, WAVELENGTH 470nm



5765

FIG. 4 SPECTROPHOTOMETRIC TITRATION OF Ni
 α -HYDROXY OXIME COMPLEX, WITH LAURIC ACID AT
470nm

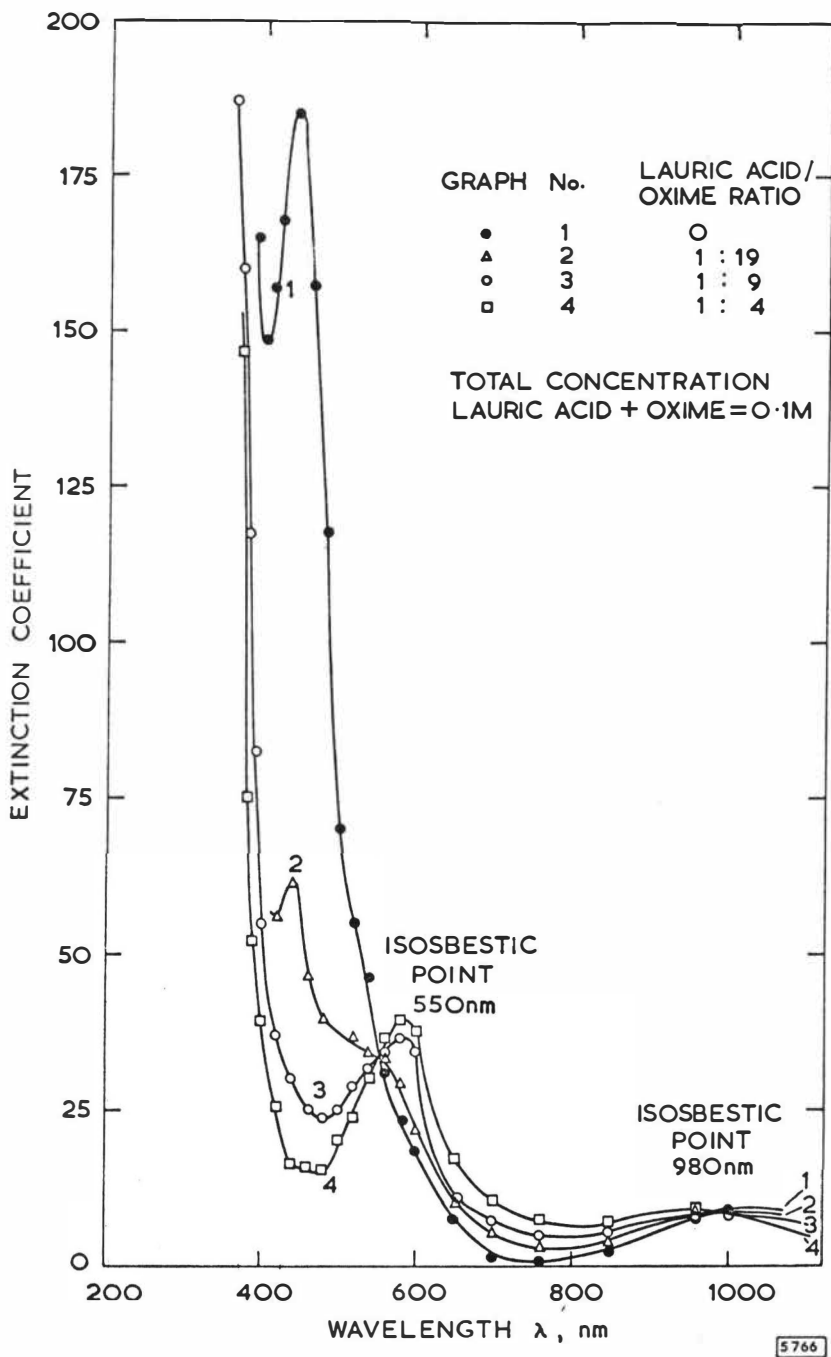
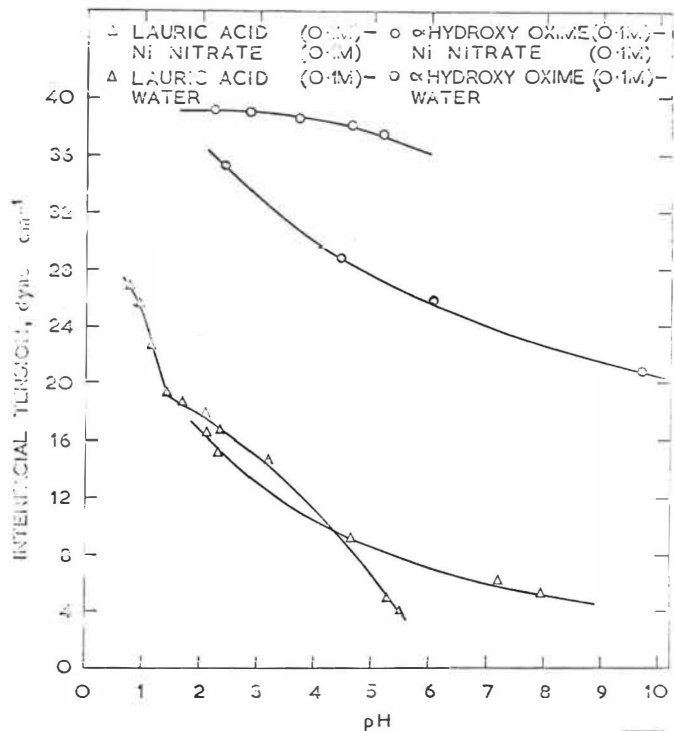
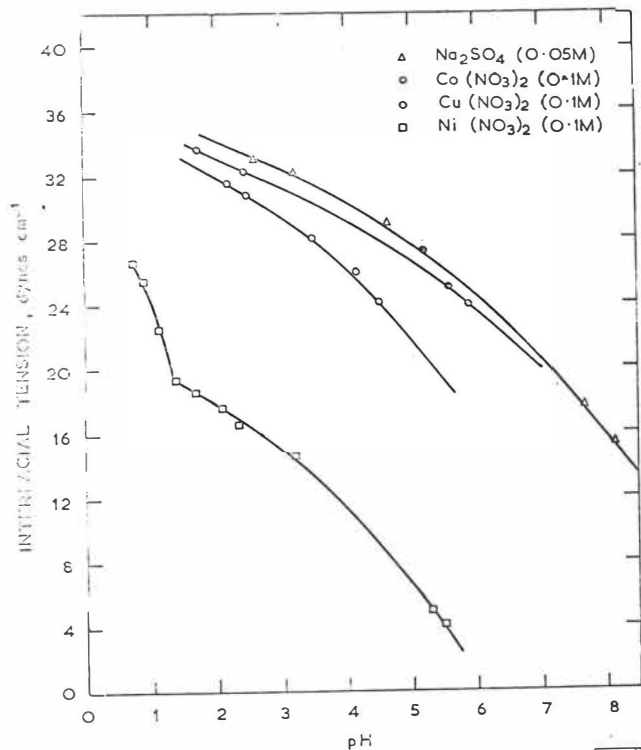


FIG. 5 VISIBLE SPECTRA OF VARIOUS Ni α HYDROXY OXIMATE/LAURIC ACID MIXTURES



5767

FIG. 6 INTERFACIAL TENSION OF HEXANE SOLUTIONS OF LAURIC ACID AND α HYDROXY OXIME OVER WATER AND NI NITRATE. EFFECT OF pH



5768

FIG. 7 INTERFACIAL TENSION OF HEXANE SOLUTIONS OF LAURIC ACID OVER NI, CO AND CU NITRATES AND Na SULPHATE. EFFECT OF pH

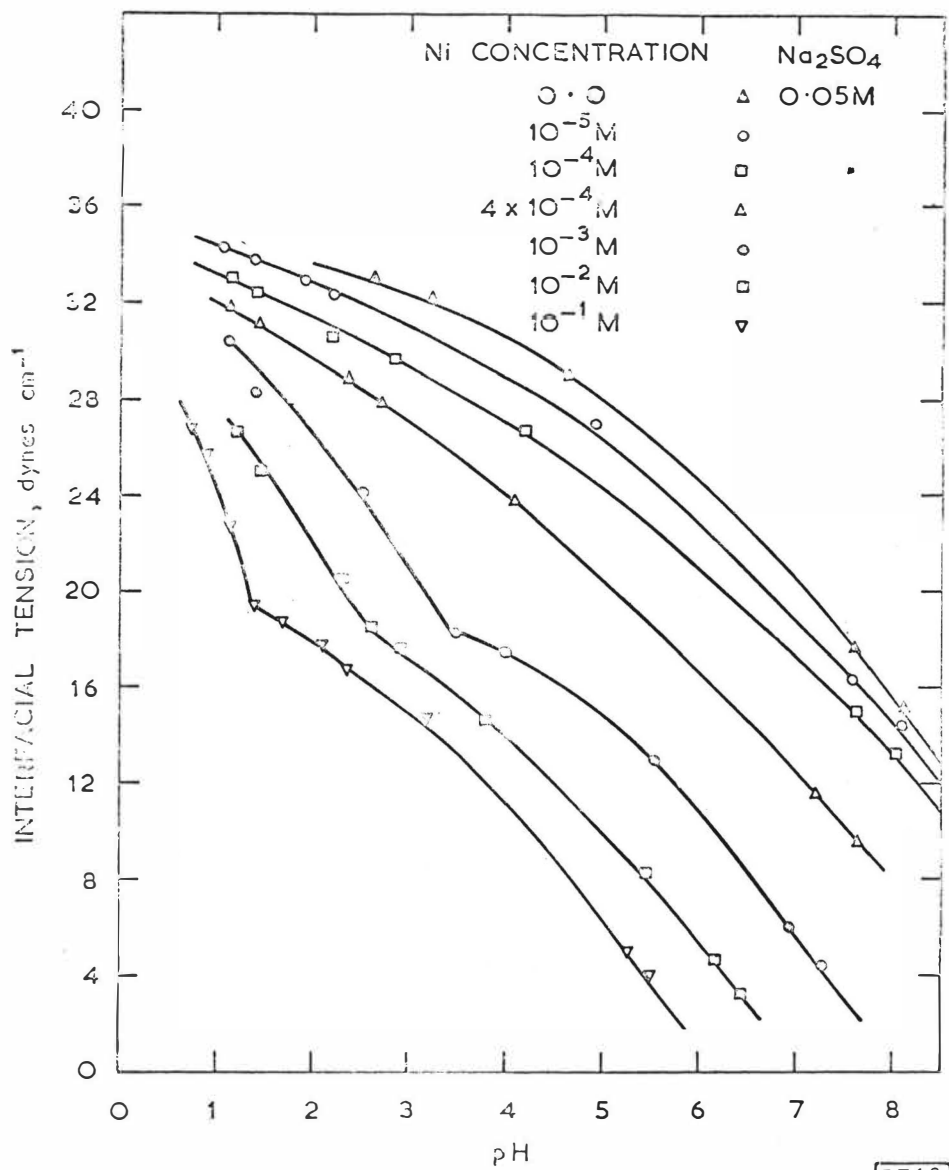
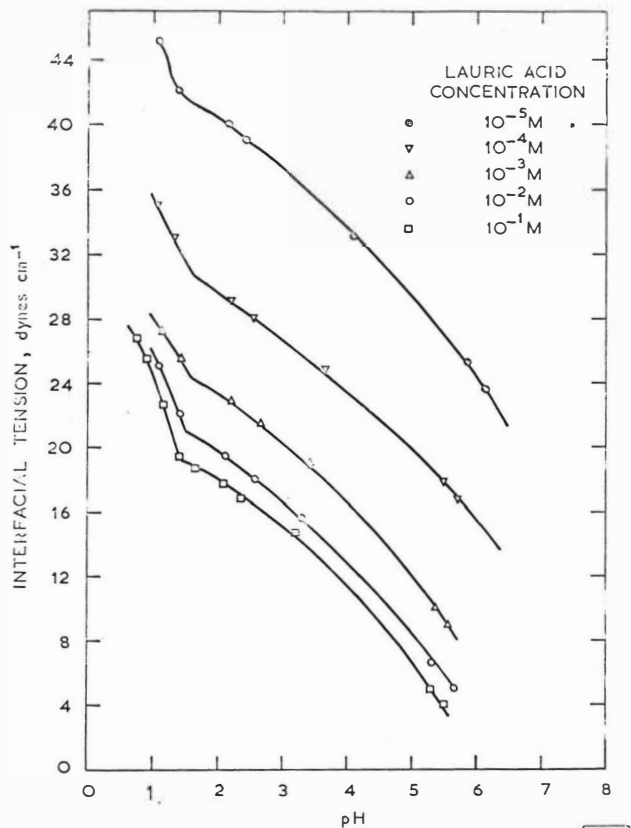
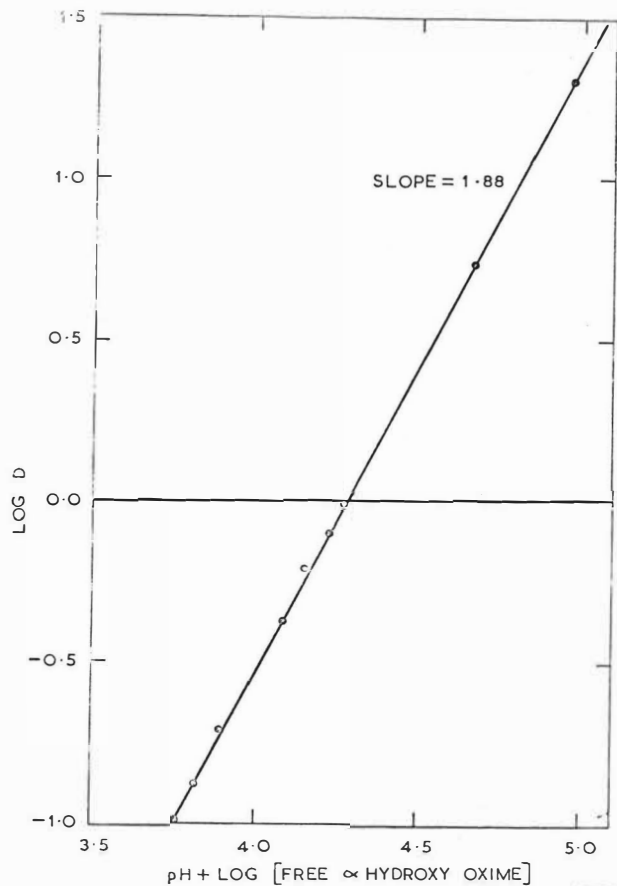


FIG. 8 INTERFACIAL TENSION OF HEXANE SOLUTIONS OF LAURIC ACID OVER WATER. EFFECT OF Ni CONCENTRATION



5770

FIG. 9 INTERFACIAL TENSION OF HEXANE SOLUTIONS OF LAURIC ACID OVER Ni NITRATE SOLUTIONS IN WATER. EFFECT OF LAURIC ACID CONCENTRATION



5771

FIG. 10 STRIPPING OF Ni FROM THE α HYDROXY OXIME COMPLEX. VARIATION OF LOG D WITH pH

Synergic extraction of metals by the mixtures of
tri-n-octylamine with a neutral extractant from
nitrate and chloride solutions

B. Ya. Spivakov, B. F. Myasoedov, B. M. Shkinev,
N. E. Kochetkova, M. K. Chmutova

Vernadsky Institute of Geochemistry and Analytical
Chemistry, U.S.S.R. Academy of Sciences, Moscow

Abstract

The solvent extraction of the trivalent transplutonium elements (TPE), Eu, Th, Zr from nitrate solutions and Am and Eu from chloride solutions by the mixtures of tri-n-octylamine (TOA) with tributyl phosphate (TBP) and trioctylphosphine oxide (TOPO) in different diluents has been studied. A considerable synergic effect has been observed in the extraction of TPE and Eu by the mixtures of TOA and TBP. The effect increases with increasing salting-out agent concentration giving extraction of TPE from nitrate and chloride solutions with high distribution coefficients. A mixture of TOA and TBP can be successfully used for the extraction of TPE from acidic nitrate solutions. A synergic effect has been also found for Th. The methods of i.r. spectroscopy and electrophoresis have been used to confirm a suggestion of the authors that the synergic effect is due to the formation of mixed anionic complexes of the metals containing inorganic ligands and co-ordinated molecules of the neutral extractant.

Introduction

In many cases some mixtures of extractants permit the extraction of metals with higher distribution coefficients than in the use of these extractants alone. (1)

It is well known that in the extraction of metals as solvates, extractant molecules are solvated with the neutral metal complex, e.g. a nitrate or a chloride. The solvation of neutral extractant molecules by anionic metal complexes with inorganic ligands is also possible. In this case a combination of a cationic extractant, which is the partner for the complex anion, with a neutral extractant can cause a synergic effect. One can expect such an effect for metal ions which form complexes with rather high co-ordination numbers (CN) because the complex solvated extractant molecules must be anionic, that is contain a sufficient number of inorganic anions. In this case the extractant molecules can lower the charge of the anionic complex and/or displace water molecules from the inner sphere of the metal; as is known, both factors promote the extraction.

Several studies have been made of the extraction of metals by mixtures of amines or quaternary ammonium salts with neutral oxygen-bearing extractants from nitrate, thiocyanate and chloride solutions.

We have studied the extraction of trivalent TPE, Eu, Th(IV) and Zr(IV) from nitrate solutions and Am(III) and Eu from chloride solutions by the mixtures of TOA and a neutral extractant. The ratio of the charge to CN in complexes of trivalent elements on the one hand and their low extraction by both amines and oxygen-bearing extractants lead to the anticipation of high synergic effects. For TPE, the problem seems of practical interest because the elements are extracted from nitrate and chloride solutions only by using high extractant concentrations and from inconveniently weak acidic solutions.

Extraction from nitrate solutions

A synergic effect ($S > 1$) was found for metal extraction by TOA nitrate and several neutral extractants. $S = D_{TOA}^{NE} / (D_{NE} + D_{TOA})$ where D_{NE} , D_{TOA} and D_{TOA}^{NE} are the distribution coefficients for the extraction of the metal by the neutral extractant (NE), TOA nitrate and their mixture respectively. TBP, TOPO and triphenylphosphine oxide all gave synergic effects with TOA nitrate, the TOA-TBP effect being particularly large.

Fig. 1 illustrates the extraction of americium by TBP-TOAHNO₃ mixtures at a constant total extractant concentration of 0.8M from 5.7M LiNO₃ and 0.1M HNO₃ solution. The extraction was carried out (a) by untreated solutions of TBP, TOAHNO₃ and their mixtures in benzene and (b) by similar solutions eight times pre-equilibrated with aqueous solutions of the same concentration to saturate the organic phase with HNO₃ initially in the absence of americium. Fig. 1 shows a marked synergic effect in both cases. Therefore, the effect is not connected with the extraction of HNO₃.

Table 1

The extraction of Am by 0.4M solutions of TBP, TOAHNO₃ and their mixture (0.4M+0.4M) in cyclohexane and its dependence on LiNO₃ concentration.

The initial HNO₃ concentration in the aqueous phase is 1M.

LiNO ₃ concentration (M)	D _{TBP}	D _{TOA}	D _{TOA} D _{TBP}	S
3.0	0.102	0.042	0.24	1.67
5.0	0.093	0.042	1.09	8.07
7.2	0.117	0.1	4.36	20.0
10.0	0.17	0.28	24.9	55.3

S-values depend very strongly on the salting-out agent concentration, as is clearly seen from the data of Table 1. Americium is extracted with a high distribution coefficient even from 1M HNO₃ solution when the LiNO₃ concentration increases up to 10M. Under such conditions D_{TBP} and D_{TOA} are approximately 100 times less than D_{TOA}^{TBP} . Analogous dependencies have been found for Cm and Cf as well as for Eu: The synergic effect follows the order: Am > Cm > Cf. It is of interest that the change from LiNO₃ to Al(NO₃)₃ of the same normality does not lead to a change of the distribution coefficients.

The extraction of tetravalent elements, thorium and zirconium, by the mixtures of TOA and TBP has been studied. Thorium was extracted from HNO₃ solutions in the presence and in the absence of LiNO₃ at different extractant concentration ratios. A synergic effect has been found in the extraction from HNO₃ solutions though its magnitudes were much lower than for trivalent elements. Maximum effects are observed at 0.5M HNO₃. The S value increases with increasing extractant concentration. This has also been observed for trivalent elements. The extraction of Th by the mixtures of TOAHNO₃ and TBP in other diluents (o-xylene, toluene, cyclohexane and CCl₄) has also been studied. It has been shown as in the case of trivalent elements that the diluent nature influences only the absolute values of the distribution coefficients and has only a small effect on the synergic effect. The extraction of Th by the extractant mixture follows the same order as in the case of amine alone; such a dependence has been found for Am and Eu as well. The S value keeps constant with increasing Th concentration up to 5×10^{-3} M and then falls. In the case of Eu the effect keeps high up to the concentration of 0.1M.

The extraction of Zr by the mixture of TOAHNO₃ and TBP from Al(NO₃)₃ solutions with different salting-out agents and HNO₃ concentrations has also been studied. A synergic effect for this metal has not been found.

Now let us come back to the mechanism of the metal extractions by a mixture of TOA and a neutral extractant. The change of distribution ratio of the ionic associate due to the addition of the neutral extractant to the system could be due to an interaction of the extractant with the cation or the anion, the changes in the properties of the organic phase or the composition of the aqueous phase due to the extraction of some component. We have already shown that the effect is not connected with the extraction of HNO₃. The practical coincidence of the extraction curves for the extraction of europium from LiNO₃ and Al(NO₃)₃ solutions of the same normality indicates that the effect is not connected with the extraction of the salting-out agent cation (for example, lithium). One of the authors with Dem'yanova and Lipovsky has shown that TBP does not interact with TOA nitrate and chloride, that is, an increase in the extraction cannot be accounted for by the interaction of the extractants.⁽²⁾ Thus indirect evidence led the authors to conclude that direct solvation of the metal (formation of a mixed complex anion containing nitrate groups and molecules of the neutral extractant in the inner sphere of the metal) may be responsible for the synergic effect.

An attempt has been made to obtain direct evidence for the solvation of TBP molecules with anionic nitrate complexes of Eu in a system with TOA. Two methods have been used. The electrophoresis of the extracted solutions with the use of traced TBP has given preliminary evidence that a synergic effect is observed in polar diluents (nitrobenzene). The electrophoresis was carried out in the TBP-TOAHNO₃-nitrobenzene system both with and without Eu. It has been found⁽³⁾ that part of the TBP is transferred to the anolyte. In other words TBP molecules are bound to the anionic part of the complex extracted with the amine.

I.r. spectroscopy was used as a second method. Here the TBP-TOAHNO₃-CCl₄ (or cyclohexane)-Eu system was initially studied. The extractant concentrations were chosen in such a way that under extraction conditions (10M LiNO₃ and 0.5M HNO₃) TBP alone, unlike its mixture with TOA, extracted Eu with a low distribution coefficient. Under such conditions a possible shift of the position of the P=O stretch band in spectra of the Eu extracts for the mixture of TBP and TOAHNO₃ can only be due to the solvation of an anionic nitrate complex of Eu. Fig. 2 shows four i.r. spectra of the organic phases in a region of P=O stretch bands for TBP solution in CCl₄; (1) alone, (2) TBP solution after a contact with the aqueous phase containing Eu, (3) solution of the mixture of TBP and TOAHNO₃ after a contact with the aqueous phase without Eu and (4) in the presence of Eu. As is seen, a band of bound TBP which can be attributed to solvated extractant molecules appears only in spectrum 4. Unfortunately, interpretation of the spectra is difficult as the P=O stretch band is masked by an NO₃⁻-group band. However, all these results together seem to be sufficient to confirm the mechanism suggested. An unambiguous spectral evidence for such a mechanism has been obtained using a chloride system.

The extraction from chloride solutions

According to different reports,⁽³⁻⁶⁾ tertiary amines extract TPE complexes of the composition MeCl₄⁻, MeCl₃²⁻ or LiMeCl₆²⁻ from concentrated chloride solutions. Water molecules add to the co-ordination sphere of such "hard" ions; this should prevent extraction of the complexes. The addition of neutral extractant molecules to the metal, forming an anionic complex, can lead to the formation of anions with a low charge and containing no water molecules, e.g.

$\text{MeCl}_4^- \cdot 2\text{S}$ or $\text{MeCl}_5^{2-} \cdot \text{S}$, where S is a molecule of the extractant. The formation of such complexes can seemingly promote the extraction if amines alone extract LiMeCl_6^{2-} under extraction conditions.

The extraction of americium and europium by solutions of TOA chloride, TBP and their mixtures in CCl_4 , o-xylene and cyclohexane has been studied. The results on the extraction of americium and europium by solutions of TBP, TOAHCl and their mixtures in CCl_4 are given in Fig. 3. A large synergic effect is observed for both elements; analogous effects have been obtained for cyclohexane and o-xylene.

The largest synergic effect has been observed in the use of CCl_4 as diluent. In the case of the two other diluents the value of S is also large. A mixture of the extractants with a total concentration of 0.8M extracts americium better than 0.8M solutions of either extractant alone.

A synergic effect has been observed in the extraction of Am and Eu by the mixture of TOA and TOPO though its magnitude is much less than in the case of TBP. In the extraction by a mixture of 0.25M TOAHCl and 0.005M TOPO, S for americium is 3.3.

Thus the synergic effect is greater using a TOA-TBP system than for the corresponding system with a weaker neutral extractant. Similar behaviour has also been observed in the extraction of TPE and Eu from nitrate solutions.^(7,8)

A mixture of 0.5M TBP and 0.3M TOAHCl in cyclohexane gives a 90% extraction of americium even from 0.5M HCl solution. A synergic effect has also been found in the use of the extractants pre-equilibrated with aqueous HCl solutions, that is HCl extraction cannot cause the effect.

As seen from Fig. 3, the distribution coefficients for americium are much higher than for Eu using TOAHCl. That is why amine systems are used for the separation of TPE and rare earths.⁽³⁾ A difference in their extraction behaviour can be probably accounted for by a higher stability of chloride complexes of TPE. A difference in the extraction behaviour of solvates must be considerably less than in the case of pure halo complexes (Fig. 3). Such a difference must be markedly less also in the case of solvated anionic complexes. In fact the distribution coefficients of Am and Eu differ less for the TBP-TOAHCl system than in the case of amine alone. This leads to a decrease in the separation factor for TPE and rare earths.

On the other hand the synergic mixtures studied show TPE extracts with higher distribution coefficients or TPE can be extracted from convenient acidic solutions at lower extractant concentrations than in the case of amines alone. The addition of a small amount of TBP to an amine solution gives high distribution coefficients for americium (particularly in cyclohexane solutions) and rather high separation factors for americium and europium. Thus the addition of 0.1M TBP in the extraction of americium from 11.1M in LiCl and 0.2M in HCl by 0.7M TOAHCl solution causes an increase of the distribution coefficient by an order of magnitude; the separation factor is 17.8 in this case.

I.r. spectroscopy has been used to study the extraction mechanism in the TBP(0.2M)-TOAHCl(0.6M)- CCl_4 (or cyclohexane)-Eu(0.1M) system. Conditions were chosen as for nitrate solutions. Fig. 4 shows i.r. spectra of the organic phases in a region of P=O stretch bands for solutions in CCl_4 . The spectra of TBP (curve 1) and its complexes with europium are similar, due to a low metal concentration in the TBP extract. The addition of the amine salt to TBP hardly changes the position of the P=O group stretch band (curve 3); the spectrum of the mixture does not change after contact with LiCl solution without

europium (curve 4). A distinct band of bound TBP (1215 cm^{-1}) appears in the spectrum of the TBP-TOA-Eu mixture (curve 5). This shows the solvation of TBP molecules by a metal complex. Under these conditions $S = 23$. Such a picture has also been observed using cyclohexane as diluent. Thus the extraction of a co-ordinatively solvated anionic complex by a mixture of TBP and TOAHCl seems to be established.

Acknowledgement

The authors express their gratitude to Professor Yu. A. Zolotov for useful discussions and advice.

References

1. Marcus Y., Kertes A., Ion Exchange and Solvent Extraction of Metal Complexes, 1969 (London, Wiley).
2. Dem'yanova T.A., Lipovsky A.A., Spivakov B. Ya., Radiokhimiya, 1972, 14, p.898.
3. Marcus Y., J. Inorg. Chem., 1966, 28, 209.
4. Moore F. L., Analyt. Chem., 1961, 33, 748.
5. Müller, W., Duyckaerts G., Fuger J., Solvent Extraction Chemistry of Metals, 1965, 233 (London, Macmillan).
6. Müller, W., Angew. Chem., 1971, 83, 625.
7. Spivakov B. Ya., Zolotov, Yu. A., Myasoedov B. F., Chmutova M. K., Kochetkova N. E., Zh. neorg. khim., 1972, 17, 3334.
8. Chmutova M. K., Myasoedov B. F., Spivakov, B. Ya., Kochetkova N. E., Zolotov Yu. A., J. inorg. nucl. Chem., 1973, 35, 1317.

Figures

Fig. 1 The extraction of Am(III) by untreated and pre-equilibrated solutions of TBP, TOAHNO₃ and their mixtures in benzene from 5.7M LiNO₃ and 0.1M HNO₃ solution.

1, 1', 1" = untreated solutions; 2, 2', 2" = pre-equilibrated solutions; 1', 2' = TBP; 1", 2" = TOAHNO₃; 1, 2 = mixtures.

Fig. 2 I.r. spectra of TBP, its mixture with TOAHNO₃ blank extract of the mixture and that with europium in CCl₄ in a region of the P=O-group stretch band.

1 - TBP, 2 - TBP extract, 3 - blank extract of the mixture, 4 - extract of the mixture with Eu.

Fig. 3 The extraction of Am(III), (1, 1', 1") and Eu(III), (2, 2', 2"), by the solutions of TBP (1', 2'), TOAHCl (1", 2") and their mixtures (1, 2) in CCl₄ from 11.1M LiCl and 0.02M HCl solution.

Fig. 4 I.r. spectra of TBP, its mixture with TOAHCl, blank extracts and those with europium in CCl₄ in a region of the P=O-group stretch band.

1 - TBP, 2 - TBP extract with Eu, 3 - mixture, 4 - blank extract of the mixture, 5 - extract of the mixture with Eu.

Fig.1. The extraction of Am(III) by untreated and pre-equilibrated solutions of TBP, TOAHNO₃ and their mixtures in benzene from 5.7M LiNO₃ and 0.1M HNO₃ solution.

1,1',1''= untreated solutions; 2,2',2''=pre-equilibrated solutions; 1; 2'-TBP; 1'',2''-TOAHNO₃; 1,2,-mixtures.

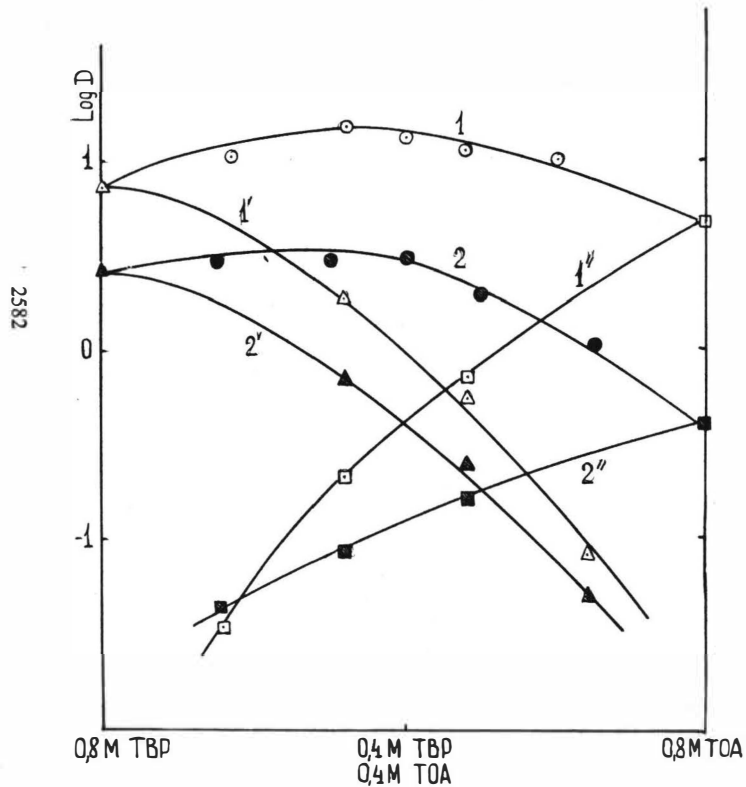


Fig.2. I.R. spectra of TBP, its mixture with TOAHNO₃, blank extract of the mixture and that with europium in CCl₄ in a region of the P=O-group stretch band. 1-TBP, 2-TBP extract, 3-blank extract of the mixture, 4-extract of the mixture with Eu.

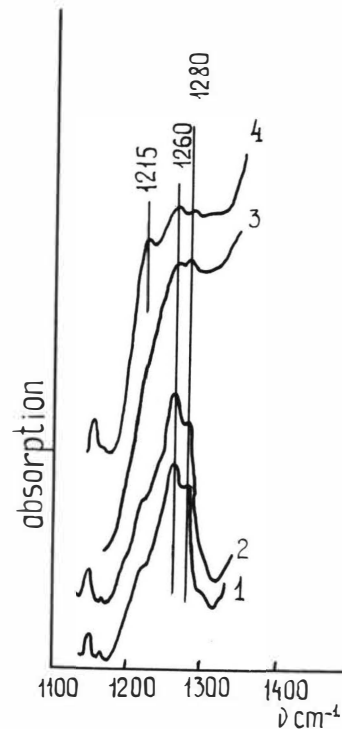


Fig.3. The extraction of Am(III) (1,1',1'') and Eu(III) (2,2',2'') by the solutions of TBP (1',2'), TOAHCl (1'',2'') and their mixtures (1,2) in CCl_4 from 11,1M LiCl and 0.02M HCl solution.

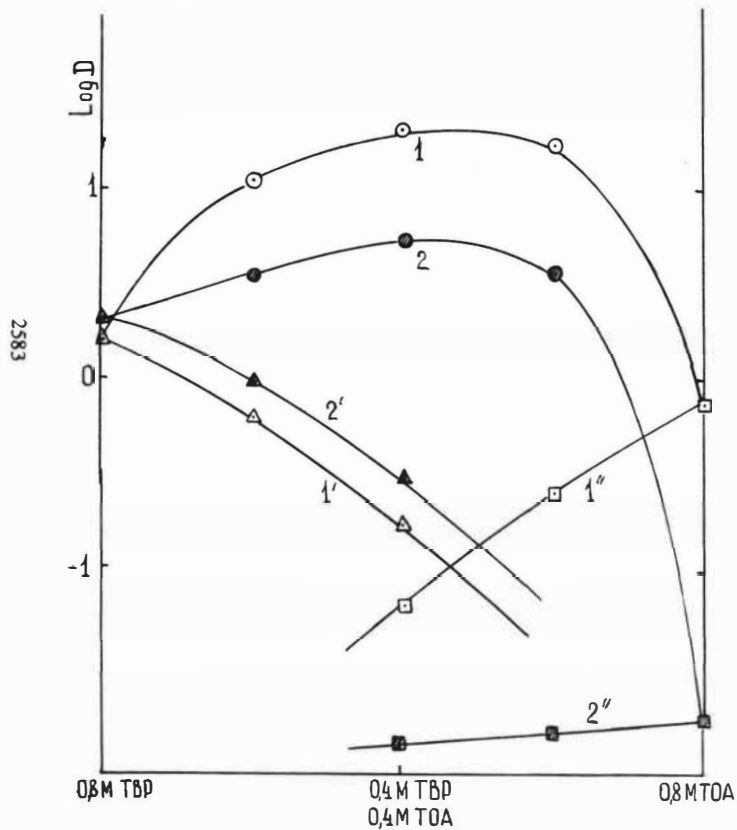
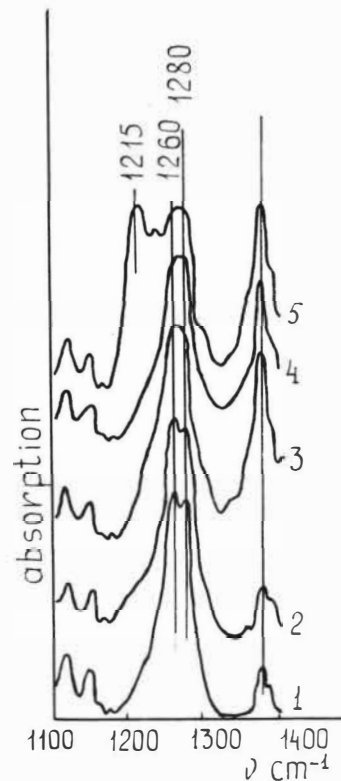


Fig.4. I.R. spectra of TBP, its mixture with TOAHCl, blank extracts and those with europium in CCl_4 in a region of the P=O-group stretch band. 1-TBP, 2-TBP extract with Eu, 3-mixture, 4-blank extract of the mixture, 5-extract of the mixture with Eu.



SYNERGIC EFFECTS IN LIQUID-LIQUID EXTRACTION OF SOME
HEAVY METALS BY 1-PHENYL-3-METHYL-4-BENZOYL-PYRAZOL-5-ONE.

O. NAVRÁTIL

Department of Radiochemistry
Purkyně University, Brno, ČSSR

The solvent extraction of zinc/II/, cobalt/II/, cerium/III/ and europium/III/ from an aqueous perchlorate and nitrate solution into benzene or toluene by mixtures of 1-phenyl-3-methyl-4-benzoyl-pyrazol-5-one /HA/ and electroneutral organic bases, S, shows a synergic effect due to the extraction of a mixed species $MA_2S_n /M = Co, Zn/$ and $MA_3S_n /M = Ce, Eu/$, $n = 1$ and/or 2. The stability of the complexes $MA_N/HA/r$, $r = 0$ or 1, and of the adducts has been calculated from the extraction curves.

1-phenyl-3-methyl-4-acyl-pyrazol-5-ones were first used practically by Jensen^{1,2}. In his papers and in the subsequent ones³⁻⁶ it is pointed out that 1-phenyl-3-methyl-4-benzoyl-pyrazol-5-one / = HA/ is a powerful extractant; the concentration products of a number of complexes with HA are very high and generally exceed the concentration products determined for complexes of the frequently employed 2-thenoyltrifluoroacetone. The synergic extraction of certain metals with the aid of HA has also been studied⁶⁻⁹. In the presence of neutral donor agents S, the complexes $MA_N S_n$ in the organic phase play an important role.

This paper concerns the problem of the complex formation of Co/II/, Zn/II/, Ce/III/, and Eu/III/ with HA by solvent extraction and the problem of their synergic extraction in the presence of S.

EXPERIMENTAL

The preparation and purification of HA was described previously¹. The other chemicals were of analytical reagent grade. The pH of the aqueous phase was adjusted with solutions of HClO₄, NaClO₄, HNO₃, NaNO₃ and NaOH in such a way that the final ionic strength was 0.1 in all cases. The working radioactive solutions of ⁶⁰Co/ClO₄², ⁶⁵Zn/ClO₄², ¹⁴⁴Ce/NO₃³ and ¹⁵²⁺¹⁵⁴Eu/NO₃³ were prepared from stock solutions by dilution with perchloric or nitric acids. Their activity was 0.02 - 2 μCi/ml and starting concentrations were 4.4 x 10⁻⁶M Co, 5 x 10⁻⁶M Zn, 1 x 10⁻⁸M Ce and 4.6 x 10⁻⁷M Eu. γ-radioactivity of the solutions was measured with a well-type scintillation counter, pH-values were measured with a glass electrode.

Equal volumes of the aqueous and the organic phases /5 to 10 ml/ were stirred for 6 hours. This time had been found sufficient for the establishment of an extraction equilibrium. After the separation of the phases aliquot portions /2 ml/ were taken from each and measured in glass ampoules. All of the procedures were carried out in a thermostated room at 20°C.

RESULTS AND DISCUSSION

Composition and stability of complexes with HA

Fig.1 shows the extraction plots of log D_{Zn} and log D_{Ce} vs. -log A⁻, where -log A⁻ is related to the equilibrium concentration of the free ligand A⁻ in the water phase by the equation

$$-\log A^- = pK_{HA} + \log (Q_{HA} + 1 + K_{HA}/[H^+]) - \log [HA]_{tot} - pH ;$$

pK_{HA} and Q_{HA} are dissociation constant and partition coefficient of HA for ionic strength μ = 0.1¹⁰, [HA]_{tot} is analytical concentration of HA. Since almost all experimental points lie on one

curve, it is evident that the aqueous phase contains complexes ZnA^+ and ZnA_2 , CeA^{2+} , CeA_2^+ and CeA_3 , only ZnA_2 and CeA_3 being extracted into the organic phase.

It may be seen from Fig.2 that, in the case of Co and Eu, and for $[HA]_{tot} \gg 0.05$ M /cobalt/ and $\gg 0.02$ M /europium/, the complexes of the type $CoA_2 \cdot HA$ and $EuA_3 \cdot HA$ are extracted into the organic phase. This conclusion follows from the fact, that all experimental points lie on one curve only for the extraction plot of $\log D/[HA]_o$ vs. $-\log A^-$ and for limiting $[HA]_{tot}$ mentioned above; the symbol $[HA]_o$ is the equilibrium concentration of HA in the organic phase. It may be assumed that the hydrolysis and polymerisation of the metal ions in pH region used in this work can be neglected ¹¹.

Employing the Dyrssen-Sillén method of two parameters ¹² we calculated the stability constants of all arising complexes in the aqueous phase. These values along with those of Q_{MA_N} and α_1 are listed in Table 1. Q_{MA_N} is the partition coefficient of uncharged complex MA_N , addition constant $\alpha_1 = [MA_N \cdot HA]_{org} / [MA_N]_{org} \times [HA]_{org}$, stability constant $\beta_n = [MA_n] / [M^{N+}][A]^{-n}$.

Table 1.
Stability and addition constants and partition coefficients of the metal complexes

Metal	Org. phase	$\log \beta_1$	$\log \beta_2$	$\log \beta_3$	$\log Q_{MA_N}$	$\log \alpha_1$
Co	benzene	3.06	6.62	-	1.42	1.96
Zn	benzene	2.94	6.56	-	3.57	-
Ce	toluene	5.22	11.08	17.58	2.80	-
Eu	toluene	3.51	8.34	14.49	3.15	1.65

Effect of neutral adducts S on the extraction of complex MA_N .

Figs. 3 and 4 show the effect of equilibrium concentration of some organic adducts S in the organic phase on the extraction of Co, Zn, Ce and Eu. The synergic effect was studied for S = tri-n-butylphosphate /TBP/, triethylhexylphosphate /TEHP/, tri-n-butylphosphinoxide /TBPO/, tri-n-octylphosphinoxide /TOPO/, quinoline /quin/ and isoamylalcohol /IamOH/. The organic phase contained $2 \times 10^{-2}M$ HA. The addition constants k_n were determined by the curve-fitting method. They are listed in Table 2. In general, the stability of the adduct complexes is reduced in the series TBPO > TOPO > chin > TBP > TEHP > IamOH; this fact agrees with the basicity of adducts used. The behaviour of cerium is, however, rather different; the destruction of synergism can be observed already in the region of $1 \times 10^{-2}M[S]_0$. This feature bears upon the different characteristic of the complex CeA_3 in contrast to the complexes EuA_3 and CoA_2 /Figs.1 and 2/.

Table 2.
Addition constants k_n of the complexes $MA_N S_n$

$$[HA]_{tot} = 2 \times 10^{-2}M; \quad k_n = \frac{[MA_N S_n]_{org}}{[MA_N]_{org} [S]_{org}^n}$$

Metal	Adduct	pH	log k_1	log k_2
Co	TBPO	4.00	5.34	7.46
	TOPO	4.00	4.96	6.52
	TBP	4.000	2.90	4.18
	TEHP	4.00	3.00	4.08
	quin	4.00	4.05	6.22
	IamOH	4.00	2.00	--
Ce	TBPO	1.75	--	7.14
	TOPO	1.75	--	6.78
	TBP	2.67	1.76	2.88

continuation of Table 2.

Metal	Adduct	pH	log k_1	log k_2
Ce	TEHP	2.67	}	destruction of synergism
	quin	2.67		
	IamOH	2.67		
Eu	TBPO	2.00	--	10.70
	TOPO	2.00	--	10.18
	TBP	2.67	--	6.56
	TEHP	2.67	--	6.48
	quin	2.67	3.17	--
	IamOH	3.35	--	3.00

Literature

1. Jensen B.S., Acta Chem.Scand. 13, 1668 /1959/.
2. Jensen B.S., Acta Chem.Scand. 13, 1890 /1959/.
3. Zolotov J.A., Lambrev V.G., Čmutova M.K., Sizoněnko N.T., Dokl.AN UdSSR 165, 117 /1965/.
4. Zolotov J.A., Čmutova M.K., Palej P.N., Zh.anal.khim. 21, 1217 /1966/.
5. Navrátil O., Jensen B.S., J.radioanal.Chem. 5, 313 /1970/.
6. Bacher W., Report KFK 1504, 1971.
7. Zolotov J.A., Gavrilova L.G., J.inorg.nucl.Chem. 31, 3613 /1969/.
8. Kočetkova N.E., Čmutova M.K., Mjasojedov B.F., Zh.anal.khim. 27, 678 /1972/.
9. Zolotov J.A., Gavrilova L.G., Radiokhimiya 11, 389 /1969/.
10. Navrátil O., Smola J., Coll.Czech.Chem.Comm. 36, 3549 /1971/.
11. Bjerrum J., Schwarzenbach G., Sillén L.G., Stability Constants of Metal-ion Complexes with Solubility Products of Inorganic Substances, Part 2, Inorg. Ligands, Chem.Soc., London 1958.
12. Dyrssen D., Sillén L.G., Acta Chem.Scand. 7, 663 /1953/.

Fig.1. The distribution of ^{65}Zn /closed symbols/ and ^{144}Ce /open symbols/ between benzene /Zn/ or toluene /Ce/ and water as a function of the concentration of free ligand A^- in the water phase; 20°C , $\mu = 0.1$.

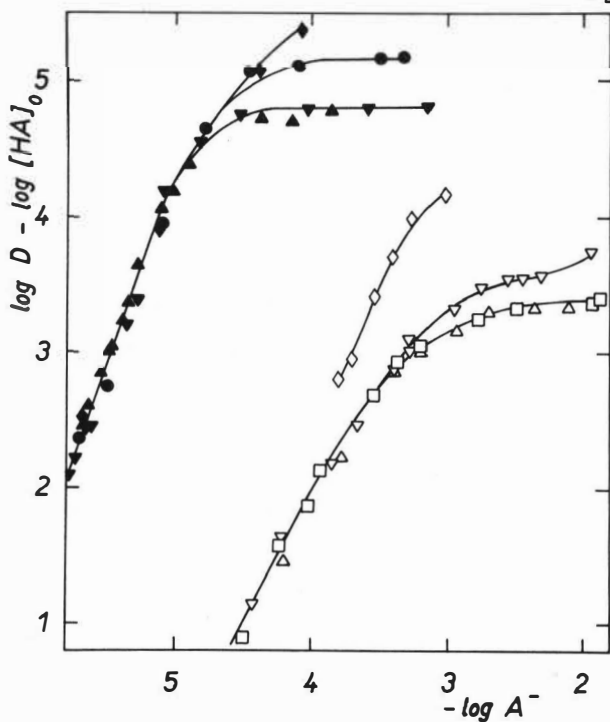
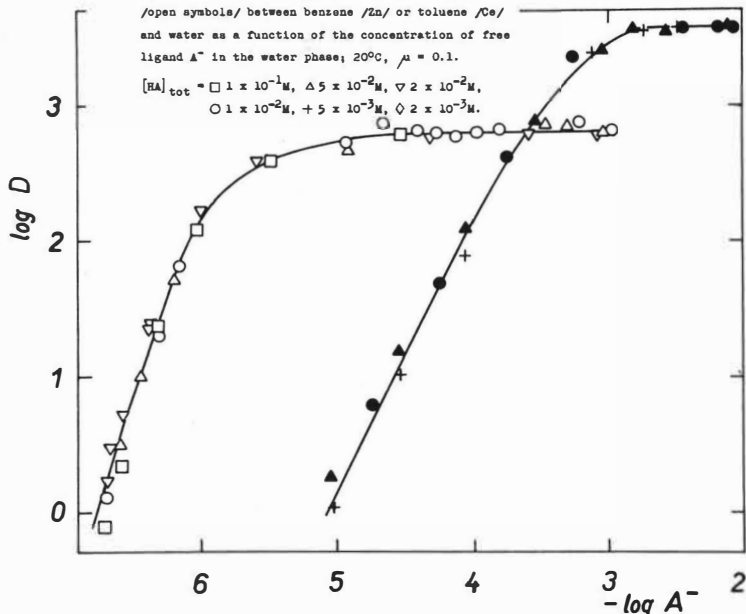


Fig.2. The dependence of $\log D - \log [\text{HA}]_0$ of ^{60}Ce /open symbols/ and $^{152+154}\text{Pu}$ /closed symbols/ on the concentration of free ligand A^- in the water phase; 20°C , $\mu = 0.1$. /the symbols are the same as in fig.1./

Fig. 3. Extraction of ^{60}Co /open symbols/ and ^{65}Zn /closed symbols/ into benzene solution containing 0.02 M HA and varying concentrations of TBP \circ , TBPO Δ , TOPO ∇ and quinoline \diamond in the organic phase from aqueous perchlorate solutions, pH 4.00; 20°C.

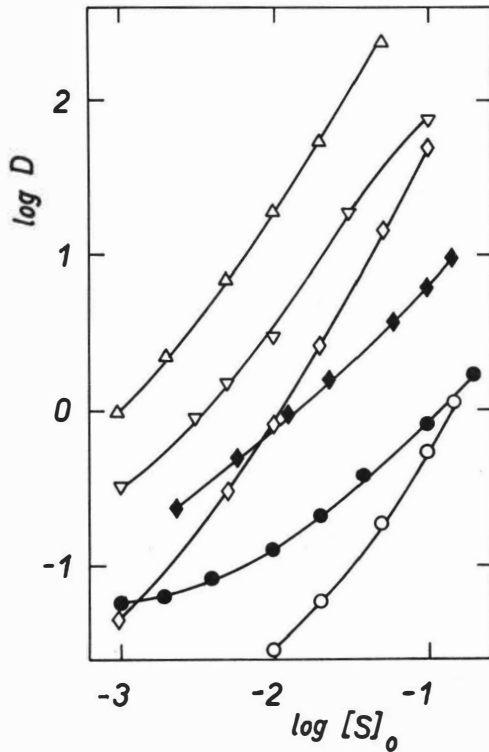
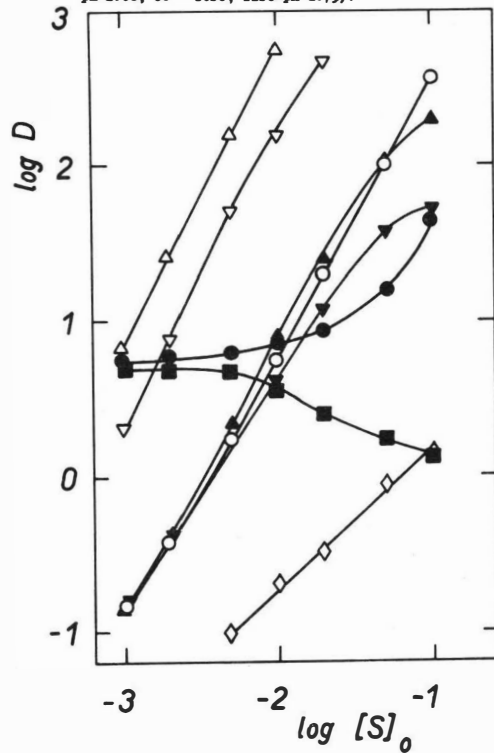


Fig. 4. Extraction of $^{152+154}\text{Eu}$ /open symbols/ and ^{144}Ce /closed symbols/ into toluene solution containing 0.02 M HA and varying concentrations of TBP \circ , TBPO Δ , TOPO ∇ , quinoline \diamond and THBP \square in the organic phase from aqueous nitrate solutions, 20°C; pH 2.67 /Eu - TOPO, TBPO pH 2.00, Ce - TOPO, TBPO pH 1.75/.



ACIDIC ORGANOPHOSPHORUS EXTRACTANTS - XXI. KINETICS AND EQUILIBRIA OF EXTRACTION OF Eu(III) BY DI(2-ETHYLHEXYL) PHOSPHORIC ACID FROM COMPLEXING MEDIA

Z. Kolařík and W. Kuhn

Institut fuer Heisse Chemie, Kernforschungszentrum Karlsruhe,
Federal Republic of Germany

Abstract: The rate and equilibria of Eu(III) extraction by di(2-ethylhexyl) phosphoric acid (HDEHP), in some cases in the presence of other organophosphates, from aqueous solutions of diethylenetriaminepentaacetic acid (DTPA) and an additional carboxylic acid complexant were studied. Under conditions of dispersion mixing the first order rate constant of the extraction reaction was found to depend on the stirring velocity as well as the nature of the diluent and the additional complexant. With n-dodecane as the former and lactic acid as the latter the rate constant and equilibrium distribution coefficient were measured as functions of the concentrations of DTPA, lactic acid and hydrogen ions in the aqueous phase and of HDEHP, tri-n-butyl phosphate and mono-2-ethylhexyl phosphoric acid in the organic phase. The extraction mechanism is discussed.

INTRODUCTION

In the Part XVIII of this Series¹ it has been shown that the rate of lanthanide(III) extraction by di(2-ethylhexyl) phosphoric acid (HDEHP) from solutions of diethylenetriaminepentaacetate (DTPA) and lactic acid decreases with increasing atomic number from La(III) to Eu(III) and that the dissociati-

on of the lanthanide(III)-DTPA complexes is the rate determining step. Of different variables the concentration of lactic acid has been shown to influence most significantly the extraction rate. In this work the extraction rate and equilibrium were studied in some detail with one single lanthanide, namely Eu(III), as functions of a number of variables. Eu(III) ^{was chosen} as a representative of lanthanides(III), because its extraction is slow enough as not to cause any experimental difficulties and a knowledge of its extraction rate under various conditions is of practical importance in the separation of transplutonides(III) from lanthanides(III), as explained previously¹. As only the latter aspect ^{was looked at,} many experiments were made with tri-n-butyl phosphate ^(TBP) present in the organic phase, ^{so} as to work under conditions similar to those of our separation studies².

EXPERIMENTAL

The experimental conditions have been described in detail previously¹. To keep the interfacial area as constant as possible at least within a series of experiments, the same impeller and extraction vessel were used and the impeller velocity was carefully controlled. The concentration of acidic organophosphates will be given in monomer formula units/l. Total concentrations of carboxylic acids will be given (if not marked as anions), including both dissociated and undissociated forms. All experiments were performed with trace metals.

RESULTS AND DISCUSSION

Also in this work the transfer of Eu(III) from the aqueous into the organic phase could be described as a reversible first order reaction with a rate constant k obtained from the slope

of the plot of $\log \frac{D_f}{(1+D_f)} \left[\frac{D_f}{(1+D_f)} - \frac{D_t}{(1+D_t)} \right]$ vs. time¹, where D_f and D_t are the distribution coefficients at equilibrium and time t respectively.

As shown in Table 1, the rate constant is dependent on the stirring velocity in the region of 1200-2400 rev/min, both in the presence and absence of lactic acid in the aqueous phase. The plot of $\log k$ vs. \log impeller speed is linear and its slope is 1.2 with lactic acid and 1.0 without lactic acid present. Obviously the dissociation of the Eu(III)-DTPA complex as the rate determining step proceeds heterogeneously on the interface and not in the bulk aqueous phase.

The importance of the presence of an additional complexing agent beside DTPA in the aqueous phase has been clearly demonstrated¹. Thus a question can arise whether the extraction of Eu(III) could not be accelerated by replacing lactic acid by any other carboxylic acid. A positive answer is given in Table 2, but it should be pointed out that of the four carboxylic acids tested only one, α -hydroxyisobutyric acid, makes the extraction reaction faster than lactic acid. In a group of mutually comparable acids with very similar dissociation constants³ the rate constant decreases in the same order as the stability of Eu(III) complexes, namely α -hydroxyisobutyric > lactic > glycollic acids⁴ (Table 2). α -Hydroxyisobutyric acid is not suitable for separation processes because of its rather high price and somewhat limited aqueous solubility; therefore all further experiments were made with lactic acid as the additional complexing agent.

The influence of the lactic acid concentration on the extraction rate was studied in this work in more detail than previously¹. The logarithmic plot of $\frac{k}{k_0}$ (with k_0 denoting the

Table 1

Effect of the stirring velocity on the rate constant k of Eu-(III) extraction by 0.3M HDEHP + 0.2M TBP in n-dodecane from 0.05M DTPA (A) and 0.05M DTPA + 1.0M lactic acid (B) at pH 3.00 ± 0.05 and 23°C

Impeller speed rev/min	k (min^{-1})	
	A	B
1200	0.024	0.41
1800	0.038	0.66
2400	0.047	0.97

Table 2

Influence of the nature of the additional complexant on the rate constant k of Eu(III) extraction by 0.3M HDEHP + 0.2M TBP in n-dodecane from 0.05M DTPA + additional complexant at pH 3.00 ± 0.05 and 23°C

Additional complexant (1.0M or 0.5M ^x acid)	⁺ pK_a Ref	⁺⁺ $\log B_1$ Ref	k (min^{-1})	$\frac{D_f}{f}$
Glycollic	3.71 3a	2.45 2	0.25	5.16
Lactic	3.74 3a	2.53 2	0.41	4.55
α -Hydroxyisobutyric	3.79 3b	2.70 2	0.73	5.58
β -Hydroxybutyric	4.39 3a	-	0.21	3.64
Citric ^x	2.94 3a	-	0.30	5.72

⁺at $\mu = 0.2$; ⁺⁺the stability constant of the 1:1 Eu(III) complex at $\mu = 2.0$

rate constant in the absence of lactic acid) vs. the lactate concentration is shown in Fig. 1. It has been observed earlier⁵ that isotopic exchange of Ce^{3+} in the $Ce(III)$ -DTPA complex is accelerated by acetate ions and this has been ascribed to the dissociation of the DTPA complex via a mixed, kinetically less stable $Ce(III)$ -DTPA-acetate complex. This plausible explanation was accepted also for the dissociation of the $Eu(III)$ -DTPA complex in the extraction system studied. The nonlinear character of the plot $\log \frac{k}{k_0}$ vs. \log lactate concentration can be explained so that the dependency is a sum of two linear components, i.e. only a fraction of the $Eu(III)$ -DTPA complex dissociates along the faster path with the intermediate formation of a mixed $Eu(III)$ -DTPA-lactate complex. At lactic acid concentrations of $\leq 0.5M$ the points of the $\log \frac{k}{k_0}$ vs. \log [lactic acid] dependence fit the "normalized" curve $\log y = \log (1+x)$. Thus the $Eu(III)$ -DTPA complex can be supposed to dissociate along two paths: one fraction, diminishing at increasing lactate concentration, without any participation of lactate ions and the other fraction, growing at an increase of the lactate concentration, via a mixed complex with the ratio $Eu:DTPA:lactate = 1:1:1$. The positive deviation of the $\log \frac{k}{k_0}$ values from the "normalized" curve at lactic acid concentrations of $> 0.5M$ gives no unambiguous evidence for the intermediate formation of a lactate-rich mixed $Eu(III)$ complex. Visual observation of the stirred phases implies that larger amounts of lactic acid can influence the dispersion of the phases and so the interfacial area.

Hydrogen ions catalyze also the dissociation of the $Eu(III)$ DTPA complex. The dependence of $\log k$ vs. pH appears also to be a sum of two linear components, because the experimental

points fit the "normalized" curve $\log y = \log (1+x^2)$ (Fig. 2). Thus one fraction of the Eu(III)-DTPA complex dissociates without any participation of hydrogen ions and the other one faster via the formation of a dihydrogen complex. A significant participation of a monohydrogen Eu(III)-DTPA complex on the dissociation reaction would require a fit of the experimental points with a more complicated curve than $\log y = \log (1+x^2)$. An analogous dependence of the rate constant on pH as in our work has been observed in isotopic exchange of Ce^{3+} in the Ce(III)-DTPA complex⁵.

A kinetic equation can be thus written for the total aqueous Eu(III) concentration, C_{Eu} :

$$\frac{dC_{Eu}}{dt} = [EuY^{2-}] \left\{ \underline{k}_1 [Lac^-] + \underline{k}_2 + \underline{k}_3 [H^+]^2 \right\} \quad (1)$$

where Y^{5-} and Lac^- are the anions of DTPA and lactic acid respectively and \underline{k}_i are individual rate constants including the respective equilibrium complex formation constants. Thus the observed rate constant \underline{k} should not depend on the DTPA concentration in the region, where Eu(III) exists in the aqueous phase predominantly as a DTPA complex, i.e. down to a value essentially lower than 0.05M used in the above experiments. However, a moderate influence of the DTPA concentration on the rate constant was observed in the range 0.003 - 0.07M; the plot of $\log \underline{k}$ vs. $\log [DTPA]$ is a straight line with the slope -0.3 (Fig. 3). Obviously an additional factor, not included in Equation (1) and not identified in this work, plays a role in the extraction reaction.

An increase of the ionic strength above the value corresponding to an aqueous Na^+ concentration of 1.4 g-ion/l lowers

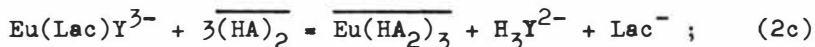
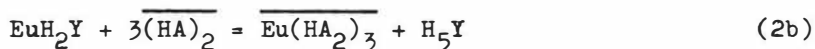
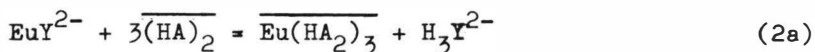
somewhat the rate constant (Table 3).

Table 3

Effect of ionic strength on the rate constant k of Eu(III) extraction by 0.3M HDEHP + 0.2M TBP in n-dodecane from 0.05M DTPA + 1.0M lactic acid + NaNO₃ at pH 3.00±0.05 and 23°C

[NaNO ₃] (M)	[Na ⁺] _{total} (g-ion/l)	k (min ⁻¹)	$\frac{D_f}{x}$
0.0	0.4	0.41	4.55
1.0	1.4	0.41	2.78
2.0	2.4	0.30	1.83

The effect of the HDEHP concentration on the rate constant is shown in Fig. 4. Here a "normalized" curve $\log y = \log (1 + x^3)$ can be fitted with the experimental points at $[\overline{\text{HDEHP}}] \leq 0.5\text{M}$. Then with increasing HDEHP concentration the fraction of the Eu(III)-DTPA complex becomes smaller which dissociates along the slower path without any participation of HDEHP and the fraction becomes larger which follows the faster paths proceeding on the interface according to the Equations



here HA is the monomeric molecule of HDEHP and the extracted Eu(III) complex is written in the well-known composition which has been shown to be valid also for extraction of Eu(III) from complexing media⁶. The levelling of the $\log k$ vs. $\log [\overline{\text{HDEHP}}]$ dependence at $[\overline{\text{HDEHP}}] > 1\text{M}$ can be ascribed to a saturation

of the interface by HDEHP species.

The rate-enhancing effect of TBP is illustrated by Table 4 and, indirectly, also by the dependence of $\log k$ on $\log [\overline{\text{HDEHP}}]$ at a constant concentration of TBP (Fig. 4). Here the decrease of the rate constant with increasing HDEHP concentration up to its value of 0.5M can be hardly due to an effect of HDEHP itself, as the analogous curve obtained in the absence of TBP intimates. If a molecular complex of HDEHP with TBP would react with the Eu(III)-DTPA complex faster than species of HDEHP alone, the $\log k$ vs. $\log [\overline{\text{HDEHP}}]$ dependence in the presence of TBP should reach a maximum at a plausible ratio of the HDEHP and TBP analytical concentrations. Thus the course of the dependence is determined most probably by the decreasing concentration of free TBP at the analytical HDEHP concentration increasing from 0,1 to 0.5M and by a saturation of the interface predominantly by HDEHP at its higher analytical concentrations. An attempt to determine the reaction order with respect to TBP after calculation of the concentration of free TBP from published data⁷ was not successful. Due to uncertainties of the calculation and imperfect consistency of the results given in Table 4 and Fig. 4, the scattering of the points of the $\log k$ vs. $\log [\overline{\text{TBP}}]_{\text{free}}$ plot was so considerable that the reaction order estimated could vary between 1 and 3. It is even impossible to suggest any qualitative explanation for the effect of TBP on the Eu(III) extraction rate.

Another molecular complexing^{agent} /, mono-2-ethylhexyl phosphoric acid (H_2MEHP), also increases the Eu(III) extraction rate, if added to the organic phase instead of TBP (Table 4). It should be noted here that in equilibrium H_2MEHP is a much more powerfull extractant for Eu(III) than HDEHP; under analogous

conditions the equilibrium distribution coefficient of Eu(III) with H_2MEHP is a factor of $\sim 10^4$ higher than that with HDEHP⁸.

Table 4

Effect of TBP and H_2MEHP on the rate constant k of Eu(III) extraction by 0.3M HDEHP in dodecane from 0.05M DTPA + 1.0M lactic acid at pH 3.00 ± 0.05 and $23^\circ C$

$[TBP](M)$	$[H_2MEHP](M)$	$k(\text{min}^{-1})$	\underline{D}_f
-	-	0.195	27.8
0.20	-	0.41	4.55
0.30	-	0.66	2.12
0.50	-	0.73	0.81
-	0.020	0.41	26.1
-	0.050	0.60	26.8

The diluent effect on the Eu(III) extraction rate is illustrated briefly in Table 5.

Table 5

Effect of the diluent nature on the rate constant k of Eu(III) extraction by 0.3M HDEHP from 0.05M DTPA + 1.0M lactic acid at pH 3.00 ± 0.05 and $23^\circ C$

Diluent	$k(\text{min}^{-1})$	\underline{D}_f
Dodecane	0.195	4.55
Benzene	0.36	0.35
Carbon tetrachloride	0.14	2.24

As for equilibria in the system studied: Of the logarithmic dependences of the Eu(III) distribution coefficient on the concentration of TBP, hydrogen ions and DTPA, each has an expected course. The $\log \underline{D}_f$ vs. $\log [\overline{\text{TBP}}]$ plot is almost parallel with an analogous curve obtained in a system involving citric and nitrilotriacetic acids⁹. The pH dependence (Fig. 2) is a curve the steepness of which is in accord with Equations (2a) - (2c) and the predominance of the species H_4Y^- and H_3Y^{2-} at the acidity studied¹⁰. The plot of $\log \underline{D}_f$ vs. $\log [\text{DTPA}]$ is a straight line with the slope -1 corroborating that Eu(III) exists in the aqueous phase of the system ^{predominantly} / as a complex with the ratio Eu:DTPA = 1:1.

The only surprising equilibrium dependence is that of $\log \underline{D}_f$ on $\log [\overline{\text{HDEHP}}]$ which in the absence of TBP has the limiting slope 2 (Fig. 5), instead of the expected value 3. Since extraction of a lactate containing Eu(III) complex, such as $\text{Eu}(\text{HA}_2)_2\text{Lac}$, is excluded by the full independence of \underline{D}_f of the lactic acid concentration, it is to be supposed that the complex $\text{Eu}(\text{HA}_2)_3$ in the organic phase is in equilibrium with the complexes EuA_i^{3-i} ($i=1-3$) in the aqueous phase. This is not

unlikely, because the aqueous concentration of A^- can be considerable at a pH value as high as 3 and in the presence of lactic acid which can increase the aqueous solubility of monoacidic organophosphates¹¹. The limiting slope 3 of the $\log \underline{D}_f$ vs. $\log [\overline{\text{HDEHP}}]$ dependence in the presence of TBP (Fig. 5) would probably be somewhat changed (but not so much as down to 2) by correcting for the amount of HDEHP bound to TBP. It should be noted that TBP lowers the aqueous concentration of A^- ¹².

The distribution coefficient of Eu(III) is not influenced

by the presence of H_2MEHP up to 0.05M in the organic phase (Table 4) and not essentially influenced, if lactic acid is substituted by an other carboxylic acid (Table 2). The distribution of Eu(III) is influenced by the ionic strength (Table 3) and, as expected, by the nature of the diluent (Table 5).

REFERENCES

1. Kolařík Z., Koch G. and Kuhn W., J. inorg. nucl. Chem. 1973, 36, in press.
2. Koch G., Kolařík Z., Haug H., Hild W. and Drobniak S., Report KFK 1651 (1972).
3. a) Sillén L. G. and Martell A. E. (Comp.), Stability Constants, Special Publ. No. 17, 1964, pp. 367, 390, 416 and 477 (The Chemical Society, London); b) Deelstra H. and Verbeek F., Bull. Soc. Chim. Belges 1963, 72, 612.
4. Choppin G. R. and Chopoorian J. A., J. inorg. nucl. Chem. 1961, 22, 97.
5. Glentworth P., Wisell B., Wright C. L. and Mahmood A. J., J. inorg. nucl. Chem. 1968, 30, 967.
6. Kolařík Z., in Gregory J. C., Evans B. and Weston P. C., Eds., Proc. Int. Solvent Extraction Conf., The Hague, Holland, 1971, p. 753 (The Soc. of Chem. Ind., London).
7. Baes C. F., Jr., Nucl. Sci. Eng. 1963, 16, 405; Yagodin R. A. and Tarasov V. V., Radiokhimiya 1969, 11, 148.
8. Kolařík Z., Dražanová S. and Chotivka V., J. inorg. nucl. Chem. 1971, 33, 1125.
9. Kolařík Z., J. inorg. nucl. Chem. 1972, 34, 2911.
10. Moeller T. and Thompson L. C., J. inorg. nucl. Chem. 1962, 24, 499.
11. Weaver B. and Kappelmann F., Report ORNL-3559 (1964).
12. Liem D. H., Acta Chem. Scand. 1972, 26, 191.

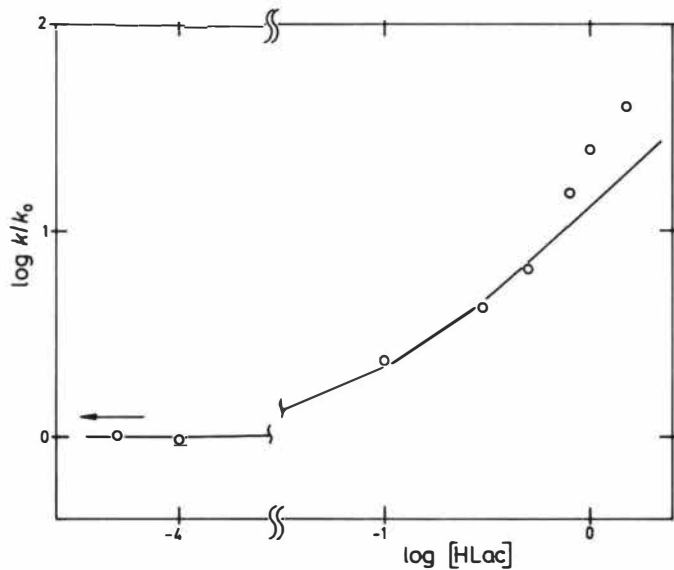


Fig. 1. The effect of lactic acid, HLac, on the rate of Eu(III) extraction by 0.3M HDEHP + 0.2M TBP in *n*-dodecane from 0.05M DTPA at pH 3.00 ± 0.05 and 23°C ; k and k_0 are the rate constants at $[\text{HLac}] \geq 0.1\text{M}$ and $[\text{HLac}] \rightarrow 0$ respectively. The point denoted by the arrow is valid for $[\text{HLac}] = 0$ and the solid curve is calculated as $\log y = \log(1+x)$.

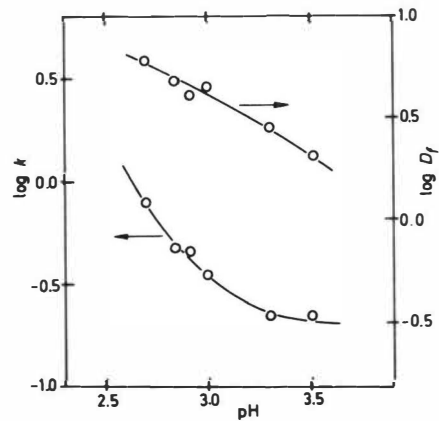


Fig. 2. The pH dependence of the rate constant k and the equilibrium distribution coefficient D_f in extraction of Eu(III) by 0.3M HDEHP + 0.2M TBP in *n*-dodecane from 0.05M DTPA + 1.0M lactic acid at 23°C . The lower solid curve is calculated as $\log y = \log(1+x^2)$.

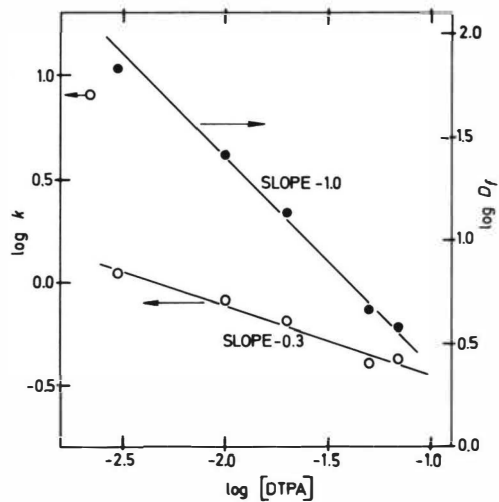


Fig. 3. The dependence of the rate constant k and the equilibrium distribution coefficient D_f on the DTPA concentration in extraction of Eu(III) by 0.3M HDEHP + 0.2M TBP in n-dodecane from 1.0M lactic acid at pH 5.00 ± 0.05 and 23°C .

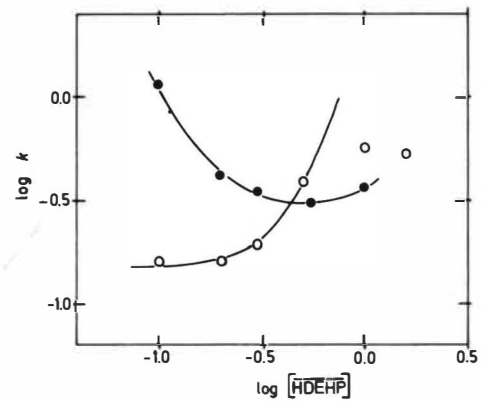


Fig. 4. The effect of the HDEHP concentration in n-dodecane on the rate constant k in Eu(III) extraction from 0.05M DTPA + 1.0M lactic acid at pH 5.00 ± 0.05 and 23°C ; measured in the absence of TBP (open points) and at 0.2M TBP (full points). A curve calculated as $\log y = \log (1+x^3)$ is fitted to the open points.

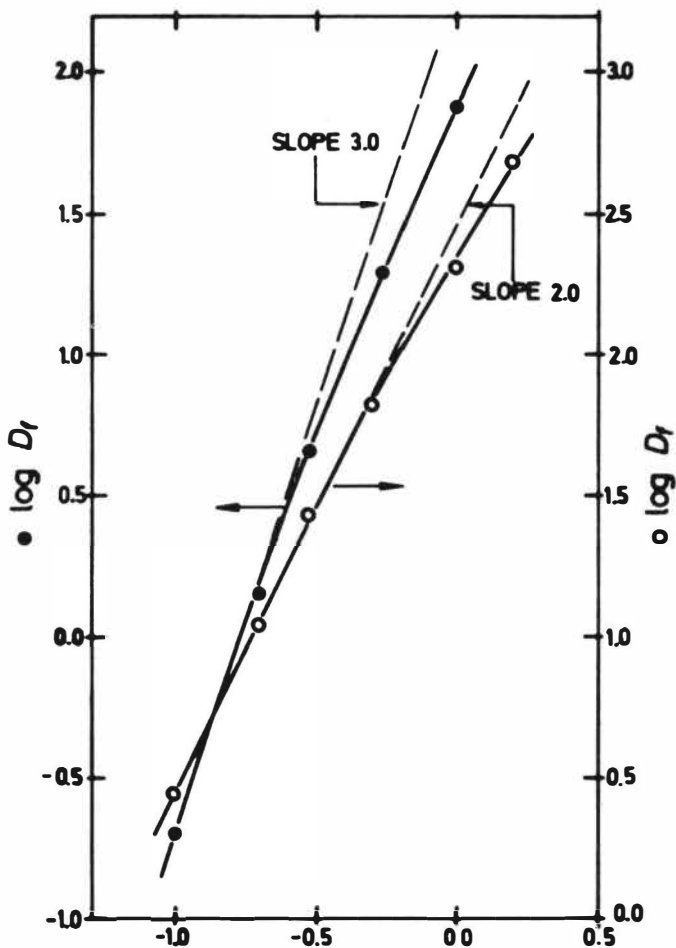


Fig. 5. The equilibrium distribution coefficient \underline{D}_f of Eu(III) at 23°C as a function of the HDEHP concentration in n-dodecane in the absence of TBP (open points) and at 0.2M TBP (full points). Aqueous phase 0.05M DTPA + 1.0M lactic acid, pH 3.00 ± 0.05 .

SESSION 25

Friday 13th September: 9.00 hrs

E X T R A C T I O N T E C H N O L O G Y

(Process Modelling & Control)

Chairman:

Dr. T. Misek

Secretaries:

Dr. E. Rushton

Mr. C. Lachme

CONTROL STUDIES ON A
SOLVENT EXTRACTION COLUMN

by

C. R. McDonald
W. L. Wilkinson

Schools of Chemical Engineering
University of Bradford, U.K.

Abstract

The dynamic behaviour and control of a multiple-mixer solvent extraction column are considered. A model is used which caters for backmixing effects and which does not involve the assumption of stage equilibrium. This model has been shown previously to be an adequate dynamic representation of columns of the type considered.

The concentration response of the column to changes in feed concentration has been studied when the column is controlled by a single feedback loop. The effect of changing the control point is considered.

The results show that feedback control is not satisfactory and a control system involving feedforward control is proposed as a more suitable arrangement for solvent extraction columns of this type. The results are also applicable to other types of contactor.

1. INTRODUCTION

In order to allow an assessment to be made of the controlled performance of a process and to permit different control strategies to be compared at the design stage, mathematical models are required which can predict the dynamic response of the controlled variables in the process to likely disturbances in the input stream and to load changes.

This work is concerned with the development of such a model for a counter-current multiple-mixer solvent extraction column which is illustrated in Figure 1. This type of contactor is widely used in industry, and with some modifications the contactor can be used for other duties such as a chemical reactor, a gas absorber or a solids dissolver. The extractor consists of a column containing a series of agitated compartments in each of which the two phases are mixed by a number of impellers carried on a central shaft. The mixing compartments are separated by a series of horizontal stator plates containing a circular central opening to allow the counter-current flow of the two phases. Vertical baffles are normally placed at the wall to assist mixing. The two liquid phases are admitted to the two ends of the column by means of sparge rings and a settling zone is provided at one end to allow the dispersed phase to coalesce before leaving the column. The continuous phase is taken off at the other end.

Deviation from plug flow occurs in both phases in agitated column contactors due to the backmixing of material counter to the direction of the main flow. Backmixing can affect the operation of large scale columns significantly and must be included in any realistic dynamic model. Likewise it is not permissible to assume that the phases in each compartment are in equilibrium, an assumption which has often been made in the past.

Solvent extraction processes have much in common with distillation processes, but whereas the dynamic behaviour of the latter has been extensively studied, analogous work on solvent extraction processes is not well developed, as can be seen from a review of the literature presented by Pollock and Johnson⁽¹⁾.

2. MATHEMATICAL MODEL OF THE PROCESS

The model to be used is that of Jones and Wilkinson, derived for a multiple mixer column (2, 3, 4). Accommodation is made for backmixing in each phase by the inclusion of the backmixing factors e_L and e_G where e_L represents the fraction of the heavy phase flow L which is flowing between stages in an opposite direction to the bulk heavy phase flow and e_G is defined similarly. The system is shown diagrammatically in Figure (2) and the analysis is subject to the following assumptions:-

- (i) e_L and e_G are constants, independent of the stage number and solute concentration.
- (ii) The volume (or weight) of each stage is constant and of this volume a constant fraction h_L is heavy phase and a constant fraction h_G is light phase.
- (iii) At each end of the column is an unmixed stage in which it is assumed that no mass transfer occurs.
- (iv) One component only is being transferred between phases according to the linear equilibrium relationship:

$$Y = mX^* + b \quad (1)$$

where Y is the concentration of solute in the light phase and X^* the concentration of solute in the heavy phase which would be in equilibrium with Y .

- (v) Mass transfer occurs according to the equation

$$Q_n = k (X_n - X_n^*) \quad (2)$$

where Q_n is the rate of mass transfer per unit interfacial area in stage n and k is the mass transfer coefficient per unit interfacial area, and is independent of stage number.

- (vi) Volume changes due to solute transfer are considered negligible.
- (vii) The stages are assumed perfectly mixed.
- (viii) There are no hydraulic lags.

With these assumptions borne in mind the mathematical model can be derived by taking a mass balance about each phase of each stage.

A solute balance on the heavy phase around stage n gives

$$L (1 + e_L) X_{n-1} - L (1 + 2 e_L) X_n + L e_L X_{n+1} - Q_n aH = H h_L \frac{dX_n}{dt} \quad (3)$$

where a is the interfacial area per unit volume and H is the height of a stage.

In a similar manner, a solute balance on the organic phase around stage n gives

$$G(1 + e_L)Y_{n+1} - G(1 + 2e_G)Y_n + Ge_G Y_{n-1} + Q_n aH = Hh_G \frac{dY_n}{dt} \quad (4)$$

At the top no mass transfer section, stage 0, the equations are

$$LX_i - L(1 + e_L)X_0 + Le_L X_1 = H' h_L' \frac{dX_0}{dt} \quad (5)$$

and

$$G(1 + e_G)Y_1 - Ge_G Y_0 - GY_0 = H'' h_G'' \frac{dY_0}{dt} \quad (6)$$

where X_i is the heavy phase feed concentration and the superscript ' denotes upper end section parameter values.

At the bottom no mass transfer section, stage N+1, the equations are

$$L(1 + e_L)X_N - Le_L X_{N+1} - LX_{N+1} = H'' h_L'' \frac{dX_{N+1}}{dt} \quad (7)$$

and

$$GY_i - G(1 + e_G)Y_{N+1} + Ge_G Y_N = H'' h_G'' \frac{dY_{N+1}}{dt} \quad (8)$$

where the superscript '' denotes lower end section values and Y_i is the light phase feed concentration.

3. SOLUTION OF THE EQUATIONS

The equations derived in the preceding section are linear with regard to concentration disturbances. Non linearities due to flow rate changes can be eliminated by assuming such disturbances to be small perturbations about a steady state value. These perturbations are assumed to be small so that products of perturbations in concentration and flow rate are negligible. In this manner Jones & Wilkinson^(2, 3) were able to solve these equations for both flowrate and concentration disturbances.

This was done in the Laplace domain. Inverse Fourier transformation yielded the impulse response which on integration gave the step or transient response. Experimental work on a 23 stage, 6" diameter column has shown that these theoretical transient responses are an adequate representation of the actual dynamic behaviour.

The method of solution quoted above is highly dependent upon equations 3 to 8 being linear. This requirement necessitates the use of the perturbation method and defines the rigidity of the model in its present form through the assumptions made in Section 2. While a solution of the closed loop problem in

the Laplace domain is not difficult, time domain calculations offer a means of simplifying the solution technique while, at the same time, enabling many of the above assumptions to be overcome.

Numerical integration and finite differencing with matrix inversion were considered as a means to obtaining the time domain solution. The matrix inversion scheme was discarded as being potentially prohibitive for a 25 stage system with respect to computing time. This decision is supported by the results of Pollock and Johnson⁽⁵⁾ who found that computational time for a matrix inversion method increased exponentially with stage number while for numerical integration, computational time increased linearly. Matrix inversion of the steady state equations, however, proved to be a most effective way of verifying the validity of the solutions by numerical integration.

The implementation of the numerical integration solution will be carried out, initially, in accordance with the assumptions of Jones and Wilkinson in order that their results may remain as a valid reference.

4. OPEN LOOP SIMULATION

4.1 Preliminary Studies on a 5 Stage column

The solution of a 5 Stage column based on the model previously discussed has been given by Ingham and Dunn⁽⁶⁾ using digital simulation. The simulation language MIMIC was used, which is based on a Runge-Kutta-Merson routine. An extension of this program to cover the 23 stage case⁽⁷⁾ produces results which are claimed to be in excellent agreement with the results of Jones and Wilkinson.

It was decided to model initially a 5 stage system, the results of which could be compared with those of Ingham and Dunn. In this manner, several integration routines were tested. Computations were carried out in Fortran IV using an ICL 1904A computer.

The steady state end sections were modelled by setting the derivatives of e.g. 5, 6, 7, 8 to zero giving

$$X_0 = \frac{X_1 - e_L X_1}{1 + e_L}$$

$$Y_0 = Y_1 \tag{10}$$

$$X_{N+1} = X_N \tag{11}$$

$$Y_{N+1} = \frac{Y_1 + e_G Y_N}{(1 + e_G)} \tag{12}$$

The integration routines to be tested were taken from the extensive Mark 3 library of subroutines developed by the Nottingham Algorithm Group (N.A.G.)⁽⁸⁾

These routines, which proved easy to implement, were each used to model the start-up situation with the test parameters used by Ingham and Dunn (Table 1).

TABLE 1

L = 0.2175	G = 0.175
$e_L = 1.0$	$e_G = 1.0$
m = 0.8	H = 7.85
$h_G = 0.2$	$k_a = 0.067$
	$y_i = 0.0$
$x_i = 0.0 + 1.0$	
Integration Step Length	20 sec
Print Interval	100 sec
Range	1080 sec

The running times of these test programmes are given in Table 2.

TABLE 2

	NAG Reference ⁽⁸⁾	Running Time Sec.
Nordsieck	DO2 ACF	134
Krogh	DO2 AHF	42
Gear	DO2 AEF	29
Runge-Kutta-Merson	DO2 ABF	35

These figures should be taken as having only relative significance since the program used has since been improved in structure. Furthermore, all runs at this stage were carried out in Trace 2 mode.

It can be seen that the methods of Nordsieck and Krogh are relatively slow and were not considered further.

In all cases excellent agreement was obtained for heavy phase concentrations. For the light phase concentrations, the predictor corrector methods were each in agreement to 5 significant figures. The

Runge-Kutta-Merson routine, however, showed slightly higher concentrations at the extract end of the column, in violation of the mass balance.

The light phase transient profiles as calculated by Gear's method are presented in Figure 3. These results are in excellent agreement with the published data of Ingham and Dunn.

Further tests with these programs were made for larger steps in X_1 . The results were in full agreement, one with another, for both heavy and light phase concentrations. The difference between the running times for Merson's and Gear's methods, however, was reduced.

It was decided to test both these methods for the solution of the 25 stage system. In addition to the methods shown in Table 2 the method of Euler is also being tested to check the assertion made recently by Luyben⁽⁹⁾ that for control problems this simple integration routine with a carefully chosen step length is superior to the complex variable step-length methods.

4.2 The 25 Stage Column

The program structure was easily modified to solve the 25 stage model with unsteady state end sections. This modified system was solved for the same conditions by Gear's method and the Runge-Kutta-Merson method. Some of the results, including mass balance information, are presented in Table 3.

Table 3

Method	Computing Time (sec)	Range (sec)	$\Delta X/\Delta Y$		A/B
			A	B	
Gear	600	7000	0.96548	0.96541	1.000073
Merson	600	5000	1.29048	0.99341	1.299041

The slight deviations from the mass balance noted when Merson's method was used to solve the 5 stage system are found to be exaggerated. Furthermore, it is seen that the computing time for the Merson's method is now significantly larger than that for Gear's method. On this evidence Gear's method was chosen for further work.

This choice would appear to be logical since these equations, like many encountered in chemical and control engineering, are almost certainly stiff; a situation for which Gear's method is most suited^(8, 10). It

might be pointed out here that the method of Krogh, discounted for this system, may be applicable for later cases when the restrictions made in the assumptions of Section 2 are dropped. Krogh's method becomes more efficient than that of Gear as the number of computations per component increases⁽¹⁰⁾.

To provide an independent check for these 25 stage results, the steady state solution was generated by setting the derivatives of equations 3, 4, 5, 6, 7 and 8 to zero. The resulting linear algebraic equations are easily solved by a matrix inversion technique. In addition to providing a check for the unsteady state profiles, these steady state data obtained by matrix inversion are useful in providing the asymptotic concentrations for $t = \infty$.

Open loop transient profiles have been calculated for the parameters shown in Table 4 below.

Table 4

L = 0.203	G = 0.187
e _L = 0.32	e _G = 0.01
m = 0.73	H = 7.45
h _G = 0.123	k _a = 0.025
	Y _i = 0.0005
X _i = 0.0 + 0.0693	
Integration Step Length	20 sec
Print Interval	100 sec
Range	5000 sec

The results of this open loop simulation agree well with the matrix inversion results. The near steady state raffinate concentration was 0.07801 gm/gm, which is compared with the matrix inversion result of 0.07803 gm/gm.

5. CONTROL SYSTEM STUDIES

Although a mathematical model capable of predicting the open-loop dynamic behaviour of a solvent extraction contractor is of value in design, particularly in assessing start-up and shut-down behaviour and the effects of changes in operating parameters, the application of the model to control system studies is

of more significance in practice. This problem will be considered here. First, a conventional feedback control system will be investigated and the inherent weaknesses of this type of control for solvent extraction plants will be discussed. The likely advantages of feed forward control techniques will then be considered.

5.1 Feedback Control

The control system to be investigated by way of example is illustrated in Figure 4. The objective will be to maintain the raffinate concentration as steady as possible in spite of disturbances in the feed concentration by regulating the flow rate of the heavy phase feed. Although other disturbances and control actions are feasible the arrangement considered here is typical and such control systems have been used on industrial plants.

Two factors have to be considered in the design of a control system of this type in order to optimise the performance. These are,

- (i) the location of the control point within the column
- (ii) the controller characteristics

In qualitative terms the selection of the control point is a compromise between two conflicting factors. In order to maintain a constant raffinate concentration it could be argued that the controlled variable should be the raffinate concentration itself. However, a disturbance which enters the top of the column and which is allowed to go undetected until it is propagated to the base of the column would result in an off-specification raffinate for a long period of time before the control system could take effective action. This is unavoidable with systems such as solvent extraction processes which involve long lags. On the other hand, if the control point is located nearer the top of the column, i.e. nearer to the point at which the disturbance enters the system, then the speed of the control will be improved at the expense of the tightness of the control, i.e. the variations in raffinate concentration could be increased. For the 25-stage column considered in this work results will be given for two control points, stage 6 and stage 12 (numbering from the top of the column), to illustrate these points.

The desired value will be taken as the initial steady state of the heavy phase concentration at the control point. It should be noted that once the feed concentration and/or the feed flow rate change from the design value, the steady state concentration profile in the column will

alter. The initial value of the concentration at the control point, i.e. the desired value imposed on the control system, will no longer be the concentration at that stage which will give the required raffinate concentration. Perfect control of the raffinate concentration could therefore not be expected with a control system of this type.

For systems with large time constants, such as the column under consideration, derivative action is not appropriate. Furthermore, as was discussed above, a change in feed concentration will, almost certainly, result in an offset in X_R . Eliminating the error at the control stage will not improve matters. Integral control would not be beneficial, only tending to reduce stability without improving the tightness of the control.

Based on these qualitative considerations, it was decided to consider proportional control only. The controller equation was of the form

$$L = L_z + K\epsilon \quad (13)$$

where L_z is the mid range constant or heavy phase feed rate at zero error, K is the controller gain, and ϵ is the error at the control point, stage c , i.e. $\epsilon = X_{CO} - X_C$.

The dynamic characteristics of the measuring element and the control valve are assumed to be negligible.

The closed loop response of the column following a feed concentration disturbance has been computed for two control points, stage 6 and stage 12, for values of the controller gain ranging from 0.1 to 100. In each case the time responses of the raffinate concentration and the concentration at the control point have been calculated and the results are presented in Figures 5 to 7.

5.2 Discussion of Feedback Control Results

The 25 stage model with proportional only control was tested by introducing an upward step of magnitude 1% (0.01 gm/gm) in the heavy phase feed concentration.

The initial conditions to be used were calculated by the matrix inversion routine for the conditions given earlier in Table 4.

The transient responses of raffinate concentration for control at stages 6 and 12 are shown in Figures 5 and 6 respectively. In both cases a controller gain of 0.1 is seen to have little effect and the response is

close to the open loop response. For a gain of 1.0 the raffinate concentration at first begins to decrease before rising in the expected manner. The explanation for this response to an upward step lies in the assumption of negligible hydraulic lags. Although a lag exists before a disturbance in feed concentration can affect the controlled variable at the control point, a change in the heavy phase feed flow rate is assumed to be instantaneously effective throughout the whole column. Thus, when an increase in the control stage concentration is detected, the controller causes a reduction in the heavy phase flow. Since the light phase flow rate is kept constant, the phase ratio will be decreased, and this results in more extraction of the solute near the base of the column. The raffinate concentration will fall slightly until such time as the concentration step reaches the base of the column to offset the effects of the reduced phase ratio. The final raffinate concentration in this case is greater than the initial value for an upward step in feed concentration.

With a gain of 10.0, control is so severe that the effects of the concentration step on the raffinate concentration is negligible compared to that of the drastically reduced phase ratio and the final ultimate concentration is lower than the initial value.

It is seen then from Figures 5 and 6 that for control at both stages 6 and 12 an increase in the gain from 1.0 to 10.0 causes the steady state error to fall from a small negative value to a large positive value. The shape of the heavy phase steady state concentration profile for $K = 10.0$ must, then, be such as to intersect the original profile. This can be seen to be the case in Figure 7 for control at stage 6. Values of the corresponding phase ratios are also given.

These steady state profiles were calculated using the matrix inversion program and substantiate the validity of the model solution, in that they agree well with the near steady state profiles obtained from numerical integration over a large range.

Evidence of the agreement of these solutions is given in Table 5. The steady state concentrations at the control stage 6 and for the raffinate as calculated by the two methods of solution are given for various values of controller gain.

Table 5

K	$X_6 (\infty)$		$X_R (\infty)$	
	Gear's method	Matrix inversion	Gear's method	Matrix inversion
0.0	0.07801	0.07803	0.02659	0.02663
0.1	0.07798	0.07798	0.02638	0.02639
1.0	0.07749	0.07749	0.02420	0.02421
10.0	0.07241	0.07242	0.01421	0.01422

A further inference is to be drawn from the fact that the error changes sign, is that, by judiciously selecting the controller gain, the steady state raffinate error can be eliminated. For control at stage 6 a gain of approximately 1.3 would seem to be effective. The profile is given in Figure 5 and the steady state raffinate concentration for this gain is 0.02344, corresponding to an error of ≈ 0.00011 .

The quality of regulation at the control point can be judged by the results shown in Figure 8. The steady state offset and speed of response vary in the expected manner as the gain is increased. For a gain of 100.0 the first traces of oscillatory behaviour are detected. Due to the high gain such oscillations are first detected in the heavy phase flow rate.

5.3 Feedforward Control

It will be apparent from the results of the preceding section that simple feedback control is not satisfactory for this system. This is due to the slow response of the column to heavy phase inlet concentration changes.

The control of such systems can often be greatly improved by the introduction of feedforward control. This involves the measurement of any load disturbances before they reach the column, enabling the simultaneous implementation of corrective action. Thus a variation in heavy phase feed concentrations can be compensated for by adjusting the heavy phase feed flowrate in order to maintain constant raffinate concentration.

The two main disadvantages with feedforward control are

- (i) the disturbance must be accurately measurable
- (ii) the feedforward controller must be an exact representation of the process dynamics

Inevitable deviation from either of these requirements will result in uncontrolled drift of the controlled variable. To prevent this, a feedback loop is usually used in conjunction with the feedforward loop and such a scheme is illustrated in Figure 9.

Since the major part of the control is effected through the feedforward loop, the feedback elements merely acting as a trim, then the problem of the large system lags is alleviated. The raffinate concentration may then be used as the feedback control variable so that the trimming action will be as effective as possible in eliminating any slight drift. Furthermore, the feedback controller need not be tuned accurately. Integral action alone may be used, but more often a minor proportional element is added.

The behaviour of the feedback system can be explained as follows.

With the assumptions of Section 2, the mathematical model is linear and can be described in terms of transfer functions, as in Figure 10, where $F_P(S)$ is the process transfer function, $F_D(S)$ is the transfer function relating X_R with load disturbances and $F_C(S)$ is the feedback controller transfer function.

The standard texts⁽⁹⁾ show that for such a system a feedforward controller, $-F_D/F_P$ would compensate exactly for any load disturbances. The transfer functions F_L and F_P have been developed by Jones and Wilkinson^(2, 3) for the system under consideration. However, if we argue that the nature or shape of the response is of secondary importance to the maintenance of zero steady state error in the controlled variable, then we can ignore the effects of all dynamic components in the feedforward controller. This amounts to setting $S = 0$ in the controller transfer function which can be denoted as $F_D(0)/F_P(0)$, and this ratio represents a constant, i.e. the ratio of the steady state gains of the disturbance and process transfer functions.

This type of feedforward controller is known as a steady state feedforward compensator⁽¹¹⁾ and represents an easily realizable physical system, which is not always the case with feedforward controllers designed in the traditional manner.

The block diagram of the feedforward-feedback system is shown in Figure 11. By straightforward block diagram algebra we can show that the load transfer function is:

$$\frac{X_R(S)}{X_I(S)} = \frac{F_D(S) - \left[\frac{F_D(O)}{F_P(O)} \right] F_P(S)}{1 + F_C(S) F_P(S)}$$

That the steady state compensator has no effect on the system dynamics follows from the fact that the characteristic equation is unchanged by the addition of feedforward control.

Furthermore, even without integral control the system will have zero steady state error as is seen by substituting for $S = 0$

$$\frac{X_R(O)}{X_I(O)} = \frac{F_D(O) - \left[\frac{F_D(O)}{F_P(O)} \right] F_P(O)}{1 + F_C(O) F_P(O)} = 0$$

The steady state feedforward compensator, then, offers an algorithm for eliminating the steady state errors of Figures 5 and 6 without introducing the undesirable features of integral control.

The introduction of non-linearities to the system does not invalidate the basic idea of the steady state feedforward compensator, only now a control computer would be required to continually update the value of $F_D(O)/F_P(O)$ which would be a function of the disturbances.

6. CONCLUSIONS

The simulation in the time domain of a 25 stage solvent extraction process has been shown to be feasible. This initial value problem, represented by 54 first order differential equations, was found to be solved most efficiently by a predictor corrector type method, due to Gear. Previous published work of this nature has involved solutions by Runge-Kutta routines (6, 12, 13)

Closed loop results for proportional only control have been presented for control at two points in the column, stages 6 and 12 respectively. A unit upward step in feed concentration was used to perturb the system. In both cases the error at the control stage could be made very small by increasing the controller gain, before instability set in.

Control of the raffinate concentration was found to be unsatisfactory for this type of control system, the error in the raffinate concentration increasing rapidly once the gain increases, above a certain value. For control at stage 6 this value was found to be about 1.3, at which point the steady state raffinate error is very nearly zero. Perfect regulation of the raffinate concentration, then, is possible for a known disturbance, by allowing an error in the control stage concentration. This error should be such that the steady

state control stage concentration lies on, and thus fixes, a new steady state concentration profile which terminates at the required raffinate concentration.

With proportional only control, the use of stage 12 rather than stage 6 as a control point results in improved control. The increased degradation of the perturbation step before reaching stage 12 means that the error develops more slowly and a smaller gain is required for a given corrective action than is required at stage 6. Thus for a given gain, control at stage 12 results in smaller raffinate concentration errors, though the response time is slightly larger than that for control at stage 6. Proportional control in both cases is unsatisfactory. By controlling nearer the raffinate end, the error in the raffinate concentration is reduced but at the expense of an increased response time.

The availability of a working model of the system suggests that feedforward control, with the addition of a feedback loop to trim the control, will be a more effective control system. A study of such a system with a steady state feedforward compensator type controller will form the basis of future work in this field.

References

- (1) Pollock, G.G., Johnson, A.I.:
The Dynamics of Extraction Processes, Part I.
Can. J. of Chem. Eng. 1969, 47, 469-476.
- (2) Jones, D.A., Wilkinson, W.L.:
The Dynamic Response of a Multiple-Mixer Solvent.
Chem.Eng.Sci. 1973, 28, 537-551.
- (3) Jones, D.A., Wilkinson, W.L.:
The Dynamic Response of a Multiple-Mixer Column to Flow Rate
Disturbances.
Chem.Eng.Sci. 1973, 28, 1577-1589.
- (4) Jones, D.A., Wilkinson, W.L.:
A Dynamic Model of a Multiple-Mixer Solvent Extraction Column.
Paper presented ISEC 1971 Conference, The Hague.
- (5) Pollock, G.G., Johnson, A.I.:
The Dynamics of Extraction Processes, Part IV.
Can. J. of Chem. Eng. 1970, 48, 711-719.
- (6) Dunn, I.J., Ingham, J.:
Modelling of Continuous Process Systems; an Introduction to
digital simulation programming.
Verfahrenstechnik 1972, 6, No. 11, 339-410.
- (7) Dunn, I.J., Ingham, J.:
Communication - Calculation of Extraction Columns with Backmixing.
Chem.Eng.Sci. 1972, 27, 1751-1752.
- (8) Nottingham Algorithms Group.
1900 Mini Manual.
- (9) Luyben, W.L.:
Process Modelling, Simulation and Control for Chemical Engineers.
McGraw-Hill 1973. P.138, 331.
- (10) Lambert, J.D.:
Computational Methods in Ordinary Differential Equations.
Wiley 1973. P.242, 113.
- (11) Henry, R.M.:
Multi-Input Control Algorithms.
University of Bradford, School of Control Engineering,
Internal Paper - 9th February 1972.
- (12) Souhrada, F., Landau, J., Prochazka, J.:
Dynamic Simulation of a Stagewise Mass Transfer Process with
Back-Mixing.
Can. J. of Chem. Eng. 1970, 48, 332-327.
- (13) Biery, J.C., Boylan, D.R.:
Dynamic Simulation of a Liquid-Liquid Extraction Column.
Ind. and Eng. Chem. Fund. 1963, 2, No. 1, 44-50.

Nomenclature.

a	Interfacial area per unit volume, cm^2/cm^3 .
b	Intercept of linear equilibrium line.
e	Backmixing coefficient.
F_C	Controller transfer function.
F_D	Disturbance transfer function.
F_P	Process transfer function.
$F(0)$	Transfer function for $S = 0$.
G	Organic phase flowrate, $\text{gm}/\text{sec. cm}^2$.
H	Height of multiple mixer component, cm.
h	Fractional hold-up, gm/cm^2 .
K	Proportional gain.
k	Mass transfer coefficient, $\text{gm}/\text{sec. cm}^2$ transfer area.
L	Aqueous phase flowrate, $\text{gm}/\text{sec. cm}^2$.
m	Distribution coefficient.
N	Total number of stage.
n	Number of n^{th} stage.
Q	Rate of mass transfer, $\text{gm}/\text{sec. cm}^2$ transfer area.
S	Laplace transform variable.
t	Time, sec.
X	Concentration of solute in aqueous phase, gm/gm.
X_D	Desired value of X, gm/gm.
X_R	Concentration of solute in raffinate, gm/gm.
X^*	Concentration of solute in aqueous phase in equilibrium with organic phase, gm/gm.
Y	Concentration of solute in organic phase, gm/gm.
e	Error between X_C and X_D .

Subscripts:

c	Value at control stage.
G	Organic phase.
i	Value at inlet.
L	Aqueous phase.
n	n^{th} stage.
O	Value at $t = 0$.
Z	Value at $\epsilon = 0$.

Superscripts:

'	Value at top compartment of column.
"	Value at bottom compartment of column.

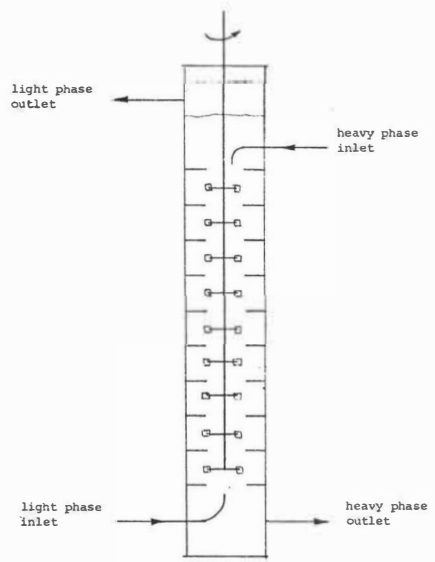


FIGURE 1 MULTIPLE MIXER COLUMN

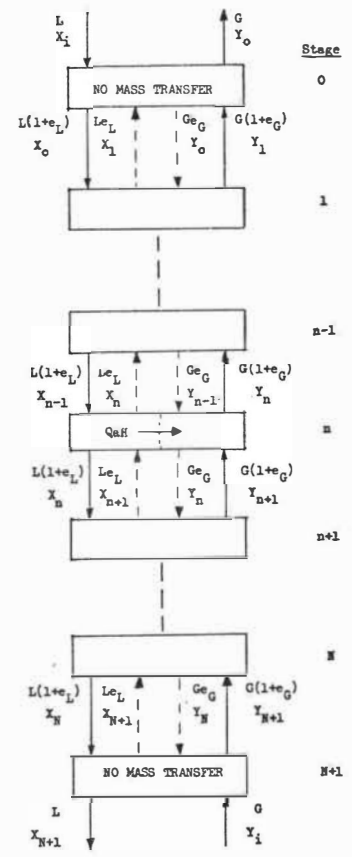


FIGURE 2. DIAGRAMMATIC REPRESENTATION OF COLUMN.

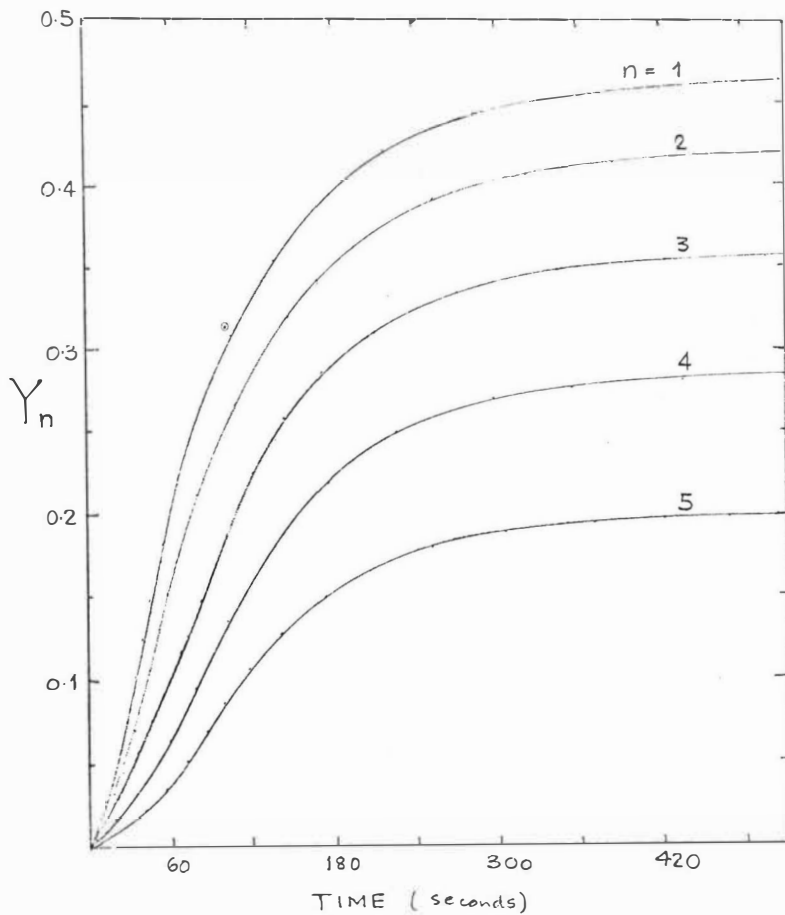


Figure 3 5 Stage model - open loop transient profiles.

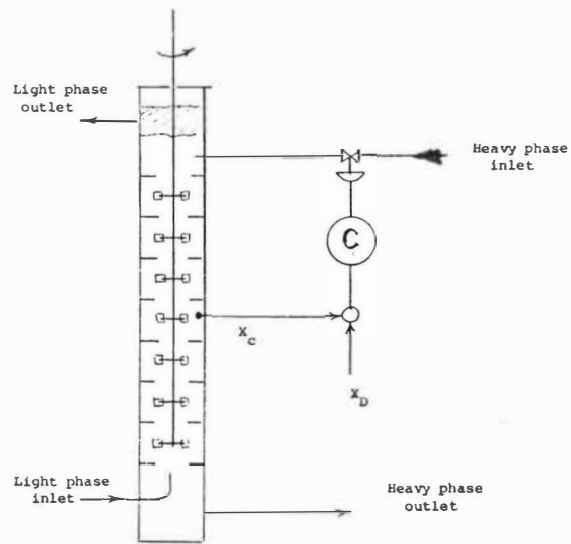
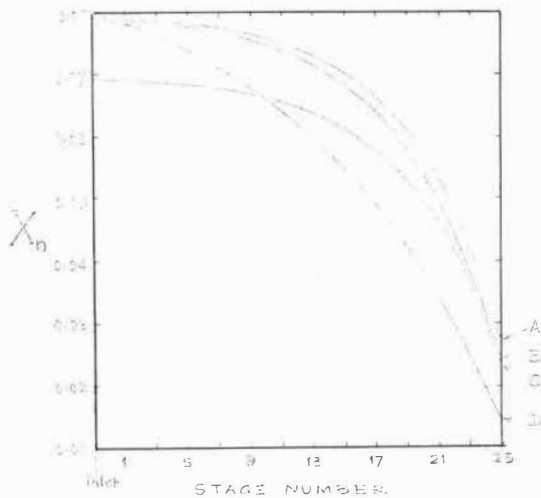


Figure 4 Feedback Control System



	X_1	K	L	1/G
A	0.0793	0.0	0.203	1.0856
B	0.0793	1.0	0.1937	1.0356
C	0.0693	0.0	0.203	1.0856
D	0.0793	10.0	0.1608	0.1599

Figure 5 25 Stage model - steady state concentration profile for control at Stage 6.

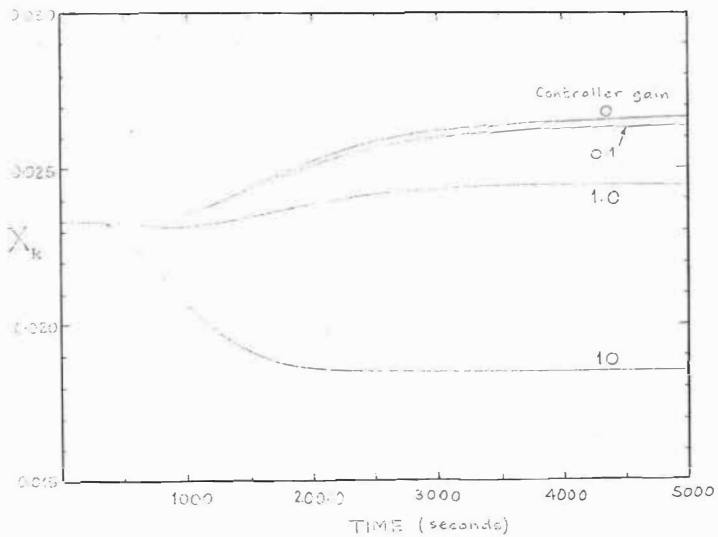


Figure 6 Closed-loop raffinate response to step change in feed concentration with control at Stage 12.

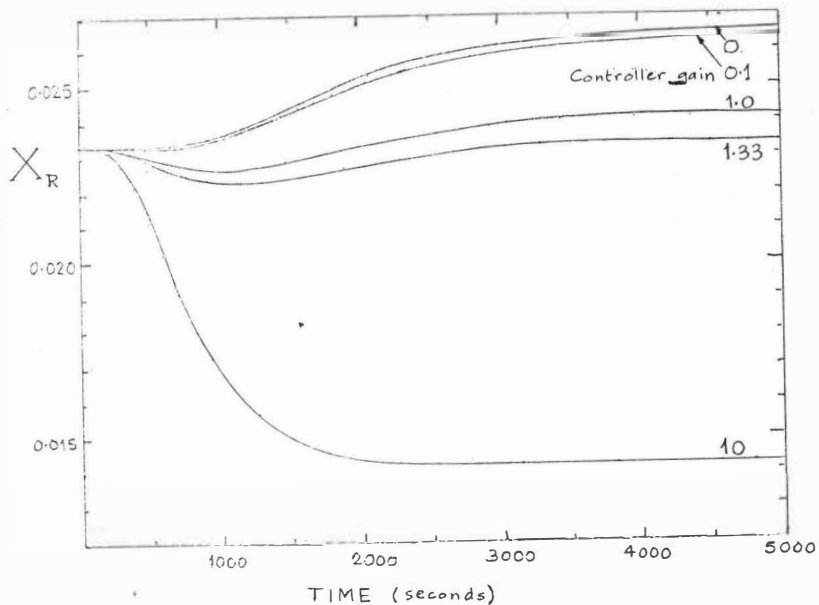


Figure 7 Closed-loop raffinate response to step change in feed concentration with control at Stage 6.

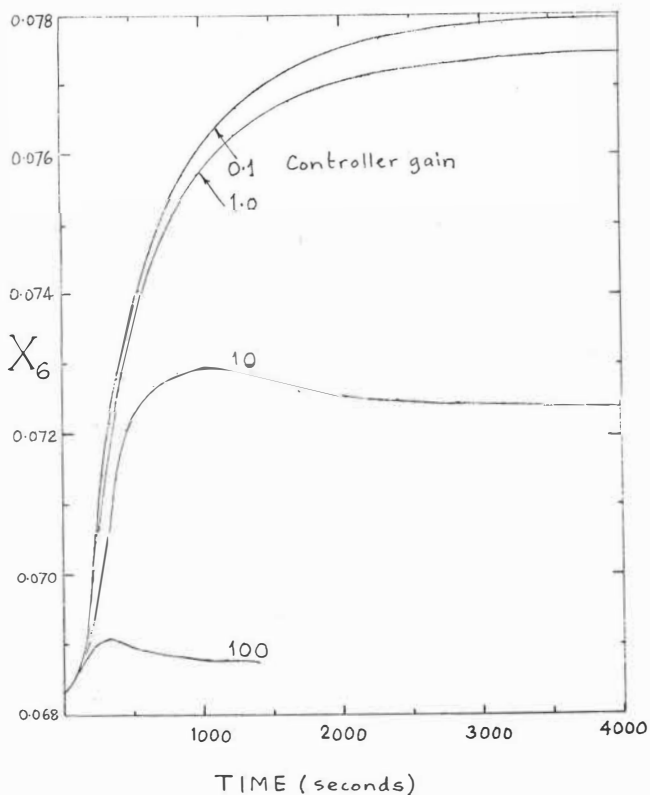


Figure 8 Closed-loop response at the control point (Stage 6).

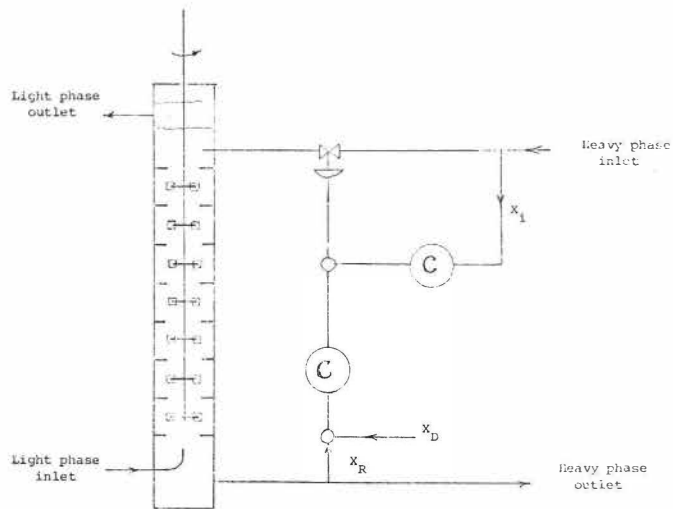


Figure 9 Feedforward-Feedback Control System

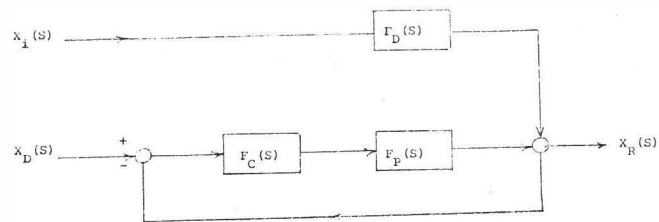


Figure 10 Block Diagram of Feedback Control System

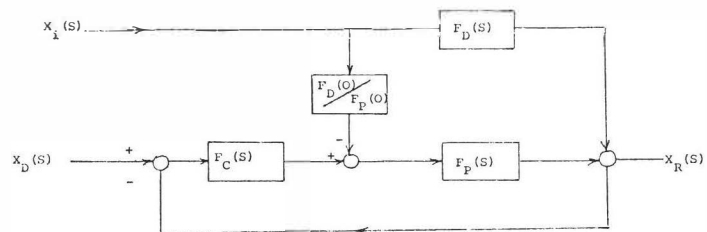


Figure 11 Block diagram of feedback/feedforward control system



SIMULATION OF THE STATIC AND DYNAMIC BEHAVIOUR OF A SOLVENT
EXTRACTION PROCESS FOR RARE EARTH SEPARATION

by - B. Gaudernack, T.B. Muller, S. Nuland and O. Ørjasæter

ABSTRACT

In connection with the development of a solvent extraction process for rare earth separation, mathematical models for static and dynamic simulation of the process as operated in an internally fed, counter-current multistage cascade were developed. The models are programmed in FORTRAN IV to be used on a CDC CYBER 70 computer. The calculation of solute concentration throughout the cascade is based on some new approaches. These were developed to retain acceptable computing times, when the models are applied for static optimization procedures, evaluation of process control methods or simulation of start-up transients.

The equilibrium conditions are described by non-linear relations obtained through the best fit correlations of experimental data.

For the static model, good agreement between computed and experimental results has been obtained. The dynamic model, however, gives slightly greater discrepancies due to uncertainties in process input and severe dynamic sensitivities.

Revealing these sensitivities has been one of the results most valuable to the understanding of the process performance.

Institutt for Atomenergi, Kjeller, Norway

INTRODUCTION

Useful separation factors for rare earth elements can be achieved by extraction with an organic solution of a quaternary ammonium nitrate from aqueous nitrate solutions of the elements. By extraction from slightly acid solutions in the presence of a suitable salting agent, e.g. ammonium nitrate, separation factors of about 2 are obtained for the lighter lanthanides. Distribution coefficients decrease regularly with increasing atomic number within the lanthanide series, and can be controlled within wide limits by adjustment of system parameters such as the aqueous acidity and salting agent concentration.

The system is also useful for yttrium separation, as yttrium remains with the heaviest lanthanides and may be separated from these in a subsequent extraction cycle, making use of a different extractant. A process for yttrium separation, based on two cycles of solvent extraction using quaternary ammonium nitrates and thiocyanates, respectively, has been developed and patented by the Norwegian company A/S Megon. (U.S. Patent 3,751,553, patents pending in other countries). The present work concerns the separation of yttrium and "heavies" by quaternary ammonium nitrate extraction, but the mathematical models described apply equally well to other rare earth separations by means of this extraction system. Similar models have also been developed for the thiocyanate system, so that the complete yttrium separation process can be simulated.

The process simulation work parallels pilot plant testing of interesting process alternatives, and the results of the two activities have been used in process optimization and economic feasibility studies, and for planning a control strategy for industrial utilization of the process.

Separation of individual rare earth or yttrium in a solvent extraction process like the one described, requires cascades comprising a relatively high number of counter-current stages. Feed compositions actually include up to 15 elements which will influence the performance of the separation process with respect to product yield and purity. A mathematical description of the process, which is based on the mass balances and equilibrium conditions for all elements at each stage of the extraction

cascade, therefore, leads to a rather extensive set of strongly coupled equations.

Besides the general computational difficulties, this means special problems for the development of mathematical models with the flexibility and moderate computing times necessary for use in static optimization procedures and for process control purposes. In this particular system, the best correlation of equilibrium data has been obtained by correlating against total molar concentration methods, which are based on correlations of equilibrium data against the concentrations in one phase only, will be less applicable.

Considering the static calculation of extraction systems, the technique used by several authors for lanthanides (1) and actinides (2) is based on Thiele and Geddes method (3). This is an iteration method where the calculations are started on a guessed concentrations distribution for all elements in one of the end streams of the cascade. For the investigated system, with equilibrium data correlated against total molar concentrations in both phases, a high number of solutes and cascades of 25 stages or more, this method was found not to give acceptable convergence and computing times. The static calculation method described in this paper was developed to overcome these difficulties.

Considering the dynamic representation of a mixer-settler cascade, non-steady state mass balances are used, taking into account the accumulation of solutes in the mixer-settler volumes on mismatch of input - output at the individual stages as well as transport delays throughout the cascade. The requirements for relevant equilibrium data correlations are the same as for steady state calculations.

In the investigated system the high number of elements and stages, as well as non-linear equilibrium data correlations, lead to a high number of differential equations which are coupled through non-linear relations.

The dynamic model described in this paper was developed for simulation of this type of multicomponent and multi-stage process on digital computers, the main requirements being acceptable accuracy, flexibility and computing times for evaluation of process control methods and simulation of start-up transients.

CORRELATION OF EQUILIBRIUM DATA

Adequate correlations for the distribution coefficients are of great importance for the dynamic as well as the static simulation. Due to the scarcity of equilibrium data available for the investigated system, however, it has been necessary to adapt some simplifying assumptions, which were previously used for a different extraction system (4):

- Interaction effects between individual solutes are negligible
- The distribution coefficient for each solute at macro-concentrations is proportional to:
 - a. the distribution coefficients at micro-concentration of the solute alone
 - b. a correction factor, which is common for all solutes, describing the effect of loading of the organic phase.

Thus, the distribution coefficients for one particular solute is given by

$$D_j = D_{mj.0}$$

D_{mj} is a function of parameters which are specific for the extraction system but independent of the concentrations of rare earths and yttrium. From the available equilibrium data for micro-concentrations, it can be approximated to an exponential function of the aqueous nitrate concentration. The exponential gain is approximately the same for all solutes, whereas the initial values decrease with increasing atomic number.

The common correction factor, ϕ is derived from equilibrium data for macro-concentrations by means of non-linear regression analysis. In the specific extraction system it is found to be a function of the total molar concentration of rare earths and yttrium in the organic phase and total molar concentration of nitrate in the aqueous phase.

From the experimental data available it has been observed that the factor, ϕ is not quite the same for all solutes, but due to the scarcity of relevant data it was found necessary, in this work, to use an average value for all solutes.

STATIC MODEL OF EXTRACTION PROCESS

Principal Description

The static model of the extraction process is based on the mass balances at steady state for each solute and each stage throughout the cascade and the distribution relations as given in the previous section. The cascade comprises a combined extraction and scrub section (Fig. 1).

Assuming that the phases are insoluble with respect to each other and neglecting volumetric variations, the mass balances are given by a set of linear equations, representing each solute concentrations at each stage of the cascade.

At an arbitrary stage number i , except the feed stage, the mass balances and equilibrium conditions for one particular solute, j , are expressed by the following equations:

$$H \cdot x_{j,i-1} + L \cdot y_{j,i+1} - (H \cdot x_{j,i} + L \cdot y_{j,i}) = 0 \quad (2)$$

$$D_{j,i} = D_j (K_{j,i} y_{j,i} - S_i) \quad (3)$$

$$\frac{y_{j,i}}{x_{j,i}} = D_{j,i} \quad (4)$$

The concentration of ammonium nitrate, S_i is considered constant in each of the two sections of the cascade.

The method for solution of this set of equations is based on the following observation: When the distribution coefficients are given, all concentrations can be found by solving some sets of linear equations with tridiagonal matrices, one set for each rare earth element in the feed.

Solving linear equations with trigidiagonal matrices can be done easily and quickly on a digital computer, and will not be described here.

We thus have the following iterative procedure:

1. Guess the values of the distribution coefficients $D^{(0)}$. The accuracy of this guess is unimportant to the following computations, and the guess is built into the programme.
2. Compute the concentrations in the cascade, resulting from the given distribution coefficients.
3. Compute new distribution coefficients $D^{(n)}$ using equation (3) ($n=1,2,\dots$)
4. If all deviations between the old and new distribution coefficients for any element in any stage are less than a given accuracy, the solution has been found.
5. If the iteration sequence has to be continued, reduce any oscillations in the distribution coefficients by the equation:
$$D^{(n)} = QD^{(n)} + (1-Q) D^{(n-1)}$$

Go to 2.

The constant Q used to subdue numerical oscillations is sometimes called a relaxation factor. Its value is usually between 0 and 1, and depends on the equilibrium relation.

Based on the described techniques a routine for calculating steady state concentration profiles of an extraction cascade was written in FORTRAN IV. This routine is used as a part of a more extensive simulation and optimization programme.

The subroutine for calculating distribution coefficients and the relaxation factor are the only parts of the routine which depend on the particular extraction system. The routine can easily be extended to cover several extraction systems, still keeping the programme fairly simple.

The programme works most efficiently with smooth equilibrium relations, but is otherwise rather intensive to the form of these relations.

Incomplete Mass Transfer

By incorporating a mass transfer resistance, stage efficiencies less than unity can be included without altering the computational method.

A mass balance may be written for each phase volume:

$$Ly_{j,i+1} - Ly_{j,i} - T_{j,i} = 0 \quad (5)$$

$$Hx_{j,i-1} - Hx_{j,i} + T_{j,i} = 0 \quad (6)$$

The mass transfer between the two phases is given by:

$$T_{j,i} = kA(y_{j,i} - j_{j,i}) \quad (7)$$

The least viscous phase, the aqueous one, is considered ideally mixed, i.e. the same concentration exists throughout the volume. Furthermore the concentrations on both sides of the boundary are in equilibrium:

$$\frac{\tilde{y}_{j,i}}{x_{j,i}} = D_j \left(x_{j,i} - \sum_{i=1}^n y_{j,i} S_i \right) \quad (8)$$

When the distribution coefficients are given these equations can be transformed to a trigidiagonal form:

$$(LD_{j,i+1} + LH_q)x_{j,i+1} - (H+LD_{j,i+1} + 2LH_q)x_{j,i} + (H+LH_q)x_{j,i-1} = 0$$

To solve this we proceed as with ideal stages.

DYNAMIC MODEL OF EXTRACTION PROCESS

Representation Based on Complete Mass Transfer

At non steady state conditions the mass balance for one solute at one particular stage, i , of the extraction cascade, expresses that the mismatch of input - output mass flows equals the rate of change in mass accumulation.

Thus, the derivative of total mass of one element in stage i may be written:

$$Z_i = Hx_{i-1} (t-x) + Ly_{i+1} (t-y) - (HX_i(t) + Ly_i(t)) \quad (9)$$

The total mass is determined by the concentrations in each phase, and the volumes of both phases in the stage:

$$Z = V_m (k_m x_i + (1-k_m) y_i) + V_{sm} (k_s x_i + (1-k_s) y_i) \quad (10)$$

The concentrations are considered to be in equilibrium:

$$y_i = D_i x_i \quad (11)$$

The distribution coefficient, D_i , is given by equation (3). It is assumed that mixing takes place in the mixer volume V_m and a fictitious part V_{sm} of the settler volume, whereas plug flow is assumed in the rest of the settler volume V_{st} and in tube connections between the stages.

The deviations of Z is given implicitly by equations (10) and (11). These have to be solved numerically at each time step of the integration of 9.

In the investigated system, with 28 stages and up to 15 solutes, this will lead to an extensive set of non-linear differential equations, which would be rather cumbersome to solve simultaneously. These difficulties are, however, overcome by a method of decoupling of the simultaneous equations in such a way that only one stage at a time is involved in the iterative procedure, which is used for solving this set of equations on a digital computer.

The decoupling of the simultaneous equations is found practicable due to the transport delays τ_x and τ_y between the neighbouring stages. Thus, the computational time increments are chosen as definite intervals of the transport delays.

The hold-up times in each mixer-settler stage are in fact represented by mixing time constants given by

$$\tau_m = \frac{k_m \cdot V_m + k_s \cdot V_{sm}}{H} \quad (12)$$

$$\tau_y = \frac{(1-k_m) \cdot V_m + (1-k_s) \cdot V_{sm}}{L} \quad (13)$$

and transport delays in the plug flow region given by

$$\tau_x = \frac{k_s \cdot V_{st}}{H} \quad (14)$$

$$\tau_y = \frac{(1-k_s) \cdot V_{st}}{L} \quad (15)$$

Characteristic values for the ratio of transport delay to mixing time are found experimentally through measurement in an actual mixer-settler, and the actual residence times are then calculated in each case from the total mixer-settler volumes and flow rates.

Incomplete Mass Transfer

This may be represented either as a mass transfer resistance or as irregularities in the flows.

The mass transfer resistance approach, similar to the one for the static model, requires repeated calculations of a small difference, $y-y$. This makes it necessary to compute y and y with many significant digits at each time step of integration. The computation time is then increased excessively.

Otherwise bypassing of a small part of the stream at each stage may be incorporated in the model. An approach like that is physically reasonable and allows fast computation. Actually an amount of the order of 1 percent of each input stream to the stage is diverted to the settler with no mass transfer taking place to the other phase.

If x_i is the concentration at the outlet of stage i , and x_i is the concentration in the ideally mixed part of the volume we have

$$x_i(t) = (1 - A)x_i(t) + Ax_{i-1}(t - x) \quad (16)$$

As a consequence equations (10) and (11) are reformulated with x and y . As to the numerical integration of the differential equations, the predictor-corrector method of Hamming is used (6). Further, the non-linear equations are solved by an iterative procedure based on the method of Wegstein (5).

Based on the described method for numerical solution of the process equations, it has been possible to simulate the dynamic behaviour at each stage of the solvent extraction process without loss of accuracy due to linearization of process equations, and retaining acceptable computing times even for long-run studies of start-up transients. The dynamic model has great flexibility as to number of stages, number of solutes and concentration distribution in the feed. The programme can handle quite complex and generally non-linear correlations of equilibrium data, and neither divergence nor other numerical problems have been experienced.

The main limitations in simulating capability are envisaged in connection with:

- disturbances due to the formation of a third phase
- local disturbances of the flow regimes and hold-up within the individual stages

A representation of these non-regularities, which might exist in the actual process, is not incorporated in the model. This may introduce some uncertainty as to the quality of the simulation and should be kept in mind by comparison of simulation results to actual process runs.

SIMULATION RESULTS AND COMPARISON TO ACTUAL RUNS

For testing purposes the static and dynamic models have been used for simulation of an actual process run with a laboratory scale mixer-settler cascade. To record the transient response, measurements of yttrium concentrations were obtained from several stages at suitable time intervals during the start-up period. The experiment was run for 70 hours, and the concentration profiles in both phases were measured. The results of the static simulation are compared to these concentration profiles, although the approach to steady state conditions is not satisfactory.

The experimental set-up and operating conditions were as follows:

Number of stages in extraction section	:	23
Number of stages in scrub section	:	5
Molar concentrations of ammonium nitrate in aqueous phase at start-up:		
- in extraction section	:	5.35 mol/l
- in scrub section and feed stage	:	2.00 mol/l
Concentration of extractant in the organic phase at start-up.	:	0.69 mol/l
The volumetric flow rates were kept constant at the following values during operation:		
- organic phase	:	2.0 l/h
- aqueous phase, scrub section	:	0.43 l/h
- aqueous feed	:	1.0 l/h

The organic feed as well as the aqueous feed to the scrub section contained no rare earths or yttrium.

Composition of aqueous feed to the extraction section:

Yttrium	:	7.97 g/l
Lanthanum	:	0.005 "
Cerium	:	0.037 "
Praseodymium	:	0.010 "
Neodymium	:	0.021 "
Samarium	:	0.015 "
Gadolinium	:	0.035 "
Terbium	:	0.060 "
Dysprosium	:	3.76 "
Holium	:	0.72 "
Erbium	:	2.30 "
Ytterbium	:	0.90 "

Concentration of ammonium nitrate:

- In aqueous feed to the scrub section : 2.0 mol/l
- In aqueous feed to the extraction section: 7.0 mol/l

Acidity in both feeds : pH = 3.0

As for the numerical calculations, the static programme required 21 iterations to reduce the maximum relative deviation between two iterations to within 1^o/100. The computing time was 82 milli-seconds per iteration on a CDC CYBER 70.

A comparison of calculated and measured concentration profiles is presented in Fig.2, which shows the concentrations (g/l) of yttrium in both phases, and in Fig.3, which shows the concentration (g/l) of erbium in the aqueous phase only.

The results of the dynamic simulation are compared to measurements of yttrium concentrations at several stages of the cascade as a function of time after start-up. At present only the first 50 hours have been simulated. On a CDC-3600 computer this simulation requires about 10 minutes of computing time, when starting with zero concentration profiles for all rare earths and yttrium.

Incomplete mass transfer is then modelled as a mass transfer resistance. (When using the bypass approach the computation on CYBER 70 would require less than 2 minutes).

Some of the results showing calculated and measured yttrium concentrations at two different stages are presented in Fig.4 and Fig.5. The accuracy of the measurements is in the order of $\pm 10\%$.

DISCUSSION

The correspondence between the experimental and simulated dynamic responses is not too good. This is mainly due to the lack of measurements and control of the input flow rates to the cascade.

Thus the experiment turned out to be more a proof for the need for modelling and controlling the process than a test of the dynamic model.

The discrepancies between computed static and measured concentration profiles (Fig.2 and Fig.3) are mainly due to the transient state of the process.

A check of the mass balance indicates that the output concentrations are too low relative to the inputs.

To provide for incomplete mass transfer is necessary, to obtain a reasonable agreement between an extraction process and its mathematical model, at least with the types of mixer-settler equipment that we have experience with.

The present extraction process is extremely sensitive to disturbances. The previous example may demonstrate that feature. If the flow rate of the scrub solution is increased a few percent the total erbium contamination will leave together with the aqueous raffinate instead of with the organic extract.

Th is is an extreme case, but the sensitivity problem has strong implications for the use of static models, especially in optimization of extraction processes. Thus, it may be meaningless to carry out a static optimization of an extraction process without a satisfactory control system.

The experiment referred to above was carried out some years ago, with the specific purpose of model testing. Since that time, both models and experimental facilities have been improved. The static model has proved to be a useful tool in experiment planning and process optimization in a pilot plant that has been operated for the last three years. The results of changing process parameters, such a feed compositions, etc., have been predicted by simulation. Generally, the agreement between predicted and actual results has been very good.

The dynamic models have been very helpful aids to understanding the transient behaviour of the processes. They are now being adapted for use in a process control system to be applied in an industrial plant for yttrium separation. As a first stage of developing this control system, the models will be utilized in an estimator which, in conjunction with an on-stream analyzer, will provide process state estimates. In this manner, data from the on-stream analyzer can be used to their full advantage, and improved communication between operator and process will result. In the next stage of development the loop will be closed, and an on-stream process computer will take care of the control functions.

NOMENCLATURE

- A = interfacial area
- D = $\frac{y}{x}$ = distribution coefficient at equilibrium
- D_j = distribution coefficient (at equilibrium) for a particular solute j at macro-concentrations
- D_{mj} = distribution coefficient (at equilibrium) for solute j at macro-concentration
- H = volumetric flow rate in aqueous phase
- i = arbitrary stage
- J = arbitrary solute
- k = mass transfer coefficient
- k_m = ratio of aqueous phase volume to total volume in mixer
- k_s = ratio of aqueous phase volume to total volume in settler
- L = volumetric flow rate in organic phase
- n = iteration counter
- N = total number of stages
- q = $\frac{1}{KA}$
- Q = relaxation factor used during the solution of the non-linear equations
- S = molar concentration of ammonium nitrate
- t = time variable
- V_m = total volume of mixer
- V_{sm} = fictitious volume of mixing flow regime in settler
- V_{st} = fictitious volume of plug flow regime in settler + volume of tube interconnections between stages
- x = molar concentration of a solute in aqueous phase
- y = molar concentration of a solute in organic phase
- \bar{y} = molar concentration of a solute in organic phase at the phase boundary
- Z = total mass (equation 10)
- ϵ_A = relative amount of aqueous phase bypassing the mixer
- ϵ_O = relative amount of organic phase bypassing the mixer
- ϕ = correction factor used in equation (1)
- τ_x = transport delay of aqueous phase between stages
- τ_y = transport delay of organic phase between stages
- τ_{xm} = mixing time constant in aqueous phase
- τ_{ym} = mixing time constant in organic phase

ACKNOWLEDGEMENT

Special thanks are due to Mr. K.O. Solberg in the Physics Department at Institut for Atomenergi for his suggestions and advice on calculation methods for digital computation.

REFERENCES

1. Sebenik, R.F., Sharp, B.M., Smutz, M: Separation Science, 1966, 1, 375.
2. Olander, D.R.,: Ind. Eng. Chem., 1961, 53, 1.
3. Thiele, E.W.,: Geddes, R.L.,: Ind. Eng. Chem., 1933, 25, 289
4. Wang, B., : Private communication, 1969
5. Frøberg, C.E.,: Introduction to Numerical Analysis, 1965. English Edition, 35.
6. Lance, G.N.,: Numerical Methods for High Speed Computer, 1960 (London)

LEGENDS AND CAPTIONS OF FIGURES

- Fig.1. Flow sheet
Fig.2. Yttrium concentrations
Fig.3. Erbium concentrations in aqueous phase
Fig.4. Yttrium concentrations at stage no.8.
Fig.5. Yttrium concentrations at stage no.28

2647

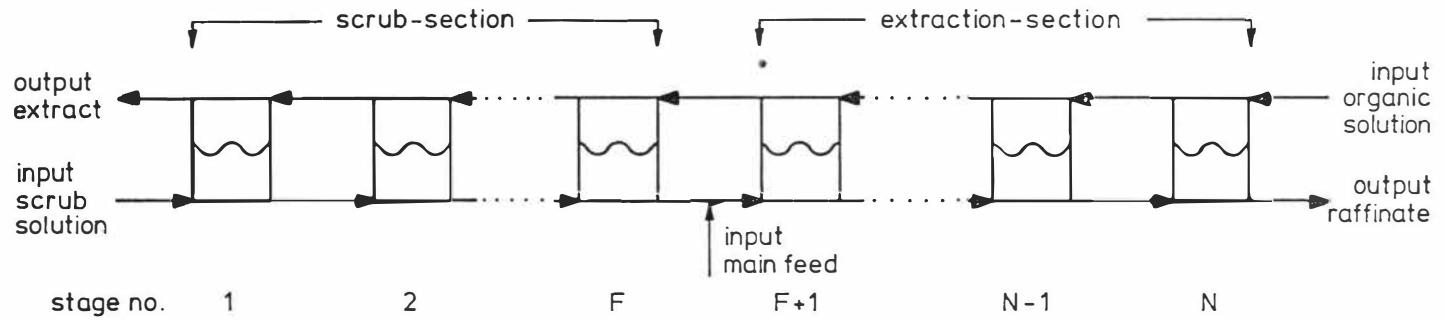


FIGURE 1.
FLOW SHEET

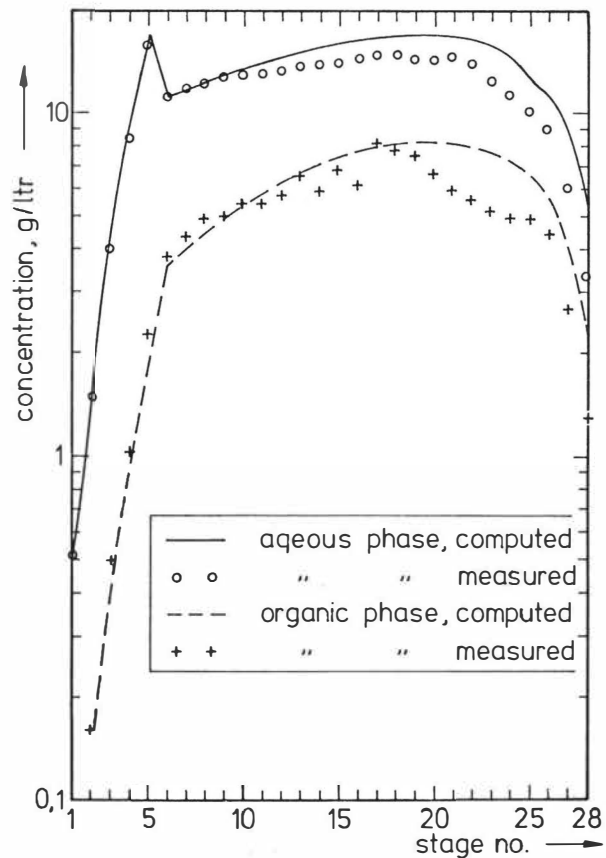


FIGURE 2
YTTRIUM CONCENTRATIONS

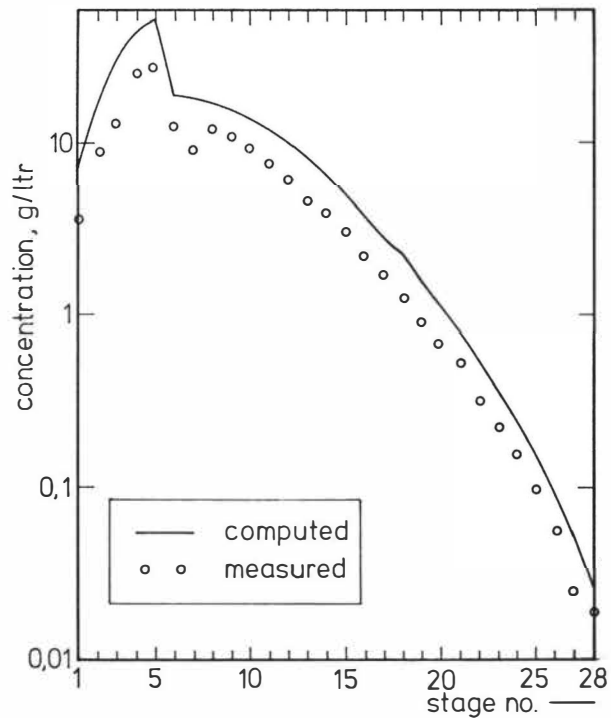


FIGURE 3
ERBIUM CONCENTRATIONS IN AQUEOUS PHASE

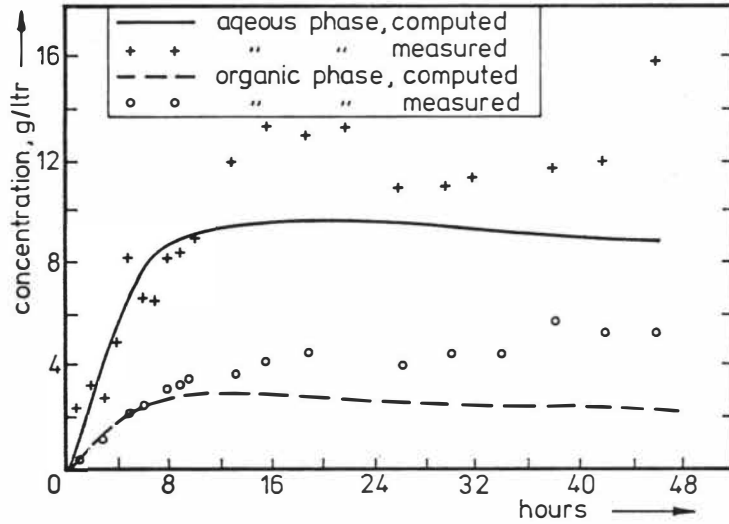


FIGURE 4
YTTRIUM CONCENTRATIONS AT STAGE NO. 8

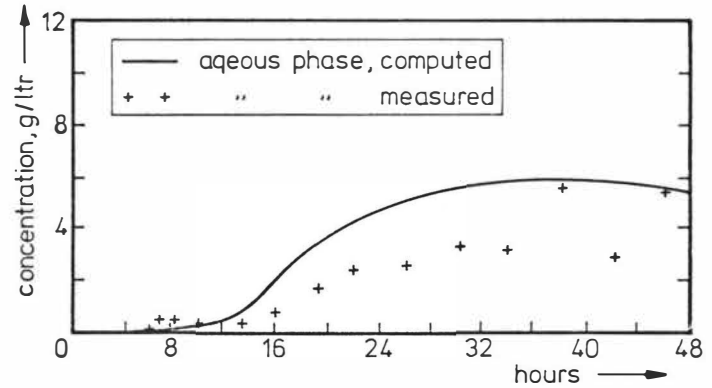
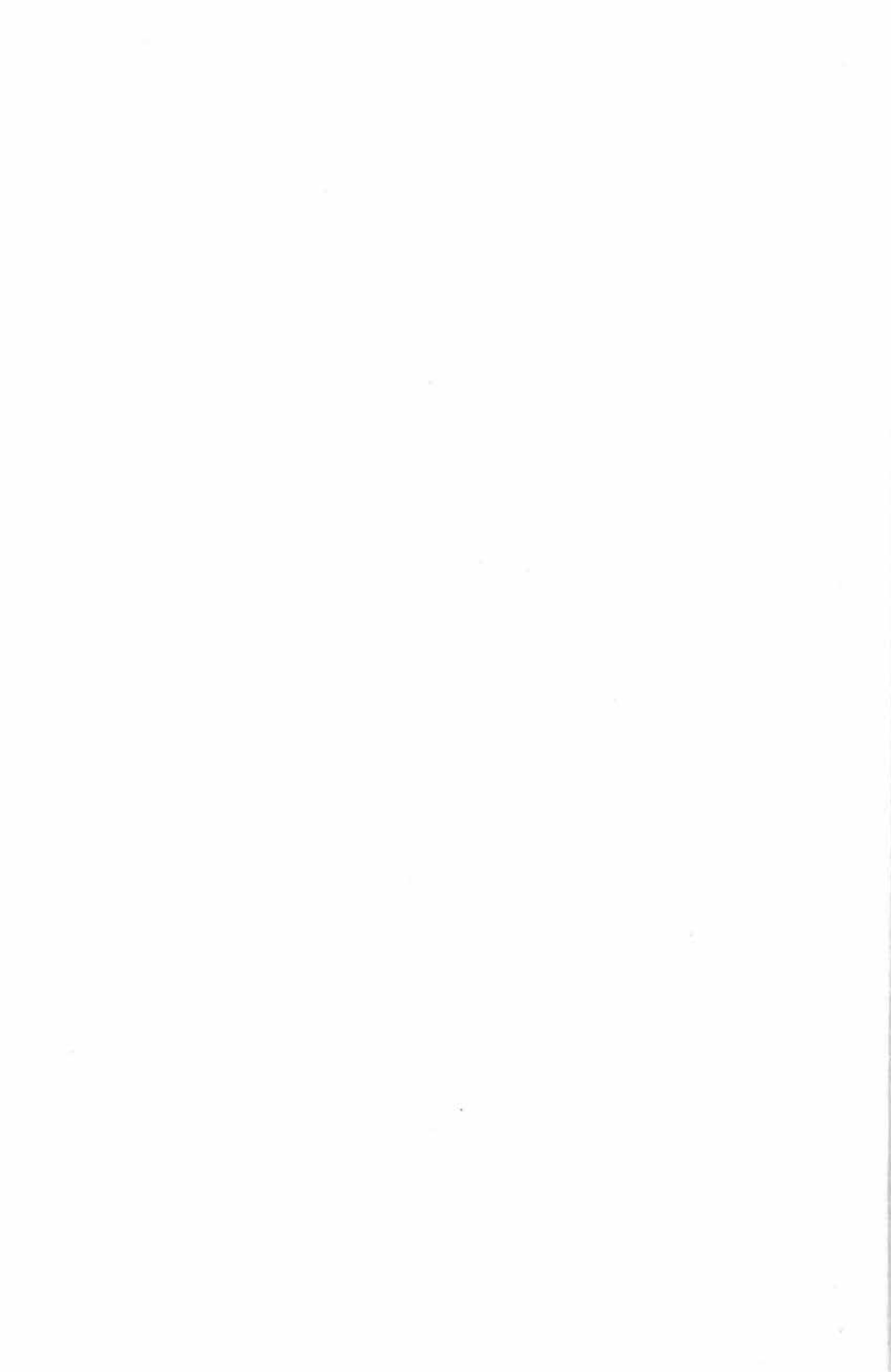


FIGURE 5
YTTRIUM CONCENTRATIONS AT STAGE NO. 28



L. Boyadzhiev

G. Angelov

ABSTRACT

A mathematical model and a method for computation of a multi-stage multicomponent extraction process, is proposed. The model deals with the general case, when fractions of the two phases are flowing backwards and the equilibrium dependence is an arbitrary function of the concentration of all components. The model and the computational method are limited by the restriction, that equilibrium in all stages is attained.

Bulgarian Academy of Sciences
Central Laboratory of Chemical Engineering
Sofia 13, Bulgaria

INTRODUCTION

The investigations on the backmixing in multistage counter-current extraction units have shown its considerable influence on the column performance. Several mathematical models and procedures have been prepared for the calculation of multistage extraction processes, taking into account the effect of backmixing¹⁻⁸. All of them deal with three component systems with only one component distributed between two phases. Multicomponent extraction is a process of great practical importance, but it has received less attention due to its complexity and the lack of equilibrium data.

In the present work a mathematical model and a method for computation of a multistage multicomponent extraction process, considering backmixing in both phases, is proposed:

Mathematical model

A scheme of a multistage countercurrent extraction cascade of NS perfectly mixed stages is shown on Fig.1. It is known¹⁵ that at these conditions the longitudinal and backmixing are practically identical. Each phase, flowing through the stages, takes away a fraction of the other phase and so E_{Bj} and R_{Bj} may be considered as flows, moving backwards to the main flows of the light (E_j) and heavy (R_j) phases. The rate of backmixing from the j -th to $(j-1)$ -th stage for the heavy phase can be expressed by^{5,6}.

$$r_j = R_{Bj}/R_j \quad (1)$$

and analogously for the light phase

$$e_j = E_{Bj}/E_j \quad (2)$$

The model assumes feed and production flows of each phase at all stages, providing to organise recirculation schemes, if necessary.

It is assumed too, that the stages are perfectly mixed and phase equilibrium is attained, so that

$$Y_{i,j} = k_{i,j} \cdot X_{i,j} \quad (3)$$

The concentration of the components is expressed as molar fractions (mol/mol) and may be written as:-

$$(4)$$

$$(5)$$

For each stage the balance of entering and leaving flows is

$$R_{j-1} + FY_j + FX_j + e_{j-1} \cdot E_{j-1} + r_{j+1} \cdot R_{j+1} + E_{j+1} = (6)$$

$$= R_j \cdot (1+r_j) + E_j(1+e_j) + PY_j + PX_j$$

and the component material balance is

$$R_{j-1} X_{i,j} + FY_j \cdot Y_{i,j} + FX_j \cdot X_{i,j} + e_{j-1} E_{j-1} Y_{i,j-1} + \\ + r_{j+1} R_{j+1} X_{i,j+1} + E_{j+1} Y_{j+4} = \quad (7)$$

$$= R_j(1+r_j) \cdot X_{i,j} + E_j(1+e_j) \cdot Y_{i,j} + PY_j + PX_j \cdot X_{i,j}$$

To make the computational procedure easier, the flows R_{NS+1} and E_{NS+1} are assumed to be equal to zero. A complete phase separation is presumed to take place at the first and the last stage, so the flows E_1 and R_{NS} , leaving the end stages, do not take away any fraction of the other phase. These circumstances change the flow balance equations. For the first stage it is

$$FY_1 + FX_1 + r_2 R_2 + E_2 = R_1 + E_1(1+e_1) + PY_1 + PX_1 \quad (8)$$

and for NS-stage

$$R_{NS-1} + FY_{NS} + FY_{NS} + E_{NS-1} \cdot E_{NS-1} = \quad (9)$$

$$= PX_{NS} + PY_{NS} + E_{NS} + R_{NS} \cdot (1+r_{NS})$$

The component material balance is for the first stage

$$FY_1 \cdot Y_{i,1} + FX_1 \cdot XF_{i,1} + r_2 \cdot R_2 \cdot X_{i,2} + E_2 \cdot Y_{i,2} = \quad (10)$$

$$= R_1 \cdot X_{i,1} + E_1 \cdot (1+e_1) \cdot Y_{i,1} + PY_1 \cdot Y_{i,1} + PX_1 \cdot X_{i,1}$$

and for the NS-stage

$$R_{NS-1} \cdot X_{i,NS-1} + FY_{NS} \cdot Y_{i,NS} + FX_{NS} \cdot XF_{i,NS} +$$

$$+ e_{NS-1} \cdot E_{NS-1} \cdot Y_{i,NS-1} = \quad (11)$$

$$= PX_{NS} \cdot X_{i,NS} + PY_{NS} \cdot Y_{i,NS} + E_{NS} \cdot Y_{i,NS} + R_{NS} \cdot (1+r_{NS}) \cdot X_{i,NS}$$

Computational procedure

Equations (1-11) may be evaluated to obtain the concentration profiles of each component ($X_{i,j}; Y_{i,j}$) and the interstage flows (R_j and E_j) through the stages of the cascade. An iteration method, developed earlier¹³ is used to compute these values. The procedure¹³ is modified to fit the requirements of the present model.

The computational procedure is:

1. The feed ($FX_j; FY_j$) and production ($PX_j; PY_j$) flowrates, the known feed concentrations ($XF_{i,j}; YF_{i,j}$), the backmixing factors ($r_j; e_j$) and the initial iterate values for the concentrations ($X_{i,j}; Y_{i,j}$) and the internal flowrates (R_j and E_j) are set.
2. The distribution coefficient $k_{i,j}$ is computed using the initial iterate values for the concentrations ($X_{i,j}; Y_{i,j}$).
3. From equations (1), (2), (3), (6) and (7) one obtains

$$X_{i,j} = BX_{i,j} / k_{i,j} \cdot B_j + (1 - k_{i,j}) \cdot R_j \cdot (1 + r_j) + PX_j \quad (12)$$

where

$$BX_{i,j} = R_{j-1} \cdot X_{i,j-1} + FY_j \cdot YF_{i,j} + FX_j \cdot XF_{i,j} + e_{j-1} \cdot E_{j-1} \cdot Y_{i,j-1} + \quad (13)$$

$$+ r_{j-1} \cdot R_{j-1} \cdot X_{i,j+1} + E_{j+1} \cdot Y_{i,j+1}$$

$$B_j = R_{j-1} + FY_j + FX_j + e_{j-1} \cdot E_{j-1} + r_{j+1} \cdot R_{j+1} + E_{j+1} \quad (14)$$

$i = 1, 2, \dots, NC$

$j = 2, 3, \dots, NS-1$

For the first and the last stage according to equations (8) - (11) the terms $BX_{i,j}$ and B_j are

$$BX_{i,1} = FY_1 \cdot YF_{i,1} + FX_1 \cdot XF_{i,1} + r_2 \cdot R_2 \cdot X_{i,2} + E_2 \cdot Y_{i,2} \quad (15)$$

$$B_1 = FY_1 + FX_1 + r_2 \cdot R_2 + E_2 \quad (16)$$

$$BX_{i,NS} = R_{NS-1} \cdot X_{i,NS-1} + FY_{NS} \cdot YF_{i,NS} + FX_{NS} \cdot XF_{i,NS} + \quad (17)$$

$$+ e_{NS-1} \cdot E_{NS-1} \cdot Y_{i,NS+1}$$

$$B_{NS} = R_{NS-1} + FY_{NS} + FX_{NS} + E_{NS-1} \cdot e_{NS-1} \quad (18)$$

where $i = 1, 2, \dots, NC$

The concentrations $X_{i,j}$ for the odd numbered stages are obtained from eq. (12), using initial assumptions for the even stages. A check, if the condition (4) is fulfilled is carried out. If not, the values of R_j in (12) are varied according to a trial and error procedure and the concentrations $X_{i,j}$ are recalculated till the condition (4) is attained.

4. The concentrations $Y_{i,j}$ for the odd stages are obtained from equilibrium equations (3).

5. The flowrates E_j for the odd stages are computed from eq (6).

6. The operations from point 3 to point 5 are repeated for the even stages using the just obtained values of $X_{i,j}$; $Y_{i,j}$; E_j and R_j for the odd stages.

The computational procedure is reiterated from point 2 to point 6 till a negligible difference between two consequently computed concentration values of each component is reached.

The expression

$$\left| \frac{X_{ij}^{(n)} - X_{ij}^{(n-1)}}{X_{ij}^{(n)}} \right| \leq \epsilon \quad (19)$$

where n is number of iterations, must be satisfied for convergence of the iteration procedure. ϵ ranges are usually taken from 10^{-3} to 10^{-6} .

The proposed model and the computational procedure are illustrated by the following example, which shows the influence of backmixing on the efficiency of the counter-current extraction process.

Example*: Acetone-ethanol mixture (molar ratio 1:1) is to be separated by means of two solvents: chloroform (heavy phase) and water (light phase). The separation is to take place in a 15-stage extraction cascade.

The number of components is four

1. Acetone
2. Ethanol
3. Chloroform
4. Water

The concentration of light and heavy phases leaving the apparatus, the concentration distribution and internal flowrates through the stages are to be computed.

Stage	Flowrate		Composition			
1	$FX_1=80$	$XF_{1,1}=0.0$	$XF_{2,1}=0.0$	$XF_{3,1}=1.0$	$XF_{4,1}=0.0$	
6	$FX_6=20$	$XF_{1,6}=0.5$	$XF_{2,6}=0.5$	$XF_{3,6}=0.0$	$XF_{4,6}=0.0$	
15	$FY_{15}=100$	$YF_{1,15}=0.0$	$YF_{2,15}=0.0$	$YF_{3,15}=0.0$	$YF_{4,15}=1.0$	

Initial assumptions

$$R_j = FX_1 \quad E_j = FY_{15} \quad X_{i,j} = XF_{i,1} \quad Y_{i,j} = YF_{i,15}$$

$$i = 1, 2, \dots, NC$$

$$j = 1, 2, \dots, NS$$

* This example is from references^{11,14}

To obtain equilibrium data the margules equation is used¹⁴:

$$\begin{aligned} \ln \gamma_{ij} = & 2C_{ij} \sum_{k=1}^{NC} C_{kj} \cdot A_{k,i} + \sum_{k=1}^{NC} C_{k,1}^2 A_{L,K} + \\ & + \sum_{k=1}^{NC} \sum_{l=1}^{NC} C_{kj} \cdot C_{lj} \cdot AS_{L,R,1} - 2 \sum_{L=1}^{NC} C_{L,1}^2 \sum_{K=1}^{NC} C_{kj} \cdot A_{L,K} - \\ & R \neq i; l \neq i; R < 1 \quad (20) \\ & - 2 \sum_{L=1}^{NC} \sum_{K=2}^{NC} \sum_{J=3}^{NC} C_{L,J} \cdot C_{K,J} \cdot C_{T,U} \cdot AS_{L,R,1} \end{aligned}$$

where $k \neq l; l \neq i; k < l$

$$AS_{L,R,1} = (A_{L,K} + A_{K,1} + A_{i,l} + A_{L,i} + A_{K,l} + A_{L,K})/2 \quad (21)$$

Equation (20) gives the activity coefficient γ_{ij} of the component i in a mixture of NC components. It gives the activity coefficients in the heavy ($\gamma_{ij}^{(R)}$) and light ($\gamma_{ij}^{(E)}$) phases and hence the values of $\gamma_{ij}^{(R)} / \gamma_{ij}^{(E)}$

The values of the constants A are those used in references
14 For the present system

$A_{11} = 0.0$	$A_{12} = 0.5446$	$A_{13} = -0.9417$	$A_{14} = 1.872$
$A_{21} = 0.599$	$A_{22} = 0.0$	$A_{23} = 1.61$	$A_{24} = 1.46$
$A_{31} = 0.674$	$A_{32} = 0.501$	$A_{33} = 0.0$	$A_{34} = 5.9$
$A_{41} = 1,338$	$A_{42} = 0.877$	$A_{43} = 4.76$	$A_{44} = 0.0$

To simplify the computation in the example, the backmixing factors are assumed to be constant through the stages. But the model and the procedure allow arbitrary chosen values of the factors r_j and e_j . Similarly, the computation of equilibrium data from the Margules equation may be easily replaced by any other useful correlation.

The changes of the internal flowrates of the heavy phase and the concentration of its components through the stages are given in fig.2. Analogous data for the light phase are given in fig.3. These results are obtained without backmixing ($e_j = r_j = 0$) for the purpose of comparison with other computational methods^{11,14}, which do not take into account the backmixing effect. The good agreement with these rigorous methods and the simplicity of the proposed method¹³ allow it to be considered as very useful and applicable to multicomponent computations.

The influence of the backmixing in the heavy phase (r_j) on the component 1 (acetone) concentration in the same phase is shown in fig.4. The tendency for the concentration smoothing throughout the stages as the backmixing factor increases, is evident. Taking into account, that acetone is fed into stage 6 and it is soluble mainly in the heavy phase flowing down, it is evident, that increase in acetone concentration in stages 1 to 6 due to backmixing, reduced the apparatus efficiency. This conclusion is confirmed by fig.5, which shows the effect of acetone concentration in the light phase outlet on the rise of the backmixing factors. In this case, the influence of the backmixing in the heavy phase (curve 1 on fig.5) is greater than those in the light phase (curve 2).

Conclusion

The proposed model and computational method predicts the concentration profile and the internal flowrates through the stages of a multistage cascade in the case of multicomponent liquid-liquid extraction. The model deals with the general case, when fractions of the two phases are flowing backwards and the equilibrium dependence is an arbitrary function of the concentrations of all components. The model and the procedure are limited by the restriction, that equilibrium in all stages is reached. But nevertheless the results obtained are in agreement with the basic concept of the backmixing influence on the process efficiency.

Symbols Used:

A	constants in eq. (20)
AS	defined by eq. (21)
B	defined by eq. (14)
BX	defined by eq. (13)
C	concentrations in eq. (20), mole fractions
E	light phase main flow, mol/s
e	light phase backmixing factor, dimensionless
E _B	light phase back flow, mol/s
FX	light phase feed flow, mol/s
FY	heavy phase flow, mol/s
k	distribution coefficient, dimensionless
NC	number of components
NS	number of stages
PX	light phase production flow, mol/s
PY	heavy phase production flow, mol/s
R	heavy phase main flow, mol/s
r	heavy phase backmixing factor, dimensionless
R _B	heavy phase back flow, mol/s
X	light phase concentration, mole fractions
XF	light phase feed concentration, mole fraction
XP	light phase production flow concentration, mole fractions
Y	heavy phase concentration, mole fractions
YF	heavy phase feed flow concentration, mole fractions
YP	heavy phase production flow concentration, mole fractions

Greek letters

γ	activity coefficient, dimensionless
ϵ	criterion for stopping of iterations

Subscripts

i component number
j stage number
k,1 subscripts in eq. (20)

Superscripts

E refers to the light phase
n iteration number
R refers to the heavy phase

R E F E R E N C E

1. Joung E.F., Chem. Eng., 1957, 64, 241
2. Miyauchi Th., Vermeulen T., Ind.Eng.Chem.(Fund),1963,2,304
3. Sleicher C.A., A.I.Ch.E.Journ., 1960, 6, 529
4. Hartland S., Mecklenburgh J.C., Chem.Eng.Sci.,1966, 21, 1209
5. Prochazka J., Landau J., Coll.Czech.Chem.Comm., 1963, 28,1927
6. McSwain C.V., Durbin L.D., Separ.Sci., 1966, 1, 677
7. Prochazka J., Landau J., Chem.Proc.Eng., 1967, 48, 51
8. Mecklenburgh J.C., Hartland S., Canad.J.Chem.Eng., 1969, 47, 453
9. Scheibel E.G., Petrol Ref., 1959, 38, 227
10. Smith B.D., Brinkley W.K., A.I.Ch.E.Journ., 1960, 6, 451
11. Hanson D.N., Duffin J.H., Somerville G.F., "Computation of multistage separation processes", 1962, N.Y. Reinhold Pb.
12. Roche E.C., Brit.Chem.Eng., 1971, 16, 821
13. Boyadzhiev L., Compt.rend.Acad.bulg.Sci., 1973, 26, 399
14. Roche E.C., D.S . Thesis, New Jersey, Stevens Inst.Technology 1966
15. Hartland S., Mecklenburgh J.C., Chem.Eng.Sci., 1968, 23, 186

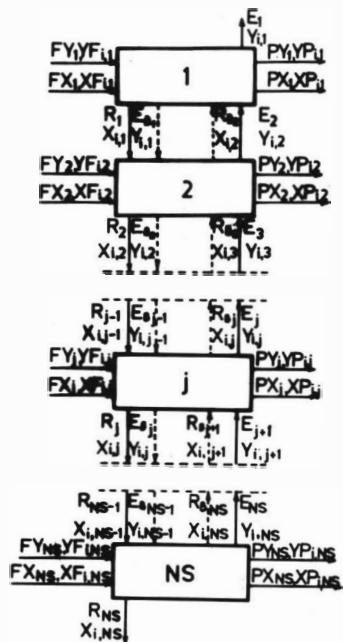


FIG. 1 A scheme of the counter-current extraction cascade

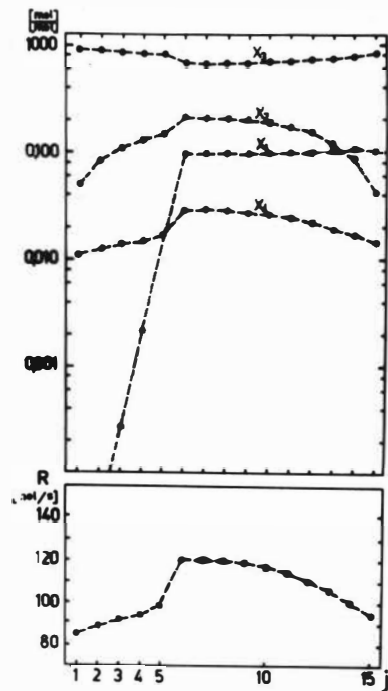


FIG. 2 The change of the internal flowrates of the heavy phase and the concentrations of its components through the stages ($r_j = e_j = 0$).

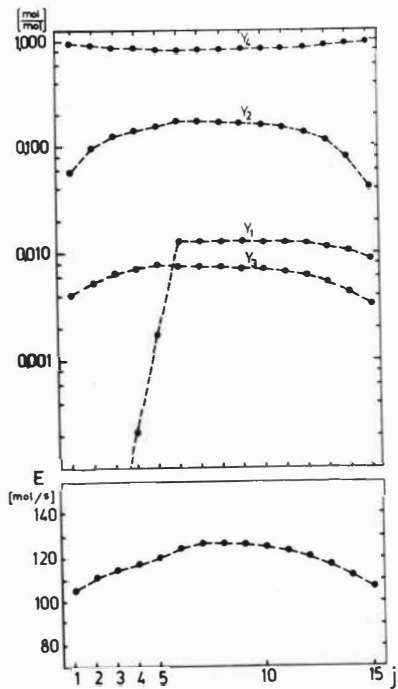


FIG. 3 The change of the internal flowrates of the light phase and the concentrations of its components through the stages ($r_j = e_j = 0$).

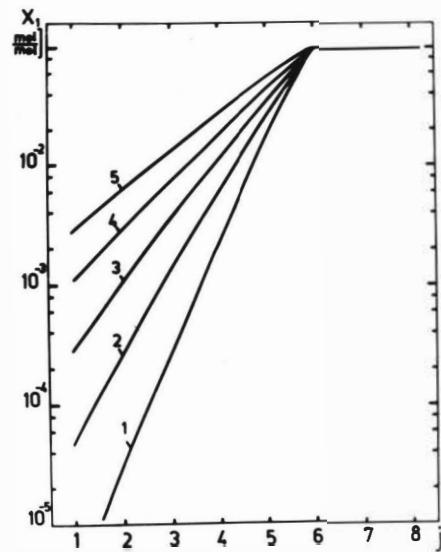


FIG. 4 The influence of the backmixing in the heavy phase (r_j) on the component 1 (acetone) concentration in the same phase ($e_j = \text{const} = 0$)

- | | |
|-----------------|-----------------|
| 1 - $r_j = 0$ | 4 - $r_j = 0.3$ |
| 2 - $r_j = 0.1$ | 5 - $r_j = 0.4$ |
| 3 - $r_j = 0.2$ | |

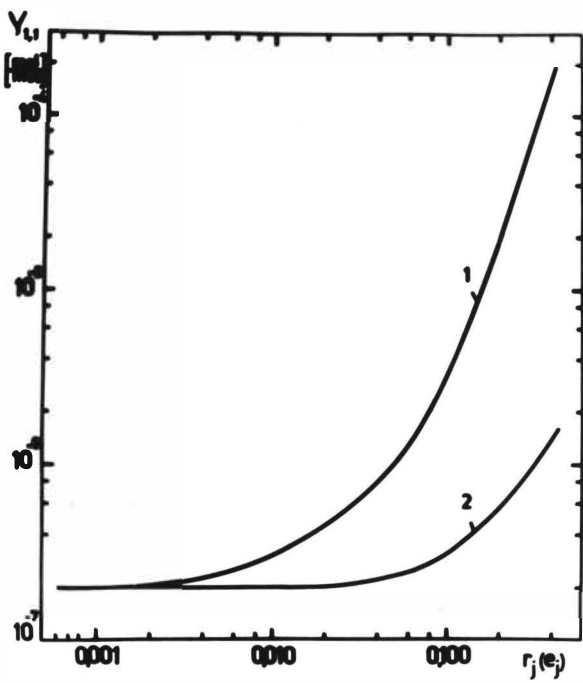


FIG. 5 The influence of backmixing on the component 1 (acetone) concentration in the light phase outlet

$$1 - Y_{1,1} = f(r_j) \quad (e_j = 0)$$

$$2 - Y_{1,1} = f(e_j) \quad (r_j = 0)$$



SCHEME TO THE ON-LINE CONTROL OF A
CONTINUOUS LIQUID EXTRACTION PROCESS

by R.N. Armfield[†] and J.B. Agnew^{*}

SUMMARY

A multidimensional optimization scheme using a search technique is described for determining the minimum of a response surface which is subject to random error and is non-stationary. The scheme is applied to a liquid extraction process in a laboratory-scale rotating disc contactor, using the system acetic acid - amyl alcohol - water. The scheme is shown to be superior to other schemes in its ability to find the optimum in a noisy environment, but is less effective once the optimum is reached.

* Department of Chemical Engineering, Monash University, Clayton, 3168, Victoria.

† Present Address: I.C.I. (Australia) Ltd., 1 Nicholson Street, Melbourne, Victoria.

INTRODUCTION

As most process systems are highly complex, they are rarely amenable to complete mathematical modelling, so that search techniques become the only feasible means by which optimum operating conditions can be determined. Search schemes have the advantage of being able to cope with the effects of unknown and unpredictable factors on system behaviour. They are also capable of adaptation as the optimum is approached.

Although numerous papers have been published on the optimisation of mathematical functions, there are not many reports in the literature on the application of optimisation techniques to process systems. Price and Rippin ⁽¹⁾ tested a sinusoidal perturbation method for simultaneous two-variable optimisation of a water-gas shift reactor. Their technique measured the gradient of the response surface in two directions by applying a small sinusoidal perturbation and then applied a gradient-dependent step; no comparison with other methods was reported. A two-pass Oxo synthesis process was studied by O'Grady and Robertson ⁽²⁾ using an optimisation scheme developed by Hooke and Jeeves ⁽³⁾. Wheeler and Aris ⁽⁴⁾ used a "questing controller" to find the optimum operating condition for a small-scale fermentation process; of the various search methods investigated, the sinusoidal perturbation and quadratic methods were found to be most successful. Terano and Tsukamoto ⁽⁵⁾ used a gradient method, with evolutionary operation for the gradient determination, to optimise the performance of a steam boiler. Numerous other authors have reported on the use of the evolutionary operations (EVOP) technique ^(6,7,8,9). It is probably the most widely used method at the present time, having the added advantage of being useful even when no on-line computer is available.

This paper is concerned with an experimental investigation of a new quadratically-dependent search technique which was developed for multivariable stochastic situations.

SEARCH TECHNIQUES

To determine the optimum operating conditions a search plan is required. This must account for both the multidimensionality and the stochastic nature of real processes if it is to be successful.

A search technique involves a sequence of experiments, the results of which are used to estimate parameters in the following Taylor's series expansion (or its discrete analogue) for the *objective function* (C) about the point \bar{x}_0 in terms of the n manipulated variables (x_1, x_2, \dots, x_n) :

$$C = C_0 + \sum_{i=0}^n \frac{\partial C}{\partial x_i} (x_i - x_{0i}) + \frac{1}{2} \sum_{i=0}^n \sum_{j=0}^n \frac{\partial^2 C}{\partial x_i \partial x_j} (x_i - x_{0i})(x_j - x_{0j}) \dots (1)$$

Optimisation techniques require the evaluation of (i) the objective function alone, (ii) the objective function and its first derivatives, or (iii) the objective function and its first and second derivatives. The results of such evaluation and re-evaluations are used to guide the search. The search itself is considered in three parts :

- (i) the *opening gambit*, which involves the selection of the starting point
- (ii) the *middle game*, in which the object is to move towards the optimum as quickly as possible
- (iii) the *end game*, in which further experiments are carried out to ensure that the point reached is the true optimum.

An important problem which occurs in dealing with real processes is the presence of random error in the measured variables. Stochastic approximation procedures deal with random error as noise superimposed on a deterministic process. Foremost among these is the basic Kiefer-Wolfowitz procedure ⁽¹⁰⁾, which has since been modified by several other workers in the field to give variable size of step.

In an earlier investigation at Monash University, Murtagh ⁽¹¹⁾ developed a univariable stochastic optimisation scheme based on the fitting of a parabola by a least-squares procedure to the response surface, with weighting of the observations in a geometric sequence based on the age of the observation. Most of the search occurred in the end-game, where the quadratic estimation was used to give the direction of the search but not the magnitude of the step, which was fixed.

Extension of Murtagh's basic algorithm to a multidimensional system has been carried out by Armfield ⁽¹²⁾.

The relationship between the objective (cost) function and n manipulated variables is assumed to be of quadratic form :

$$C = C_0 + \underline{x}^T \underline{a} + \frac{1}{2} \underline{x}^T \underline{H} \underline{x} \dots (2)$$

where : \underline{x} is the vector of the n independent manipulated variables

\underline{a} is the vector of coefficients of the linear terms

\underline{H} is the Hessian matrix

If \underline{H} is positive definite, the minimum of the objective function is obtained for :

$$\underline{x}_{\min} = -\underline{H}^{-1} \underline{a} \quad \dots(3)$$

To obtain this estimate of the minimum, the elements of \underline{H} and \underline{a} must first be evaluated. This can be done by expressing equation 2 in an alternative linear form :

$$C = \underline{z}^T \underline{b} \quad \dots(4)$$

in which the elements of \underline{z} are obtained from the elements of \underline{x} , while the elements of \underline{b} are obtained from the elements of \underline{a} and \underline{H} and the value C_0 . Using this linear form, the weighted sum of squares (S) of the deviations of the predicted cost (C) and the actually observed cost (C^*) is represented by the quadratic expression, for m observations :

$$S_m = (\underline{Z}\underline{b} - \underline{C}^*)^T_m W_m (\underline{Z}\underline{b} - \underline{C}^*)_m \quad \dots(5)$$

where W_m is the weighting matrix (to be specified) and

$$\underline{Z}_m^T = (z_1, z_2, \dots, z_m)$$

$$\underline{C}_m^{*T} = (C_1^*, C_2^*, \dots, C_m^*)$$

The minimum value of S is found by standard means ⁽¹³⁾ to occur for :

$$\underline{b}_m = (\underline{Z}^T \underline{W} \underline{Z})_m^{-1} (\underline{Z}^T \underline{W} \underline{C}^*)_m \quad \dots(6)$$

The weighting matrix is taken as a diagonal matrix with diagonal elements given by :

$$W_{ii} = \begin{cases} W^{m-t-i+1} & \text{for } i \leq m-t \\ 1 & \text{for } (m-t) < i < m \end{cases} \quad \dots(7)$$

where t is the number of elements in \underline{z} , i.e. the least number of observations required to solve equation 4 without a degenerate solution.

OUTLINE OF PROPOSED SEARCH TECHNIQUE

The *opening gambit*, which initiates the main part of the algorithm, consists of t experiments carried out at a series of points to cover the search space broadly so that the coefficients \underline{b} in equation 4 can be determined. The following method is used to specify the points :

- (i) commence at some arbitrary starting point : independent variables at their initial values;
- (ii) increment each independent variable in turn by an amount Δ , until all variables have been so incremented;

- (iii) first variable is incremented a further amount Δ ; subsequent variables are set back to initial values, and are then incremented in turn by Δ until all have been so incremented.
- (iv) second variable is incremented a further amount Δ ; subsequent variables are set back to initial values, and are then incremented in turn by Δ until all have been so incremented;
- (v) continue with higher variables as in (iii) and (iv) until all variables have been incremented 2Δ above their initial values.

Once the first quadratic has been found, the *middle game* is used to obtain the next prediction of the optimum using the quadratic obtained in the opening gambit. After moving to this point the regression coefficients are updated using a recursive procedure in which the weighting coefficients do not form a pure geometric sequence; instead, those most recent observations necessary to fit the quadratic are given unit weight, while the remaining observations are weighted geometrically with respect to age. The elements of \underline{a} and \underline{H} are determined from \underline{b} and the position of the new optimum is determined using equation 3. If a minimum is unobtainable (e.g. quadratic inverted or degenerated), a gradient-dependent step is taken using the following optimum gradient algorithm :

$$\underline{x}_{\min} = \underline{x}_m - \hat{\underline{H}}^{-1} (\underline{a} + \underline{H}\underline{x}_m) \quad \dots (8)$$

where \underline{a} and \underline{H} have the values obtained from the last curve which was successfully fitted and $\hat{\underline{H}}$ is the last positive definite matrix obtained. After predicting the position of the minimum, the actual point at which the next observation is made may be modified depending on the magnitudes of the changes in the independent variables. The step size for each independent variable is constrained by the following criteria :

$$\beta \alpha_m < | \underline{x}_m - \underline{x}_{\min} | < \alpha_m \quad \dots (9a)$$

$$\alpha_{\min} < \alpha_{m,i} < \alpha_{\max} \quad \dots (9b)$$

where α_m and $\beta \alpha_m$ are the constraints and the step size and α_{\min} and α_{\max} are the limits of the constraints.

The *end game* is entered when all the $\alpha_{m,i} \leq \alpha_{\min}$. The procedure followed is based on the EVOP scheme of Spendley et al (14) using a simplex tableau in which the spacing between vertices is α_{\min} . If during the use of the end game a point is predicted such that any of the elements of α_m become larger than α_{\min} , then the middle game is re-entered.

Theoretical evaluation of the scheme has been described elsewhere (12). Application of the technique to an experimental system will now be discussed.

EXPERIMENTAL DETAILS

A liquid extraction process was used for the experimental studies. The process flow diagram is shown in Figure 1.

A rotating disc contactor was constructed following the design of Vermijs and Kramers (15). The basic dimensions of the column were :

Column internal diameter	44.0 mm
Rotor diameter	15.0 mm
Disc diameter	25.5 mm
Compartment height	17.3 mm
Number of compartments	52

The ternary system used consisted of water, amyl alcohol and acetic acid. The solvent, water, was the dispersed phase.

Instruments used to measure solute concentrations were :

- (i) continuous-flow differential refractometer for acetic acid in feed;
- (ii) specific gravity meter, for acetic acid in raffinate;
- (iii) conductivity meter, for acetic acid in extract.

Flow rates were determined from valve stem positions of Honeywell motorized valves in feed, solvent and extract lines. An independent measure of solvent rate was obtained using a hot-wire flow meter. Interface level at the top of the contactor was detected using a proximity meter. Temperatures were measured by thermistors in half-bridge circuits.

The computer used was a general-purpose Ferranti *Sirius* machine with a storage capacity of 7,000 words each of 10 decimal digits. Details of the process interface unit which was specially constructed are given by Murtagh (11); program details are given by Armfield (12). Ten process variables were measured on-line, enabling mass balances to be computed and the interface to be controlled directly.

Experimental runs were carried out for both single-variable optimisation (manipulating solvent rate) and two-variable optimisation (manipulating both solvent and feed rates), with feed concentration held constant at 9 percent by weight acetic acid in amyl alcohol.

Objective Functions

For the single-variable optimisation study, the following objective function was employed with solvent flowrate (V_w) as the manipulated variable; x_c is the acid concentration in the extract :

$$\text{Function 1 : } C = 0.01 V_w^3 - V_w x_c \quad \dots(10)$$

This function is shown plotted in Figure 2. Functions used in the two-variable studies, in terms of solvent flowrate, feed flowrate (V_a) and acid concentration in raffinate (x_r) were :

$$\text{Function 2 : } C = 0.01 V_w^3/V_a + 0.05 V_a^2 - 1.5 V_w x_c \quad \dots(11)$$

$$\text{Function 3 : } C = (V_w - 15.0)^2 + (V_a - 12.5)^2 - k V_w x_c / (V_a x_r) \quad \dots(12)$$

where k was assigned values of 125 (Function 3A) and 12.5 (Function 3B).

These functions are shown in Figures 3-5.

Optimisation Schemes

The following schemes were compared :

Scheme 1 : The proposed method, already described.

Scheme 2 : The gradient-dependent method of Sharp ⁽¹⁶⁾ modified to operate in two dimensional situations by using the gradient from a quadratic approximation.

Scheme 3 : A quadratic method of Murtagh ⁽¹¹⁾ modified for two-dimensional situations by using the quadratic approximation with constant step sizes in both dimensions.

Scheme 4 : The EVOP procedure of Spendley, Hext and Himsworth ⁽¹⁴⁾ based on the simplex design for the test pattern.

RESULTS

Typical paths taken by Scheme 1 for locating the optimum are shown in Figure 2 for the single-variable case and Figures 6 and 7 for the two-variable case. Fifty-three successful runs were made in all.

In order to compare the results from different runs, the following parameters were employed :

- (i) the *optimisation interval* (I), which was the elapsed time between optimisation calculations;
- (ii) the *minimum step size allowable* (S), which was the smallest change in the manipulated variables allowed;

- (iii) the *number of steps* (N) required to reach the optimum;
- (iv) the *total error* (E) involved in reaching the optimum, which was the sum of all the deviations from the true optimum up to the stage when the optimum had been reached;
- (v) the *average deviation* (D) once the optimum had been reached;
- (vi) the *loss factor* before the optimum had been reached (L_1), which was defined by :

$$L_1 = \frac{EI}{N_{th} t_{ss} D_o} \quad \dots(15)$$

where : N_{th} refers to the theoretical minimum number of steps for a quadratic method of optimisation to reach the optimum (i.e. the minimum number of experimental points required to determine the quadratic function, plus one.); t_{ss} is the time required to reach steady state following a step change in flow rate; D_o refers to the deviation existing between the starting point of the search and the position of the true optimum.

- (vii) the *loss factor* after the optimum had been reached (L_2), which was defined by :

$$L_2 = \frac{D}{S} \quad \dots(16)$$

These last two parameters were defined to facilitate comparison of the different optimisation methods for the two different parts of the search.

DISCUSSION

Loss factors for those runs in which the optimum was not constrained are listed in Table 1. The proposed Scheme 1 was superior to the other techniques in its ability to find the optimum operating conditions for each test function used, as indicated by the lower values of L_1 . However, it was not as successful in holding the optimum as Schemes 3 and 4 due to the variability of the step size employed.

Whilst functions 3A and 3B are of similar form, the former was in general a more difficult surface for the different schemes to handle. The proposed scheme once again showed the best performance, indicating that it is less affected by a change in response surface and that it could have an even greater advantage on a more difficult surface.

The effect of variation in initial deviation from the optimum was checked using Function 2. The number of steps required to reach the optimum was significantly lower for the proposed scheme than for Scheme 3. Scheme 4 would not have been expected to perform any better than Scheme 3 because of the similar limitation in variation of step size. The performance of Scheme

2 could not be estimated because it does not allow for variation in step size; its performance might well have been superior to the other methods because it did not permit over-stepping the constrained optimum.

One of the obvious limitations of steady-state search techniques is the large time delay between implementing a change and the final attainment of the new steady-state conditions when the objective function is re-evaluated and further changes are implemented. The actual time necessary for steady-state conditions to be reached following a step change in solvent flow-rate was determined to be 30 minutes. In an effort to speed up the optimisation procedure, the optimisation interval was reduced. The averaged results, shown in Table 2, indicated a lower loss factor prior to attainment of the optimum even when the five-minute interval was used and more steps were required; however, the loss factor after reaching the optimum increased as the time interval was reduced. These effects suggest that an adaptive procedure for setting the optimisation interval could be an improvement. By using a shorter time interval before the optimum had been reached, the first loss factor would be reduced, while a longer interval after this stage would reduce the second loss factor.

The shorter optimisation interval still indicates the gradient of the cost function at the experimental point, provided sufficient time is allowed to establish the correct gradient. Steps then taken move towards the optimum, even though the quadratic approximation may be seriously in error. However, once the region of the optimum is reached the changes in independent variables are small and the dynamic errors become important. Thus to obtain the correct step size, the quadratic approximation has to be good and this necessitates reduction of dynamic error to a minimum.

CONCLUSIONS

The proposed search technique was shown to be superior to three other techniques in its ability to find the optimum operating conditions, employing several different types of objective functions. Once the optimum has been reached, however, the proposed scheme was not as satisfactory at holding the optimum due to the variability of step size employed.

It was found experimentally that the optimisation interval could be reduced considerably below the time required to attain steady-state without affecting the performance of the scheme in finding the optimum.

REFERENCES

1. Price, R. and Rippin, D., Proc. U.K. Aut. Control Convention, Bristol, C21, 1-20 (1967).
2. O'Grady, W. and Robertson, H., I.F.A.C. Congress, London, Paper 32E (1966).
3. Hooke, R. and Jeeves, T., J.A.C.M., 8, 212 (1961).
4. Wheeler, J. and Aris, R., C.E.Sc, 25, 3, 445 (1970).
5. Terans, T. and Tsukamoto, Y. I.F.A.C. Congress, London, Paper 16B (1966).
6. Hunter, W. and Kittrell, J., Technometrics, 8, 3, 389 (1966).
7. Baasel, W., Chem. Eng., 72 14, 147 (1965).
8. Bacon, D., Canad. Min. & Met. Bull., 60, 1178, (1967).
9. Carpenter, B. and Sweeney, H., Chem. Eng., 72, 14, 117 (1965).
10. Kiefer, J. and Wolfowitz, J., Annals of Math. Stat. 23, 462 (1952).
11. Murtagh, R.W., PhD Thesis, Monash University, Australia, (1967).
12. Armfield, R.N., PhD Thesis, Monash University, Australia (1971).
13. Linnick, Y., "Method of Weighted Least Squares", Pergamon (1961).
14. Spendley, W., Hext, G. and Himsforth, F., Technometrics, 4, 441 (1962).
15. Vermijs, H. & Kramers, H., C.E.Sc, 3, 2, 55 (1954).
16. Sharp, A.K., M. Eng. Sc. Thesis, Monash University, Australia, (1965).

TABLE 1 : Average Loss Factors

	L_1	L_2
<u>Cost Function 1:</u>		
Scheme 1	1.0	2.6
Scheme 2	1.7	6.0
Scheme 3	1.2	2.3
<u>Cost Function 3B:</u>		
Scheme 1	0.18	2.2
Scheme 2	0.23	3.5
Scheme 3	0.20	1.4
Scheme 4	0.23	2.0
<u>Cost Function 3A:</u>		
Scheme 1	0.19	2.2
Scheme 2	0.24	-
Scheme 3	0.24	1.5
Scheme 4	0.28	-

TABLE 2 : Effect of Variation of Optimisation Interval in Proposed Scheme 1.

<u>Optimisation Interval</u> (min)	<u>Number of Steps</u> (N)	L_1	L_2
30	6	2.3	1.8
15	6	1.0	2.6
10	6	0.9	2.8
5	9	0.5	4.3

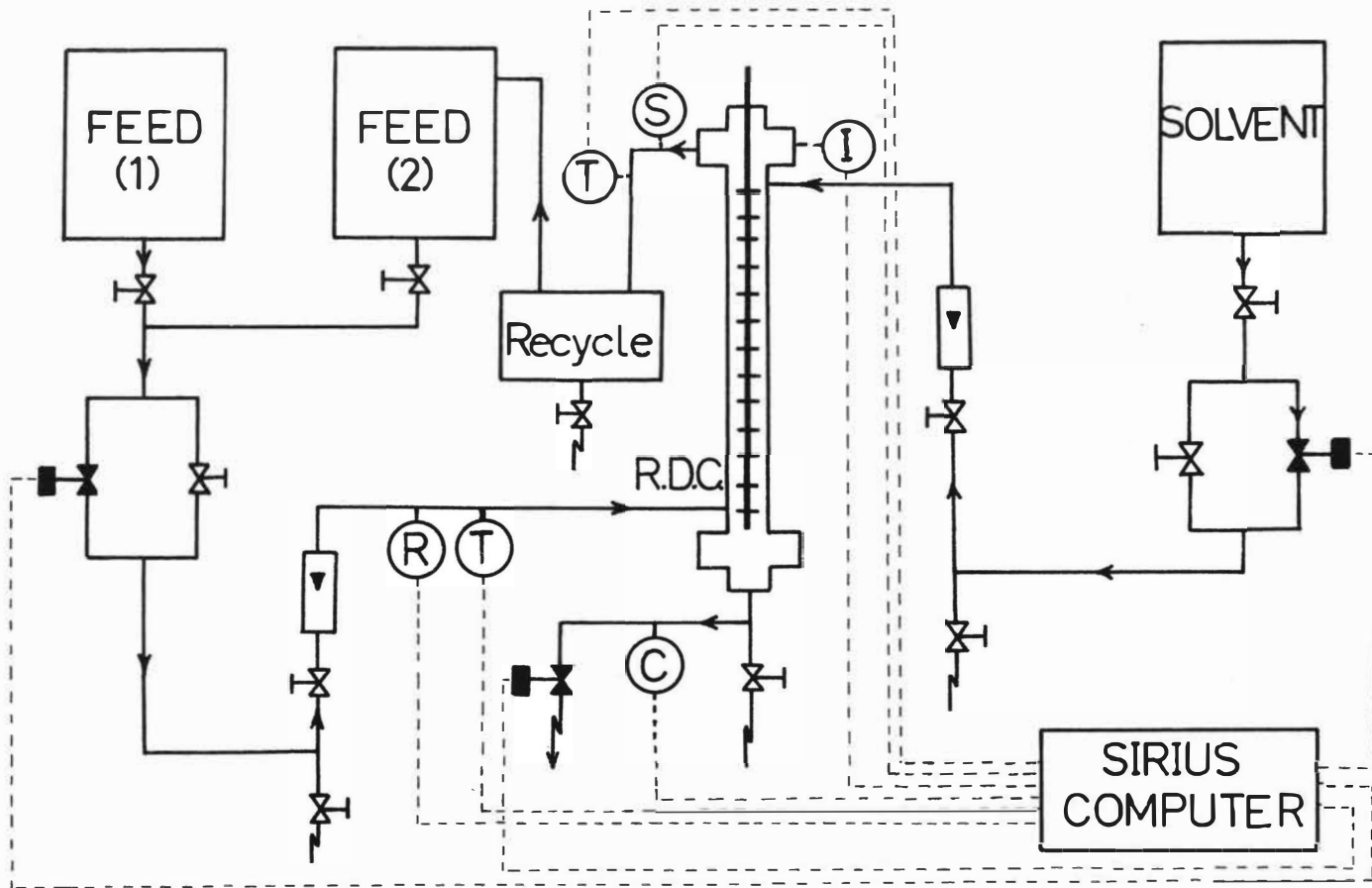


FIGURE 1: FLOW DIAGRAM OF EXPERIMENTAL LIQUID EXTRACTION SYSTEM.

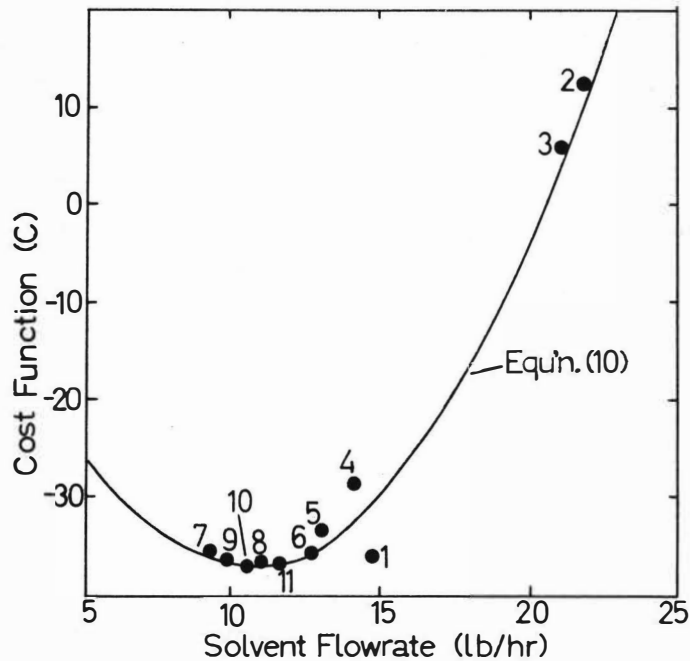


FIGURE 2: SINGLE-VARIABLE SEARCH, SCHEME 1.

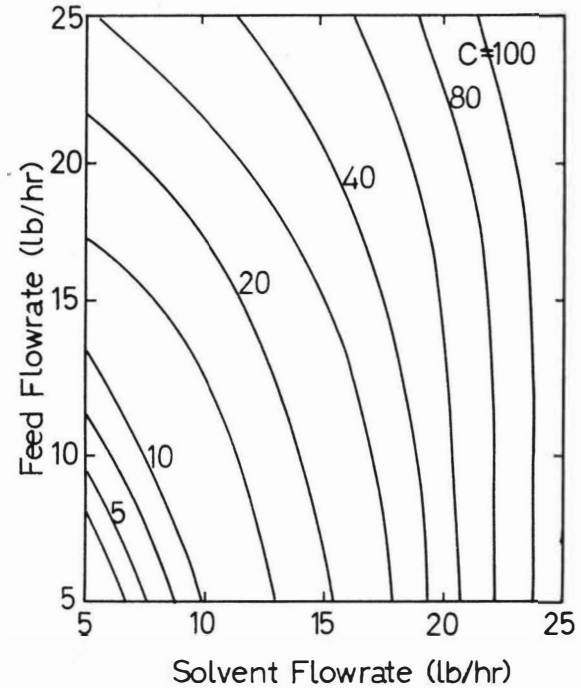


FIGURE 3: CONTOURS FOR OBJECTIVE FUNCTION 2.

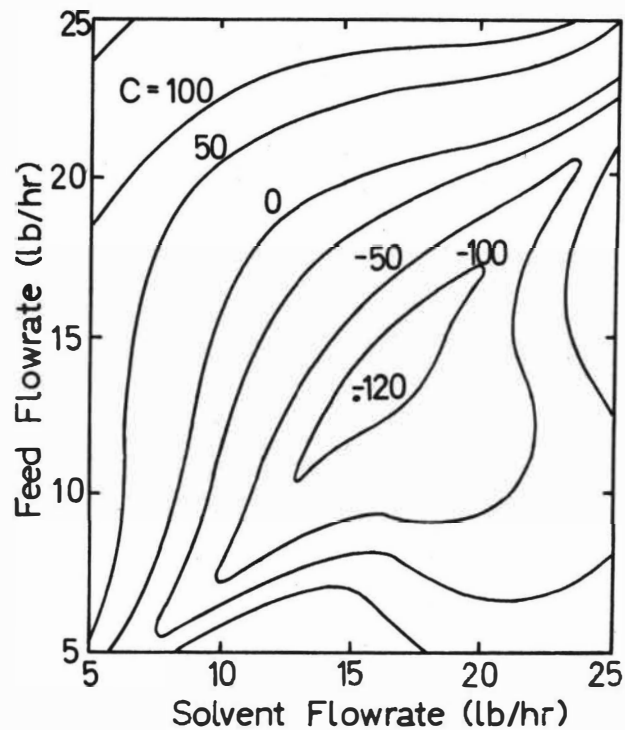


FIGURE 4: CONTOURS FOR OBJECTIVE FUNCTION 3A.

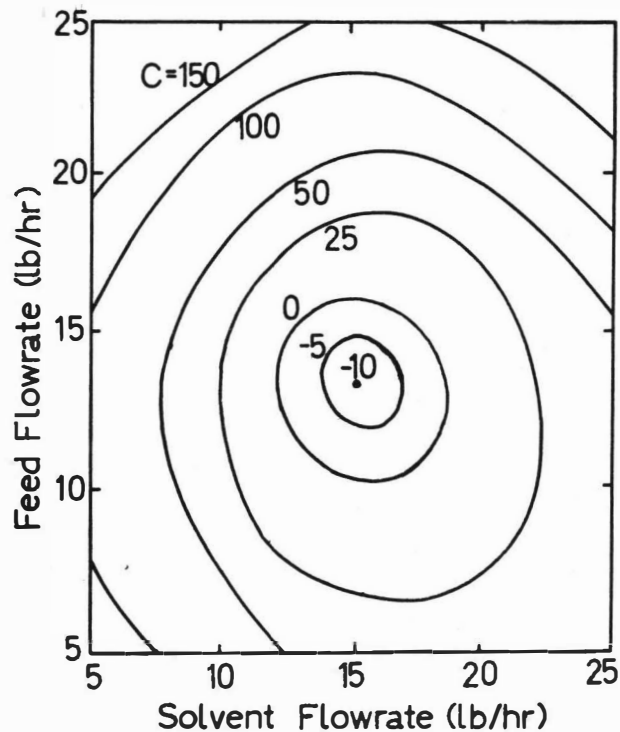


FIGURE 5: CONTOURS FOR OBJECTIVE FUNCTION 3B.

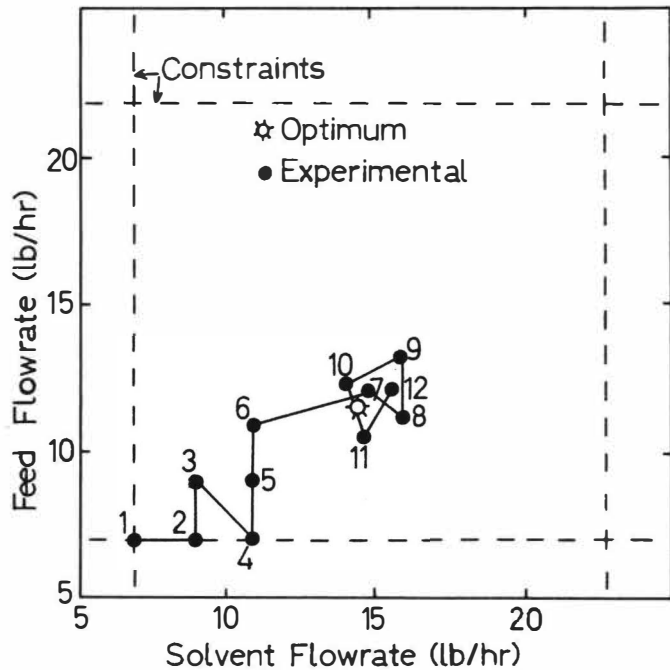


FIGURE 6: TYPICAL PATH TAKEN BY SCHEME 1.

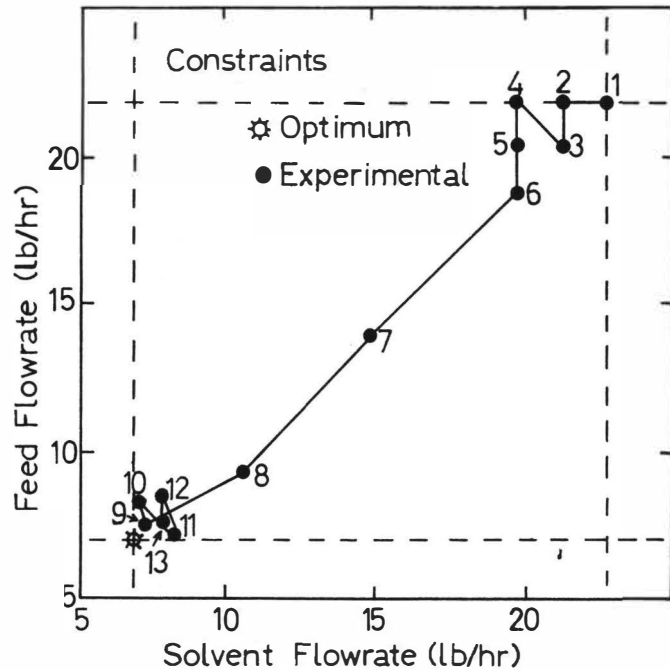


FIGURE 7: TYPICAL PATH TAKEN BY SCHEME 1.

SESSION 26

Friday 13th September: 9.00 hrs

C H E M I S T R Y O F E X T R A C T I O N

(Rare Metals)

Chairman:

Mr. A. Fontaine

Secretaries:

Dr. M.A. Hughes

Mr. A. Bathellier

EXTRACTION OF PLATINUM GROUP METALS FROM

CYANIDE MELTS WITH LIQUID METALS

K.F. Fouché, J.G.V. Lessing and P.A. Brink

Atomic Energy Board, Chemistry Division, Private Bag X256, Pretoria
South Africa

Abstract: *The extraction of the platinum group metals, gold, silver and copper, by liquid bismuth, tin and zinc, and alloys of these elements from molten (Na, K)CN eutectic, was investigated. A separation scheme for rhodium, iridium, ruthenium and osmium, based on the selective extraction into liquid metals and alloys, was also developed and it was shown that the method can be integrated with separation methods where rhodium, iridium and ruthenium are first concentrated in tin or lead buttons. This technique also provides a method for purifying rhodium of iridium impurity with a separation factor of more than 10^3 .*

INTRODUCTION

PRACTICALLY ALL PREVIOUS INVESTIGATIONS dealing with the distribution of solutes between molten salts and liquid metals were confined mainly to systems of interest in the reprocessing of liquid-metal-fueled nuclear reactors¹, molten salt breeder reactors^{2,3} and, to some extent, also liquid-metal-cooled fast breeder reactors⁴. The salt phases in such systems are composed of either chloride or fluoride salts where all platinum group and related elements will be expected to concentrate exclusively in the metal phases. This is due mainly to the unfavourable free energies of formation

of the halide salts of these elements in such systems⁵.

In an experimental survey ¹⁶ of find molten salt systems in which platinum group metals would have comparable affinities for the salt phase and another immiscible phase, it was established that molten alkali cyanide-liquid metal systems may be useful in this respect. Although very little information is available regarding the free energy of formation of platinum group metal cyanide compounds at high temperature, the high stability of such compounds in aqueous systems⁶ suggests that platinum group metals contained in molten cyanide solutions should be stable and would probably not be reduced as readily as from halide melts.

The present investigation was therefore undertaken to establish the viability of molten cyanide-liquid metal extraction systems, and also to find out if such systems could be of any use for separating platinum group and related metals.

EXPERIMENTAL

Apparatus: Extractions were carried out in vessels of the type shown schematically in Fig. 1. The lower portion (200 mm) of the stainless steel tube (62 mm OD, 250 mm long) was inserted in a well-type furnace. The titanium crucible (35 mm OD, 100 mm long), fabricated from titanium rod, had a slightly conical base to facilitate complete removal of the liquid metal phase. A chromel-alumel thermocouple contained in a thin quartz tube was inserted between the crucible and a quartz liner (45 mm ID). The stirrer was constructed by cutting open and flattening the lower portion (75 mm) of a 9 mm OD titanium tube. The upper part of the tube was clamped in a Heidolph stirrer and the opening was connected to the argon supply. The control thermocouple of an Ether temperature controller was inserted on the outside of the stainless steel tube.

Reagents: The salt mixture used in all experiments consisted of a 1 : 1 molar mixture of analytical grade NaCN and KCN. The salt was vacuum-dried at room temperature for at least one week before use. Laboratory grade Bi, Zn, Sn and Pb were further purified by filtering through porosity-2 sintered glass filters under argon atmosphere. Radioactive tracers were prepared by neutron irradiation of Specpure metals or chloride salts. ^{105}Rh tracer was obtained from neutron-irradiated RuCl_3 ⁷.

Procedure: In experiments for studying the extraction behaviour of individual metals (Fig. 2), 10 mg quantities of the elements (as chloride salts), spiked with radioactive tracers, were mixed with 10 - 15 g of salt in titanium crucibles. The mixture was melted under argon and stirred for 30 min before addition of metal phases. Metal pieces were added to the melt through a quartz tube which was inserted through the sampling port. Mixing of the phases was continued (1 - 2 h) until the radioactivity in the salt phase, as determined from samples drawn from the melt into quartz tubes, remained constant, before the composition of the alloy was changed by addition of more Sn or Zn to Bi - Sn or Sn - Zn systems respectively. The fraction extracted at each alloy composition was calculated from the loss of activity in the salt phase.

A different procedure was followed when investigating the separation of mixtures of metals. Metal chloride (anhydrous) salts were dissolved in the salt phase, stirred for 30 min under argon and then equilibrated for 1 h, each time with successive metal phases (Table 1). Metal phases were removed quantitatively by suction into quartz tubes inserted through the sampling port. The quantities extracted into various metal phases were determined from the gamma spectra (corrected for matrix absorption effects) obtained from a Ge(Li) detector coupled to a 4000-channel analyzer.

In some experiments platinum metals and radioactive tracers were

concentrated in Sn by the classical fire-assay method⁸. This was done by fusing a total of 1 g of platinum group metals with 35 g SnO₂, 50 g Na₂CO₃, 10 g Borax, 10 g SiO₂ and 40 g flour at 1200°C for 1 h. The separated tin button was treated with HCl, and the residu was chlorinated in a quartz tube⁸ at 700°C for 16 h to remove all tin and to convert the platinum metals to chloride salts. Two glass-wool stoppers were inserted in cooler parts of the tube to collect sublimed products. The chlorinated residu was subsequently leached with aqua regia, and the dried solid was treated as shown in Fig. 2.

Rhodium was analyzed for iridium impurity by mixing 20 mg RhCl₃ with 200 mg SiO₂ and irradiating for 30 min at a thermal neutron flux of 1×10^{14} n/cm²/sec. Samples and standards were analyzed gamma-spectrometrically after a cooling period of three to four days.

RESULTS AND DISCUSSION

Extraction of metals

The extraction behaviour of the platinum group metals, of silver and of gold is shown in Fig. 2 where percentage extraction into the metal phase is plotted as a function of the atom fraction of tin in bismuth. In addition to the results shown in the figure, it was found that the extraction of ruthenium into tin can be improved by the addition of zinc. A tin alloy containing 0.2 at.% Zn will extract 80 % ruthenium, while 95 % is extracted by 0.5 at.% Zn at 550°C. Osmium can further be recovered from the salt phase by extraction into zinc at 700°C. The percentage extracted into the metal phase was calculated as $\%E = (D/(D+1))100$, where

$$D = \frac{\text{Specific activity of metal}}{\text{Specific activity of salt}}$$

and is thus applicable to a system with equal weights of metal and salt phases.

These extractions, in which metal ions in the salt phase are reduced by and extracted into the metal phases, are probably of the type



where M(CN)_m represents the metal ions being extracted from the salt phase and R is Bi, Sn or Zn. For simplicity the species in the salt phase are shown as neutral compounds; it is, however, likely that at least the extracted metals are present as anionic cyanide complexes. Although the equilibrium constant

$$K = \frac{a_M}{a_{\text{M(CN)}_m}} \cdot \frac{\left[\frac{a_{\text{R(CN)}_n}}{a_R} \right]^{\frac{m}{n}}}{\left[\frac{a_{\text{R(CN)}_n}}{a_R} \right]^{\frac{m}{n}}} = \exp \left[-\frac{m}{n} \Delta G_{\text{R(CN)}_n}^{\circ} - \Delta G_{\text{M(CN)}_m}^{\circ} \right] \quad (2)$$

where a denotes activity, can in principle be calculated from the difference in the free energies of formation of R(CN)_n and M(CN)_m , the actual distribution behaviour is clearly also dependent on the activity coefficients of the solutes. The distribution of M between an alloy, in which R acts as reductant, and a salt phase is given by

$$D_M = \frac{N_{\text{M(metal)}}}{N_{\text{M(CN)}_m \text{ (salt)}}} = K \frac{\gamma_{\text{M(CN)}_m}^{\frac{m}{n}} \gamma_R^{\frac{m}{n}}}{\gamma_M^{\frac{m}{n}} \gamma_{\text{R(CN)}_n}^{\frac{m}{n}} \gamma_{\text{R(CN)}_n}^{\frac{m}{n}}} \quad (3)$$

where N denotes mole fraction and γ designates activity coefficient. With the exception of γ_R (which remains close to one for solutions of tin in bismuth), none of the activity coefficients or K , as shown in (3), are known for the systems under investigation. Considering the factors which normally affect extractions from molten halide systems⁹, and also the stable intermetallic compounds that are formed between platinum group metals and Bi, Sn or Zn¹⁰, as well as the well-known high stability of platinum group metal cyanide complexes in aqueous solutions, it is probable that K and γ_m are the

extraction-determining factors. This is qualitatively in agreement with the above results which show that Pt, Pd, Au, Rh and Ag, all elements which form stable intermetallic compounds with bismuth (resulting in low values for γ_m in (3)), are extracted quantitatively into bismuth. Iridium and ruthenium, which do not form stable compounds with bismuth, can however, be extracted when tin, with which they do form stable compounds, is added to bismuth. That this (γ_m) is not the only extraction-determining factor is shown by the fact that iridium and ruthenium are extracted by bismuth from chloride melts, and that iridium can be removed from bismuth into a chloride melt by the addition of cyanide to the system¹¹.

The fact that the oxidized forms of bismuth and tin (eq. (3)) are stable in molten cyanide is surprising as cyanide compounds of these elements are rather unstable - at least in aqueous chemistry. The results for the extraction of iridium (Fig. 2) show that the extraction is reversible and that tin, which is oxidized during the extraction of iridium from the salt, must therefore be present in a stable, readily reducible form. Since the same results are obtained for microgram as well as tens of milligram quantities of the elements investigated here, the above behaviour can obviously not be the result of solubility factors or impurities in the metal phases.

Clearly, more basic information on extractions from molten cyanide (e.g. activity coefficients, free energy of formation, oxidation states of solutes, etc.) is required before a more quantitative discussion of the above results can be attempted. It is, however, evident from these results that the present system is unique among molten salt-liquid metal systems in that not all platinum group metals behave as noble metals, and that this property may have potential use for the separation of rhodium, iridium, ruthenium and osmium. This possibility was further investigated and the results will be outlined below.

Separation Studies

A scheme for the separation of Rh, Ir, Ru and Os based on the above results was tried out on a mixture containing 20 mg each of these elements, as chloride salts dissolved in 10 g cyanide eutectic. Extractions for 1 h each with 10 g portions of metal phases yielded the results shown in Table 1.

TABLE 1

Percentage extraction of Rh, Ir, Ru and Os from molten cyanide after removal of successive metal phases

Metal Phase	°C	% Extraction			
		Rh	Ir	Ru	Os
Bi (1)	550	90	0	0	0
Bi (2)		>99	3	0	0
Bi-Sn (1)	550		85	<1	0
Bi-Sn (2) $X_{\text{Sn}} = 0.5$			>95	<3	0
Sn-Zn (1)	550			80	0
Sn-Zn (2) $X_{\text{Sn}} = 0.2$				>95	2
Zn	700				99

The potential use of this separation scheme in the refining of platinum metals was investigated further through experiments in which the concentrations were increased considerably, and also by initially concentrating the platinum group metals in tin or lead by the fire-assay method, as is normally done for industrial concentrates¹². The separation scheme that was developed for a mixture of Ir, Rh and Ru (ratio 1 : 4 : 8) containing 10 % each of Pt, Pd and Au, all marked with radioactive tracers, is given in Fig. 3. The total concentration of platinum metals in the salt (15 g)

was about 5 %, and extractions were carried out each time with 10 g quantities of metal phase. Although these extractions were probably not obtained under equilibrium conditions (1 h equilibration times), it was nevertheless found that efficient and reproducible results can be obtained in this manner.

Separation of Au, Pt and Pd: More than 90 % of the Au, Pt and Pd present is removed during chlorination and subsequent leaching with aqua regia. If desired, extraction with lead can be carried out at 520°C before the rhodium extraction. The remaining Au, Pt and Pd, together with 2 - 3 % rhodium, will be extracted into lead.

Extraction of rhodium: The extraction of rhodium with three portions of bismuth is practically quantitative (>95 %). Although it may be expected that a small fraction of iridium will be co-extracted (Fig. 2), it is found in practice that iridium will only be extracted into bismuth when practically no rhodium is left in the salt phase. This effect is illustrated in Table 2 where the effect of rhodium on the extraction of iridium into tin is shown. In the absence of rhodium, iridium will be extracted quantitatively into Sn (Fig. 2). This is probably due to the equilibrium



whereby any iridium that is being reduced by tin is immediately reoxidized by $\text{Rh}^{\text{n}+}$.

TABLE 2

Percentage extraction of Ir (10 mg) and Rh - Ir (120 and 10 mg respectively) mixture from 10 g cyanide eutectic into 10 g Sn at 550°C as function of time

Time (min)	Ir	Mixture	
		Rh	Ir
10	>99	83	0
40		88	0
120		95	0
180		>99	<1
240			21
280			71
300			90

Rhodium can be recovered from the bismuth phase by extraction into molten zinc¹³. The excess zinc is dissolved in HCl, and the precipitate is chlorinated at 700°C to remove zinc and to form insoluble $RhCl_3$ which is digested with aqua regia as a further purification step before reduction, in hydrogen, to the metal.

Typical recoveries (as determined from the weight of metal) of rhodium when carried through the whole separation scheme are between 80 and 85 %. Gamma-spectrometric analysis of the radioactivity in purified rhodium showed the presence of <0.01 % of all elements which had been radioactively marked. Neutron activation analysis of iridium (normally the major contaminant of rhodium) in several rhodium samples yielded concentrations of 0.001 to 0.005 % Ir.

Effect of nickel: During these experiments it was also observed that nickel (added as $NiCl_2$) may have a profound effect on the extraction of Rh, Ir and Ru. It is, for example, impossible at any temperature to extract iridium or

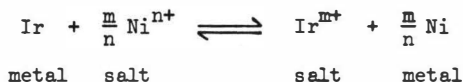
ruthenium from a cyanide melt containing 3 % nickel into tin. Rhodium, however, can still be extracted into tin under these conditions. This observation was utilized for developing a method of purifying rhodium of iridium (or ruthenium) impurity, as is shown in Table 3. These results were obtained by extracting RhCl_3 from a eutectic melt at 600°C , containing 3 % nickel, into tin. The excess tin, as well as some nickel, was dissolved in HCl , and the remaining tin and nickel in the Ni-Rh-Sn alloy was removed by chlorinating at 700°C and digestion of RhCl_3 with aqua regia.

TABLE 3

Purification of Rh from Ir impurity
by extracting Rh into Sn at 600°C from
cyanide eutectic containing nickel

Ir ppm	
Before	After
60	0.05
30	0.02

The above behaviour indicates that nickel falls between rhodium and iridium in the electrochemical series for cyanide melts so that the equilibrium



prevents reduction of iridium while Ni^{n+} is still present in the salt. This is in agreement with experimental observations carried out with radioactive nickel (<1 % concentration) which showed that iridium can be extracted into tin only when no nickel is left in the salt phase. The extraction behaviour

of nickel into tin is rather erratic and no consistent results could be obtained at the concentration levels used in the above extractions. A fraction of the nickel in solution is apparently extracted faster than the rest. This behaviour is in agreement with electronic spectra obtained on quenched cyanide melts as well as on molten cyanide solutions, which showed that, in addition to Ni(II), at least one other oxidation state (probably Ni(0)) is also present¹⁴.

Extraction of iridium: Although iridium can be extracted quantitatively into three portions of Bi-Sn alloy at 550°C (Table 1), it was found that <5 % Ru is co-extracted when pure tin is used at 520°C for the extraction of iridium. As in the case for Rh - Ir, this is probably due to oxidation of ruthenium in the metal phase by iridium in the salt. This method is preferred as it simplifies the recovery of iridium from the metal phase. The combined tin phases (30 g) containing iridium can be purified of ruthenium impurity by contacting it with molten cyanide (15 g) containing 1.5 % nickel. Ruthenium, as well as part of the iridium, is oxidized into the salt phase by nickel. The nickel content of the system is, however, such that it will be fully extracted into tin, and within 1 h >99 % Ir will be contained in the metal phase while >90 % Ru will be contained in the salt phase.

If desired, the metal phase containing iridium and nickel can be purified of rhodium by contacting it with molten cyanide containing 3 % nickel. Iridium passes quantitatively into the salt phase, while rhodium remains in the metal phase. Iridium can be recovered from the salt phase by contacting it with a zinc alloy containing 0.5 at.% tin at 600°C. Iridium is recovered from tin or tin-zinc phases by dissolving the excess metal in HCl, chlorinating the residu at 700°C, and finally digesting IrCl₃ with aqua regia before reduction to the metal in hydrogen.

Gamma-spectrometric analysis of the recovered iridium (about 80 %) showed <0.01 % of all radioactively marked elements.

Extraction of ruthenium: Ruthenium in the original cyanide melt, as well as the small fraction that was co-extracted with iridium and subsequently transferred to a salt phase, can be extracted with Sn-Zn (0.5 at.% Zn) at 600°C . Excess tin and zinc in the combined metal phases are dissolved in HCl. The remaining Sn-Zn-Ru alloy, combined with the trapped volatile products during the initial chlorination, as well as the dried residue of the aqua regia wash of the chlorinated residue (see experimental), can be rendered soluble in water by fusion with sodium peroxide. Ruthenium can subsequently be recovered by chlorine distillation¹⁵, and the recovered RuCl_3 can be reduced to the metal in hydrogen.

Yields of ruthenium were normally about 80 %. Gamma-spectrometric analysis of the final products showed the purity to be >99.9 % as compared with other radioactively marked elements.

Osmium: Although osmium was not included in the separation scheme, as it would probably be volatilized quantitatively during the chlorination step, any osmium present in the system would still be in the salt phase from which it can be extracted with zinc at 700°C .

Stability of melt

Infrared spectra and argentimetric cyanide determinations on quenched melts¹¹ revealed that cyanide melts under argon or nitrogen atmosphere are stable for many hours for systems containing low concentrations (<0.5 %) of platinum metals. At higher concentrations, and also at temperatures above 650°C , the rate of degradation increases considerably when the system is not completely oxygen-free. Cyanate and, to a lesser extent, carbonate are the main decomposition products under such conditions. Low concentrations of

these impurities do not appear to have significant effects on the above separation scheme. Extractions from molten cyanides containing higher concentrations (~15 % cyanate + carbonate) caused by prolonged exposure of a melt with high platinum metal content to the atmosphere, were less selective and some iridium and ruthenium followed rhodium during extraction into bismuth.

ACKNOWLEDGEMENTS

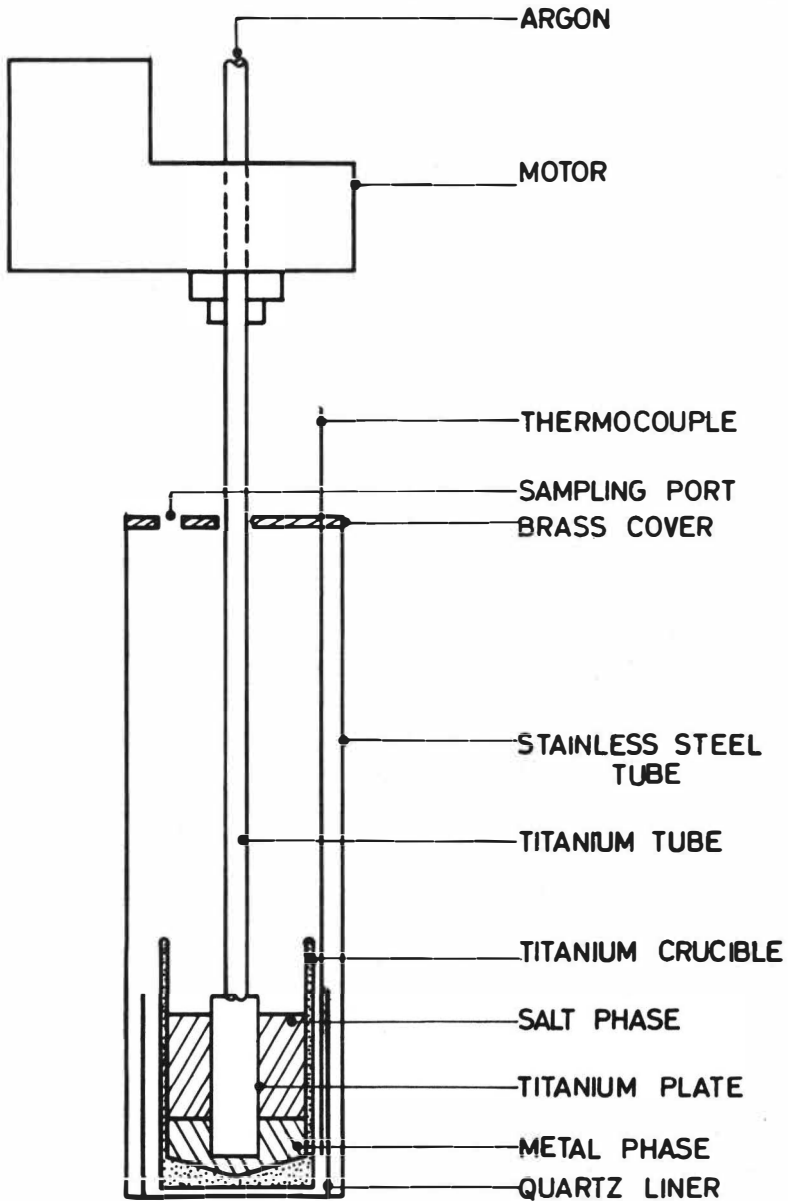
The authors wish to thank the South African Atomic Energy Board for permission to publish these results. They are also grateful to Mr. C.R. de Jager and Mr. T.T. Retief for technical assistance, and to Dr. P. Crowther for helpful discussions.

REFERENCES

1. R.H. Wiswall and J.J. Egan, in Thermodynamics of Nuclear Materials, Proceedings of I.A.E.A. Symposium 1962, p. 345, I.A.E.A., Vienna (1962).
2. M.W. Rosenthal, P.N. Haubenreich, H.E. McCoy and L.E. McNeese, *At. En. Rev.*, 9, 601 (1971).
3. B.R. Harder, G. Long and W.P. Stanaway, in Nuclear Metallurgy 15, 405. USAEC Rep. CONF-69081 (1969).
4. R.K. Stenuenberg, R.D. Pierce and I. Johnson, in Nuclear Metallurgy 15, 325. USAEC Rep. CONF-69081 (1969).
5. Y. Marcus, in Advances in Molten Salt Chemistry (Ed. by J. Braunstein, G. Mamantov and G.P. Smith), p. 63, Plenum Press, New York (1970).
6. B.M. Chadwick and A.G. Sharpe, in Advances in Inorganic and Radiochemistry (Ed. by H.J. Emeleus and A.G. Sharpe), Vol. 8, p. 83, Academic Press, New York, 1966.
7. J.G.V. Lessing and K.F. Fouché, To be published.
8. F.E. Beamish, The Analytical Chemistry of the Noble Metals, p. 162, Pergamon Press, London 1966.
9. I. Johnson, in Applications of Fundamental Thermodynamics to Metallurgical Processes, (Ed. by G.R. Fitterer), p. 153, Gordon and Breach, New York, 1967.
10. M. Hansen, Constitution of Binary Alloys, McGraw-Hill, New York, 1958.
11. J.G.V. Lessing, Unpublished results.
12. S.E. Livingstone, in Comprehensive Inorganic Chemistry, (Ed. by J.C. Bailar, H.J. Emelens, R. Nyholm and A.F. Trotman-Dickenson), Vol. 3, p. 1170, Pergamon Press, Oxford, 1973.
13. O.E. Dwyer, H.E. Howe and E.R. Avrutik, *Nuclear Sci. and Eng.* 12, 15. (1962).

14. K. de Haas, Unpublished results.
15. F.E. Beamish, The Analytical Chemistry of the Noble Metals, p. 39, Pergamon Press, London, 1966.

Fig. 1. Schematic diagram of extraction apparatus.



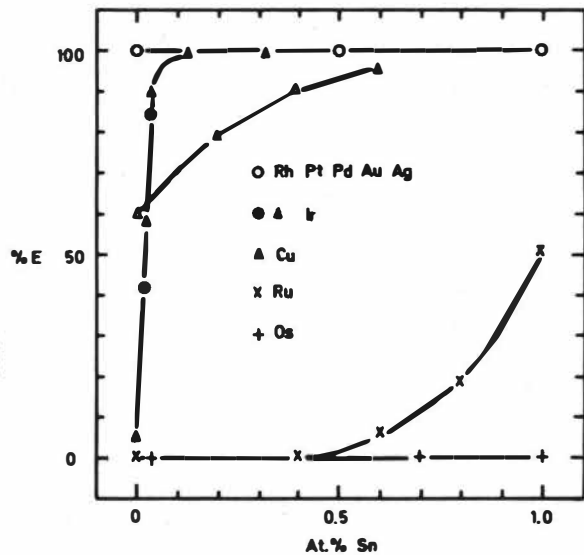


Fig. 2. % Extraction of platinum group and related elements from molten cyanide as function of atom fraction Sn in Bi. Results marked ● on iridium-extraction curve were obtained by adding Bi to Sn-rich alloy.

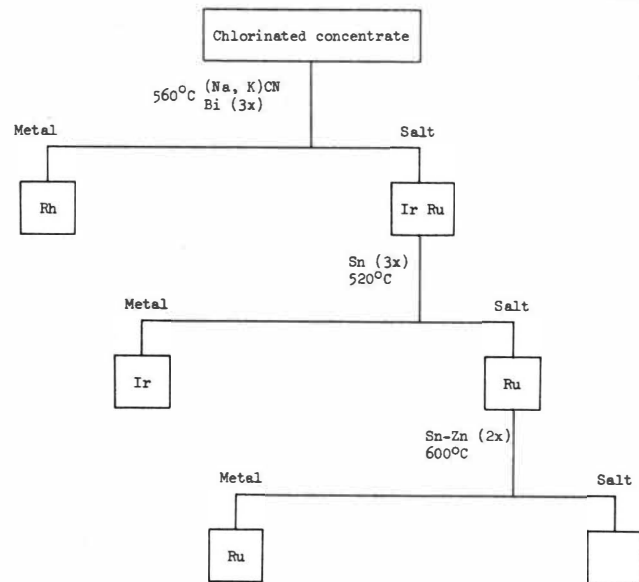


Fig. 3. Separation scheme for Rh, Ir and Ru.

EXTRACTION OF RUTHENIUM AND OSMIUM NITROSOCOMPLEXES.

The extraction of ruthenium and osmium nitrosocomplexes $/M NO X_5/2-$ has been studied. In these compounds M stands for Os and Ru and X stands for Cl, Br, J, NO_2 , OH ligands, aliphatic amine salts, quaternary ammonium and phosphonium compounds, neutral phosphoric reagents - R_3PO and sulfur contained compounds - R_2SO . The dependence of osmium and ruthenium extraction on the nature and concentration of acids in aqueous phase and on the nature of internal ligands in osmium and ruthenium nitrosocomplexes as well as on the nature of extractants and diluents in organic phase is shown. Coordinating compounds of nitroso-osmium and ruthenium which are obtained during extraction have been synthesized and studied. The mechanism of extraction of osmium and ruthenium nitrosocomplexes is discussed.

The systematic study of extraction of nitrosocomplex compounds of osmium and ruthenium such as $/M NO X_5/2-$ and $/M NO (NO_2)_2 OH/2-$ where M stands for Os and Ru and X stands for Cl, Br, or J ligands, is only recent. The extraction of some ruthenium nitrosocomplexes with long chain aliphatic amines $/L,2/$, salts of quaternary ammonium compounds $/3/$, and some neutral phosphoric extractants $/4/$ has been studied. No reports of the extraction of the equivalent nitrosocomplexes exist. Furthermore, we have no data on the extraction of complex compounds of ruthenium and osmium with such extractants such as sulfur containing compounds or salts of quaternary phosphonium compounds; these extractants are comparatively recent.

Amine salts are the most effective extractants of anion complexes of metals. That is why the possibility of their use for extraction of osmium and ruthenium nitrosocomplexes should be considered first. It is known that while traversing from primary to secondary and then to tertiary amines in accordance with increase of their electron donor properties the extraction of metal containing complex anions increases $/5/$. The similar relation has been observed during the extraction of $/Ru NOCl_5/2-/I/$ and $/OsNOCl_5/2-$ complexes. For example, during the extraction of 0.01 m $(NH_4)_2/Os NOCl_5/$ from 1 m HCl with solution of 0.03 m tri - n - octylamine (TOA) in benzene the distribution coefficient for osmium $D_{OS} = 9.3$, for di - n - octylamine (DOA) $D_{OS} = 3.7$. In case of extraction of 0.005 m $(NH_4)_2/Os NOCl_5/$ from 1 m HCl with 0.03 m TOA in benzene $D_{OS} = 22$, for DOA $D_{OS} = 11$ and the trialkylmethylamine, Primene JM - T - $(R_1) (R_2) (R_3) CNH_2$ (mol. wt. is equal to 320), $D_{OS} = 3$.

The nature of the neutral phosphoric extractant has also a great influence upon the extraction. The substitution of either groups RO in a molecule of neutral phosphoric reagents by more electrondonor alkyl radikals R results in the increase of extraction of nitrosocomplexes of osmium and ruthenium of TBP $/(C_4H_9O)_3 PO/$ DAMP $/(iC_5H_{11}O)_2 CH_3PO/$ BDBP $/(C_4H_9O)(C_4H_9)_2 PO/$ TBPO $/(C_4H_9)_3 PO /$.

The experimental data for the extraction with sulfur contained reagents (table I) show that dialkylsulfoxides (R_2SO) extract ruthenium nitrosocomplexes less effectively than amines and phosphoric compounds. The maximum extraction of ruthenium into the organic phase is observed when di-n-heptylsulfoxide $(C_7H_{15})_2SO$ is used as an extractant. In the case when di-n-heptylsulfone $(C_7H_{15})_2SO_2$ and di-n-octylsulfide are used ruthenium distribution coefficients are reduced.

TABLE 1

Extraction of ruthenium from 1m HCl with 0.4 m solutions of sulfur contained compounds in benzene.

Extractant	Distribution coefficient	
	$(NH_4)_2/RuNOCl_5/$	$(NH_4)_2/RuNO Br_5/$
$(C_7H_{15})_2SO$	0.045	0.062
$(C_7H_{15})_2SO_2$	0.005	0.010
$(C_8H_{17})_2S$	0.002	0.003

For single-type nitrosocomplexes of osmium the same regularity can be observed e.g. R_2SO R_2SO_2 R_2S .

Of great interest for the extraction of nitroso-osmium and nitroso-ruthenium complexes are salts of quaternary phosphonium compounds R_4PX , which are slightly inferior as extractants to the salts of quaternary ammonium compounds.

During extraction of 0.005 m $(\text{NH}_4)_2/\text{RuNOCl}_5/$ from 1 m HCl with 0.02 m solution of $(\text{C}_9\text{H}_{19})_4\text{NBr}$ in chloroform distribution coefficient $D_{\text{Ru}}=6.2$, but during extraction with 0.02 m $(\text{C}_{10}\text{H}_{21})_4\text{PBr}$, $D_{\text{Ru}}=5.2$ are observed.

The nature of radical R in the molecule R_4PX influences greatly the extraction of the nitrosocomplexes of ruthenium and osmium. During transition from $(\text{C}_{10}\text{H}_{21})_4\text{PBr}$ to $(\text{C}_{12}\text{H}_{25})_4\text{PBr}$, D_{Ru} decreases from 5.2 to 2.0 respectively which is evidently due to steric hindrance. The introduction into the molecule R_4OBr of strong electron acceptor phenyl radicals instead of alkyl radicals causes the decrease of D_{Ru} for $\text{Ru NO Cl}_5/2^-$ up to 1.2 for the extraction by a 0.02 m solution of tetraphenylphosphoniumbromide in chloroform. In the case of the extraction of 0.001 m $(\text{NH}_4)_2/\text{Os NO Cl}_5/$ from 1 m HCl with 0.02m solutions of extractants in chloroform, $D_{\text{Os}}=13.0$ for $(\text{C}_9\text{H}_{19})_4\text{HBr}$, $D_{\text{Os}}=9.6$ for $(\text{C}_{10}\text{H}_{21})_4\text{PBr}$ and $D_{\text{Os}}=5.0$ for $(\text{C}_6\text{H}_5)_4\text{PBr}$.

The value of the distribution coefficient of osmium and ruthenium depends considerably on the nature of organic diluent. For example, while extracting nitrocomplex of nitroso-osmium $\text{Os NO}(\text{NO}_2)_4\text{OH}/2^-$ with tetra - n - octylammonium nitrate, D_{Os} decreases approximately by an order of magnitude in passing from benzene to chloroform (table 2).

TABLE 2

Extraction of $\text{Na}_2/\text{Os NO}(\text{NO}_2)_4\text{OH}/. \text{H}_2\text{O}$ from 1 m HNO_3 with solutions of $(\text{C}_8\text{H}_{17})_4\text{N NO}_3^-$.

Diluent	benzene	Cl-benzene	NO_2^- benzene	dichlor-ethane	Heptyl-alcohol	chloro-form
D_{Os}	1.8	1.8	1.1	0.7	0.6	0.15

Let us consider further the influence of the character and concentration of acids in aqueous phase as well as that of the nature of ligands in the nitrosocomplexes of ruthenium and osmium on their extraction,

The acidity of the aqueous phase may have different influences on the extraction of ruthenium and osmium nitrosocomplexes (table 3).

TABLE 3

Extraction of $(\text{NH}_4)_2 / \text{Ru NO Cl}_5 /$ from HCl with different extractants

Concentration of HCl, m	0.5	1	3	5	7	10
0.1 m $(\text{C}_8\text{H}_{17})_3\text{NHCi}$ in benzene	54	45	40	26	20	12
0.04m $(\text{C}_8\text{H}_{17})_4\text{NBr}$ in chloroform	24	17	4.8	2.9	1.5	0.28
0.04m $(\text{C}_{12}\text{H}_{25})_4\text{PBr}$ in chloroform	9.9	6.5	2.2	1.3	0.9	0.3
0.2m $(\text{C}_8\text{H}_{17})_3\text{PO}$ in benzene	0.06	0.13	0.8	0.84	0.4	0.08
0.2m $(\text{C}_7\text{H}_{15})_2\text{SO}$ in benzene	0.01	0.013	0.04	0.08	0.46	0.86

In the case of amines, salts of quaternary ammonium and phosphonium compounds the distribution coefficients decrease as aqueous phase acidity increases. This is connected with the increased competitions of the anions for the extractant. In the case of neutral phospho-organic extractants the D_{Ru} and D_{Os} dependence on the concentration of hydrochloric acid goes through a maximum in the region of 4 m HCl (Fig.1). The increase in the distribution coefficients can be explained by protonation of the phospho-organic extractant which later forms ionic pairs with the complex metal containing anions [6]. Further increases in the HCl concentration causes both the increased competition of hydrochloric acid for extractant and the consequent suppression of the extraction of osmium and ruthenium nitrosocomplexes.

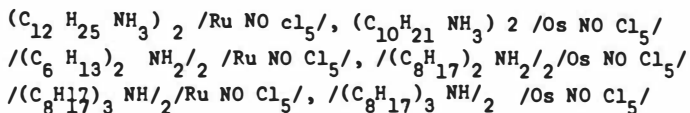
During the extraction of the nitrosoosmium and nitroso-ruthenium pentahalogenocomplexes by solutions of sulfoxides - R_2SO , and increase in the distribution coefficients is observed as the hydrochloric acid concentration in the aqueous phase increases up to 10m. At the same time the character of the D_{Ru} dependence on acid concentration in aqueous phase is quite different in the case of extraction of $/Ru NOX_5/^{2-}$ from nitric acid solutions by sulfoxides. Thus as the concentration of nitric acid increases distribution coefficients of ruthenium decrease. Apparently this is connected with the competing action of the extractant for the nitric acid which can be extracted much better by di - alkylsulfoxides than is HCl /7/. Thus the nature of the organic phase and the nature of the mineral acid in the aqueous phase both influence the extraction of the osmium and ruthenium complexes.

The nature of the ligands in the internal sphere of $/MNOX_5/^{2-}$ complexes considerably influence the extraction of ruthenium and osmium. During extraction of $/OsNOHal_5/^{2-}$ from 1m H_2SO_4 by TOA solutions in benzene and of $/RuNOHal_5/^{2-}$ from 1m HCL by $(C_{12}H_{25})_4$ PBr solutions in chloroform the increase in metal extraction is observed in a number of complexes $/M NOCl_5/^{2-}$ $/M NOBr_5/^{2-}$ (Fig. 2). Probably, the D_{Ru} increase observed is associated with the increase of the solvation of the extracting complexes in organic phase and with the decrease of hydration of these complexes in the aqueous phase.

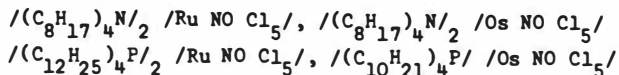
It should be noted that depending on the nature of the organic reagent used we observe that osmium nitrosocomplexes are better extracted than the analogous ruthenium nitrosocomplexes. For example, during the extraction of osmium from 0.005m solution of $(NH_4)_2 /Os NOCl_5/$ in 1 m HCL by 0.05m solution of TOA in benzene $D_{Os}=30$, whereas for the extraction of $(NH_4)_2 /RuNOCl_5/$ under the same conditions the distribution coefficient of ruthenium is $D_{Ru}=10$.

Let us consider in detail the extraction mechanism of osmium and ruthenium nitrosocomplexes by amines. The attempt to determine solvate numbers on the basis of extraction data from $\log D - \log /S/$ (slope of $\log D - \log /S/$) leads to fractional values of solvate numbers. It seemed to us unlikely that fractional values of solvate numbers can characterize the composition of compounds transferring to organic phase at extraction.

In order to obtain more precise data on the composition of compounds formed on extraction we prepared the solid states nitrosocomplexes of osmium and ruthenium with nitrogen and phosphorus containing reagents:



The analogous bromo- and iodocomplexes of nitroso-osmium and nitroso-ruthenium were also prepared. In addition, complexes with cations of quaternary ammonium and phosphonium compounds are synthesized:



In infra red spectra of the synthesized compounds shared a strong band in the region of 1800 cm^{-1} characteristic of valence oscillations of the nitroso-group - NO /9-12/. The bands observed at 615 cm^{-1} and 580 cm^{-1} are attributed to valence Vos-N and distortion Os NO oscillations of nitroso-group (Table 4). Broad absorption bands in the region of 3000-3200 I/cm according to literature data available /13/ we referred to valence oscillations of N-H connection disturbed by hydrogen connection of N-H ... X type where X stands for halogen-ligands in complexes of nitroso-osmium and nitroso-ruthenium. If the state of NH in IR compound absorption spectra is taken for the criterion of the stability of hydrogen bonding then one may draw a conclusion that the most stable hydrogen bonding is realized in the case of complexes with tertiary amines, and the least stable with primary amines. At the same time the nature of internal ligand in nitrosocomplexes of osmium and ruthenium does not markedly influence the hydrogen bonding.

In order to study the behavior of synthesized compounds in anhydrous solutions their conductivity was investigated. In polar solvents of the type involving low molecular weight alcohols, the substituted ammonium complexes of nitroso-osmium and nitroso-ruthenium are considerably dissociated. At the same time the decreased solvation power and dielectric constant of the solvent leads to decreased dissociation of the synthesized compounds (Table 5).

TABLE 4

Wave numbers (cm^{-1}) of maxima of absorption bands in IR-spectra of nitrosocomplexes of osmium and ruthenium.

Compound	$(\text{AmH})_2 / \text{Os NO X}_5 /$		$(\text{Am H})_2 / \text{Ru NO X}_5 /$	
	NO	NH	NO	NH
R_4N^+	1795	-	1830	-
R_3NH^+	1825	3035	1867	3020
R_2NH_2^+	1840	3070 3130	1883	3040 3090
RNH_3^+	1845	3150 3180	1890	3140 3185
I	1815	3020	1838	3030
Br	1820	3030	1800	3030
Cl	1825	3035	1867	3020

In non-polar solvents of type involving benzene rings, like another amine salts /I4/, produce intermolecular association. For example, in a 0.04 m solution of $(\text{TOAH})_2 / \text{OsNOCl}_5 /$ in benzene, the average value of the degree of association is $\bar{n} = 1.8$. Thus, substituted aminocomplexes of nitroso-osmium are much greater associated in non-polar dissolvents than complexes of nitroso-ruthenium of the same type ($\bar{n} = 1$ for $(\text{TOAH})_2 / \text{Ru NOCl}_5 /$ under the same conditions).

TABLE 5

Molecular conductivity ($\text{cm}^2/\text{oh mole}$)
under $25 \pm 0.05^\circ\text{C}$.

SOLVENT	:	dilution, 10-1 mole			
		500	1000	2000	4000
CH_3OH	:	113	134	159	186
$\text{C}_2\text{H}_5\text{OH}$:	28.6	34.0	41.2	49.3
$\text{C}_4\text{H}_9\text{OH}$:	3.9	4.8	7.0	10.0
$\text{C}_8\text{H}_{17}\text{OH}$:	0.1	-	-	-
$\text{CH}_3\text{-CO-CH}_3$:	38.6	49.6	63.2	79.0
$\text{NO}_2\text{-benzene}$:	7.9	10.8	13.1	16.4
Cl-benzene	:	0.1	-	-	-

The nitrosocomplexes of osmium and ruthenium of the same type are chemically very similar and the better extraction of osmium is best explained by the fact that in the organic phase, extracted complexes containing osmium produce intermolecular associations.

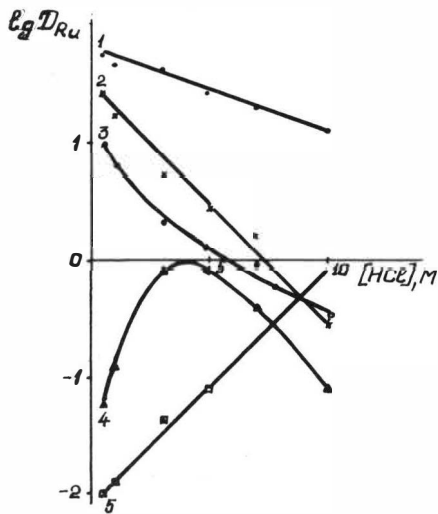
Thus the extraction of nitrosocomplexes of osmium and ruthenium by amine salts, quaternary ammonium and phosphonium compounds follows the mechanism of outer-sphere substitution which is not connected with the destruction of the internal sphere of nitrosocomplexes of osmium and ruthenium.

In the case of the extraction of pentahalogenocomplexes of ruthenium and osmium by neutral phosphoric R_3PO and sulfur containing R_2SO reagents from acidic media it seems most likely that a hydration-solvation mechanism is realised. This process leads to the formation in organic phase of $[\text{S}_x(\text{H}_3\text{O})(\text{H}_2\text{O})_y]_2/\text{MNOX}_5/$ complexes /15/. For the extraction of nitrosocomplexes of nitroso-ruthenium by R_3PO the mechanism of inter-sphere substitution /16/ with the formation of $[\text{Ru NO}(\text{NO}_2)_2(\text{R}_3\text{PO})_2 \text{OH}]$ complexes is observed.

- I. N.M. Sinitzin, O.E. Zvjagintzev, V.F. Travkin, Russ. J. Inorg. Chem., 13, 2788 (1968).
2. N.M. Sinitzin, V.N. Pichkov, O.E. Zvjagintzev, Russ. Radiochem., 8, 545 (1966).
3. N.M. Sinitzin, F.J. Rovinsky, V.I. Ispravnikova, Reports of Science Academy of USSR, 176, 1320(1967).
4. N.M.Sinitzin, F.J. Rovinsky, V.F. Travkin, News of Siberia Department of Science Academy of U.S.S.R., Ser. of Chem. Sciences, N. 9, printing 4, 101(1970).
5. R.M. Diamond, "Solvent extraction chemistry", Moskow, Atomizdat, 1971, p. 180.
6. A.T. Casey, E.Devies, T.Z. Meek, E.S. Wagner, "Solvent extraction chemistry, North-Holland, Amsterdam, 1967, p. 327.
7. W. Korpek, Nucleonica, 7, 715, 8, 747(1963).
8. K.A. Bolshakov, N.M. Sinitzin, V.F. Travkin, G.L. Plotinsky, Russ. J. Inorg. Chem., 18, 1424(1973).
9. P.Gans, A. Sobatini, L. Sacconi, Inorg. Chem., 5, 1877(1966).
10. N.M. Sinitzin, K.J. Petrov, Russ. J. Structure Chem., 9, 45, (1968).
11. W.P. Griffith, J. Chem. Soc., A, 372(1969).
12. M.J. Cleare, H.P. Fritz, W.P. Griffith, Spectrochim. Acta, 28A, 2013(1972).
13. K.J. Petrov, N.M. Sinitzin, M.V. Rubtsov, Russ. J. Inorg. Chem., 13, 2614(1968).
14. D.T. Copenhofor, C.A. Kraus, J. Am. Chem. Soc., 73, 4457(1951)
15. N.M. Sinitzin, F.J. Rovinsky, V.J. Ispravnikova, Russ. Radiochem., 14, 826(1972).

16. O.F. Zvjagintzev, N.M. Sinitzin, V.N. Pichkov, Russ.
J. Inorg. Chem., II, 128(1966).

Allen
A. Curran
Neof. J. P. S.



1. $-0,1 \text{ m } (\text{C}_8\text{H}_{17})_3 \text{ N HCl}$ in benzene,
2. $-0,04 \text{ m } (\text{C}_8\text{H}_{17})_4 \text{ NBr}$ in chloroform,
3. $-0,04 \text{ m } (\text{C}_{12}\text{H}_{25})_4 \text{ PBr}$ in chloroform,
4. $-0,2 \text{ m } (\text{C}_8\text{H}_{17})_3 \text{ PO}$ in benzene,
5. $-0,2 \text{ m } (\text{C}_7\text{H}_{15})_2 \text{ SO}$ in benzene.

Fig. 1. Extraction of $(\text{NH}_4)_2[\text{RuNOCl}_5]$ from HCl by different extractants:

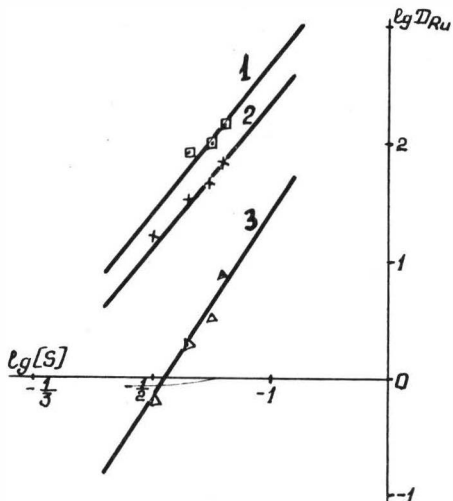


Fig. 2. Extraction of $(\text{NH}_4)_2[\text{RuNOHal}_5]$ from 1 m HCl by

$(\text{C}_{12}\text{H}_{25})_4 \text{ PBr}$ in chloroform:

- 1 $-(\text{NH}_4)_2[\text{RuNOJ}_5]$, 2 $-(\text{NH}_4)_2[\text{RuNOBr}_5]$,
- 3 $-(\text{NH}_4)_2[\text{RuNOCl}_5]$.

2813

A MODIFIED DILUENT FOR THE SOLVENT EXTRACTION
OF GOLD(I) CYANIDE FROM ALKALINE SOLUTION

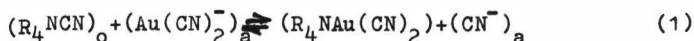
T. GROENEWALD, Chamber of Mines of South Africa
P.O. Box 61809, Johannesburg, South Africa.

SYNOPSIS

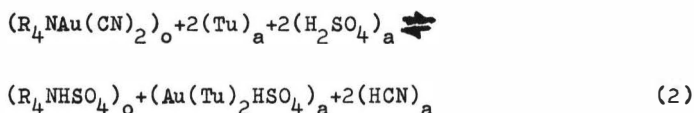
The solvent extraction of gold(I)cyanide from alkaline cyanide medium into kerosene containing methyl tri-n-alkyl (C_8 to C_{10}) ammonium ion was investigated. If instead of the long-chain alcohols which are traditionally used as modifiers, highly polar solvents such as the sparingly soluble ketones were added to the kerosene diluent, the severe emulsification of the phases was eliminated, and the extraction efficiency of the amine extractant was enhanced synergistically.

INTRODUCTION

The solvent extraction of the gold(I)cyanide ion from alkaline cyanide leach liquors by means of long-chain amines dissolved in organic diluents has been investigated quite widely.¹⁻⁸⁾ For a quaternary ammonium salt, the extraction process may be written as⁽⁸⁾



For some amines the equilibrium constant for this reaction is so high that it is difficult to find aqueous cyanide solution conditions which will reverse the reaction with any efficiency. However, the gold(I) may be stripped into acidic solutions of thiourea(Tu)⁴⁻⁷ as the cationic complex⁽⁹⁾ $Au(Tu)_2^+$



where the subscripts refer to the organic(o) and aqueous(a) media.

The choice of diluent for the amine extractant in an industrial process is virtually restricted to solvents of the hydrocarbon type such as kerosene because a large solvent loss due to solubility of the diluent in the aqueous phase is unacceptable. It is thus not possible to use many organic diluents which by virtue of their different aliphatic or aromatic contents⁽¹⁰⁾ or increased polarity^(11a) would result in improved extraction efficiency.

It has been found that the efficiency of extraction increases along the series secondary⁽¹⁾ to tertiary⁽²⁻⁶⁾ to quaternary ammonium salts^(7,8), but that this advantage is reduced by an increasing tendency towards emulsion formation. Modifiers such as long-chain alcohols are often used to decrease the extent of emulsion and of third-phase formation, but this type of modifier was found to have the disadvantage of reducing the extraction efficiency of the amine extractant^(11a) to a level unsuitable for practical application⁽⁷⁾. It was thought that it might be possible to avoid this disadvantage by selecting as

modifier one of the sparingly soluble ketones which have been used as diluents for quaternary ammonium compounds in the extraction of gold(I)cyanide from aqueous solution^(8,12). On the basis of the solubility data^(11b,13) (see table 1), the loss due to solubility of a ketone such as diisobutyl ketone from the system would compare favourably with that found for some of the long-chain alcohols such as decanol which is used widely as a modifier in some solvent extraction process⁽¹⁴⁾.

This paper summarises the results obtained in a study of the extraction of gold(I)cyanide from alkaline solutions using methyl tri-n-alkyl (C₈-C₁₀) ammonium salt in a kerosene diluent modified with diisobutyl ketone, as well as the stripping of the gold into acidic solutions of thiourea. This extractant was reported to have a relatively high extraction efficiency⁽⁷⁾. The effect of the concentration of ketone modifier was investigated, and it was found that a diluent containing 30% diisobutyl ketone offered the best balance of conditions for an extraction process; the more detailed investigations were restricted to the use of this diluent composition.

The extraction process

The extraction equilibrium constant (K) is given by⁽⁸⁾

$$K = \frac{(R_4NAu(CN)_2)_o (CN^-)_a}{(R_4NCN)_o (Au(CN)_2^-)_a} \quad (3)$$

and provided the activity coefficients of gold in the organic and aqueous phases are equal, which is reasonable when the concentrations are low,

$$K = D(CN^-)_a / (R_4NCN)_o \quad (4)$$

where D is the distribution ratio of the gold. A plot of

$\log((R_4NAu(CN)_2)_o (CN^-)_a / (R_4NCN)_o)$ versus $\log(Au(CN)_2^-)_a$ should be linear and of unit slope with an intercept on the y-axis at $\log(Au(CN)_2^-)_a = 0$ of $\log K$.

$$\text{Also, } (15) \quad D = (\text{Au})_o / (\text{Au})_a \quad (5)$$

$$= c((\text{R}_4\text{N}^+)_o^i - n(\text{Au})_o)^d \quad (6)$$

where the superscript i indicates initial concentration, c is a proportionality constant equal to $K/(\text{CN}^-)_a$ and n is the number of extractant molecules associated with each molecule of the gold species in the organic phase. Since the power term d equals unity, a plot of $1/(\text{Au})_o$ versus $1/(\text{Au})_a$ is linear with slope $1/c(\text{R}_4\text{N}^+)_o^i$ and y-axis intercept $n/(\text{R}_4\text{N}^+)_o^i$.

EXPERIMENTAL

Methyl tri-n-alkyl ($\text{C}_8\text{-C}_{10}$) ammonium chloride was commercially available as Aliquat 336 (General Mills Inc.) The organic phases were prepared by dissolving weighed amount of Aliquat 336 in kerosene containing known percentages of diisobutyl ketone. The Aliquat 336 was converted to the cyanide form by pre-equilibration with alkaline cyanide solution. The solutions of gold in cyanide medium were prepared using potassium aurocyanide ($\text{KAu}(\text{CN}_2)$) and potassium cyanide. In some instances the pH of the solutions was maintained at fairly constant levels with carbonate/bi-carbonate buffers. The presence of buffer salts did not appear to affect the extent of extraction of the gold significantly. The pH was measured by means of a glass electrode.

All experiments involved the use of separating funnels, usually under ambient conditions of temperature (20 to 25°C). In the case of the stripping experiments, the gold(I)cyanide was first taken into the organic phase in the same way as for forward extraction studies, and then stripped into the acidic solutions of thiourea; occasionally, precipitation of solid salts of gold was observed in the aqueous phase, in which case these experiments were repeated at 50 or 70°C. The concentrations of gold in the aqueous and organic phases were determined by atomic absorption spectrometry (12, 16).

The loss of diisobutyl ketone from the kerosene solutions due to solubility in the aqueous phase was determined by measurement of the refractive index of the kerosene solutions.

RESULTS

The extraction of gold(I)cyanide

In preliminary experiments it was noticed that there was an apparent loss of gold from the system. This was traced to the formation of very small amounts of a dense third liquid-phase, which was immiscible with water or pure kerosene, but which was miscible with pure diisobutyl ketone; such small volumes were difficult to isolate, but one sample had a gold concentration of over 0.8M. The apparent loss of gold could be used to identify the onset of third-phase formation. Figure 1 shows the lowest concentration of Aliquat 336 which was tested and at which there was definitive evidence of third-phase formation, the figure also shows the highest concentration tested without there being a significant loss of gold. It was thus possible to select a safe maximum concentration of Aliquat 336; e.g. up to 4 or 8×10^{-3} M Aliquat 336 in 30% diisobutyl ketone in kerosene could be used before onset of third-phase formation.

Equilibrium studies

In the light of the above, the present studies were largely confined to the diluent composed of 30. diisobutyl ketone in kerosene. The concentration of Aliquat 336 was varied between 4×10^{-4} and 4×10^{-3} M, the cyanide concentration between 0.01 and 0.1M and the initial concentration of gold(I)cyanide in the aqueous phase between $(0.1 \text{ and } 4.0) \times 10^{-5}$ M, i.e. less than 0.1 times the stoichiometric amount of Aliquat 336 in the organic phase. The phase volume ratio (organic to aqueous) was 1:30. The equilibrium pH depended primarily upon the cyanide concentration, but also upon the Aliquat 336 concentration. When $(\text{CN}^-) = 10^{-2}$ M, pH=10.4 (4×10^{-3} M Aliquat 336) and pH=10.2 (4×10^{-4} M Aliquat 336) and when $(\text{CN}^-) = 10^{-1}$ M, the pH values were 11.2 and 10.8, respectively. Correction⁽¹⁷⁾ was made for the activity coefficients of the aurocyanide and cyanide ions ($\gamma = 0.74$ at an ionic strength $I=0.1$ M, and $\gamma = 0.90$ at $I=0.01$ M) and for the equilibrium $\text{H}^+ + \text{CN}^- \rightleftharpoons \text{HCN}$ ($K_a = 10^{9.3}$).

The results are shown in Figure 2, plotted according to Eq.3. The slope of the line was 0.96 with a standard deviation of 0.05 and correlation coefficient 0.968. Calculation of K directly by Equation 3 gives $K=9.0 \times 10^4$ with a standard deviation of 2.4×10^4 .

When the concentration of gold in the aqueous phase was varied between $(0.15 \text{ and } 2.0) \times 10^{-4} \text{ M}$, and contacted with a diluent containing $3.5 \times 10^{-3} \text{ M}$ Aliquat 336 using a phase volume ratio of 1:30, a typical extraction equilibrium isotherm was obtained (Figure 3); calculation by Equation 6 indicated $K=5.96 \times 10^4$ (standard deviation 0.75×10^4), and $n=1.5$.

A few exploratory studies were performed in which the gold was extracted from 0.01M cyanide solution at pH10, and the concentrations of gold were measured using radiotracer techniques with the isotope ^{198}Au ($t_{1/2} = 2\frac{1}{7}$). When pure kerosene was used as diluent for the Aliquat 336, exceedingly stable emulsions were formed which could not be broken. In pure diisobutyl ketone, $K = 3 \times 10^5$ and in 20% decanol in kerosene, $K = 6 \times 10^3$. These values should really be regarded only as indicative of the order of magnitude of K in these systems.

The stripping of gold(I) by acidic solutions of thiourea

The extent to which gold was stripped from diluents containing 10^{-2} M Aliquat 336 and 10^{-4} M gold(I)cyanide into equal volumes of 1.0M sulphuric acid containing between 0.01 and 1.0M thiourea decreased with decreasing concentration of thiourea and with increasing proportion of diisobutyl ketone in the kerosene (Figure 4). Variation of the concentration of Aliquat 336 between $(0.5 \text{ and } 1.5) \times 10^{-3} \text{ M}$ had little effect upon the result.

Equilibrium studies

Stripping equilibrium curves (20°C) using solutions of thiourea (1.0, 0.5, and 0.2M) and sulphuric acid (1.0 and 0.1M) at a phase volume ratio (organic to aqueous) of unity are shown in Figure 5. When the phase volume ratio was changed to 20:1 and to 50:1, and the gold in the aqueous phase exceeded $3 \times 10^{-3} \text{ M}$, a third phase consisting of a fine white crystalline solid was formed, which could account for as much as 25% of the gold in the system.

The precipitation of the solid phase was promoted by an increase in the sulphate concentration in the aqueous phase. This solid was more soluble in the aqueous phase at elevated temperatures, and stripping equilibrium curves were determined at 50°C with a phase volume ratio of 50:1 (Figure 6); the concentration of gold in the aqueous phase was found to reach almost 0.1M.

The validity of the equilibrium reaction (Equation 2) could not be confirmed with the data obtained in this investigation. Only the concentrations of the gold in the respective phases and the pH were measured, and the concentrations of the other terms were calculated by assuming that the cyanide in the diluent was replaced by bisulphate ion, and that hydrogen cyanide itself was not removed from the aqueous phase, by distribution between the diluent, or by loss to the small gas space in the apparatus, or by rapid hydrolysis or decomposition in the system. Any one of these assumptions could be invalid under the conditions obtaining in this experiment.

Alternative stripping reagents

When the gold was stripped into 1M hydrochloric acid solution containing 1M thiourea, the maximum concentration of gold attained was only $3.4 \times 10^{-3} \text{M}$.

Perchloric acid solutions containing thiourea were found to be effective for stripping the gold. Stripping equilibrium curves for a phase volume ratio of 50:1 at 20°C and at 50°C are shown in Figure 7. The concentrations of the gold in the perchloric acid solutions were found to be as high as $1.9 \times 10^{-1} \text{M}$. Often supersaturation of the aqueous phase appeared to occur, and the phases could be separated before precipitation of the gold as a white needle-like crystalline compound occurred. This formation was promoted by addition of perchlorate ion. In cases where the gold precipitated before the phases could be separated, the precipitate was redissolved by heating both phases to 70°C. This accounts for the S-shape of the equilibrium curves in Figure 7.

The solubility of diisobutyl ketone in water

The solubility of the diisobutyl ketone in water in contact with a diluent system containing various proportions of diisobutyl ketone in kerosene is shown in Figure 8. The distribution ratio of diisobutyl ketone between kerosene and water was 2×10^3 (relative standard deviation of 18% for 12 determinations).

DISCUSSION

The results obtained in this investigation are summarised in Table 2. Equilibrium curves for the extraction of gold(I)cyanide from 0.021M cyanide at pH 8 to 9 into 30% decanol in tetradecane containing a variety of quaternary ammonium salts have been reported.⁽⁷⁾ From these data the relevant extraction equilibrium constants have been calculated and compared (Table 2); the extraction efficiency of the methyl tri-n-alkyl (C_8 to C_{10}) ammonium salt compares favourably with those found for the other extractants.

As the proportion of polar solvent such as diisobutyl ketone (dipole moment 2.74 Debye) in the kerosene (dipole moment approximately zero) increased; the value of the equilibrium constant K increased by as much as two orders of magnitude as the composition of the phase changed from pure kerosene to pure diisobutyl ketone. A less polar solvent such as n-decanol (dipole moment 1.63 Debye) appeared to have little beneficial effect upon the extraction efficiency of the Aliquat 336. This may be due to some chemical interaction between the alcohol and amine in the organic phase^(11a).

Optimum extraction of the gold from cyanide solutions, and the subsequent stripping of the gold was effected by an organic phase consisting of about $4 \times 10^{-3}M$ Aliquat 336 in 30% diisobutyl ketone in kerosene. This solution could be loaded to about $2.6 \times 10^{-3}M$ gold, and it was found that the extraction and stripping cycle could be repeated with no apparent decrease in efficiency of the processes. By using the McCabe-Thiele construction, it could be predicted that the gold may be extracted in about three

theoretical stages, thereby increasing the concentration of the gold by a factor of between 25 and 50. The resultant organic phase can be stripped in about four theoretical stages, giving a further overall increase in the concentration of the gold by a factor of between 50 and 70. It was assumed that the cyanide solution would initially contain either 5×10^{-5} or 1×10^{-4} M gold, and the raffinate 10^{-8} M gold, and also that the loaded solvent would contain 2.5×10^{-3} M, and the scrubbed solvent 2.5×10^{-5} M, while at 70°C the acidic thiourea (perchlorate) could be loaded to 0.15 M gold, and be stripped electrochemically^(18,19) to 2.5×10^{-3} M.

The saturation solubility of diisobutyl ketone in water can be estimated (Figure 8) as about 270 p.p.m. in reasonable agreement with the previous estimate⁽¹³⁾ of 600 p.p.m. at 20°C . The loss of diisobutyl ketone by solution in water from a kerosene diluent containing 30% diisobutyl ketone would thus be less than 100 p.p.m. and of the same order of magnitude as the solubility loss of n-decanol, which has been used in proportions up to 30% in tetradecane to prevent formation of emulsions with alkaline cyanide solutions; not more than about 1% of the diisobutyl ketone in the diluent should be lost per cycle, assuming a phase volume ratio of 1:30.

CONCLUSIONS

Whereas the extent of extractions of gold(I)cyanide increases as the proportion of a polar modifier such as diisobutyl ketone in the kerosene diluent increases, the extent of stripping into acidic solutions of thiourea decreases accordingly. The composition of the diluent must therefore be selected to ensure optimum recovery, bearing in mind that the solvent losses due to solubility of the diluent medium in the aqueous phase will increase with the proportion of polar solvent used.

The modifiers which are used to prevent the emulsification of diluents such as kerosene with alkaline aqueous media, as well as the formation of third phases, should also be chosen with a view to enhancing the extraction efficiency of the amine.

In this regard the sparingly soluble ketones appear to have an advantage over the alcohols which do not appear to enhance the extraction efficiency.

ACKNOWLEDGEMENTS

The technical assistance of Miss. L.M.D. Jones and Mrs. H.S. Stenton is gratefully acknowledged, as is the least square-analysis of some of the results by means of the computer by Mr. D.A. Roberts. Permission to publish this paper was granted by the Chamber of Mines of South Africa.

REFERENCES

1. MADIGAN, D.G., "The amine extraction of gold from cyanide solution", Amdel Bull., (1968), No.6, 1-6
2. PLAKSIN, I.N. and SHIVRIN, G.N., "The mechanism of extraction by amines in alkali" Dokl.Akad.Nauk.SSSR(1963), 150, 870-3.
3. ZVYAGINTSEV, O.E., ZAKHAROV-NARTSISOV, O.I., and OCHKIN, A.V. "Extraction of hydrogen dicyanoaurate(I) with tri-n-octylamine, Russ. J. Inorg.Chem., (1961),6, 1012-3.
4. PLAKSIN, I.N., LASKORIN, B.N., and SHIVRIN, G.N., "Solvent extraction of complex gold and silver cyanides from cyanide solution", Tsvet.Metal.,(1961),34 19-22.
5. CHERNYAK, A.S., SKOBEEV, I.K. NAVTANIVUCH, M.L., IVANOV,O.P., ORECHKIN, O.B., and SHEPOT'KO, O.F., "Extracting gold and silver from cyanide solutions using technical mixtures of amines", Tsvet.Metal.,(1967),40,24-7.
6. PLASKIN, I.N., and SHIVRIN, G.N., "The rules governing the distribution of cyanide complexes of noble metals during extraction", Izv. VUZ, Tsvet.Met.(1965) 2, 50-7.

7. SHIVRIN, G.N., BASOV, A.S., LASKORIN, B.N., and SHIVRINA, E.M., "Extracting noble metals from cyanide solutions with quaternary ammonium compounds", *Tsvet.Metal.*, (1966), 39, 19-23
8. IRVING, H.M.N.H., and DAMODARAN, A.D., "The extraction of complex cyanides by Liquid ion-exchangers". *Anal.Chim.Acta*, (1971), 53, 267-75.
9. KAZAKOV, V.P., LAPSHIN, A.I., and PESHCHEVITSKI, B.I., "Redox potential of the gold(I)thiourea complex" *Russ.J.inorg.Chem.*, (1964), 9, 708-9.
10. RITCHEY, G.M., "Solution purification by ion exchange or solvent extraction", Information Circular IC 237, November, 1971, Department of Energy, Mines and Resources, Ottawa, Canada.
11. MARCUS, Y., and KERTES, A.S., "Ion exchange and solvent extraction of metal complexes" Wiley-Interscience (1969), (a)783-7(b)932-3(c)757-65.
12. GROENEWALD, T., "Determination of gold(I) in cyanide solutions by solvent extraction and atomic absorption spectrometry", *Anal.Chem.*, (1968), 40, 863-6.
13. MARSDEN, C., "Solvents Manual" Cleaver-Hume Press Ltd., London (1954).
14. MEYBURGH, B.G., "The design, erection and operation of a Purlex plant at Buffelsfontein Gold Mining Company Ltd.", *J.S.Afr. Inst.Min. Metall.*, (1970), 71, 55-66.
15. LLOYD, P.J.D., AND OERTEL, M.K., "A theoretical basis for the evaluation of long-chain amine extractants and its application in design calculations for separation efficiencies and the number of theoretical stages", *Unit Processes in Hydrometallurgy*, (1963), 24, 453-77.

16. GROENEWALD, T. and JONES, B.M., "Determination of gold in solutions of thiourea", Anal.Chem.(1971), 43 1689-91.
17. BUTLER, J.N., "Ionic equilibrium - a mathematical approach" Addison-Wesley Publ.Co.(1963).
18. BEK, R. Yu, MASLII, A.I. and LAVROVA, T.A., "Electrode reactions in the electrolytic recovery of gold from thiourea solution", Tsvet.Metal-, (1969), 42 69-73.
19. MASLII, A.I. and ZADONSKAYA, A.Y., "Kinetics of the electrolytic separation of gold from thiourea solutions", Siverian J.Chem., (1970), 2, 61-5.

T A B L E 1

Physical properties of some organic solvents (11b)

Solvent	Di-electric constant	Dipole moment (Debye)	Solubility(%w/w)	
			Water in organic	Organic in water
n-Hexane	1.910	0.0	--	0.001
n-Heptane	1.924	0.0	--	0.0003
n-Octane	1.948	0.0	--	0.0001
Kerosene	2*	0.0*	--	0.0001*
Cyclohexane	2.10	0.0	--	0.006
Benzene	2.28	0.0	0.072	0.178
Toluene	2.38	0.4	0.042	0.050
o-xylene	2.57	0.5	--	0.018
Di-n-propylether	3.39	1.18	0.45	0.49
Di-n-butylether	3.08	1.22	--	0.03
Di-n-hexylether	--	--	0.12	0.01
Me-i-butyl ketone	13.11	2.76	1.9	1.7
Diisobutyl ketone	13*	2.74	0.45	< 0.06
n-butyl acetate	5.1	1.85	1.37	1.0
i-butyl acetate	5.3	1.86	1.65	0.67
n-hexanol	13.3	1.64	7.2	0.56
n-octanol	10.3	1.68	--	0.03
n-decanol	8.1	1.63	3.0	0.02

* Estimated value.

TABLE 2

Summary of extraction data for the extraction of
gold(I)cyanide by a variety of quaternary ammoni-
um compounds(QAC)

Quaternary ammonium compound	Extraction Equilibrium Constant(K)		* n	Medium	Remarks	Ref.
	K.	Std. Error of K.				
Dimethyl dialkyl (C ₁₇ -C ₂₀)	2x10 ²		1.4	0.03M QAC in 30% decanol/tetradecane	--	7
Dimethyl alkyl (C ₁₇ -C ₂₀)benzyl	5x10 ²		2.1	"	--	7
Dimethyl alkyl (C ₁₀ -C ₁₆)benzyl	5x10 ²		2.0	"	--	7
Methyl Dialkyl (C ₁₇ -C ₂₀)benzyl	2x10 ³		2.8	"	--	7
Trialkyl(C ₈)benzyl	2x10 ³		2.2	"	--	7
Trimethyl alkyl (C ₁₇ -C ₂₀)	--		--	"	Stable emulsion formed	7
Trimethyl alkyl (C ₁₀ -C ₁₆)	--		--	"	"	7
Methyl trialkyl(C ₈)	1.1x10 ³	0.2x10 ³	1.75	"		7
Methyl trialkyl(C ₈)	3.2x10 ³	0.7x10 ²	1.75	7.8x10 ⁻³ M QAC in diesel fuel.		7
Methyl trialkyl (C ₈ -C ₁₀) (Aliquat 336)	3x10 ⁵	--	--	10 ⁻⁶ to 10 ⁻² M QAC in diisobutyl ketone.		this study
Methyl trialkyl (C ₈ -C ₁₀) (Aliquat 336)	6x10 ³	--	--	10 ⁻⁶ to 10 ⁻² M QAC in 20% decanol/kerosene.		"
Methyl trialkyl (C ₈ -C ₁₀) (Aliquat 336)	6.0x10 ⁴	0.7x10 ⁴	1.5	4x10 ⁻⁴ to 4x10 ⁻³ M QAC in 30% diisobutyl ketone/kerosene		"
Tetra-n-hexyl	1.58x10 ¹	--	--	Methyl isobutyl ketone		8

*n = ratio of QAC molecules to gold atoms in the organic phase.

FIGURE 1 CONDITIONS FOR THE FORMATION OF A THIRD PHASE DURING SOLVENT EXTRACTION OF $Au(CN)_2^-$ BY ALIQUAT 336 IN DIISOBUTYL KETONE / KEROSENE SOLUTION.

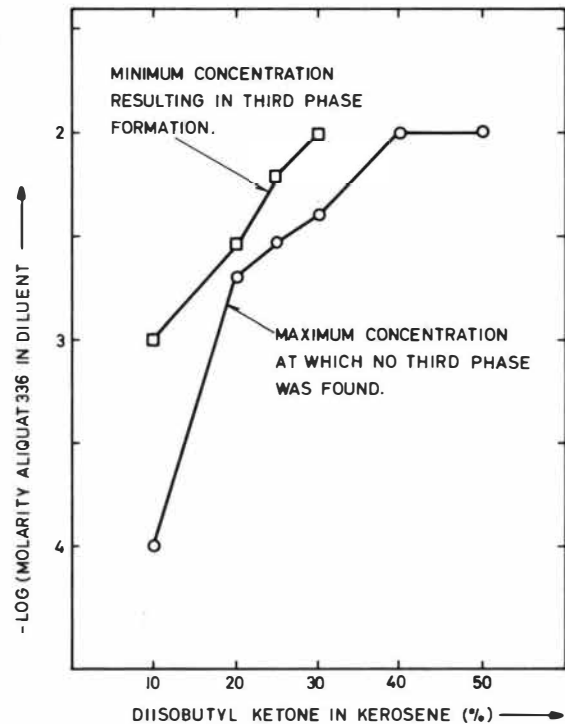


FIGURE 2. THE EXTRACTION OF $Au(CN)_2^-$ BY SOLUTIONS OF ALIQUAT 336 IN 30% DIISOBUTYL KETONE IN KEROSENE AT 20°C.

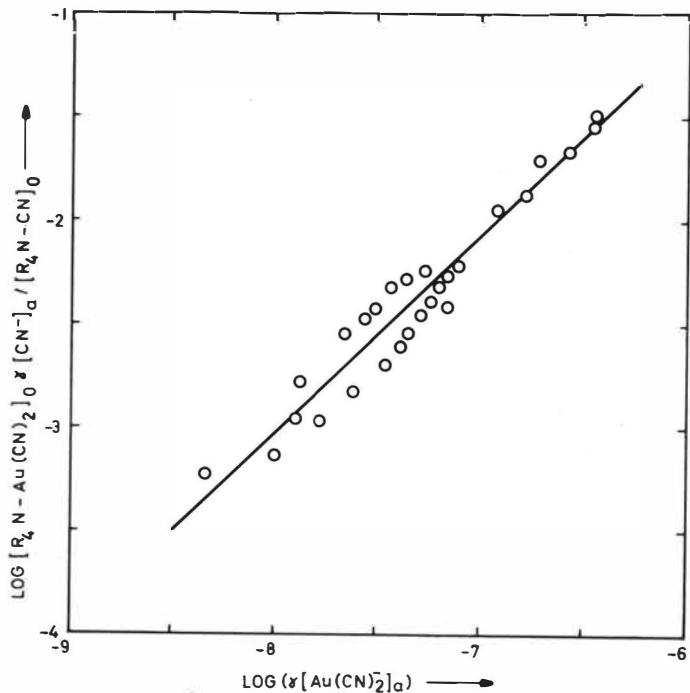


FIGURE 3. EXTRACTION OF $\text{Au}(\text{CN})_2^-$ BY SOLUTIONS OF $3.5 \times 10^{-3} \text{ M}$ ALIQUAT 336 IN 30% DIISOBUTYL KETONE IN KEROSENE AT 20°C .

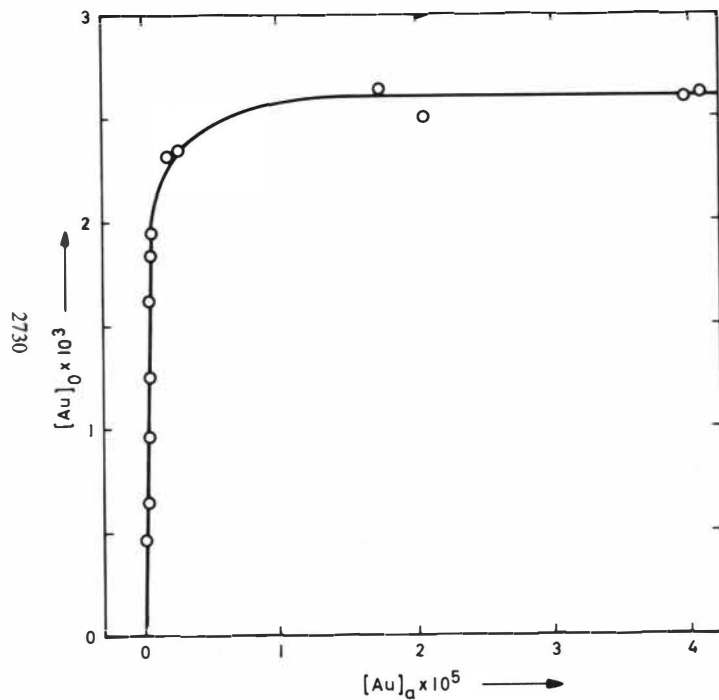


FIGURE 4. STRIPPING OF $\text{Au}(\text{CN})_2^-$ FROM DIISOBUTYL KETONE / KEROSENE MIXTURES CONTAINING $4 \times 10^{-3} \text{ M}$ ALIQUAT INTO SOLUTIONS OF THIOUREA (Tu) AND 1.0 M SULPHURIC ACID AT 20°C (INITIAL CONCENTRATION OF GOLD IN THE KEROSENE = $1.0 \times 10^{-4} \text{ M}$.)

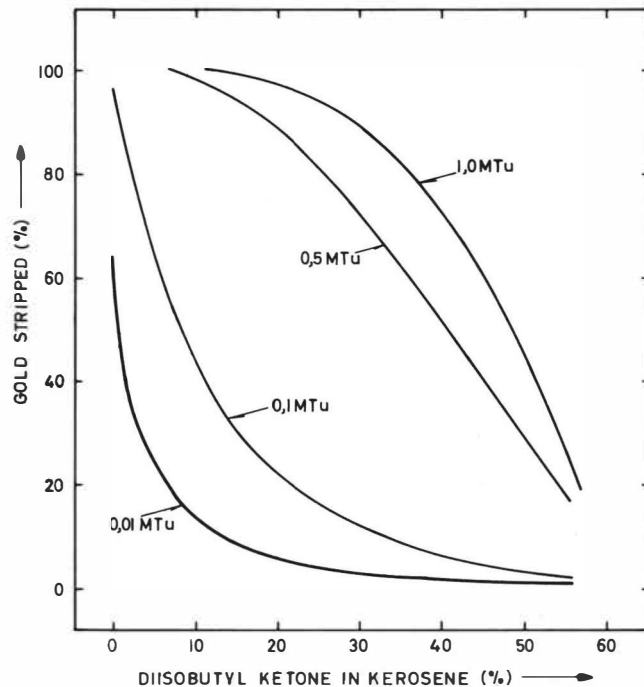


FIGURE 5. STRIPPING OF $\text{Au}(\text{CN})_2^-$ FROM 30% DIISOBUTYL KETONE / KEROSENE CONTAINING $4 \times 10^{-3} \text{ M}$ ALIQUAT 336 INTO SOLUTIONS OF THIOUREA (Tu) AND SULPHURIC ACID AT 20°C (PHASE VOLUME RATIO = 1:1)

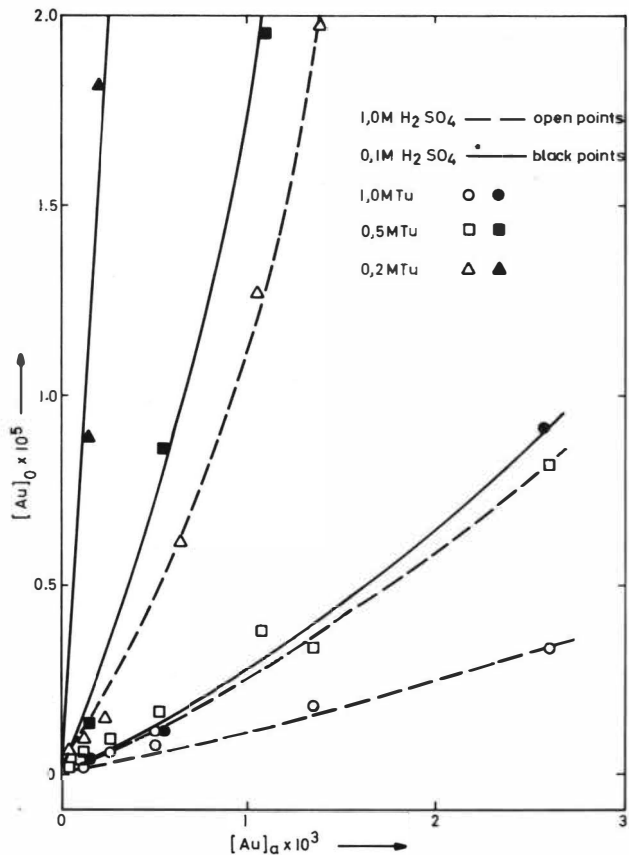


FIGURE 6. STRIPPING OF $\text{Au}(\text{CN})_2^-$ FROM 30% DIISOBUTYL KETONE / KEROSENE CONTAINING $4 \times 10^{-3} \text{ M}$ ALIQUAT 336 INTO SOLUTIONS OF THIOUREA (Tu) AND $1,0 \text{ M}$ H_2SO_4 AT 50°C (PHASE VOLUME RATIO = 50:1)

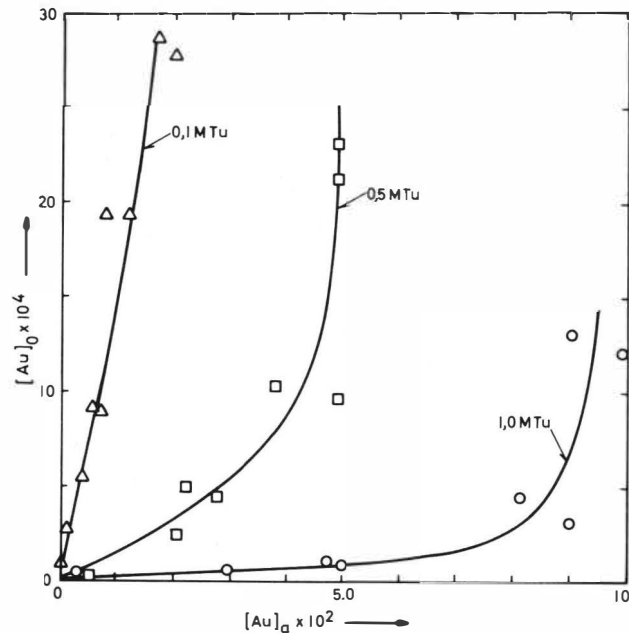


FIGURE 7. STRIPPING OF $\text{Au}(\text{CN})_2^-$ FROM 30% DIISOBUTYL KETONE / KEROSENE CONTAINING $4 \times 10^{-3} \text{M}$ ALIQUAT 336 INTO SOLUTIONS OF THIOUREA (Tu) AND PERCHLORIC ACID. (PHASE VOLUME RATIO = 50:1)

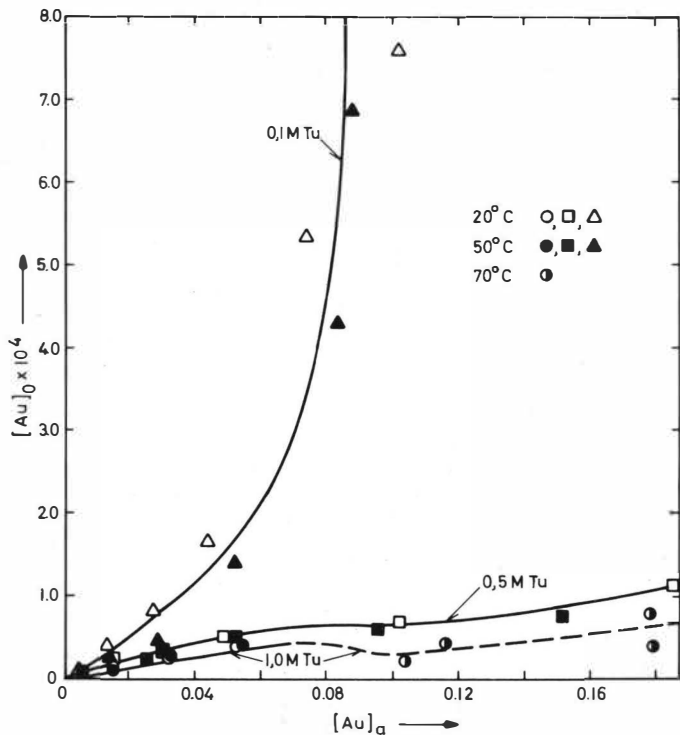
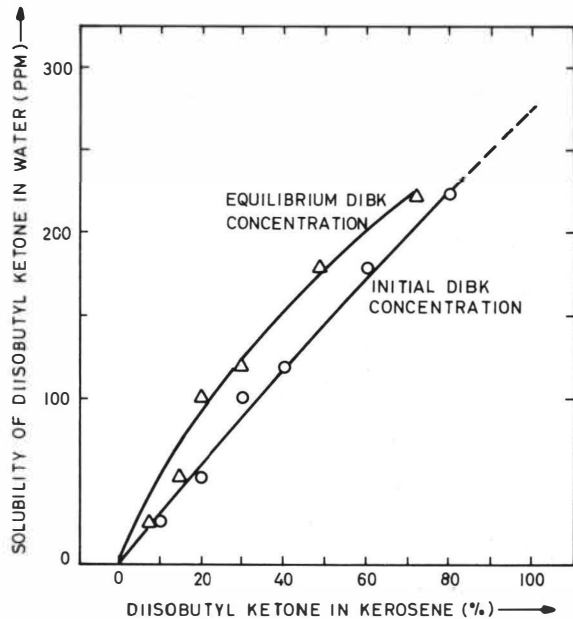


FIGURE 8. SOLUBILITY OF DIISOBUTYL KETONE IN WATER IN EQUILIBRIUM WITH A SOLUTION OF DIISOBUTYL KETONE (DIBK) IN KEROSENE.



SOLVENT EXTRACTION OF SILVER(I) AND MERCURY(II) WITH
SULPHUR CONTAINING LIGANDS

by D. Sevdic

Institute "Rudjer Bošković", Zagreb, Yugoslavia

SYNOPSIS

The solvent extraction of silver(I) and mercury(II) with tetradentate (TTP) and octadentate (OTO) macrocyclic ligands containing only sulphur as donor has been studied. The experiments were carried out from chloride and perchlorate solutions. The extraction dependence of silver and mercury on chloride, perchlorate and ligand concentrations has been investigated. In the presence of perchlorate ions different extraction behaviour, especially for silver, has been found. On the basis of the results obtained, the extraction mechanism is discussed.

INTRODUCTION

Recently cyclic polyethers and related cyclic ligands have attracted much interest because of their unusual metal binding properties^{1,2}. During the last few years several macrocyclic ligands containing only thioether donors have been synthesized^{3,4} and their metal ion complexes have been prepared and characterized^{5,6,7}. These new complexes illustrate the relationships among macrocycle ring size, donor atom type and mode of chelation. The formation of complexes of macrocyclic polyether ligands with alkali, alkaline earth and silver cations was investigated by Pedersen⁸. It was found that macrocyclic polyether sulfides are poorer complexing agents for sodium and potassium than the oxygen analogs, but that are good for complexing silver.

In our earlier investigations we studied the solvent extraction of mercury(II)^{9,10} and silver(I)¹¹ with thiophosphorus compounds. Since silver and mercury have a good affinity toward sulphur containing ligands, we chose two tetradentate and octadentate macrocyclic ligands containing only sulphur donors for our new solvent extraction investigations. We synthesized 1,4,8,11-tetrathiacyclotetradecane (TTP)³ and 1,4,8,11,15,18,-22,25-octathiacyclooctacosane (OTO)⁶ to investigate the solvent extraction of silver and mercury with them.

EXPERIMENTAL

Reagents

1,4,8,11-tetrathiacyclotetradecane (TTP) was prepared according to the method described by Rosen and Busch³.

1,4,8,11,15,18,22,25-octathiacyclooctacosane (OTO) was synthesized by the method similar to that of Travis and Busch⁶.

Nitrobenzene (Merck p.a.) was used as a solvent in all experiments.

Radioactive tracers and standard metal solutions

Radioactive tracers ^{110}Ag and ^{203}Hg were obtained from the New England Nuclear Corp. The initial concentrations of mercury in the aqueous phase were 10^{-6}M , while silver was in tracer concentrations. Sodium chloride, hydrochloric and perchloric acids (Merck p.a.) were used to adjust the ionic strength. Sodium perchlorate was prepared from sodium carbonate (Merck p.a.) and perchloric acid.

Distribution measurements

It has been found that the equilibrium in investigated systems is attained after ten minutes. A stirring time of twenty minutes was used in all experiments. The investigations were carried out at 24°C . Equal volumes (2 ml) of organic and aqueous phases were used. After stirring, the phases were separated by centrifugation and the γ -activity of the organic and water aliquots (1 ml) were determined using a γ -scintillation counter.

RESULTS

Nitrobenzene was used as a solvent because in the other solvents such as benzene, carbon tetrachloride and chloroform, a loss of activity has been observed.

Dependence of the extraction on the reagent concentration

The experiments were carried out from $/H^+/=0.5M$, $/Cl^-/=0.5M$, $/H^+,Na^+,Cl^-,ClO_4^-/=2M$ and $/H^+/=0.5M$, $/Cl^-/=0.5M$ aqueous solutions. The dependence of silver and mercury extraction on TTP concentration is shown in Fig. 1. Depending on the kind of anions present in the aqueous phase, a different extraction behaviour was observed. Linear dependencies were obtained from chloride solutions, with slopes of 0.9 and 1 for silver and mercury respectively. When extraction was carried out from solutions containing both chloride and perchlorate ions, similar results were obtained for mercury, except that the distribution coefficients were somewhat higher. However, a rather different extraction behaviour was observed for silver. In the linear portion of the curve, the slopes vary from 1 to 2.5, depending on the reagent concentration. In addition, the distribution coefficients are about three orders of magnitude higher in comparison with those obtained from solutions containing only chlorides.

The extraction dependence of silver and mercury on OTO concentration is represented in Fig. 2. The same slopes were obtained for TTP and OTO as ligand, except that the distribution coefficients are only about one order of magnitude higher for OTO.

Dependence of the extraction on chloride concentration

The experiments were carried out from solutions containing both chloride and perchlorate anions with constant ionic strength ($/H^+/=0.5M$, $/H^+,Na^+,Cl^-,ClO_4^-/=2M$), as well as from solutions containing chloride ions only. In the latter case the ionic strength was not constant. Therefore, the activity of the chloride ions was calculated for each concentration and the values were plotted in graphs.

The dependence of silver and mercury extraction with TTP on chloride ion concentration is shown in Fig. 3. From the solutions containing perchlorate ions, the slopes in the linear parts of the curve range from -1.5. to -2.5 for mercury, while the slope for silver is -2. From chloride solutions slopes vary from -1.5 to -2.2 and -2 for silver and mercury respectively.

In Fig. 4. experimental results for the extraction dependence of silver and mercury with OTO as reagent on chloride ion concentration are given. From solutions containing both perchlorate and chloride ions slopes of -2.1 for silver and -2.5 for mercury were obtained. The results from solutions containing only chloride ions show that in the linear parts of the curves slopes vary from -1.5 to -2.3 and -2 for silver and mercury respectively.

Dependence of the extraction on perchlorate concentration

The dependence of silver and mercury extraction with TTP and OTO on perchlorate ion concentration from solutions with constant hydrogen (0.2M) and chloride (0.2M) ion concentrations is represented in Fig. 5. The activity of the perchlorate ions was calculated and plotted in the graph. With TTP as the reagent,

slopes of 0.4 for silver and 0.5 for mercury were obtained. When OTO was used as the reagent, these slopes are 0.3 and 0.45 for silver and mercury respectively.

DISCUSSION

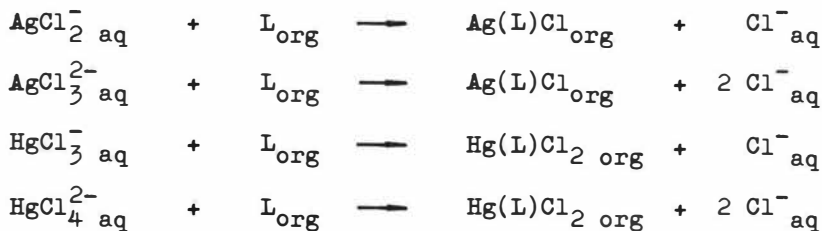
In our previous investigations of the solvent extraction of silver and mercury with thiophosphorus compounds from chloride solutions with constant ionic strength ($[H^+, Na^+, Cl^-, ClO_4^-] = 1M$), we have found that, depending on the reagent concentration, the number of ligands in complexes varies from one to four and one to two for mercury and silver respectively^{9,10}. It was also found that the presence of perchlorate ions in solutions did not affect the extraction of silver and mercury.

However, quite different results were obtained in investigations of the extraction of silver and mercury with macrocyclic ligands having thioether as donors. A pronounced dependence of the extraction on perchlorate ions has been established for both metals. Distribution coefficient values increase with increasing perchlorate ion concentration. Investigations of the extraction dependence of mercury on reagent concentrations indicate that one ligand is always bound to mercury regardless of the presence or absence of perchlorate ions. Distribution coefficients are only slightly higher when the extraction is carried out in the presence of perchlorate ions. Studies of extraction dependence of silver on ligand concentrations show that one ligand is bound to

silver when the extraction is carried out from chloride solutions. From perchlorate solutions the ligand/metal ratios for silver are always 2.5. In addition, the distribution coefficients were about three orders of magnitude higher which indicate that perchlorate ions have a greater influence on the formation and stability of silver complexes than on mercury complexes.

Depending on the chloride ion concentration in the aqueous phase, one and two chloride ions are probably released in the extraction of silver and mercury with both macrocyclic ligands. In the presence of perchlorate ions slopes of -2 and -2.5 for silver and mercury respectively were obtained.

The composition of the ionic species of silver and mercury in chloride solutions is well known¹². The complexes of silver and mercury with TTP which have the composition $\text{Hg}(\text{TTP})\text{Cl}_2$ and $\text{Ag}(\text{TTP})\text{X}$, where $\text{X}=\text{BF}_4^-$ and NO_3^- , have already been prepared and characterized⁷. On the basis of this data and our extraction studies, a simple extraction mechanism of silver and mercury with TTP and OTO from chloride solutions could be supposed:



The extraction mechanism from the solutions containing both chloride and perchlorate ions is rather complicated.

Without further extraction studies, and the isolation and characterization of the extracting species, it is very difficult to presume any kind of extraction mechanism. It could be only supposed that chloride ions are partially displaced by perchlorate ions.

On the basis of the results obtained by the investigation of the solvent extraction of silver and mercury with TTP and OTO from solutions containing both chloride and perchlorate ions, it can be assumed that a partial exchange of chloride ions with perchlorate ions takes place during the extraction process. So, in addition to Hg(L)Cl_2 , Hg(L)Cl/ClO_4 is probably formed, while for silver, the formation of Ag(L)Cl and $\text{Ag(L)}_2\text{ClO}_4$ complexes can be proposed. This different behaviour of silver and mercury can be explained by the fact that mercury complexes more strongly with halides than silver. Further studies are continuing in our laboratory.

Acknowledgement. The autor wishes to thank Dr. Henrike Meider for continual interest in this work and for valuable discussions.

REFERENCES

1. Pedersen C.J., J. Am. Chem. Soc., 1967, 89, 7017.
2. Lindoy L.F. and Busch D.H., Preparative Inorganic Reactions, 1971, 6, 1 (New York: John Wiley).
3. Rosen W. and Busch D.H., J. Am. Chem. Soc., 1969, 91, 4694.
4. Rosen W. and Busch D.H., Inorg. Chem., 1970, 9, 262.
5. Rosen W. and Busch D.H., Chem. Commun., 1969, 148.
6. Travis K. and Busch D.H., Chem. Commun., 1970, 1041.
7. Travis K., Dissertation, The Ohio State University, 1971.
8. Pedersen C.J., J. Org. Chem., 1971, 36, 254.
9. Sevdic D. and Meider-Goričan H., Proc. Int. Solvent Extraction Conf., 1971, 2, 1091 (London: Soc. of Chem. Industry).
10. Sevdic D. and Meider-Goričan, J. inorg. nucl. Chem., 1972, 34, 2903.
11. Sevdic D. and Meider H., unpublished work.
12. Marcus Y., Coord. Chem. Rev., 1967, 2, 257.

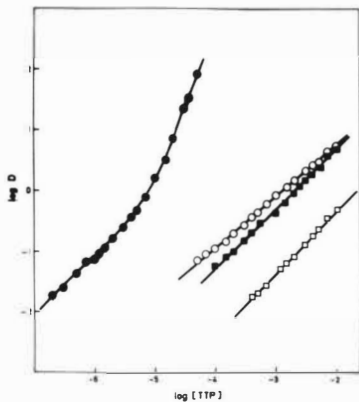


Fig. 1. Dependence of the extraction of Ag(I) (●, ○) and Hg(II) (■, □) on TTP concentration from $/H^+/=0.5M$, $/Cl^-/=0.5M$, $/H^+, Na^+, Cl^-, ClO_4^-/=2M$ (●, ■) and $/H^+/=0.5M$, $/Cl^-/=0.5M$ (○, □) aqueous solutions.

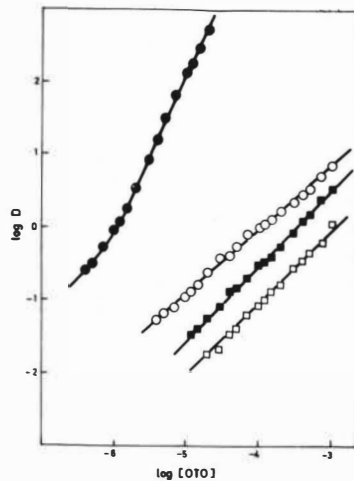


Fig. 2. Dependence of the extraction of Ag(I) (●, ○) and Hg(II) (■, □) on OTO concentration from $/H^+/=0.5M$, $/Cl^-/=0.5M$, $/H^+, Na^+, Cl^-, ClO_4^-/=2M$ (●, ■) and $/H^+/=0.5M$, $/Cl^-/=0.5M$ (○, □) aqueous solutions.

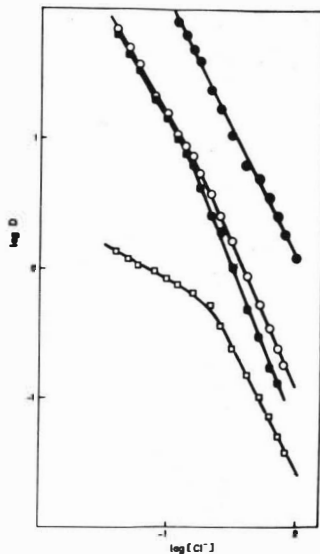


Fig. 3. Chloride ion dependence of the extraction of Ag(I) (●, ○) and Hg(II) (■, □) with TTP from $/H^+/=0.5M$, $/H^+, Na^+, Cl^-, ClO_4^-/=2M$: ● /TTP/ $=10^{-5}M$; ■ /TTP/ $=10^{-4}M$ and from chloride aqueous solutions: ○ /TTP/ $=10^{-4}M$; □ /TTP/ $=10^{-3}M$.

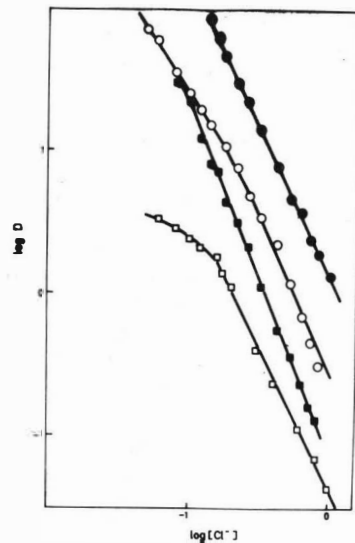


Fig. 4. Chloride ion dependence of the extraction of Ag(I) (●, ○) and Hg(II) (■, □) with OTO from $/H^+/=0.5M$, $/H^+, Na^+, Cl^-, ClO_4^-/=2M$: ● /OTO/ $=10^{-6}M$; ■ /OTO/ $=10^{-4}M$ and from chloride aqueous solutions: ○ /OTO/ $=10^{-5}M$; □ /OTO/ $=10^{-4}M$.

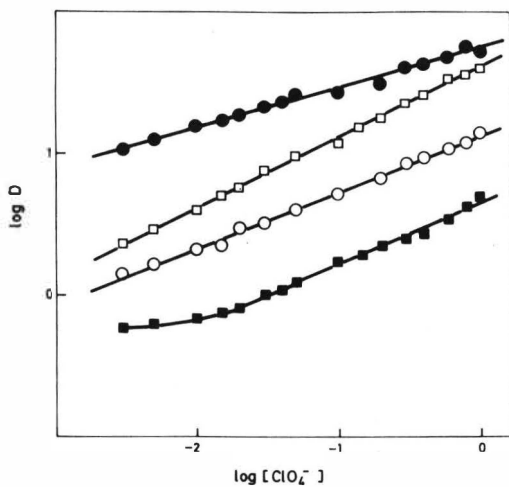


Fig. 5. Perchlorate ion dependence of the extraction of Ag(I) (●, ○) and Hg(II) (■, □) with TTP and OTO from $[H^+] = 0.2M$, $[Cl^-] = 0.2M$ aqueous solutions:
 ● /OTO/ = $10^{-6}M$, ○ /TTP/ = $10^{-5}M$ and ■ /OTO/ = $10^{-4}M$,
 □ /TTP/ = $10^{-2}M$.

THE CHEMICAL EQUILIBRIA AT DISTRIBUTION OF MERCURY (II)
CHLORIDE BETWEEN WATER AND SOLUTIONS OF TBP AND DI-n-OCTYL
SULPHOXIDE IN DIFFERENT DILUENTS

by V.A.Mikhailov, N.A. Korol and D.D.Bogdanova

Institute of Inorganic Chemistry, Novosibirsk, USSR.

The results of computer analysis of HgCl_2 distribution isotherms between water and dilute solutions of TBP and di-n-octyl sulphoxide (DOSO) in CCl_4 , C_6H_6 , CHCl_3 and 1,2- $\text{C}_2\text{H}_4\text{Cl}_2$ are given. For extraction by dialkyl sulphides the following species with TBP and DOSO are found in the organic phase: HgCl_2L , HgCl_2L_2 , $(\text{HgCl}_2\text{L})_2$, $(\text{HgCl}_2)_2\text{L}_2$. Experimental values of mean molecular weight of the solutes in benzene solutions containing mixtures of HgCl_2 and extractant are close to calculated ones. Extraction equilibrium constants and formation constants of complexes in different diluents are given and discussed.

Introduction

The distribution of HgCl_2 between water and solutions of dialkyl sulphides from $(\text{C}_4\text{H}_9)_2\text{S}$ to $(\text{C}_8\text{H}_{17})_2\text{S}$ in a row of diluents had been studied earlier. Computer analysis of the distribution isotherms established the formation of $\text{HgCl}_2\text{R}_2\text{S}$, $\text{HgCl}_2(\text{R}_2\text{S})_2$, $(\text{HgCl}_2\text{R}_2\text{S})_2$, and $(\text{HgCl}_2)_2\text{R}_2\text{S}_2$ in organic phase and the corresponding extraction equilibrium constants and formation constants of complexes in the organic phase were determined. We report here the results of such investigation for HgCl_2 distribution between water and solutions of TBP and DOSO in different diluents.

When extracting the tracer amounts of HgCl_2 by diluted solutions of TBP in n-hexane the complexes HgCl_2TBP and $\text{HgCl}_2(\text{TBP})_2$ are produced in organic phase². In the solid state, 1:1 complexes with ligands containing oxygen are found and dimers are formed $(\text{HgCl}_2\text{L})_2$ ³. The extractant and ligand DOSO is a close analogue of TBP^{4,5}. In addition individual crystalline compounds of HgCl_2 with dialkyl sulphoxides and dialkyl sulphides with molar ratios HgCl_2 to L of 1:1, 2:1 and 3:2 are similar structures^{6,7}, despite the R_2SO molecule's co-ordination to mercury through oxygen⁶. Due to these facts one can assume that interaction of HgCl_2 with TBP, DOSO and R_2S in different diluents leads to

formation of the complexes of the same stoichiometry and similar structure.

Experimental

Reagents

DOSO was prepared as described elsewhere⁸ and purified by threefold recrystallization from heptane. The sulphur content was determined by potentiometric titration with perchloric acid in dioxane as solvent⁹, Calcd. for $(C_8H_{17})_2SO$: S, 11,68. Found: S, 11,62: 11,69.

TBP and diluents were purified in the usual manner. Pharmacopoeia mercury (II) chloride was recrystallized from water.

Distribution isotherms.

Equal volumes of an aqueous solution of $HgCl_2$ and 0.05, 0.1, 0.2M solutions of TBP or DOSO in given diluents were stirred at $25 \pm 0.1^\circ C$ (for the systems with C_6H_6 $10 \pm 0.1^\circ C$) was also investigated for one hour. This time was shown to be sufficient to ensure equilibrium between the phases. The equilibrium concentration of $HgCl_2$ in aqueous phase was varied from 3×10^{-4} to 0.268M (0.188M at $10^\circ C$) the latter corresponds to the saturated solution of $HgCl_2$ at three phase equilibrium. After stripping with an excess of 0.0125M solution of complexone III the concentrations of $HgCl_2$ in equilibrium aqueous phase and in strip liquor were determined by titration of excess of complexone III with standard magnesium sulphate using Eriochrome Black as the indicator¹⁰. The sum of $HgCl_2$ concentrations in both phases was different from the initial $HgCl_2$ concentration in the aqueous phase less than by 3%.

The distribution of $HgCl_2$ between water and pure diluents was studied by similar procedure. At $25^\circ C$ the values of partition coefficients $P_{HgCl_2} = \frac{[HgCl_2]_{org}}{[HgCl_2]_{aq}}$ calculated taking account of the $HgCl_2$ dimerisation and dissociation processes in aqueous phase were equal to $CCl_4 - 0.00201$, $CHCl_3 - 0.0152$, $1,2-C_2H_4Cl_2 - 0.289$, $C_6H_6 - 0.0850$. The latter value is in a close agreement with other data¹¹. For C_6H_6 at $10^\circ C$ we found $P_{HgCl_2} = 0.0740$.

Mean molecular weight.

Different amounts of HgCl_2 were added to weighed quantities of either 0.2M TBP or 0.1M DOSO solutions in benzene. The freezing temperature depression was measured on such solutions in which extractant, HgCl_2 , and products of their interaction were present. The mean molecular weight of the solutes (M) calculated from such data is equal to $X_i M_i / X_1$, where X_i is molar concentration of i-th species in solution. The nature of these species and values of their concentrations are initially unknown.

Computer analysis of distribution isotherms.

HgCl_2 distribution isotherms for eight investigated systems are shown in Fig.1 and 2 in the form of the dependences $\log (C_{\text{HgCl}_2} - \text{HgCl}_2)$ against $\log C_{\text{HgCl}_2}^{\text{aq}}$. For the initial part of isotherms C_{HgCl_2} is proportional to $C_{\text{HgCl}_2}^{\text{aq}}$, i.e. only monuclear complexes exist in organic phase. In accordance with previous results^{1,2} one can assume that these complexes are HgCl_2L and HgCl_2L_2 with equilibrium constants,

$$\beta_{1s} = \frac{\text{HgCl}_2\text{L}_s}{a_{\text{HgCl}_2} \text{L}^s}, \quad (1)$$

where a_{HgCl_2} is the thermodynamic activity of HgCl_2 which approximately coincides with $C_{\text{HgCl}_2}^{\text{aq}}$ (formula for calculation of a_{HgCl_2} is given below). In this case one can easily show that

$$q / a_{\text{HgCl}_2} [\text{L}] = \beta'_{1,1} + \beta'_{1,2} \text{L}, \quad (2)$$

where $q = C_{\text{HgCl}_2} - \text{HgCl}_2$ and $\text{HgCl}_2 = r_{\text{HgCl}_2} a_{\text{HgCl}_2}$. At low a_{HgCl_2} the value of L is close to the total extractant concentration C_L .

Plots of $q/a_{\text{HgCl}_2} C_L$ against C_L are really linear ones in accordance with equation (2) (Fig.3). It allows one to determine the approximate values of $\beta'_{1,1}$ and $\beta'_{1,2}$. However, the distribution isotherms so calculated in which only two complexes are assumed are placed far below the observed isotherms at higher a_{HgCl_2} . Since the formation of increasing amounts of HgCl_2L_s , with $s \geq 2$, in this part of isotherm contradicts the law of mass action, then this disagreement proves the formation of polynuclear complexes at higher a_{HgCl_2} .

Thus one needs to take into account a set of complexes with general formula $(\text{HgCl}_2)_r L_s$ and thus extraction equilibrium constants.

$$\beta_{rs} = (\text{HgCl}_2)_r L_s / a_{\text{HgCl}_2}^r [L]^s \quad (3)$$

If the set of β_{rs} is known, the distribution isotherms are determined by the following system of equations

$$C_{\text{HgCl}_2} = P_{\text{HgCl}_2} a_{\text{HgCl}_2} + \sum_{rs} r \beta'_{rs} a_{\text{HgCl}_2}^r [L]^s \quad (4)$$

The calculations of β_{rs} were carried out with the help of computer "Minsk-32". Sillen's algorithm¹² which reduces the transition from on approximate set of β_{rs} to more exact one to the solution of a linear algebraic equation system (programme LETAGROP) was used after small improvements. The sum of the squares of relative difference between experimental and calculated values of q for all experimental points $U = \sum (q_j^{\text{exp}} / q_j^{\text{calc}} - 1)^2$ was used as the minimized function in multidimensional space of β'_{rs} . Initial approximations for β'_{11} and β'_{12} were determined by formula (2). Initial approximation for other constants were found by direct seeking at fixed values of β'_{11} and β'_{12} .

In aqueous solutions of HgCl_2 the processes of dimerization and dissociation take place with equilibrium constants $K_{\text{dim}} = \text{Hg}_2\text{Cl}_4 \text{ aq} / \text{HgCl}_2^2 \text{ aq}$ and $K_{\text{diss}} = \text{HgCl}^+ \text{ aq} \text{ Cl}^- \text{ aq} / \text{HgCl}_2 \text{ aq}$. Thermodynamic activity a_{HgCl_2} was taken equal to $\text{HgCl}_2 \text{ aq}$ and determined by formula,

$$a_{\text{HgCl}_2} = \left\{ 1 + 8K_{\text{dim}} \left[C_{\text{HgCl}_2}^{\text{aq}} - K_{\text{diss}} C_{\text{HgCl}_2}^{\text{aq}} \right]^{1/2} \right\}^{1/2} 1/4K_{\text{dim}} \quad (5)$$

which is valid for small K_{diss} . In accordance with previous results^{13,14} K_{diss} were taken equal to 0.3 and 5×10^{-7} respectively. When assuming no HgCl_2 dimerization in organic phase, this value of K_{dim} is in good agreement with observed decreasing values of D_{HgCl_2} and with increasing values of $C_{\text{HgCl}_2}^{\text{aq}}$ in the systems water-pure diluent at both temperatures. The temperature dependence of K_{diss} was also not taken into account since correction due to dissociation was small even for the lowest HgCl_2 concentrations used.

The calculations were carried out for every system assuming first the formation of three 1:1, 1:2 and then 1:1, 1:2, 2:2 and 4:2 complexes in the organic phase. The calculated values of β'_{11} and β'_{12} for both variants are close to those obtained by means of equation (2). The values of β'_{22} decrease slightly when the complex 4:2 is taken into consideration, the description of distribution isotherms being improved.

The most remarkable improvement of the experimental data description takes place in systems DOSO- $C_2H_4Cl_2$ and DOSO - C_6H_6 . This corresponds to the greatest contribution of complex 4:2 to the total $HgCl_2$ concentration in organic phase for these two systems at high a_{HgCl_2} (the calculations with four complexes show these contributions to be 45 and 37%, respectively, when two liquid phases are in equilibrium with solid $HgCl_2$). Contribution of the complex 4 : 2 to the total mercury concentration in systems DOSO - $CHCl_3$ and DOSO- CCl_4 does not exceed 10%. Therefore the transition to the case with four complexes does not give an essential improvement of isotherms' description. For the systems with TBP the contribution of 4 : 2 complex to mercury concentration is less than that for systems with DOSO and for the diluents $C_2H_4Cl_2$, C_6H_6 , CCl_4 and $CHCl_3$ it does not exceed 20, 14, 8 and 4%, respectively. The difference between the descriptions of these systems assuming existence of three or four complexes is also small. In addition, for the system TBP - $CHCl_3$ unlike the other systems the contribution of 1:2 and 2:2 complexes to mercury concentration is negligible (not greater than 0.5% and 2% respectively). So this system can be satisfactorily described assuming formation of the 1:1 complex only in organic phase.

Thus, the formation of complexes 1:1, 1:2 and 2:2 was reliably ascertained for all studied systems excluding TBP - $CHCl_3$ (adducts between $HgCl_2$ and sulfoxides with mole ratio 1:2 are unknown in crystalline state). As for complex 4:2 its formation is unequivocally ascertained only for the systems DOSO - $C_2H_4Cl_2$ and DOSO - C_6H_6 , and its existence in the rest of the systems is doubtful. Nevertheless, since the isotherms' description is slightly improved by introducing this complex we consider such a description almost in all the cases to be more preferable. According to Biscarini and co-workers¹⁵ the formation of $(HgCl_2)_2L_2$ in a solution is due to the dimerization of the unstable intermediate $(HgCl_2)_2L$ preceded by the formation

of a crystalline adduct with mole ratio $\text{HgCl}_2 : \text{L} = 2:1$.

In Table 1 the values of β_{rs} calculated for the case with four complexes, U and $\beta_{rs} = U/(k-1)^{1/2}$ are given. β_{rs} is mean relative difference between calculated and measured values of q and for description with four complexes it does not exceed 0.04 (4%) in accordance with the expected experimental error. The values of β_{22} , U and β_{rs} for the second case (without the 4:2 complex) are presented in parenthesis.

TABLE 1

Extraction equilibrium constants for HgCl_2 extraction by TBP

Diluent	C_6H_6	C_6H_6	CCl_4	CHCl_3	$1,2\text{-C}_2\text{H}_4\text{Cl}_2$
t, °C	25	10	25	25	25
Log β_{rs}					
11	0.505 $\pm 0.012^a$	0.586 ± 0.010	0.068 ± 0.010	-0.382 ± 0.006	0.504 ± 0.012
12	0.941 ± 0.040	1.184 ± 0.023	0.880 ± 0.016	-2 ^c	0.810 ± 0.048
22	1.77 ± 0.10 (1.91 ± 0.08)	1.94 ± 0.11 (2.08 ± 0.07)	1.15 ± 0.10 (1.26 ± 0.05)	-1 ^c	1.72 ± 0.10 (1.97 ± 0.09)
42	2.4 ± 0.2	2.9 ± 0.2	1.6 ± 0.3	0.32 ± 0.07	2.55 ± 0.10
U	0.0188 (0.0324)	0.0149 (0.0248)	0.0089 (0.0108)	0.0178	0.0305 (0.0500)
	0.031 (0.039)	0.025 (0.032)	0.021 (0.023)	0.031	0.035 (0.046)
k	24	28	24	22	27

^a Errors for $\log \beta'_{rs}$ values are given for a confidence interval of P = 0.95.

^b The values of $\log \beta'_{11}$ and $\log \beta'_{12}$ for C_6H_{14} which are 0.14 and 1.78, respectively, can be calculated from data of Sekine and Ishii² using the equation (8). For C_6H_{14} $\log p_{\text{HgCl}_2} = -2.1^2$. ^c The contribution of the appropriate form to C_{HgCl_2} is too small for more accurate determination of β_{rs} . Computed values are: $\log \beta'_{12} = -1.96 \pm 0.15$ and $\beta'_{22} = -0.99 \pm 0.11$.

On Fig.1 and 2 the distribution isotherms calculated for the first descriptive case are shown by dashed and solid lines for 10 and 25°C respectively.

TABLE 2

Extraction equilibrium constants for HgCl₂ extraction by DOSO

Diluent	C ₆ H ₆	C ₆ H ₆	CCl ₄	CHCl ₃	1,2-C ₂ H ₄ Cl ₂
t, °C	25	10	25	25	25
Log 11	0.915 ±0.028	1.118 ±0.036	0.303 ±0.044	0.013 ±0.009	1.081 ±0.013
Log 12	2.003 ±0.021	2.283 ±0.031	1.762 ±0.015	0.21±0.06	1.37±0.06
Log 22	3.22±0.08 (3.43±0.13)	3.57±0.09 (3.75±0.11)	2.64±0.09 (2.70± 0.05)	0.848 ±0.006 (0.99±0.05)	2.81±0.11 (3.12±0.19)
Log 42	4.18±0.07	4.72±0.11	2.8±0.5	1.47±0.06	4.11±0.08
U	0.0165 (0.199)	0.0384 (0.150)	0.0206 (0.30301)	0.0096 (0.0127)	0.0254 (0.284)
=	0.026 (0.089)	0.040 (0.078)	0.031 (0.036)	0.022 (0.025)	0.033 (0.103)
k	28	28	26	24	27

Comparison of calculated and measured
mean molecular weights

If the β'_{rs} values are known, it is easy to calculate $[L]$ using the second equation of (4), then molar concentration of each complex and mean molecular weight of the solutes, the latter is determined by

$$\bar{M} = \sum X_i M_i + [L] M_L + [HgCl_2] M_{HgCl_2} / \left(\sum X_i + [L] + [HgCl_2] \right). \quad (6)$$

To calculate \bar{M} the values of r_s at benzene freezing temperature were used. They were obtained by means of Vant-Hoff's equation using data on r_s at 10 and 25°C.

Measured and calculated values of \bar{M} are compared in Fig.4. For system with TBP the difference between them is approximately 3%, for system with DOSO that is about 10%. These little discrepancies seem to be arising from performing of cryoscopic measurements with dry benzene while the β'_{rs} values used at \bar{M} calculation correspond to water saturated organic phase.

A good consistency of calculated values of \bar{M} with those measured is an independent evidence of the correctness of the β'_{rs} values and the complex formation scheme itself.

Discussion

Relative efficiency of extractants

At low $HgCl_2$ concentration in aqueous phase the values of D_{HgCl_2} can be calculated by the formula

$$D_{HgCl_2} = P_{HgCl_2} + \beta'_{11} [L] + \beta'_{12} [L]^2. \quad (7)$$

The calculated magnitudes D_{HgCl_2} at 25°C are listed in Table 3.

TABLE 3

The values of D_{HgCl_2} for $HgCl_2$ extraction by TBP, DOSO and DOS.

Diluent	n-C ₆ H ₁₄	C ₂ H ₄ Cl ₂	C ₆ H ₆	CCl ₄	CHCl ₃
0.05M TBP	0.23	0.46	0.27	0.08	0.04
0.1M TBP	0.75	0.67	0.49	0.20	0.06
0.2M TBP	2.79	1.17	1.07	0.54	0.10
0.05M DOSO	-	0.95	0.75	0.25	0.07
0.1M DOSO	-	1.73	1.92	0.78	0.13
0.2M DOSO	-	3.64	5.77	2.72	0.28
0.05M DOS	-	1.98	0.43	-	0.56
0.1M DOS	-	5.71	1.18	-	2.08
0.2M DOS	-	19.3	3.93	-	8.08

Data for di-n-octyl sulphide (DOS) are also included in the table for comparison. As in all previously investigated cases^{4,5} DOS is more effective extractant than TBP. When $C_2H_4Cl_2$ or $CHCl_3$ are used as diluents DOS proves the most effective extractant for $HgCl_2$, being simultaneously the most selective one (from chloride media it also extracts only gold and palladium^{4,5}).

Formation constants of complexes in different diluents

Almost nothing is known about the formation constants of complex non-electrolytes in non-aqueous media. However, these constants are of great interest for co-ordination chemistry. In the case considered here the full formation constants of complexes in different media can be calculated by the expression

$$\beta'_{rs} = \frac{[HgCl]_r [L]_s}{[HgCl_2]^r [L]^s} = \beta'_{rs} / [HgCl_2]^r \quad (8)$$

The values of β'_{rs} are listed in Table 4. Equilibrium constants for some other reactions which can be useful in evaluation of media influences on complex formation are also included to the table. These constants are following: stepwise formation constant for $HgCl_2L_2$, $K_2 = \frac{[HgCl_2L_2]}{[HgCl_2L][L]} = \beta'_{12} / \beta'_{11}$; dimerization constant for $HgCl_2L$, $K_d = \frac{[(HgCl_2L)_2]}{[HgCl_2L]^2} = \beta'_{22} / \beta'_{11}^2$; equilibrium constant of $HgCl_2$ addition to $HgCl_2L_2$, $= \frac{[HgCl_2L_2]_2}{[HgCl_2L_2][HgCl_2]} = \beta'_{22} / \beta'_{12}$. The processes of the complex formation succeed best in the CCl_4 medium. In $C_2H_4Cl_2$, which is the best diluent from a view point of extraction efficiency, these processes go to the least extent. The variations of equilibrium constants for different diluents are the same for TBP and DOSO. For instance, $CCl_4 > C_6H_6 > CHCl_3 > C_2H_4Cl_2$ is such a series for β'_{11} and β'_{22} .

TABLE 4

Equilibrium constants of the various reactions in non-aqueous media at 25°C

Diluent	C_6H_6	CCl_4	$CHCl_3$	$1,2-C_2H_4Cl_2$	$n-C_6H_{14}$
TBP					
Log 11	1.576	2.767	1.436	1.043	2.24 ²
Log 12	2.012	3.579	0	1.349	3.88 ²
Log 22	3.91	6.55	3	2.80	-
Log 42	6.7	12.4	7.6	4.7	-
Log K_2	0.436	0.812	-1	0.306	1.64 ²
Log K_d	0.76	1.02	0	0.72	-
Log	1.90	2.97	3	1.45	-
DOSO					
Log 11	1.986	3.002	1.831	1.620	-
Log 12	3.074	4.461	2.03	1.91	-
Log 22	5.36	8.0	4.484	3.89	-
Log 42	8.46	14	8.74	6.27	-
Log K_2	1.088	1.459	0.20	0.29	-
Log K_d	1.39	2.04	0.82	0.65	-
Log	2.29	3.58	2.45	1.98	-

Dependence of extraction equilibrium constants on diluent nature

The way that equilibrium constants change as the medium changes is due to the varying intermolecular interactions of reactants and products with solvent. If a standard state for each reactants and products is chosen such that it is a state which is independent of the medium, then the equilibrium constant will not depend on the medium where the reaction occurs, and the condition of equilibrium for any of considered heterogeneous reactions can be written in the following form (compare with (3)):

$$x_{rs} \gamma_{rs} / \bar{a}_{\text{HgCl}_2}^r x_L^s \gamma_L^s = \text{const.} \quad (9)$$

where x_{rs} and γ_{rs} are mole fraction and activity coefficient of the complex rs . Each reaction is characterized by its own value of const. In a dilute solution $x_{rs} = [(\text{HgCl}_2)_{rs}^L] / n$, where n is the number of moles in one litre of water saturated diluent. Then the latter equation can be rewritten in the form:

$$\beta'_{rs} \gamma_{rs} n^{s-1} / \gamma_L^s = \text{const.} \quad (10)$$

Following (10), the way in which γ_{rs} change with media is due to change of activity coefficients of the extractant and extracted complex and to a much less extent is due to change of n .

In an analogous manner it can be shown that

$$\beta_{rs} \gamma_{rs} n^{r+s-1} / \bar{a}_{\text{HgCl}_2}^r \gamma_L^s = \text{const.} \quad (11)$$

Thus, the dependence of this equilibrium constant on media is determined by the greater number of parameters and is more complicated. One can consider the β_{rs} change to be determined by independent changes of β_{rs} and γ_{HgCl_2} , the latter being proportional to the ratio n/P_{HgCl_2} .

According to equation (9), $\gamma_{rs} \gamma_L^s / \beta_{rs} n^{s-1}$ and the value of γ_{rs} can be determined if γ_L^s and β_{rs} are known. At 25°C the values of $\log \gamma_{\text{TBP}}$ in infinitely dilute solutions of TBP in dry $n\text{-C}_7\text{H}_{16}$, C_6H_6 , CCl_4 and CHCl_3 are equal¹⁶ to 0.618, -0.442, -0.448, -1.979 respectively (the standard state is pure TBP). Practically the same values of γ_{TBP} were found by other authors^{17,18}. In the Table 5 the $\log \gamma_{rs} / (\gamma_{rs})_{\text{CCl}_4}$ values for TBP are given. These values were calculated by

$$\gamma_{rs} / (\gamma_{rs})_{\text{CCl}_4} = \gamma_{\text{TBP}}^s (\beta'_{rs})_{\text{CCl}_4} n_{\text{CCl}_4}^{s-1} / (\gamma_{\text{TBP}})_{\text{CCl}_4} \beta'_{rs} n^{s-1} \quad (12)$$

Similar values for DOSO which were calculated using assumption $\gamma_{\text{DOSO}} \sim \gamma_{\text{TBP}}$ are also given in this table. The values of γ_{TBP} in $n\text{-C}_6\text{H}_{14}$ and $n\text{-C}_7\text{H}_{16}$ were supposed to be equal.

TABLE 5

The values of $\log \gamma_{rs} / (\gamma_{rs})_{CCl_4}$ for different complexes.

Diluent	$n-C_6H_{14}$	CCl_4	C_6H_6	$CHCl_3$
TBP				
$\log \gamma_{11} / (\gamma_{11})_{CCl_4}$	0.99	0	-0.43	-1.08
$\log \gamma_{12} / (\gamma_{12})_{CCl_4}$	1.30	0	-0.07	-
$\log \gamma_{22} / (\gamma_{22})_{CCl_4}$	-	0	-0.62	-
$\log \gamma_{42} / (\gamma_{42})_{CCl_4}$	-	0	-0.8,	-1.8
DOSO				
$\log \gamma_{11} / (\gamma_{11})_{CCl_4}$	-	0	-0.60	-1.23
$\log \gamma_{12} / (\gamma_{12})_{CCl_4}$	-	0	-0.35	-1.57
$\log \gamma_{22} / (\gamma_{22})_{CCl_4}$	-	0	-0.59	-1.33
$\log \gamma_{42} / (\gamma_{42})_{CCl_4}$	-	0	-1.3	-1.7

The values of γ_{rs} for all considered complex non-electrolytes decrease in the series $C_6H_{14} > CCl_4 > C_6H_6 > CHCl_3$, which does not coincide with those of γ_{TBP} and γ_{HgCl_2} change. The same series of activity coefficients change is observed for dimer of di-n-butyl phosphoric acid (HDBP)₂¹⁹, its salts Eu [H(DBP)₂]₃ and Am [H(DBP)₂]₃¹⁹, dimer of di-2-ethylhexyl phosphoric acid (HD2EHP)₂²⁰ and its salt UO₂[H(D2EHP)₂]₂²⁰. In all these cases the interaction between solute and solvent is determined mainly by hydrocarbon radicals placed on the periphery of a molecule. General regularities of $\log \gamma$ change for such substances are revealed by the existence of linear correlations between their \log values in different solvents.

The dependence of $\log \gamma_{\text{TBP}}^s / n^{s-1} \beta'_{\text{rs}}$ (corresponding to $\log \gamma_{\text{rs}}$ with accuracy of a constant) on $\log \gamma_{(\text{HR})_2}$ (there HR is HDBP) are shown in Fig.5. as well as similar dependences for activity coefficients of $(\text{HD2EHP})_2$ and $\text{UO}_2 [\text{H}(\text{D2EHP})_2]_2$.

Frolov and co-workers^{21,22} found in a number of cases the linear correlation between logarithms of activity coefficients of a given substance in its infinitely dilute solutions in different solvents and the empiric polarity parameters E_T ²³ for those. Such correlations as for $\log \gamma_{\text{TBP}}^s / n^{s-1} \beta'_{\text{rs}}$ so as for activity coefficients of $(\text{HDBP})_2$, $(\text{HD2EHP})_2$ are shown in Fig.6. When plotting Figures 5 and 6 it was supposed the activity coefficients of $(\text{HDBP})_2$ in $n\text{-C}_6\text{H}_{14}$ and $n\text{-C}_7\text{H}_{16}$ as well as the E_T values for these solvents to be equal each to other. The deviations of points for hydrocarbons from linear dependence $\log \gamma - E_T$, observed for all considered substances, take place also for some β -diketones²¹.

Thus, the way β'_{rs} change with variation of the diluent nature as HgCl_2 is extracted by TBP and DOSO is connected with sensibly regular changes of activity coefficients for a great group of substances in different solvents.

NOMENCLATURE

$$a_{\text{HgCl}_2} = [\text{HgCl}_2]_{\text{aq}}$$

thermodynamic activity of HgCl_2

$$C_{\text{HgCl}_2}, C_{\text{HgCl}_2}^{\text{aq}}$$

total analytical concentration of HgCl_2 in organic and aqueous phases, respectively; mole/l.

$$[X], [X]_{\text{aq}}$$

molar concentration of species X in organic and aqueous phases, respectively; mole/l.

D_{HgCl_2}	distribution coefficient of HgCl_2
E_T	empiric polarity parameter of diluent or solvent
k	number of experimental points
K_2	the second stepwise formation constant in organic phase
K_d	dimerization constant for HgCl_2 in organic phase
K_{dim}	dimerization constant for HgCl_2 in water
K_{diss}	dissociation constant for HgCl_2 in water
\bar{M}	mean molecular weight of solutes, see Equation (6).
M_i	molecular weight of i-th substance
n	number of moles in 1 l of water saturated diluent
P_{HgCl_2}	partition coefficient for HgCl_2
$q = C_{\text{HgCl}_2} - [\text{HgCl}_2]$	total concentration of HgCl_2 in complexes in organic phases, mole/l.
U	sum of the squares of relative differences between experimental and calculated values of q for all experimental points
x_{rs}, x_L	mole fraction of $(\text{HgCl}_2)_{rL_s}$ or L in organic phase
β_{rs}	formation constant for complex $(\text{HgCl}_2)_{rL_s}$ in organic phase, see Equation (8)
β'_{rs}	extraction equilibrium constant for complex $(\text{HgCl}_2)_{rL_s}$, see Equation (3).
$\delta_{rs}, \delta_L, \delta_{\text{HgCl}_2}$	activity coefficient of $(\text{HgCl}_2)_{rL_s}$, L or HgCl_2 in organic phase

- α equilibrium constant for process of HgCl_2 addition to $\text{HgCl}_2 \cdot \text{L}_2$ in organic phase
- $\bar{\sigma}$ mean relative difference between experimental and calculated values of q .

References

- ¹Mikhailov, V.A., Korol', N.A., & Ochirzhapova, D.D., Proceedings of the XV-th International Conference on Coordination Chemistry, 1973, p.633 (Moscow: Nauka)
- ²Sekine, T., & Ishii, T., Bull. Chem. Soc. Japan, 1970, 43, 2422
- ³Brill, T.B., & Hugus, Z.Z., J. Inorg. Nuclear Chem., 1971, 33, 371
- ⁴Mikhailov, V.A., Torgov, V.G., Gil'bert, E.N., Mazalov, L.N., & Nicolaev, A.V., Proceedings International Solvent Extraction Conference 1971, 1971, vol 2, p.1112 (London: Society of Chemical Industry)
- ⁵Mikhailov, V.A., Torgov, V.G., & Nicolaev, A.V., Izv. Sibirsk. Otd. Akad. Nauk SSSR, Ser. Khim. Nauk, 1973, No 7, vyp 3, 3
- ⁶Biscarini, P., Fusina, L., & Nivellini, G.D., J. Chem. Soc. (A), 1971, 1128
- ⁷Biscarini, P., Fusina, L., & Nivellini, G.D., J. Chem. Soc. Dalton Transactions, 1972, 1003
- ⁸Methoden der organischen Chemie (Houben-Weyl), 1955, Band 9, S.213 (Stuttgart: Georg. Thieme Verlag)
- ⁹Gal'pern, G.D., Girina, G.G., & Luk'janitsa, V.G., In "Metody analiza organicheskikh soedinenii, ikh smesei i proizvodnykh", 1960, vol.1, p.85 (Moscow: izd-vo AN SSSR)
- ¹⁰Pribil, P., Kompleksy v chemicheskoy analize, 1960, p.505 (Moscow: izd-vo inostrannoi literatury)
- ¹¹Marcus, Y., & Kertes, A.S., "Ion exchange and Solvent extraction of metal complex", 1969, p.445 (London, New-York, Sydney, Toronto, Wiley-Interscience)

- ¹²Sillén, L.G., Acta Chem.Scand., 1962, 16, 159
- ¹³Linhart, G.A., J.Chem.Soc., 1915, 37, 258
- ¹⁴Marcus, Y., Acta Chem.Scand., 1957, 11, 599
- ¹⁵Biscarini, P., Fusina, L., & Nivellini, G.D., Inorg.Chem., 1971, 10, 2564
- ¹⁶Kharchenko, S.K., Mikhailov, V.A., Afanas'ev, Yu.A., & Ponomareva, L.I., Izv.Sibirsk.Otd.Akad.Nauk SSSR, Ser.Khim. Nauk, 1964, No 11, vyp.3, 30
- ¹⁷Rozen, A.M., Khorkhorina, L.P., Yurkin, V.G., & Novikov, I.M., Dokl. Akad.Nauk SSSR, 1963, 153, 387
- ¹⁸Pushlenkov, M.F., & Shuvalov, O.N., Radiokhimiya, 1963, 5, 536
- ¹⁹Mikhailov, V.A., & Kharchenko, S.K., Izv.Sibirsk. Otd. Akad. Nauk SSSR, Ser. Khim. Nauk, 1967, No 2, vyp.1, 3
- ²⁰Rozen, A.M., & Yurkin, V.G., Dokl.Akad.Nauk SSSR, 1972, 207, 1165
- ²¹Frolov, Yu.G., & Sergievsky, V.V., In "Khimiya protsessov ekstrakttsii", 1972, p.97 (Moscow:Nauka)
- ²²Frolov, Yu.G., Pushkov, A.A., & Sergievsky, V.V., Proceedings International Solvent Extraction Conference 1971, 1971, vol 2, p.1236 (London: Society of Chemical Industry)
- ²³Reichardt, D.S., Angew.Chem., 1965, 77, 30

Captions to the Figures:

Fig.1. Distribution isotherms of HgCl_2 between water and 0.05 , 0.1 and 0.2M TBP solutions in C_6H_6 (a), $1,2\text{-C}_2\text{H}_4\text{Cl}_2$ (b), CCl_4 (c) and CHCl_3 (d) at 25°C . Dashed lines - C_6H_6 at 10°C .

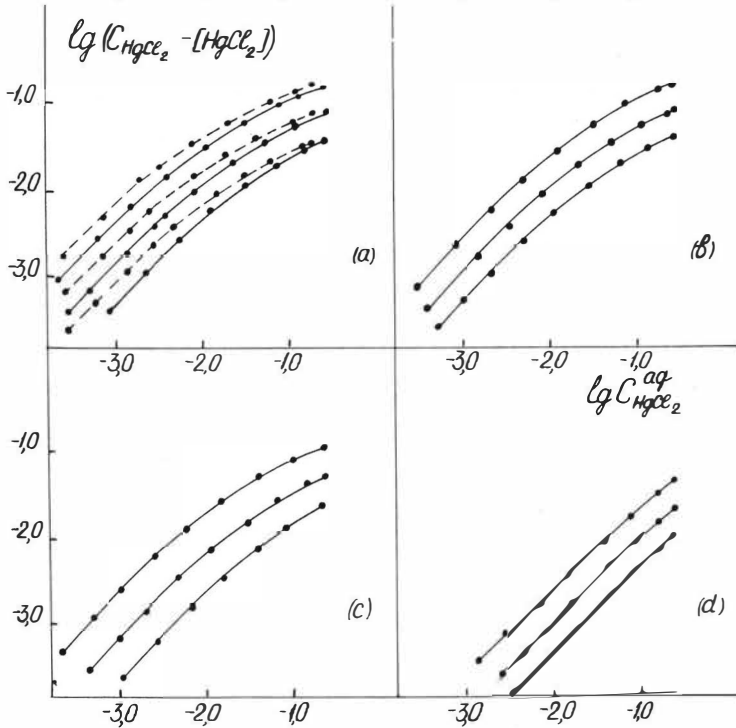
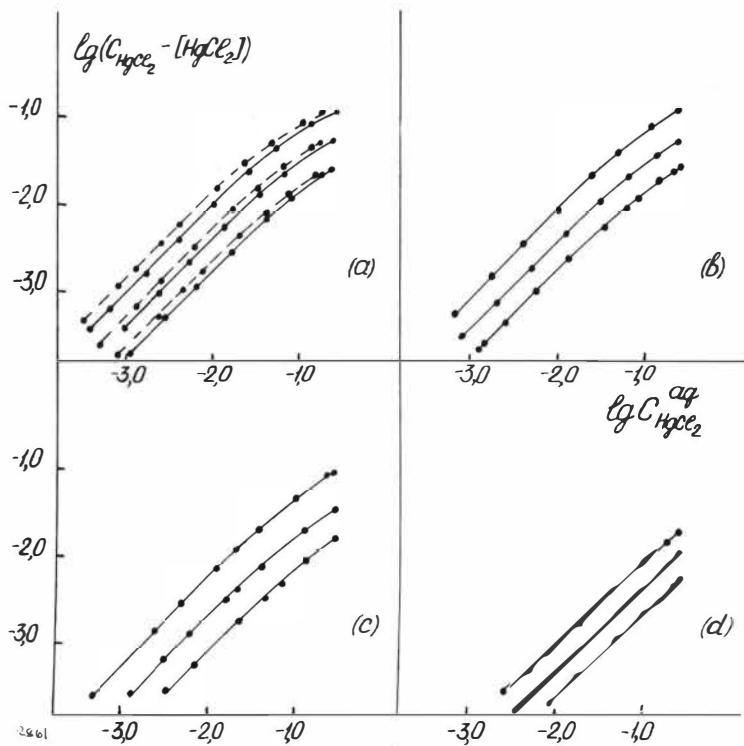
Fig.2. Distribution isotherms of HgCl_2 between water and 0.05, 0.1 and 0.2M DOSO solutions in C_6H_6 (a), $1,2\text{-C}_2\text{H}_4\text{Cl}_2$ (b), CCl_4 (c) and CHCl_3 (d) at 25°C . Dashed lines - C_6H_6 at 10°C .

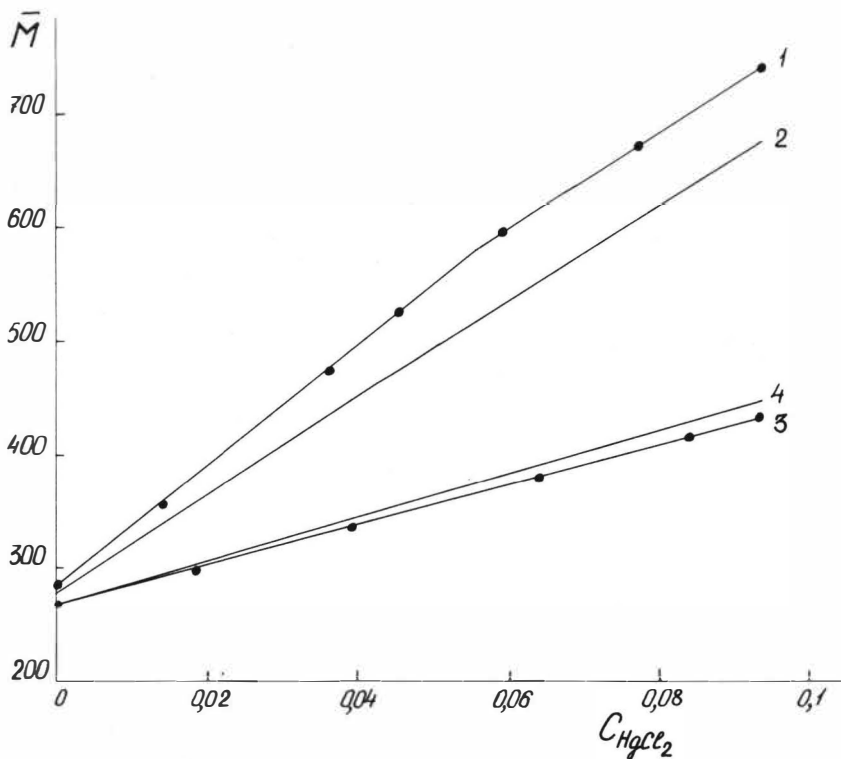
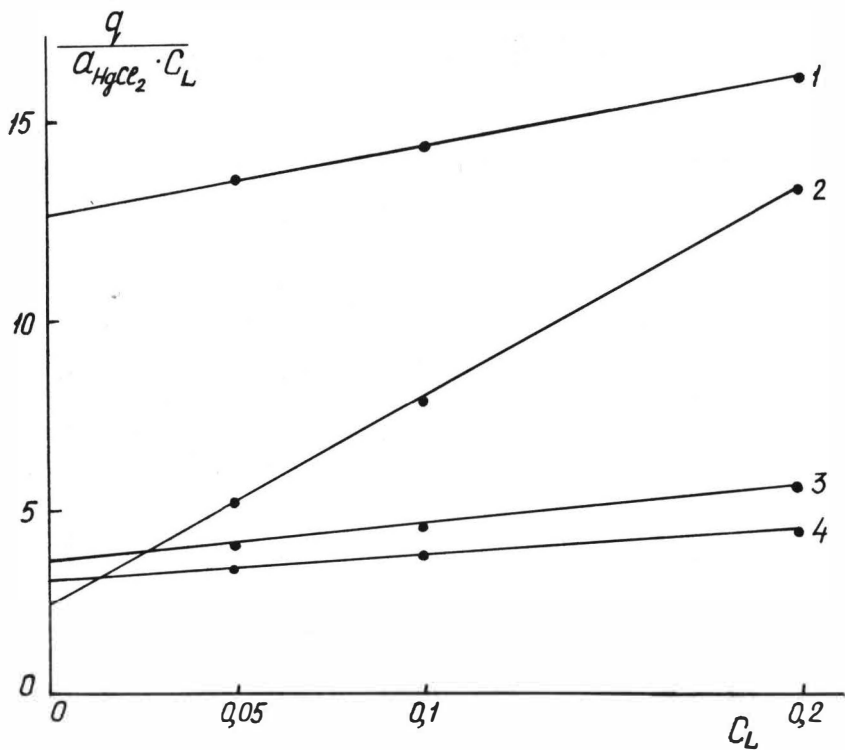
Fig.3. Dependences of $q/a_{\text{HgCl}_2} C_L$ on C_L . 1- DOSO in $1,2\text{-C}_2\text{H}_4\text{Cl}_2$; 2 - DOSO in CCl_4 ; 3 - TBP in C_6H_6 ; 4 - TBP in $1,2\text{-C}_2\text{H}_4\text{Cl}_2$.

Fig.4. Mean molecular weights of solutes in benzene solutions of mixtures DOSO + HgCl_2 (1 - measured, 2 - calculated, $C_{\text{DOSO}} = 0.1\text{M}$) and TBP + HgCl_2 (3 - measured, 4 - calculated, $C_{\text{TBP}} = 0.2\text{M}$).

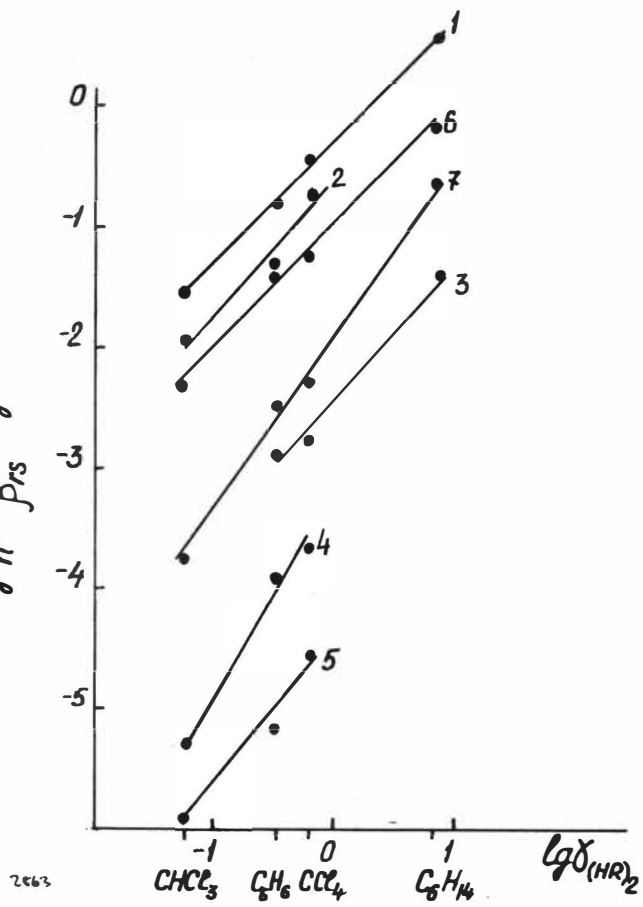
Fig.5. Linear correlations between logarithms of activity coefficients of HgCl_2TBP (1), HgCl_2DOSO (2), $\text{HgCl}_2(\text{TBP})_2$ (3), $\text{HgCl}_2(\text{DOSO})_2$ (4), $(\text{HgCl}_2\text{DOSO})_2$ (5), $(\text{HD2EHP})_2$ (6), and $\text{UO}_2[\text{H}(\text{D2EHP})_2]_2$ (7) in their infinitely diluted solutions in different diluents and logarithm of the activity coefficient of $(\text{HDBP})_2$ ($\log \gamma_{(\text{HR})_2}$).

Fig.6. Correlations between logarithms of the activity coefficients of HgCl_2TBP (1), HgCl_2DOSO (2), $(\text{HDBP})_2$ (3), $\text{HgCl}_2(\text{DOSO})_2$ (4), $(\text{HgCl}_2\text{DOSO})_2$ (5), $(\text{HD2EHP})_2$ (6) and $\text{UO}_2[\text{H}(\text{D2EHP})_2]_2$ in different diluents and E_T .



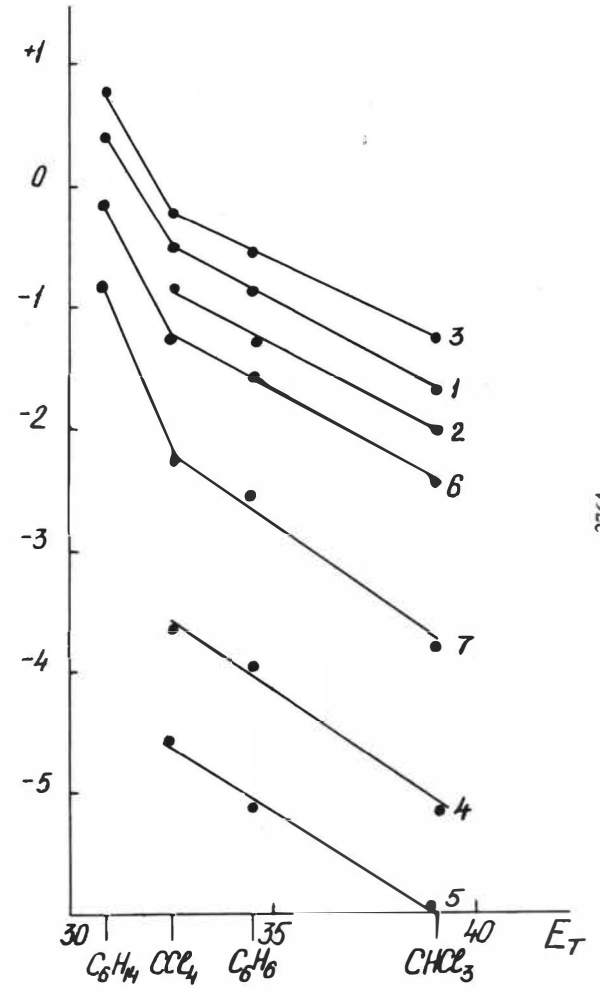


$\lg \frac{\delta_{TAP}^s}{\beta_{rs}} \cdot \lg \delta$



2663

$\lg \frac{\delta_{TAP}^s}{\beta_{rs}} \cdot \lg \delta$



2764

SEPARATION OF MOLYBDENUM AND TUNGSTEN BY
A LIQUID-LIQUID ION-EXCHANGE METHOD

F. ESNAULT*, M.ROBAGLIA**, J.M. LATARD***, J.M.DEMARTE**

* Director of Department "Poudres metalliques" Ste UGINE-CARBONE

**C.E.A., Societe D'Etudes Chimiques

***Chef de fabrication, Societe UGINE-CARBONE

Travaux effectues au Commissariat a l'Energie Atomique
(Department de Genie Radioactif C,E.A.

B.P. no. 6

92260 FONTENAY-AUX-ROSES

FRANCE

SUMMARY

A process for the recovery of molybdenum values and tungsten values from a molybdenum contaminated alkaline solution of tungsten values, was carried out on a laboratory scale. This process included acidifying the solution to a pH of 3 to 3.5 contacting the solution with an organic extractant di-2-ethyl hexyl phosphoric acid, diluted in an inert hydrocarbon in the presence of ethyl 2 hexanol 1. Thus molybdenum is selectively extracted, more readily when the tungsten concentration is low. Then molybdenum is stripped by an aqueous ammonia solution.

The mother liquor, now molybdenum free, is contacted with an amine dissolved in an organic diluent capable of forming a tungstate amine complex. Then tungsten is stripped by an aqueous ammonia solution.

INTRODUCTION

The chief source of tungsten now is scheelite (plentiful in South Korea), mainly a calcium tungstate (CaWO_4). Wolframite (Fe, Mn) methods are used to enrich the ores.

Scheelite concentrates are generally attacked by hot hydrochloric acid at medium concentration so as to precipitate the tungstic acid and remove the soluble calcium chloride. The tungstic acid is then dissolved in ammonia (11N) and the paratungstate is precipitated by evaporating the ammonia. Impurities in the ammonium tungstate solutions (silicotungstate, phosphotungstate and molybdotungstate polymers) limit the crystallisation yield. The mother liquors from crystallisation can contain from 5 to 10% of the tungsten initially present in the ore and their characteristics are as follows:

pH 8; WO_3 70 to 110 g/l; Mo 3 to 10 g/l; SiO_2 2 to 4 g/l

These mother liquors must be treated to eliminate some of the impurities and to recycle the tungsten.

The separation of tungsten and molybdenum by liquid-liquid extraction consists in adjusting the pH of the mother liquors to around 3.5 with hydrochloric acid, extracting the MoO_2^{++} formed at these pH's by the di 2-ethyl hexyl phosphoric acid and separating the tungsten from the residual impurities with a primary amine.

The tungsten and molybdenum are stripped by means of ammoniacal liquors so as to obtain ammonium tungstates and molybdates.

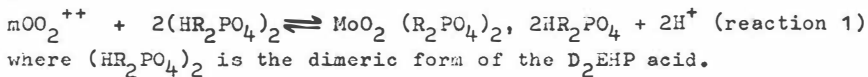
EXTRACTION OF THE MOLYBDENUM

Extraction of pure molybdenum VI is present in solution as anions which are increasingly polymeric as the pH decreases (MoO_4^{--} , HMoO_4^- , $\text{Mo}_7\text{O}_{24}^{6-}$, $\text{Mo}_6\text{O}_{24}^{4-}$, etc). The equilibrium of these various kinds also depends on the molybdenum concentration (I).

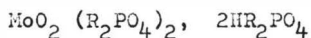
When the pH drops below 3, MoO_2^{++} cationic forms appear in solution and these polymerise as the pH diminishes ($\text{Mo}_2\text{O}_5^{++}$, $\text{Mo}_3\text{O}_8^{++}$) (I).

The curve giving the molybdenum distribution coefficient in terms of the pH reaches a maximum at around pH 2 to 2.5 and calclcs out for pH's above 5 (Fig.1.) (I).

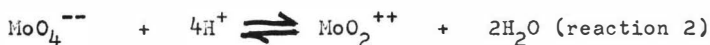
The increase in the distribution coefficient when the pH increases is usual for all cation exchanger extractants when the form extracted is that existing in the aqueous phase, thus for pH 2:



When the pH of the aqueous phase is greater than 3, most of the molybdenum is anionic in form. The D₂EHP acid extracts the few cationic forms present in the medium. This extraction breaks the equilibrium between the various forms of molybdenum and shifts the equilibria towards the formation of new cations which will be extracted in turn. It has been shown that the principal form extracted is the non-condensed cation MoO₂⁺⁺ which in the organic phase forms an anhydrous complex:



But in order to describe the extraction it is necessary to add to the extraction reaction (1) anion cation transformation reactions in an aqueous phase of the type:



The conjunction of reactions one and two enables the decrease in the distribution coefficient with increasing pH to be explained. Further, the greater the concentration of the D₂EHP acid (Fig.1, reaction 1), the greater the distribution coefficients.

Figure 2 represents the variations in the pH of the aqueous phase following extraction. So long as the cationic forms predominate their extraction brings about a drop in the pH (reaction 1) and when anionic forms are present, the extraction of the MoO₂⁺⁺ causes the pH to rise again (reaction 1 + 2). There appear to be self stabilisation areas which are very difficult to foresee for they depend on the ionic state of the molybdenum in the initial aqueous phase. But these areas are very useful if liquid-liquid extraction is carried out in several stages.

Effect of the presence of tungsten on molybdenum extraction

a) Molybdenum distribution curves

Pure molybdenum may be extracted by the D_2EHP acid as a cation, thanks to the transformations in the ionic state of this metal (anion \rightleftharpoons cation equilibria). But the presence of the tungsten modifies this state and affects the transformation kinetics. It is known that molybdenum is extracted in the presence of tungsten traces (2).

Figure 3 shows that the molybdenum percent extraction drops considerably in the presence of tungsten (at a pH of 3) tending towards a limit of around 25%. This non-zero asymptotic value, even for very low molybdenum contents, appears to indicate that it will be possible to extract all the molybdenum.

The molybdenum distribution curves (Fig.4) for pH's of around 3 to equilibrium, show that it can be hoped to obtain distribution coefficients varying from 1.3 to 2.2 in the most favourable cases (20 g/l of WO_3 , pH = 2.8) and of 0.5 to 0.6 in the least favourable cases (40 g/l of WO_3 , pH = 3.5) when the molybdenum contents range from 1 to 4 g/l. When the aqueous phase becomes poor in molybdenum the K_d drops to around 0.2 to 0.3 for the initial $\frac{WO_3}{Mo}$ ratio soon exceeds 50 at which value the percent extraction drops to its limit value.

These curves were plotted as from synthetic $WO_3 - Mo$ solutions. Their value was checked in the case of industrial solutions by using the mother liquors of the first paratungstate crystallisation, brought to the desired pH and WO_3 dilution. The agreement is good.

b) Extraction selectivity

The variation in the WO_3/Mo ratio in the organic phase was studied in terms of initial aqueous WO_3/Mo ratios for various molybdenum concentrations (Fig.5).

The greater the quantity of molybdenum in the organic phase, the lower the organic WO_3/Mo ratio, therefore the better is the selectivity. But it was observed that the molybdenum distribution coefficients in the presence of tungsten were very reduced. Therefore, it will not be possible to charge the D_2EHP acid to saturation point (4 moles of D_2EHP acid per mole of molybdenum) and the excess solvent will have a depressive effect on the selectivity. Therefore the extraction scheme will have to include a scrubbing section in order to bring the tungsten back to the aqueous phase.

c) Effect on contact time

We have studied the effect of the pH and the presence of the tungsten on the equilibrium of the solutions, therefore on the distribution of the molybdenum on equilibrium. But in the continuous application of a process, the equilibrium state is only an asymptote and the rate of the reactions is a fundamental parameter.

Figure 6 shows the total extraction kinetics to be slow, the more so as the tungsten content is high and the molybdenum content low (with synthetic and industrial solutions alike). The extraction reactions with D_2EHP acid being rapid in general, it seems that it is the anion-cation transformation kinetics which limit the system. Incidentally the effect of the tungsten on the kinetics can only be explained by considering the ionic state modifications in the aqueous phase.

In applying the process it will therefore be necessary to have long contact times. The contact time has no effect on selectivity.

d) Means envisaged to increase the distribution coefficients
in industrial solutions

The concentrations in the crystallisation mother liquors can vary from 40 to 120 g/l of WO_3 owing to the variety of ores treated (WO_3 richness and contained impurities). Molybdenum becomes increasingly difficult to extract as the impurities in the solutions increase. This phenomenon is most certainly due to the increasingly greater polymerisation of the ions present which limit the anion cation equilibrium shift.

As we have seen, lower pH, longer contact time and amount of D_2EHP acid provide for better extraction conditions but they cannot offset the effect of polymerisation. It seems that the only efficient way is to use a depolymeriser. The addition of fluorine to aged industrial solutions (Fig.7.) improves extraction to a marked degree.

This effect is noticeable as soon as the fluorine is added but it only becomes appreciable with very polymerised solutions (one year old) at the end of 2 or 3 days.

Moreover the addition of fluorine to solutions improves the distribution coefficients (Fig.4) the extraction kinetics and appears to improve selectivity.

CONCLUSION

It may generally be concluded that the extraction of molybdenum must be carried out:

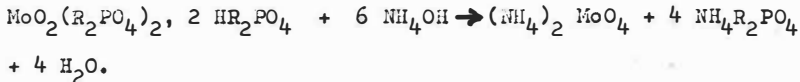
- at around a pH of 3 in order to stabilise the solutions and have better distribution coefficients,
- with tungsten contents under 50 g/l (around 40 g/l to avoid precipitation) in the aqueous phase,
- in the presence of fluorine in the aqueous phase and preferably in an HCl medium, to depolymerise the solutions and raise the K_d 's and the kinetics.

- with a fairly high D_2EHP acid content (positive effect on the K_d 's)
- with a high organic to aqueous (O/A) volume ratio to offset the low K_d 's in the presence of tungsten,
- with long contact times, owing to the slow kinetics,
- using selective solvent scrubbing to improve extraction selectivity.

STRIPPING CONDITIONS

In the case of cationic solvents, stripping is generally effected in a highly acid medium in order to shift the $M^{(n+)}/nH^+$ equilibrium. With molybdenum, the mechanics are more complex and acids have not turned out to be good stripping agents; on the other hand, the contact of the organic phase charged with a basic solution destroys the affinity of the molybdenum for the D_2EHP acid.

The stripping reaction is then total and fast. The MoO_2^{++} species being unable to exist in basic media:



If molybdenum-rich aqueous solutions are desired for the remainder of the treatment, stripping will have to take place in an ammoniacal (or ammonium carbonate) medium and with a recycling of the aqueous phase including an adjustment of pH to 9 by concentrated ammonia in the recycling vessel, so as to prevent any contact between the D_2EHP acid and the concentrated ammonia (emulsion hazard).

It should be noted that the ammonium salt of the D_2EHP acid forms a third phase in an organic diluent. A modifier is therefore required.

After stripping, the D_2EHP acid is entirely in the $NH_4R_2PO_4$ form. By stoichiometric contact with an acid (HCl or H_2SO_4), it must be transformed into HR_2PO_4 in order to recycle. Ammonium sulphate or chloride will be a by-product in this stage.

TESTS CARRIED OUT WITH CRYSTALLISATION MOTHER LIQUORS
IN MIXER-SETTLERS

The preceding results enabled an extraction scheme to be defined, comprising a dilution and an adjustment of the pH of the mother liquors before they pass to the mixer-settlers (Fig.3.0).

The various tests (Table 1) showed that:

- the pH stabilises at around 3 and 3.5,
- the WO_3 content must not exceed 50 g/l for the solutions to remain stable,
- the molybdenum distribution coefficients are acceptable and correspond to those determined,
- the $\frac{O}{A}$ ratio must be great if it is desired to exhaust the molybdenum solution (and it is necessary to have appliances enabling good emulsions to be obtained in these conditions).
- the contact times must be long,
- most of the molybdenum is extracted by the D_2EHP acid in 2 or 3 stages, the major part of the mixer-settlers serving to exhaust the solution,
- scrubbing at a pH ≈ 3 is efficient,
- concentrated stripping at a regulated pH (~ 9) is feasible.

Finally, various tests on the raffinates show that the extraction is not blocked and that molybdenum concentrations of under 50 mg/l (3) can be reached. The use of depolymerisers is particularly efficient. By adding an adequate number of stages or by increasing the solvent flow, the tungsten purity desired can therefore be reached in the raffinate.

EXTRACTION OF THE TUNGSTEN

The molybdenum having been extracted, the solution to be treated contains all the tungsten as well as the impurities (P, As, Si) which form the polyanions and which were not extracted by the cationic extractant (D_2EHPA). Therefore it is necessary in the second stage to find a specific tungsten solvent in order to purify the tungsten.

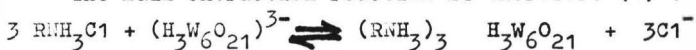
Study of the main extraction parameters

Amines of all classes completely extract the tungsten from the acid solutions: quaternary ammonium salts extract it again in the pH's exceeding 6 (4) (5). At acid pH's the secondary amines and particularly the tertiary amines form a complex with the tungsten whose solubility in the organic phase is very low. Polymers appear, aggregating and forming a gelatinous precipitate. The addition of alcohol slightly improves solubility. Some primary amines, on the contrary, extract the tungsten without forming any precipitate and the addition of alcohol prevents the third phase formation. Also the primary amines only extract very little silicon as SiO_3^{--} .

A primary amine was chosen: the JMT primene, an aliphatic amine with a branched alkyl chain, which possesses good settling qualities. It has been used in the hydrochloride form (RNH_3Cl) 5% diluted (or $0.13 M l^{-1}$) in dodecane (91 %) modified by ethyl 2 hexanol 1 (4%) to stay uniform in the first part of the process.

The extraction of the tungsten depends on the pH of the aqueous solution. At a pH of 8, the tungsten is present as mono-tungstate WO_4^{--} . At a pH of 6, the anion $(HW_6O_{21})^{5-}$ forms; at more acid pH's $(H_3W_6O_{21})^{3-}$ is found.

The main extraction reaction is therefore (4) :



The distribution coefficients at pH 3 and 4 (Fig.9) are significant and there is saturation of the solvent at around 60 g/l.

The extraction reaction is very fast. When the aqueous phase contains silicon and phosphorus, anionic silicotungstic and phosphotungstic acids are co-extracted. It is possible to add to the aqueous phase a certain quantity of depolymeriser, fluorine for instance; so as to form compounds of the SiF_4 and PF_4 types which are not extracted by the amines. According to (5) 100% excess is required in relation to the stoichiometric quantity (5 times the Si and P molarity) to complex the silicon and the phosphorus adequately. But it is necessary to avoid forming SiF_6^{---} or PF_6^{---} which are extractable kinds.

If the solution from which the tungsten is to be extracted still contains molybdenum, the latter is entirely co-extracted when the tungsten is totally extracted.

STRIPPING CONDITIONS

The use of ammonia based stripping reagents is a great advantage to the extent that this provides easy precipitation of the ammonium paratungstate. This precipitation can be effected at the same time as the stripping (7) (4) but generally it is preferred to strip the tungsten in soluble form and then precipitate it (5) (8) for the three phase extraction appliances are complex and costly.

It has been observed that the anion present in the organic phase is mainly $(\text{H}_3\text{W}_6\text{O}_{21})^{3-}$, the stripping reaction is then:

$$(\text{RNH}_2)_3 (\text{H}_3\text{W}_6\text{O}_{21}) + 12 \text{NH}_4\text{OH} \rightarrow 3 \text{RNH}_2 + 6(\text{NH}_4)_2 \text{WO}_4 + 9 \text{H}_2\text{O}$$

If the pH of the aqueous phase is more than 8 after stripping the organic phase can be checked for complete discharge (7)(4).

But although the stripping in one single contact can be virtually total, given the output pH, it does lead to an aqueous phase containing white ammonia paratungstate precipitates as soon as the WO_3 concentration therein exceeds 40 g/l.

The reason for this is that the simultaneous stripping of large amounts of tungsten brings about a surfeit of unstable anionic forms. The transformation reactions then release numerous H^+ ions and precipitation conditions can appear locally. Therefore, stripping with recycling of the aqueous phase must be envisaged so that a small quantity only of tungsten is stripped at each run to ensure proper transformation of the anionic form of the tungsten. During this recycling, the pH of the aqueous stripping phase must be readjusted by adding ammonia. Finally, the amine in basic form emulsifies if it is contacted with an aqueous solution of a pH above 10.

TESTS EXPECTED IN MIXER-SETTLERS

The solution feeding the tungsten extraction bank is the raffinate from the extraction of the molybdenum. Its pH is therefore around 3 to 3.5 (Fig.8).

A test made on the raffinate of the sixth molybdenum extraction run gave the following results (table 2).

TABLE 2
Molybdenum-tungsten separation test. Tungsten recovery

	WO_3 g/l	Mo g/l	F^-
Mother liquors	95	6.2	$5 \cdot 10^{-2}$
Raffinate from the extraction of the molybdenum + F^- = feed	39	0.34	$5 \cdot 10^{-2}$
Raffinate from the WO_3 extraction	0.057	0.004	
Stripping solution	96.5	1.09	

WO₃ percentage recovered over both runs : 99.5%
Separation factor: (Mo/WO) mother liquor / (Mo/WO₃)
stripping solution = 6.38³

(Mo/WO₃) stripping solution: = 1.02 (by weight).

This test showed that:

- 3 or 4 stages suffice completely to extract the tungsten,
- concentrated stripping is feasible but it uses too much ammonia,
- there is no molybdenum-tungsten separation in the tungsten extraction stage. The total separation factor for tungsten therefore only depends on the prior extraction of the molybdenum.

SEPARATION OF THE IMPURITIES AND COST

It was found, from a number of determinations effected during run 6, that scrubbing the aqueous phase from molybdenum stripping with a diluent, enables the D₂EHP acid solubilised in the aqueous phase (150 mg/l for D₂EHPA 10%) to be recovered. The $\frac{P}{Mo}$ ratio is then under 0.05%. The arsenic and the silica are not extracted.

The extraction of the tungsten enables the $\frac{As}{WO_3}$ ratio to be divided by three. On the other hand, the silica and the phosphorus were almost entirely extracted, probably because the fluorine content was badly adjusted.

Finally, a calculation of the costs shows that the reagents for such a process work out at around Fr. 4.50 per kg of WO₃ (including solvent losses and without any ammonia recycling).

CONCLUSIONS

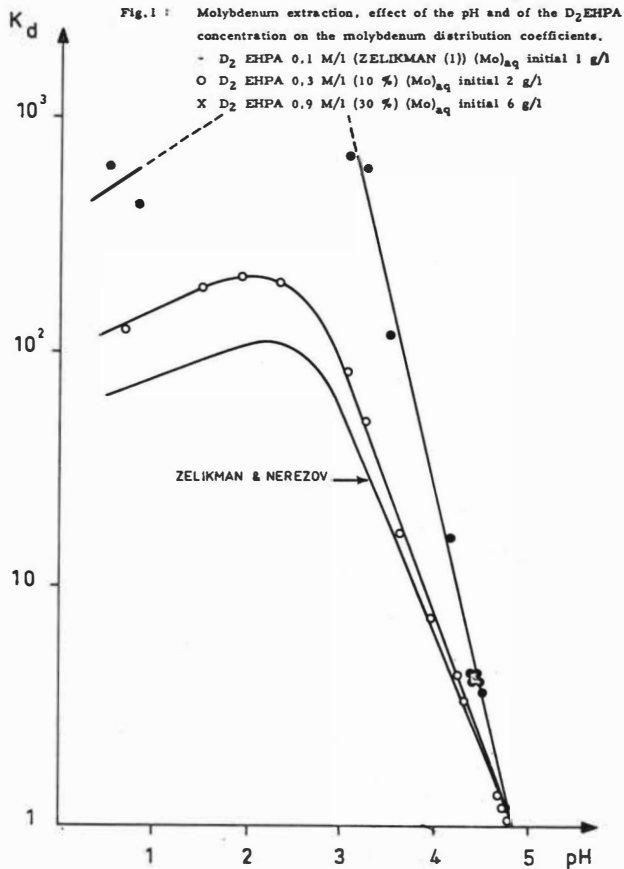
Thus, the entire molybdenum extraction process followed by the extraction of the tungsten can be used for solutions where the WO_3/Mo ratio is not too great. The molybdenum is then easily separated and the tungsten can then be purified by successive precipitations, or by extraction followed by a precipitation, or yet again by several extraction runs.

The molybdenum was not totally extracted where the solutions contained tungsten in greater concentrations but this extraction seems feasible.

As concerns the tungsten, extraction was found to be feasible, purification, on the other hand, does not appear to be complete. Numerous patents and articles have studied this problem and it would appear that it is not possible to achieve total purification in one single extraction stage. However, fluorine used in the aqueous phase or a second tungsten extraction run could lead to pure tungstate solutions.

REFERENCES

- (1) A.N. ZELIKMAN, V.M. NIEREZOV
Russ. J. of Inorg. Chem. 5. (1969) 685
- (2) V. CHIOLA and all (Sylvania Electric Products Inc.)
U.S.P. 3 607 007 (21 sept. 1971)
U.S.P. 3 607 008 (" ")
- (3) F. ESNAULT, M. ROBAGLIA, J.M. LATARD, J.M. DEMARTHE
Bulletin d'Information Scientifique et Technique C.E.A. n° 185 (oct 73)
p. 59
- (4) P.E. CHURCHWARD, D.W. BRIDGES
U.S. BM-RI 6845 (1966)
- (5) J.L. DROBNICK, C.L. LEWIS
Met. Soc. Conf. A.I.M.E. 24 (1963) 504-514
- (6) BLAIR BURNWELL
B.P. I 013 364 (15 déc. 1965)
U.S.P. 3 256 057 (14 juin 1966)
U.S.P. 3 256 058 (14 juin 1966)
A. ROBIETTE
B.B. 671 325 (12 nov. 1965)
B.P. I 089 913 (8 nov. 1967)
- (7) GENERAL MILLS INC.
B.P. 895 402 (2 mai 1962)
- (8) UNION CARBIDE CORPORATION
B.P. 889 295 (14 février 1962)



-1990

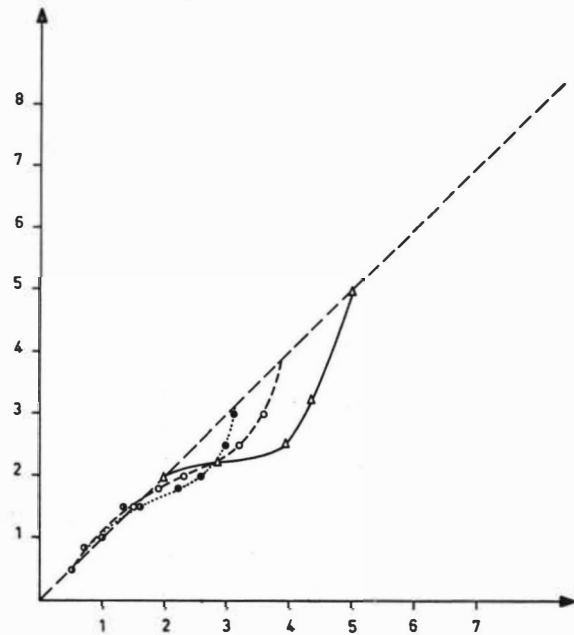
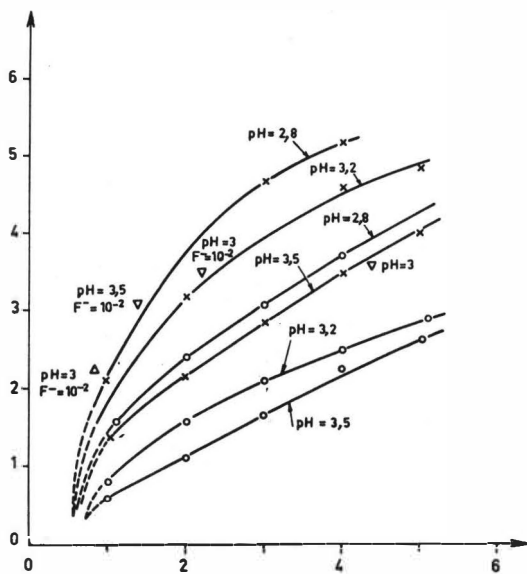
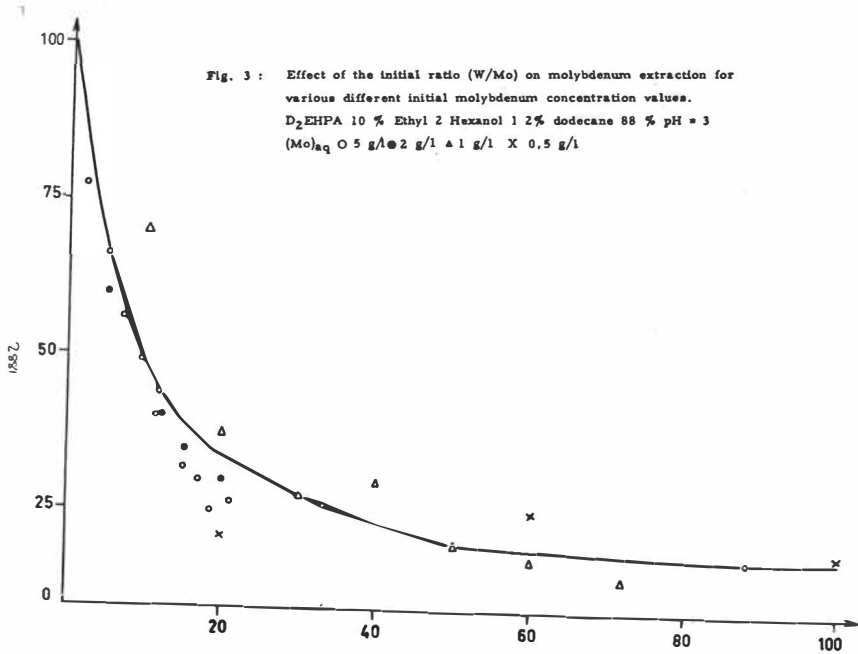


Fig. 2 : Relation between the pH's before and after molybdenum extraction.

- Δ D₂ EHPA 0,1 M/l (Mo)_{aq} initial 1 g/l
 ○ D₂ EHPA 0,3 M/l (Mo)_{aq} initial 2 g/l
 X D₂ EHPA 0,9 M/l (Mo)_{aq} initial 6 g/l



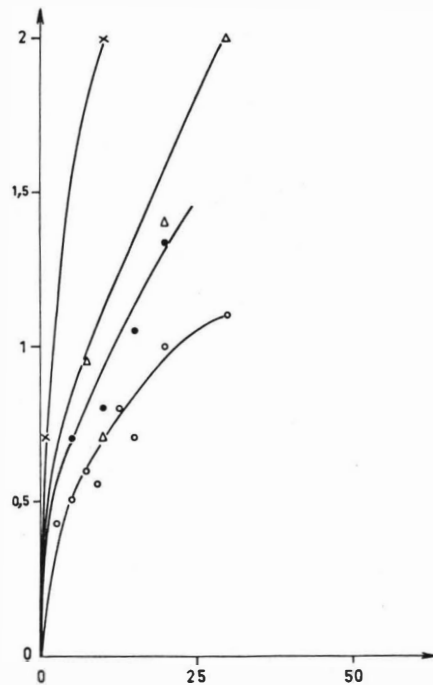


Fig. 5 : Molybdenum extraction - Effect of the initial ratio (WO_3/Mo) on extraction selectivity for various different molybdenum concentrations.

D_2EHPA 10 % ethyl 2 hexanol 1 2 % dodecane 88 % pH = 3

1 - $(WO_3)_{aq} = 40$ g/l $(Mo)_{aq} = 2$ g/l
 2 - $(WO_3)_{aq} = 20$ g/l $(Mo)_{aq} = 2$ g/l
 3 - $(WO_3)_{aq} = 40$ g/l $(Mo)_{aq} = 4$ g/l

Fig. 6 : Effect of contact time on molybdenum extraction :

D_2EHPA 10 % , ethyl 2 hexanol 1 2 % , dodecane 88 % pH = 3

X synthetic solutions 1 - $(WO_3)_{aq} = 40$ g/l $(Mo)_{aq} = 2$ g/l
 2 - $(WO_3)_{aq} = 20$ g/l $(Mo)_{aq} = 2$ g/l
 3 - $(WO_3)_{aq} = 40$ g/l $(Mo)_{aq} = 4$ g/l
 4 - $(WO_3)_{aq} = 20$ g/l $(Mo)_{aq} = 3.5$ g/l

Δ industrial solutions 1 - $(WO_3)_{aq} = 30$ g/l $(Mo)_{aq} = 1.5$ g/l
 2 - $(WO_3)_{aq} = 35$ g/l $(Mo)_{aq} = 1.5$ g/l
 3 - $(WO_3)_{aq} = 40$ g/l $(Mo)_{aq} = 1.5$ g/l

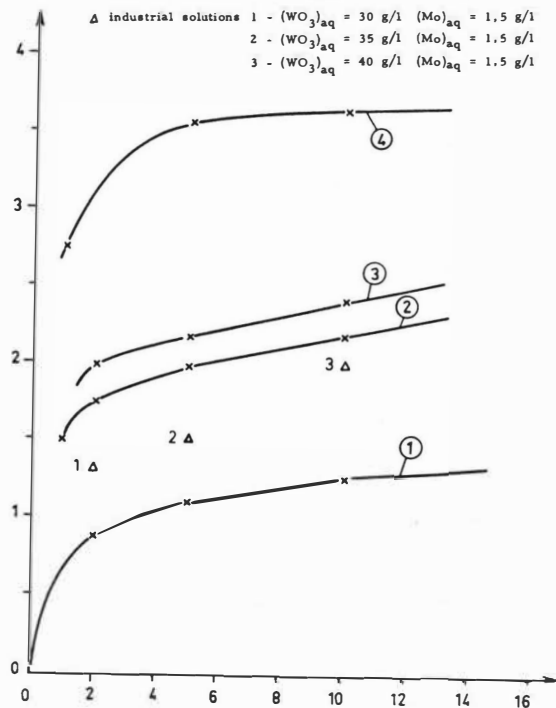


Fig. 7 : Molybdenum extraction. Change in the distribution coefficients with the time interval separating the adjustment of the pH and extraction with respect to various different industrial solutions. D_2EHPA 10 %, ethyl 2 hexanol 1 2 %, dodecane 88 % pH = 3

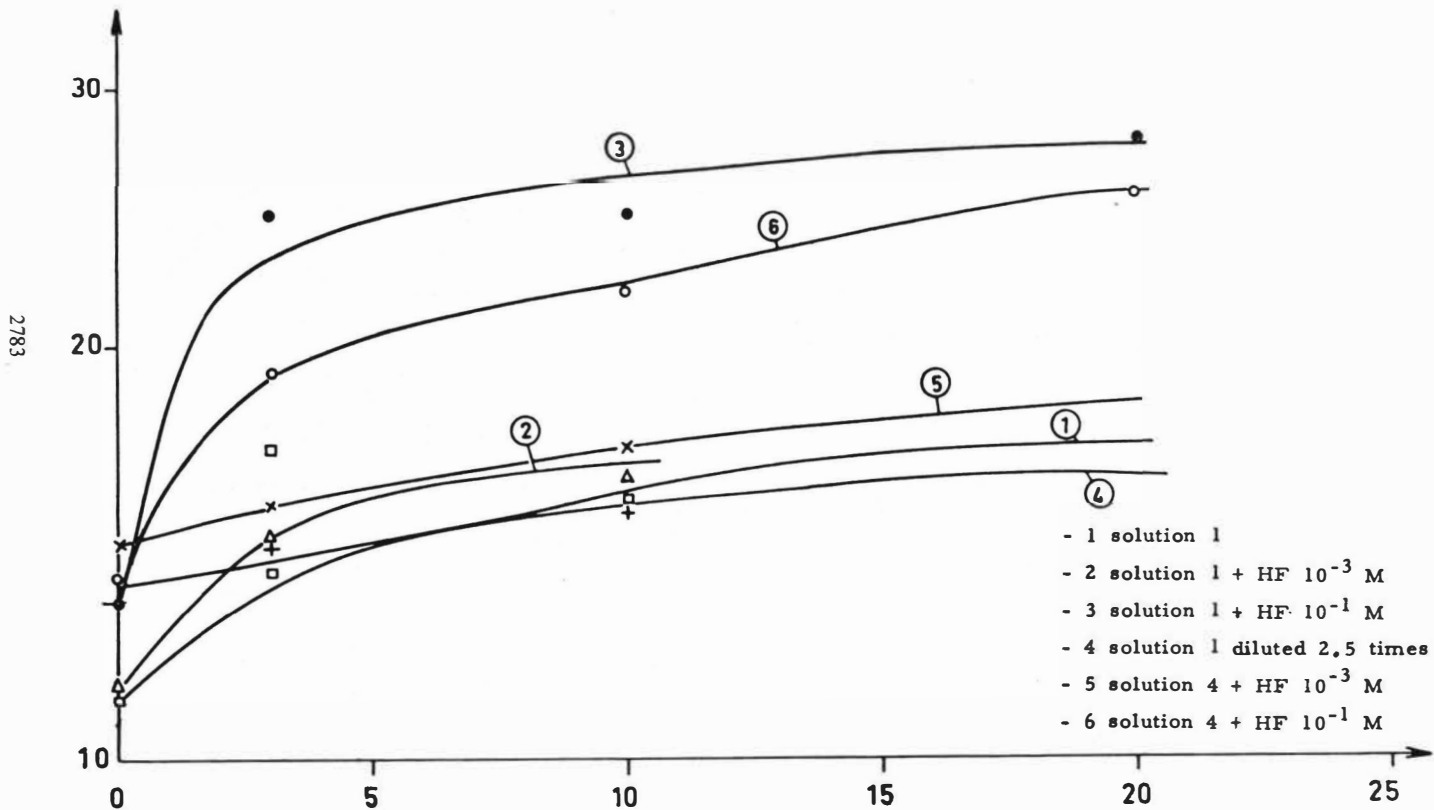
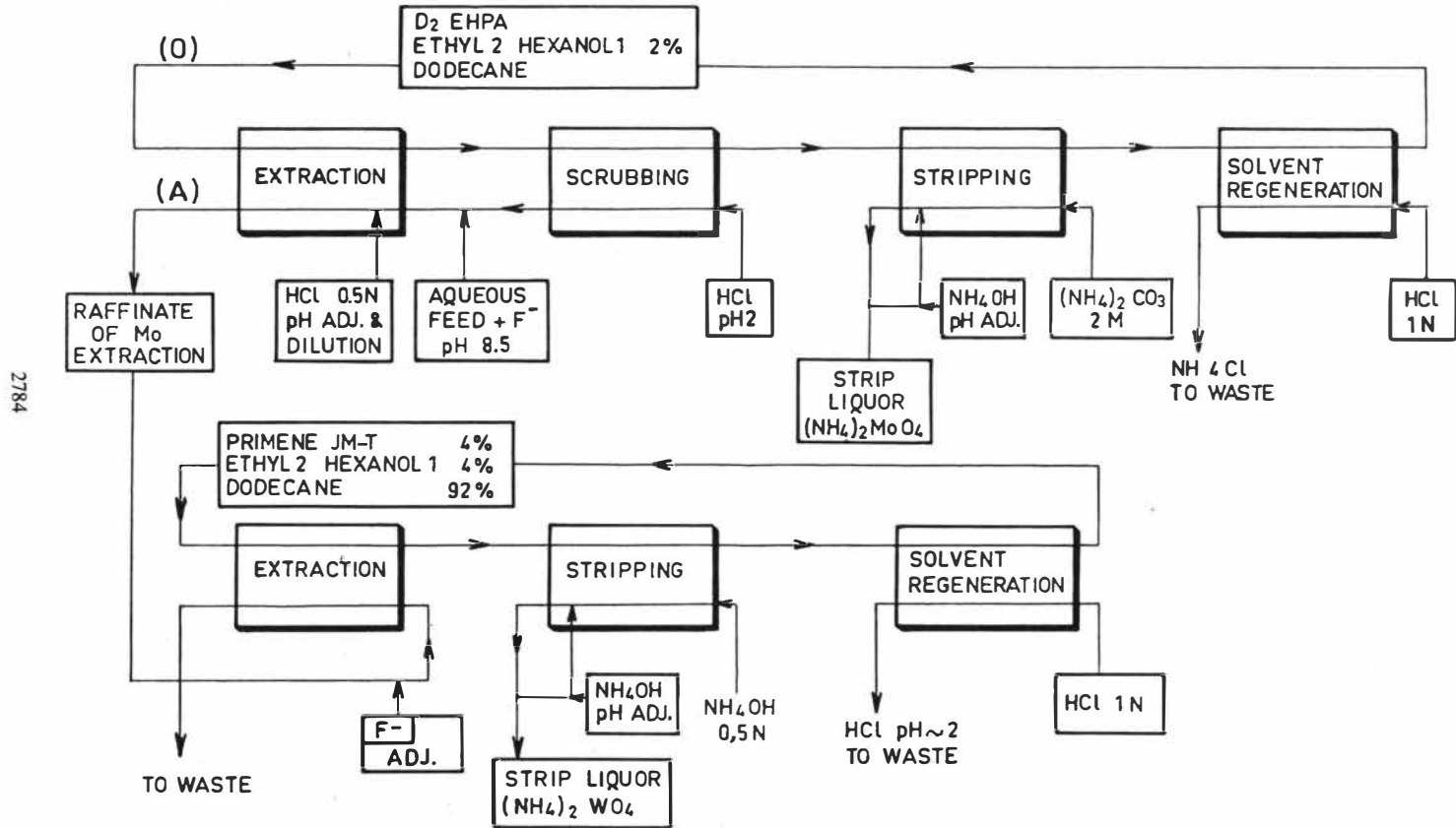


Fig. 8 : Extraction scheme used for molybdenum-tungsten extraction



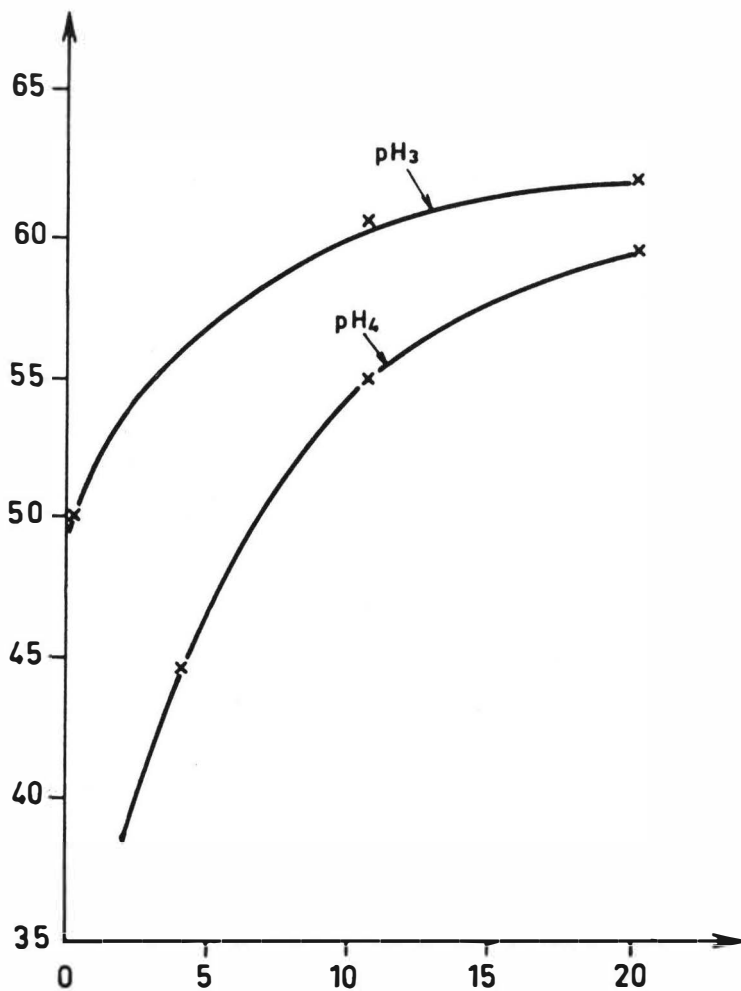


Fig. 9 : . Extraction of tungsten : equilibrium lines.
 J.M.T. primene 5 % (HCl salified)
 dodecane 93 %
 ethyl 2 hexanol 1 2 %

SESSION 27

Friday 13th September: 9.00 hrs

INDUSTRIAL PROCESSES

(Development, Performance and Economics)

Chairman:

Mr. B.F. Warner

Secretaries:

Dr. P.J. Boiles

Mr. J. Coste

INTERESTING ASPECTS IN THE DEVELOPMENT OF A NOVEL SOLVENT EXTRACTION
PROCESS FOR PRODUCING SODIUM BICARBONATE

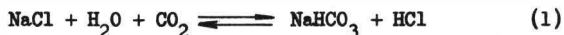
R. Blumberg, J.E. Gai and K. Hajdu.

IMI-Institute for Research and Development,
P.O.B. 313, Haifa, Israel.

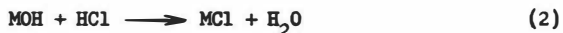
A novel process has been developed for converting sodium chloride and carbon dioxide into sodium bicarbonate and hydrochloric acid. Conceptually a simple multicycle system was defined for achieving the process aims; in practice this entails two liquid-liquid extractions using an amine as the means for hydrochloric acid transfer. Solubilities and acid/base relationships impose very fine limits of reversibility on the amine system selected. Amine/diluent interactions are exploited, as well as the degrees of freedom of the phase rule. The interplay of chemistry and technology make this an unusual liquid-liquid extraction process.

INTRODUCTION

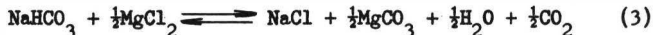
A novel process ¹⁾ has been developed for converting sodium chloride and carbon dioxide into sodium bicarbonate and hydrochloric acid. The equilibrium reaction represented by the equation (1)



is unfavourable and requires removal of HCl if it is to proceed to the right. Conceptually the simplest way to achieve this is by the introduction of a suitable base "MOH" to give the reaction represented by the equation(2).



Since it is the aim of the process to produce also hydrochloric acid, it is necessary to select MOH so as to permit the reverse reaction to be achieved under suitable technological conditions, in order to liberate the HCl again. Presently magnesium chloride is the most suitable chloride from the point of view of thermo-hydrolytic decomposition, hence magnesium hydroxide has been selected as the neutralising base. Unfortunately magnesium hydroxide cannot be used directly within the reaction between sodium chloride and carbon dioxide since the equilibrium represented by the equation (3) lies far to the right.



This has necessitated the selection of a second base to be interposed as chloride acceptor so as to obviate direct contact of Mg^{2+} and HCO_3^- . Since the strong basicity of many simple high molecular weight amines, relative to aqueous solutions of acids has been known for some time, it was thought to utilise an amine as the intermediate base in the process for coproduction of sodium bicarbonate and hydrochloric acid. The equations (4) (5) and (6) represent, therefore, the sequence of reactions constituting the process.



From a technological point of view it is clearly desirable that the amine components (free amine and hydrochloride) should constitute a separate liquid

phase, thus facilitating separation of feed components, recycle streams, and products. This of course leads directly to liquid-liquid extraction systems for equations (4) and (5).

Although this basic idea seems simple enough, there are various features which distinguish it from most other such systems. Thus in equation (4) the sodium bicarbonate is to be precipitated as a solid phase, and the carbon dioxide is potentially present as a gas phase, so that this system is nominally composed of four phases instead of the usual two. Many aspects are rather different, therefore, from those normally encountered by solvent extraction technologists.

In the following a description will be given of the considerations required to translate the basic idea into a technologically feasible process. However this paper is not a case history of process development, but a discussion of physico-chemical aspects of the liquid-liquid extraction systems which have relation to the practical process application. The paper falls, therefore, in the "no-man's land" between pure chemistry and chemical technology.

AMINE-DILUENT COMBINATION

The first requirement of any solvent is that it must perform the extraction for which it is intended. In the present case this means, firstly, that the amine, in its diluent or carrier solvent has to be sufficiently basic to cause reaction (4) to proceed from left to right. Since the solvent has to be recycled and it is also necessary to strip out the HCl, this means that the amine salt must be sufficiently acidic to permit reaction (5) also to proceed from left to right.

In the following, the stage involving execution of reaction (4) is termed "reaction", while that of reaction (5) is termed "regeneration". In general, the former stage is the one that will be discussed in this paper, but the latter has to be considered, too, in order to understand the choice of solvent.

If both stages are performed at ambient temperature, and the carbon dioxide pressure in the reaction stage is atmospheric, it can be calculated that the basicity of the amine/diluent system should be equivalent to that of a water-soluble base having pK_b lying between 4 and 6. A more practical form of the requirement is that an aqueous solution, in equilibrium with the hydrochloride

form of the amine in carrier solvent, should have as low a pH as possible while still not causing decomposition of the bicarbonate under the given carbon dioxide pressure. One of the methods used for characterizing this, was the measurement of half-neutralization pH, i.e. the pH of an aqueous solution in equilibrium with solvent containing equivalent amounts of free amine and of amine salts.

Various commercially available tertiary, secondary and primary amines were tested in polar and non-polar diluents. Typical results are presented in Table 1. It appeared that secondary and primary amines are generally too strongly basic to permit convenient regeneration with magnesium hydroxide. The amine finally selected in practice was a tertiary amine containing eight to twelve carbon atoms per chain, referred to here as TCA. As can be seen from Table 1 there is a strong influence of polarity of solvent on the basicity of the system. Thus TCA in a non-polar diluent, such as xylene, gives a half-neutralization pH which is too low (2.4) for reasonable conversions of the amine into its hydrochloride in the reaction system. Since it could be concluded that a more polar diluent was required, nitrobenzene was initially selected for further study based on information derived from the literature.^{2,3)} This diluent caused the amine to have about the correct basicity, but it introduced a different problem, namely one of solubility. Whereas the amine hydrochloride is suitably soluble in nitro-benzene, the free amine has only limited solubility. This is the reverse of the more common solubility problems in liquid-liquid extraction, where limited solubility of polar constituents in non-polar diluents is usually encountered. Furthermore, for technological reasons, in view of the high molecular weight of the amine, it is desirable to work with concentrated solutions, in other words with maximum ratio of amine to diluent. The possibility of working with systems containing three liquid phases is very tempting since additional separations are thus inherent in the system, but, technologically, it is inconvenient. A recognised procedure for preventing third phase formation is the addition of a higher aliphatic alcohol and, indeed, addition of decanol to the nitro-benzene eliminated the problem. While investigating the optimum concentration of decanol required, it was observed that the conversions of amine to amine hydrochloride were increased by the presence of the alcohol.*

* This led later to a rather detailed study of interactions in such a system⁴⁾ in which it was found that the combined diluent effect was non-additive, i.e. that mixtures of nitrobenzene and decanol could make the amine more basic than either of them taken alone.

Finally, various alcohols were studied by themselves and these were found to give increased conversions to amine hydrochloride as the chain length decreased, as shown in Table 2.

TABLE 1: Half titration pH values of Amine-HCl systems in the presence or absence of diluents.

Amine : Diluent ratio = 1 : 1 by weight.

Amine Formula	Mol.Wt.	Diluent		
		Xylene	i-AmOH	No diluent
$N(C_{13}H_{27})_3$ branched	563	2.2	3.8	2.5
$N(C_{12}H_{25})_3$ straight chain	521	2.5	5.0	Precipitate
NR_3 (R = C ₈ - C ₁₀ straight chain)	351 - 437	2.8	4.5	3.0
$ \begin{array}{c} \text{CH}_3 \quad \text{CH}_3 \\ \quad \\ \text{CH}_2 - \text{CH} = \text{CH} - \text{CH}_2 - \text{C} - \text{CH}_2 - \text{C} - \text{CH}_3 \\ \quad \\ \text{CH}_3 \quad \text{CH}_3 \\ \text{C}(R_1, R_2, R_3) \end{array} $	341 - 393	4.0	5.6	4.4
$R_1 + R_2 + R_3 = C_{11} - C_{14}$				
H_2NR	269-325	Higher than 6.0		
R = C ₁₈ to C ₂₂ branched				

TABLE 2: Conversion of TCA to its hydrochloride - in equilibrium with a saturated NaCl brine at 1 atmospheric CO₂ pressure - as a function of dilution with alcohols of different chain length.

Diluent (alcohol)	1 solvent/mole amine	
	0.5	0.8
	Conversion percent *	
i-PrOH	90	95
n-BuOH	74	91
n-AmOH	67	86

$$* \text{ Conversion percent} = \frac{\text{mole Amine.HCl}}{\text{mole total Amine}} \times 100$$

The lower limit in the choice of the molecular weight of the alcohol for practical purposes is governed by its miscibility with water, so the final choice of diluent was n-pentanol. This choice obviated altogether the necessity of using nitrobenzene as diluent component and thus eliminated the problem of the third phase formation. In subsequent process development work, a 50/50 weight mixture of amine and n-pentanol was used.

In addition to the half-neutralization pH, another aspect examined in the screening studies was the absorption of carbon dioxide. Typical data for comparison of diluents on the basis of carbon dioxide absorption are presented in Table 3. The data were determined by connecting a gas burette containing the gas to a vessel containing a mixture of TCA, diluent and sodium chloride brine (in the presence of solid sodium chloride) and stirring until no more absorption was observed. Since carbon dioxide is also physically absorbed in the liquid phases, there was absorption in every case; however, in the presence of alcohol or nitrobenzene, where amine hydrochloride was formed, the volume of absorbed carbon dioxide is almost an order of magnitude higher than in the case of other diluents where no reaction occurs.

TABLE 3: CO₂ volumes absorbed by systems composed of 10 mmole of TCA in the presence of various diluents and saturated NaCl brine (at 25°C and 1 atmospheric CO₂).

Diluent	ml	NaCl brine ml	CO ₂ absorbed ml
Iso-propanol	5	5.0	218
"	10	5.0	228
Iso-amyl alcohol	5	5.0	194
Nitrobenzene	5	5.0	124
"	8	5.0	218
Xylene	8	5.0	38
Kerosene	11	5.7	36

Up to this point we have considered only the physico-chemical interactions of the amine/diluent system aimed at satisfying the requirements of equation (4), the reaction. However, each increase in solvent basicity, which favours the reaction, has a deleterious effect on the regeneration as expressed by equation (5). Here the acidity of the Mg(OH)₂/MgCl₂ aqueous phase as a function of magnesium chloride concentration defines the limitations of the system, since it is technologically desirable to attain as concentrated a solution of aqueous magnesium chloride as possible. This influence can clearly be seen in Table 4.

TABLE 4: pH values of MgCl₂/Mg(OH)₂ aqueous solutions.

MgCl ₂ Wt. %	Mg(OH) ₂ saturation Wt. %	pH
6.3	0.003	8.5
9.0	0.005	8.7
12.6	0.008	8.6
17.7	0.022	8.0
34.3	0.212	6.5

Since equation (5) represents an equilibrium reaction, there is a relationship between the magnesium chloride concentration in the aqueous phase and the free amine/amine hydrochloride ratio in the solvent phase, as can be seen in Table 5.

TABLE 5: Equilibrium in the system $MgCl_2-H_2O$ /Amine-Am.HCl-AmOH as a function of $MgCl_2$ concentration.

Aqueous Phase		Solvent Phase (Wt.%)				TCA/TCA.HCl
$MgCl_2$	Wt. %	TCA	TCA.HCl	H_2O	AmOH	equiv.ratio
23.3		40.2	11.3	1.8	46.7	3.8
14.4		49.8	1.4	1.9	46.9	40.0

Technologically this implies counter-current operation. In practice four stages were found satisfactory for the amine/diluent combination selected on the basis of the considerations defined above. This solvent system limited the concentration of magnesium chloride obtainable to about twenty eight percent.

As a matter of general interest, the amine was virtually insoluble in the process brines (< 10 ppm), while two typical pentanol solubilities were 1.2 g/l in the reaction brine and 4 g/l in the concentrated magnesium chloride solution.

OTHER THERMODYNAMIC PARAMETERS

Although the choice of amine-diluent combination is the one which fixes the most important thermodynamic parameter of the system, namely the solvent basicity, there are also several others to be considered. In a system with a multiplicity of possible phases, there are phase rule limitations under certain possible conditions and it is instructive to consider them. For this purpose it is sufficient to regard the amine as a single component (even though there may be additional minor amine compounds present in practice).

The reaction system contains 6 components: amine, diluent, CO_2 , NaCl, $NaHCO_3$ and H_2O . The extreme case occurs when there is a brine simultaneously saturated with both NaCl and $NaHCO_3$ (i.e. these are considered present also as solids), two organic liquid phases (e.g. as with nitrobenzene), and a CO_2 -

containing gas phase. For a given carbon dioxide pressure and a given temperature (see below), the system is invariant, but, practically speaking, when the phase rich in free amine disappears during the course of the reaction, one degree of freedom becomes available.

For the latter case, i.e. with only one organic liquid phase present, the degree of freedom available relates to the concentration of amine in the diluent. One expects that as the concentration of amine is increased, the amount of HCl transferred per unit volume of solvent will increase, this being a relevant technological consideration. However, with highly solvating diluents this is true only up to a certain point because of the loss of the effect as the ratio of diluent to amine decreases. This can be seen clearly from Figure 1.

If the brine is not saturated with NaCl, an additional degree of freedom is introduced which expresses itself merely as a decrease in amine hydrochloride concentration with decreasing NaCl concentration. Technologically, this occurs when the initial feed brine is nearly saturated but becomes depleted as the reaction proceeds. In a typical practical application the feed brine contained 26% NaCl and was not permitted to drop below 24%, the latter already causing about 10% loss in the HCl-transport ability of the solvent, compared to the former.

Since sodium bicarbonate is the least soluble salt, and its solubility varies only slightly over the ranges considered, it can be assumed that the brine will remain saturated with respect to it at all times; hence this does not affect the degrees of freedom and it is therefore not a process control factor.

Considering, firstly, only the equilibrium of the reaction (4), the effect of increasing the temperature is to shift the equilibrium to the left, as is to be expected for an exothermic reaction. This would indicate that reaction (4) be executed at as low a temperature as possible. The heat of reaction for equation (4) was determined as being approximately - 19 Kcal/mole (exothermic), and this heat has to be removed. Actually, the question of cooling, and temperature of operation, has several aspects which will be referred to again under technological considerations. In contrast to the reaction, the regeneration is apparently only slightly endothermic, to the extent of 1-2 Kcal/mole, and is favoured by higher temperatures.

The last parameter to be considered is that of carbon dioxide pressure. As shown in Figure 2, the amine-hydrochloride/free-amine equivalent ratio in the equilibrium organic phase was found to be a straight-line function of the partial pressure of carbon dioxide, over the pressure range investigated, namely one to three atmospheres absolute of carbon dioxide. This means that the influence of pressure for each specific case can easily be evaluated.

KINETIC AND TECHNOLOGICAL CONSIDERATIONS

Although this paper is intended as a study of interactions in complex, multi-component, multiphase systems, kinetic and technological considerations cannot be excluded.

Reaction

The simplest form of executing reaction (4) would be to introduce all the feed components together and to let the reaction proceed under invariant conditions. This would then involve mass transfer between the following phases:

gas to liquid (CO_2)
liquid to liquid (HCl)
nucleation of solids, followed by liquid to solid
 ($\text{precipitation of NaHCO}_3$)
solid to liquid (dissolution of NaCl)

If, for practical reasons, it is convenient to avoid the possibility of contamination of the solid sodium bicarbonate by solid sodium chloride, it is possible to assume that the sodium chloride feed be initially dissolved in the aqueous feed brine; there are then still three feed streams, namely aqueous, solvent and gas, to be considered.

Since the system is no longer invariant, the technological possibility of counter-current operation presents itself. However, since of the three inter-phase transfers listed that of gas to liquid is much the slowest, especially if it cannot be performed under conditions favourable for gas-liquid contact, it was decided to pre-absorb the amount of carbon dioxide needed for the reaction into the solvent (which has a carbon dioxide solubility about eight times that of the brine) under pressure, ahead of the reaction, thus reducing the feed streams to two. In order to avoid having to perform phase separations

under pressure, as would probably be required in counter-current operation, cocurrent operation was chosen.

Stoichiometric considerations and equilibria determine the phase ratios of solvent to aqueous phase per unit of HCl transferred. This then determines also the quantity of carbon dioxide required for the reaction; its solubility in the quantity of solvent, as a function of pressure, determines the pressure under which the initial absorption must be performed. Using pure carbon dioxide, this was found to be eight atmospheres absolute, for the amine/diluent combination selected. A certain amount of the overall heat of reaction is liberated in this step. In a pilot scale packed column there was a temperature rise of about 8°C.

The reaction proper was tested continuously, in stirred tank reactors operating under pressure. A minimum of three reactors in series was required. The reason for reactors in series is partly to avoid short-circuiting of reactants but also, more important, to avoid flashing out of dissolved carbon dioxide. Thus, if only one reactor were used, with the products existing at atmospheric pressure, the carbon dioxide dissolved in the feed solvent would largely flash out before having time to react. This was obviated by maintaining the reactors at successively decreasing hydrostatic pressures, with throttling between them. The overall residence time for all the reactors together is approximately six minutes. It was found that when clear feed brine was used, there was a tendency to supersaturation of sodium bicarbonate; this means an increase in concentration of one component on the product side of equation (4), tending to reverse the equilibrium reaction; the result of this was that the reaction did not proceed to the desired extent. For this reason the presence of a minimum amount of bicarbonate crystals in the feed brine was essential to provide seeding. Reaction rates were not sensitive to the degree of agitation, as long as the latter was good according to accepted practice.

Phase Separation

The reactor products have to be separated into a reasonably clear solvent phase, recycle brine and a slurry of sodium bicarbonate crystals. This was achieved in a single vessel incorporating in a particular way the features of a settler for liquid-liquid separation and a thickener for solid-liquid separation. The solvent was removed by periferial overflow while the recycle

brine was removed through a side outlet somewhat below the brine-solvent interfacial zone.

The recycle brine is sent to be resaturated with sodium chloride, the solvent goes to regeneration, and the sodium bicarbonate crystals are separated, washed and dried. Figure 3 gives a schematic presentation of the flowsheet.

ACKNOWLEDGEMENTS

Apart from the authors of this paper, all those listed as inventors of the process had a very active part in the development described. D. Gonen was in charge of piloting and various persons participated in operation. This paper is published with the permission of the management of IMI-Institute for Research and Development.

REFERENCES

- 1) Blumberg, R.; Baniel, A.; Gai, J.E.; Hajdu, K.; Neuberger, M.; Shorr, L.M.
A process for the manufacture of alkali metal bicarbonates.
1969, Israel Pat. 33552
- 2) Wilson, A.S. and Wogman, N.A.
J. Phys. Chem., 1962, 66, 1552
- 3) Muller, W. and Diamond, R.M.
J. Phys. Chem., 1966, 70, 3469
- 4) Gai, J.E.
Solvation Phenomena in the system: Tri-octyl amine-Nitrobenzene-Decanol-Hydrochloric Acid.
1971, Ph.D thesis (Technion, Israel Institute of Technology, Haifa.)

FIG. 1

CONCENTRATION OF HCl IN ORGANIC PHASES IN EQUILIBRIUM WITH AN AQUEOUS BRINE SATURATED WITH NaCl AND NaHCO₃ AT 1 ATM. CO₂ PRESSURE AND 25°C. AS A FUNCTION OF TCA CONCENTRATION IN SOLVENT (TCA-AMOH)

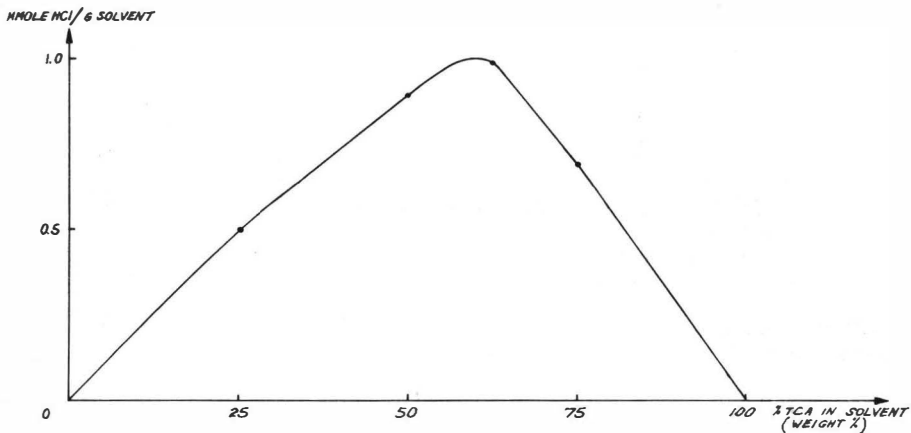


FIG. 2

EQUILIBRIUM AMINE · HCl/AMINE RATIOS IN THE PRESENCE OF A SATURATED NaCl BRINE - AT VARIOUS CO₂ PRESSURES.
 SOLVENT COMPOSITION: 38.0% TCA
 37.2% NITROBENZENE
 24.8% DECANOL

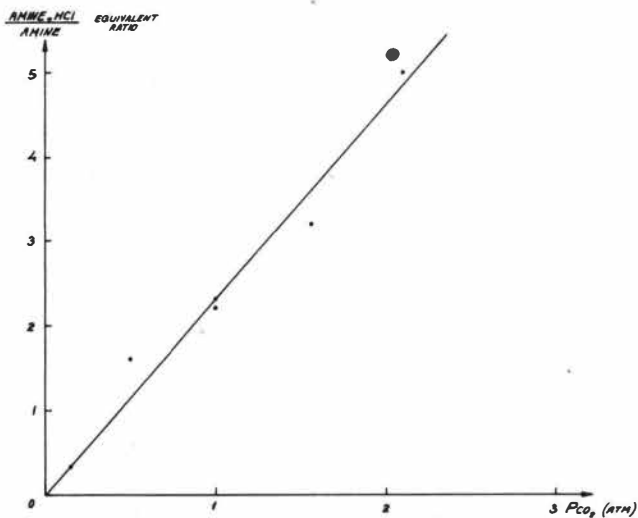
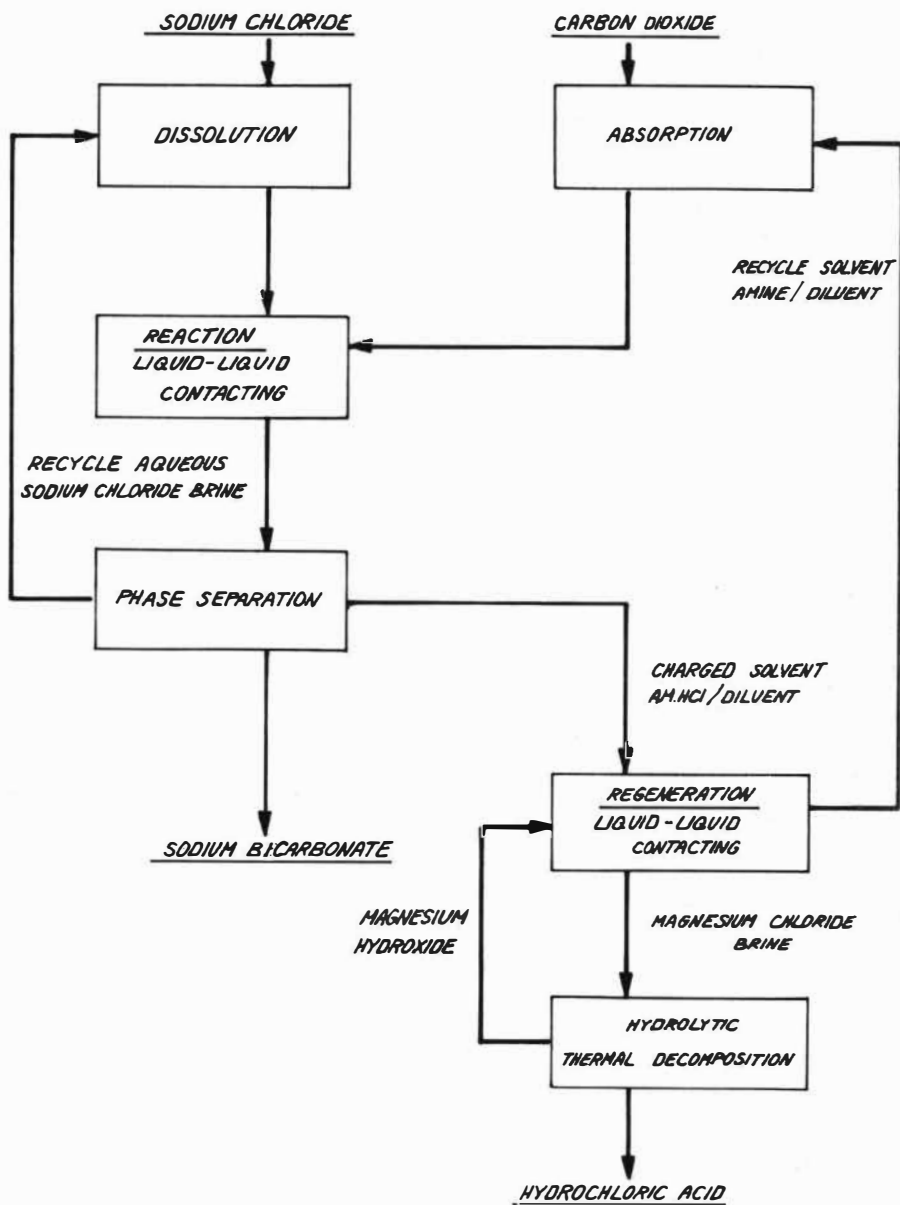


FIG. 3 SCHEMATIC FLOWSHEET



BY

U. Kuylenstierna x)
Stora Kopparbergs Bergslags AB
S-791 01 Falun 1
Sweden

H. Ottertun x)
Department of Nuclear Chemistry
Chalmers University of Technology
S-402 20 Göteborg 5
Sweden

A solvent extraction process for the recovery of acids and metals from the waste solutions produced by stainless steel pickling plants is described. The pickling acids, the monovalent acids HNO_3 and HF are extracted by tributylphosphate (TBP). The metals are recovered from the raffinate by precipitation (1).

Alongside a theoretical evaluation of the process, pilot plant experiments on both mixer-settlers and pulsed sieve-plate columns have been carried out. Based on the development work, a plant has been built by Stora Kopparbergs Bergslags AB at their Stainless Steel Works in Söderfors, Sweden.

x) Present address:
MX-Processer AB
Frötallsgatan 19
S-421 32 Västra Frölunda, Sweden.

The recovery process for acids and metals.

The stainless steel pickling solution is processed according to the flow scheme in Figure 1.

Concentrated sulphuric acid is added to the pickling solution in proportion to the total metal content. The temperature, raised by the heat of solution, is reduced to about 25 °C in a heat exchanger, where the cooling medium is the process water used to strip extracted acids.

Nitric acid, hydrofluoric acid and molybdenum are extracted counter-currently with 75% TBP in kerosene. The extraction efficiency for the acids is primarily dependent on the concentration of sulphuric acid, the phase flow ratio and the number of theoretical stages. A low temperature favours the extraction.

The loaded organic solution is stripped of the acids and some 50% of the molybdenum by contacting it with pure water. A high temperature is favourable for stripping in that it enhances phase separation and reduces the distribution factors. The stripping efficiency is primarily dependent on the phase flow ratio and the number of stages.

The evaporation of water from the pickling liquor in the bath permits a higher aqueous flow in the stripping operation than in the extraction operation. At a ratio of 1.3 (strip liquor flow to pickling liquor flow) and with at least 10 theoretical stages in both extraction and stripping a total theoretical recovery of 95% nitric acid and 65% hydrofluoric acid is attained.

In the Söderfors process pneumatically-pulsed sieve-plate columns are used as contactors both for extraction and stripping.

The non-stripped acids, molybdenum and degradation products are removed in a caustic wash before the solvent is recycled. A mixer-settler is used as contactor in this unit.

The weakly acidic raffinate from the extraction operation containing the metals, mainly as sulphates but also as fluorides, is treated with limestone and NaOH to precipitate the fluoride as CaF_2 and the metals as hydroxides.

Apart from precipitating the fluoride, the limestone also facilitates filtration of the slurry. At the Söderfors plant, the caustic wash solution is mixed together with the raffinate in the precipitation unit, whereby molybdenum (as CaMoO_4) is recovered together with the other metals.

Single stage experiments. Distribution data.

Tributylphosphate (TBP) forms adduct complexes with acids, which are soluble in many organic solvents, e.g. kerosene. From a pickling solution containing the acids HNO_3 , HF and H_2SO_4 , the preferential order of extraction is HNO_3 , HF and H_2SO_4 . The distribution factor for H_2SO_4 is so small that extraction of this acid is negligible. Various species have been proposed between the extracted acids and TBP and water (2,3,4).

The thermodynamics of the extraction of HNO_3 and HF is too complicated to be represented by a simple chemical model. Neither the activity factors in the two phases nor their variations are known. The simultaneous extraction of HNO_3 and HF has been studied experimentally in systems having aqueous solutions comparable to those in the industrial process. The experiments were carried out to obtain data of the type D_{nitrate} , $D_{\text{fluoride}} = f([\text{NO}_3^-]_{\text{tot, aq}}, [\text{F}^-]_{\text{tot, aq}})$ at constant $[\text{TBP}]_{\text{org}}$, $[\text{SO}_4^{2-}]_{\text{tot, aq}}$ and temperature.

The distribution factors are defined as the concentration of the respective acid in the organic solution divided by the total concentration of the anion in the aqueous solution.

To achieve high distribution factors, a TBP-concentration of 75% (by volume) was selected for the investigations, though a concentration of 50% has also been studied. A concentration higher than 75% is not

feasible because unfavourable physical properties make phase separation too slow. A matrix of distribution data was thus obtained both for the extraction and for the stripping system. The matrix for the extraction system comprised data for three different $[\text{SO}_4^{2-}]_{\text{aq}}$ -values.

Some of the experimental data obtained are shown in Figures 2 and 3. In Figure 2 it is seen that in the extraction system HF has lower D-values than HNO_3 . The low D-values for HF are due to formation of strong complexes between the metal and fluoride ions. The D_{fluoride} -values decrease at high nitrate concentrations because of competition with HNO_3 in the organic phase. In a multistage extraction (see Figure 4) nitric acid is completely extracted within a few stages after which the extraction of hydrofluoric acid starts. The concentration of HF in the organic solvent passes a maximum which implies an internal recirculation of HF inside the extraction system. This is a consequence of the decreasing D-value for HF as the nitrate concentration increases towards the extract exit. For these reasons both many stages and a high organic to aqueous flow-rate are required for maximum recovery of HF. The latter factor is, however, restricted by the water balance of the entire process.

Figure 3 shows the conditions prevailing during stripping. The extract containing HNO_3 and HF meets pure water. The conditions for the stripping of HF are unfavourable because the D-value for HF increases with decreasing nitrate and fluoride concentrations. The stripping of HNO_3 is more favourable and is restricted only by the aqueous phase flow provided a sufficient number of stages are available.

Most of the experimental data shown in Figures 2 and 3 have been collected by means of the AKUFVE-technique (5). A synthetic pickling solution prepared by dissolving the metal sulphates in an aqueous solution containing appropriate concentrations of HNO_3 , HF and H_2SO_4 was used as a standard solution, in order to maintain controlled conditions with those metal concentrations known to be optimal in a pickling solution. Experiments with real pickling liquors have confirmed the AKUFVE-experiments.

Multistage calculations.

Numerical interpolations have been made, from the distribution data collected, to produce the equilibrium information needed to perform multistage calculations. This was necessary because it proved difficult to find a theoretical model capable of describing the experimental data with acceptable accuracy.

A multistage computer program was used to calculate the stage concentrations of HNO_3 and HF in extraction and stripping. The data fed to the computer are: the data matrix for interpolating the distribution factors D_{nitrate} and D_{fluoride} , the values of $[\text{NO}_3^-]_{\text{tot,aq}}$, $[\text{F}^-]_{\text{tot,aq}}$ and $[\text{SO}_4^{2-}]_{\text{tot,aq}}$ in the pickling solution, the organic to aqueous flow ratios in extraction and stripping, and the number of theoretical stages in each section.

The calculations are based on an iterative procedure, starting with a standard assumption as to the concentrations of nitrate and fluoride in the aqueous effluent from the last stage. Using the distribution factors and the mass balances the concentrations of the acids in the aqueous influent are evaluated. The values are compared to the "right" ones and the sign and magnitude of the differences are used to make new assumptions as to the nitric and fluoride concentrations in the effluent. Maintaining the concentration of one of the acids constant, iteration proceeds with respect to the concentration of the other acid until convergence is achieved. Iterations are alternately performed with respect to the concentrations of the two acids until a satisfactory convergence is achieved with respect to both.

The program has been used to assess the influence of variables such as the

1. Number of theoretical stages in extraction and stripping.
2. Concentration of sulphuric acid in the pickling liquor.
3. Organic to aqueous flow ratios in extraction (ϕ) and in stripping (θ).

In Figure 5 the percentage yields of the recovered acids are given as functions of ϕ (the extraction flow ratio) at $\phi/\theta=1.5$ (where θ is the stripping flow ratio) for different numbers of stages (the numbers of stages for extraction and stripping being equal), and as functions of

ϕ/θ for different ϕ with 11 extraction and stripping stages.

In these calculations the pickling liquor has the following composition:

$$[\text{NO}_3^-]_{\text{tot, aq}} = 2.5\text{M}, [\text{F}^-]_{\text{tot, aq}} = 1.5\text{M}, [\text{SO}_4^{2-}]_{\text{tot, aq}} = 1.5\text{M} \text{ and } [\text{Me}^{n+}]_{\text{tot, aq}} = 2\text{N}$$

From Figure 5 it is seen that a recovery of almost 100% HNO_3 and 70% HF is theoretically possible with $\phi/\theta = 1.5$, $\phi = 2.4$ and at least 10 stages. The optimal values of ϕ and θ depend on ratio ϕ/θ (fixed by the pickling process) and on the number of stages.

Multistage Pilot Plant Experiments.

Two types of contactor, the mixer-settler and the pulsed sieve-plate column, were used in the pilot plant experiments. The mixer-settlers were of pump-mix type having a cylindrical mixer with an effective volume of 60 ml placed centrally in a cylindrical settler of volume 850 ml. The mixer-settler arrangement contained 10 stages. Perspex was used as construction material.

The pulsed column had an internal diameter of 0.090 m and a height of 3 m. The diameter was chosen to give a capacity 1/10 of that required for the full scale column in Söderfors. The pulse was generated by a teflon bellow pulser. The top section of the column was made of glass to permit visual observation. The parts were made in HD-polyethylene. A mixer-settler coupled to the column was available for caustic wash of the solvent.

The extraction, stripping and washing steps were tested both separately and in series in a mixer-settler array. In the pulsed column, only one operation could be studied at a time.

Parallel to the theoretical calculations, experiments were carried out to study the influence of the variables below on the recovery of the acids:

1. Organic to aqueous flow ratio in extraction and stripping.
2. Concentration of sulphuric acid in the pickling liquor (mixer-settlers only).
3. TBP concentration in the organic phase (mixer-settlers only).
4. Flow capacity (pulsed column only).
5. Number of stages and HETS-values.

The dependence of the yields of HNO_3 and HF on the variables in 1 above agreed well with theoretical predictions.

The influence of the sulphuric acid concentration in the aqueous phase (see 2 above) was investigated in separate mixer-settler experiments, since equilibrium data did not permit an accurate calculation of the optimal value of this variable. As mentioned above an increase in the concentration of H_2SO_4 will give a higher extraction yield of HF. However, additional H_2SO_4 will also cost more caustic soda to precipitate the raffinate metals. The price of these different chemicals determine the desired optimum. Mixer-settler experiments were carried out in which the sulphuric acid concentration in the pickling liquor feed was varied under otherwise constant conditions. The results showed that sulphuric acid should be added to a concentration close to the metal equivalent concentration.

The effect of varying the TBP concentration (see 3 above) was also investigated in separate mixer-settler experiments. In two runs, each with four extraction stages, five stripping stages and one washing stage, the concentrations 75% and 50% were examined. The experiments were carried out under conditions identical except for a change in the organic phase flow. For the lower TBP concentration a 50% higher flow was required to give the same flow ratios TBP to pickling liquor and TBP to water as for the higher concentration. The results in Table 1 show no significant differences in the recoveries of the two acids. It seems that decreasing the TBP concentration leads to a small loss of HF and a small gain of HNO_3 .

T A B L E 1.

Conc. TBP %	Acid concentrations in the strip liquor	
	M HNO ₃	M HF
50	1.26	0.21
75	1.23	0.24

The main purpose of the pulsed column experiments was to investigate the variables in 4 and 5 above. It turned out that the column capacity for the extraction system was much higher than that for the stripping system. This is due mainly to the greater difference in phase densities for the extraction system. Both extraction and stripping were accomplished with the organic phase as the continuous medium. This decision was determined by the column material (plastic), which is wetted by the organic phase.

Theoretical equations based on available physico-chemical data such as densities, viscosities and surface tensions have been used to calculate flooding characteristics for the actual systems. A theoretical model was checked against the pilot plant data, and then used for scale-up.

HETS-values for the pilot column of height 3 m have been determined for both the extraction and stripping systems. Since real pickling liquors with varying metal compositions were used in the pilot experiments, equilibrium data collected for synthetic pickling solutions could not be used to calculate the number of theoretical stages for the extraction system. Because of this experiments were carried out with identical solutions in contactors of the two types. Data from these experiments are given below in Table 2. The 10-stage mixer-settler experiment given in Table 2 is also illustrated in a McCabe-Thiele diagram in Figure 4. In our studies of the stripping system the number of theoretical stages could be calculated. The number of stages was five to seven for both the extraction and the stripping system. Since the HETS-value depends on the extraction factor and the distribution factors for both extracted acids vary considerably with height in the column the HETS-values must also vary up the column. The average HETS-value was about 0.5 m. The full scale column height of 10 m should give an extractive capacity corresponding to more than ten stages.

T A B L E 2.

REPRESENTATIVE RESULTS FROM PILOT PLANT RUNS.

EXTRACTION	Flow rate			Conc. Pickling bath (Aq _{in})				Conc. Org _{out}				Raffinate				% Extraction of acids	
	Aq ml/m	Org ml/m	Org/ Aq	HNO ₃ M	HF M	Me g/l	Mo g/l	HNO ₃ M	HF M	Me g/l	Mo g/l	HNO ₃ M	HF M	Me g/l	Mo g/l	HNO ₃	HF
Pulsed column	1070	2530	2.4	2.25	1.87	Fe=44 Cr= 7.2 Ni=11.5	1.13	0.91	0.35	-	0.48	<0.01	1.05	-	0.02	>99	44 x)
10 stage mixer- settler	49	127	2.6	2.25	1.87	Fe=44 Cr= 7.2 Ni=11.5	1.13	1.07	0.42	-	-	<0.01	0.84	-	-	>99	55 x)
x) $2 \cdot [\text{SO}_4^{2-}]_{\text{tot.aq}} = [\text{Me}^{\text{n+}}]_{\text{tot.aq}}$, where $[\text{Me}^{\text{n+}}]_{\text{tot.aq}}$ is normalized.																	
STRIPPING	Flow rate			Extract (Org _{in})				Stripped solvent				Strip liquor				% Stripping	
	Aq ml/m	Org ml/m	Org/ Aq	HNO ₃ M	HF M	Me g/l	Mo g/l	HNO ₃ N	HF M	Me g/l	Mo g/l	HNO ₃ M	HF M	Me g/l	Mo g/l	HNO ₃	HF
Pulsed column	1000	1780	1.8	0.91	0.35	-	0.48	0.11	0.09	-	0.25	1.38	0.38	-	0.39	88	74
5 stage mixer- settler	53	102	1.9	1.10	0.39	-	-	0.23	0.16	-	-	1.39	0.39	-	-	79	59

Features of a contactor suitable for a full-scale plant.

The limitations imposed on the choice of materials by the highly corrosive process liquids can be summarized in two points:

1. Tributylphosphate excludes many of the classic polymer materials.
2. The combination HNO_3 -HF excludes all metals.

Long duration tests have been carried out on a wide variety of materials at different temperatures. High density polyethylene (HD-PE), graphite and PTFE were found to be resistant while ceramics, polyesters, polypropylene and low density polyethylene were only partially resistant.

For components subjected to the action of both TBP and acids the material chosen in the Söderfors plant was HD-PE. The temperature must not be allowed to exceed 50 °C.

The multistage calculations mentioned above indicated that a large number (>10) of theoretical stages is necessary both for extraction and stripping. This fact strongly influenced the choice of pulsed sieve-plate columns for the contactors in the plant built at Söderfors.

The main arguments for the choice of pulsed columns are summarized below:

1. Low investment cost.
2. Low floor space requirement.
3. Small solvent volume in the system.

However, mixer-settlers have some important advantages.

1. The possibility of repair without a total shut-down.
2. High flexibility.
3. Large residence time.
4. Low hydrostatic head resulting in insignificant stresses in the construction material.
5. Ease of scale-up.
6. Ease of control.

Tests have shown that the stripping of HF is limited by slow kinetics, so that a high residence time in the mixing operation is essential. A high temperature is desirable both from equilibrium and kinetic considerations. The temperature is easy to control in a mixer-settler while it is very difficult to control in a pulsed column.

Discussion.

During three months of nearly continuous operation of the plant at Söderfors the solvent extraction equipment has worked very well. It seems probable that mixer-settlers could compete with a pulsed column as contactor for stripping operation owing to the kinetic limitation in the stripping of HF.

As an alternative to dumping the Söderfors plant is economically advantageous.

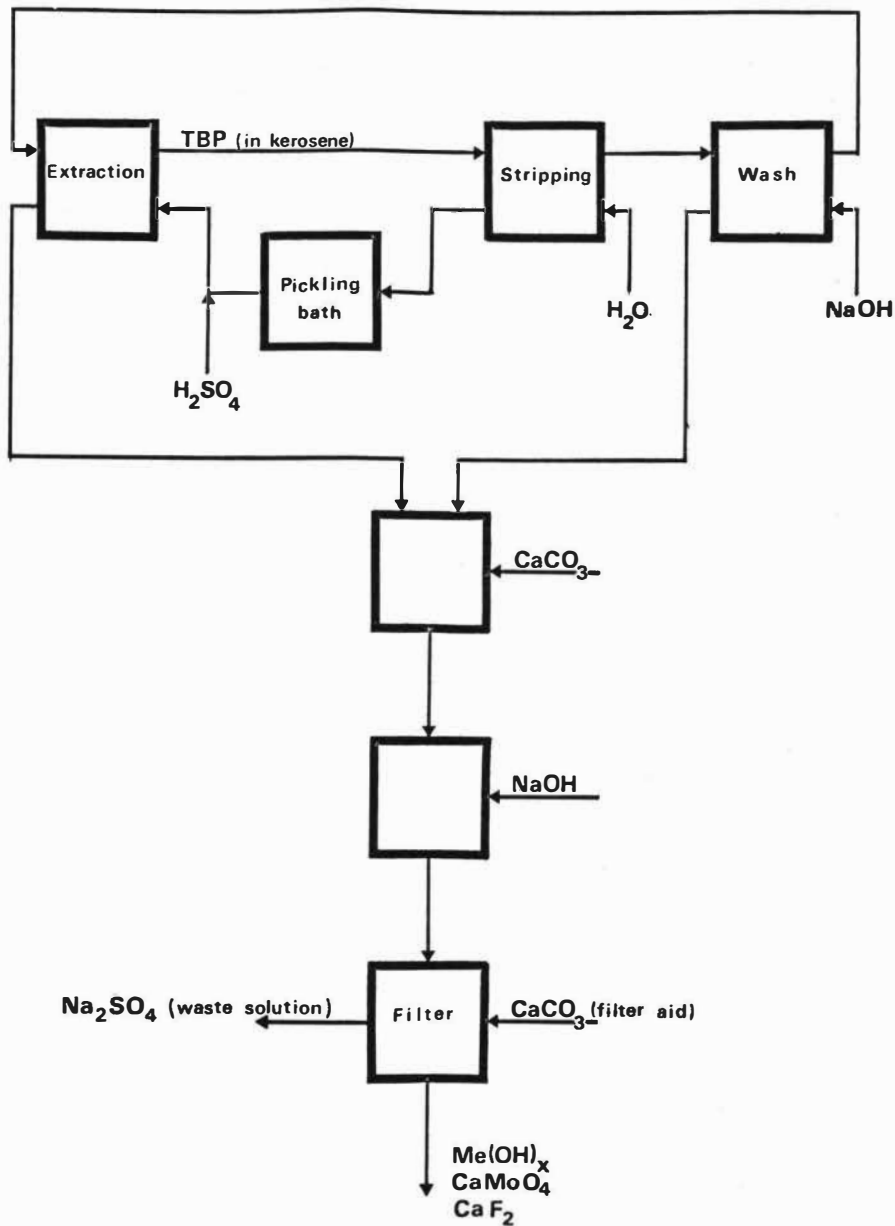
Acknowledgements.

The authors wish to express their sincere appreciation to Professor Jan Rydberg and Dr. Hans Reinhardt for their valuable critical comments. The work described has been supported by grants from the Swedish Technical Research Council.

References.

1. Rydberg J. et al.,
Proceedings from the International Symposium on Hydrometallurgy, Chicago 1973.
2. Marcus Y. and Kertes S.,
Ion Exchange and solvent extraction of metal complexes.
J. Wiley and Sons, London 1969.
3. Davies W., Jr.,
Nucl. Sci. Eng. 14 (1962) 159,169,174.
4. Korovin S.S. et al.,
Russ. J. Inorg. Chem. 11 (1966) 96.
5. Reinhardt H. and Rydberg J.
Chem. Ind. (1970) 488.

Fig. 1 Flow scheme for the process developed.



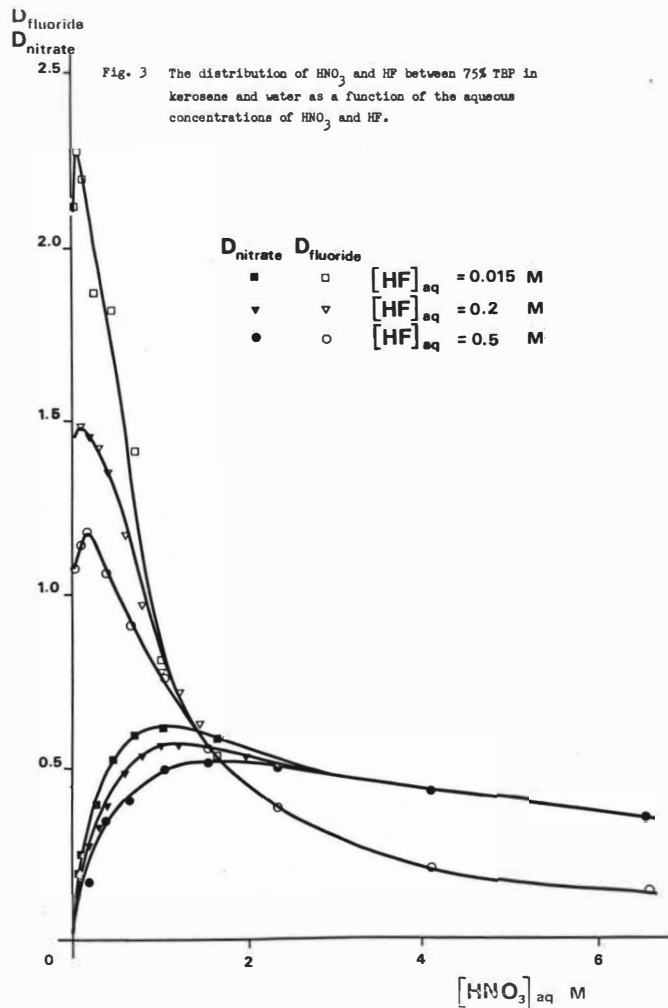
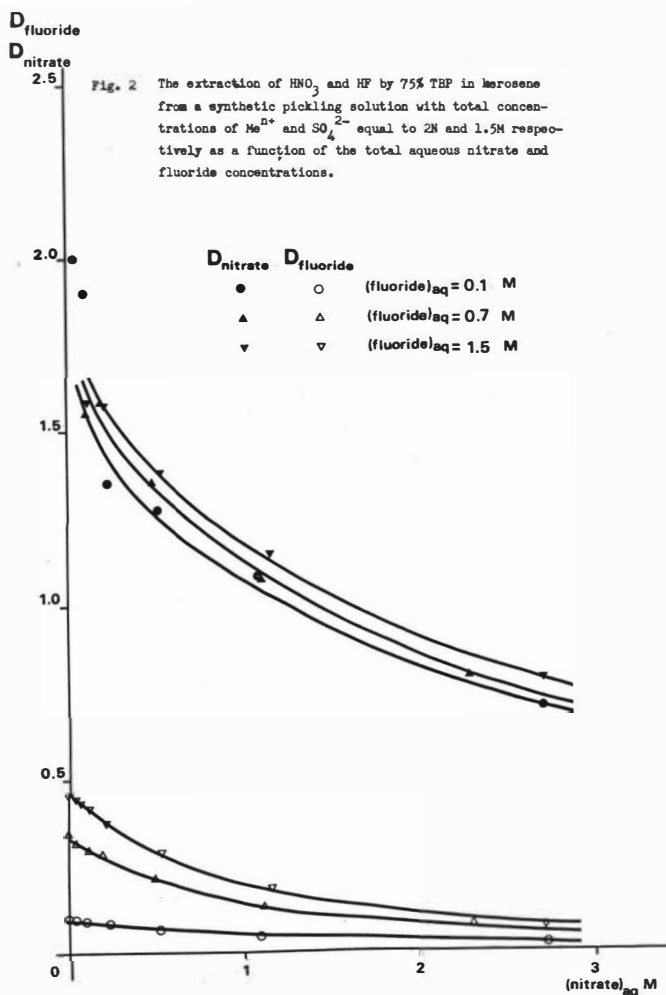


Fig. 4 McCabe-Thiele diagram from a 10-stage mixer-settler experiment showing the extraction of HNO_3 and HF from a pickling liquor.

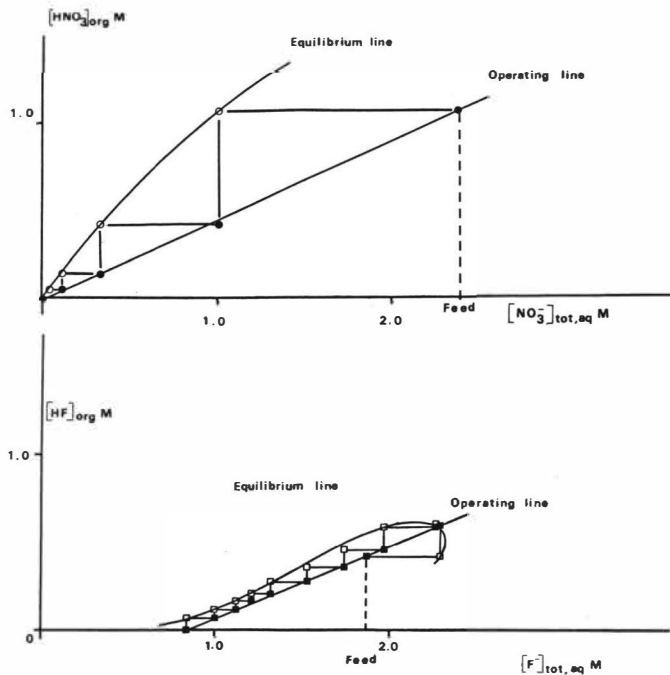
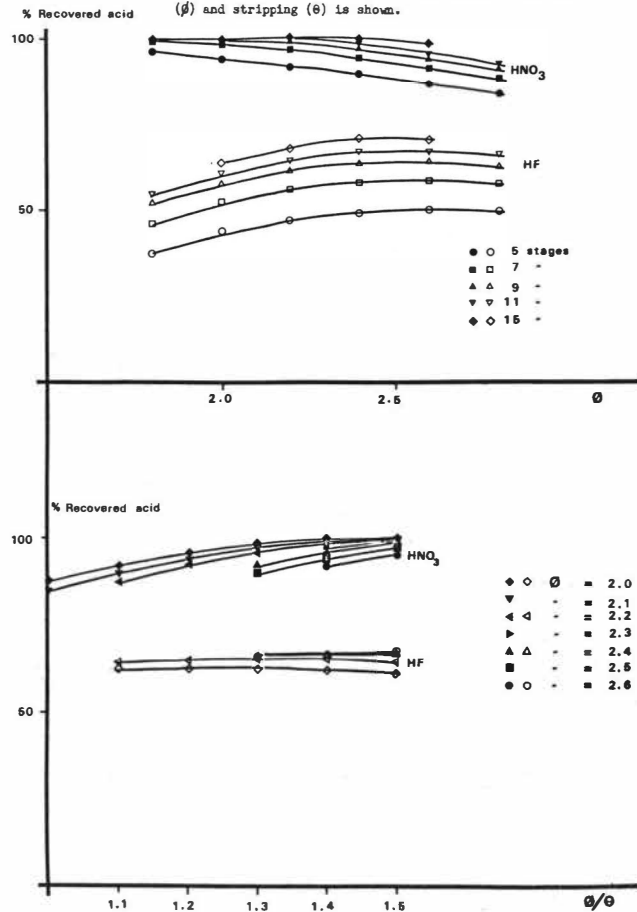


Fig. 5 Theoretical yields of HNO_3 and HF. The influence of the number of stages and the phase flow ratios in extraction (β) and stripping (θ) is shown.



Paper 199
INTERNATIONAL SOLVENT EXTRACTION
CONFERENCE 1974

ECONOMICS OF
SX AND ITS ALTERNATIVES
FOR URANIUM AND COPPER

JOHN DASHER
Principal Engineer
M&M Division



San Francisco, USA

ABSTRACT

When uranium mill construction ceased about 1962, SX(Solvent eXtraction) was indicated for uranium - either alone in new plants or helping IX(resin Ion eXchange) in older plants. During the next decade IX became cheaper via new resins and new equipment, and SX showed it can save refining costs. The selective carbonate leach still has its place.

For copper, SX is being economically applied to dump, heap and agitation leach solutions (acid and ammoniacal) to get copper from waste rock, oxide ores, scrap and sulfide concentrates for electrowinning, but copper is also obtained economically from these materials without benefit of SX.

SX has established a beachhead, but the defenders are far from conquered.

INTRODUCTION

For SX to be used it must not only obtain good metallurgical results, but also do so at a cost below that of alternative processes. Costs will be given first for uranium then for copper, first for old processes then for new, first for lean sources then for richer ones.

Published costs have not been escalated, but for comparability have been converted (if indicated) to US currency at rates of Dec. 1973.

URANIUM

Ion Exchange

Late in 1948 a real breakthrough was scored with the discovery that strong base ion exchange resin has a great affinity for uranyl sulfate complex ions. Our group at MIT, which was concerned with recovering a uranium by-product from South African gold ores, gave up all other approaches and went to piloting (1, 2). When this technology was declassified, I reported at the '56 AIME annual meeting as typical, the IX costs of Table 1(3). These are less than half of anything we had previously known. I then forecast that IX would not be used to recover metals less valuable than copper.

TABLE 1
COST OF ION EXCHANGE - 1 T/d U₃O₈

	<u>\$/day</u>	<u>¢/lb U₃O₈</u>
Resin at 20%/year on \$54,000	33	1.65
Elution acid, HCl or HNO ₃	92	4.6
Precipitation alkali, MgO or NH ₃	65	3.25
Miscellaneous chemicals	<u>10</u>	<u>0.5</u>
Sub-Total, Reagents	200	10.0
Equipment at 10%/year on \$320,000	100	5.0
Labor, supervision, and overhead	128	6.4
Maintenance at 4%/year on equipment	40	2.0
Water	7	0.35
Power	<u>12</u>	<u>0.6</u>
Total	\$487	24.35¢

This IX technology had by then been applied in South Africa to sixteen plants treating CN residues averaging under 0.5 lb. U₃O₈/T, in the Elliot Lake district of Canada and in several plants in our Western States.

Several of these Western ores had montmorillonite and, after leaching, wouldn't thicken or filter (Separan was as yet unknown). This led us in 1950 to RIP (Resin-In-Pulp) (4, 5, 6). The initial RIP plants had the resins in baskets and costs on 0.5% ore were 9¢ for the resin and baskets and 16¢ to elute and precipitate a pound of U₃O₈.

Solvent Extraction

SX found promise over IX in the recovery of uranium from phosphoric acid (7) before its application to sulfate liquors well before declassification (8, 9). At the '57 AIME annual meeting, Brown reported on uranium extraction from sulfate leach solutions with alkyl phosphoric esters and with amines. Costs are in Tables 2 and 3.

TABLE 2
ESTIMATED REAGENT COSTS
FOR PHOSPHORIC ESTER EXTRACTION

<u>Chemical</u>	<u>Use</u>	<u>Per Pound U₃O₈</u>		
		<u>Consump-</u> <u>tion</u>	<u>Unit</u> <u>Price</u>	<u>Cents</u>
Na ₂ CO ₃	Stripping	2.0 lb	2.3¢	4.6
H ₂ SO ₄	Precipitation	1.3 lb	1.5¢	2.0
NH ₃	Precipitation	0.25 lb	5.8¢	1.5
D2EHPA	Extractant	0.01 lb	\$1	1.0
TBP	Modifier	0.22 lb	60 ¢	1.3
Kerosene	Diluent	0.02 gal	56 ¢	<u>2.8</u>
Total				13.2

TABLE 3
ESTIMATED CHEMICAL REAGENT COSTS
FOR AMINE EXTRACTION

<u>Chemical</u> <u>Reagent</u>	<u>Use</u>	<u>Per Pound U₃O₈</u>		
		<u>Consump-</u> <u>tion</u>	<u>Unit</u> <u>Cost</u>	<u>Cents</u>
NaCl	Stripping	2.3-3.2 lb	0.8¢	1.8-2.6
H ₂ SO ₄	Stripping	0.2-0.3 lb	1.5¢	0.3-0.5
NH ₃	Precipitation	0.25-0.30 lb	5.8¢	0.8-2.9
Amine	Distribution loss	0.008-0.029 lb	\$1.	0.8-2.9
Organic	Entrainment	0.05 gal	44-52¢	2.2-2.6
Na ₂ CO ₃	Regeneration	0-1.6 lb	2.3¢	<u>0 -3.7</u>
Total				6.6-14.1

Compared to the IX chemical costs of 10¢ only the lower amine figure has an appreciable advantage. SX, however, was able to avoid the various poisoning problems resins had. Table 4 compares IX costs for three Canadian plants vs. those obtainable by SX (10). Poisoning problems at Uranium City are responsible not only for 1.5¢ more chemicals, but also for 2¢ more resin. Stripping chemicals are less in each example.

TABLE 4
IX VS SX OPERATING COSTS

	Cents per Pound U ₃ O ₈					
	<u>Elliot Lake</u>		<u>Bancroft</u>		<u>Uranium City</u>	
	<u>IX</u>	<u>SX</u>	<u>IX</u>	<u>SX</u>	<u>IX</u>	<u>SX</u>
Resin or Solvent	1.0	3.0	1.0	3.0	3.0	3.0
Elution or Strip	5.7	1.2	3.2	1.2	9.8	3.2
Remove Poisons	-	-	<u>0.6</u>	-	<u>1.5</u>	-
Chemicals Subtotal	6.7	4.2	4.8	4.2	14.3	6.2
Labor & Maintenance	<u>2.5</u>	<u>2.5</u>	<u>6.5</u>	<u>6.5</u>	<u>5.5</u>	<u>5.5</u>
Total	9.2	6.7	11.3	10.7	19.8	11.7

Table 5 compares capital costs of an Elliot Lake IX plant and its SX alternate (10). SX has a lower inventory and, if mixer settlers are used, 0.9¢/lb. lower equipment cost. So SX was generally used for plants built after '60.

TABLE 5
IX VS SX CAPITAL COSTS, 3000 T/d

		<u>Thousand Dollars</u>	<u>Amortization, ¢/lb U₃O₈*</u>
IX	Resin Inventory	135	0.7
	Equipment	400	<u>2.2</u>
	Total	535	2.9
SX	Solvent Inventory	7	0.04
	Mixer-Settlers	225	1.3
	Columns	400-660	2.2-3.7
	Centrifugal Contactor	<u>450</u>	<u>2.5</u>
	Total	232-667	1.34-3.74

* at 10%/year

Combinations

SX also was married to IX and RIP in several existing plants. This combination was called Eluex in the US and Bufflex in South Africa. It aimed at a pure product that wouldn't need to be redissolved and solvent extracted and at eluting with inexpensive H₂SO₄, instead of with HCl or HNO₃.

Canadians found that the desired purity could be obtained by SX of nitrate eluates with tributyl phosphate or dibutyl-butyl-phosphonate and also by SX of sulfuric eluate with tri-capryl amine. Costs are in Table 6. The credit with amine is due to the H₂SO₄ being useful in leaching (11).

TABLE 6
COSTS OF PURE PRECIPITATES

<u>Elution</u>	<u>Extractant</u>	<u>¢/lb. U₃O₈</u>
HNO ₃	NH ₃ precipitation	Base
HNO ₃	Tributyl Phosphate	21
HNO ₃	Dibutyl-butyl-phosphonate	3
H ₂ SO ₄	Tricapryl amine	-11

Table 7 compares conventional IX, estimated at 22¢ (due largely to importing nitric into South Africa) with Bufflex at under 6¢(12). This IX-SX combination overcame the cost disadvantage the older plants had vs. the newer SX plants and gave a pure product also.

TABLE 7
IX VS IX + SX (BUFFLEX) REAGENT COSTS

<u>Chemical</u>	<u>Use</u>	<u>Per Pound U₃O₈</u>	
		<u>Pounds</u>	<u>Cents US</u>
<u>Conventional IX</u>			
HNO ₃	Elution	2.86	17.6
H ₂ SO ₄	Regenerate resin	0.07	0.04
NaOH	Regenerate resin	0.03	0.26
Lime	Fe precipitation	0.97	1.06
NH ₃	ADU precipitation	0.512	<u>4.4</u>
Total			22.4
<u>Bufflex</u>			
Alamine 336	Make-up	0.006	0.56
Isodecanol	Make-up	0.009	0.21
Kerosene	Make-up	0.108	0.54
H ₂ SO ₄	Regenerate resin	1.0	0.71
NH ₃	Precipitation, scrub	0.352	3.01
NaOH	Regenerate resin, solvent and deionizer	0.058	0.50
Na ₂ CO ₃	Regenerate solvent	0.019	0.11
HCl	Regenerate deionizer	0.005	0.04
Water	Scrub		<u>0.06</u>
Total			5.75

Divorce!

It was then found that SX could get a pure uranium precipitate directly from South African leach solutions. Now that a market for uranium is again developing, most South Africa plants are employing SX alone (13). This is called "Purlex" (for Pregnant URanium Liquor EXtraction).

Return of IX

But IX is not yet out of it. The new macroreticular resins are tough. Weak base resins are more easily and cheaply eluted. Some new mills have installed these. Costs in Table 8 are hard to beat (14).

TABLE 8
MACRORETICULAR WEAK BASE IX REAGENT COSTS

<u>Chemical</u>	<u>Per Pound U₃O₈</u>	
	<u>Pounds</u>	<u>Cents</u>
NaCl	1.1	1.0
NH ₃	0.25	0.75
Activated Carbon	0.01	0.375
Resin	0.1	<u>0.125</u>
Total		2.25

Who Needs Thickeners or Filters?

Although RIP was initially intended for ores that were virtually impossible to thicken and filter, it has become obvious that it is always easier and cheaper to desand the slurry than to get a clarified solution. Various forms of multi-stage up-flow fluid bed IX have been developed (15, 16, 17, 18, 19).

Rosenbaum estimates upflow IX as 27¢/lb U₃O₈ cheaper than conventional SX, due largely to a 26% saving in capital costs (16). Work has also been done on SIP (Solvent-In-Pulp) processing (20). Ritcey et al estimated IX and SX on clear solutions as equals, and both SIP and continuous IX at 10 percent solids were 18¢/lb U₃O₈ cheaper (21). Not quite as much, but still impressive!

This large advantage of RIP and SIP is not available at locations where rainfall exceeds evaporation and where suspended solids and/or radioactivity in effluents are limited.

Carbonate Leach

This discussion of alternatives to SX for uranium is not complete until the selective carbonate leach has been mentioned. This was used in many early plants and is still applied economically for high lime ores.

COPPER

Copper leach solutions from mines, from waste dumps, from oxide, silicate, sulfide and native ores, from scrap and from sulfide concentrates have surrendered their values with and without benefit of SX. Let us discuss alternatives vs. SX, material by material.

Dump Leaches and Mine Water

My '56 prophesy about IX for metals down to the value of copper has not yet come true. Table 9 shows results obtained earlier with carboxylic cation resins in the calcium form at Cerro de Pasco on mine waters that had been neutralized to pH 3.5 to remove ferric (22). That resin has a loss estimated at 15 percent per year which made this uneconomic. There are better resins available now. The low current efficiency was due to iron wasting current by going from ferric to ferrous and back to ferric and to having only 10 g/l Cu to start with.

TABLE 9
IX for Cu

	<u>Single</u> <u>Column</u>	<u>2 in</u> <u>Series</u>
Cu recovered, %	91	95
Fe rejected, %	92	95
Current efficiency, %	33	50

Copper at pH4 or higher can also be separated from ferrous iron by weak base anion resins (23).

Until recently the standard method of recovering copper from acid mine waters and dump leach solutions was by cementation on light scrap iron--in launders. An improved form of cementation is the Kennecott cone (24). Table 10 gives several estimates of cementation costs. Jacobi did his estimate when Cu was 30¢ (25). Shoemaker commented that capital costs are low (26). McGarr estimated for higher Fe costs and only to blister copper (27). Refining cost would be additional. Jones' costs are actual for 1969 at Bagdad (28).

TABLE 10
CEMENTATION COSTS, ¢/lb. Cu

Author	Jacobi	Shoemaker	McGarr	Jones
Product	cathodes	cathodes	anodes	cathodes
Year	1963	1968	1969	1969
<u>ITEM</u>				
Iron		3.8	3.8-9.8	5.011
Other Cementation	4	1.3	1.3	1.048
(S) melting				
Freight	-	7	3-7	7.72
Refine				
Ship & Sell	4	-	-	
Total	<u>8</u>	<u>12.1</u>	<u>8.1-18.1</u>	<u>13.78</u>

SX entered when General Mills reported in Fall '65 the specific extractant LIX-64 (29). This was aimed at extraction of copper from dump leach liquors whose initial pH drops no lower than 1.7 when 1 g/l Cu is exchanged. Pilot plants were set up by Duval to treat 100 gal/min of waste dump liquor, (30) and by Bagdad whose oxide ore heap was giving only 1 g/l Cu in the leach solution (31). Results were reported Fall '67.

Bagdad went ahead with the 3rd Commercial LIX plant (32). Its economics, estimated and actual, are in Table 11 (28, 33). Estimated costs for solvent extraction and electrowinning were less than half those for cementation, and actual costs turned out to be 11.27¢/lb cheaper. At 14.6 million lb/yr, this is \$1.64 million, which will equal the \$5 million capital costs in about three years. Capital costs for various flows of 1 g/l solution, per McGarr, (27, 33) are in Table 12.

TABLE 11

<u>Item</u>	<u>SX-ELECTROWIN OPERATING COST @ 1 g/l Cu</u>		
	<u>Cents (US) per pound Cu</u>		
	<u>A Priori Estimates per</u>		<u>Bagdad 1971</u>
	<u>McGarr</u>	<u>Jones</u>	<u>Actual</u>
Labor, SX	} 2.3-3.0 }	2.203	0.325
Elwin			0.652
O'head			0.694
Power	0.9-1.0	0.895	1.109
Steam	-	0.175	0.637
Reagents	2.0-3.0	1.815	0.63
Acid Credit	-(2.2-2.3)	-(1.539)	-(2.537)
Misc., SX	-	} 0.385	.586
Elwin	-		.435
Total	3.0-4.7	4.184	2.531

TABLE 12
SX-ELECTROWIN AT 1 g/l Cu
CAPITAL COSTS

<u>Thousand Gal(US)/min</u>	<u>Million Dollars</u>
1	1.5 - 2.3
2	2.7 - 4
3	3.4 - 5.6
4	4.1 - 7.2
5	5.0 - 8.7
6	5.5 - 10
8	6.8 - 12.2

Most of the difference in operating costs comes from the cost of smelting and refining cements. This may cost Bagdad more than accountants would charge within an integrated company for treatment at its smelter.

Oxide Ores

Solutions from ores are richer than dump leach solutions or mine waters. Most heap leaches give from 2 to 4 g/l Cu, while vat leaching obtains over 10 g/l. Dilute solutions have generally been cemented. Strong solutions are generally directly electrowon.

The Ray (Arizona) vat leach and electrowinning plant for 10000 t/d silicate ore plus a roaster and an acid plant for it cost \$35 million (34). However, at ASARCO's new vat leach plant at San Xavier, which treats 4000 T/d of ore and cost \$13 million (35), all the copper is cemented.

Another alternative hydrometallurgical process for oxidized copper ores is ammoniacal leaching (36). Copper is usually precipitated from these solutions as an oxide by boiling and tailings are steamed to minimize ammonia loss.

Cyanide leaching also has its advocates. Concerning its economics, Rose notes that at 7000 T/d it would be economic on tailing having 7 lb. Cu/T (37). That's almost ore.

Two weeks after visiting the Duval Pilot plant in April 1967, we started a SX-electrowinning study for Ranchers Exploration and Development, who were heap leaching an oxide ore which gave a difficult solution for SX. This contained about 4 g/l each Cu and free H_2SO_4 , and was being cemented. LIX-64 was only able to extract about two-thirds of its copper before it became too acid. This study also involved the alternative of using a strong extractant later to be named Kelex 100. Ranchers decided to use the more thoroughly tested LIX-64 for the first commercial copper SX-electrowinning plant. Miller reported the investment for 1000 gpm and 15 T/d Cu (39) as \$3 million including the inventory of organic and starter sheets.

Shoemaker estimated 7¢/lb. Cu for SX-electrowinning from such heap leach solutions which, with a 1¢ to 3¢ lb. Cu. credit for needing less acid than cementation, gave a 5¢ to 7¢/lb. differential in favor of this new route. Capital cost was stated at \$170 000 to \$190 000 per daily ton of copper, which would be recovered in about four years (26).

Table 13 gives estimated capital costs for 3 g/l Cu solutions under Australian conditions separately for the SX and electrowinning facilities (40). The last column is an estimate of an electrowinning plant operating directly on a stronger (vat leach) solution at a lower current density. The saving shown in electrowinning from use of SX is not near enough to pay for it but the extra cost of the vat leaching facilities required when SX is not used wasn't estimated.

TABLE 13
SX - ELECTROWIN AT 3 g/l Cu
CAPITAL COSTS

<u>US GPM</u>	<u>ST/d Cu</u>	<u>\$(U. S.) Millions</u>		
		<u>SX</u>	<u>Elwin A*</u>	<u>Elwin B*</u>
1000	18	3.9	0.95	1.65
2000	36	5.8	1.85	2.7
3000	54	7.3	2.6	3.7
4000	72	8.2	3.3	4.6

*A - when combined with SX, 25-30 Amp/ft²

B - without SX, stronger solution, 12 - 15 Amp/ft. ²

Table 14 compares SX-electrowinning with cementation for a hypothetical oxide ore leaching operation in Australia producing 5000 long tons per year copper. Mining costs are excluded, but leaching costs weren't reported separately. Big difference is in the revenue from cathodes being so much greater than that for cements. Including depreciation, costs are about equal (40). SX-electrowinning is clearly preferable - providing, Brown said, a life of at least seven years is expectable. Incidentally, Ranchers only expected a 7-year life for the Bluebird Mine when our study indicated a switch from cementation to SX (41). They have no reason to regret this decision, especially as General Mills came up with a stronger reagent - LIX-64N (42) - and as they found so much more ore they installed another rectifier, are now pushing the present plant to more than 150% of design capacity (43) and plan a four-fold expansion (44).

TABLE 14
ELECTROWINNING VS CEMENTATION (5000 T/yr)

<u>Item</u>	<u>US Cents per Pound Cu</u>	
	<u>SX-Elwin</u>	<u>Cementation</u>
Labor	2.4	2.4
Power	3.2	1.5
Scrap Iron	-	5.7
Water	1.5	2.3
Organics	0.8	-
Utilities/Supplies	1.1	0.8
Maintenance	3.3	1.6
Depreciation	10.0	4.9
Extra Acid	-	4.0
Total	21.5	23.2
Revenue	56.7	43.4
Gross Income	35.2	20.2

Nchanga, already a giant leach-electrowin operation, planned expansion and evaluated several ways to treat various new materials. Later, a second round of studies, assuming a still larger tonnage compared cementation with SX-Elwinning (45). Results in Table 15 indicated the largest SX plant yet, but scale-up work was needed. This was done by Power-Gas and resulted in the publication of several economic analyses (46) besides that of Brown (40) already given.

TABLE 15
NCHANGA EXPANSION ALTERNATIVES

Process	Product	% Cu	Cents per Pound Cu		
			Operating	Capital*	Total
<u>First Round Studies, 23,000 T/D</u>					
LPF-H ₂ S	Sulfide	25	11.3	3.0	14.3
Scrap Iron	Cements	85	19.1	2.3	21.4
Sponge Iron	Cements	85	15.8	2.7	18.5
Liming	Hydroxide	17	7.5	2.6	10.1
<u>Second Round Studies, 28,700 T/D</u>					
Scrap Iron	Cements	85	24.0	3.4	27.4
Refining	Cathodes	99.9	4.9	2.2	7.1
Total			28.9	5.6	34.5
SX-Elwin	Cathodes	99.9	15.7	6.8	22.5

* at 1%/month

Warwick estimated the operating cost of SX only for 2 g/l Cu solutions at 3.2¢ to 4.4¢/lb. Cu. Table 16 gives his capital costs estimates for the SX facility only along with those from Brown. Also shown are the combined SX electrowin costs from Brown and McGarr. This table mainly goes to prove that published capital costs for hypothetical SX plants vary from many factors and are not directly comparable.

TABLE 16
SX CAPITAL COSTS, \$(US) Million

US gal/min.	SX Only		SX + Elwin	
	Warwick (2 g/l Cu)	Table 13 (3 g/l Cu)	Table 13 (3 g/l Cu)	Table 12 (1 g/l Cu)
1000	1.0-1.3	3.9	4.85	1.5-2.3
2000	1.6-1.9	5.8	7.65	2.7-3.0
3000	2.2-2.5	7.3	9.9	3.4-5.6
4000	2.6-2.9	8.2	11.5	4.1-7.2
5000	3.0-3.4	-	-	5.0-8.7
6000	3.5-3.9	-	-	5.5-10.0
8000	4.3-4.8	-	-	6.8-12.2

Other numbers will soon be available. An AMAX-Anaconda joint venture has announced a 10000 T/d oxide ore agitation leach SX-electrowinning plant at Twin Buttes (47) and, after nearly 60 years of vat leaching and direct electrowinning, Chuquicamata has decided to install SX for Exotica ore (48, 49).

All these figures show SX-electrowinning better than making cements, assuming this cathode copper is saleable at a cathode price and that cements need to be melted in the convertor, cast into anodes and electro-refined. There are two things which may narrow the gap. One is if the cements could be melted and fire-refined for sale. As residuals in iron scrap - especially in light scrap - are uncontrollable, this help for cementation becomes reasonable only if it is done with sponge iron of known purity as Hecla plans at Lakeshore (50) and which Nchanga found cheaper (45). The other possible evener is if electrowon cathodes contain objectionable quantities of impurities such as lead or sulfate and are marketable only at a discount. One way of preventing the lead impurity is to replace the lead cathodes with those of dimensionally stable coated titanium (51). Another way of excluding lead was found in Nchanga's piloting (52). Adding a few ppm of cobalt coats the lead anodes and reduces lead in cathodes. This is already being used by the others (53).

SCRAP

In the early 50's, I worked on a process to leach low-grade copper scrap with ammonium carbonate and to H_2 reduce copper powder from the solution (54, 55). A plant was built (56) which was too small to be economic. There is also at Bagdad a plant using hydrogen reduction of copper sulfate which could refine scrap (57). Sherritt Gordon reported improved ammoniacal scrap processes including alternatives to hydrogen reduction (58).

The first commercial application of SX to scrap treatment (second commercial SX plant for copper) is the Capital Wire and Cable operation at Casa Grande (43). This uses an ammoniacal leach and LIX-64N. The ammoniacal route has an advantage for the concentrated solutions from leaching scrap because no matter how much copper is extracted, the solution does not become acid.

Without quantitative economics of SX or its alternative scrap treatment operations, it is obvious that prompt scrap, and heavy scrap which can be sorted, are more economically recycled by melting than by leaching. It is also important to remember that scrap dealers have a justly deserved reputation for charging all the traffic will bear. This leaves little margin for the processor.

SULFIDE CONCENTRATES

There are many ways that copper sulfide concentrates can be put into solution (59, 60). A recent in-house study compares commercialized methods for a hypothetical operation treating 440 T/d Arizona chalcopyrite concentrate. Results are in Table 17. The commercial copper concentrate hydrometallurgy operations to date are small, involve some other non-ferrous metal value e. g., Co, Zn, Ni, and use the sulfating roast (61, 62).

Second is a less expensive way which involves a partial roast (61, 63), and an autoclave leach (64). It was practiced for only a short time commercially at Fredericktown and with air, not oxygen (65, 66). These routes don't use SX, nor does the leach with ammonia and air combined with H₂ reduction shown third (67). It is commercial only on nickel but Evans published the conditions recommended for chalcopyrite (68). These were used in this study.

TABLE 17

HYDROMETALLURGY FOR ARIZONA
CHALCOPYRITE CONCENTRATE

<u>Process</u>	<u>Capital</u> <u>Millions\$</u>	<u>Cents per Pound Cu</u>			<u>Total</u>
		<u>Capital*</u>	<u>Operating</u>	<u>Credits</u>	
1. Sulfating, Dilute acid leach Electrowin }	31.0	5.3	6.8	(3.3)	8.8
2. Partial roast, Autoclave + O ₂ , Electrowin }	28.5	4.9	6.9	(4.4)	7.4
3. NH ₃ + air - H ₂ Reduction }	45.1	7.7	13.0	(1.9)	18.8
4. NH ₃ + O ₂ - H ₂ Reduction }	41.3	7.1	13.5	(1.9)	18.7
5. NH ₃ + O ₂ - SX - Electrowin }	26.3	4.5	10.9	(1.9)	13.5
6. NH ₃ + air - SX - Electrowin }	30.1	5.2	10.5	(1.9)	13.8
7. Hotter NH ₃ +O ₂ - Ammine - Electrowin }	29.2	5.0	10.4	(3.7)	11.7

* @ 1% a month

The Arbiter process uses ammonia with oxygen to avoid the need for autoclaves (69). Examples 4 and 5 involve leaching with NH₃ and oxygen using the same leach time, temperature, oxygen partial pressure, and copper extraction as in 3. These are not the conditions used in the plant we built at Anaconda, Montana to treat a concentrate which is largely cuprous sulfides and pyrite (70). We are adding a separate circuit to treat a small quantity of chalcopyrite from Nevada which will require conditions similar to those assumed in this study (71). The Arbiter process uses SX and electrowinning instead of H₂ reduction. This was assumed for examples 5 and 6. Fonseca (74) used NH₃ at 150 C (vs 75C for 3 to 6) and precipitated the ammine salt by pressurizing with NH₃. This can be thermally decomposed and electro-won. This is example 7.

Regarding credits, each of the ammoniacal routes is assumed to make 100 T/d of cathodes with most of the remaining copper floated and sent to the smelter as suggest by Evans (68) and Kuhn (70). This is credited @ 30¢/lb. Acid routes are credited for additional cathodes at 50¢/lb and for acid at \$6/T. Fonseca's route gets half the S as acid.

Comparisons show, where acid can be sold and under the conditions assumed, oxygen is a little better than air and SX-Electrowin is much better than H₂ reduction. However, the hotter NH₃ route without SX is even better. The acid routes, which don't use SX, are best. These numbers for hydrometallurgy may be compared with the cost of pyrometallurgy now that SO₂ can't go up the stack, which has now grown to 12¢ (72), 13¢ (73), or 14¢ (59), per pound of copper from chalcopyrite concentrates.

There are other promising routes that don't use SX, including sulfate roasting of pellets containing lime plus countercurrent leaching to limit iron extraction (75) or electrolysis with SO₂ to avoid the adverse effect of iron on current efficiency (76). At least \$10 million is being spent on each of three acid processes that oxidize the sulfide only to the element (73, 77, 78) and whose published descriptions ignore solvent extraction.

Solvent extraction of strong solutions of copper not as the ammine has been advocated using Kelex 100 (79) which also extracts some of the acid formed (80).

SUMMARY

For uranium, SX, IX, IX plus SX combination and selective leaches which use neither, all have their own economic niche.

For copper, SX has been shown economic for treating all types of leachable materials but the same types have all been economically treated without it.

SX has been found increasingly useful for uranium, and for copper but its alternatives are still found to be competitive.

BIBLIOGRAPHY

1. A. M. Gaudin: Principles and New Developments in Uranium Leaching, International Conference on the Peaceful Uses of Atomic Energy, UN, Geneva, 1955, vol. 8, pp. 8-12.
2. A. M. Gaudin, R. Schuhmann, Jr., and J. Dasher, "Development of the Extraction Process for Uranium for South African Gold Uranium Ores", Jnl. of the So. African Institute of Mining & Metal, vol. 50, No. 5, p. 287, December 1956. Also an abridged version in Journal of Metals, p. 1065, August 1956 and Mining Engineering, August 1956.
3. John Dasher, A. M. Gaudin, and R. D. Macdonald, Engineering Aspects of Ion Exchange in Hydrometallurgy, TP 4296 D, Trans AIME, vol. 209. Also Jnl. of Metals, January 1957, p. 185.
4. R. F. Hollis and C. K. McArthur, The Resin-in-Pulp Process for Recovery of Uranium, International Conference on the Peaceful Uses of Atomic Energy, UN, Geneva 1955. Also Mining Engineering, May 1957, p. 443.
5. G. F. Richards, H. D. Webb, G. T. Bator, Resin-in-Pulp Process at Mines Development, Paper to AIME, Annual Meeting 1957.
6. K. W. Lentz, Union Carbide's Uranium Operation at Maybell, Colorado, Paper to AIME, San Francisco, February 1959.
7. R. S. Long, D. A. Ellis and R. H. Bailes, International Conference on Peaceful Uses of Atomic Energy, UN, Geneva 1955, vol 8. pp. 77-80.
8. K. B. Brown, D. J. Crouse and C. F. Coleman, Some New Solvent and Extraction Processes for Use in the Treatment of Uranium, Thorium and Vanadium Ores, Paper to AIME, New Orleans, February 1957. Also ORNL-1734 (1954), 1859, 1903, 1922, 1959 (1955), 2099, 2172, 2173, (1956). Also Proc. 2nd UN International Conference PUAE, vol. 3, p. 472, 1958.
9. E. H. Crabtree and C. J. Lewis, Comments on Uranium Recovery by Solvent Extraction, Paper to AIME, New Orleans, February 1957. Also Mining Congress Jnl., December 1956.
10. S. O. Anderson, A. Ashbrook, D. S. Flett, G. M. Ritcey and D. R. Spink, Solvent Extraction in Process Metallurgy, University of Waterloo, 1971.
11. K. W. Downes, Recent Developments in the Treatment of Uranium Ores from the Elliot Lake District, Processing of Low-Grade Uranium Ores, IAEA, Vienna 1967, pp. 79-88.
12. A. Faure, et al, Production of High Purity Uranium at a South African Gold Mine, J. South Africa IMM, vol. 66 No. 8, p. 319, March 1966.
13. A. Faure, T. H. Tunley, Uranium Recovery by Liquid-Extraction in South Africa, IAEA paper SM-135/30, Recovery of Uranium, Proc. Sao Paulo Symposium, August 1970, p. 241, IAEA, Vienna 1971. Also A. Faure, T. H. Tunley, The Purlux Process, S. Air. Atomic Energy Board, Pelindaba, S. Africa, July 1969.
14. M. I. Ritchie, Utah Construction and Mining Company's Unique Shirley Basin Uranium Mill, IAEA Sao Paulo Symposium, loc. cit p. 147. Also H. E. Gardner, R. Kunin and R. E. Kerollis, Application of Weak Base Resin Ion-Exchange for Recovery of Uranium at Uravan, Colorado, Paper to AIME, Chicago, February 1973.
15. D. R. George, J. R. Ross and J. D. Prater, By-Product Uranium Recovered With New Ion Exchange Techniques, Mining Engineering, January 1968, p. 73. Also U.S. Bur. Mines RI 7471 (1971). Also J. R. Ross, D. R. George, "Recovery of Uranium from Natural Mine Waters by Counter-Current Ion Exchange", U. S. Bureau of Mines, R.I., 7471, Jan., 1971. Also D. R. George, and J. R. Ross, "New Developments in the Recovery of Uranium by Ion Exchange". Paper presented at Uranium Symp., S. E. Utah Section. AIME. Moab. Utah. June 1967.

16. J. B. Rosenbaum, D. R. George, Cost Reductions in Ion Exchange Processing of Uranium Ores, IAEA paper SM-135-24, Recovery of Uranium, Sao Paulo Symposium, August 1970, p. 297, IAEA, Vienna 1971. Also J. B. Rosenbaum and J. R. Ross, A Countercurrent Column for Fluid-Bed Ion Exchange of Uranium Ore Slurries, Chap. 20, 2nd International Symposium on Hydrometallurgy, Chicago, February 1973.
17. P. J. Lloyd, Economic Recovery of Low-Grade Uranium Values from Witwatersrand Ores, IAEA paper SM-135-31. Recovery of Uranium, Proc. Sao Paulo Symposium, August 1970, p. 437, IAEA, Vienna 1971.
18. J. D. Lloyd, Unit Operations of Solid-Liquid Separation Product Concentration and Recovery in Hydrometallurgical Processing Systems, Advances in Extractive Metallurgy, IMM Symposium, London, October 1971, p. 189.
19. F. L. D. Cloete and M. Streat, U.S. Patent 3,551,118. Also F. L. D. Cloete and M. Streat, Nature, vol. 200, p. 1199, 1963. Also M. Streat and R. Y. Qassim, Recovery of Uranium from Unclearified Liquors by Ion Exchange, Chap. 18, International Symposium on Hydrometallurgy, Chicago, February 1973.
20. G.M. Ritcey, E.G. Joe, and A.W. Ashbrook, "Solvent-in-Pulp Extraction of Uranium from Acid Leach Slurries", AIME Trans., vol. 238, pp. 330-334 (1967). Also E.G. Joe, G.M. Ritcey, A.W. Ashbrook, "The Eldorado Process for Liquid Ion Exchange-in-Pulp of Uranium and Copper", Journal of Metals, January, 1966, pp. 18-21. Also G.M. Ritcey, "Solvent-in-Pulp Processing Using Sieve Plate Pulse Columns". Society of Chemical Industry, Nov. 6, 1971. Also G.M. Ritcey, "Solvent-in-Pulp Processing Using Sieve Plate Pulse Columns", Mines Branch, Dept. Energy, Mines and Resources, Ottawa, EMA 71-10. Presented to the Solvent Extraction Group of the Society of Chemical Industry, University of Aston, Birmingham, May, 1971. Also R.R. Grinstead, K.G. Shaw, and R.S. Long, "Solvent Extraction of Uranium from Acid Leach Slurries and Solutions", Proceedings of the Int. Conf. on the Peaceful Uses of Atomic Energy, vol. 8, p. 1523 (1955). Also A.A. North, and R. A. Wells, "Solvent Extraction of Uranium from Slurries by Means of a Rotary-Film Contactor". Trans. IMM Vol. 74, Part 8, pp. 463-488 (1964-65).
21. G.M. Ritcey, M.J. Slater, B.H. Lucas, A Comparison of the Processing and Economics of Uranium Recovery from Leach Slurries by Continuous Ion Exchange or Solvent Extraction, Chapter 17, 2nd International Symposium On Hydrometallurgy, Chicago, February 1973.
22. T.A.A. Quarm, Recovery of Copper from Mine Drainage Water by Ion Exchange. Trans. IMM, vol. 64, pp. 109-117 (1954-55).
23. R.C. Knupp, I.M. Abrams, C.J. Lewis, New Resin Technique in the Recovery of Copper from Dilute Process Streams. Paper to AIME, New York, February 1964.
24. H.R. Spedden, E.E. Malouf, and J.D. Prater. Cone-Type Precipitators for Improved Copper Recovery. Min. Engineering, vol. 18, No. 4, April 1966, pp. 57-62.
25. J.S. Jacobi, The Recovery of Copper from Dilute Process Streams, Min. Engineering, September 1963, pp. 56-62.
26. R.S. Shoemaker and R.M. Darrah, The Economics of Heap Leaching, Mining Engineering, December 1968, p. 68.
27. H. J. McGarr, N.H. Berlin, and W.F.A. Stolk, "The Cost of Copper - Solvent Extraction and Electrowinning Look Great on Paper". E. & M.J. pp 66-67, December 1969.
28. R. L. Jones, Paper to Pacific-Southwest Minerals Conference, Phoenix AZ, Apr., 1973
29. D.W. Agers, J.E. House, R.R. Swanson, and J.L. Drobnick, A New Reagent for Liquid Ion Exchange Recovery of Copper. Min. Engineering, vol. 17, No. 12, December 1965, pp. 76-80. Also D.W. Agers, J.E. House, R.R. Swanson, and J.L. Drobnick, "Copper Recovery from Acid Solutions Using Liquid Ion Exchange", Journal of Metals, pp. 191-198, June 1966.
30. R.R. Nelson and R.L. Brown, The Duval Corp. Copper Leach, LIX Pilot Plant, The Design of Metal Producing Processes, R.M. Kibby ed., TMS of AIME, 1969, p. 324.
31. D.W. Agers and E.R. DeMent, LIX-64 as an Extractant for Copper, Paper to SME of AIME, September 1967.

32. Anon, How Bagdad Uses LIX to Recover Copper From Dump Leach Solutions, World Mining, April 1971, p. 46-48.
33. H. G. McGarr, "Liquid Ion-Exchange Recovers Copper from Wastes and Low-Grade Ores", E. & M. J., pp. 79-81, October 1970. Also H. J. McGarr, "Solvent Extraction Starts in Making Ultrapure Copper", Chemical Eng'ng, pp. 82-84, August 10, 1970.
34. Anon, E. & M. J., October 1967, p. 114. Also anon, Sulfur, No. 71, July-August 1967, p. 29.
35. D. N. Skillings, Jr., Asarco Starts Up San Xavier Copper Project in Arizona, Skillings Min. Rev., March 10, 1973, p. 1. Also anon., Chem. Eng'ng., April 2, 1973, p. 72. Also, Anon., Metals Source-book, February 26, 1973.
36. E. J. Duggan, Flotation and Leaching, E. & M. J., vol. 126, No. 26, pp. 1008-1015, December 29, 1928. Also E. J. Duggan, Ammonia Leaching at Kennecott, Trans. AIME, vol. 106, pp. 547-558, 1933. Also R. E. Wilmshurst, R. L. Parker, The Burra Treatment Process, Paper No. 10, Australasian IMM, Adelaide, 1971. Also Anon., Leach Extraction of Copper, Austral. Mining, June 1972, p. 24. Also R. S. Shoemaker, Ammonia Revival for the Keweenaw, Mining Eng'ng., May 1972, p. 45. Also R. P. Frants, T. P. McNulty, Leaching a Copper Silicate Ore With Aqueous Ammonium Carbonate. Paper to 2nd International Hydrometallurgical Symposium, AIME, Chicago, February 1973.
37. Anon., Copper Leaching with Cyanide - A Review of 5 Inventions, E. & M. J., September 1967, p. 123. Also C. Chamberlain et al, How Cyanidation Can Treat Copper Ores, E. & M. J., October 1969, p. 90. Also G. W. Lower et al, Recovery of Copper by Cyanidation, Min. Eng'ng., November 1965, p. 56. Also D. H. Rose et al, White Pine Experiments with Cyanide Leaching of Copper Tailings, Min. Eng'ng, August 1967, p. 60.
38. J. A. Hartlage, "Kelex 100 - A New Copper Solvent Extraction Reagent". Presented to SME of AIME, Salt Lake City, Utah, September 1969. Also E. & M. J. October 1969, p. 93.
39. A. Miller, Process for the Recovery of Copper from Oxide Cu-Bearing Ores by Leach LIX and Electrowinning at Ranchers Bluebird Mine, Miami, Ariz. The Design of Metal Producing Processes, TMS of AIME, 1969, p. 337.
40. R. F. M. Brown, Solvent Extraction and Electrowinning for the Recovery of Metals, Paper No. 10, Australasian IMM, Adelaide, 1971.
41. K. L. Power, Operation of the First Commercial Copper Liquid Ion Exchange and Electrowinning Plant, Copper Metallurgy, R. P. Ehrlich, Ed., Proc. AIME Symposium, Denver, 1970, p. 1. Also J. Dasher and K. L. Power, "Copper Solvent-Extraction Process: From Pilot Study to Full Scale Plant", E. & M. J., April, 1971, pp. 111-115. Also K. L. Power, "Operation of the First Commercial Liquid Ion-Exchange and Electrowinning Plant". Presented at the International Solvent Extraction Conference, The Hague, April, 1971. Also K. R. Rawling, "Commercial Solvent Extraction Plant Recovers Copper from Leach Liquors", World Mining, pp. 34-37, December 1969.
42. E. R. DeMent, C. R. Merigold, LIX-64N - A Progress Report on the LIX of Copper, Paper to AIME, Denver, February 1970. Also C. R. Merigold, D. W. Agers, and J. E. House. "LIX64N - The Recovery of Copper from Ammoniacal Leach Solutions", Presented at the International Solvent Extraction Conference, The Hague, April, 1971.
43. D. W. Agers, Economic Considerations in the Selection of Solvents and Design of Solvent Extraction Plants. Proc. 1st Annual Meeting of Canadian Hydrometallurgists, Ottawa, October 1971, p. 34. Also Joe Rosenbaum, U.S. Bur. Mines IC 8502, p. 4.
44. Anon., Mining Engineering, March 1973, p. 4.
45. J. A. Holmes, and J. F. C. Fisher, Development of a Process for the Extraction of Copper from Tailing and Low-Grade Materials at the Chingola Division of Nchanga Consolidated Copper Mines, Zambia, Advances in Extractive Metallurgy, IMM Symposium, October 1971, London, p. 169.
46. G. C. I. Warwick, J. B. Scuffham and J. B. Lott, Solvent Extraction - Today's Exciting Process for Copper and Other Metals, World Mining, October 1970, p. 38. Also S. A. Gardner, G. C. I. Warwick, Pollution Free Metallurgy: Copper via Solvent Extraction, E. & M. J., April 1971, p. 110.

47. Anon., LIX Plant for Anaconda, Mining J., February 16, 1973, p. 129. Also Anon., Skillings Min. Rev., January 13, 1973. Also Metals Sourcebook, Feb. 26, 1973
48. Anon., Solvent Extraction Plant, Mining J., March 23, 1973, p. 237.
49. Anon. Metals Week, Oct. 29, 1973, p. 1
50. W. A. Griffith et al., Development of the Roast-Leach-Electrowinning Process for Lakeshore, AIME, February 1973, Chicago, Preprint A-73-64.
51. Anon., Metal Anodes Are Winning New Converts, Chemical Week. April 5, 1972, p. 35.
52. Anon., Anode Corrosion Overcome, Mining Journal, October 20, 1972, p. 317.
53. Anon., Anaconda Company's Arbiter Process, Engineering and Mining Journal, February 1973, p. 74.
54. U. S. Patents 2,647,825, -829, -830, -831, -832; 2,675,842, -843.
55. J. O'Connor, Chemical Refining of Metals, June 1952, p. 164. Also Anon., New Chemical Method Recovers Ni, Co, Cu Metal, Mining Eng'g., June 1952, p. 565.
56. V. H. Ryan and H. J. Tschirner, Production and Characteristics of Chemically Precipitated Cu Powder, Proc. Metal Powder Assn. 1957 (13th Annual), p. 25-32. Also J. F. Whitaker. Wire and Wire Products, vol. 36. October 1961, p. 1346.
57. W. J. Yurko, Continuous Processing and Process Control, p. 55, Gordon & Breach, 1968. Also E. & M. J., January 1967, p. 97. Also Chemical Engineering. August 29, 1966, p. 66. Also Skillings Min. Rev., November 5, 1966, p. 19.
58. W. Kunda, H. Veltman and D. J. I. Evans, Production of Copper from the Ammine Carbonate System, Copper Metallurgy, AIME Symposium, 1970, Denver, p. 27.
59. J. Dasher, Hydrometallurgy for Copper Concentrate, Paper to 2nd CIM Hydrometallurgy Group Meeting, Montreal, October 1972, and CIM Bulletin, May 1973. Also J. Dasher, How Can the Industry Produce Copper Legally and Still Make a Profit, Paper to AIME, February 1972, and Mining Mag., April 1972, p. 279.
60. K. N. Subramanian et al., Can. Met. Quarterly, vol. 11, No. 2, 1972. Also R. J. Roman and B. R. Benner, The Dissolution of Copper Concentrates, Mineral Sci. and Engineering, vol. 5, No. 1, January 1973, p. 3.
61. Dorr-Oliver, "Par. 3" FluoSolids Seminar, May 1967
62. E. S. Howell et al., E. & M. J., July 1959, p. 86. Also H. Kurushima et. al. J. Metals, May 1955, p. 634. Also Anon., Can. Chem. Processing, February 1971, p. 20
63. Met. Mining and Proc., November 1964, p. 33. Also, Min. Mag. July 1973, p. 77
64. G. P. Lutjen, E. & M. J., December 1953, p. 72 Also W. R. McCormick, Paper to AIME, St. Louis, October 1958. Also H. L. Hazen et al., Metal Min. and Proc. April 1964, p. 47. Also H. L. Hazen et al., Deco Trefoil, March/April 1964, p. 7. Also E. & M. J., September 1965, p. 122.
65. P. J. McGauley et al., U. S. Pat. 2,736,859 (1956).
66. W. R. McCormick, Personal Communication. Also P. J. McGauley, Personal Communication.
67. F. A. Forward, Trans CIMM, vol. 56 (1953), p. 373. Also S. Nashner, CIM Bull., vol. 48, No. 519, p. 396 (1955)
68. D. J. I. Evans et al., CIM Bull., No. 628, p. 857, August 1964

69. Anaconda Press Release, January 4, 1973, summarised in Wall Street Jnl., January 5, 1973, p. 5; Metals Week, January 8, 1973, p. 2; Iron Age, January 1973, p. 51; Skillings Min. Rev., January 13, 1973, p. 12; Mining Record, January 17, 1973; Mining Engineering, February, 1973, p. 22. Also E&MJ, Feb 1973, p. 74. Also N. Arbiter, Anaconda's Ammonia Leach Process, Paper to Am Mining Cong., Denver, Sept. 1973.
70. M. C. Kuhn et. al. Anaconda's Arbiter Process for Copper, Paper to Hydrometallurgy Group, CIM, Edmonton, October, 1973.
71. Anon., Skillings Min. Rev. July 14, 1973, p. 16. Also E&MJ, Aug. 1973, p. 127
72. R. H. Leseman, E. & M.J., March 1973, p. 86.
73. E. S. Allen, P. R. Kruesi, Cymet Electrometallurgical Processes for Treating Base Metal Sulfide Concentrates, Paper to MMIJ-AIME, Tokyo, May 1972. Also P. R. Kruesi et. al, Cymet Process - Hydrometallurgical Conversion of Base Metal Sulfides to Pure Metals, CIM Bull, June 1973, p. 81. Also P. R. Kruesi, Paper to Am. Min. Cong. Denver, Sept. 1973.
74. A. G. Fonseca, Ammonia-Oxidative Leach of Chalcopyrite, Paper No. 48, CIMM Annual Meeting, April 1973.
75. Anon. Stanford Earth Scientist, April-June 1963, p. 6. Also R. W. Bartlett & H. H. Haug, The Lime-Concentrate-Pellet-Roast Process for Treating Copper Sulfide Concentrates, J of Metals, Dec. 1973, p. 28
76. G. F. Pace & J. C. Stauter, Direct Electrowinning of Copper from Synthetic Leach Solutions SO₂ and Graphite Electrodes-Pilot Plant Results, CIM Bull, Jan 1974, p. 85.
77. Anon. Sherritt and Cominco to Test New Hydrometallurgical Process, Skillings Min. Rev. Nov. 17, 1973, p. 6
78. Anon. E&MJ, July 1973, p. 123, Also Chem. Eng'ng Oct. 1, 1973, p. 73
79. G. M. Ritcey, Recovery of Copper from Concentrated Solution by Solvent Extraction Using Kelex 100, CIM Bulletin, Apr, 1973, p. 75.
80. J. A. Hartlage, A. D. Cronberg, Chemical and Physical Factors to be Evaluated upon Designing a Kelex Extraction System, Paper to CIM Conf. of Metallurgists, Quebec City, Aug. 1973.

Author: C. P. BIRCH

Abstract:

The ability of the new copper extractant 'P-1' to treat feed solutions of both low (3 g/litre) and high (40 g/litre) copper concentration, was tested. It was demonstrated that P-1 was effective in both systems; high recoveries ($\approx 90\%$) could be achieved with compact mixer-settler circuit configurations, due to the high chelating strength and loading capacity of the extractant. Additional advantages were: rapid copper transfer and high selectivity against Fe(III) and Co(II) in the sulphate system. Chemical and physical performance of P-1 were confirmed in a pilot circuit.

With the presently acceptable strip solution copper tenor of 30 g/litre the acid tenor necessary to strip P-1 effectively was 225 g/litre.

Place of origin:

Research and Development Department of Nchanga Consolidated Copper Mines, Kitwe, Zambia.

1. Introduction

Nchanga Consolidated Copper Mines Limited has a considerable commitment to copper solvent extraction, presently embodied in the new 55,000 litre/minute plant at the company's Chingola Division. The interest of NCCM in new copper extractants lies partly in the desire to improve the performance, and ultimately to uprate substantially the copper throughput, of the Chingola plant. A further application for new extractants involves the copper recovery stage of a new projected cobalt/copper process developed by NCCM, in which it is required to produce copper of electrolytic quality from a 40 g/l Cu, 70 g/l Co, 10 g/l H₂SO₄ leach solution.

The new extractant 'ACORGA-P-1', an ortho-hydroxy-aryl-oxime, in the process of being developed by ICI Organics Division, in the United Kingdom, was received by the Research and Development Department of NCCM in Kitwe, Zambia, in October 1972. The main findings of this work are presented.

2. Experimental Techniques

The experimental methods employed to evaluate the main properties of P-1 are listed as follows.

Loading capacity as a function of aqueous equilibrium pH

The extractant was dissolved at a strength of 20 g/l in the diluent. A series of solutions of composition 4 g/l Cu(II) as sulphate, was prepared, the pH values being 0.5, 1.0, 1.3, 1.9, 3.0. The loading capacity of the solvent for each of these pH values was obtained by a 'repeated contacting'

technique. Thus, equal volumes of fresh aqueous and solvent were contacted by vigorous shaking, in a separating funnel, to equilibrium. After phase separation, the aqueous phase was removed and replaced with a fresh aliquot of aqueous. The process was repeated until the pH values of raffinate samples from successive contacting steps were equal. The copper analysis of the final solvent was the loading capacity at the equilibrium aqueous pH.

Kinetics of extraction and stripping

'Kinetics' in this context refers to the rate of solute transfer under specified conditions of agitation and is expressed as the percentage approach to equilibrium in a given time. The vessel and agitator size and configuration, solution compositions, phase continuity, and temperature were fixed.

Experiments with P-1 were conducted at two levels of impeller speed. The apparatus is illustrated in Fig. 1.

The essentials of the technique were as follows:

(i) starting solutions were brought to the reaction temperature of 25°C, (ii) 400 ml of the solvent were agitated in the vessel at the appropriate impeller speed, (iii) 400 ml of aqueous were added rapidly with simultaneous starting of a stop watch, (iv) after the chosen time interval, the agitation was stopped, (v) immediately sufficient clear phase was generated, samples of

both aqueous and solvent were withdrawn for analysis, (vi) the process was repeated, starting with fresh 'feed' solutions, with agitation for different time intervals, (vii) the equilibrium copper tenor in both phases was established by agitation for ten minutes.

Phase disengagement

This is characterised by the time required for coalescence to a clear interface, after agitation of the aqueous and organic phases in the apparatus depicted in Fig. 1. The phases were equilibrated before phase disengagement was commenced; exploratory tests with P-1 have shown that there was no detectable effect of mass transfer on phase separation.

Extraction and strip isotherms

Isotherms were determined by contacting the appropriate aqueous and organic starting solutions to equilibrium at a range of volumetric ratios, normally 10:1, 5:1, 2:1, 1:1, 1:2, 1:5, 1:10. At each ratio, fresh portions of the feed solutions were employed. The contacting was achieved by shaking of a separating funnel containing the two phases by hand in a laboratory where the air temperature was controlled to 25°C. Adequate time was allowed to ensure equilibrium; 10 minutes in the intermediate values of O/A ratio, 30 minutes at the more extreme values. Both phases were analysed for copper content before and after contacting. The validity of each equilibrium point was checked by calculating

the solute balance. The isotherms were plotted as copper concentration in solvent versus copper concentration in aqueous. Each point on the isotherm represents a different value of equilibrium aqueous acidity, the acid 'equivalent' of the aqueous phase (i.e. H_2SO_4 concentration + Cu concentration x 98/63.5) is, however, constant for the whole isotherm.

Continuous tests

The extraction and stripping performance of P-1 for a variety of multistage countercurrent configurations was checked using a small mixer-settler system. The mixer volume was 0.25 litres and the settler volume 0.50 litres. Agitation and interstage pumping were effected simultaneously by the mixing impeller. Both the mixer residence time and the settler area were considerably oversized to ensure that each mixer-settler behaved as a discreet equilibrium stage.

Pilot mixer-settler circuit

The pilot circuit employed for testing of P-1 in the copper/cobalt separation system, consisted of three extraction and two strip stainless steel mixer-settler units. The mixer-settler design is depicted in Fig. 2. The mixer had a six-bladed turbine impeller, with a separate pumping impeller mounted on the bottom of the common shaft. A ring baffle around the pumping impeller prevented any agitation of the mixer contents by this impeller. The agitating impeller speed could be varied without any constraint arising from the pumping requirement. The circuit was arranged

such that the mixer-settler units pumped one phase between stages, the other phase flowing by gravity.

The settler design was conventional, with a fixed central, horizontal discharge slot for dispersion entry, and a full width aqueous discharge weir. Interface level control was by means of an adjustable jack-leg. The mixer volume was 2.1 litres, the settler volume 6.3 litres. An internal recycle was provided on all mixer-settlers to generate a phase ratio of 1.0 in each unit. The aqueous feed rate to the extraction circuit was 50 ml/minute. The overall phase ratio was normally approximately 4.0 in the extraction circuit, and 0.5 in stripping. Hence the total flowrate through each mixer-settler was greater in stripping than in the extraction units. The presence of the recycle, together with the differential between solvent and aqueous flow, lead to different mean residence times of each phase in the mixers. The mean residence time provided in the extraction circuit was excessive, but unavoidable as all the mixer-settlers were of the same capacity. Organic phase continuity was employed in all mixers throughout the testwork.

The settler area was varied by the provision of a moveable end baffle. Samples of each phase for determination of secondary entrainment of the other phase were removed from points adjacent to the baffle.

Analysis of entrained solvent in the aqueous phase was achieved

by extraction using carbon tetrachloride, followed by infra-red analysis of the P-1 content of the extract. The total solvent entrainment level was then back-calculated, the P-1 strength of the solvent being known. Entrainment of aqueous in organic was determined by centrifugation using specially designed tubes.

Operation of the plant was on a continuous basis. Shift composite samples of each stream were taken during periods of steady operation, for analysis of circuit performance.

3. Results and discussion

The experimental data and their interpretation are presented according to the following format:

- (i) Equilibrium extraction and stripping data to characterise generally the copper transfer properties of P-1.
- (ii) The specific application of P-1 to treatment of a 3 g/l Cu feed, in respect of circuit configurations and performance levels. Data indicative of required equipment size are also discussed.
- (iii) Application of P-1 to treatment of a high copper tenor solution. In addition the findings of preliminary piloting of P-1 are presented.

A range of different diluents was considered for P-1. Exploratory

tests on four diluents demonstrated that those with relatively low aromatic contents, i.e. up to 20% by volume, were all acceptable. The single pure aromatic diluent tested, Shellsol A, was unacceptable as the phase disengagement of the P-1/Shellsol A solvent was extremely slow. Of the diluents immediately available, Shell MSB 210 (<4% aromatics) and Esso Escaid 100 (~20% aromatics), were both employed in P-1 testing.

Equilibrium characteristics of P-1

The copper loading capacity of 20 g/litre P-1 in the diluent Shell MSB 210, is presented as a function of aqueous phase pH in Fig. 3. It is apparent that the extractant has a high loading capacity even at low pH.

The ability of any extractant to transfer copper depends both on its loading characteristics and on the ease of stripping copper from the solvent phase.

The equilibrium copper concentration in the solvent, as a function of the copper and acid tenor of the aqueous phase at equilibrium has been determined for 40 g/litre P-1 in Shell MSB 210. The results are presented in Fig. 4 on a 20 g/litre basis assuming that the residual copper level in stripped solvent is directly proportional to the extractant concentration. It is apparent from Fig. 4 that the copper level in the solvent is clearly strongly dependent on both the copper and acid tenor. Using these data, an indication may be given of the transfer

capacity of P-1, as a function of the strip solution composition. Such a correlation is illustrated in Fig. 5, where solvent transfer capacity is defined thus:

$$\frac{(\text{loading capacity of solvent g/l}) - (\text{residual copper tenor after stripping})}{(\text{loading capacity of solvent})} \times 100\%$$

Fig. 4 shows that for a 30 g/l copper concentration in the strip solution, the lowest practicable value consistent with acceptable cathode quality in present 'conventional' electrowinning equipment, the acidity level of 150 g/l would give a transfer capacity of 37%, which represents poor extractant utilisation. However, the transfer capacity is increased to 55% at 200 g/l H₂SO₄ and 72% at 250 g/l H₂SO₄, at the 30 g/l Cu level.

It is stressed that reduction of the strip solution copper tenor is an equally effective means of extending the transfer capacity of P-1. Thus, Fig. 4 shows that for a 15 g/l Cu level in the strip solution, at 150 g/l H₂SO₄ acidity level, a 55% transfer efficiency is obtainable.

4. Low copper tenor system

Equilibrium performance of P-1

The distribution isotherms for extraction and stripping of P-1 were determined and are presented in Figs. 6 and 7. The extraction isotherm is clearly very 'steep'. A McCabe-Thiele

diagram has been constructed on the isotherm of Fig. 6.

For a phase ratio of 1:1, a high extraction is obtainable in three equilibrium stages, with the system operating at close to the solvent loading capacity (defined in the limit by the feed pH in a continuous system). It is evident that the maximum stripped solvent copper tenor consistent with high copper transfer is 1.65 g/litre. The acid tenor of a 30 g/litre Cu strip solution required to achieve this level is estimated, from strip equilibrium data to be 225 g/litre.

The ability of P-1 to perform effectively in a continuous circuit was demonstrated in the laboratory scale mixer-settler cascade. Results are presented for two circuit configurations in Table 1.

TABLE 1 : Performance data from laboratory scale mixer-settler circuit

		Run Number		
		1	2	3
<u>Circuit Parameters</u>				
Number of stages	Extraction	3	2	3
	Strip	2	1	2
Phase ratio	Extraction	1.1	1.0	3.5
	Strip	1.0	1.0	0.5
<u>Solvent</u>				
P-1 strength	g/litre	40	50	150
Cu tenor g/l	Stripped	1.65	2.35	6.00
	Loaded	4.30	5.25	16.00
<u>Extraction circuit</u>				
Feed	Cu g/litre	3.05	2.90	31.2
	pH	1.88	1.97	13.2 *
Raffinate	Cu g/litre	0.19	0.03	2.2
Recovery from feed	%	93.8	99.0	93.0
<u>Strip circuit</u>				
Strip solution	Cu g/litre	29.3	29.5	29.0
	H ₂ SO ₄ g/litre	225	216	245
Strip liquor	Cu g/litre	36.7	32.2	33.4

* g/litre H₂SO₄

The data from Run 1, Table 1, show that a reasonably high recovery is obtainable from a 3.05 g/l Cu, pH 1.9 feed, using three extraction and two strip stages and 40 g/l P-1, and a strip solution containing 29.3 g/l Cu, 225 g/l H₂SO₄. The copper transfer per litre of solvent was in this case, 56% of the solvent loading capacity.

The possibility of reducing the number of extraction and strip stages was tested in the continuous circuit. Results of this run (Run 2, Table 1) show that by using 50 g/l P-1 and a phase ratio of 1:1 in strip, two stages of extraction and one of stripping could recover 99% of the copper from the feed.

Rate of copper transfer in extraction and stripping

The rate of copper extraction in a P-1 system was determined for intense agitation (1270 rpm) and mild agitation (420 rpm).

The power input in a given impeller/mixer configuration in a baffled tank¹ is proportional to N^3D^5 , where N = the impeller rotational speed, and D = the impeller diameter. Hence the lower agitation level used represents: $420^3/1270^3$, 1/28 of the power applied at the higher level.

Data for the rate of approach to equilibrium in both extraction and stripping are presented in Table 2.

TABLE 2 : Kinetics - rate of approach to equilibrium in extraction and stripping

Time - seconds	15	30	60
	% of equilibrium		
Extraction:			
Impeller speed 1270 rpm	-	100	100
420 rpm	54	76	-
Strip:			
Impeller speed 1270 rpm	-	100	100

Conditions:

Extraction - Starting solutions: Aqueous 4 g/l Cu (II) sulphates
 4 g/l Fe (III)
 pH 1.90

Solvent 40 g/litre P-1 (stripped)

Strip - Starting solutions: Aqueous 25 g/l Cu (II)
 150 g/l H₂SO₄

Solvent 40 g/litre P-1, loaded to maximum capacity at pH 1.90

Diluent - Shell MSB 210.

The rate of both processes under strong agitation is shown to be extremely rapid, with equilibrium having been achieved in 30 seconds. At a low agitation rate, the extraction rate is still regarded as acceptable. Scale-up data from laboratory batch kinetic tests to large scale continuous pilot equipment, in the

existing Chingola solvent extraction system, are available. These results have demonstrated that a rate of approach to equilibrium, in the laboratory equipment, of 75% in 30 seconds and 90% after 60 seconds, is sufficiently rapid to generate stage efficiencies generally greater than 95% in continuous mixer-settlers with 2-3 minutes' mixer residence time, provided that sufficient agitation intensity is applied. It would appear probable that in a P-1 circuit, using relatively mild agitation in the mixers, a retention time of dispersion in the mixers of 2-3 minutes would be adequate for high stage efficiency.

Phase disengagement rates

The phase disengagement time in the standard test was determined at two levels of P-1 strength, and a range of aqueous compositions in respect of iron(III) and acidity. Exploratory tests had indicated a significant effect of these latter components. Results are presented in Table 3.

TABLE 3 : Time for complete phase disengagement in extraction and strip systems, as a function of aqueous composition

Solvent * g/l P-1	Composition of aqueous solution at equilibrium			Time for phases to disengage completely - seconds
	Cu g/l	Fe ³⁺	pH	
60	4	0	2.0	96
60	4	4	2.0	144
60	4	4	1.75	105
60	4	4	1.50	90
40	4	4	1.97	105
40	4	4	1.76	78
40	4	4	1.52	69

* Diluent - Esso 'Escaid 100'

The time for complete phase disengagement appears to be dependent upon the aqueous acidity level, in the presence of iron. As with mass transfer rates, scale-up data from laboratory batch experiments to continuous pilot scale equipment are available. The phase disengagement times in Table 3 imply an acceptable settler area requirement.

Selectivity against Fe (III)

The main impurity existing in copper acid leach solutions, which has a tendency to be co-extracted with copper by hydroxy-oxime-type extractants, is iron in the ferric form.

The iron concentration in the solvent as a function of time for the extraction and the stripping systems is presented in Table 4.

TABLE 4 : Level of iron in solvent vs time (from kinetic tests), for extraction and strip systems

Time, seconds	0	15	30	60	600
Test conditions:					
Extraction system:					
1. Low impeller speed (420 rpm):					
Fe concentration in solvent, mg/litre	5(4)*	10(10)	9(9)	-	8(8)
Cu - % of equilibrium extraction	0	55	76	-	100
2. High impeller speed (1270 rpm):					
Fe concentration in solvent, mg/litre	2	-	9	8	6
Cu - % of equilibrium extraction	0	-	100	100	100
Strip system:					
High impeller speed (1270 rpm):					
Fe concentration in solvent, mg/litre	11	-	3	4	4
Cu - % of equilibrium stripped	0	-	100	100	100

* Figures in brackets from duplicate test. Diluent - Shell MSB 210

It is evident that relative to copper, the rate of iron extraction is rapid. An equilibrium value of approximately 10 mg/litre iron in the solvent was established within 15 seconds, even with mild agitation. This equilibrium level represents a low value for the partition coefficient, i.e. approximately 2.5×10^{-3} under the conditions of the test. The removal of iron from loaded solvent is shown to be essentially complete after 30 seconds, with rapid agitation; the level of 4 mg/l Fe in solvent is close to the limit of detection for the methods available.

The kinetic and equilibrium behaviour of iron distribution refers only to a single set of chemical conditions in the extraction and strip systems. The most realistic assessment of the selectivity characteristics is provided by data from a continuous system.

Iron transfer data are presented in Table 5. These results were obtained from the laboratory continuous runs 1 and 2 (see Table 1 for circuit parameters).

TABLE 5 : Iron transfer data from continuous laboratory mixer-settler circuit

Continuous run number	Feed			Fe tenor in solvent, mg/l					*Relative iron transfer (overall)
	Cu g/l	Fe(III) g/l	pH	Extraction stages E1 E2 E3			Strip stages S1 S2		
1	3.05	1.13	1.88	7	8	10	2	2	1.8×10^{-3}
2	2.90	0.95	1.97	8	17	-	4	-	1.4×10^{-3}

* $\frac{\text{Fe transferred per litre of solvent}}{\text{Cu transferred per litre of solvent}}$

Diluent - Esso 'Escaid 100'.

The overall iron transfer is clearly low. A convenient indication of the degree of selectivity is the 'relative impurity transfer' which is defined:

$$\frac{\text{Impurity transferred per litre of solvent}}{\text{Cu transferred per litre of solvent}} = \frac{(\text{Impurity concentration in loaded solvent})}{(\text{Copper concentration in loaded solvent})} \cdot \frac{(\text{Impurity conc. in stripped solvent})}{(\text{Cu Conc. in stripped solvent})}$$

In both tests, low values of ≤ 0.002 were obtained. Also, the

solvent was stripped to a very low iron level, indicating that all iron extracted was transferred to the strip circuit.

5. High copper tenor system

Laboratory results

This evaluation was aimed at establishing the required parameters to enable P-1 to extract > 90% of the copper from a feed containing 40 g/l copper, 70 g/l cobalt, 1 g/l Fe(III) (all as sulphates), and 10 g/l sulphuric acid. It was necessary to establish a suitable operating strength for P-1; this involved a compromise between copper transfer capacity of the solvent, (constrained ultimately by the solubility of the Cu/P-1 co-ordination compound in the diluent) and the rate of phase disengagement. Static phase disengagement tests using a range of P-1 concentrations indicated that 150-200 g/l P-1 was an acceptable concentration.

Kinetic tests in this system demonstrated rapid transfer of copper, i.e. 97% of equilibrium transfer after 30 seconds in both the extraction and strip systems, with the high impeller speed.

Extraction and stripping distribution isotherms were determined with a 150 g/l P-1 solution; these are presented in Figs. 7 and 8. It is apparent from the McCabe-Thiele constructions that with a three extraction, two strip stage system, a high recovery from the 40 g/l copper feed is obtainable.

Results from a laboratory scale continuous test (run 3) with a three extraction stage, two strip stage circuit, are presented in Table 1. These results confirm the ability of P-1 to extract copper from a feed of high copper content; a 93% recovery from a 31.2 g/l copper, 13 g/l H_2SO_4 feed, was obtained.

The selectivity of P-1 against cobalt was tested by contacting a 40 g/l P-1 solvent with an aqueous phase containing 40 g/l Co, 41 g/l Cu and 9 g/l H_2SO_4 using intense agitation for 10 minutes. Subsequent analysis of the solvent showed that the cobalt level was below the detection limit of 1mg/litre.

Pilot plant results

The purpose of the piloting work was to establish the long term consistency of P-1 extraction and strip performance in a practical operating system, and to identify any problems in physical handling, particularly phase disengagement.

The P-1 sample employed in these tests was from a different sample batch from the material evaluated in the laboratory. The latter had a loading capacity of 0.113 g of copper per gram of extractant at aqueous pH 1.9; the newer batch loaded to 0.090 g copper maximum capacity at pH 1.9. An extractant strength of 210 g/l P-1 was employed, generating a solvent loading capacity of 19 g/l Cu at pH 1.9.

The pilot circuit was in operation for nineteen days.

Performance data for three extended periods of reasonably steady operation are presented in Table 6. The degree of fluctuation of many of the operating parameters was fairly large. However, the overall copper recovery was very consistent, and was normally $>90\%$. Thus, the laboratory results are largely confirmed; further, it is evident that a P-1 circuit has sufficient flexibility for the extraction efficiency to be relatively insensitive to normal operational fluctuations.

It is stressed, however, that the consistent copper transfer results would not have been achieved without maintenance of the correct strip solution acid and copper levels, due to the known sensitivity of the strip efficiency of P-1 to this parameter. The other strip circuit parameters (given high stage efficiency) i.e. phase ratio and number of stages, are less critical. Thus, it was found that a single strip stage operating at a phase ratio of 1.0, was still capable of stripping the loaded solvent to an acceptable level of 5 g/l Cu. A higher phase ratio increases the copper content of the strip liquor;

TABLE 6 : P-1 pilot plant - copper extraction and strip performance data

	Run 1	Run 2	Run 3
Hours on line	88	56	40
Phase ratio - Extraction: Average	3.9	3.5	3.6
	(3.1 - 5.1)	(3.0 - 4.7)	(3.4 - 3.7)
Strip: Average	0.50	0.47	0.49
	(0.32 - 0.57)	(0.33 - 0.52)	(0.48 - 0.51)
Feed - * Copper g/l: Average	36.6	39.5	42.7
	(35.6 - 38.4)	(36.4 - 40.0)	(42.2 - 43.2)
H ₂ SO ₄ g/l: Average	10.7	6.8	5.2
	(5.9 - 16.1)	(3.5 - 13.3)	(3.4 - 8.1)
Raffinate - Copper g/l: Average	2.3	2.7	3.7
	(1.2 - 3.1)	(2.0 - 4.0)	(3.1 - 4.8)
H ₂ SO ₄ g/l: Average	67.6	67.9	73.7
	(65.4 - 69.8)	(63.4 - 73.3)	(68.4 - 79.7)

TABLE 6 continued

	Run 1	Run 2	Run 3
Hours on line	88	56	40
Spent electrolyte - Copper g/l: Average	33.2 (27.3 - 40.0)	29.9 (27.8 - 33.3)	31.3 (27.6 - 34.1)
H ₂ SO ₄ g/l: Average	256 (234 - 269)	244 (238 - 252)	247 (242 - 253)
Advance electrolyte copper g/l - Average	38.3 (31.1 - 47.9)	34.5 (32.4 - 37.7)	36.5 (32.8 - 39.2)
Solvent - loaded Cu g/l: Average	13.8 (10.5 - 16.6)	13.2 (11.2 - 14.7)	15.0 (12.3 - 16.3)
Stripped Cu g/l: Average	4.9 (4.2 - 6.6)	4.9 (4.5 - 5.3)	4.6 (3.7 - 5.4)
% copper recovery from feed:	93.7 (91.6 - 96.8)	93.1 (89.4 - 94.5)	91.4 (89.6 - 92.8)

Figures in brackets refer to the maximum and minimum values in each run.

All stream compositions quoted above are based upon analyses of 8-hour shift composite samples.

* The feed cobalt tenor was in the range 53-74 g/litre, as sulphate.

Diluent - Esso Escaid 100.

at the 1.0 phase ratio a minimum temperature of 30°C was necessary to prevent crystallisation of copper sulphate.

The reduction of strip solution flowrate, to equal the solvent flow, is desirable in that the strip mixer-settler size is reduced; this is important as the solvent flow in the system discussed is already three to four times that of the feed flow.

Stage efficiencies (i.e. degree of approach to equilibrium) in the mixer-settlers were determined, though mixer residence times (4-6 minutes in extraction, 2.6-3.5 minutes in strip) were excessive. Generally, stage efficiencies were well over 90%.

Phase disengagement in the settlers was monitored throughout the pilot plant testwork. In general, no serious difficulties were encountered. Some initial flooding of the S2 settler was observed initially, however this phenomenon did not subsequently reappear; this could not be explained as there were no major changes in the relevant operating parameters.

A wide scatter of the dispersion band width results was observed. No meaningful correlation of dispersion band widths with parameters such as temperature was detected. There was no general difference between dispersion band widths in the extraction and strip systems, and between individual settlers.

The plot of dispersion band widths against the flowrate of

dispersion per unit settler area, is presented in Fig. 9. The majority of results lie within a fairly well defined scatter band. A specific flowrate of $50 \text{ l/m}^2\text{min}$ would generate a dispersion band of between 40 and 110 mm. Higher values of specific flowrate might be acceptable, particularly as it is NCCM's experience in other systems that scale-up of settlers from small scale results, using constant specific dispersion flow, leads to substantial spare settler capacity on the large scale.

Entrainment levels of organic in the raffinate, and in strip liquor, were found to be, on average, approximately $100 \mu\text{l/litre}$ of aqueous in both cases. The majority of results were in the range $65\text{-}120 \mu\text{l/litre}$. Only limited data are available for the entrainment level of aqueous in the solvent phase. However, the entrainment of aqueous in the stripped solvent was generally higher than that in loaded solvent, values of $> 500 \mu\text{l/litre}$ having been obtained. No operational difficulties were caused by the resulting carryover of strip solution to the extraction circuit.

6. Chemical stability

Experimental work on the stability of the extractant under a range of representative conditions has been commenced. At the moment of writing this work is at too early a stage for any conclusions to be drawn.

7. Conclusions

P-1 has been demonstrated to be an effective copper extractant for the treatment of copper-bearing sulphuric acid leach solutions. It possesses certain desirable properties, which may be listed as follows:

(i) P-1 has a high chelating strength in the presence of relatively large concentrations of sulphuric acid, and a high loading capacity. This enables it to extract copper effectively from high tenor solutions (e.g. 40 g/l Cu), in three equilibrium stages.

In low copper tenor systems, a circuit using P-1 would require only two stages of extraction and one strip stage, whilst maintaining a high efficiency of copper extraction from the feed. The high chelating strength of P-1 would also ease any constraint on the leach solution acid tenor in a low copper tenor system, thus simplifying leach circuit acidity control.

(ii) The copper transfer rate in both the extraction and strip processes is very rapid. This might be exploited by employing mild agitation, which would tend to minimise entrainment levels in both phases. It would also allow a less stringent mixer design requirement.

The rapid kinetics of P-1 might allow the use of a differential contactor rather than mixer-settlers. A much reduced solvent inventory requirement would result.

(iii) The selectivity of P-1 against Fe(III) is high, a P-1 circuit would thus require a low bleed from the electrowinning circuit to

prevent accumulation of iron in the electrolyte.

The fact that P-1 does not extract cobalt, even from high cobalt tenor solutions, enables it to be employed effectively in a copper/cobalt separation process in a sulphuric acid system.

A disadvantage of P-1 is that within existing electrowinning constraints, it is necessary to employ a strip solution with a high acid tenor, preferably $>225 \text{ g/l H}_2\text{SO}_4$, to provide reasonably effective stripping.

Acknowledgements

Acknowledgement is due to the members of the Research and Development staff who conducted the experimental work. The assistance of the Analytical section of Research and Development, and the Rokana Analytical laboratory are also noted.

The contribution of Mr J R Orjans (Project Leader in Research and Development), who directed the pilot plant work and designed the mixer-settler units, is also acknowledged.

References

1. Perry, J H Chemical Engineers' Handbook, Fourth edition.
McGraw-Hill, New York 1963. p 19 - 9.

List of symbols

- N = impeller speed, rpm.
- D = impeller diameter, mm.
- E₁ = first extraction stage in mixer-settler cascade
(where aqueous feed enters).
- E₂, E₃ = subsequent extraction stages.
- S₁ = first strip stage in mixer-settler cascade,
where loaded solvent enters.
- S₂ = second strip stage, where strip solution enters.

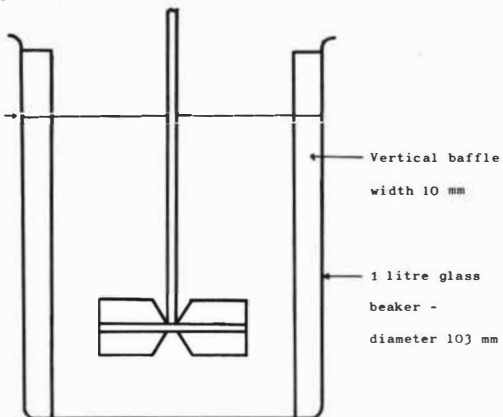
Fig. 1 Mixing apparatus used for kinetic and phase disengagement tests

Cross section -

side view:

Solution level

Depth 104 mm

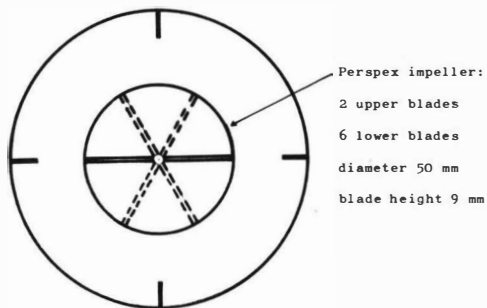


Vertical baffle

width 10 mm

1 litre glass
beaker -
diameter 103 mm

Plan view:



Perspex impeller:

2 upper blades

6 lower blades

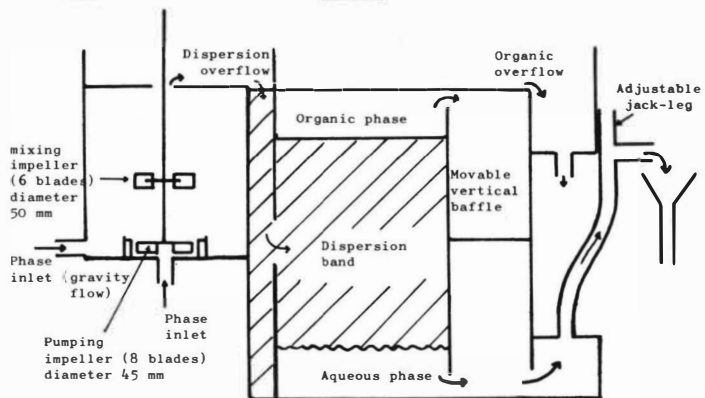
diameter 50 mm

blade height 9 mm

Fig. 2 Diagram of mixer-settler employed in P-1 pilot circuit

mixer

settler



Dispersion
overflow

Organic
overflow

Organic phase

Adjustable
jack-leg

Movable
vertical
baffle

mixing
impeller
(6 blades)
diameter
50 mm

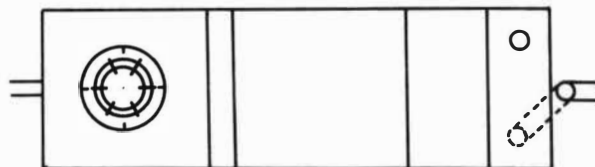
Phase
inlet (gravity
flow)

Phase
inlet

Pumping
impeller (8 blades)
diameter 45 mm

Dispersion
band

Aqueous phase



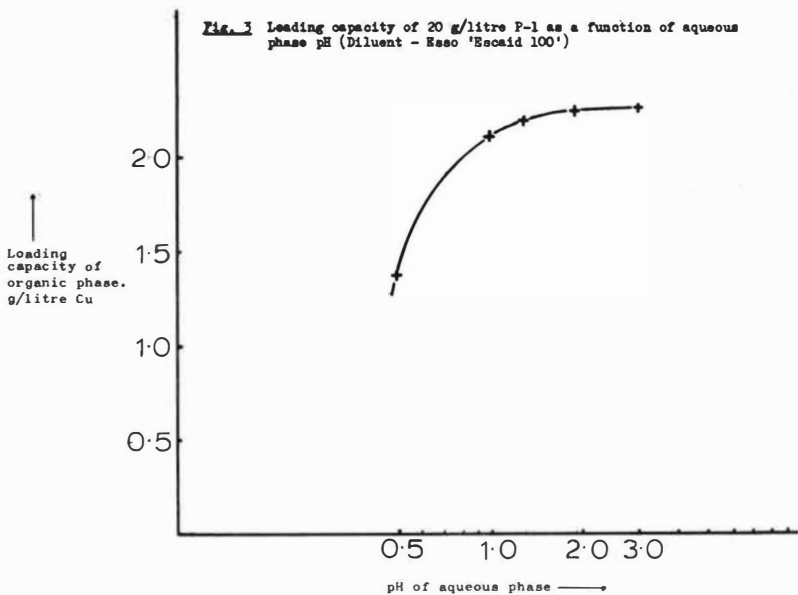


Fig. 4 Copper tenor of 20 g/l P-1 (diluent Shell 'MSB 210') as a function of aqueous acidity, at two levels of copper tenor in aqueous

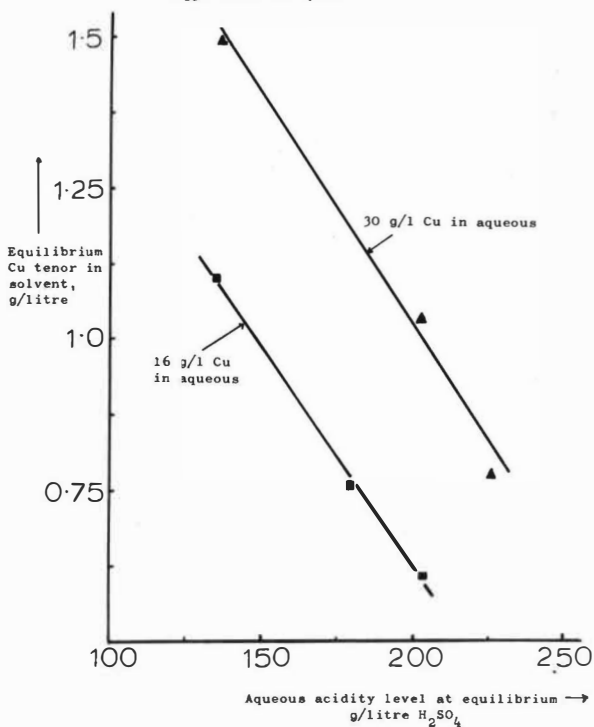


Fig. 5 Transfer capacity of P-1 as a function of strip solution composition.

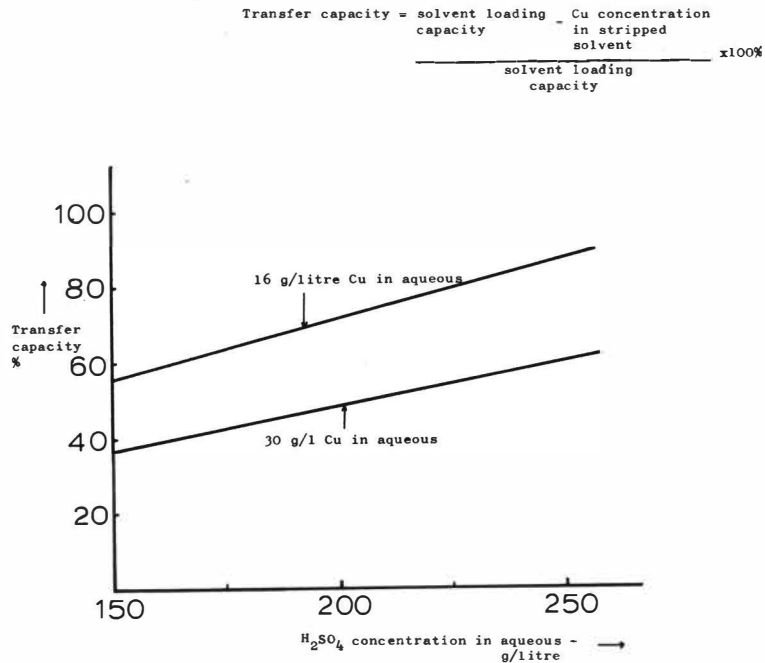


Fig. 6 Extraction isotherm and McCabe-Thiele Diagram: 40 g/litre P-1 (diluent: Shell 'MSB 210') with feed of composition 3.15 g/l Cu, pH 2.1

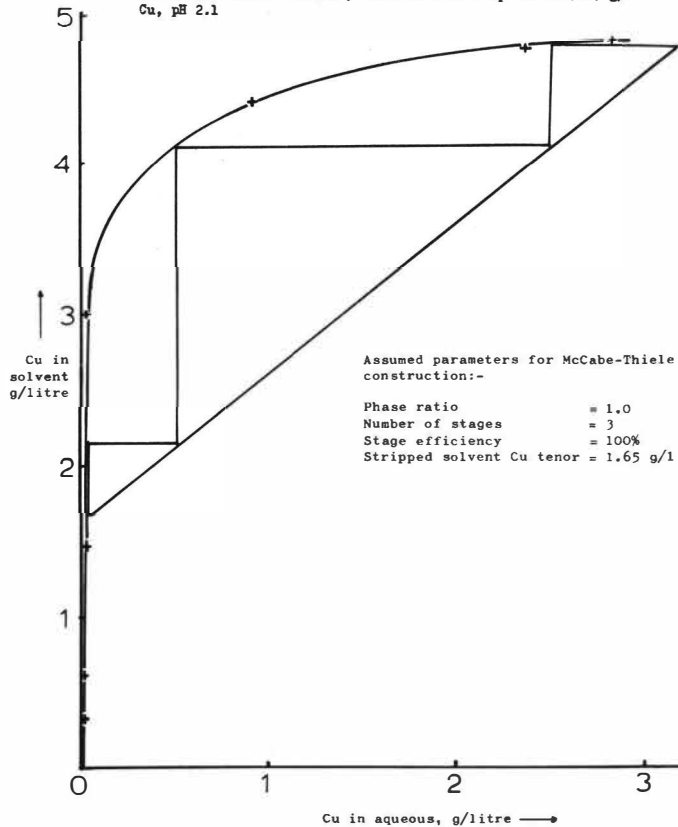
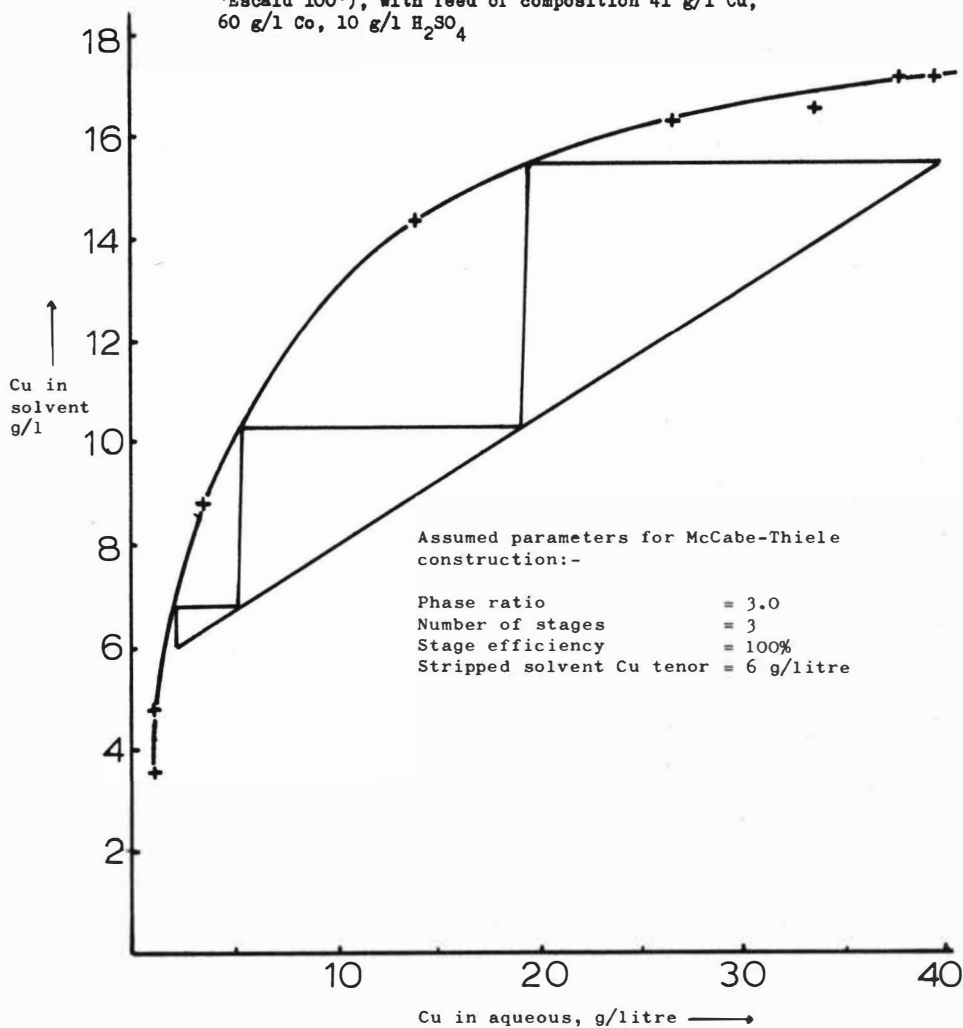
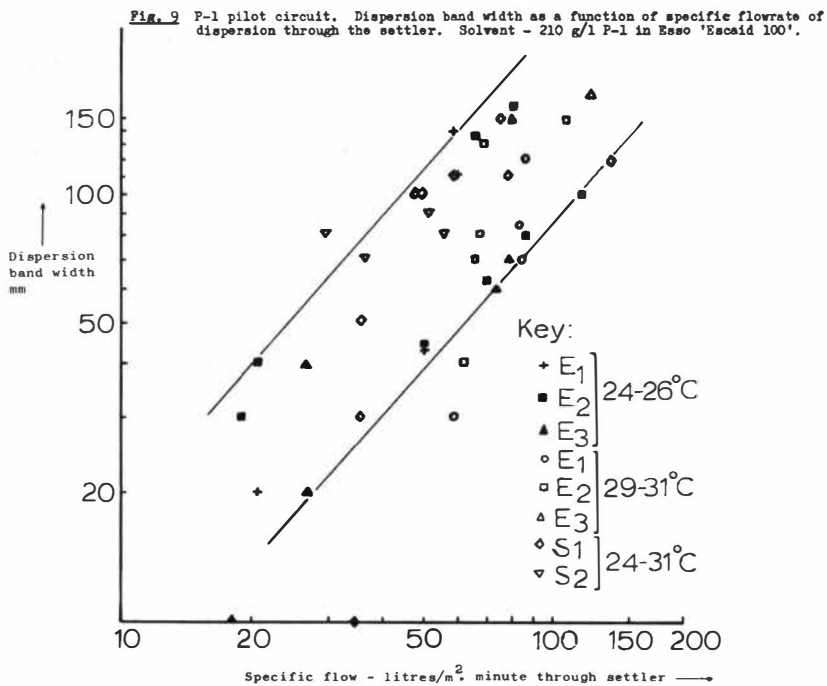
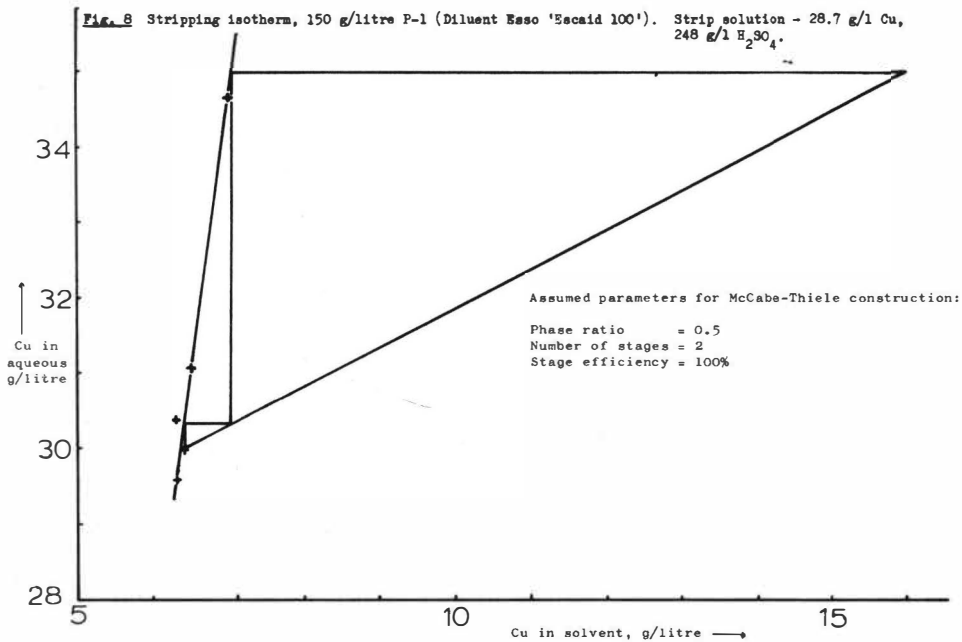


Fig. 7 Extraction isotherm for 150 g/litre P-1 (Diluent Esso 'Escaid 100'), with feed of composition 41 g/l Cu, 60 g/l Co, 10 g/l H_2SO_4







Some Comments on the Loss, and Environmental Effects of
Solvent Extraction Reagents used in Metallurgical Processing

G.M. Ritcey, B.H. Lucas and A.W. Ashbrook

INTRODUCTION

There is, at the present time, apparently little emphasis being placed on environmental effects resulting from solvent components lost from solvent extraction processes. Rather, the emphasis is on the economic aspects as they directly affect the process. This position will undoubtedly change in the future; the emphasis on both aspects of solvent loss can thus be expected to equalise.

Loss of solvent from solvent extraction processes may occur by solubility and entrainment in the aqueous phase, by volatilisation, or as a result of degradation of one or more solvent components producing a soluble degradation product. There is also the situation where degradation of the extractant results in the formation of an inactive compound which is not lost to the aqueous phase, but builds up in the solvent. This might give the same symptoms as extractant loss by solubility. A further possibility is loss due to the solubility of a metal-extractant complex, which may be of environmental significance if a metal thereby contaminates an effluent stream (see below).

Information on overall extractant losses in solvent extraction processes is given in ref. (1). Data on the solubility in water of various extractants, diluents and modifiers will be found in (2), and further data on the solubility of alcoholic modifiers in sulphate media in (3). Diluent stability in nitric acid media is considered in (4). In general, however, information on solvent losses is rather sparse, and often refers only to total losses, irrespective of cause.

Organics that are present in the mine or milling property, and which frequently appear in the mine water or effluent, are traces of lubricants and oils

that are associated with the various pieces of process equipment. These organic compounds, in addition to any solvent from the solvent extraction circuit, can if present in a stream which is being recycled within the mill, cause problems within the mill such as: (1) attack rubber linings of ball mills, thickeners, or leach vessels; (2) inhibit the dissolution process; (3) cause poor filtration or difficult liquid/solids separation; (4) may appear in the final product, causing poor electrodeposition, poor precipitation

TABLE 1

Extractant Losses Reported for Some Processes

Metal Extracted	Extractant	Extraction pH	Loss ppm
	Naphthenic acid	4.0	90
Ni	Naphthenic acid	6.5	900
	Versatic 911	7.0	900
			300
Co	Versatic 911	7.7	100
Rare Earths	D2EHPA	2.0	7
Co	D2EHPA	5.5-6.5	30
U	Tert. Amines	1.5-2.0	10-40
Cu	LIX-64	1.5-2.0	4-15
U	TBP	2.0	25-40
Cu	Kelex 100	1-2	10
Hf	MIBK	1-5M HCl	20,000

and filtration, or problems with drying; (5) in treating a bacterial leach solution by solvent extraction, the organic may inhibit the bacteria activity⁽⁵⁾.

Solvents passing out in effluent streams may eventually provide irrigation to grazing lands. Metals in the solvent may prove hazardous to animals because of the suspected high metal uptake by plants growing in such areas.

Although many present operating plants treat their effluents by lime neutralization, this procedure will probably be slowly phased out as emphasis is placed more on residual mill reagent concentration, nutrient concentration in mine-mill effluents, and on total oxygen demand of mine and mill wastes.

ENVIRONMENTAL CONSIDERATIONS

Perhaps the area of environmental pollution most pertinent to solvent extraction processing is that of water pollution, and consequently the toxicity of solvent extraction reagents to aquatic life then becomes important. Thus the primary consideration in the development of water quality criteria for these reagents is to determine their toxicity towards fish, and their biodegradability.

Toxicity of Some Petrochemicals to Fish

Since different species of fish may differ widely in their tolerance to the same reagent, four fish types are usually used, such as the fathead minnow, blue gill, goldfish and guppy. These four species have been used by Pickering and

Henderson in the study of tolerance limits for a number of petrochemicals⁽⁶⁾.

Median tolerance limits (TL_m) were computed in different concentrations of solvent causing 50 percent mortality of the fish under the experimental conditions during the time period of 96 hours. In general, the toxicity was greater when soft water was used in the tests. In Table 5 are shown the TL_m for the fish in the presence of a number of different petrochemicals, using soft water in the tests, at a temperature of 25°C, for a 96 hour retention time⁽⁶⁾. Except for isoprene and methyl methacrylate which were less toxic, values for all four species in the presence of the other petrochemicals ranged from 10 to 97 mg/l. In general it was found that 100 percent survival occurred at test conditions of about one half of the TL_m value.

Samples of two solvents were subjected to toxicity tests on juvenile coho salmon; (i) 0.1 M Alamine 336 in kerosene containing 5 vol percent isodecanol; (ii) 10 vol percent LIX 64N in kerosene. The TL_{m96} showed 110 ppm and 240 ppm respectively for these two mixed solvent systems⁽⁷⁾. It is interesting to speculate whether the levels indicated are in fact soluble in the aqueous phase to the extent at which the tests were performed.

In most mining and metallurgical operations, water-soluble organics, in the form of flotation agents, filter or settling aids, etc., are used and are present in the feed solution to solvent extraction. These water-soluble organic

reagents not only can affect the solvent extraction process, as regards mass transfer and phase separation, but could also interact with the organic reagents in the raffinate from the solvent extraction process. Data on the toxicity of most of these water-soluble reagents, used in the mining industry, to fish life has been compiled by Hawley of the Ontario Ministry of the Environment⁽⁸⁾.

TABLE 2

Median Tolerance Limits for Some Petrochemicals (6)

Compound	TL _m 96 (mg/l)			
	Fatheads	Bluegills	Goldfish	Guppies
Benzene	33.47	22.49	34.42	36.60
Chlorobenzene	29.12	24.00	51.62	45.53
0-Chlorophenol	11.63	10.00	12.37	20.17
3-Chloropropene	19.78	42.33	20.87	51.08
0-Cresol	12.55	20.78	23.25	18.85
Cyclohexane	32.71	34.72	42.33	57.68
Ethyl Benzene	48.51	32.00	54.44	97.10
Isoprene	86.51	42.54	180.00	240.00
Methyl Methylacrylate	159.1	311.0	232.2	368.1
Phenol	34.27	23.88	44.49	39.19
Styrene	46.41	26.05	64.74	74.83
Toluene	34.27	24.00	57.68	59.30

Biodegradability

A biodegradable substance is a compound which can be broken down via intermediate metabolites by an organism or a series of organisms to carbon dioxide and water⁽⁹⁾. If the stabilities of the particular solvent components are known, then the treatment and retention time needed in a tailings area to degrade the component(s) can be estimated.

Petroleum hydrocarbons are bio-degraded to form CO₂; several factors⁽¹⁰⁾ may limit the rate of biodegradation, and are as follows:

1. organism availability
2. nutrient availability
3. oxygen
4. refractory nature of some petroleum fractions to biodegradation
5. temperature (low temp. slows the rate)
6. ecological effects

The hydrocarbons that are considered here, and which are common in solvent extraction processing, contain: normal paraffins, branched chain paraffins, cycloparaffins(naphthenes), aromatics, and olefinic hydrocarbons.

The degradation of a hydrocarbon occurs through oxidation to simpler compounds, either directly by exposure to oxygen (autooxidation), or through metabolism by microorganisms (microbiol oxidation). Air oxidation of paraffins, olefins, and many aromatics proceeds by a free radical chain reaction which is initiated by sunlight. First, hydroperoxides

(RCH_2OOH) are formed which break down into alcohols or other compounds containing an oxygen atom. Subsequently, the alcohols are further oxidized to yield ketones, aldehydes, or carboxylic acids. Alternatively, the hydroxy compounds may condense with other oxidation products to form higher molecular weight compounds which resist further degradation⁽¹⁰⁾. The rate of autooxidation depends on the temperature, intensity of sunlight, and the type of oil. The presence of some metals and salts in the oil-aqueous system may accelerate the process⁽¹⁰⁾, and in the case of solvents in streams resulting from solvent extraction, trace metals may be present as well as high salt concentrations.

Microbial metabolism of alkane hydrocarbons is by oxidation of the terminal methyl group to a primary alcohol, then to an aldehyde, and eventually to a fatty acid having the same number of carbon atoms as the original alkane. Further oxidation decomposes the fatty acid. The presence of side chains on the alkanes reduces their biodegradability. The more branched the alkane, the more resistant the hydrocarbon is to biodegradation.

Alkenes are degraded at a saturated or unsaturated carbon atom. At a saturated carbon, an unsaturated fatty acid is formed. At an unsaturated carbon either a primary alcohol or fatty acid is formed.

The biodegradation of aromatic hydrocarbons is more difficult, and slower than aliphatic hydrocarbons, and a series of complicated steps are involved.

An excellent review of oil-oxidizing microorganisms for biodegradation of oil on sea water has been given⁽¹⁰⁾. The rate at which crude oil is degraded on the sea was estimated to be 0.1 to 1.0 grams oil per cubic meter of water per day. In the biodegradation of a mixed solvent from solvent extraction processing, since no single organism can degrade all the compounds present, a mixed population of microorganisms may be required for seeding the effluent stream. However, the various microorganisms must be carefully selected so that by-products can be controlled, because some organisms may produce toxic compounds.

Biodegradation is expected to remove the aliphatic fraction more rapidly than the other constituents.

Studies carried out at Washington University have been reported on the use of an activated sludge sewage treatment plant for biodegradation of organic compounds⁽¹¹⁾. Two of the parameters selected to indicate the rate and degree of completeness of biodegradation were oxygen uptake and soluble carbon removal. In Table 3 are tabulated several organic compounds according to whether they are easily, significantly less, or very resistant to, biodegradation.

Biodegradability of organic compounds such as oils can be enhanced by the presence of bacteria which eat the oil and related hydrocarbons, breaking them down into innocuous materials. Strains of such microorganisms are being developed at the University of Western Ontario⁽¹²⁾. Also, it has been reported that Rosenberg at Tel Aviv University has developed a fast-multiplying strain of arthrobacter bacteria for clean-up

of oil-tanker ballast water⁽¹²⁾. Ruel of Environment Canada states some practical considerations in the use of bacteria⁽¹²⁾:

1. Biodegradation of oil requires the presence of bacteria, nutrients, oxygen, and water, all at the same time and in the proper proportions.
2. Even if the proper nutrients are supplied, all of the necessary elements will be found together only at the interface between oil and water.
3. If the oxygen used in the decomposition comes from the dissolved oxygen in the water, the reduction in oxygen available to marine life may be more damaging than the original spill.

TABLE 3

Biodegradability of Some Organics⁽¹¹⁾

<u>Easily Biodegradable</u>	<u>Significantly Less Biodegradable</u>	<u>Very Resistant* to Biodegradation</u>
n-propanol	ethylene glycol	aniline
ethanol	isopropanol	methanol
benzoic acid	o-cresol	monoethanolamine
benzaldehyde	diethylene glycol	methylethylketone
ethylacetate	pyridine	acetone
	triethanolamine	

*Lost to the atmosphere in appreciable amounts.

Thus by choice of the right condition many of these limitations can be avoided. The products of the biooxidation are CO_2 , a residual soluble BOD (biochemical oxygen demand), TOD (total oxygen demand) and bacterial cells. The latter often constitute a difficult solid-liquid separation⁽¹³⁾.

A few data indicate that the bacteria thiobacillus ferrooxidans, used in the leaching of copper or uranium ores, is affected differently by different organics reagents⁽⁵⁾.

While these bacteria thrive in the presence of aliphatic diluents or di-(2-ethylhexyl)phosphoric acid, the presence of LIX 64N, Kelex 100, amines, or Solvesso 150 (an aromatic diluent) inhibits bacterial growth.

Effects of Soluble Metal-Extractant Complexes

One general observation regarding the toxicity of metals to fish is that if the metal ion is complexed in some way, its toxicity decreases. Thus metal ions such as copper are less toxic to salmon in hard water than in soft water, presumably as a result of complexation with the materials providing the hardness to the water.

This interesting observation may also hold for metal ions complexed by solvent extraction extractants. It is unlikely that, at the pH values normally existing in rivers and streams, the metal complex would be decomposed unless, for example, the organic moiety were biodegradable. Thus, one might suppose that the complexed metal ion would be preferable to an uncomplexed ion, at least as far as fish are concerned.

On the other hand, the conditions prevailing in a fish (or other consumer of the water) may be such as to strip the metal from the complex, thus resulting in the formation of toxic species, especially if the organic moiety were also toxic.

We can only speculate on these matters, but it is an area where studies are needed. For example, studies on the uptake of metals by plants indicate that metal-organic complexes can cross cell membranes much more easily than metal salts presumably because of their organic-like structure⁽¹⁴⁾. Thus metals can in this way move to the plant foliage, which can then be eaten by animals on which man feeds. This seems to be an area which might be of particular interest in view of the metal-organic complexes present in solvent extraction raffinates which find their way into areas where animals graze.

Another interesting aspect of this line of thinking is that concerning the uptake of metal organic complexes by animals and humans. Thus the acidity of the stomach of the animal will determine, in large part, whether the metal complex is decomposed, that is, in solvent extraction jargon, whether the metal is stripped. This would appear to depend on the stability of the metal-organic complex. However, this seems to be of little interest in solvent extraction processing at the present time.

In conclusion, it is apparent that considerably more research into the losses of solvent components to the aqueous phase is required, because of both the economic and environmental importance of this aspect of solvent extraction processing. This will include greater emphasis in the fields of analytical, inorganic and biochemistry. Unless more emphasis is placed in the areas discussed in this paper, the solvent extraction process could fall foul of environmental legislation.

REFERENCES

1. Ashbrook, A.W., *Min. Sci. Eng.*, 5, 169 (1972).
2. Ziezyk, P.R., and MacKay, D., *Can. J. of Chem. Eng.*, 49, 747 (1971).
3. Blake, C.A., Brown, K.B., Coleman, C.F., Horner, D.E. and Schmidt, J.M., USAEC Report ORNL-1903 (1955).
4. Marston, A.L., West, D.L., and Wilhite, R.N., pp. 213-236, in *Proceedings of International Solvent Extraction Conference*, Pub. CRC Press, Ohio, (1965).
5. Ritcey, G.M., and Lucas, B.H. Dept. Energy, Mines and Resources, Mines Branch, Ottawa, unpublished data.
6. Pickering, Q.H., and Henderson, C. *Journal WPCF*, p.1419, Sept. 1966.
7. Ritcey, G.M., personal communication.
8. Hawley, J.R., "Use, Characteristics and Toxicity of Mine-Mill Reagents in Ontario", Ministry of the Environment of Ontario, Toronto, 1972.
9. Painter, H.A., *Chemistry and Industry*, p.818, 1973.
10. Friede, J., Guire, P., Gholson, R.K., Gaudy, E., and Gaudy, A.F., (Oklahoma State University, Okalahoma), U.S. Dept. of Commerce, Report No. AD-759-848 (1972).
11. Technical Editor, *Chem. Eng. News*, p.42, Dec. 8, 1969.
12. Editor, *Eco/Log Report*, p.4, Aug. 10, 1973, Pub. Corpus Services, Toronto.
13. Fox, R.D., *Chem. Eng.*, p.72, Aug. 6, 1973.
14. Ashbrook, A.W., personal communication.

AUTHOR INDEX

<u>AUTHOR</u>	<u>SESSION</u>	<u>PAPER NO.</u>	<u>PAGE</u>
ABRAMOV, L A	10	79	1057
AGNEW, J B	25	260	2667
ALESSI, P	8	265	969
AL-HEMERI, A A A	15	24	1591
ALLAK, A	3	11	265
ALLARD, B	13	142	1419
ALSTAD, J	10	141	1083
ALY, G S	2	219	189
AMBROSE, P T	12	119	1319
AMMON, R V	24	6	2511
ANGELINO, H	12	140	1341
ANGELOV, G	25	250	2651
ANVILINA, V N	18	28	1891
ANWAR, M M	8	26	893
ARMFIELD, R N	25	260	2667
ARNOLD, D R	15	25	1619
ASHBROOK, A W	8	193	943
" " "	27	274	2873
ASHTON, N	17	117	1813
AUGUSTSON, J H	10	141	1083
BAGREEV, V V	17	242	1883
BAILES, P J	9	32	1011
BAIRD, M H I	15	17	289 1571
BALAKIREVA, N A	20	187	2137
BARNEA, E	2	102	141
BARTON, Mrs C J	11	246	1263
BATHELLIER A	19	257	2075
BAUMGARTNER, F	19	109	1997
BAUTISTA, R G	13	59	1399
BENMALEK, M	20	66	2109
BERARD, P	19	257	2075
BERTS, L	7	131	829
BIRCH, C P	27	261	2837
BLUMBERG, Dr R	27	103	2787
BOGDONOVA, D D	26	158	2745
BOIKOVA, D	21	186	2263
BORG, K O	20	209	2173
BORRELL, A	12	140	1341
BOUDRY, C J	14	253	1551
BOURGUIGNON, J R	18	154	1949
BOURNE, J R	12	77	1297
BOUSE, D G	19	220	2035
BOYADEHLEV, L	25	250	2651
BOZEC, C	11	201	1201
BREZHNEVA, N E	16	205	1737
BRINK, P A	26	64	2683
BRONZAN, P	21	128	2235
BRUIN, S	6	100	643
BYKHOVSKAYA, I A	20	187	2137

<u>AUTHOR</u>	<u>SESSION</u>	<u>PAPER NO.</u>	<u>PAGE</u>
CAPUANO, V	16	213	1716
CAVERS, S D	12	119	1319
" " "	3	121	399
" " "	3	147	417
CELEDA, J	4	202	477
" "	1	204	49
CHALEB, M T	22	155	2269
CHEKMAROV, A M	21	36	2209
CHERMETTE, H	20	66	2109
CHIARIZIA, R	16	213	1761
CHICHAGOVA, G N	13	41	1389
CHEMUTOVA, M K	24	136	2577
" " "	10	167	1103
CHOUDHURY, P R	12	119	1319
CHRISTIE, P G	6	125	685
CLINTON, S D	23	192	2483
COLEMAN, C F	20	148	2123
COOK, S T M	8	26	893
COX, M	24	91	2559
COX, P R	23	53	2415
CRABTREE, H E	7	67	791
CROIX, J M	8	65	913
CRONBERG, A D	6	222	747
CUER, J P	11	152	1185
DANESI, P R	16	213	1761
DANIELSSEN, T	10	141	1083
DANILOV, N A	10	206	1109
DASHER, J	27	199	2877
DAVIES, G A	3	18	289
" " "	5	87	533
" " "	5	138	567
DAVIES, G R	22	266	2379
DEMARTHE, J M	11	201	1201
" " "	11	251	1275
" " "	26	252	2765
DOULAH, M S	5	87	533
DROZDOVA, M K	7	157	849
DRYGIN, A I	10	206	1109
DUNCAN, A	14	61	1481
DWORSCHAK, H	14	14	1451
DZEVITSKII, B E	1	80	19
" " "	5	81	515
" " "	18	82	1907
DZIAMKO, V M	18	28	1891
DZUBUR, I	3	115	379

<u>AUTHOR</u>	<u>SESSION</u>	<u>PAPER NO.</u>	<u>PAGE</u>
EDGE, R M	3	90	347
EGER, I	16	163	1729
EINAGA, H	16	47	1689
EKSBORG, S	20	194	2149
ELLIS, S R M	17	117	1813
ESNAULT, F	26	252	2765
EUZEN, J P	5	130	551
FARBU, L	23	95	2427
" "	10	141	1083
FIDELIS, I	10	134	1073
FISCHER, G	17	242	1883
FISH, L W	12	119	1319
" " "	3	147	417
FLETT, D S	24	91	2559
FORSYTH, J S	3	121	399
" " "	3	147	417
FOUCHE, K F	26	64	2683
FRID, O M	20	187	2137
FROLOV, Yu G	21	33	2197
" " "	17	34	1791
GABRIELSSON, M	20	209	2173
GAI, J E	27	103	2787
GALLE, A A	18	264	1971
GALIN, M	4	15	441
GALTSOVA, E A	7	157	849
GANDON, L	11	201	1201
GAUDERNACK, B	25	211	2631
GENET, M	4	15	441
GERMAIN, M	19	257	2075
GINDIN, L M	13	41	1389
" " "	16	94	1711
GLOE, K	16	94	1717
GOLDACKER, H	19	109	20
GORBANEV, A I	1	80	19
" " "	5	81	515
" " "	18	82	1907
GOUMONDY, J P	11	251	1275
GRAUER, F	13	178	1441
GRIMM, R	7	7	765
GROENWALD, T	26	123	2715
GULLAMONT, R	4	15	441
GUNKLER, T	6	137	725
GUTTIPIREZ, M	5	130	551

<u>AUTHOR</u>	<u>SESSION</u>	<u>PAPER NO.</u>	<u>PAGE</u>
HABSLIEGER, D	22	155	2269
HAFEZ, M M	15	78	1671
HAJDU, K	27	103	2787
HALASI, R	18	139	1937
HALL, A	14	14	1451
HANSON, C	8	26	893
" "	7	50	779
" "	23	51	2399
HARTLAGE, J	6	222	747
HARTLAND, S	22	216	1845
HARTMAN, A	8	113	927
HASEGAWA, Y	17	69	1803
HAUSEBERGER, H	19	109	1997
HEALY, T V	4	57	459
HEELS, J D	24	91	2559
HENRY, E	22	256	2339
HILL, J S	6	100	643
HODGKINSON, F	15	55	1651
HOSHINO, T	19	72	1983
HUGHES, M A	11	2	1145
" " "	23	51	2399
HUMMELSTEDT, L	6	107	669
" "	7	131	829
HUPPERT, K L	19	241	2063
INGHAM, J	12	77	1297
ISSEL, W	19	241	2063
IVANOV, I M	13	41	1389
IVANOV, O V	18	28	1891
IVANOV, V D	2	233	231
IVASCHENKO, A V	18	28	1891
IYER, P V R	9	114	1029
IZARD, J A	3	121	399
JACKSON, I D	5	138	567
JAKOVLEV, G N	4	226	1853
JASNOVITSKAYA, A L	4	226	1853
JEDINAKOVA, V	4	202	477
" "	4	203	487
" "	1	204	49
JEFFREYS, G V	3	11	265
" " "	15	25	1619
JENSEN, W H	11	223	1231
JOHANNISBAUER, W	2	247	243
JOHANNSON, G	8	113	927
JOHNSSON, S	13	142	1419
JONSSON, T E	20	209	2173
JORDANOV, N	21	186	2263

<u>AUTHOR</u>	<u>SESSION</u>	<u>PAPER NO.</u>	<u>PAGE</u>
KADLECOVA, L	16	73	1705
KAISER, G	2	247	243
KALAFATOGLU, I E	3	90	347
KARJALUOTO, J	7	131	829
KARPACHEVA, S M	2	233	231
KASAKOVA, T S	18	28	1891
KASAS, T S	13	74	1409
KASIMOV, F D	4	226	493
KERTES, A S	13	177	1433
" " "	13	178	1441
KHOLKIN, A I	16	94	1717
KIKIC, I	8	265	969
KIZIM, N F	24	35	2541
KNOCH, W	19	241	2063
KOKISO, M	17	69	1803
KOLARIK, Z	24	269	2593
KOMAROV, E V	17	227	1853
KOMAROV, V N	17	227	1853
KOPUNEC, R	4	46	451
KOROL, N A	26	158	2745
KORPUSOV, G V	16	205	1737
" " "	10	206	1109
KORPUSOVA, R D	10	206	1109
KOTANI, S	21	182	2249
KOTCHETKOVA, N E	24	136	2577
" " "	10	167	1103
KOTLIAROV, R V	10	79	1057
KRASNOV, K S	13	74	1409
KROEBEL, R	20	56	2093
KRYLOV, Yu S	10	206	1109
KUHN, W	24	269	2593
KUPFER, M J	19	220	2035
KUTYREV, I M	17	242	1883
KUYLENSTIERNA, U	27	145	2803
KUZNETSOV, G I	4	226	493
KUZNETSOV, V S	13	74	1409
KYRS, M	16	73	1705

<u>AUTHOR</u>	<u>SESSION</u>	<u>PAPER NO.</u>	<u>PAGE</u>
LABROCHE, C	8	65	913
LACKME, C	8	65	913
LAKSHEMANAN, V I	11	124	1169
" " "	6	125	685
" " "	6	126	699
LANGDON, W M	3	62	319
LASKORIN, B N	16	236	1775
" " "	1	237	63
LATARD, J M	26	252	2765
LAURENCE, G J	18	154	1949
" " "	22	155	2269
LAWSON, G J	11	124	1169
" " "	6	125	685
" " "	6	126	699
" " "	6	127	711
LEAVER, T M	11	2	1145
LEBOUHILLEC, J	22	256	2339
LESSING, J G V	26	64	2683
LEVIN, I S	20	187	2137
LEWIS, L C	14	153	1535
LILLYMAN, E	14	110	1499
LOGSDAIL, D H	11	246	1263
LUBOSHENIKOVA, K S	16	94	1717
LUCAS, B H	23	174	2437
" " "	8	193	943
" " "	27	274	2873
LUNDQVIST, R	4	143	469
MACASEK, F	4	46	451
MAKSIMOVIC, Z B	18	139	1937
" " "	17	218	1845
MALEK, Z	4	202	477
MANFROY, W	6	137	725
MARDEZHOVA, G A	7	157	849
MARGULIS, V B	1	80	19
" " "	5	81	515
" " "	18	82	1907
MARKLAND, S	21	27	2183
MARSLAND, J G	23	51	2399
MARTELET, C	20	66	2109
MATTILA, T K	2	106	169
MEIDER-GORICAN, H	21	128	2235
" " "	16	213	1761
MERIGOLD, C R	11	223	1231
MERLE, A	8	65	913
MEYER, A	20	56	2093
MEYER, D	2	102	141
MEZHOV, E A	17	229	1867
MICHEL, P	18	154	1949
" " "	22	256	2339
MIHALOP, P	11	246	1263
MIKHAILIGHENKO, A I	10	79	1057
MIKHAILOV, V A	7	157	849
" " "	26	158	2745

<u>AUTHOR</u>	<u>SESSION</u>	<u>PAPER NO.</u>	<u>PAGE</u>
MIKULAJ, V	4	46	451
MILLS, A L	14	110	1499
MILNES, M H	8	267	983
MIOGINOVIC, Mrs Lj	17	218	1845
MIQUEL, P	19	197	2019
" "	11	251	1275
" "	14	253	1551
MIROKHIN, A M	16	236	1775
MISEK, T	22	258	2365
MIZRAHL, J	2	102	141
MOGLI, A	12	77	1297
MOHRING, D	22	248	2315
MORGUNOV, A F	21	33	2197
MRNKA, M	4	202	477
" "	4	203	487
" "	1	204	49
MUHL, P	16	94	1717
" "	17	242	1883
MULLER, T B	25	211	263
MUMFORD, C J	15	24	1591
" " "	15	25	1619
MURATET, G	12	140	1341
MARATOV, V M	2	233	231
MURTHY, S L N	7	50	779
MYASOEDOV, B F	24	136	2577
" " "	10	167	1103
McDONALD, C R	25	9	2607
McDOWELL, W J	20	148	2123
McKAY, H A C	23	95	2427
McKAY, H A C	11	246	1263
McNAB, G S	12	119	1319
McNEESE, L E	12	191	1371
NAKASUKA, N	7	75	823
NAVRATIL, O	24	195	2585
NAYLOR, A	14	61	1481
NEKOVAR, P	9	185	1047
NEL, V W	14	150	1519
NEMECEK, M	15	78	1671
NEMOTO, S	19	72	1983
NOVOSEITSEVA, L A	20	187	2137
NULAND, S	25	211	2631
NYHOLM, P S	6	126	699
NYMAN, B G	6	107	669
" " "	7	131	829

<u>AUTHOR</u>	<u>SESSION</u>	<u>PAPER NO.</u>	<u>PAGE</u>
O'BRIEN, W G	13	59	1399
OBUKHOVA, M E	10	228	1129
OCHKIN, A V	1	37	1
OKUHURA, D N	24	12	2527
OLDSHUE, J Y	15	55	1651
ORJASAEFER, O	25	211	2631
OTTERTUN, H	27	145	2803
PATIGNY, P	19	197	2019
PAULES, B	9	23	995
PAVLOVA, M	21	186	2263
FERRUT, M	9	23	995
PETRUKHIN, C M	1	135	35
PEARAMOND, J C	15	55	1651
PILBEAM, A	4	57	459
PILGRIM, R F	2	49	107
PLOTINSKY, G L	26	88	2703
PONTER, A B	5	263	591
PRATT, M W T	8	26	893
PRIBYLOVA, G A	10	167	1103
PRIDDEN, B J	6	127	711
PROCHAZKA, J	15	78	1671
PROKHOROVA, N P	16	205	1737
PROKOPCHUK, Yu Z	16	205	1737
PROSKURYAKOV, V A	18	264	1971
PUSHEENKOV, M F	4	226	493
" " "	10	228	1129
RAGINSKY, L S	2	233	231
RAIS, J	16	73	1705
REGNIER, G	19	197	2019
RICE, N M	7	67	791
RIPOCHE, J	5	130	551
RITCEY, G M	15	17	1569
" " "	2	49	107
" " "	23	174	2437
" " "	8	193	943
" " "	27	274	2873
ROBAGLIA, M	26	252	2765
RODINA, T F	20	187	2137
ROHDE, K L	14	153	1535
ROSENFELD, J I	3	62	319
ROUYER, H	22	256	2339
ROVINSKY, F J	26	88	2703
ROWDEN, G A	2	45	79
RUSSETON, E	3	18	289
RUVARAC, A Lj	18	139	1937
RYDBERG, J	13	142	1419

<u>AUTHOR</u>	<u>SESSION</u>	<u>PAPER NO.</u>	<u>PAGE</u>
SANDINO, D	20	66	2109
SATO, T	7	181	871
" "	21	182	2249
SATROVA, J	1	204	49
SAWISTOWSKI, H	9	114	1029
" "	3	115	379
SCARGILL, D	11	246	1263
SCHILL, G	20	194	2149
SCHMIEDER, H	19	109	1997
SCHROTTEROVA, D	4	202	477
SCHULZ, W W	19	220	2035
SCIBONA, G	16	213	1761
SCUFFHAM, J B	2	45	79
" " "	5	138	567
SEIDLOVA, B	22	258	2365
SEKINE, T	17	69	1803
SERGEEV, V P	1	80	19
SERGEEVA, V V	20	187	2137
SERGIEVSKY, V V	17	34	1711
SERYAKOVA, I V	18	83	1923
SEVDIC, D	26	129	2733
SHALYGIN, V M	18	82	1907
SHARAPOV, B N	1	237	63
SHCHEPETILNIKOV, N N	4	226	493
SHELOUMOV, M V	2	233	231
SHESTERIKOV, V N	17	229	1867
SHKINEV, B M	24	136	2577
SHMIDT, V S	17	229	1867
SHVARTSMAN, V Ya	10	206	1109
SINEGRIBOVA, O A	21	36	2209
SINITZIN, N M	26	88	2703
SLADKOVSKA, J	4	203	487
SLATER, M J	2	49	107
SOARES, L de J	17	117	1813
SOKOLOVA, N P	10	79	1057
SOLDATENKOVA, N A	21	33	2197
SPATHE, R	22	248	2315
SPINK, D R	24	12	2527
SPIVAKOV, B Ya	1	135	35
" " "	24	136	2577
STEINER, L	22	216	2289
STRACHAN, A N	23	53	2415
STUCKENS, W	11	152	1185
SUND, H	7	131	829
SVETLAKOV, V I	16	205	1737
SVETLOV, A A	26	88	2703

<u>AUTHOR</u>	<u>SESSION</u>	<u>PAPER NO.</u>	<u>PAGE</u>
TAILLARD, D	19	197	2019
TALBOT, J	22	155	2269
TANAKA, M	7	75	823
TANAKA, T	19	72	1983
TARASOV, V V	24	35	2541
TARASOVA, V A	20	187	2137
TARNERO, M	11	251	1275
TERAO, O	21	182	2249
TEXLER, N	11	152	1185
THAI, Mrs T L	18	154	1949
THORNTON, J D	9	32	1011
TISCHENKO, L I	20	187	2137
TODD, D B	22	266	2379
TORGOV, V G	7	157	849
TOUSSET, J	20	66	2109
TRAVKIN, V F	26	88	2703
TRUKHANOV, S Ya	16	205	1737
TSERYUTA, Yu S	17	242	1883
TSIMERING, L	13	177	1433
TSUBOYA, T	19	72	1983
TUNLEY, T H	14	150	1519
UEDO, M	7	181	871
UHLEMANN, E	18	224	1965
UL'YANOV, V S	16	236	1775
VACEK, V	9	185	1047
VAN DER MEER, D	6	100	643
VARENTSOVA, V I	20	187	2137
VIJAYAN, S	5	263	591
VODEN, V G	10	228	1129
VOROBYEVA, G A	18	83	1923
VORSINA, I A	20	187	2137
WAIN, A G	23	95	2427
WARNECKE, E	19	109	1997
WARNER, B F	14	61	1481
WARWICK, G C I	2	45	79
" " " "	5	138	567
WASAN, D T	3	62	319
WATSON, J S	12	191	1371
WEISS, S	22	248	2315
WILKINSON, W L	25	9	2607
WILSON, P D	14	61	1481
WURFEL, R	22	248	2315

<u>AUTHOR</u>	<u>SESSION</u>	<u>PAPER NO.</u>	<u>PAGE</u>
YAGODIN, G A	24	35	254,1
" " "	21	36	2209
YAKSHIN, V V	16	236	1775
" " "	1	237	63
YAMADA, H	7	75	823
YUDUSEKINA, L M	17	242	1883
YUKHIN, Yu M	20	187	2137
ZAGORETS, P A	1	37	1
ZOLARIK, Z	7	7	765
ZOLOTOV, Yu A	18	83	1923
" " "	1	135	35
" " "	17	242	1883



INDEX OF PAPERS

Paper No	AUTHORS	SESSION	Page
2	Hughes and Leaver	11	1145
6	Ammon	24	2511
7	Grimm and Zolarik	7	765
9	McDonald and Wilkinson	25	2607
11	Jeffreys and Allak	3	265
12	Spink and Okuhara	24	2527
14	Dworschak and Hall	14	1451
15	Guillamont, Genet and Galin	4	441
17	Baird and Ritcey	15	1569
18	Rushton and Davies	3	289
23	Paules and Perrut	9	995
24	Mumford and Al-Hemeri	15	1591
25	Arnold, Jeffreys and Mumford	15	1619
26	Arwar, Cook, Hanson and Pratt	3	893
27	Markland	21	2183
28	Dziomko, Ivanov, Anvilina, Ivashchenko and Kasakova	18	1891
32	Bailes and Thornton	9	1011
33	Frolov, Morgunov and Soldatenkova	21	2197
34	Frolov and Sergievsky	17	1791
35	Yagodin, Tarasov and Kizim	24	2541
36	Yagodin, Sinegribova and Chekmarev	21	2209
37	Zagorets and Ochkin	1	1
41	Ivanov, Gindin and Chichagova	13	1389
45	Rowden, Scuffham and Warwick	2	79
46	Macasek, Mikulaj and Kopunec	4	451
47	Einaga	15	1689
49	Slater, Ritcey and Pilgrim	2	107
50	Hanson and Murthy	7	779
51	Hanson, Hughes and Marsland	23	2399
53	Cox and Strachan	23	2415
55	Oldshue, Hodgkinson and Pharamond	15	1651
56	Kroebele and Meyer	20	2093
57	Healy and Pilbeam	4	459
59	O'Brien and Bautista	13	1399
61	Warner, Naylor, Duncan and Wilson	14	1481
62	Wasan, Rosenfeld and Langdon	3	319
64	Fouche, Lessing and Brink	26	2683
65	Croix, Labroche, Lackme and Merle	8	913
66	Benmalek, Chermette, Martelet, Sandino and Tousset	20	2109
67	Crabtree and Rice	7	791
69	Sekine, Kokiso and Hasegawa	17	1803
72	Tsuboya, Tanaka, Nemoto and Hoshino	19	1983
73	Rais, Kyrs and Kadlecova	16	1705
74	Krashov, Kasas and Kuznetsov	13	1409
75	Nakasuka, Tanaka and Yamada	7	823
77	Ingham, Bourne and Mogli	12	1297
78	Hafez, Nemecek and Prochazka	15	1671
79	Mikhailichenko, Kotliarov, Sokolova and Abramov	10	1057
80	Gorbanev, Sergeev, Dzevitskii and Margulis	1	19
81	Gorbanev, Dzevitskii and Margulis	5	515
82	Gorbanev, Margulis, Dzevitskii and Shalygin	18	1907

Paper No.	AUTHORS	SESSION	Page
83	Zolotov, Seryakova and Vorobyeva	18	1923
87	Doulah and Davies	5	533
88	Sinitzin, Travkin, Plotinsky, Svetlov and Rovinsky	26	2703
90	Edge and Kalajatoglu	3	347
91	Flett, Cox and Heels	24	2559
94	Muhl, Gindin, Kholkin, Gloe and Luboshnikova	16	1717
95	Farbu, McKay and Wain	23	2427
100	Bruin, Hill and Van Der Meer	6	643
102	Mizrahi, Barnea and Meyer	2	141
103	Blumberg, Gai and Hajdu	27	2787
106	Mattila	2	169
107	Nyman and Hummelstedt	6	669
109	Schmieder, Baumgartner, Goldacker, Hausberger and Warnecke	19	1997
110	Mills and Lillyman	14	1499
113	Johannson and Hartman	8	927
114	Iyer and Sawistowski	9	1029
115	Dzubur and Sawistowski	3	379
117	Ashton, Soares and Ellis	17	1813
119	Choudhury, Ambrose, McNab, Fish and Cavers	12	1319
121	Izard, Cavers and Forsyth	3	399
123	Groenwald	26	2715
124	Lakshmanan and Lawson	11	1169
125	Christie, Lakshmanan and Lawson	6	685
126	Lakshmanan, Lawson and Nyholm	6	699
127	Lawson and Pridden	6	711
128	Bronzan and Meider-Gorican	21	2235
129	Sevdic	26	2733
130	Euzen, Ripoche and Guttieprez	5	551
131	Hummelstedt, Sund, Karjaluoto, Berts and Nyman	7	829
134	Fidelis	10	1073
135	Spivakov, Petrukhin and Zolotov	1	35
136	Spivakov, Myasoedov, Shkinev, Kotchetkova and Chmutova	24	2577
137	Manfroy and Gunkler	6	725
138	Jackson, Scuffham, Warwick and Davies	5	567
139	Maksimovic, Ruvarac and Halasi	18	1937
140	Borrell, Muratet and Angelino	12	1341
141	Alstad, Augustson, Danielssen and Farbu	10	1083
142	Allard, Johnson and Rydberg	13	1419
143	Lundqvist	4	469
145	Kylenstierna and Ottertun	27	2803
147	Forsyth, Fish and Cavers	3	417
148	McDowell and Coleman	20	2123
150	Tunley and Nel	14	1519
152	Cuer, Stuckens and Texier	11	1185
153	Lewis and Rohde	14	1535
154	Laurence, Thai, Bourguignon and Michel	18	1949
155	Laurence, Habsieger, Talbot and Chaieb	22	2269
157	Torgov, Mikhailov, Drozdova, Mardezhova and Galtsova	7	849
158	Mikhailov, Korol and Bogdonova	26	2745
163	Eger	16	1729
167	Myasoedov, Chmutova, Kotchetkova and Pribylova	10	1103
174	Ritcey and Lucas	23	2437
177	Tsimering and Kertes	13	1433
178	Grauer and Kertes	13	1441
181	Sato and Uedo	7	871
182	Sato, Kotani and Terac	21	2249

Paper No	AUTHORS	SESSION	Page
185	Nekovar and Vacek	9	1047
186	Jordanov, Pavlova and Boikova	21	2263
187	Levin, Sergeeva, Rodina, Tarasova, Yukhin, Varentsova, Vorsina, Balakireva, Bykhovskaya, Novoseltseva, Tischenko and Frid	20	2137
191	Watson and McNeese	12	1371
192	Clinton	23	2483
193	Ritcey, Lucas and Ashbrook	8	943
194	Eksborg and Schill	20	2149
195	Navratil	24	2585
197	Patigny, Regnier, Taillard and Miquel	19	2019
199	Dasher	27	2877
201	Bozec, Demarthe and Gandon	11	1201
202	Malek, Schrotterova, Jedinakova, Mrnka and Celeda	4	477
203	Sladkovska, Jedinakova and Mrnka	4	487
204	Mrnka, Satrova, Jedinakova and Celeda	1	49
205	Brezhneva, Korpusov, Prokhorova, Prokopchuk, Svetlakov and Trukhanov	16	1737
206	Korpusov, Danilov, Krylov, Korpusova, Drygin and Shvantsman	10	1109
209	Borg, Gabrielsson and Jonsson	20	2173
211	Gaudermack, Muller, Nuland and Orjasaeter	25	2631
213	Danesi, Meider-Gorican, Chiarizia, Capuano and Scibona	16	1761
216	Steiner and Hartland	22	2289
218	Maksimovic and Miocinovic	17	1845
219	Aly	2	189
220	Schulz, Bouse and Kupfer	19	2035
222	Hartlage and Cronberg	6	747
223	Merigold and Jensen	11	1231
224	Uhlemann	18	1965
226	Pushlenkov, Shchepetilnikov, Kuznetsov, Kasimov, Jasnovitskaya and Jakovlev	4	493
227	Komarov and Komarov	17	1853
228	Pushlenkov, Voden and Obukhova	10	1129
229	Shmidt, Mezhev and Shesterikov	17	1867
233	Karpacheva, Raginsky, Muratov, Ivanov and Sheloumov	2	231
236	Laskorin, Yakshin, Ul'Yanov and Mirokhin	16	1775
237	Laskorin, Yakshin and Sharapov	1	63
241	Huppert, Issel and Knoch	19	2063
242	Bagneev, Zolotov, Tseryuta, Yudushkina, Kuttyrev, Fischer and Muhl	17	1883
246	Mihalop, Barton, Logsdail, McKay and Scargill	11	1263
247	Johannisbauer and Kaiser	2	243
248	Weiss, Spathe, Wurfel and Mohring	22	2315
250	Boyadzhiev and Angelov	25	2651
251	Demarthe, Tarnero, Miquel and Goumondy	11	1275
252	Esnault, Robaglia, Latard and Demarthe	26	2765
253	Boudry and Miquel	14	1551
256	Rouyer, Lebouhellec, Henry and Michel	22	2339
257	Germain, Bathellier and Berard	19	2075
258	Seidlova and Misek	22	2365
260	Armfield and Agnew	25	2667
261	Birch	27	2837
263	Vijayan and Ponter	5	591
264	Proskuryakov and Gaile	18	1971
265	Kikic and Alessi	8	969
266	Todd and Davies	22	2379
267	Milnes	8	983
269	Kolarik and Kuhn	24	2593
274	Ritcey, Lucas and Ashbrook	27	2873

FRENCH WORKING GROUP

Chairman: Mr C LONG, President de la Section Centre-Est de la Societe de chimie industrielle

Vice-Chairman: Prof. GERMAIN, Directeur de l'Ecole Superieure de chimie industrielle de Lyon

Mr M JAYMOND, Directeur du Laboratoire de Recherches de Decines

Mr N VACHET, President du Syndicat des fabricants de produits chimiques de Lyon & de la region

Secretary: Mlle Y GIROD, Secreteaire Generale du Syndicat des fabricants de produits chimiques de Lyon

Representants de la chimie:

Mr P DOMINJON, Vice-President de l'Union des Industries chimiques

Mr M GAILLARD, Directeur de la Ste des usines chimiques RHONE-POULENC

Mr LAFONT, Centre de Recherches Les Carrieres

Mr SACONNEY, Directeur du Centre de Recherches Lyonnais

Mr TRIPARD, Directeur a la Ste des usines chimiques RHONE-POULENC

Prof PORTAULT, Universite LYON I et Societe de chimie industrielle de Lyon

Representants de l'industrie du Petrole:

Mr GROLLIER-BARON, Institut Francais du Petrole

Mr LAGOUTTE, Societe ELF

Representant l'industrie textile:

Mr P ROCHAS, Directeur General du Centre de recherches de la soierie & des industries textiles

Representant les produits a usage pharmaceutique:

Mr P RAJOT, Directeur de la Societe ROUSSEL-UCLAF

Representant les produits a usage parfumerie:

Mr M GATTEFOSSE, Directeur de la Societe GATTEFOSSE

Representant la Metallurgie:

Mr J COURSIER, Directeur a la Ste, PECHINEY UGINE KUHLMANN

Mr ROBATEL, President-Directeur General, ROBATEL S.L.P.I.

Representant les recherches nucleaires:

Mr ROSTAING, Centre d'Etudes Nucleaires